
Final Reports of the U.S. Experiments Flown on the Russian Biosatellite Cosmos 2229

James P. Connolly, Michael G. Skidmore, Denice A. Helwig, Editors
Ames Research Center, Moffett Field, California

April 1997



National Aeronautics and
Space Administration

Ames Research Center
Moffett Field, California 94035-1000

PREFACE

On December 29, 1992, Russia launched Cosmos 2229, an unmanned spacecraft carrying biological experiments from several countries. Those participating included the United States, Canada, France, Germany, Kazakhstan, Ukraine and the European Space Agency. This mission included 11 U.S./Russia joint experiments.

Cosmos 2229 represents the eighth consecutive Cosmos biosatellite mission involving U.S. and USSR/Russia joint experiments. Earlier flights included Cosmos 782 in November 1975, Cosmos 936 in August 1977, Cosmos 1129 in September 1979, Cosmos 1514 in December 1983, Cosmos 1667 in July 1985, Cosmos 1887 in September 1987, and Cosmos 2044 in September 1989. These Cosmos Biosatellite Missions, involving experiments with monkeys, rats, plants, and insects, have provided scientists with valuable information on how the basic biology of living organisms is affected by the space environment.

For Cosmos 2229 (referred to as Bion 10 by Russian participants), the U.S. focus for the mission shifted away from research with rats and concentrated on nonhuman primate studies. To allow room on the spacecraft for additional research equipment, no rats were flown on the Cosmos 2229 mission.

Cosmos 2229 returned to Earth successfully on January 10, 1993, near the city of Karaganda in Kazakhstan. It was a complex mission that required nearly three years of preparation for flight and ground test hardware to support the mission. On behalf of all American participants, I wish to thank the Institute of Biomedical Problems, SKTB Biophyspribor, CSDB Samara, and the many fine Russian scientists, engineers and other specialists who provided outstanding support for the U.S./Russia joint experiments on Cosmos 2229.

Two people who contributed extensively to the Cosmos (Bion) Biosatellite Program and to Cosmos 2229 are no longer with us. They are Drs. Rodney Ballard and Arkady Truzhennikov. Dr. Ballard was the U.S. Project Scientist for Cosmos Missions 1887, 2044 and 2229. Dr. Truzhennikov worked on many biosatellite teams for the primate flights and filled the critical role of science support manager and test schedule coordinator for Cosmos 2229. His support was essential to the smooth flow of preflight and postflight science testing for the mission. This volume is dedicated to the memory of Drs. Rodney Ballard and Arkady Truzhennikov, and others like them, who have helped to establish and maintain the quality and vitality of the Cosmos (Bion) Biosatellite Program.

James P. Connolly
Cosmos 2229 Project Manager
NASA Ames Research Center

TABLE OF CONTENTS

PREFACE	iii
TABLE OF CONTENTS	v
SUMMARY	1
I. COSMOS 2229 MISSION DESCRIPTION	2
A. INTRODUCTION	2
B. MISSION OVERVIEW (E.A. Ilyin and V.I. Korolkov).....	3
1. Background	3
2. Primate Experiments	3
3. Gravitational Biology Experiments	4
4. Radiation Dosimetry Studies	5
5. Radiation Biology Studies	6
C. RUSSIAN HARDWARE SUPPORT OF EXPERIMENTS (V.K. Golov, V.S. Magedov, V.I. Korolkov)	6
D. PREPARING THE PRIMATES FOR SPACE FLIGHT (V.I. Korolkov, B.A. Lapin, A.N. Truzhennikov, Yu.V. Gordeev, D. Helwig).....	8
E. U.S. MISSION MANAGEMENT	9
1. U.S. Experiments	9
a. Primate Experiments	9
b. Primate-Bios.....	10
2. Mission Management Plan	10
a. Hardware Development	11
b. Training	11
c. Hardware and Experiment Verification Tests	11
d. Science Integration Tests.....	11
e. Data/Specimen/Hardware Transfer for Postflight Analysis.....	11
f. Documentation	12
F. PRIMATE EXPERIMENT OPERATIONS	12
1. Flight Group	12
a. Preflight Events.....	12
b. Launch, On-Orbit, and Reentry Events.....	12
c. Postflight Events.....	13
2. Control Groups.....	13
TABLES AND FIGURES FOR SECTION I	14

II. U.S. FLIGHT AND GROUND-SUPPORT HARDWARE	35
A. HARDWARE OVERVIEW	35
1. Flight Hardware and Test Plan.....	35
2. Ground-Support Hardware and Test Plan.....	36
3. Hardware/Software Documentation and Data Transfer.....	36
B. EXPERIMENT-SPECIFIC HARDWARE	36
1. Circadian Rhythm/Temperature Regulation Experiment	36
a. Flight Hardware	36
b. Ground-Support Hardware.....	37
2. Neurovestibular Experiments.....	37
a. Flight Hardware	37
b. Ground-Support Hardware.....	37
3. Neuromuscular Experiment	38
a. Flight Hardware	38
b. Ground-Support Hardware.....	38
4. Bone Experiments	38
a. Flight Hardware	38
b. Ground-Support Hardware.....	38
 TABLES AND FIGURES FOR SECTION II	 39
III. SCIENCE REPORTS	63
K-8-01 (1)	65
Bending Stiffness of the Tibia in Young Rhesus Monkeys after Two Weeks in Space Aboard the Cosmos 2229 Biosatellite <i>S.B. Arnaud, et al.</i>	
K-8-01 (2)	81
Calcium Metabolism and Correlated Endocrine Measurements in Primates During Cosmos 2229 <i>C.E. Cann, et al.</i>	
K-8-01 (3)	91
DEXA Measurements: Cosmos 2229 Rhesus Flight Experiment <i>A. LeBlanc, et al.</i>	
K-8-02	109
Reduction of Ocular Counter-Rolling by Adaptation to Space <i>B. Cohen, et al.</i>	
K-8-03	131
Studies of Vestibular Neurons in Normal, Hyper- and Hypogravity <i>M.J. Correia, et al.</i>	
K-8-04 (1)	169
Functional Neuromuscular Adaptation to Space Flight <i>V.R. Edgerton, et al.</i>	

K-8-04 (2)	185
Morphologic and Metabolic Properties of Single Muscle Fibers in Hindlimb Muscles of the Rhesus <i>S.C. Bodine-Fowler, et al.</i>	
K-8-05	215
Circadian Rhythms and Temperature Regulation in Rhesus Monkeys During Space Flight <i>C.A. Fuller, et al.</i>	
K-8-06	239
Rhesus Monkey Metabolism During Space Flight: Measurement of Energy Expenditure Using the Doubly Labeled Water Method <i>C.A. Fuller, et al.</i>	
K-8-07	249
Cosmos 2229 Rhesus Monkey Immunology Study <i>G. Sonnenfeld, et al.</i>	
K-8-08	291
Adaptation to Microgravity of Oculomotor Reflexes (AMOR): Otolith-Ocular Reflexes <i>D.L. Tomko, et al.</i>	
Supplemental Data Analysis	353
Plasma Hormone Concentrations in Rhesus Monkeys After Space Flight <i>R.E. Grindeland, et al.</i>	

LIST OF TABLES

SECTION I

1. Cosmos biosatellite missions with U.S. participation	14
2. Summary list of papers presented at the Cosmos 2229 Final Results Symposium	15
3. Primate food, juice and water consumption	20
4. Primate cardiovascular data before and after flight	21
5. Primate examinations and tests postflight	22
6. Electrodes and sensors implanted	23
7. Physiological signals recorded inflight.....	24

SECTION II

1. Summary list of hardware by experiment	39
---	----

LIST OF FIGURES

SECTION I

1. Cosmos spacecraft	25
2. Capsule oxygen and relative humidity	26
3. Capsule temperature	27
4. Heart rate of monkey 151 (Ivasha)	28
5. Heart rate of monkey 906 (Krosh).....	29
6. Body temperature of monkey 151 (Ivasha)	30
7. Body temperature of monkey 906 (Krosh).....	31
8. Primate-Bios	32
9. Monkey in Bios restraint chair.	33
10. Psychomotor Response System	34

SECTION II

1. Cosmos 2229 inflight bioinstrumentation	44
2. U.S. Signal conditioning - Cranial cap	45
3. U.S. Signal conditioning - Other than cranial cap	46
4. CR/T flight hardware	47
5. Head electronics assembly	48
6. Head Electronics Signal Simulator (HESS)	49
7. Head Motion Velocity (HMV) unit.	50
8. EEG/EOG hybrid chip	51
9. Optokinetic rotator	52
10. Computer-controlled, multi-axis rotator	53
11. Portable Linear Sled (PLS)	54
12. Ground Test Unit-1 (GTU-1)	55
13a. Tendon force sensor assembly	56
13b. Tendon force sensor	57
14. Tendon force signal conditioner	58
15. EMG/ECG board	59
16. Ground Test Unit-2 (GTU-2)	60
17. Mechanical Response Tissue Analyzer (MRTA)	61

SUMMARY

Cosmos 2229 was launched on December 29, 1992, containing a biological payload including two young male rhesus monkeys, insects, amphibians, and cell cultures.

The biosatellite was launched from the Plesetsk Cosmodrome in Russia for a mission duration of 11.5 days. The major research objectives were:

- Study adaptive response mechanisms of mammals during flight
- Study physiological mechanisms underlying vestibular, motor system and brain function in primates during early and later adaptation phases

American and Russian specialists jointly conducted 11 experiments on this mission including extensive preflight and postflight studies with rhesus monkeys. Biosamples and data were subsequently transferred to the United States. The U.S. responsibilities for this flight included development of flight and ground-based hardware, verification testing of hardware and experiment procedures, and postflight analysis of biospecimens and data for the joint experiments.

A description of the Cosmos 2229 mission is presented in this report including preflight, on-orbit and postflight activities. The flight and ground-based bioinstrumentation which was developed by the U.S. and Russia is also described, along with the associated preflight testing of the U.S. hardware. The major hardware components for this mission (Bios systems and major instrumentation systems) were developed by SKTB Biophyspribor in St. Petersburg, Russia. Final Science Reports for each of the U.S./Russia joint experiments are also included.

Richard Mains, Greg Leonard and the staff of Mains Associates expended a great deal of effort on the compilation and organization of materials for this Cosmos 2229 report. Their assistance in the preparation of this document is greatly appreciated.

I. COSMOS 2229 MISSION DESCRIPTION

A. INTRODUCTION

The Cosmos 2229 biosatellite was launched from Plesetsk on December 29, 1992, at 16:30 hours Moscow time. Recovery was at 07:16 hours on January 10, 1993. Total mission duration was 11.5 days. Cosmos 2229 was the eighth consecutive USSR/Russia biosatellite mission to include the participation of U.S. scientists. Table 1 lists all Cosmos missions with joint U.S.-USSR/Russia experiments and summarizes mission parameters for each. Other countries that participated in the Cosmos 2229 mission were Canada, France, Germany, Kazakhstan, and Ukraine. The European Space Agency also sponsored some experiments. Table 2 provides a complete listing of the papers presented at the Cosmos 2229 Final Results Symposium in December 1993.

The Cosmos 2229 biosatellite carried two male rhesus monkeys and an assortment of amphibians, insects and cell cultures. The U.S.-Russia joint experiments conducted on Cosmos 2229 included eleven primate experiments studying neurovestibular, musculoskeletal, circadian rhythm and metabolic responses.

B. MISSION OVERVIEW
E.A. Ilyin and V.I. Korolkov
Institute of Biomedical Problems (IMBP), Moscow

1. Background

On December 29, 1992, at 16:30 hours Moscow time, the Cosmos 2229 biological satellite (Figure 1) was launched from the Plesetsk cosmodrome in the Arkhangelsk area of Russia. The flight, planned for a length of up to 14 days, was terminated after 11 days, 16 hours. Cosmos 2229 landed on January 10, 1993, 100 km to the north of the city of Karaganda at 07:16 hours.

The main objective of the Cosmos 2229 mission was to investigate the mechanisms of adaptation to microgravity at the organism, cellular and subcellular levels. Primate studies were conducted to investigate the central mechanisms underlying the development of space motion sickness, central nervous system, musculoskeletal and cardiovascular function at early and intermediate stages of adaptation to microgravity, and time course variations of circadian rhythms. Other non-primate experiments were carried out in the fields of cell and population biology, developmental biology, chronobiology, and radiation biology.

The biosatellite carried two rhesus monkeys, Spanish newts, fruit flies, desert darkling beetles, silkworm larvae and clawed frog eggs. Experiments were also carried out on plant and animal cell cultures. Various bio-objects, detectors and dosimeters were flown inside and outside the spacecraft in support of radiation investigations. All biological experiments survived the flight.

During the nearly 12-day flight, the biosatellite completed more than 185 orbits around the Earth. Orbital parameters were as follows: apogee–396.8 km; perigee–226 km; angle of inclination–62.8°; initial rotation period–90.4 minutes. Environmental parameters within the biosatellite were:

- total barometric pressure: 720-760 mm Hg
- partial O₂ pressure: 140-180 mm Hg (Figure 2)
- partial CO₂ pressure: up to 1 mm Hg
- relative humidity: 30-70% (Figure 2)
- ambient temperature, first 9.5 days: 20-26 °C (Figure 3)
- ambient temperature, last 2 days: 30-31.3 °C (Figure 3)
- light cycle: 16 hours light, 8 hours dark
- illumination level: 60 lux (light), 2 lux (dark)

The Cosmos 2229 flight, dedicated to the 1992 International Space Year, was an international project with American, Russian, German, French, Czech, Canadian, Chinese, Dutch, Lithuanian, Ukrainian, Uzbek and European Space Agency (ESA) scientists represented on the mission.

2. Primate Experiments

The primate experiments used rhesus (*Macaca mulatta*) monkeys, raised in the primate nursery in the city of Sukhumi. Primate selection and training began eighteen months before launch. From the original group of 36 animals, twelve were selected for implantation and eventually seven were delivered to the launch site. This constituted three crews—a prime, a backup and a reserve—and an individual monkey for making technical recordings.

The primate selection procedures included extensive clinical and veterinary monitoring. Skin and hair were evaluated, a detailed set of blood and immunological parameters was tracked, heart rate and ECG were evaluated, behavioral patterns were monitored, intestinal and skin microflora were evaluated, and fluctuations in body temperature and weight were assessed.

The training regimen included instrumented reflexes required to perform arm and leg motor tasks, and acclimatization to and use of the flight hardware. To evaluate animal tolerance to launch and reentry stresses, +Gz acceleration tests were also performed. Surgical implantation of electrodes and sensors followed. Of a pool of six flight candidates, two monkeys, Ivasha (#151) and Krosh (#906), were selected and placed in the Primate-Bios capsules three days before launch. The capsules were then loaded into the biosatellite one day prior to launch.

Krosh adapted well to space flight as evidenced by physiological parameters. Ivasha appeared to develop space motion sickness. Krosh's mean daily heart rate ranged from 110 to 195 bpm. Ivasha's mean heart rate ranged from 65 to 168 bpm. Body temperature of both animals was in the range of 36.6–39.9 °C (Figures 4–7).

Inflight food and juice consumption for Krosh and Ivasha are shown in Table 3. Krosh's food and juice consumption was almost equal to baseline. Ivasha consumed approximately 30% of food and juice baseline amounts. Pre-, during and postflight, the monkeys were fed a paste flight diet to ensure comparable metabolic data. On days 2, 3 and 5, while exhibiting space motion sickness, Ivasha consumed significantly less food than normal.

The biosatellite landed on January 10 at 07:16 Moscow time 100 km north of the city of Karaganda. A field laboratory was set up at the landing site. The Primate-Bios capsules were removed from the biosatellite and taken to the field laboratory. The monkeys were removed from the capsules and given physiological examinations to determine their health status. Examination of the monkeys at the site showed Krosh to be in satisfactory condition, active and responsive to environmental stimuli. Ivasha was sluggish and exhibited orthostatic intolerance. His condition improved markedly after countermeasures were taken. Krosh showed a 5% body weight decrease while Ivasha showed a 13% decrease. As called for in the experiment protocols, blood, sublingual cell and urine samples were collected from the monkeys at this time. Pre- and postflight cardiovascular data for each monkey are shown in Table 4.

After preliminary examinations and sample collection, the primates, other bio-objects and experimental hardware were shipped to Moscow and delivered to the Planernaya campus of the Institute of Biomedical Problems (IMBP) 16 hours after recovery. Ivasha began participation in postflight testing one or two days later than Krosh. Six weeks after recovery, ground-based control experiments were conducted with the flight subjects. The schedule of postflight examinations and tests is shown in Table 5.

3. Gravitational Biology Experiments

Several gravitational biology experiments flew on the Cosmos 2229 mission supported by Russian and ESA hardware. These studies encompassed a number of disciplines within biology, including cell, developmental, chrono-, and population biology. Scientists representing Russia, former Russian republics, Canada, China and ESA conducted the experiments. Most of the experiment payloads were placed in the biosatellite two days before launch. One plant container was loaded 4.5 hours before launch. The research subjects were examined at the recovery site field laboratory and then transported to Moscow in temperature controlled biotransporters.

- Fruit Fly Experiment

Three strains of fruit flies (*Drosophila melanogaster*) were cultivated prior to the launch. The strains, housed either in a clinostat, centrifuge or normal conditions, were each adapted to a different gravity field. Their responses to microgravity were compared. The clinostat and normal gravity strains showed the highest fertility rates while the centrifuge strain showed the lowest fertility rate.

- Beetle Experiment

The effect of microgravity on circadian rhythms of motor activity was studied using darkling beetles (*Trigonoscelis gigas R.*). The flight group experienced microgravity in orbit and ground controls experienced seven days of 2 g hypergravity on a centrifuge. This study demonstrated for the first time that the circadian rhythms of motor activity are gravity dependent.

- Silkworm Experiment

The silkworm caterpillars were in good condition and completed normal pupation.

- Tadpole Experiment

To study the effect of microgravity on organ development, 53 African clawed frog (*Xenopus laevis*) eggs at the tail bud stage were flown. During flight, 45 larvae hatched and developed as freely swimming tadpoles. Compared to ground controls, the flight tadpoles developed smaller bodies and lungs. After adaptation to Earth gravity, the flight tadpoles also exhibited negative buoyancy: when not swimming, they remained at the bottom of their water bowls.

- Newt Experiment

Fifteen adult female Spanish newts (*Pleurodeles waltlii*) were launched to study the effect of microgravity on tissue regeneration. Specific tissue types included limb, muscle, bone, eye lens, brain, vestibular and olfactory organs, as well as blood formation, calcium metabolism, oogenesis, and genetic parameters. Of those fifteen, only eight survived. Tissue that regenerated during space flight exhibited some abnormalities, but the significance of specific findings remained unclear.

- Cell Culture Experiments

Fibroblast cells were isolated from fifteen-day mouse embryos. Two culture types flew on the mission. One was a monolayer culture, obtained from F-208 mice, attached to a solid substrate; the other was a three dimensional histoculture obtained from A-Sn mice, on a gel support. The experiment was flown in an ESA Biobox unit. The cell cultures were recovered in good condition. Postflight analysis showed evidence that microgravity can cause significant changes in the morphology and function of cells growing on a solid substrate.

4. Radiation Dosimetry Studies

The purpose of the radiation studies was to monitor the experimental environment generated by nuclear and electromagnetic solar radiation during space flight. Radiation levels are dependent on biosatellite orientation and orbit parameters. Detailed data were to be gathered on ionizing radiation both outside the capsule, with thin or no shielding, and inside the capsule behind shielding. This ongoing series of studies is gathering information on the entire spectrum of ionizing radiation at the Cosmos orbital inclinations.

Of the four containers housing passive dosimetry detectors attached to the outside of the biosatellite, two were found to be only partially closed upon recovery. The surfaces of these two containers were badly burned. Temperatures in the containers ranged from below -60 °C to above 60 °C.

Flight measurements yielded new data concerning neutron dose spectra typical of a minimum solar activity time period. A correlation was also established between an absorbed dose and detector material thickness. Maximum surface dose during flight was 2200 rad per day and the distribution curve indicates that the dose consists primarily of low energy protons and radiation belt electrons.

Along with these measurements, doses absorbed by the primates were measured. Their total dosage was 445 ± 23 mrem during the course of the flight.

An investigation was also carried out to explore the use of dielectric material as radiation shielding. It was hypothesized that high-ohmage dielectrics irradiated to elicit strong internal electric fields would significantly reduce the absorbed radiation dose without increasing shield thickness and weight. Glass plates were precharged on the ground and then exposed to cosmic radiation while on the biosatellite.

Results showed that the penetration depth of electrons in the dielectric was reduced, the back scattering coefficient increased, the coefficient of electron passage across thin dielectric layers decreased and the absorbed dose behind the charged dielectric layers decreased. The absorbed dose behind the charged glass decreased by 30–40% and it was determined that this material increases shielding efficiency by 1.5–1.8 times without an increase to shielding thickness or weight.

5. Radiation Biology Studies

The purpose of the radiation biology investigation was to study the effects of cosmic radiation, and heavy ions in particular, on actively metabolizing higher aquatic plants (*Wolffia arrhiza*). Using plastic detectors, for the first time it was possible to identify specimens hit by single heavy ion particles.

During the 11.5 days of space flight, 16.5% of the plant specimens were hit by radiation particles. Upon recovery, the detectors were processed and the ten-month ground-based portion of the study was carried out. Over that period, the following parameters were measured: specimen death rate, developmental abnormalities, and remote effects. It was found that specimens hit or passed closely by particles experienced a 50% death rate. Controls only experienced a 27% death rate. Flight specimens also exhibited the highest number of developmental abnormalities.

C. RUSSIAN HARDWARE SUPPORT OF EXPERIMENTS AND ENVIRONMENTAL PARAMETERS *V.K. Golov, V.S. Magedov, V.I. Korolkov* IMBP, Moscow

The experiment hardware flown on Cosmos biosatellites fulfills several functions. These include:

- 1) providing life support to experimental animals and other biological specimens during a long-term space flight
- 2) monitoring health status of the flight animals and controlling experimental protocols
- 3) maintenance of predetermined environmental parameters, i.e., temperature, humidity, oxygen supply, and removal of carbon dioxide and toxic gases
- 4) generation of special effects, e.g., animal lifting at a predetermined speed, presentation of light signals
- 5) operating life support and data recording systems in an automated mode
- 6) ensuring data collection, preliminary processing and storage during flight

In terms of design and development, animal life support and research systems (Bios) present the greatest challenge. The Primate-Bios capsules for rhesus monkeys have been used in four flights without significant modifications. The Primate-Bios consists of an animal capsule containing a primate chair and life support subsystems such as ventilation, light, food supply, juice supply and waste management. (A description of the Primate-Bios is found below in section 1.b of the U.S. Mission Management segment of this report.)

Physiological measurements for the Cosmos 2229 mission were performed using hardware procured by the Institute of Biomedical Problems (IMBP) from several companies, particularly SKTB Biophyspribor, St. Petersburg, Russia. Some experiments were performed by means of hardware supplied by principal investigators from Germany, the United States and Czechoslovakia. The research hardware included:

- Implanted and applied sensors and electrodes for measuring physiological parameters
- Biopotential amplifiers and signal conditioners
- Multiplexers for sending required data to tape recorders
- Two types of analog tape recorders
- Control unit that regulated lights, operator's tasks, data recording, food and juice supply, command translation and forwarding

During the Cosmos 2229 flight, 21 physiological parameters arranged in eight programs were recorded by four flight recorders. In addition, biorhythm parameters were recorded using an eight-channel signal processor (U.S.), and galvanic skin reflexes were measured by a custom-made unit (Germany). A list of physiological signals recorded from the two monkeys and recording programs are shown in Tables 6 and 7.

Although there were several hardware failures, the science program was implemented and important information on how to modify the hardware was obtained.

Air regeneration was ensured by using potassium peroxide as in manned spacecraft. Partial oxygen pressure was maintained within the range 140–180 mm Hg. Toxic contaminants were removed by means of activated charcoal filters. Sources of these toxic contaminants are construction materials (porolone, polyethylene, lacquers, etc.), animal bodies and, mainly, animal wastes. Chromatographic analysis of air contaminants, according to IMBP methods, demonstrated that their concentration was significantly lower than maximally allowable concentrations recognized for manned missions. For more detailed information on the environmental conditions within the biosatellite, see the "Habitation Conditions" section of the Cosmos 2044 mission report (NASA Technical Memorandum 108802).

Cosmos 2229 also carried various pieces of hardware developed for the gravitational biology experiments by the Ukraine, Lithuania, Uzbekistan, China, and ESA. ESA developed the Biobox, a thermally controlled unit which included a cultivator and a centrifuge generating 1 g.

The flight was 11 days and 16 hours in duration. During flight the health status of both animals remained satisfactory. However, beginning with flight day 5 a food dispenser in one Primate-Bios failed and an emergency food supply system was activated. The emergency system was flown on Cosmos 2229 for the first time.

By flight day 10, most experiments were completed. In terms of weather conditions at the recovery site, the biosatellite could be recovered on flight days 11 through 15. However, on flight day 10 the biosatellite continuously remained under solar light which caused the inside temperature to rise to 31.3 °C (see Figure 3). Taking this into account, the decision was made to land the biosatellite on flight day 12.

Primate examinations immediately after recovery were performed in a field laboratory deployed at the recovery site and equipped with all necessary hardware.

D. PREPARING THE PRIMATES FOR SPACE FLIGHT
V.I. Korolkov, B.A. Lapin, A.N. Truzhennikov, Yu.V. Gordeev, D. Helwig
IMBP, Moscow and Ames Research Center, Moffett Field

Primate selection and training began 18 months before launch. Approximately 90 male juvenile monkeys were initially selected at the Institute of Experimental Pathology and Therapy, Sukhumi, Georgia in the former Soviet Union. These free-ranging animals were put into single cages. They were observed clinically and a determination of their morphological suitability (weight, height, girth) for the flight hardware configuration was made.

From this initial group, 60 were selected and trained to sit in primate chairs. Each animal's behavior and adaptability to minimal restraint were recorded. As a result, further culling of the animal pool took place and approximately 30 animals continued with the training regimen. They were trained to use the feeding and drinking systems and to perform motor tasks critical to the inflight neurophysiology experiments. About a year before flight, the best 20 animals were selected and shipped to the Institute of Biomedical Problems (IMBP) in Moscow, Russia where more refined training and preparation for flight occurred.

At IMBP, training of the animals to the flight environment and test paradigms was pursued. The monkeys were trained to two programs, using a juice supply as a reward. For Program 1 (head-eye-hand coordination), a light signal is presented in the center of a semi-circular panel. The animal is required to turn off the signal by pushing the lit target with a finger. Then another lit target is presented to the right or to the left at random. The animal is rewarded with juice if he performs correctly. If he makes a mistake, the next signal will be presented after a delay. Program 2 light signals are located in the center of the panel, at a slightly lower level than the Program 1 signals. According to the program, the monkey is required to move his foot and to push the foot pedal in response to a stimulus. In response to a light triggering signal the animal must push the foot pedal three times within a certain time period and within a certain range. If the animal performs the task correctly, another light stimulus is presented. In this case the animal must keep the pedal depressed within a certain range for a specific amount of time. As soon as the motor performance criteria have been met, the animal can be presented at random with more difficult tasks, e.g. applying greater force. Previous investigations demonstrated that preparation for Program 2 requires more time than training on Program 1.

The basic criteria for selection of flight candidates at this phase were the rate of adaptation to isolation and the ability to learn essential motor tasks. Throughout the process of selection, general health and morphological characteristics were evaluated. Following acceleration, noise and prolonged isolation tests, 12 animals were selected as the prime flight candidates. These animals underwent a series of six surgical procedures, beginning 4 1/2 months before flight, including implantation of multiple sensors (e.g. EMG, EEG, ECG, electro-oculogram, tendon force, temperature) and collection of biopsies (muscle, bone, marrow).

After postoperative recovery, the animals were tested to obtain baseline physiological and behavioral data. Approximately 40 days preflight, the animals were placed on the paste diet used for flight. Seven animals were selected and shipped to the launch site approximately three weeks before launch. These animals were selected and ranked based on health, size (3.5–4.5 kg), adaptability to the flight capsule, performance on motor tasks and condition of implanted sensors. The animals selected for flight, #151 (Ivasha) and #906 (Krosh), were placed in the satellite two days before launch. They were approximately three years old at launch.

Inflight, each animal was maintained in a Primate-Bios capsule which included life support and experiment systems. Each monkey was seated in a primate restraint couch equipped with an upper right arm restraint strap and a lap restraint plate with a leg separator. A waste collection system used unidirectional airflow to direct excreta toward a receptacle underneath the chair. The primate

chair was designed to provide adequate support to the monkey for launch accelerations and for the deceleration levels associated with re-entry. (Typically, deceleration levels measure up to 40 g for 10 msec at different stages of descent and less than 30 g for 40 msec at impact.) A detailed description of the Primate-Bios system used for Cosmos 2044 is contained in NASA Technical Memorandum 108802. While the Cosmos 2229 Primate-Bios is different in some respects, most features of the system remained the same.

Each Primate-Bios contained separate primate-activated dispensers for a water/juice mixture and a paste diet. These dispensers were designed so that presentation to the animal could be controlled via an uplinked signal from the ground. The orientation of the two primate capsules in the spacecraft enabled the monkeys to view each other. A television camera mounted in each Bios allowed periodic inflight video monitoring of the subjects from the ground.

At recovery, the monkeys were in satisfactory condition. They were active and showed appropriate responses to environmental stimuli. After preliminary examinations, the primates were shipped to Moscow and arrived at the IMBP test facility approximately 16 hours after landing. Testing for the neurovestibular experiments began almost immediately, although Ivasha began participation in postflight testing one day later than Krosh. The postflight testing in all disciplines continued through the seventeenth day after recovery.

Following space flight, data from Ivasha and Krosh were compared with their preflight data and with data from the remainder of the flight pool, which made up the control group. A control study was performed 40 days after recovery to assess readaptation following space flight. The flight animals were housed in flight-like capsules and physiological data were recorded as in flight. Four of the control animals were housed in lower fidelity flight-type primate chairs and capsules, which did not have the capability to record physiological data. After a mission-length restraint period, biopsies were taken from all six animals to acquire bone, muscle and bone marrow samples. The control study also provided an opportunity to retest the flight experience of Ivasha, who had a reduced food intake. Since the animals were fed the flight paste diet, this experience was mimicked with one of the control animals.

Cosmos 2229 adds an important segment of data to existing information about the physiological effects of weightlessness on restrained rhesus monkeys. The mission has helped to extend the understanding of the impact of space flight on neurovestibular, musculoskeletal, immunological, cardiovascular, endocrine and thermoregulatory systems. Further, results of these studies can be expected to add to the understanding of some mechanisms of human response to microgravity. Animal care and use throughout all phases of this project conformed to World Health Organization guidelines.

E. U.S. MISSION MANAGEMENT

1. U.S. Experiments

The joint U.S./Russian experiments conducted aboard Cosmos 2229 included 11 primate experiments using rhesus monkeys (*Macaca mulatta*) as subjects. The primates were provided by the Institute of Biomedical Problems (IMBP), Moscow.

a. Primate Experiments

These experiments were designed to study adaptive physiological responses to microgravity in primates. The goals of the experiments were to study the effect of microgravity on: bone and calcium metabolism, neurovestibular responses, neuromuscular functioning, circadian rhythms and temperature regulation, metabolism, and immune responses. Specific objectives were to:

- Study bone density, bone stiffness and calcium metabolism before and after exposure to microgravity
- Study the effect of microgravity on the vestibulo-ocular reflex during vestibular and optokinetic stimulation
- Compare eye movement responses, vestibular primary afferent responses and vestibular nuclei responses under normal gravity and microgravity conditions
- Study linear vestibulo-ocular reflexes during gravity receptor stimulation before and after exposure to microgravity
- Determine the effect of weightlessness on flexor and extensor muscles of the leg using functional, biochemical and morphological measurements
- Study the circadian timekeeping system, the effectiveness of circadian rhythm synchronizers and the thermoregulatory system of rhesus monkeys during space flight
- Determine the metabolic rate in rhesus monkeys during space flight, as measured by CO₂ production using the doubly-labeled water method
- Determine the effects of space flight on the immune responses of rhesus monkeys through analysis of leukocyte subpopulation distribution

b. Primate-Bios

Each Cosmos 2229 flight monkey was housed in a Russian Primate-Bios capsule for the duration of the mission (Figure 8). Each Bios was equipped with a seating and restraint system, life support and environmental enrichment systems, and experiment-related instrumentation. Based on specific morphological features and natural posture, the restraint couch provided seating for the monkey and support commensurate with dry land impact following parachute descent (Figure 9). Restraint was effected by a lap-restraint plate and straps on the upper right arm. The degree of thoracic restraint was adjustable by ground command. A chain link bib protected percutaneous leads from the monkey's grip. The Bios offered a clear visual pathway allowing the monkeys to view one another throughout the flight.

Life support in the Primate-Bios included illumination controllable for light/dark cycles and air circulation and filtration. Unidirectional air flow directed waste into a receptacle under the restraint couch. Food and liquid in the form of a paste diet and a water/juice mixture were stored in the base of the Bios. The monkey obtained food or drink by sucking on the appropriate dispenser spout. The availability of food or drink could be controlled by ground command. In the event of a failure in the primary food dispenser, an emergency feeder could be introduced. For purposes of both verifying primate well-being and gathering experimental data, the Bios was equipped with a video monitoring system for periodic observation of the animal from the ground.

A Psychomotor Response System installed in the Bios measured behavioral and vestibular parameters as well as providing environmental enrichment for the subjects (Figure 10). A display screen presented task stimuli to which the monkey had been trained to respond. By making the correct response using either a hand lever, foot lever or touch screen, the monkey received reinforcement in the form of a juice reward. An incorrect response resulted in a delay before presentation of the subsequent task. The Bios was also equipped with a motorized unit to raise and lower the restraint couch in order to provide further vestibular stimulation.

2. Mission Management Plan

The U.S. responsibilities for experiments on the Cosmos 2229 mission were to: a) develop U.S. flight and ground-based hardware; b) train Russian specialists in the use of U.S.-developed flight and ground-based hardware; c) complete flight hardware and experiment verification testing; d) conduct science integration tests; e) develop, with Russian specialists, procedures for postflight data, specimen

and hardware transfer; and f) provide essential documentation for experiment procedures and for U.S. flight hardware.

a. Hardware Development

Flight hardware developed and supplied by the Ames Research Center (ARC) included: 1) Circadian Rhythm/Temperature Regulation (CR/T) hardware; 2) angular rate, tendon force and EMG sensors; and 3) preamplifiers and power supply for measuring various physiological parameters inflight. Ground support hardware supplied by ARC included software and test equipment for the CR/T experiment, a Portable Linear Sled to support the neurovestibular experiments, and the Mechanical Response Tissue Analyzer (MRTA) for bone measurements. Other ground test hardware was provided by U.S. investigators to support their specific experiments. The U.S. hardware development and testing processes for the mission are described in detail in Part II of this document.

b. Training

Russian personnel were trained by U.S. specialists in the set-up, use, and testing of most flight and ground hardware systems. Specifically, the Russian engineering team was trained in integrated system testing using the U.S. preamplifiers, transducers and power supply; testing and use of the CR/T hardware; and operation of the MRTA.

c. Hardware and Experiment Verification Tests

All U.S. flight hardware underwent environmental, verification and functional tests to ensure mission readiness. Ground-based hardware was subjected to rigorous functional testing only. A series of feasibility studies was performed to verify individual experiment protocols. These studies culminated in three Science Integration Tests.

d. Science Integration Tests

Each Science Integration Test (SIT), lasting fourteen days, was designed to assess the compatibility of experimental procedures. The specific objectives of these tests were to: 1) determine the effect of the Russian restraint chair on a subject's physiology in a normal gravity environment, 2) integrate experiment procedures and hardware, 3) gain experience with surgical techniques and flow, 4) verify performance of U.S. flight instrumentation designs, and 5) gather baseline data.

The first SIT dealt with the various musculoskeletal procedures. Specifically, it verified compatibility between the muscle biopsy procedure, tendon force buckle operation and EMG measurements. The second SIT assessed the suite of bone procedures. These included bone densitometry, radiography, iliac crest and tibial biopsies, marrow aspiration, blood analysis, bone strength tests and sublingual cell collection. The third SIT tested compatibility between the regulatory physiology brain temperature implants and the neurovestibular eye coil implants.

e. Data/Specimen/Hardware Transfer for Postflight Analysis

A large quantity of U.S. flight and ground-based hardware to support preflight, inflight and postflight studies was shipped to and returned from IMBP in Moscow. Data captured on the Russian flight recorder were copied tape-to-tape following the flight. CR/T data stored in solid state memory were transferred to computer disks. Investigators receiving tissues preflight and postflight were responsible for the transfer of their own biosamples.

f. Documentation

The Experiment Management Plan (EMP) document provided the essential information required to conduct each experiment. The EMP included: 1) a list of the joint investigators (U.S./Russian); 2) experiment objectives; 3) protocols for the flight and control experiments; 4) an overview of experiment verification tests; 5) procedures for specimen collection and labeling; 6) procedures for animal preparation and tests; 7) log sheets for experiment data; 8) requirements and procedures for data transfer and analysis; and 9) a listing of experiment hardware and equipment.

To coordinate science reporting by both countries, the U.S. investigators agreed to submit postflight science reports to the Russians prior to submitting manuscripts to scientific journals for publication. Preliminary Science Reports were submitted to the Russians nine months postflight, and Final Science Reports were submitted fifteen months postflight. These Final Science Reports are included in Section III of this document.

F. PRIMATE EXPERIMENT OPERATIONS

This section focuses on mission operations associated with the joint U.S./Russian experiments.

1. Flight Group

a. Preflight Events

Two male rhesus monkeys were selected as flight subjects from six flight-prepared candidates three days prior to launch. The subjects were then installed in the Primate-Bios units. Preflight procedures for the bone experiments included subject growth rate measurements; bone stiffness and densitometry measurements; bone marrow aspiration; blood samples; and sublingual cell samples. These procedures were conducted preflight and continued after recovery.

Neurovestibular preflight procedures included mounting of the electrode platform; implantation of a head restraint ring, eye coils, and EOG and orthodromic stimulation electrodes; placement of brain electrodes and evaluation of implants. Testing measurements and studies were performed using ground support hardware, including the Portable Linear Sled and U.S. investigator-provided motor-driven rotators.

Preflight procedures for the neuromuscular study included implantation of EMG electrodes and the tendon force buckle. Muscle biopsies were taken from each flight candidate, intermittent unrestrained and flight chair studies of EMG activity were conducted, and tendon force transducer calibration and testing was completed with animals in restraint.

For the CR/T study, preflight procedures involved implantation of the axillary temperature transmitters and brain temperature sensors, placement and securing of skin temperature probes, and tests on flight candidates. The metabolism study preflight procedures included collection of baseline urine samples from all flight candidates, administration of doubly-labeled water (DLW), collection of a series of urine samples from flight candidates, and collection of urine samples from the non-flight animals. Blood and bone marrow samples for the immunology study were taken from the entire flight pool approximately six weeks before launch.

b. Launch, On-Orbit and Reentry Events

No flight procedures were required for the bone or metabolism studies. Neurovestibular flight procedures included the presentation of visual cues to produce head and eye movements, the recording of these movements and the recording of neural activity. Flight procedures for the neuromuscular

study involved the recording of EMG activity, tendon force, foot lever activity and foot lever position during motor task performance. The CR/T study recorded skin temperature, axillary temperature, brain temperature, motor activity, heart rate, and Bios ambient temperature.

c. Postflight Events

Postflight procedures for the bone experiments were a continuation of the series of preflight procedures, as well as analysis of iliac crest biopsy tissue obtained by the Russians. The neurovestibular experiments repeated preflight study procedures which included vestibulo-ocular reflex (VOR) measurements, eye movement, vestibular primary afferent response (VPAR), vestibular nuclei response (VNR) recordings, and linear vestibulo-ocular reflex (LVOR) measurements.

For the neuromuscular study, postflight procedures included muscle biopsies with various histochemical assays on each biopsy; EMG, tendon force and foot lever recordings; locomotion studies; restraint chair tendon force recordings; and unrestrained EMG recordings.

Postflight procedures for the CR/T experiment involved removal of sensors and postflight calibration and testing of the CR/T Signal Processor (CR/T-SP). For the metabolism experiment, two postflight urine samples were collected. The immunology study collected a series of blood and bone marrow samples between the third and twelfth days postflight.

2. Control Groups

Forty-five days following recovery (R+45), a postflight study to control for restraint effects was conducted using the flight animals and four additional monkeys. The flight animals were housed in Bios capsules with the flight scenario duplicated as closely as possible. Physiological data were collected as in the flight. The control animals were housed in lower-fidelity restraint chairs. No physiological data were recorded from these animals. Following the flight-equivalent period of restraint, biosamples were obtained from all animals.

Other experiment-specific controls were required by certain protocols. For the neuromuscular study, muscle biopsies were taken from ten control subjects, and restraint chair tendon force recordings and unrestrained EMG recordings were taken from two control subjects. For the immunology study, four flight candidate monkeys and two vivarium monkeys were used as assay controls. Blood and bone marrow samples were obtained from these animals. The metabolism study maintained one ground control monkey in restraint during the flight period of the R+45 control study as a synchronous control. Urine samples were collected from this animal on the same schedule as for the flight subjects. The metabolism study also collected urine samples from three vivarium controls on a schedule similar to that of the flight animals.

TABLE 1
COSMOS BIOSATELLITE MISSIONS WITH U.S. PARTICIPATION

Mission Parameters	782	936	1129	1514	1667	1887	2044	2229
Launch	11/25/75	08/03/77	09/25/79	12/14/83	07/10/85	09/29/87	09/15/89	12/29/92
Recovery	12/15/75	08/22/77	10/14/79	12/19/83	07/17/85	10/12/87	09/29/89	01/10/93
Duration (days)	19.5	18.5	18.5	5.0*	7.0	12.5	14.0	11.5
Orbital Period (min.)	90.5	90.7	90.5	89.3	89.4	90.7	89.3	90.4
Apogee (km)	405	419	406	288	270	403	294	397
Perigee (km)	226	224	226	226	211	222	216	226
Inclination (deg.)	62.8	62.8	62.8	82.3**	82.4**	62.3	82.3**	62.8
NASA TM No.***	78525	78526	81299/ 81289	88223	108803	102254	108802	this volume

* Mission duration shortened for the first rhesus monkey flight

** Higher orbital inclination for radiation experiments

*** NASA Technical Memorandum (TM)—available through the Life Sciences Division (SL), NASA Ames Research Center

TABLE 2

PAPERS PRESENTED AT COSMOS 2229
FINAL RESULTS SYMPOSIUM, DECEMBER 1993

I. Primate Experiments

Neurological Studies

Primary Afferent Response of Rhesus Monkeys Before and After Exposure to Space Flight	M.J. Correia, J.D. Dickman, A.A. Perachio (USA); I.B Kozlovskaya, M.G. Sirota (Russia)
Reduction of Ocular Counter-Rolling by Adaptation to Space	M. Dai, B. Cohen, L. McGarvie, T. Raphan (USA); I.B Kozlovskaya, M.G. Sirota (Russia)
Adaptation to Microgravity of Oculomotor Reflexes (AMOR): Otolith-Ocular Reflexes	D. Tomko (USA); I.B Kozlovskaya (Russia)
Investigation of Attention Processes in Primates Exposed in Microgravity. Does the Rhesus Monkey's Attention Change in Space Flight? Measurements of Electrocardiogram during the Biocosmos 2229 Mission	C. Graille (France); G.G. Shlik, M.A. Shirvinskaya, B.S. Magedov, R. Buser (Russia)
Effect of Microgravity on Sleep in Rhesus Monkeys	D. Lagarde, C. Graille, P. Van Beers (France); G.G. Shlik (Russia)

Immunology and Microbiology Studies

The Immune System of Primates Exposed in the Space Flight Environment	L.V. Konstantinova (Russia)
Effect of Space Flight on Immune Parameters of Rhesus Monkeys	G. Sonnenfeld (USA)
Phenotypic Analysis of Blood Cells and Functional Parameters of Polynuclears in Monkeys following Space Flight	D. Schmitt (France)
Peculiarities of the Microbial Status of Primates during Preparation for and the Flight on Biosatellites	N.N. Lizko, V.K. Ilyin, A.A. Naumov (Russia)
Space Flight Effects on the System of Natural Cytotoxicity in Animals	D.O. Meshkov, M.P. Rikova, A.T. Lesnyak (Russia)

Biological Rhythms Studies

Circadian Rhythms and Temperature Regulation in Rhesus Monkeys	C.A Fuller, T.M. Hoban-Higgins, D.W. Griffin (USA); V. Ya. Klimovitsky, A.M. Alpatov (Russia)
Electrocutaneous Resistance and Biorhythms in Primates during Space Flight	E.L. Wachtel, H.-U. Balzer, K. Hecht (Germany); M.A. Shirvinskaya, G.G. Shlik (Russia)

Muscle Studies

Differential Modulation of Recruitment of Motor Pools in the Rhesus in Response to Space Flight	V.R. Edgerton (USA)
Changes in the Muscular Structure in Monkeys during the Flight of Biocosmos 2229	B.S. Shenkman, S.L. Kuznetsov, A.V. Tolokolnikov, T.L. Nermirovskaya, V.V. Stepanov (Russia)
Problems of Muscular Adaptation to Microgravity	S.L. Kuznetsov (Russia)
Response of Primate Flexor and Extensor Hindlimb Muscles to Space Flight	S. Bodine-Fowler, D. Pierotti, V.R. Edgerton (USA)
Muscular Plasticity in Upper Limb of Monkeys on Biocosmos 2229	D. Desplanches, M.H. Mayet, (France); B. Shenkman, M. Heissler, H. Hoppeler, I.B. Kozlovskaya (Russia)
Evolution of the Structure-Function Relationship of the Contractile Proteins on Monkey Triceps Muscles in Weightlessness Conditions (Biocosmos 2229)	J. Mounier, C. Cordonnier, S. Helles, V. Montel, F. Picquet, L. Stevens (France)
Electromyographic Activity of the Monkey Upper Limb Musculature during Space Flight (Biocosmos 2229)	M. Falempin, X. Messeles (France)

Circulation, Blood Formation and Thermoregulation Studies

Selection Training and Preparation of Monkeys for Space Flight	V.I. Korolov, A.N. Truzhennikov, G.G. Shlik, Mh. Shirvinskaya, Yu.V. Gordeev, I.O Guiryayeva (Russia); D. Helwig (USA)
Changes in Water Spaces in the Primates' Bodies following Exposure in Microgravity	V.I. Lobachik (Russia)
Alteration in Oxygen Delivery to the Brain and the Endocranial Pressure of Monkeys in Space	V.P. Krotov, E.V. Trambovetsky (Russia)

Effects of Space Flight on the Bone Marrow Blood Formation in Monkeys	T.E. Burkovskaya, L.O. Guiryayeva (Russia); C.A. Fuller (USA)
Temperature Homeostasis of Primates in Flight on Biocosmos	V.Ya. Klimovitsky, A.M. Alpatov (Russia); C.A. Fuller (USA)
Psychoemotional and Sympathetic Activity Studies on Primates in Flights on Biocosmos	E.L. Wachtel, H.-U. Balzer, K. Hecht (Germany); G.G. Shlik, M.A. Shirvinskaya (Russia)
Changes in the Vegetative Nervous Parameters in Monkeys during Space Flight	A.M. Badakva, I.O. Guiryayeva, D.V. Zalkind, N.V. Muller (Russia)

Bone Studies

DEXA Measurements: Cosmos 2229 Rhesus Flight Experiment	A. LeBlanc (USA); A.S. Rakhmanov (Russia)
USI Findings in Monkey's Bones	V.E. Novikov (Russia)
Histological Investigation of Monkey's Bones	E. Zerath, H. Holy, A. Alexandre, A. Malovier, S. Reno, K. Andre (France); V.E. Novikov, V.I. Korolkov (Russia)
Regenerative Processes in Bone Tissues in Space	A.S. Kaplansky, G.N. Durnova, T.E. Burkovskaya (Russia)
Hormonal Regulation of Bone Metabolism	C. Cann (USA); M. Dotsenko (Russia)
Bones of Animals in the Period of Readaptation to 1 g (Biosatellite Experience)	V.S. Oganov (Russia)

Metabolism Studies

Water-Salt Metabolism in Monkeys Prior to and Post Flight	M.A. Dotsenko, V.I. Korolkov, Yu.V. Natochin, R.I. Rudneva (Russia)
The Effects of Gravity on the Metabolism of Rhesus Monkeys	C.A. Fuller, T.P. Stein, D.W. Griffin (USA); M.A. Dotsenko, A.N. Truzhennikov, V.I. Korolkov (Russia)
Non-Invasive Measures on Bone Function and Electrolyte Metabolism in Young Rhesus Monkeys after Space Flight	S. Arnaud, T. Hutchinson, C. Steele, B. Silver (USA); A.T. Bakulin, R.I. Rudneva, M.A. Dotsenko (Russia)
Plasma Hormone Concentrations of Rhesus Monkeys after Space Flight	R.E. Grindeland, V.R. Mukku, K.L. Gosselink (USA); M.A. Dotsenko (Russia)

II. Gravitational Biology Experiments

Impact of Microgravity and Hypergravity on the Free-Running Circadian Rhythmicity of the Desert Beetles <i>Trigonoscelis Gigas</i>	W.J. Rietveld (The Netherlands); A.M. Alpatov (Russia); L.B. Oryntaeva (Kazakhstan)
Arthropods as Promising Objects for Chronobiological Research in Space Flight	G. Fleissner (Germany)
Effect of Microgravity on Circadian Rhythms and Geotaxis of <i>Drosophila</i>	E. De Juan Navarro, R. Marco (Spain)
Possible Effects of Microgravity on in vitro Long Bone Growth and Mineralization	J.P. Veldhulzen, J.J.W.A. van Loon (The Netherlands)
Effect of Microgravity on the Osteogenic Cell Line Being Stimulated with System and Local Effectors Metabolism	L. Bierkens, G. Schoeters (Belgium)
Peculiarities of the Embryonal Bone in vitro Development in Microgravity	N.V. Rodionova, O.P Berezovskaya (Ukraine)
Culture of Osteoblast-Like Cells (ROS 17/2.8) during the Last Biosatellite Mission: Effects of Six Days Microgravity	C. Alexandre, C. Genty, S. Palle, L. Vico (France)
Growth and Motility of Cells in Culture in vitro	A.V. Gabova, M.G. Tairbekov, B.A. Baibakov, L.B. Margolis (Russia)
Peculiarities of Structure of <i>Lepidium sativum</i> L. Root Columella Cells under Microgravity Conditions	R. Laurinavicius (Lithuania); A. Sievers, B. Buchen, A. Stockus (Germany)
Structural/Functional Properties and Peroxidation in the Membrane of Plant Cells in vitro in Microgravity	E.L. Kordium, S.L. Zhadko, D.A. Klimchuk, A.V. Popova (Ukraine)
Experiment "Chlamydomonas" in the Biocosmos 2229 Mission	E. Van Spronsen, H. Van den Ende (The Netherlands); O.V. Gavrilova (Russia)
Regeneration of Nervous, Muscular and Bone Tissues in Space Flight	S. Grinfeld, F. Folke, A. Duprat (France); V.I. Mitashev, N.V. Brushlinskaya (Russia)
Development of <i>Xenopus Laevis</i> Larva in Space	E.V. Snetkova, N.A. Chelnaya, L.V. Serova, S.V. Saveliev, E.V. Cherdantseva (Russia); S. Pronich, R. Wassersug (Canada)

Effects of Space Flight on the Population of <i>Drosophila melanogaster</i> Preliminarily Adapted to a Changed Gravity	R. Marco (Spain); I.A. Ushakov (Russia)
Peculiarities of Organ and Tissue Regeneration In and Post Space Flight	V.I. Mitashev, E.N. Grigorian, S.Ya. Tuchkova, N.V. Brushlinskaya (Russia); S. Grinfeld, A.P. Duprat, G.J. Anton (France)

III. Radiobiology Experiments

Biological Effects of Heavy Charged Particles of the Galactic Cosmic Rays and Other Space Flight Factors on Higher Plants	L.V. Nevzgodina, E.N. Maksimova, E.V. Kaminskaya (Russia); G. Horneck, G. Reitz, R. Facius (Germany)
Comparative Analysis of the Genetic Effects Induced by some Components of Cosmic Radiation	N.L. Delone, V.V. Antipov (Russia)
Present Results of the Joint Radiobiological Experiments ESA/IBMP SEEDS aboard Cosmos 2044 and 2229	K.E. Gartenbach, A.R. Kranz, M.W. Zimmermann, C. Heilmann, E. Schopper, J.-V. Schott (Germany); V. Shevchenko, B. Baican, E.E. Kovalev, A. Mareny (Russia)
Correlation of Dosimetric Data and Different Biological Endpoints in <i>Arabidopsis Thaliana</i>	K.E. Gartenbach (Germany)

TABLE 3

FOOD, JUICE AND WATER CONSUMPTION (g/day)

	Preflight		Inflight		Postflight	
Monkey ID	906	151	906	151	906	151
Food intake	300	340	380	113	205	245
Juice intake	300	300	127	78	118	154
Water intake	510	538	390	150	261.5	325.5

TABLE 4

PRIMATE CARDIOVASCULAR DATA BEFORE AND AFTER FLIGHT

Parameter	Krosh (906)		Ivasha (151)	
	Before	After	Before	After
Age (years)	3.5		4.5	
Body weight (g)	3950	3750	4700	4100
Blood pressure (mm Hg)	110/70	125/80	120/80	100/80
Heart rate (beats/min)	185	165	182	172
Hematocrit (%)	39	36	39	42
Erythrocyte sedimentation rate (mm/hr)	2	3	2	2

TABLE 5
PRIMATE EXAMINATIONS AND TESTS POSTFLIGHT

Day	Procedures
R + 0	Clinical examination, skin cleaning, blood draw and urine collection for biochemistry; primate shipment to Moscow
R + 0-2	Vestibular and motor activity tests
R + 3	Tilt test; blood draw for biochemistry and immunology; bone marrow puncture; bone studies; muscle biopsy
R + 4-5	Vestibular and motor activity tests
R + 6-8	Metabolic studies
R + 9	Blood draw and urine collection for biochemistry and immunology; data recording in a flight capsule
R + 10	Vestibular tests
R + 11	Tilt test; blood draw; bone studies; bone marrow puncture
R + 12-15	Data recording in a flight capsule
R + 16	Iliac crest biopsy
R + 30	Bone studies

TABLE 6
ELECTRODES AND SENSORS IMPLANTED IN PRIMATES

Central electrodes	#
Active electrocorticographic electrodes (ECoG)	2
Subcortical monopolar electrodes for four neurographic leads (Vestibular nerve-1, vestibular nuclei-4, flocculo-nodular area-1)	6
Skull indifferent electrode for two ECoG leads (ECoGi)	1
Electrodes for two electrooculographic leads (EOG)	4
Eye coils	2
Skull common electrode for biopotentials from central and peripheral electrodes (Ec)	1
Neck electromyographic electrodes (EMGn)	2
Brain pO ₂ electrodes	2
Intracranial pressure sensor	1
Brain Temperature	1
Peripheral electrodes and sensors	
Electrocardiographic electrodes (EKG)	2
Arm and leg electromyographic electrodes (EMGc) (pairs)	10
Body temperature transducer	1
Tendon force transducer	1
Rheoplethysmographic electrodes (ZpG)	3
Gastrointestinal activity electrodes	2

TABLE 7
PHYSIOLOGICAL SIGNALS RECORDED INFLIGHT

Recording Program Number	1	2	3	5	6	7	8	9
Recording Program Name	BL Neuro	Lift	Gaze Fixation Reaction	Motor Control 1	Motor Control 2	Attention	Cardiovascular System	Sleep
Exposure Type	None	Lift	Motor Task Electric Stimulation	Motor Task Electric Stimulation	Motor Task Electric Stimulation	Motor Task		
Recorder Type	HF	HF	HF	LF	LF	LF	LF	LF
HF Recorder Number	1 & 2	1 & 2	1 & 2	1 or 2	1 or 2	1 or 2	1 & 2	1 or 2
Recording Speed	1	1	1	2	2	1	1	1
Channel Number:								
1	VNR-1	VNR-1	VNR-1	1EMG-1	1EMG-3	1ECOG-1	RPG	1ECOG-1
2	VNR-2	VNR-2	VNR-2	1EMG-2	1EMG-4	1ECOG-2	RPG Zo	1ECOG-2
3	VNR-3	VNR-3	VNR-3	1Tendon Force	1Tendon Force	1EOG-yaw	*	1EOG-yaw
4	VNR-4	VNR-4	VNR-4	1Foot Pedal	1Foot Pedal	1EMG	EKG	1EMG-1
5	EOG-yaw	EOG-yaw	EOG-yaw	1Pedal Torque	1Pedal Torque	1EKG	BP	1EKG
6	EOG-pitch	EOG-pitch	EOG-pitch	1Ref. Signal	1Ref. Signal	1Ref. Signal	Systolic BP	-
7	ECOG-1	EMG-1	EMG-5	2EMG-1	2EMG-3	2ECOG-1	EMG	2ECOG-1
8	EMG-1	EMG-2	EMG-6	2EMG-2	2EMG-4	2ECOG-2	*	2ECOG-2
9	ECOG-2	ECOG	ECOG	2Tendon Force	2Tendon Force	2EOG-yaw	PO2	2EOG-yaw
10	Head position	Head position	Head position	2Foot Pedal	2Foot Pedal	2EMG	PO2	2EMG
11	EKG	EMG-1	*	2Pedal Torque	2Pedal Torque	2EKG	-	EKG
12	-	Chair Position	Ref. Signal-1	2Ref. Signal	2Ref. Signal	2Ref. Signal	Chair Position	-

* Translation from Russian source material was unavailable

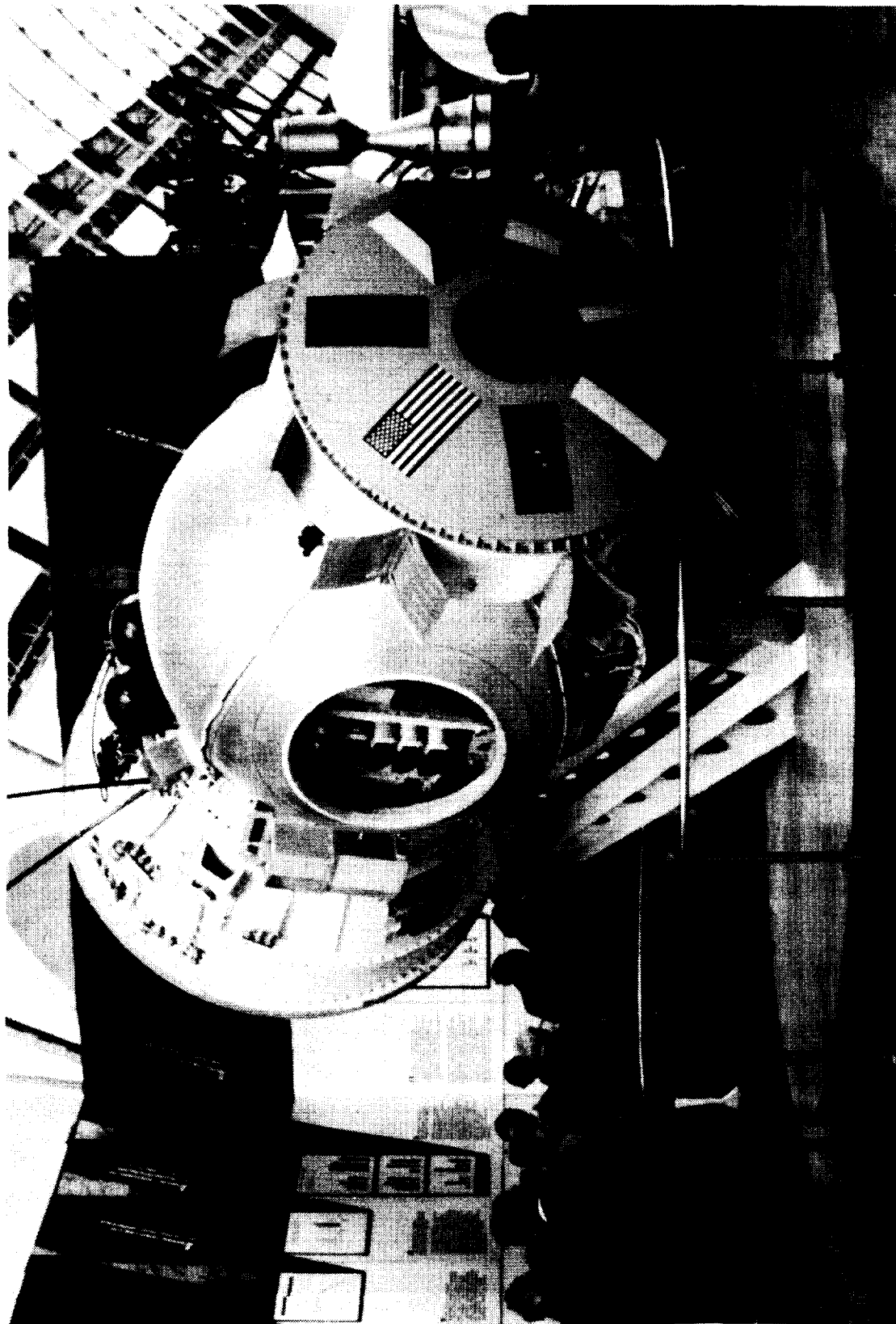
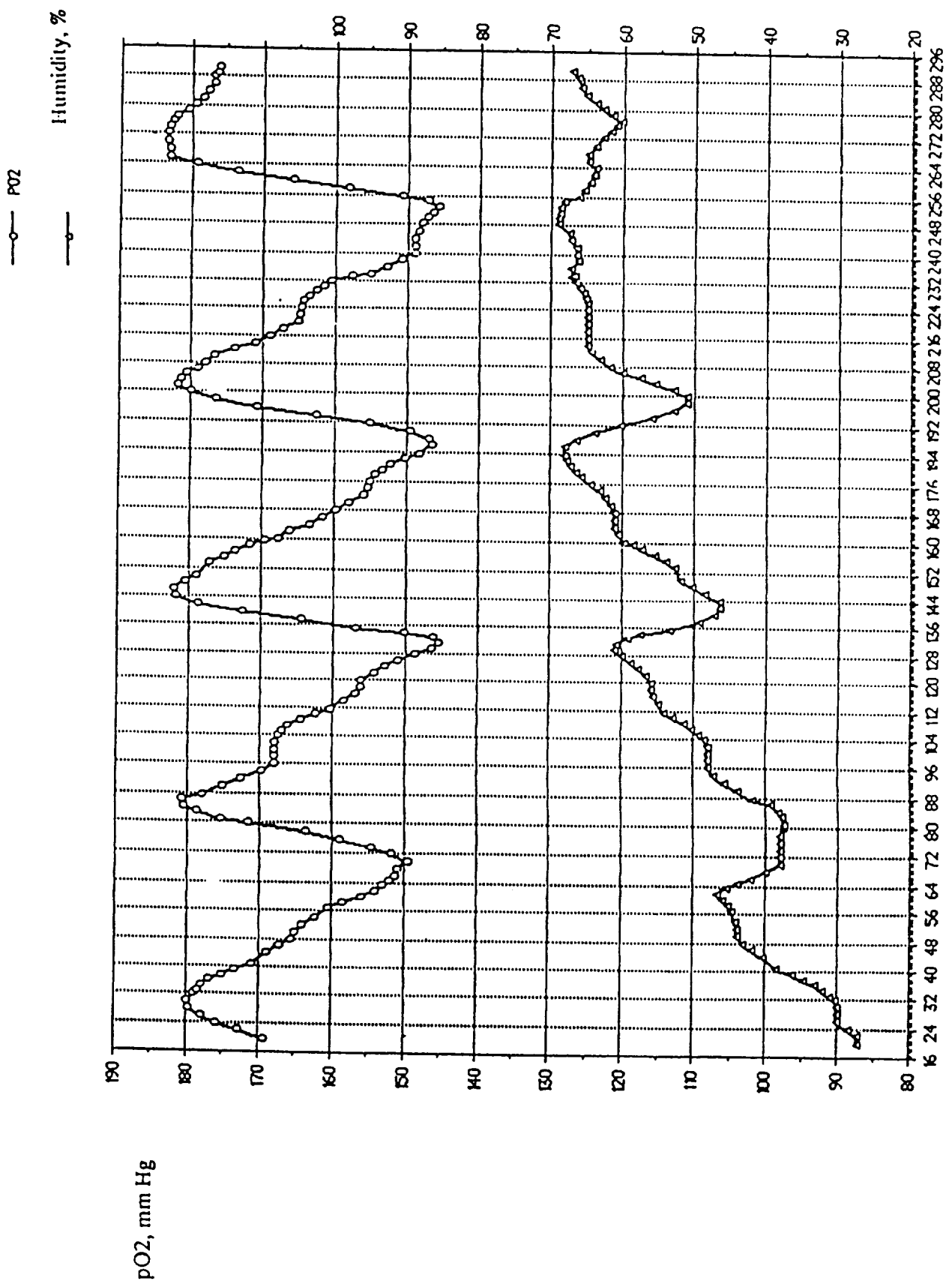


Figure 1. Cosmos spacecraft.



Flight time, hours

Figure 2. Capsule oxygen and relative humidity.

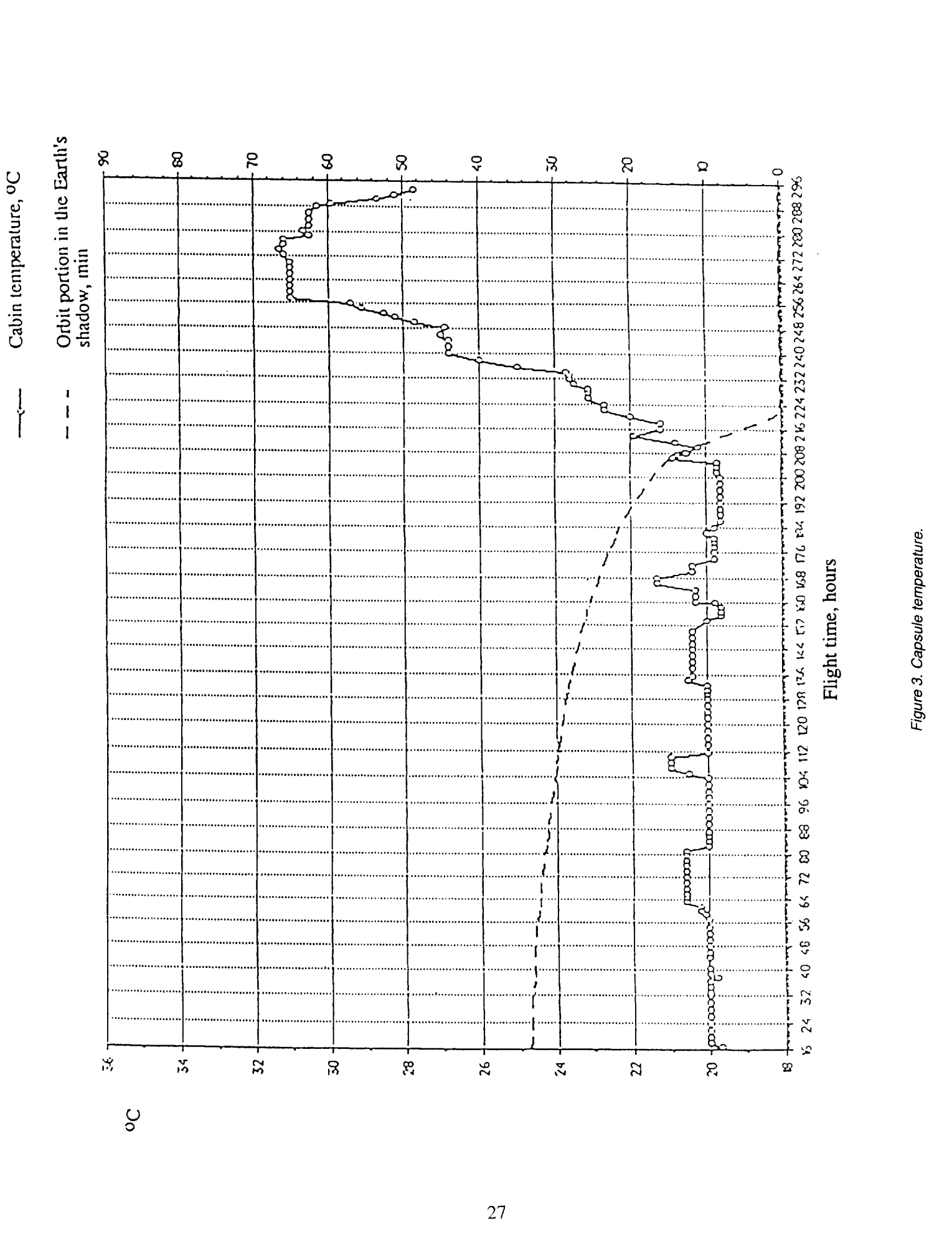


Figure 3. Capsule temperature.

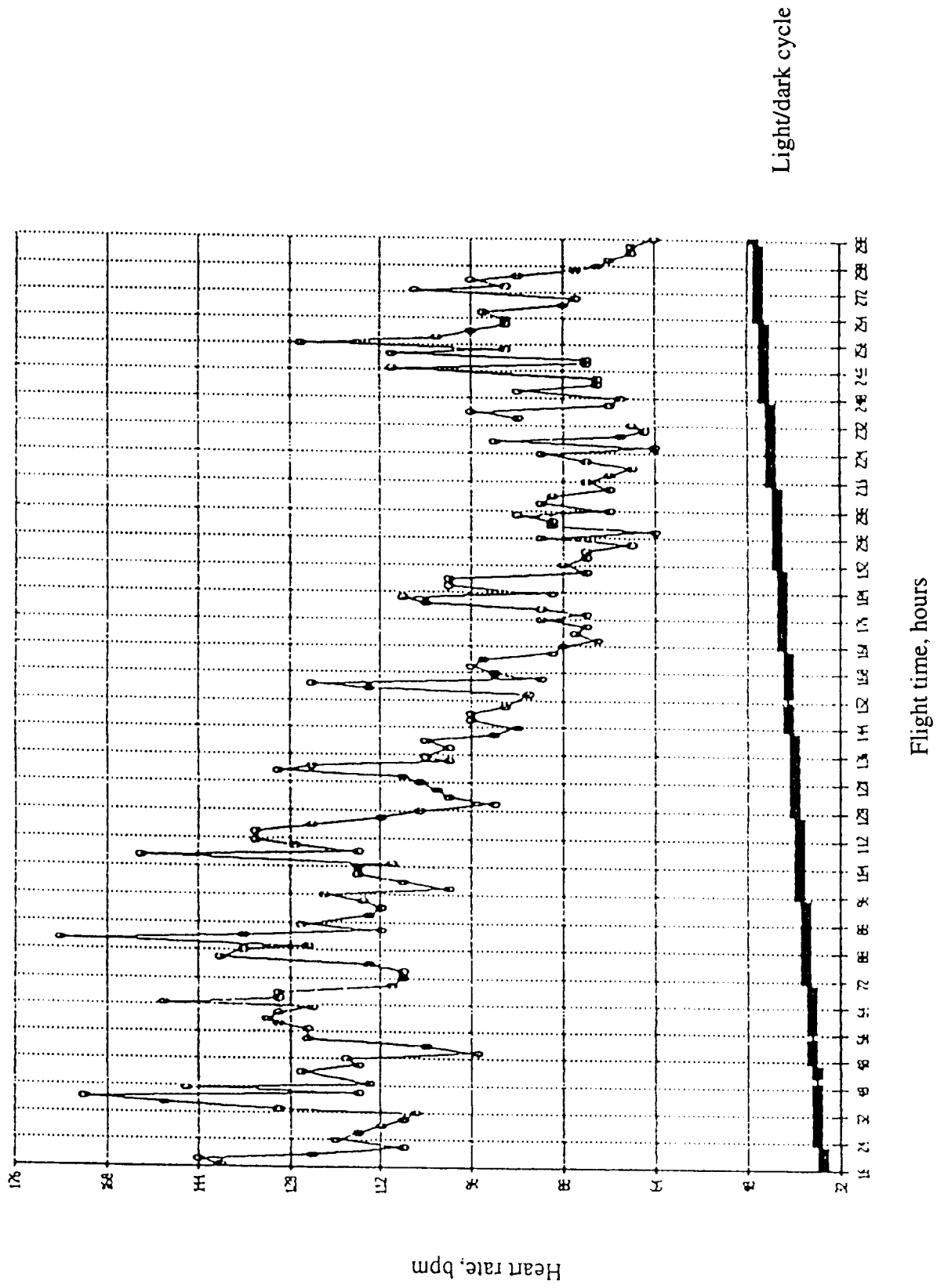


Figure 4. Heart rate of monkey 151 (Ivasha).

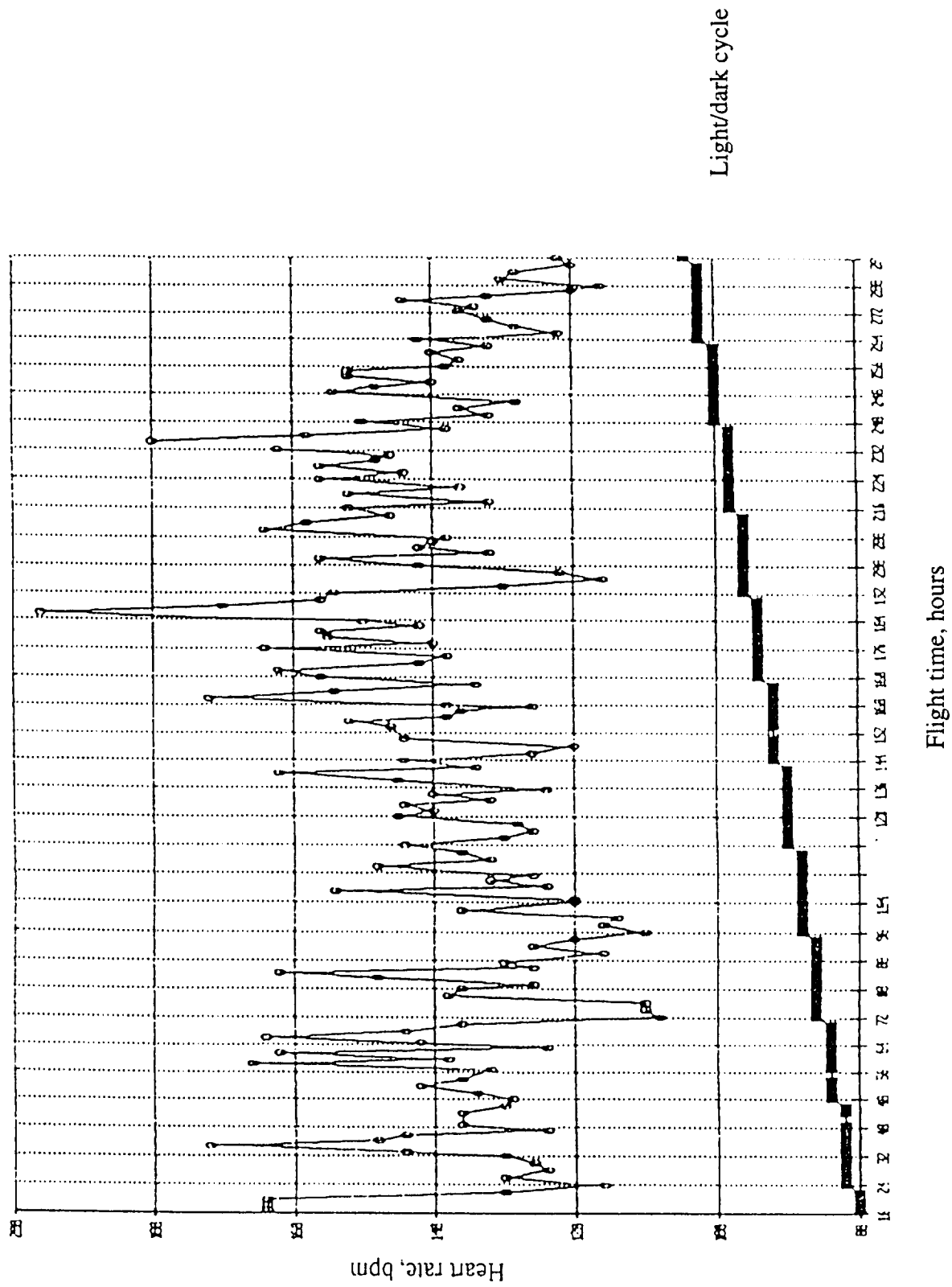


Figure 5. Heart rate of monkey 906 (Krosh).

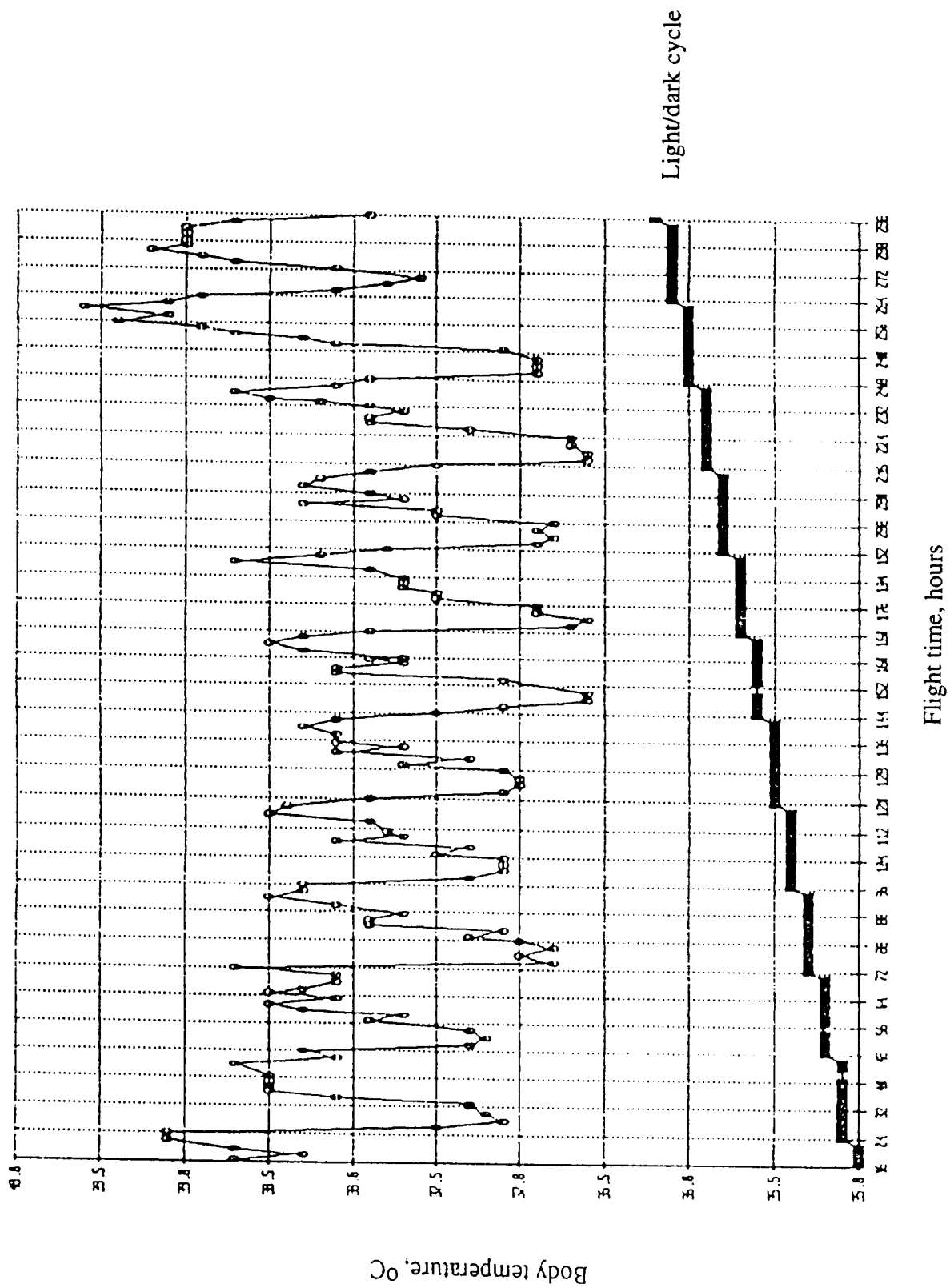


Figure 6. Body temperature of monkey 151 (Ivasha).

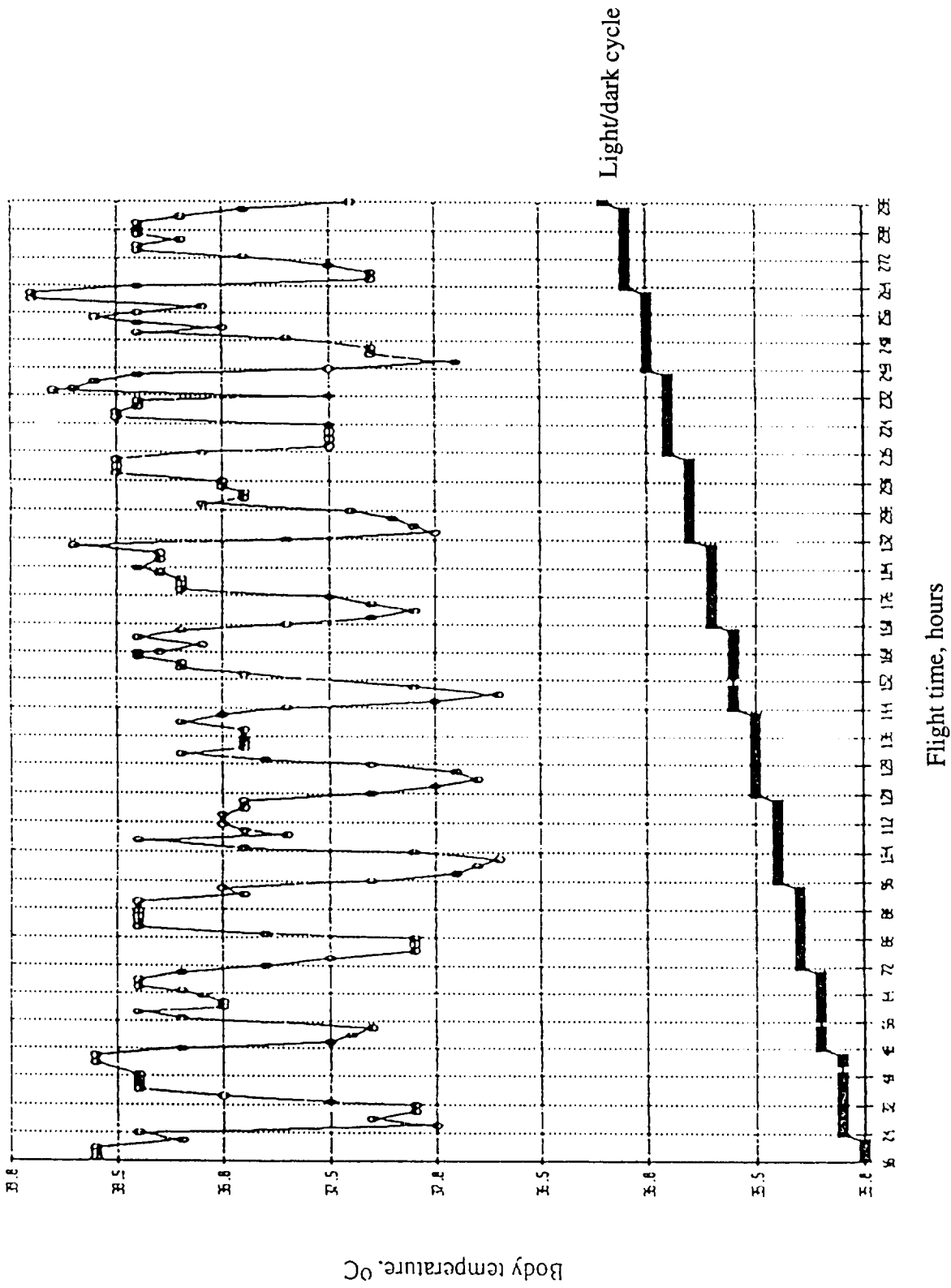


Figure 7. Body temperature of monkey 906 (Krosh).

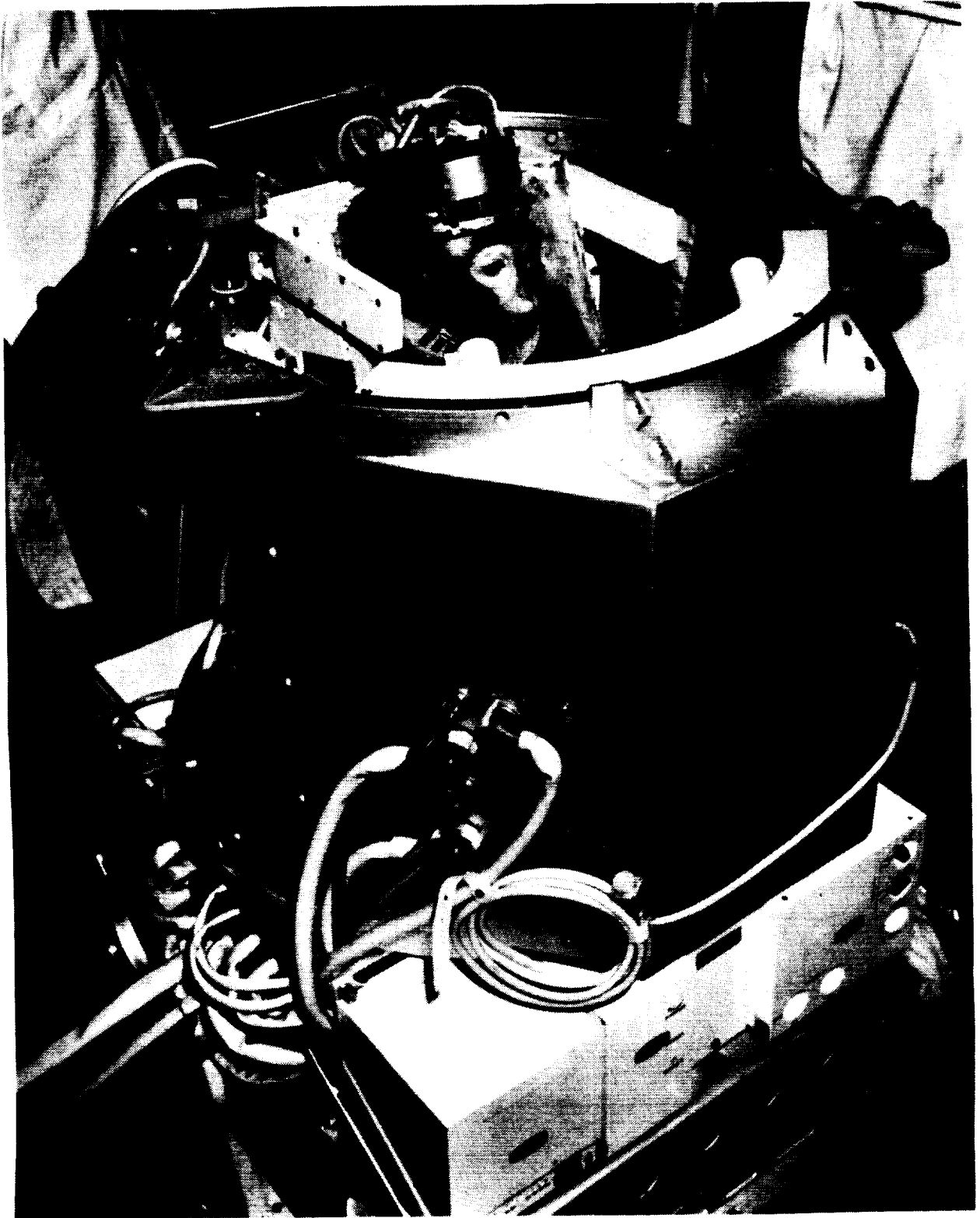


Figure 8. Primate-Bios.



Figure 9. Primate in Bios restraint chair.

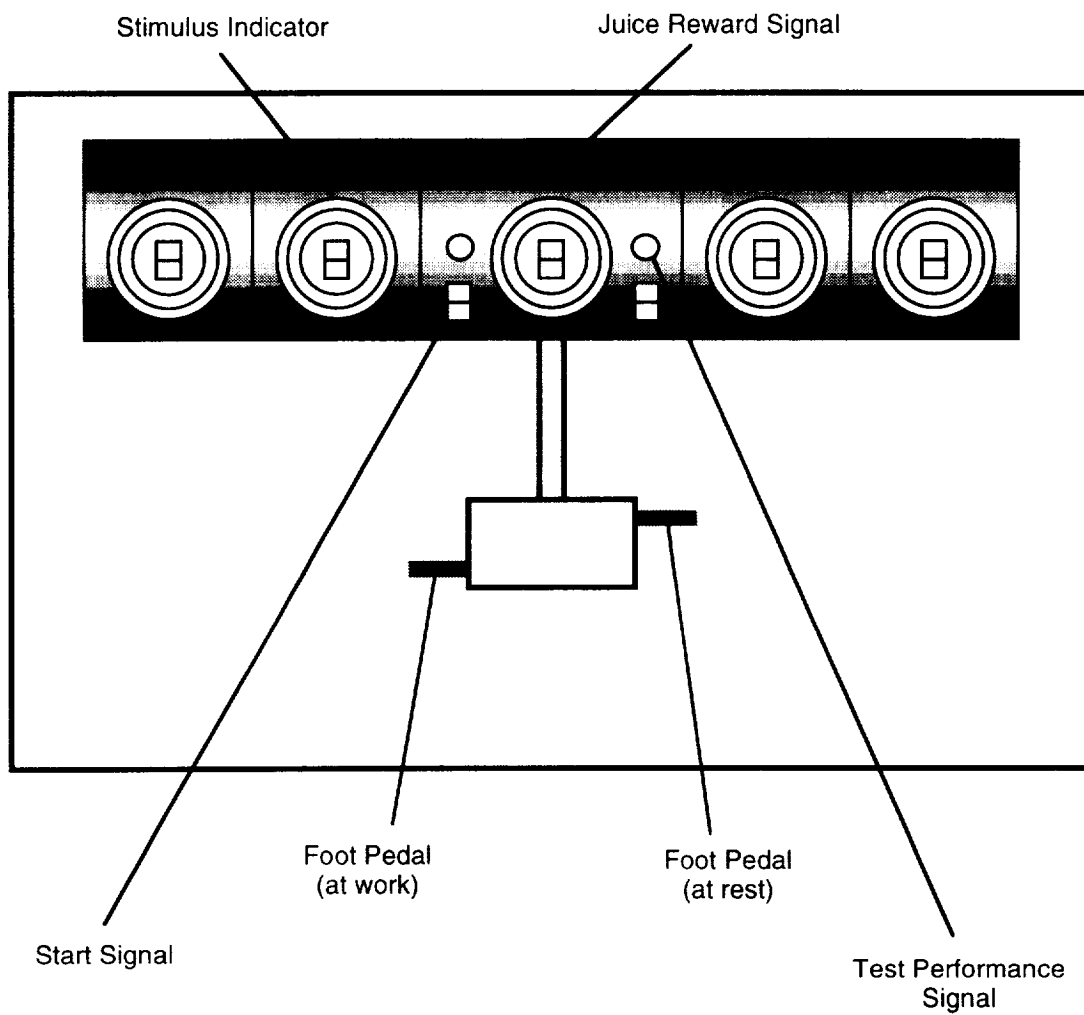


Figure 10. Psychomotor Response System.

II. U.S. FLIGHT AND GROUND-SUPPORT HARDWARE

A. HARDWARE OVERVIEW

This chapter describes the U.S.-developed hardware for U.S./Russian joint experiments on Cosmos 2229. The hardware consisted of both flight and ground-support hardware. The U.S. flight equipment acquired physiologic data from two Rhesus monkeys during the 11.5-day mission and the resultant data were recorded on spacecraft analog tape recorders for later analysis. The ground-support hardware (some developed for Cosmos 2229 and some upgraded following Cosmos 2044) was used for science verification tests and for experiment-unique preflight and postflight studies. A summary list of the flight and ground hardware, by experiment, is shown in Table 1.

1. Flight Hardware and Test Plan

Cosmos 2229 represents the highest level of U.S./Russian flight hardware integration yet attempted in the joint Cosmos Biosatellite Program. Hardware development for the mission required an unprecedented degree of cooperation, with U.S. and Russian engineers collaborating on the design of several flight instrumentation subsystems. This mission also marked the first time U.S. personnel participated in the preparation of payload hardware at the Plesetsk Cosmodrome.

The U.S. provided hardware for neuromuscular, neurovestibular and circadian rhythm/temperature regulation experiments. Neuromuscular equipment included implants and preamplifiers for EMG signals, and transducers and preamplifiers for tendon force measurements. For the neurovestibular experiments, U.S.-supplied flight hardware included: angular rate sensors to measure the pitch and yaw of each monkey's head; electrodes, multiplexer and preamplifiers for VNR measurements; and preamplifiers for EOG and EEG measurements. Circadian Rhythm/Temperature Regulation (CR/T) instrumentation included sensors and signal conditioning to measure skin temperature, brain temperature, ambient temperature, and motor activity. Deep body temperature and heart rate were recorded from existing Russian signals for a total of eight digitally recorded parameters.

The U.S. flight hardware was integrated with Russian spacecraft hardware and consisted of head and body electronics for monitoring physiological parameters from the Rhesus monkeys. Figures 1-3 illustrate the flight configuration and inflight recording plan for U.S. and Russian-supplied flight hardware. The head electronics were designed to interface with physiologic sensors and precondition signals for further amplification and recording on board the spacecraft. This included preamplification for eye coil, PO₂, VNR, EEG, EOG, brain temperature, electrostimulation, rheoplethysmography, and intracranial pressure sensors. It also served as a platform for mounting the head-motion angular rate sensors. The primate body electronics provided signal conditioning for EMG/ECG, Tendon Force and various body temperature sensors. The U.S. power supply derived its power from the Russian spacecraft's 27Vdc power source. It provided regulated and battery power to all the U.S.-supplied electronic hardware, except for the CR/T instrumentation (which had its own internal battery power). The power supply's battery was recharged inflight from the spacecraft power source.

All flight hardware supplied by the U.S. underwent environmental tests to qualify for flight. One unit of each hardware assembly was subjected to Qualification Testing, while all remaining units completed Acceptance Testing. The Qualification Test procedures were nearly identical to those of Acceptance Tests except that hardware was subjected to increased levels of stress. A Burn-In Test screened the assemblies for weak or marginally performing components which might fail under continuous use. The hardware was powered and exposed to temperatures of 80+/-2 °C for either 96 or 120 hours. To verify the ability of the hardware to perform under varying temperatures, a Thermal Cycle Test was performed. With the equipment powered, the temperature chamber was cycled between 62+/-2 °C and -16+/-2 °C. A total of five cycles was performed. To insure that the hardware

met the operational and structural stress requirements of the mission, Random Vibration Tests in the X, Y and Z axes were performed. A High Humidity Test was completed to verify hardware function and integrity under conditions of extreme humidity. The powered assemblies were exposed for 96 hours to 40+/-2 °C and 98+2/-15% relative humidity. Following each of the tests described above, a Functional Test was completed to verify continued performance of the hardware to documented specifications.

2. Ground-Support Hardware and Test Plan

The U.S. ground-support hardware was used for preflight and postflight ground experiments and for tests of U.S. flight hardware. The ground-support hardware consisted of the HESS, GTU-1, and GTU-2 (to support head and body electronics systems), and other experiment-specific ground equipment. This equipment supported preflight testing of flight hardware and ground-based data gathering both preflight and postflight. The neurovestibular studies, in particular, made use of complex ground-support hardware to assess the effects of microgravity on the vestibular system of primates. All ground-support hardware underwent thorough functional testing prior to the mission to verify appropriate operation. The various ground support hardware will be described briefly in a following section.

3. Hardware/Software Documentation and Data Transfer

Experiment Management Plans (EMPs) were developed for all U.S. experiments. These documents detailed all procedures, specifications and hardware needed to carry out the science protocols. Where required, experiment data sheets were included in the EMPs.

A documentation package for the U.S. flight hardware was provided to the Russians. This package included system descriptions, specifications, diagrams and instructions for hardware installation, testing and operation. A separate document detailing operation of the CR/T data recorder and software was also provided.

B. EXPERIMENT-SPECIFIC HARDWARE

1. Circadian Rhythm/Temperature Regulation Experiment

a. Flight Hardware

The Circadian Rhythm/Temperature (CR/T) Regulation experiment used an enhanced version of the hardware system flown on Cosmos 2044 (Figure 4), with some change to the eight parameters measured. These parameters included: motor activity, ambient temperature, brain temperature, three channels of skin temperature, and the two Russian-supplied parameters of heart rate and deep body temperature. Motor activity was monitored via a piezoelectric sensor attached to the monkey's restraint jacket. Thermistors attached directly to the monkey's ankle, thigh and temple measured skin temperature, and a thermistor at the bottom of the primate chair monitored ambient temperature. Brain temperature was monitored via a brain-implanted thermistor with leads to the Head Electronics Assembly (Figure 5). Brain temperature data were recorded at one-minute intervals while all other parameters were recorded at ten-minute intervals.

The Circadian Rhythm/Temperature Signal Processor (CR/T-SP) recorded all parameters. Providing its own battery power supply, the CR/T-SP functioned as a self-contained signal processing and digital data storage device that conditioned incoming physiological signals for processing and stored data for later recovery by a ground-based computer. The CR/T-SP used a VITARTS/VITACORD software package to collect and record data. The CR/T Interface Box (CR/T-IB) provided an interconnect point between the sensors and the CR/T-SP.

b. Ground-Support Hardware

The Head Electronics Signal Simulator (HESS) (Figure 6) supported the CR/T experiment as well as the neurovestibular studies. Simulated brain temperature, VNR, EEG, and EOG signals were generated by the HESS to test the Head Electronics Mother Board. The Ground Readout Unit (GRU) tested the operation of the CR/T-SP and was used to begin data sampling and to recover data stored in the CR/T-SP. The GRU consisted of an IBM compatible computer; a CR/T Interface Board in the computer, to provide an interconnect between the computer and the CR/T-SP; and a printer. The GRU ran the VITARTS/VITACORD software to recover the stored flight data. A Signal Simulator provided test signals for all parameters measured.

2. Neurovestibular Experiments

a. Flight Hardware

Three neurovestibular experiments flew on Cosmos 2229. For experiments K-8-02 and K-8-03, angular rate sensors measuring head motion velocity (HMV), one each for yaw and pitch, were mounted on the Head Electronics Assembly of each subject. The HMV sensors were driven by the HMV Signal Conditioner Module (Figure 7) with output to the Russian Final Amplifier Box. Head motion data measured responses to visual stimuli generated by the Russian Psychomotor Response System. Data were recorded by the Russian flight recorder.

The U.S. also supplied amplifiers and preamplifiers in the form of hybrid integrated circuits for experiment K-8-03. A multiplexing vestibular nuclei response (VNR) amplifier preconditioned a total of seven signals. Two logic signals controlled a multiplexer in selecting among four serially switched VNR inputs for recording on a single Russian recorder channel. The EEG/EOG hybrid conditioned EEG and EOG signals (Figure 8).

b. Ground-Support Hardware

Each of the neurovestibular studies employed ground-based apparatus to provide vestibular and/or optokinetic stimulation to the primates pre- and postflight. Experiment K-8-02 used a four-axis vestibular and optokinetic rotator (Figure 9). The computer-controlled, motor-driven rotator was surrounded by an optokinetic sphere with 10° vertical black and white stripes on its inner surface. The primate chair, attached to the rotational axis of a C gimbal, could be fixed in positions about the subject's vertical, naso-occipital and interaural axes $\pm 90^\circ$. This arrangement allowed the rotator to tilt in any position while the subject was pitched or rolled and stimulated visually by the optokinetic sphere. The science report for experiment K-8-02 provides a more detailed description of the optokinetic rotator.

Experiment K-8-03 used a computer-controlled multi-axis rotator for preflight and postflight studies of primate eye position, VNR and vestibular primary afferent responses (VPAR) (Figure 10). A hand-driven two-axis rotator was used for testing of the animals at the launch site. See pp. 49–50 of NASA Technical Memorandum 108802, Volume I and pp. 303–331 of Volume 2 for more detail on this experiment.

Experiment K-8-08 used a specially designed Portable Linear Sled (PLS) (Figure 11). The PLS allowed vestibular measurements to be made during horizontal and vertical oscillations of specified frequency and sinusoidal acceleration. Housed in the light-tight Specimen Test Container (STC), subjects traveled along ceramic rails on air bearings providing vibration-free motion. The STC was also gimballed to allow yaw, pitch or roll stimulation of each monkey. The L-shaped PLS could be rotated on end with a manually operated gantry for vertical oscillations. See the "Ground Support Requirements for Portable Linear Sled" document appended to the science report for more details.

The Ground Test Unit-1 (GTU-1) (Figure 12) was used to test the Head Electronics Mother Board and to support ground-based neurovestibular studies. In both situations, GTU-1 received signals from the Mother Board for conditioning and provided buffered outputs for either equipment testing or data recording.

3. Neuromuscular Experiment

a. Flight Hardware

A Tendon Force Sensor (Figures 13a and 13b) was surgically implanted in each flight subject on the distal tendon of the medial gastrocnemius of the left leg. The sensor used was an active strain gauge half bridge. The other half of the bridge consisted of the Tendon Force Compensation Module. The module provided temperature compensation and voltage scaling. An integral cable connected the sensor to the module. Excitation to the Tendon Force Sensor was provided by the Tendon Force Signal Conditioner Board (Figure 14). The Board also controlled offset, gain and filtering of the tendon force signal.

EMG electrodes were implanted in six muscle sites. The EMG/ECG Board (Figure 15), located in the Russian Preamplifier Box, provided preamplification of the electrode signals.

b. Ground-Support Hardware

The Ground Test Unit-2 (GTU-2) (Figure 16) was used to test the tendon force and EMG/ECG Boards. GTU-2 provided power and simulated tendon force and EMG signals to the boards as well as connections to monitor the board output signals. The Lab Test Unit (LTU) was used for ground-based animal studies requiring EMG/ECG and tendon force measurements. The LTU, with hardware identical to the flight suite, contained the EMG/ECG and tendon force boards and provided preamplification of the EMG/ECG and tendon force signals.

4. Bone Experiments

a. Flight Hardware

No flight hardware was required for the bone experiments on Cosmos 2229.

b. Ground-Support Hardware

Two pieces of ground-support hardware were used to make pre- and postflight measurements for the bone experiments. The Mechanical Response Tissue Analyzer (MRTA) (Figure 17), a NASA-modified version of a commercial system, provided non-invasive measurement of tibial bone strength using a low frequency vibratory stimulus. To measure bone mass and overall body composition, a commercially available densitometer, Hologic QDR-1000W, was used. The densitometer scanned the subjects by means of dual-energy X-ray absorbitometry (DEXA).

TABLE 1
SUMMARY OF HARDWARE BY EXPERIMENT

Experiment: Country	Flight	Ground
General U.S. Supplied Equipment:		
		Head Electronics Signal Simulator (HESS) (for testing of head electronics assembly) Battery Packs (to power ground-based hardware) Battery Charger
General Russian Supplied Equipment:		
	Cosmos Biosatellite Flight Primate Chair and Accompanying Hardware (Primate-Bios) Flight Data Recording Systems	Field Laboratory with Generators and Environmental Control Equipment (set up at recovery site) Biosatellite Mock-Up (Synchronous Flight Simulation)
Bone and Mineral Changes in Young Rhesus Monkeys (K-8-01):		
I. U.S. Supplied		Mechanical Response Tissue Analyzer (Gaitscan, Inc.) Dual Photon Bone Densitometer (Lunar DPX) Intracellular Ion Kit (Intracellular Diagnostics) Cell Culture Facility Axiophot Epifluorescence Microscope (Zeiss) Centrifuge Balances
II. Russian Supplied		

TABLE 1 (Cont.)
SUMMARY OF HARDWARE BY EXPERIMENT

Experiment: Country	Flight	Ground
Reduction of Ocular Counter-Rolling by Adaptation to Space (K-8-02):		
I. U.S. Supplied		Ground Test Unit #1 (GTU-1) (to test HMV signal) Primate Chair (with modified head restraint) Head-Fixed Field Coil System Computer-Controlled Rotator Optokinetic Stimulator Eye Coil Assemblies, Frontal and Roll (shared with K-8-08) Eye Coil System (Neurodata) Computer System and Software (for eye position data recording) Stereo Amplifier (Techron) High Frequency Filter (for multi-unit recordings) Power Transformers (220V, 50 Hz/110V, 50 Hz)
II. Russian Supplied		

TABLE 1 (Cont.)

SUMMARY OF HARDWARE BY EXPERIMENT

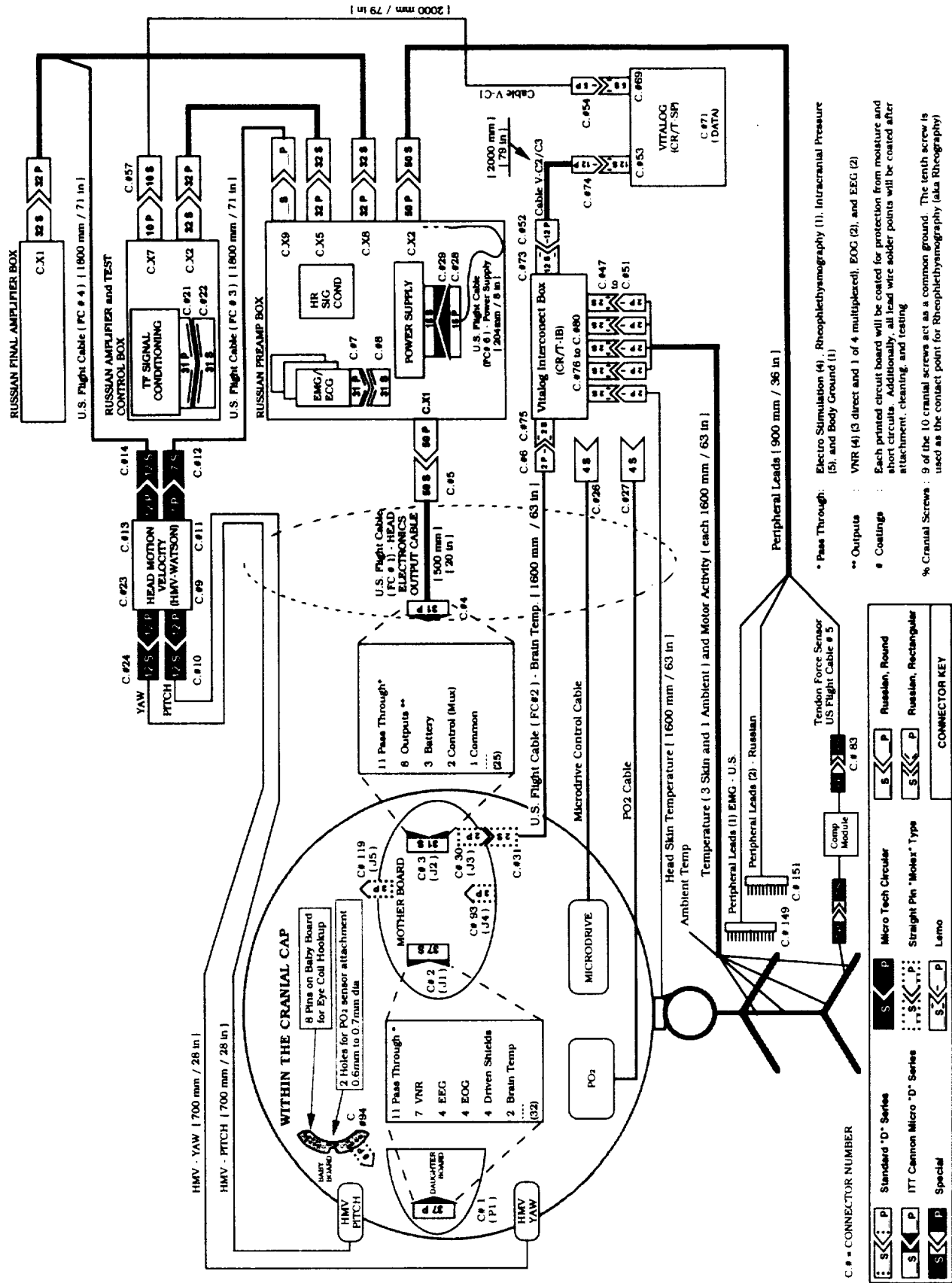
Experiment: Country	Flight	Ground
Studies of Vestibular Neurons in Normal, Hyper- and Hypogravity (K-8-03):		
I. U.S. Supplied	Multiplexing VNR Preamplifier EEG/EOG Preamplifier	Ground Test Unit #1 (GTU-1) (to test HMV, VNR, EEG and EOG signals) Two-Axis Motor-Driven Rotator and Animal Restraint with Controlling Computer and Software Two-Axis Hand-Driven Rotator with Animal Restraint Computer and Software (for template isolation of single action potentials from multiple train unit) Buffer Amplifiers Hydraulic Microdrive, Microelectrodes and Electrode Platforms Physiological Amplifiers Multi-Axis Rotator Tape Recorder (TEAC XR-510)
II. Russian Supplied	Stimulator (to provide electrical stimulation)	Active Head Movement Test Apparatus Stimulator (flight type)

TABLE 1 (Cont.)
SUMMARY OF HARDWARE BY EXPERIMENT

Experiment: Country	Flight	Ground
Functional Neuromuscular Adaptation to Spaceflight (K-8-04):		
I. U.S. Supplied	EMG Implants EMG Preamplifiers Tendon Force Transducer Tendon Force Signal Conditioner	GTU-2 (for testing EMG and tendon force signals) Lab Test Unit (LTU) (to provide preamplifiers for EMG and tendon force signals) EMG Implants Tendon Force Transducer Calibration Systems for Tendon Force Transducer Two-Channel Telemetry System Ground-Based EMG Recording System Cameras and Recorders for Locomotion Studies
II. Russian Supplied	Modified Foot Lever System	Training Bios and Flight-Type Couch Tape Recorder (TEAC XR510)
Biological Rhythms and Temperature Regulation (K-8-05):		
I. U.S. Supplied	Circadian Rhythm/Thermoregulation Signal Processor (CR/T-SP) CR/T Interface Box (CR/T-IB) Brain Temperature Sensors Motor Activity Sensors Skin Temperature Sensors Ambient Sensors	Ground Readout Unit (GRU) Portable GRU GRU-CR/T-SP Software Signal Simulator Data Listing Software
II. Russian Supplied	Temperature Transmitters ECG Lead Implants Skull Cap Assembly	

TABLE 1 (Cont.)
SUMMARY OF HARDWARE BY EXPERIMENT

Experiment: Country	Flight	Ground
Rhesus Monkey Metabolism During Spaceflight (K-8-06):		
I. U.S. Supplied		Doubly-labeled Water Kit
II. Russian Supplied		
Rhesus Monkey Immunology Study (K-8-07):		
I. U.S. Supplied		Microcentrifuge Small Centrifuge Portable Laminar Flow Hood
II. Russian Supplied		Tools (for bone marrow sampling)
Adaptation to Microgravity of Oculomotor Reflexes (AMOR) (K-8-08):		
I. U.S. Supplied		GTU-1 (for testing EOG signals) Eye Coils (shared with K-8-02) CNC Coil System EOG Amplifier Portable Linear Sled Primate Chair (with modified head restraint) Computer System (for eye position recording, on-line display, and on-site data reduction)
II. Russian Supplied		Operating Microscope (Zeiss) 14-Channel Videocassette Recorder (TEAC XR510)



* Pass Through: Electro Stimulation (4), Rheoplethysmography (1), Intracranial Pressure (5), and Body Ground (1)

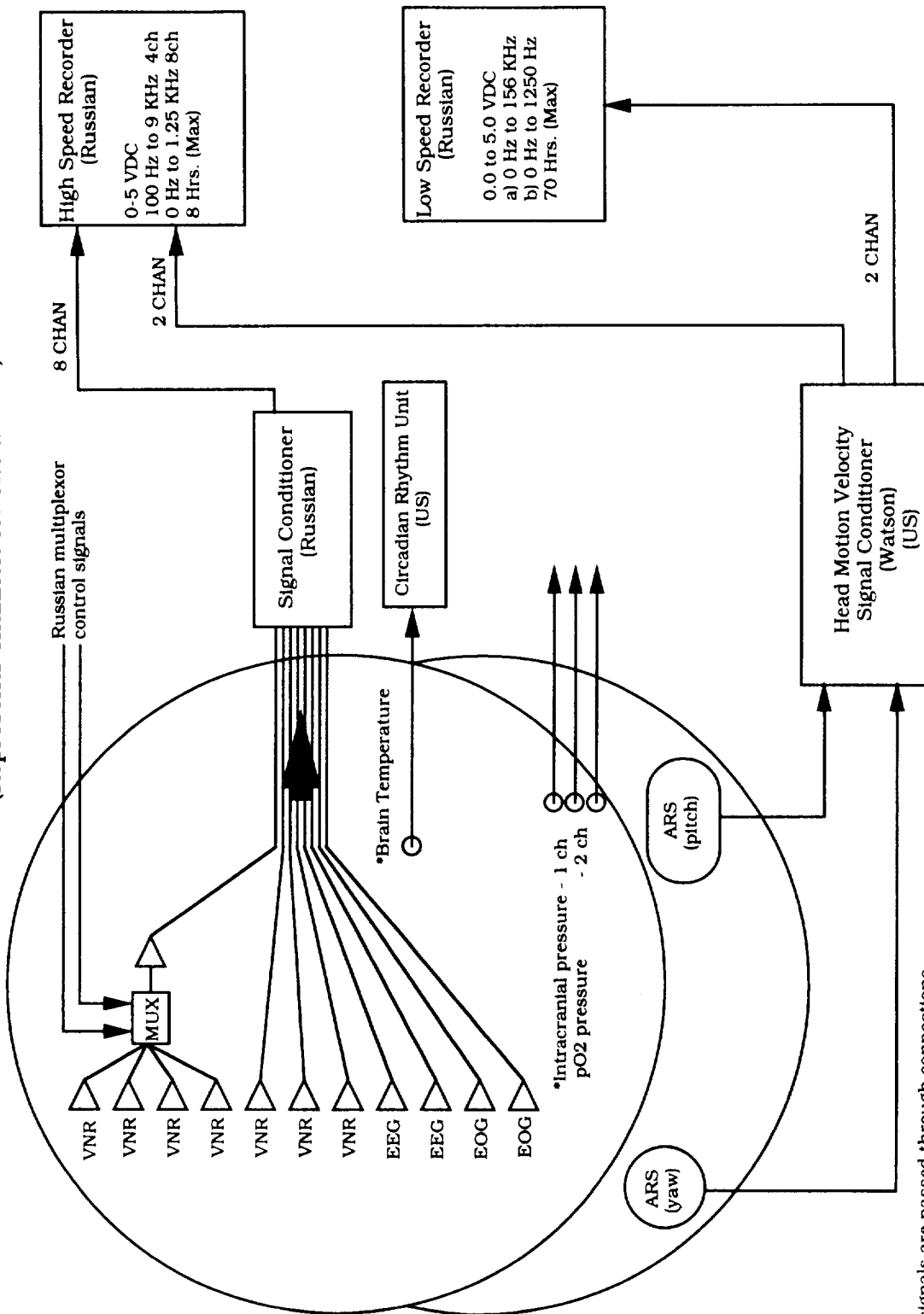
** Outputs: VNR (4) (3 direct and 1 of 4 multiplexed), EOG (2), and EEG (2)

• Coatings: Each printed circuit board will be coated for protection from moisture and short circuits. Additionally, all lead wire solder points will be coated after attachment, cleaning, and testing

% Cranial Screws: 9 of the 10 cranial screws act as a common ground. The tenth screw is used as the contact point for Rheoplethysmography (aka Rheography)

Figure 1. Cosmos 2229 inflight bioinstrumentation.

(Represents channels for one animal)



* These signals are passed through connections on the cranial cap electronics boards but are not processed by skull cap signal conditioners.

Figure 2. U.S. Signal conditioning - Cranial cap.

(Represents channels for one animal)

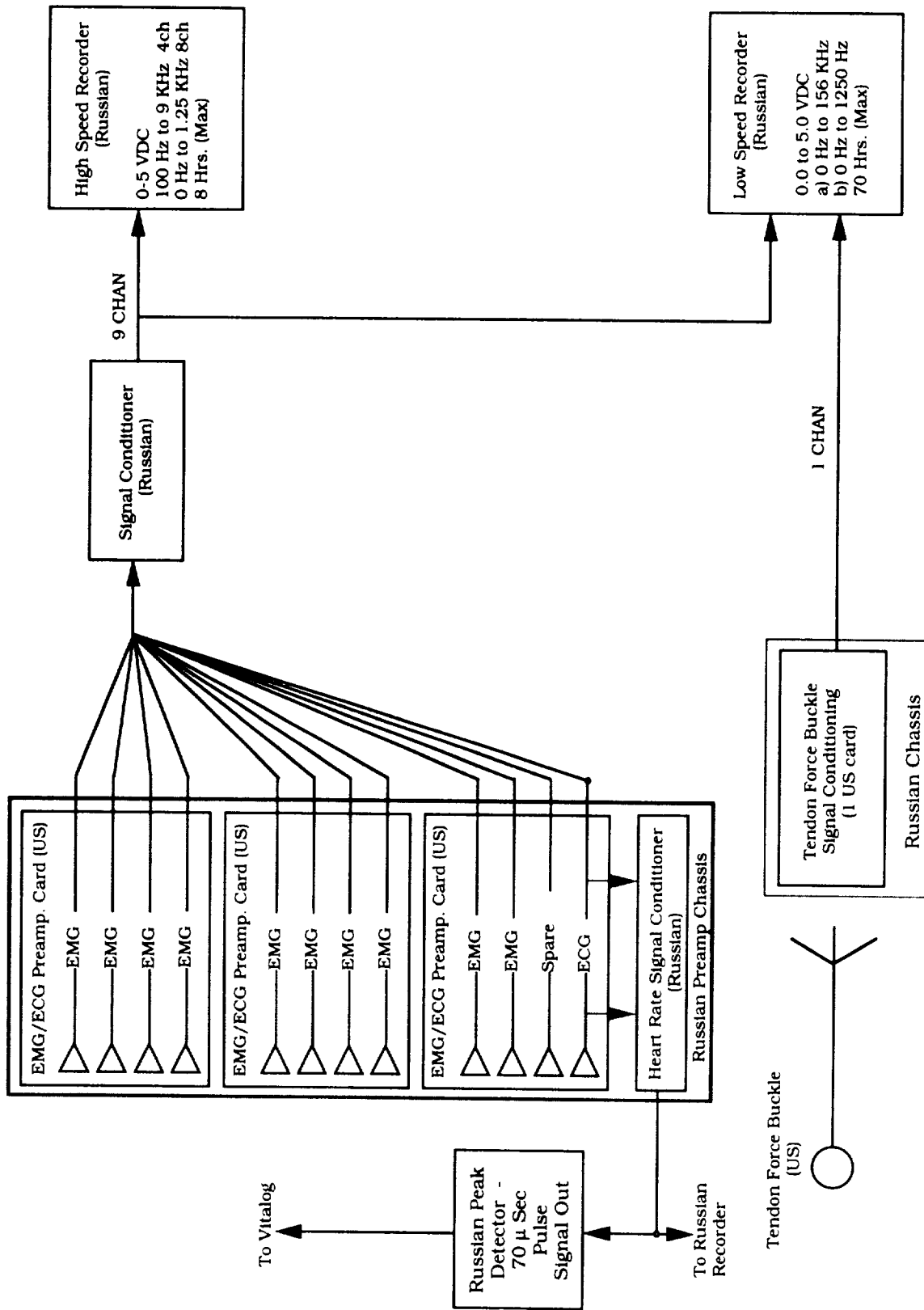


Figure 3. U.S. Signal conditioning - Other than cranial cap.

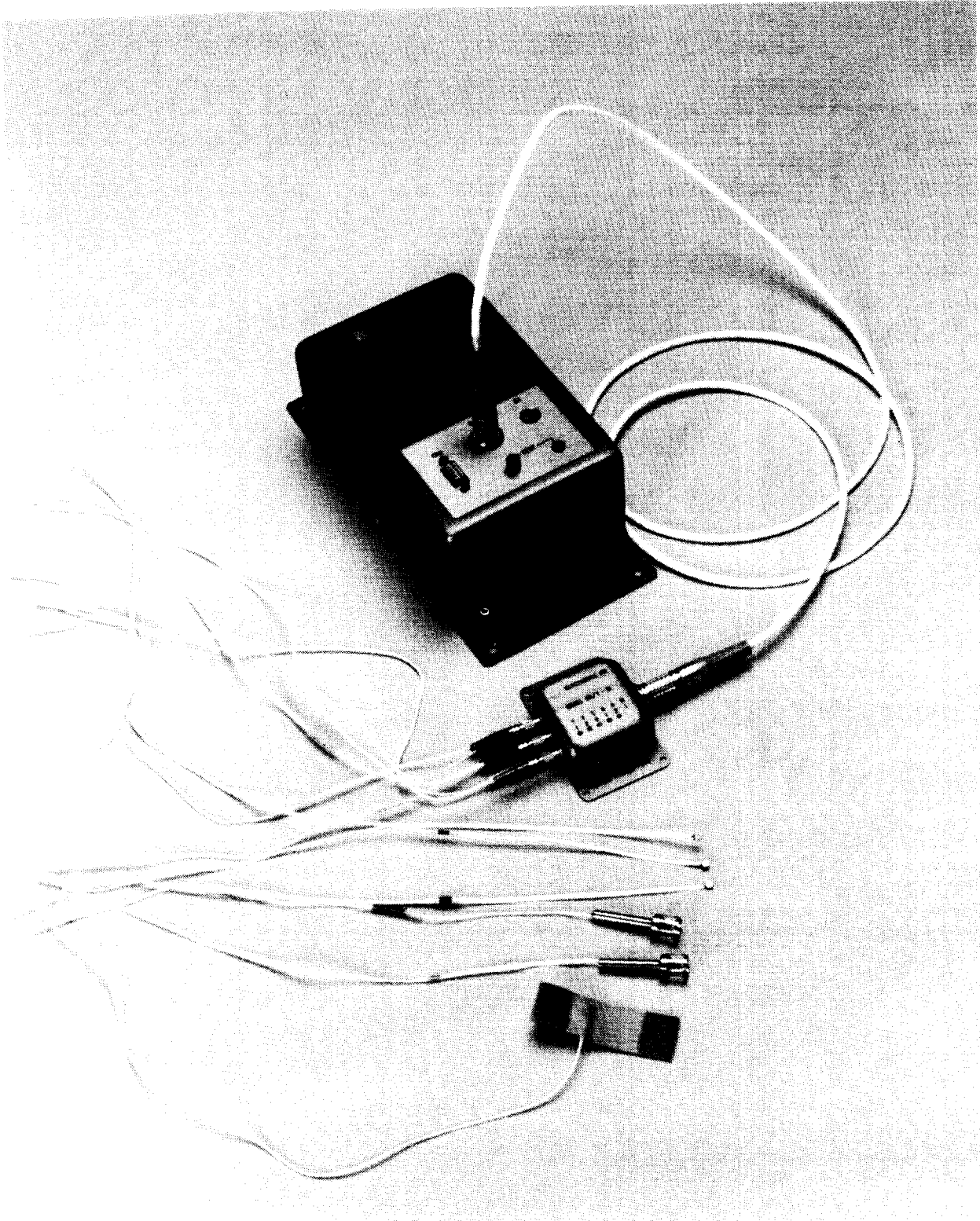


Figure 4. CR/T flight hardware.

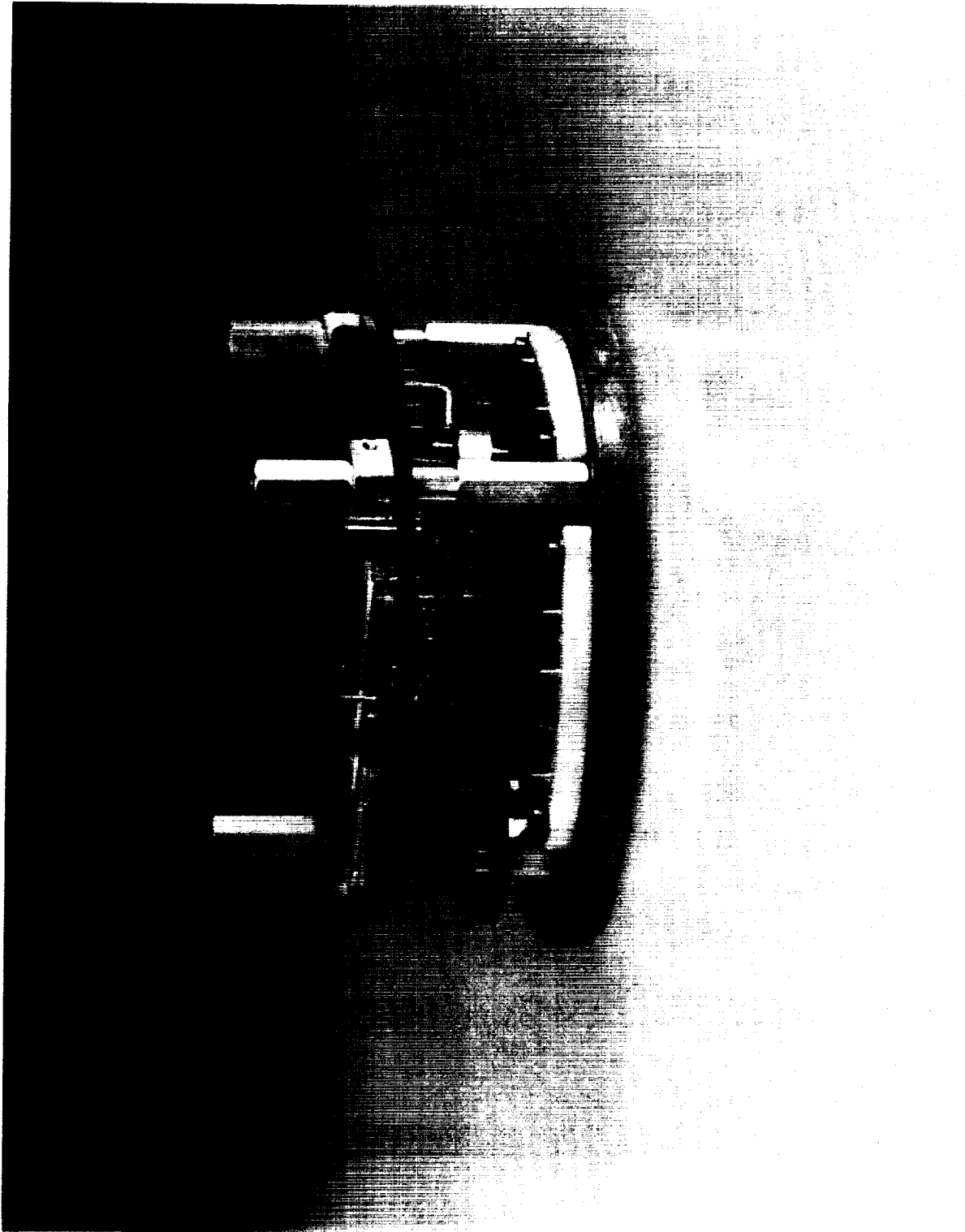


Figure 5. Head electronics assembly.

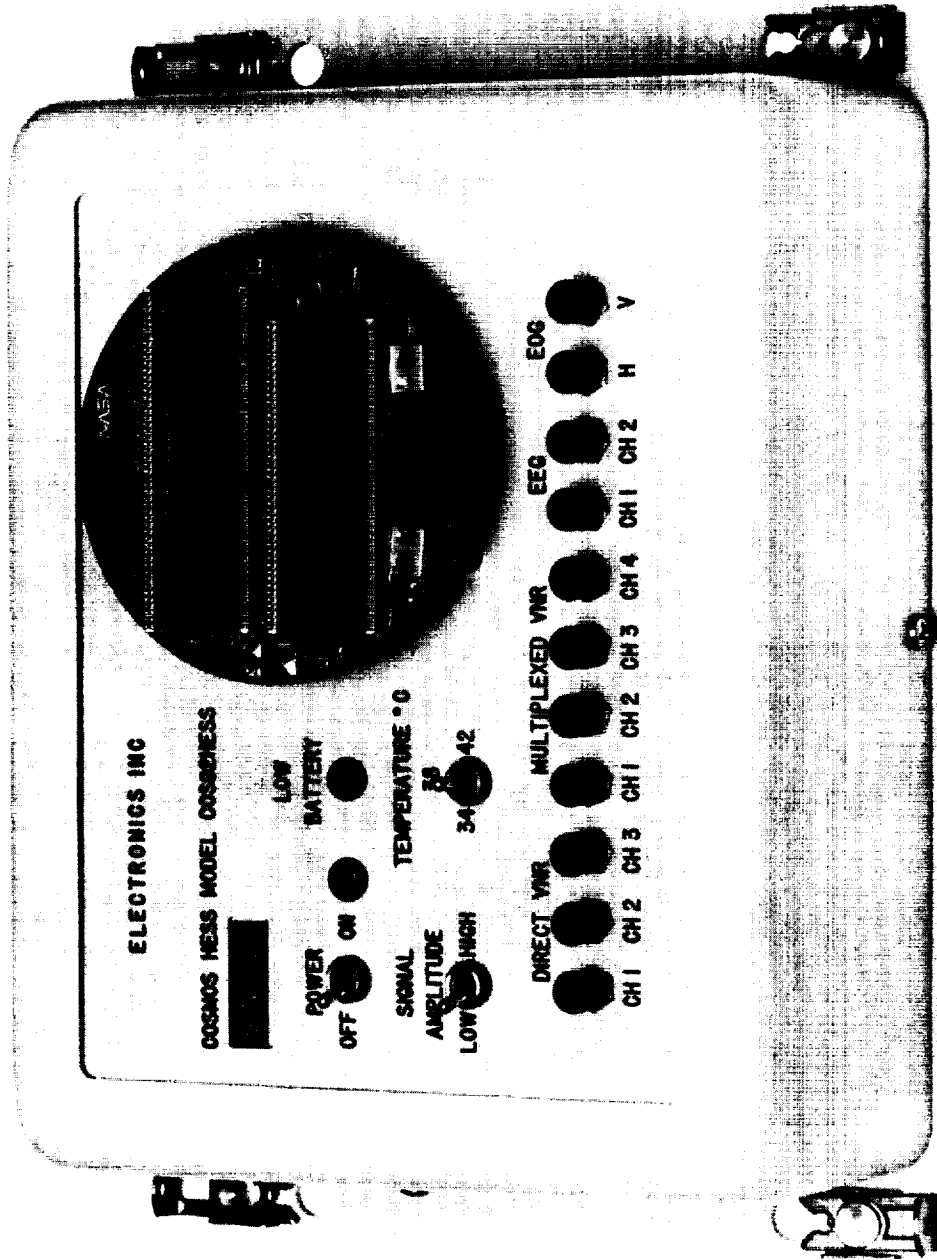


Figure 6. Head Electronics Signal Simulator (HESS).



Figure 7. Head Motion Velocity (HMV) unit.

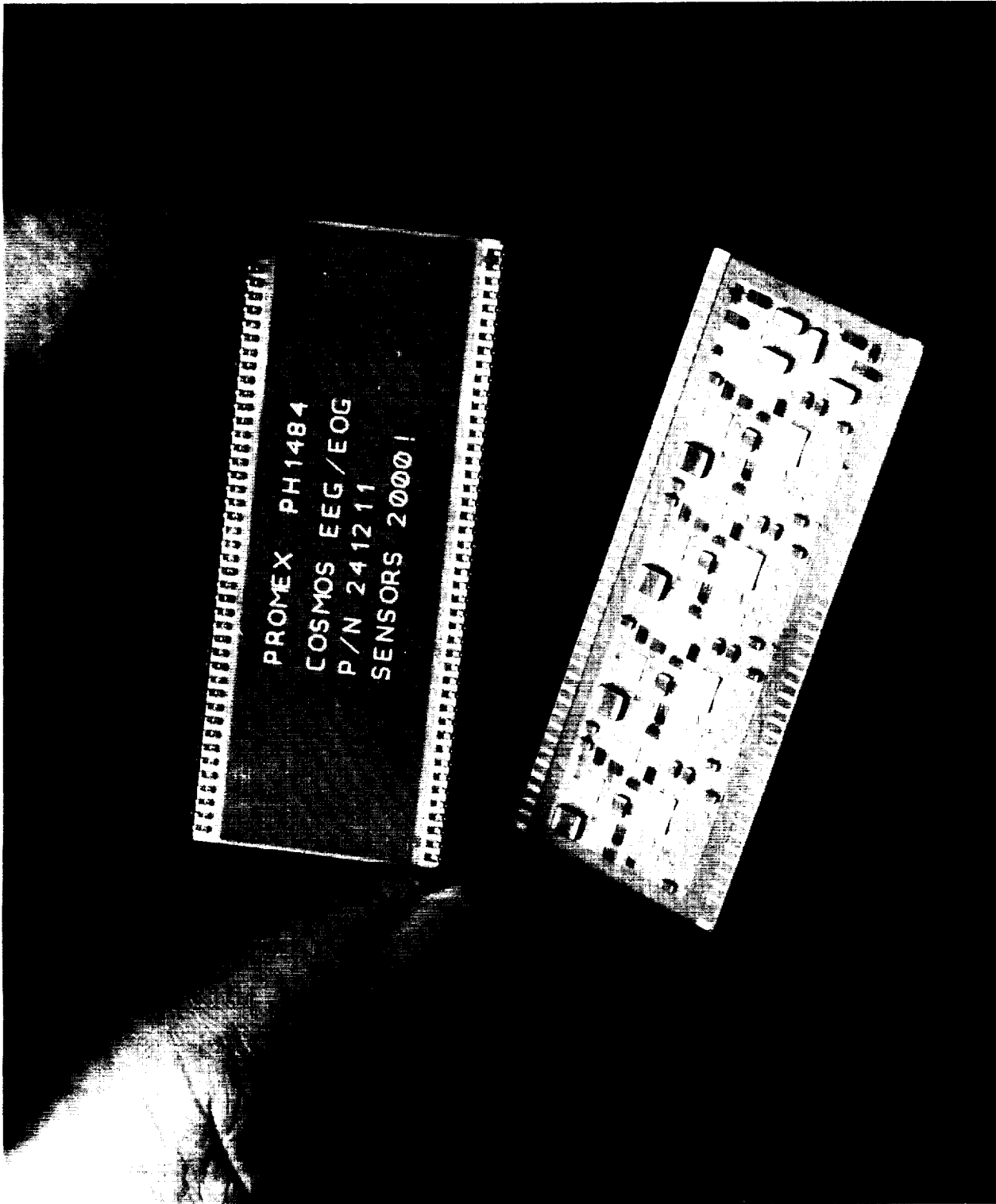


Figure 8. EEG/EOG hybrid chip.

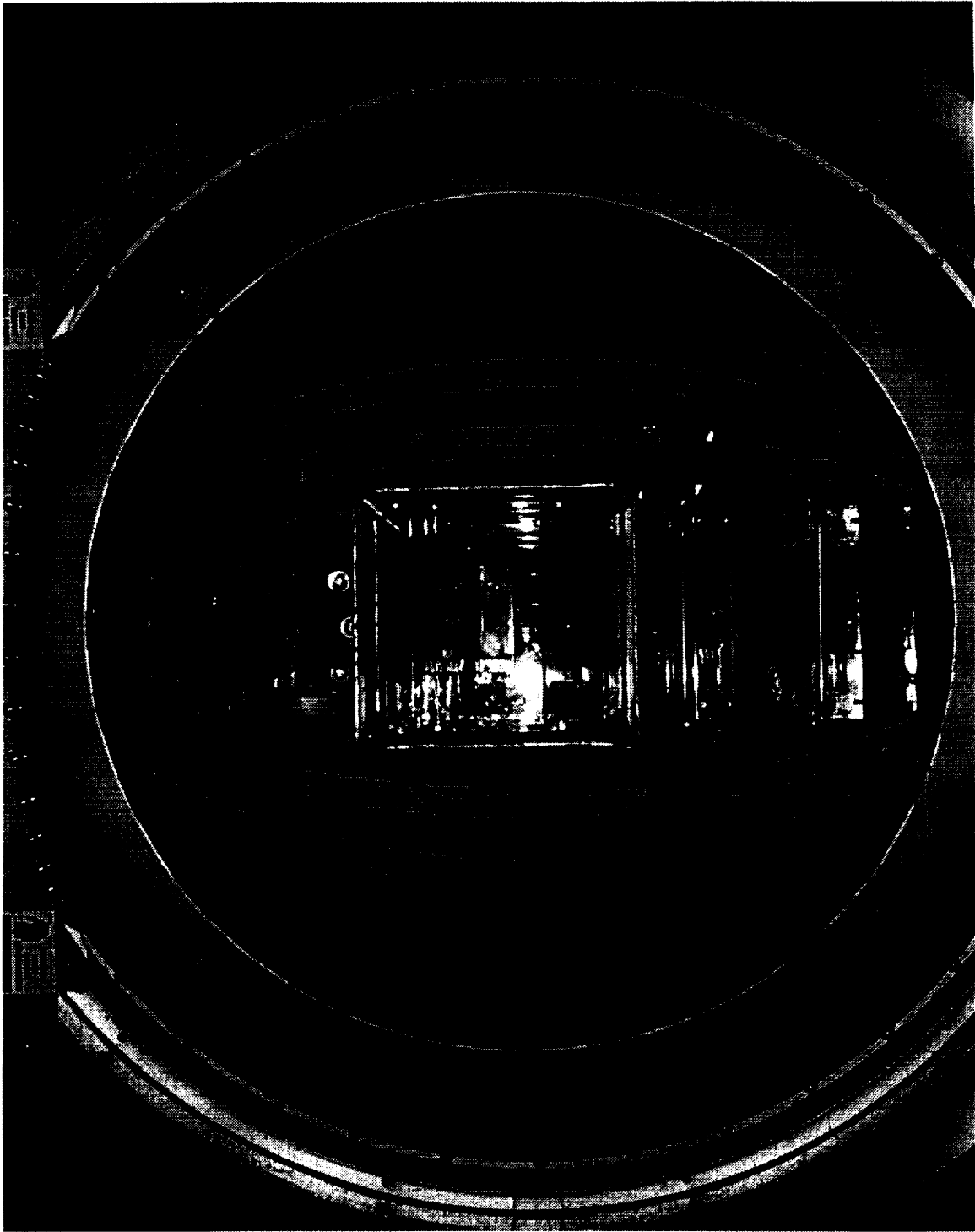


Figure 9. Optokinetic rotator.

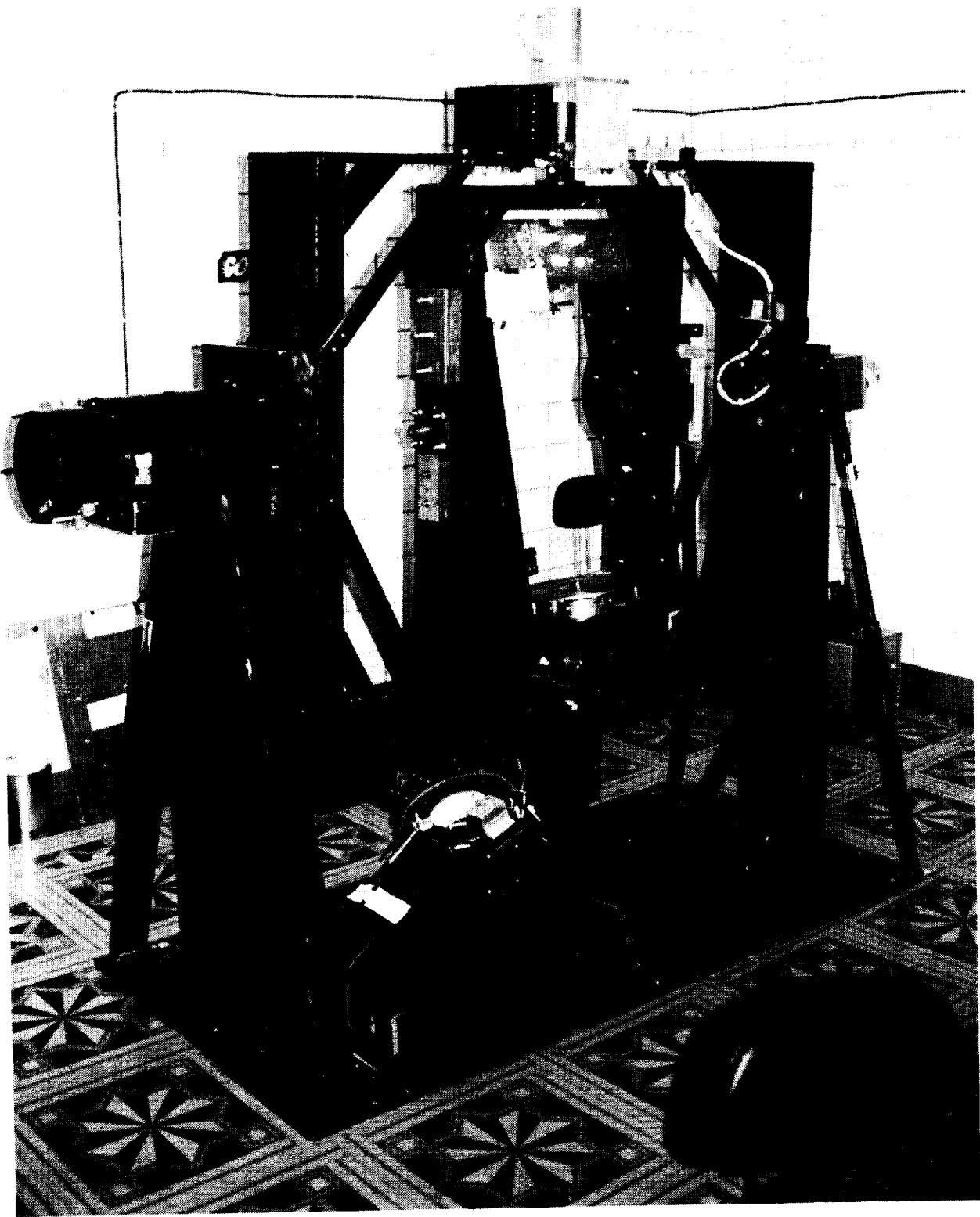


Figure 10. Computer-controlled, multi-axis rotator.

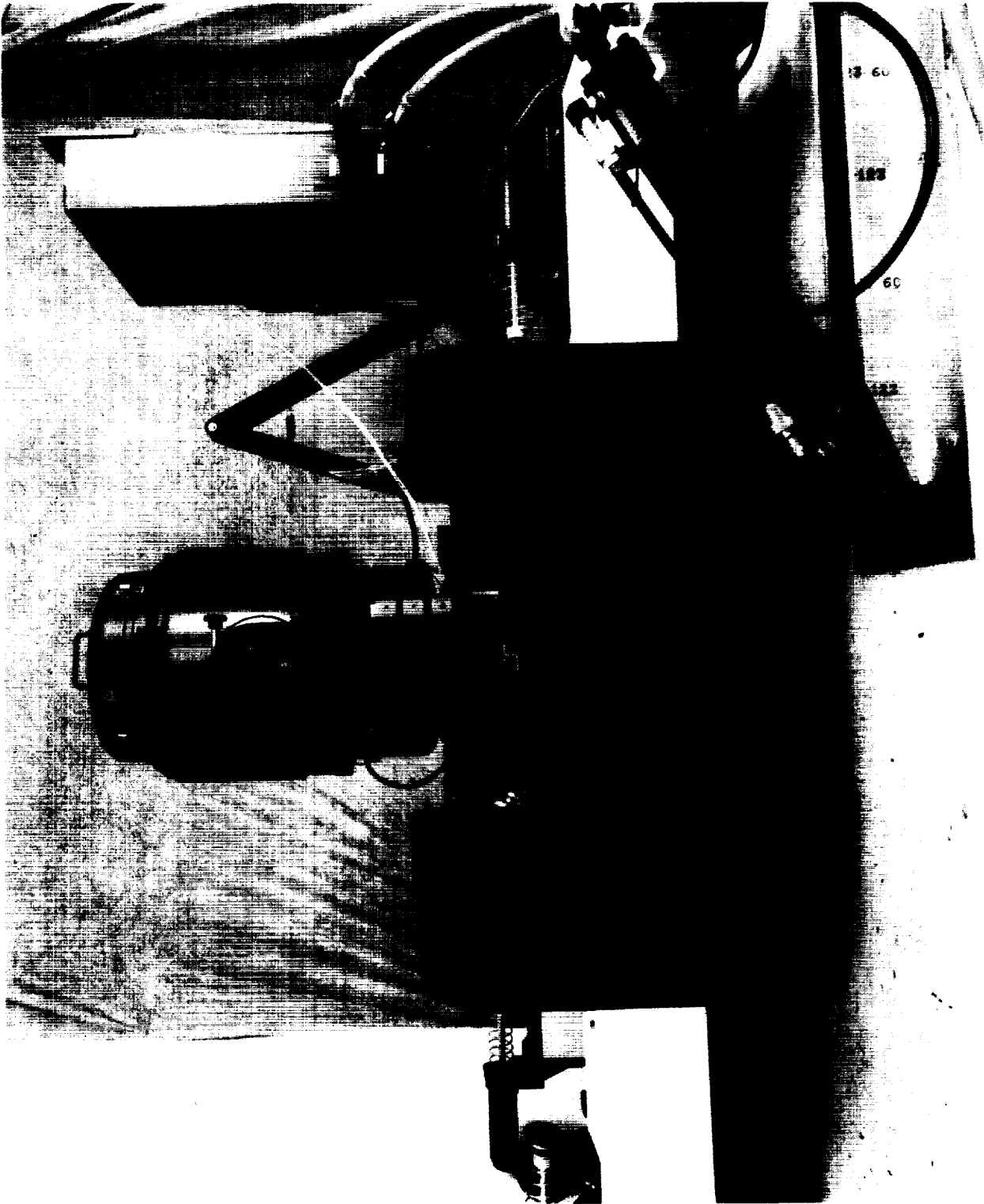


Figure 11. Portable Linear Sled (PLS).

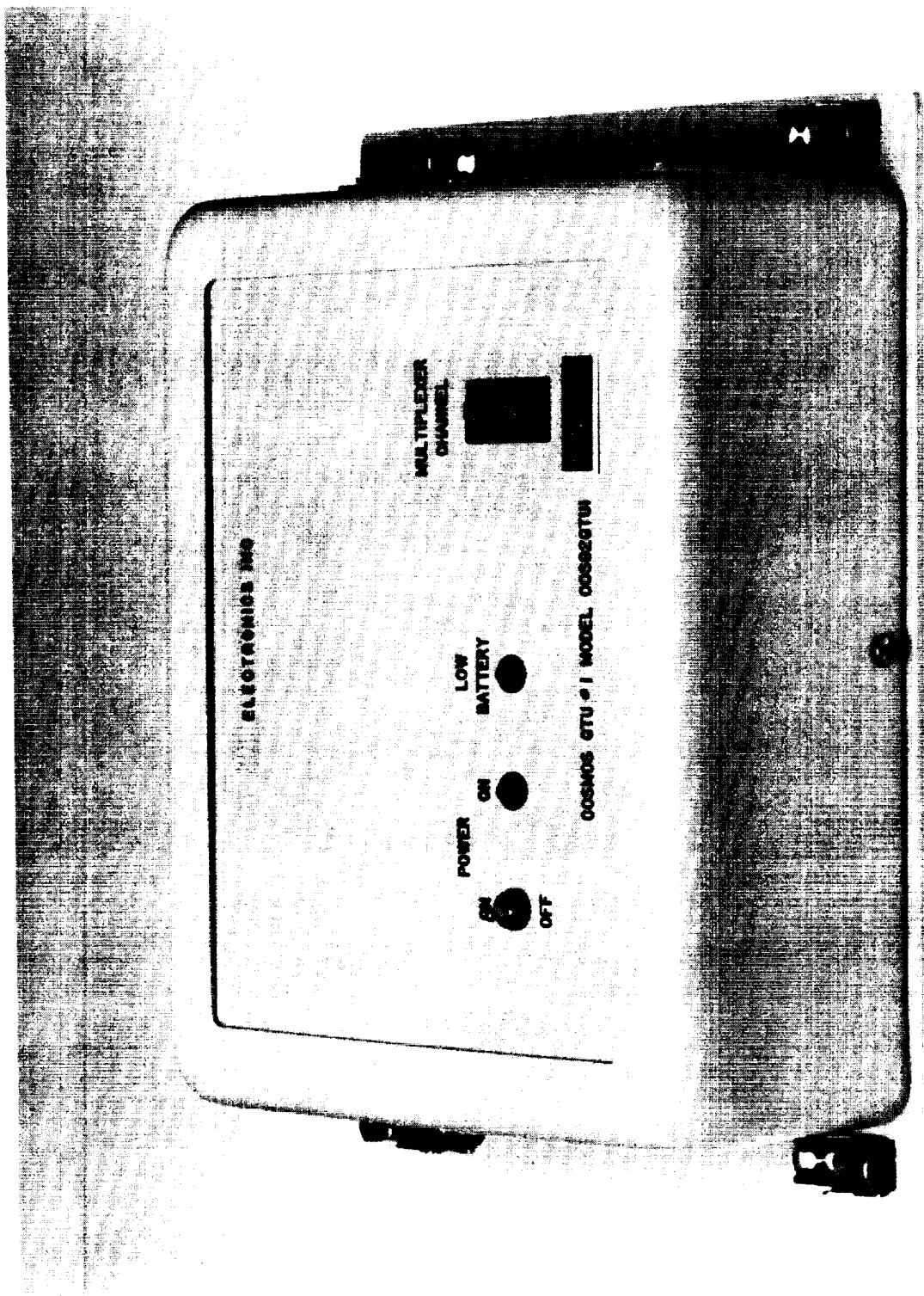


Figure 12. Ground Test Unit-1 (GTU-1).

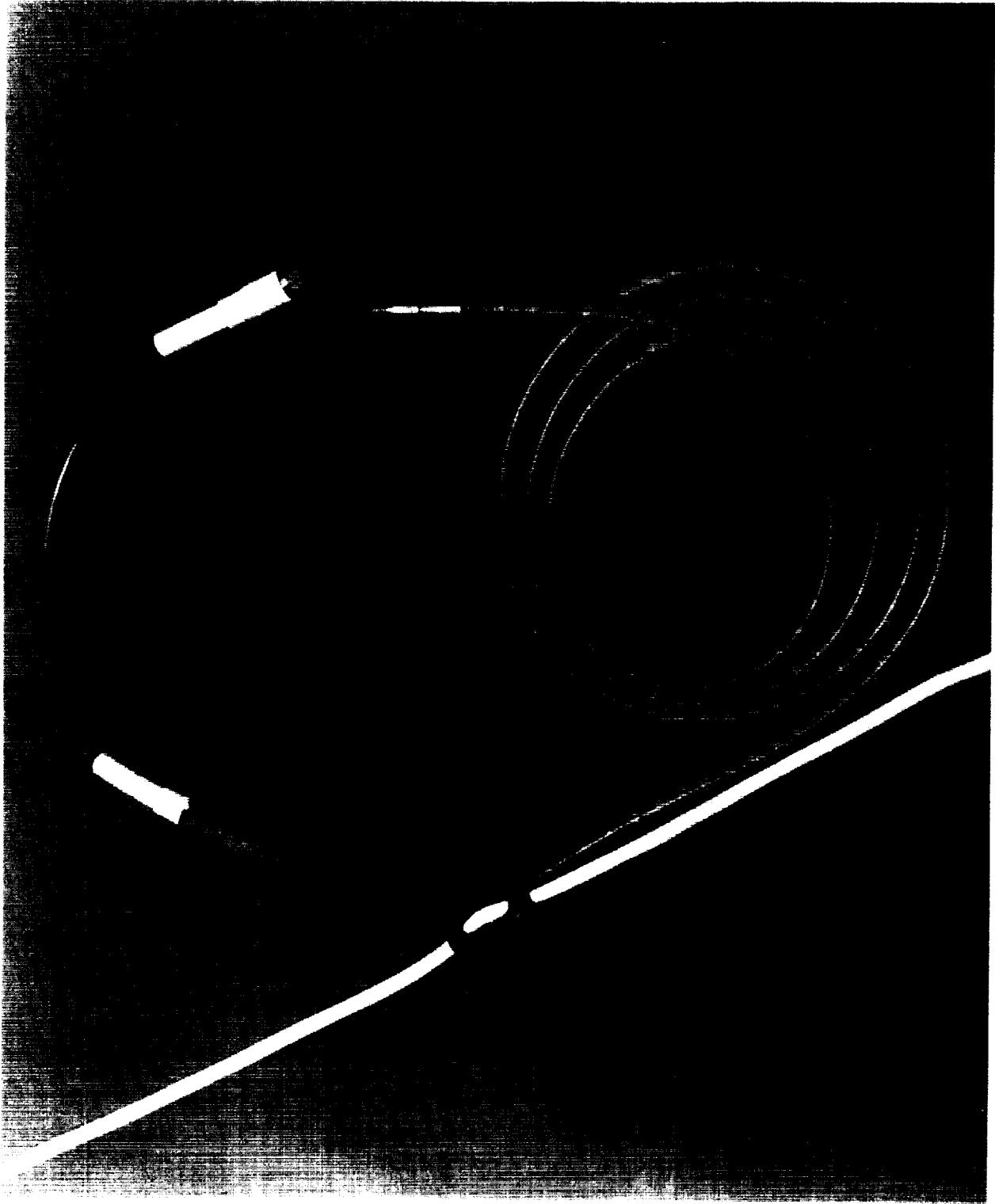


Figure 13(a). Tendon force sensor assembly.

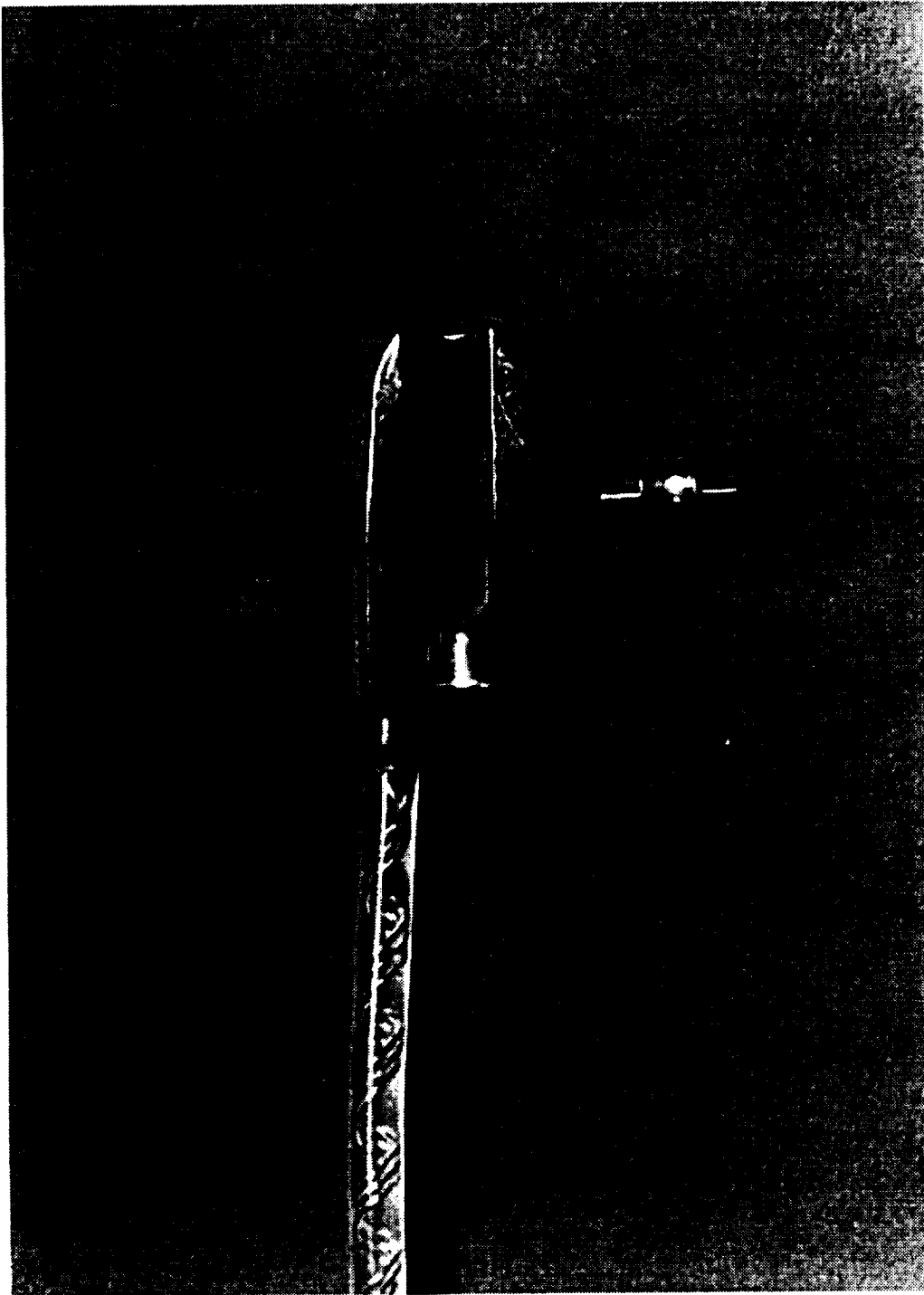


Figure 13(b). Tendon force sensor.

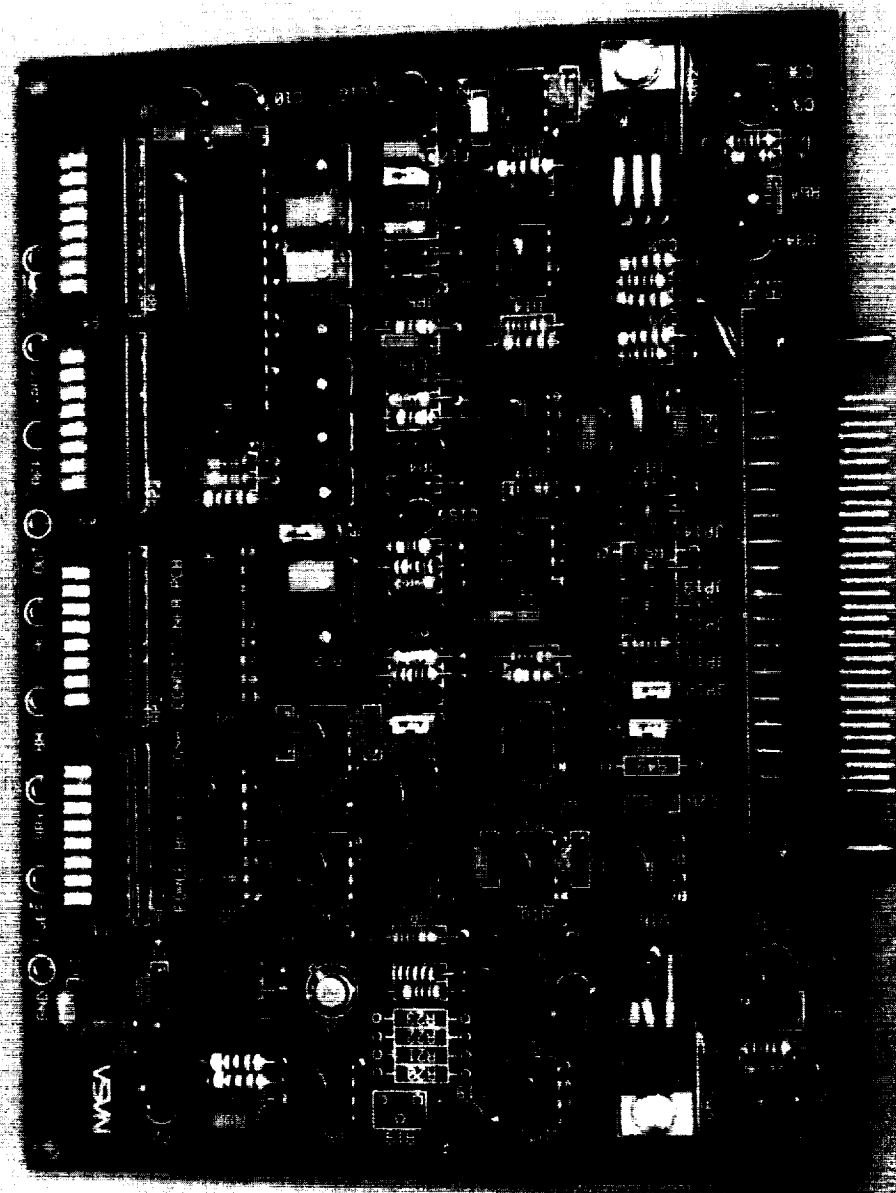


Figure 14. Tendon force signal conditioner.

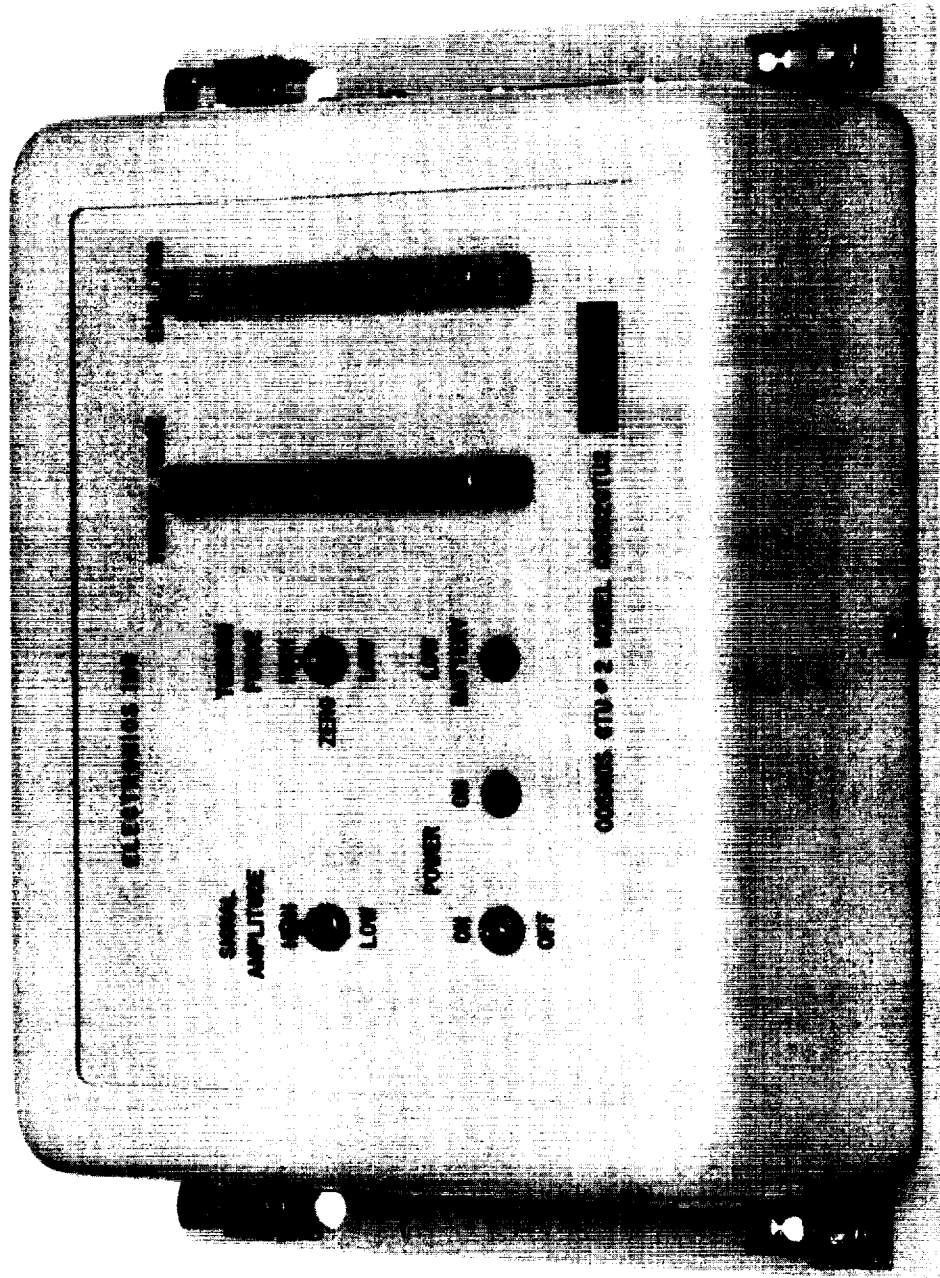


Figure 16. Ground Test Unit-2 (GTU-2).

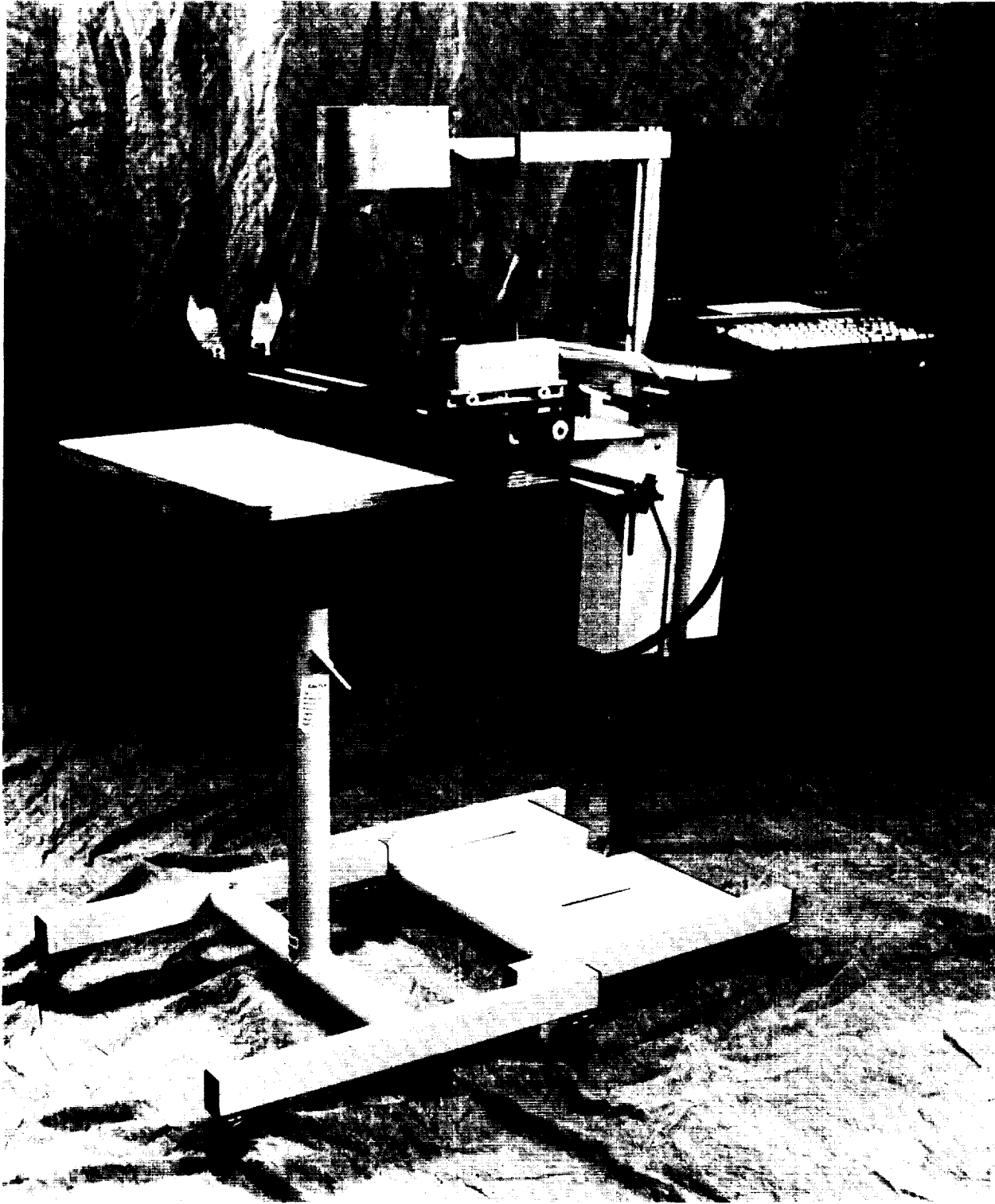


Figure 17. Mechanical Response Tissue Analyzer (MRTA).

III. SCIENCE REPORTS

EXPERIMENT K-8-01 (Part 1)

BENDING STIFFNESS OF THE TIBIA IN YOUNG RHESUS MONKEYS AFTER TWO
WEEKS IN SPACE ABOARD THE COSMOS 2229 BIOSATELLITE

Principal Investigator:

Sara B. Arnaud
NASA Ames Research Center
Moffett Field, CA

Co-Investigators:

Teresa Hutchinson
NASA Ames Research Center
Moffett Field, CA

Alexey V. Bakulin
Institute of Biomedical Problems
Moscow, Russia

Charles R. Steele
Stanford University
Stanford, CA

with the technical assistance of:

Shawn Bengston
NASA Ames Research Center
Moffett Field, CA

BENDING STIFFNESS OF THE TIBIA IN YOUNG RHESUS MONKEYS AFTER TWO WEEKS IN SPACE ABOARD THE COSMOS 2229 BIOSATELLITE

Sara B. Arnaud, Teresa Hutchinson, Alexey V. Bakulin, Charles R. Steele

ABSTRACT

Localized demineralization has been documented in the proximal tibia of young monkeys after 2 weeks exposure to microgravity. It is not known whether this decrease in mineralization is the consequence of unloading the bone from weightlessness *per se* or the chair restraint during the flight. It is also not known if the acquired mineral deficit impairs the function of the tibia, i.e. its loading capability. To evaluate the bone non-invasively before and after unloading by flight or chairing, we measured its cross-sectional bending stiffness (EI, Nm²) with an instrument, the Mechanical Response Tissue Analyzer (MRTA). The MRTA was modified for use in animal bones and the *in vivo* method verified for accuracy by comparing EI in the same set of tibias pre- and post-mortem by a standard mechanical testing device (Instron, Inc.)($r=0.94$, $p<.0001$). In the course of this flight experiment we found objective evidence of higher stiffness in the right than left tibia in 80% of the young monkeys tested. Five male Rhesus monkeys (3.7 ± 0.2 kg), restrained in a replica of the biosatellite chair for a 2 week pilot study in the U.S., showed an average decrease of 33% in tibial EI ($p<.05$). Repeated measures ($n=5$) in 5 unrestrained controls (4.2 ± 0.3 kg) in Moscow during a 4 month period of testing revealed similar mean values ranging from 4.2 ± 1.1 to 4.4 ± 1.2 in tibial EI. The variation in individuals of the control group did not show a consistent directional change as observed in the 2 flight monkeys. Relative to 45 days prior to launch, the 3.4 kg monkey who tolerated the space flight well, showed postflight decreases in EI to 37% by 20 days after landing. The 4.3 kg monkey who was dehydrated on landing showed variable responses in each leg postflight. Based on our validation and ground-based studies, the MRTA provides an accurate non-invasive measure of bone mechanical properties of sufficient precision in small groups of subjects for us to conclude that chair restraint alone has a major impact on bending stiffness. These short term changes in EI suggest that the loading capability of the tibia is reduced by chair restraint through acute mechanisms that affect mechanical properties in microgravity or in 1 g where these same phenomenon may account for individual variation observed in young animals.

INTRODUCTION

A deficit in the mineral content of weight bearing bones is a well documented consequence of exposure to microgravity. The proximal tibia of the young Rhesus monkey is particularly vulnerable to bone mineral loss (Rakhmanov et al., 1991), but it is uncertain if this localized loss of bone affects the loading capability of the whole bone. Young used a model of restraint that unloaded the tibias of non-human primates to study the evolution of disuse osteoporosis in the tibia (Howard et al, 1971). In addition to documenting the changes that occurred in the mineral content (Cann et al., 1980) and morphology of the tibia (Young et al., 1989), he initiated a program to develop a non-invasive biomechanical test to estimate the physical properties of the bone and its strength (Young et al., 1979). The approach to this problem was to perform impedance measurements on the bone and evaluate the response by a spring in series model. In this model the effective spring constant of a uniform bone loaded at its midpoint is determined, or $K_b = 48 EI/L^3$ where EI is the bending stiffness of the cross section, E is the elastic modulus, I the cross-sectional moment of inertia and L, bone length. The instrument developed for this measurement applied a low frequency vibration with a magnetic shaker to the center of a long bone. The resonant response over the 100-250 Hz range was used to compute bending stiffness. The first results that showed promise were carried out in the *ulnas and tibias of 2 monkeys after 3 (Young et al., 1979) and 6 months restraint (Young et al., 1983)*. Correlations of bending stiffness with bone mineral content were generally good, but

changes in bending stiffness exceeded those in mineral loss during immobilization and on recovery EI returned to control levels earlier than restoration of mineral.

A number of revisions in instrument hardware and software have been completed. These have culminated in considerable experimental data in the human ulna (Steele et al., 1988, McCabe et al., 1991, Myburgh et al., 1992, Myburgh et al., 1993). A new MRTA instrument that was designed for use in the clinical setting and manufactured by a small company, was used to determine EI in the human tibia, a bone with more complex geometry and resonance response than the ulna (Arnaud et al., 1991). We used this instrument to measure EI in the young monkeys involved in the Cosmos 2229 mission to assess the effects of inactivity during chair restraint and weightlessness.

METHODS AND PROCEDURES

Equipment

The instrument used to determine EI was the prototype of a portable table top model for use in humans (Gait Scan, Inc., Ridgeway, N.J., USA). A number of modifications, illustrated in Figure 1 (see end of report) were made to accommodate small bones. The limb supports were reduced in size and width. Contact of the tibia with the proximal supports was improved by adding a more flexible ball and socket joint and posts for adjusting the height with pins. The diameter of the curvature of the probe tip was reduced. A counterweight system that used weights ranging from 50 to 800 grams to offset the 1.3 kilogram load of the magnetic shaker and impedance head was attached. A metal ruler was attached to the base frame of the instrument to facilitate centering of the probe. A 6-parameter mathematical model that accounted for mass, stiffness and damping of skin and bone was developed.

Validation of Instrument

Scheduled necropsies at ARC and the California Regional Primate Center were the source of 22 monkey tibias from 2.5-13 kg animals which could be tested *in vivo* with the MRTA, excised and later tested by 3-point bending with a standard mechanical testing device (Instron) in the Laboratory of Orthopedic Research, University of California, Davis directed by Dr. B. Martin. Support for 3-point bending was provided by steel pins inserted through the proximal and distal ends of the tibia. The mineral content and density was measured in frozen bones in the laboratory of Dr. J. Kiratli at the Veterans Administration Hospital in Palo Alto, California by dual-energy x-ray absorptometry (Hologic QDR 1000/W). The relationship between EI *in vivo* determined with the MRTA and the objective measure of bending stiffness is illustrated in Figure 2 ($r=0.92$, $p<.0001$). EI *in vivo* was also related to bone mineral density ($r=0.81$, $p<.0001$), width at the midpoint of the bone ($r=0.57$, $p<.001$), bone area ($r=0.75$, $p<.001$) and body weight ($r=0.69$, $p<.001$).

Protocol for EI Measurements

A quality control procedure for checking the condition of the instrument by a measure of EI in an aluminum rod was carried out before each set of measurements. All protocols were approved by the Animal Care and Use Committee. Monkeys were anesthetized with intramuscular Telazol, 2.5-9 mg/kg (50 mg tiletamine hydrochloride and 50 mg zolazepam hydrochloride/ml) prior to the MRTA test and the leg shaved. A metal tape was used to measure the leg, flexed at the knee and ankle along its medial aspect from the lower edge of the medial malleolus to upper edge of the tibia. Leg lengths obtained in this manner agreed well with x-ray measurements. The leg was placed on the proximal leg support in a manner to establish good contact of the bone with the metal plates. The heel was then rested on the distal support and fixed firmly in place by closing 2 metal plates against the malleoli. The curved surface of the probe, automatically centered, was then placed on the skin surface of the tibia. Counterweights were estimated and added. A 2-second stimulus was given by

the computer prompt. The response curve was reviewed and if satisfactory, the measurement repeated 3 times. If the response curve was unsatisfactory, the position of the leg or counterweights was adjusted. The probe was lifted off the leg in between each test. Approximately 10 minutes were required to measure EI in each limb.

Ground-based Pilot Experiment

To determine the effects of chair restraint on tibial EI, both right and left tibias from 5 young male Rhesus monkeys, 3.7 ± 0.2 kg, were tested before and after 14 days restraint in a chair constructed to resemble the biosatellite chair. Instrumentation for the neuroscience and muscle experiments was in place in all the animals and did not appear to influence EI, as shown on Table 1. EI measurements were acquired at weekly intervals on 2 occasions before and after the period of chair restraint.

Flight Experiment

Right and left tibias of ten 3.4 ± 0.5 year old male monkeys who were candidates for the flight experiment were tested before the institution of any measure, including surgery, necessary for the flight. Five monkeys who could be tested on 5 separate occasions served as the controls for the 2 flight monkeys who were tested at 2.5 and 1.5 months prior to launch, and at 7, 20, and 30 days after landing.

Statistical Analyses

For all estimates, right and left tibias were treated as separate functional units with analysis of 10 values in 5 monkeys, 8 in 4 etc. Paired t-tests were used to evaluate right and left sided differences and changes in the pilot study. One way analysis of variance by repeated measures was used to determine changes in EI in control animals to assess reproducibility of the method. Correlation coefficients were determined by linear regression analysis.

RESULTS

Mean \pm SD values for age, body weight, and EI in the right and left tibias from all the young monkeys in each of the 3 studies are given in Table 2. When all EI values were combined, EI was higher in the right than left tibia ($p < .001$). Although body weights were the same in all 3 groups, EI was higher in IMBP animals than in either of the US groups. IMBP monkeys were 0.5 to 1 year older, on the average, than US monkeys.

The effects of 2 weeks chair restraint on EI in the 10 tibias of the 5 monkeys in the pilot study is illustrated on Figure 3. An average decrease of 33% (3.6 ± 1.5 to 2.4 ± 1.2 , $p < .001$) during 2 weeks of chair restraint was observed at the end of chairing and was still 28% lower than basal 1 week later.

Repeated measures over a 5.5 month period resulted in very consistent EI values in 5 control IMBP monkeys. See Figure 4. The values ranged from 4.4 ± 1.2 to 4.2 ± 1.1 Nm². Flight monkey #27906, whose food and water consumption were the same inflight as preflight, showed a maximum decrease of 24% in EI (4.1 ± 0.3 to 3.1 ± 0.2 Nm²) in the right and a 37% decrease (4.6 ± 0.2 to 2.9 ± 0.1 Nm²) in the left tibia on the 20th day post flight relative to the test 45 days preflight.

The flight monkey (#26151) who did not tolerate the flight well, consuming 30 % of preflight food in flight, had EI values that were erratic. Relative to preflight values, the right tibia showed a 7% decrease on R+7 and a 4% increase on R+20 (7.1 ± 0.4 to 6.6 ± 0.3 to 7.4 ± 0.2 Nm²); the left tibia showed a 35% increase on R+7 that was sustained (24%) at R+20 (4.6 ± 0.1 to 6.2 ± 0.2 to 5.7 ± 0.2

Nm²), as illustrated on Figure 5. Pre- and postflight changes in EI were unrelated to the changes in body weight.

DISCUSSION

This is the first application of a non-invasive technology to measure the mechanical properties of intact long bones after exposure to microgravity. Although the possibility of quantifying changes in mechanical properties of bone after a space flight mission of 2 weeks seemed remote, there were observations of decreases of 7.6 and 15.7% in radiographic density of the tibias of young monkeys in a previous flight of the same duration (Rakhmanov et al., 1987) that could alter bone composition sufficiently to influence its bending stiffness. The estimations of regional density used in this flight experiment did not show similar changes in tibial mineral density in the tibias during this flight. Although EI is known to be related to the mineral density of bone in cross-sectional (Steele et al., 1988) and longitudinal studies of disuse osteoporosis (Young et al, 1983), there is no evidence that the changes we observed after chair restraint or in one flight animal were associated with alterations in mineral density. More precise estimations of the mineral content in the proximal tibia than were accomplished in this study may be required to show such a relationship although the brevity of the flight and the chair experiment precluded the documentation of measurable decreases in bone mineral content by techniques currently available. Young found mineral density and stiffness of the tibias of adult Rhesus monkeys well correlated in a disuse osteoporosis model over a period of 12 months with measurements taken every 2-3 months, but did not examine the early responses (Young et al., 1983).

Our observation of decreases in tibial bending stiffness on the day that young monkeys were released from chair restraint is not in keeping with prevailing concepts of the stability of bone and the long duration required to change mechanical properties through changes in bone composition or structure. The measurement, EI, represents Young's modulus of elasticity, E, a material property of bone reflecting its chemical composition or mineral content primarily, and I, the cross-sectional moment of inertia, that represents the geometric characteristics of the bone. Aside from biceps strength, the best predictor of stiffness in ulna of adult humans was bone width or geometry (Myburgh et al., 1993). Our validation study showed the best predictor of EI in the Rhesus monkey tibia to be mineral content although correlations with area and width were good. This phenomenon may be due to the more homogeneous cylindrical conformation of the human ulna than the tibia or, perhaps, the weight bearing function of the tibia. It is well known that the mineral content of skeletons exposed to high body weights or high gravitational loads have high mineral densities (Whalen, 1988). In these brief studies the changes in body weight were not related to the changes in EI. We did not acquire bone width or mineral data in the tibia during chair restraint, but bone histology in the iliac crest where biomechanical loads may have been increased during chair restraint revealed significant increases in bone formation rates. The histologic data in monkeys suggests that rates of mineral deposition of sufficient magnitude to be measurable in bone occurs in as short a period of time as 2 weeks (Wronski, 1993). We have similar findings for decreases in bone formation rates in adult male volunteers for bed rest studies in whom iliac crest biopsy showed quantifiable histologic changes in as short a time as 1 week (Arnaud, 1992). Based on our awareness of how relatively rapidly bone responds to biomechanical stress at the microscopic level, the EI measurements at the whole bone level in chaired animals may reflect mineral losses undetectable by radiographic techniques.

The possibility that changes in mechanical properties of bone can occur rapidly following brief periods of exposure to changes in physical activity has some support from experimental data. Rubin et al. (1987) used ultrasonic velocity *in vivo* to determine the effects of the 26 mile Boston Marathon run across the tibia. Post-race velocities at the narrowest section of the tibial diaphysis were slightly, but significantly higher than pre-race velocities at the same site. These investigators speculated that these acute changes were not likely due to microdamage, since that would decrease ultrasound velocity, but rather the initiation of an adaptive mechanism that resides in the molecular structure and organic constituents of bone that may respond to brief intense activity by reorientation of tissue elements or other means. It is not likely that the bones of young monkeys would acquire fatigue damage manifested by microfractures from the lowered biomechanical stress to which they were exposed. A well known feature of young bone tissues, however, is the relatively higher water and collagen content, relative to the mineral content. While it is not known how dehydration or alterations in the protein composition of bone might affect EI, the results in our flight animals and the high individual variability in stiffness in these young animals suggest the potential importance of metabolic status in tibial EI. The monkey whose food and water consumption was unaltered by space flight showed a pattern of changes in EI similar to those of contented chair-restrained monkeys of the same age, whereas the monkey who was clinically dehydrated on landing showed no consistent decrease and even a trend to increased stiffness in one limb.

Until we were able to conduct a study which compare the EI *in vivo* measurement to objective biomechanical tests in the same bone, the possibility that the results obtained were an artifact of the method was considered most likely. Differences in operator techniques were removed from the study. Each set of measurements were obtained by the same person who began a set of measurements by checking the instrument with a quality control test that used an aluminum rod. While acceptable response curves at the time of testing were chosen by the operator, the final data was processed by a computer program equipped with a statistical evaluation of the curve fitting process. For the present, our view is that the data reported represent real biological variations in biomechanical properties of young monkey tibias. Further experimentation is needed to understand how metabolic problems that affect fluid balance and mineralization influence bending stiffness.

Experience in quantifying EI in other studies with the same instrument indicates the measurement to be of sufficient sensitivity to quantify small differences in EI. Right and left sided ulnas of same individual show differences in EI consistent with use and independent of mineral density (Arnaud, 1991). Although lower limb dominance and use in the Rhesus monkey is not as well documented as in the upper extremity (Dhall and Singh, 1977) the right tibia in 80 % of the population we studied shows higher EI than the left. This evidence for primate lower limb laterality appears to be genetic in origin since our observations were all in animals less than 4 years of age.

The loading capability of the tibias is defined as $P_{cr} = EI (p/L)^2$ and is proportional to EI. A 30% decrease in EI would indicate a similar reduction in the buckling load. The loading capability of the tibia appears to be reduced by chair restraint, a necessary part of any flight experiment in the monkey. Further investigation regarding the effects of alterations in nutrition or fluid and electrolyte metabolism on the mechanical properties of bone is needed to determine the cause of the more acute changes we observed in EI in this flight experiment.

ACKNOWLEDGMENTS

Our thanks to Dr. Bruce Martin, Dr. Jenny Kiratli, Jeffrey Emery, Dr. Lin-Jun Zhou, David Mayer, Mr. Anthony Mauriello, President and his associates at Gait Scan, Inc. for assistance and support of this flight experiment.

REFERENCES

1. Arnaud, S.B., D.J. Sherrard, N. Maloney, R.T. Whalen, and P. Fung. Effects of 1 Week Head-Down Tilt Bed Rest On Bone Formation and the Calcium Endocrine System. *Aviat. Space & Environ. Med.* 63:14-20, 1992.
2. Arnaud, S.B., C.R. Steele, L-J. Zhou, T. Hutchinson, and R. Marcus. A Direct Non-Invasive Measure of Long Bone Strength. *Proc. Annual Inter. Cong. of the IEEE Engineering in Med. and Biol. Soc.* 13:1984-1985, 1991.
3. Arnaud, S.B., T.J. Wronski, P. Fung, M. Navidi, and R. Ballard. Calcium Metabolism and Bone Histomorphometry in Mature and Young Rhesus Monkeys During Reduced Activity. *J. Bone and Mineral Res.* 8:S281, 1993.
4. Cann, C.E., H.K. Genant, and D.R. Young. Comparison of Vertebral and Peripheral Mineral Losses in Disuse Osteoporosis in Monkeys. *Radiology* 134:525-529, 1980.
5. Dhall, U. and I. Singh. Anatomical Evidence of One-Sided Forelimb Dominance in the Rhesus Monkey. *Anat. Anz.* 141:420-425, 1977.
6. Howard, W.H., J.W. Parcher, and D.R. Young. Primate Restraint System for Studies of Metabolic Responses During Recumbency. *Lab Animal Sci.* 21:112-117, 1971.
7. McCabe, F., L-J. Zhou, C.R. Steele, and R. Marcus. Non-invasive Assessment of Ulnar Bending Stiffness in Women. *J. Bone and Min Res.* 6:53-59, 1991.
8. Myburgh, K.H., S. Charette, L-J. Zhou, C.R. Steele, S. Arnaud, and R. Marcus. Influence of Recreational Activity and Muscle Strength on Ulnar Bending Stiffness in Men. *Med. Sci. Sports Exerc.* 25:592-596, 1993.
9. Myburgh, K.H., L-J. Zhou, C.R. Steele, S. Arnaud, and R. Marcus. In Vivo Assessment of Forearm Bone Mass and Ulnar Bending Stiffness in Healthy Men. *J. Bone and Mineral Research* 7:1345-1530, 1992.
10. Rakhmanov, A.S., A.V. Bakulin, S.L. Dubonos, V.Y. Novikov, C. Cann, and S. Nogues. Study of the State of Bone Tissue in Monkeys Flown on Cosmos-1887. *Kosmicheskaya Biologiya i Aviakosmicheskaya Meditsina* 25:42-44, 1991.
11. Rubin, C.T., G.W. Pratt, A.L. Porter, L.E. Lanyon, and R. Poss. The Use of Ultrasound *in vivo* to Determine Acute Change in the Mechanical Properties of Bone Following Intense Physical Activity. *J. Biomechanics* 20:723-727, 1987.

12. Steele, C.R., L-J. Zhou, D. Guido, R. Marcus, W.L. Heinrichs, and C. Cheema. Non-invasive Determination of Ulnar Stiffness From Mechanical Response- in vivo Comparison of Stiffness and Bone Mineral Content in Humans. *J. Biomech. Eng.* 110:87-96, 1988.
13. Whalen, R.T., D.R. Carter, and C.R. Steele. Influence of Physical Activity on the Regulation of Bone Density. *J. Biomechanics* 21(10):825-837, 1988.
14. Young, D.R., W.H. Howard, C. Cann, and C.R. Steele. Non-invasive Measures of Bone Bending Rigidity in the Monkey (*M. nemestrina*). *Calcif. Tiss. Int.* 27, 109-115, 1979.
15. Young, D.R., W.J. Niklowitz, and C.R. Steele. Tibial Changes in Experimental Disuse Osteoporosis in the Monkey. *Calcif Tissue Int.* 35:304-308, 1983.

TABLE 1. EFFECT OF TENDON FORCE BUCKLE AND MUSCLE BIOPSY ON TIBIAL EI MEASUREMENTS (MEAN±SD).

Procedure	EI, Nm ²
Tendon Force Buckle ^a	3.4 ± 1.9
No Tendon Force Buckle	3.8 ± 1.3
Muscle Biopsy ^b	2.9 ± 1.6
No Muscle Biopsy	2.3 ± 0.6

^a Tendon Force Buckle was in place 1 week-3 months prior to Pre #1 (-7 days chair restraint)

^b Muscle biopsies occurred 1-5 days prior to Post #2 (+7 days chair restraint)

TABLE 2. RIGHT VERSUS LEFT TIBIA EI IN 2-4 YEAR OLD RHESUS MONKEYS (MEAN \pm SD).

	N	AGE yr	BODY WEIGHT kg	LIMB LENGTH			TIBIA EI	
				RIGHT cm	LEFT cm	RIGHT Nm2	LEFT Nm2	
U. S. Monkeys	8	2.5 \pm 0.1	3.7 \pm 0.2	13.1 \pm 0.6	13.1 \pm 0.6	4.0 \pm 1.4	2.9 \pm 1.4†	
IMBP Monkeys	10	3.4 \pm 0.5	3.5 \pm 0.4	14.9 \pm 0.7	14.8 \pm 0.8	4.3 \pm 1.0	3.8 \pm 1.2††	
Validation Monkeys	6	3.0 \pm 1.0	3.6 \pm 0.9	13.3 \pm 1.4	13.2 \pm 1.4	5.2 \pm 2.4	4.5 \pm 2.1††	
All Monkeys	24	3.0 \pm 0.7	3.6 \pm 0.6	13.9 \pm 1.2	13.8 \pm 1.2††	4.4 \pm 1.6	3.7 \pm 1.6*	

right versus left by paired t test †p<0.005, ††p<0.028, *p<0.0001.

MRTA Modifications by NASA

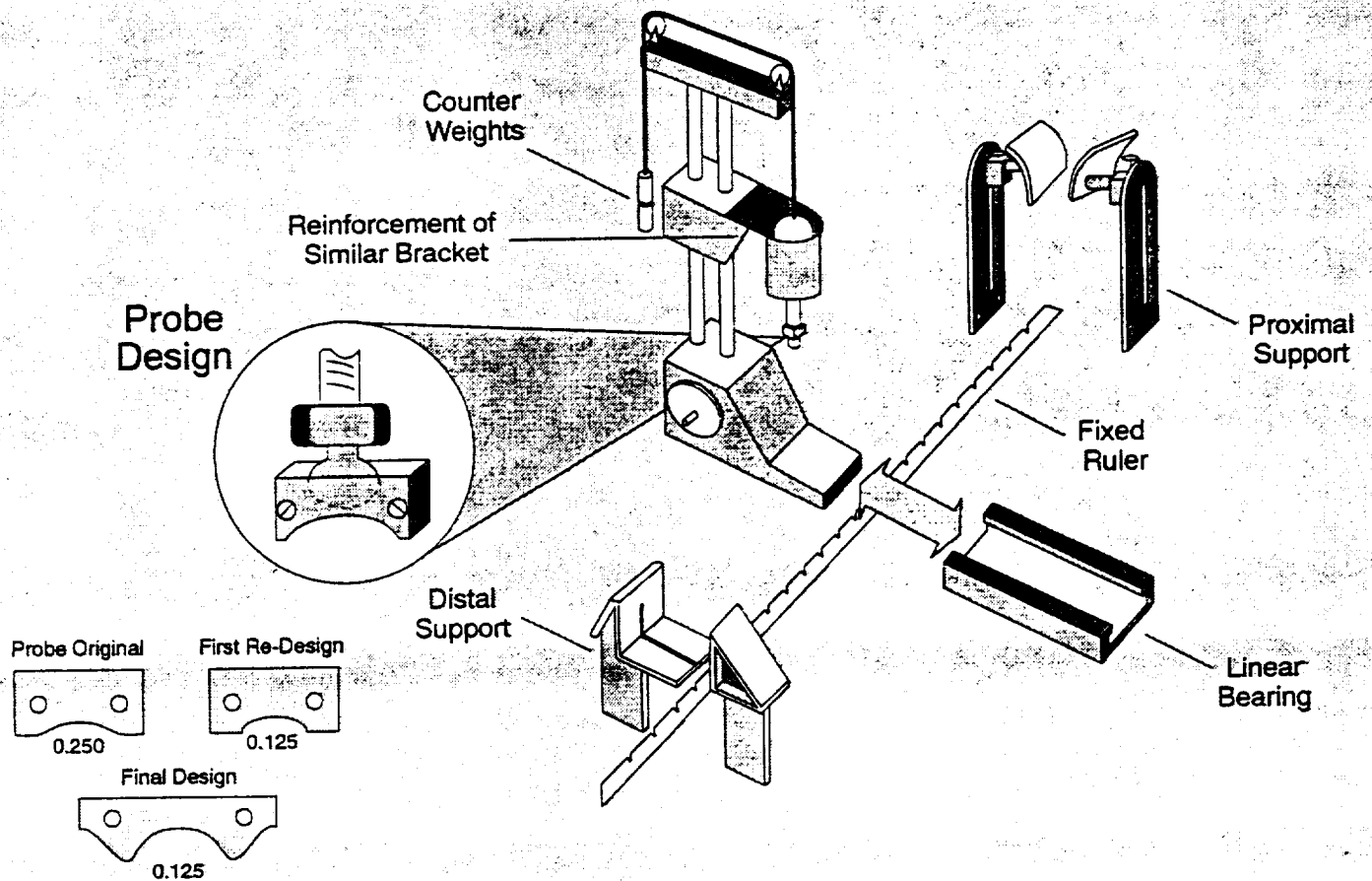


Figure 1. Modifications to the portable table top MRTA by NASA Ames Research Center.

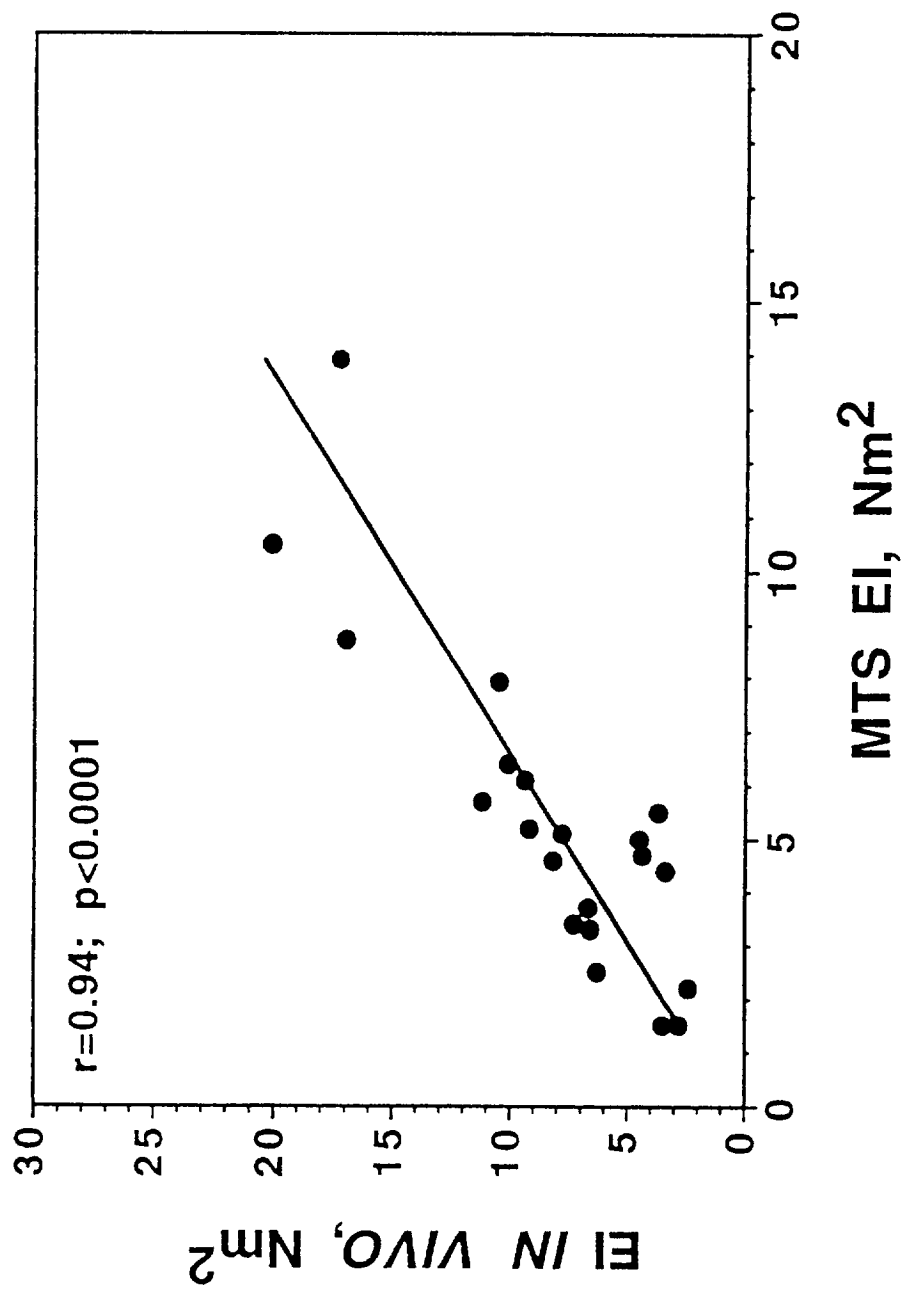


Figure 2. Relationship between in vivo EI and MTS bending stiffness.

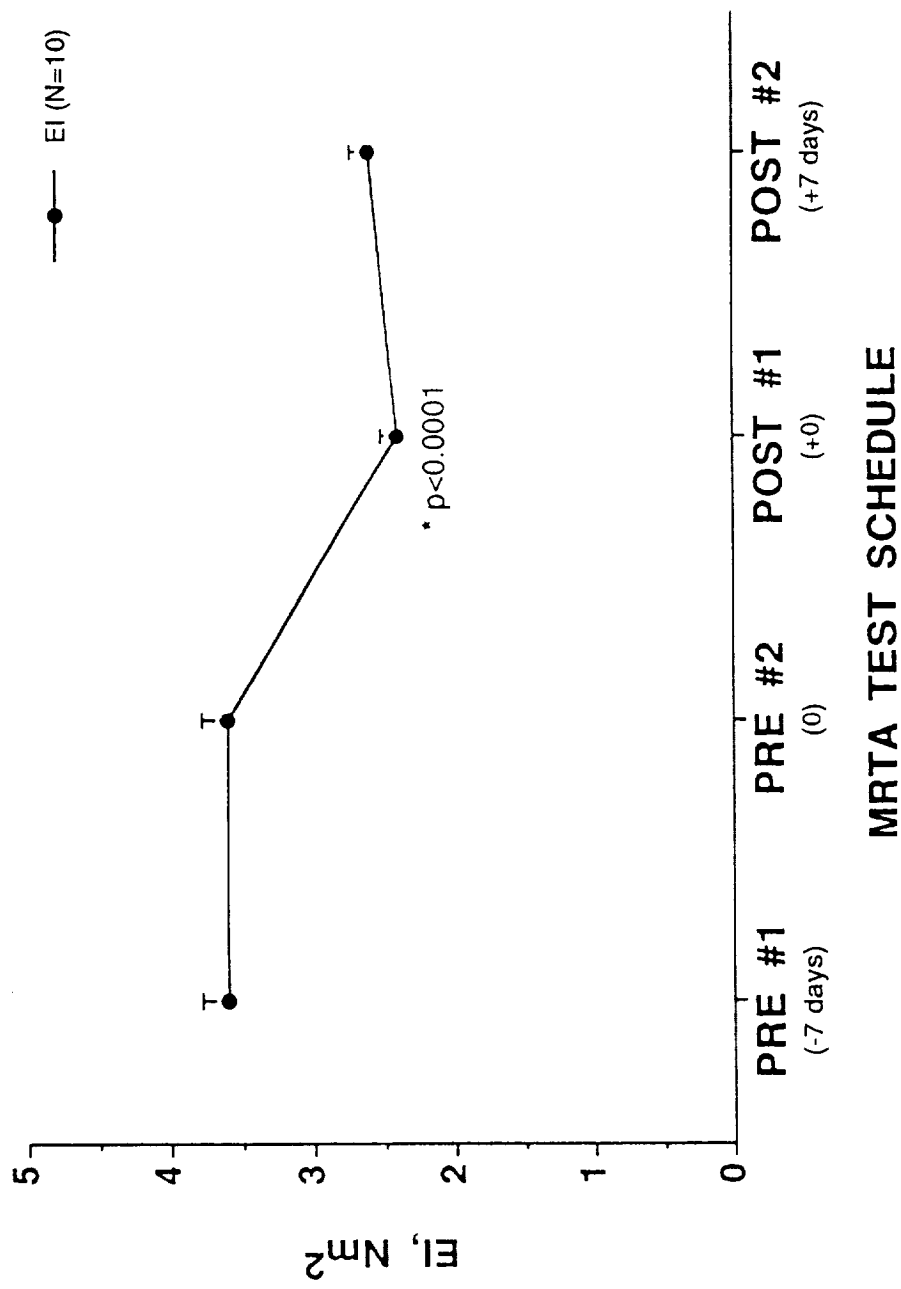


Figure 3. Right and left combined MRTA EI values for the U.S. pilot monkeys.

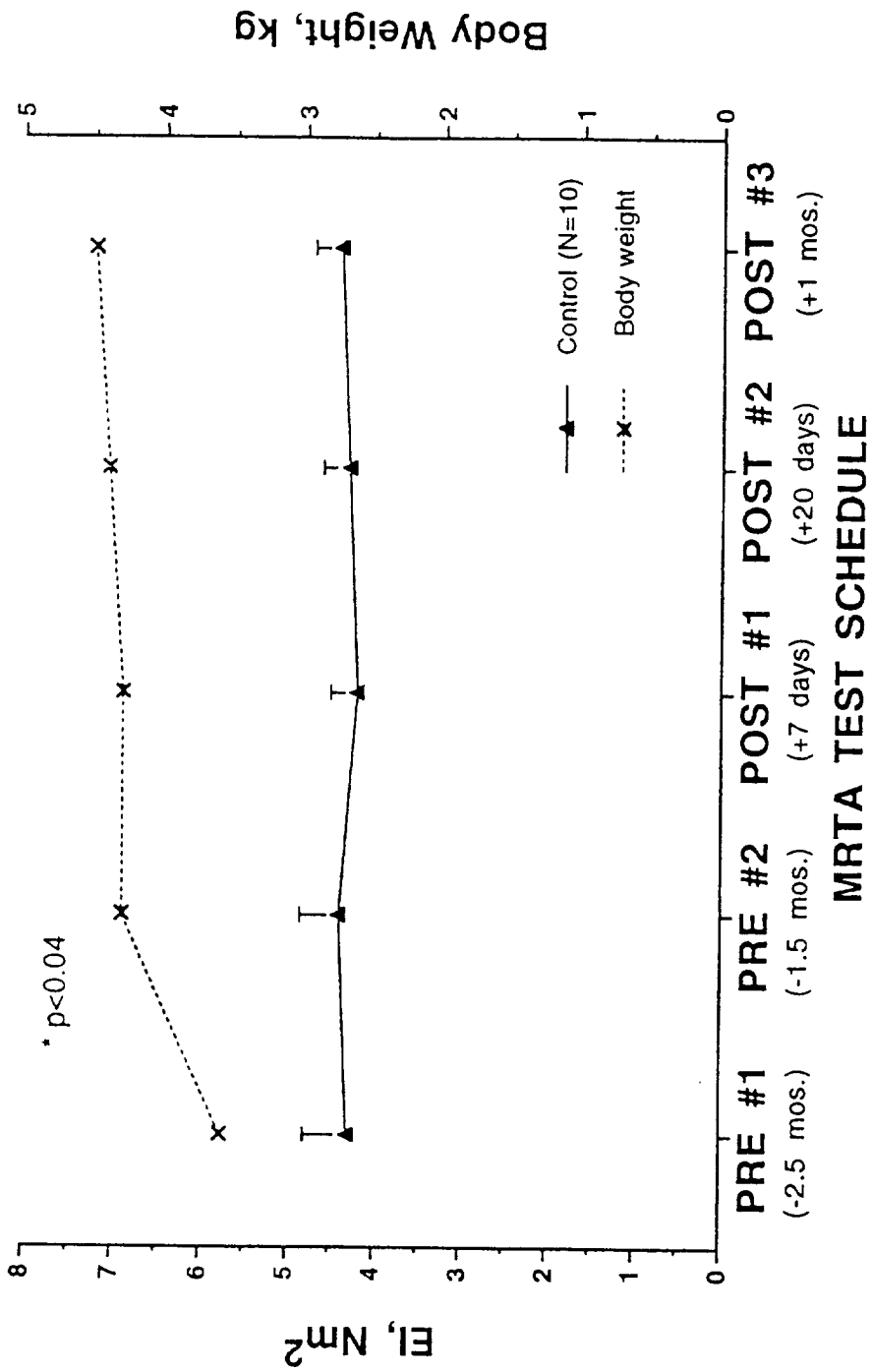
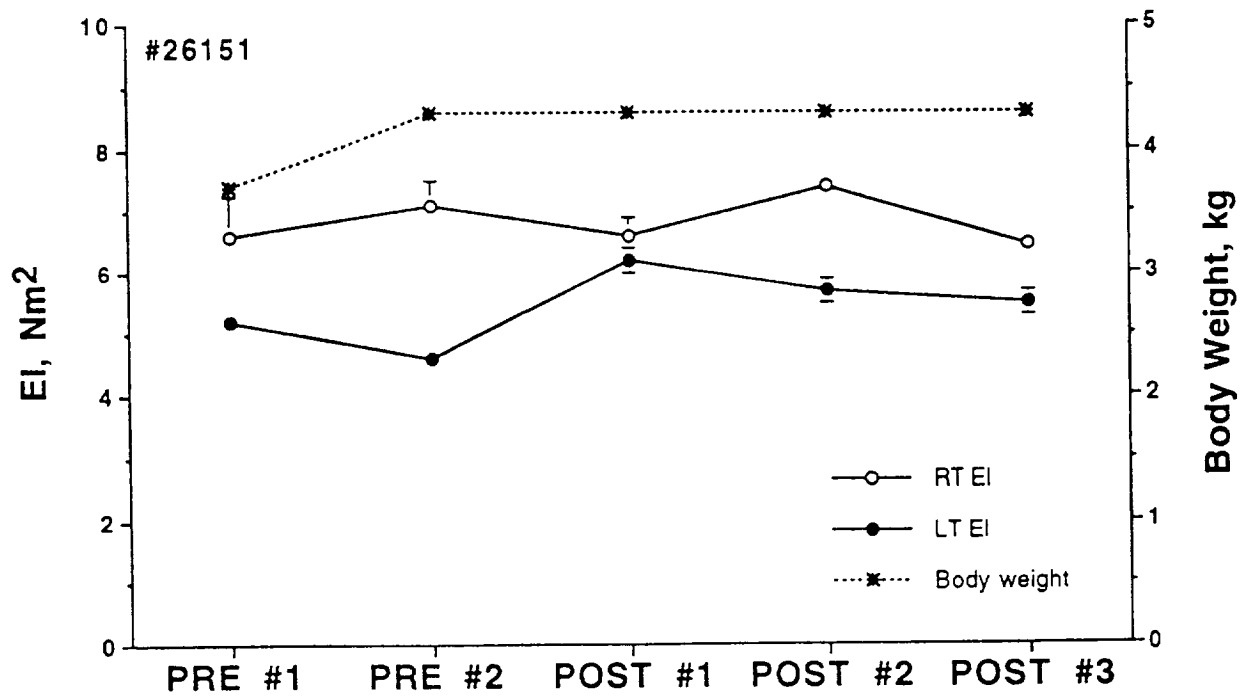
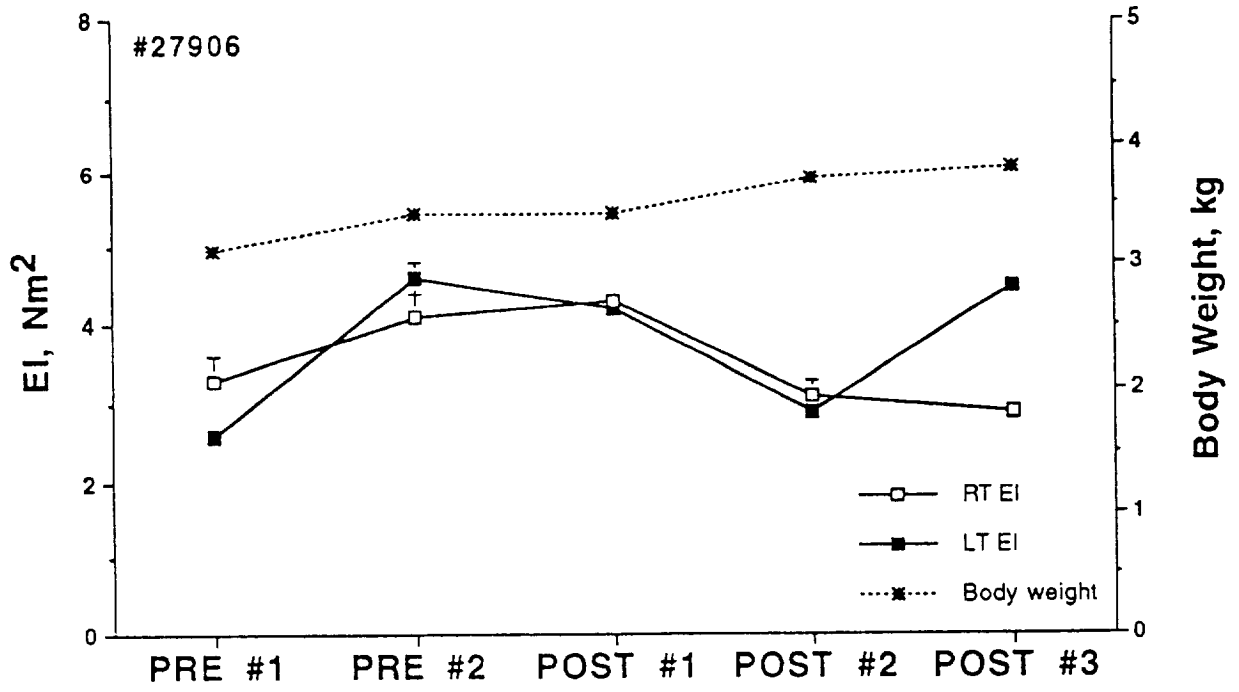


Figure 4. Right and left combined MRTA EI values for the IMBP control monkeys.



MRTA TEST SCHEDULE

Figure 5. MRTA EI values for flight monkeys #27906 and #27907.

EXPERIMENT K-8-01 (Part 2)

CALCIUM METABOLISM AND CORRELATED ENDOCRINE
MEASUREMENTS IN PRIMATES DURING COSMOS 2229

Principal Investigator:

Christopher E. Cann
University of California
San Francisco, CA

Co-Investigators:

Patricia Buckendahl
University of California
San Francisco, CA

Claude D. Arnaud
University of California
San Francisco, CA

CALCIUM METABOLISM AND CORRELATED ENDOCRINE MEASUREMENTS IN PRIMATES DURING COSMOS 2229

Christopher E. Cann, Patricia Buckendahl, Claude D. Arnaud

INTERPRETATION

Cosmos 1514

Metabolic and Calcium Tracer Studies

Cosmos 1514 metabolic studies are consistent with increased bone resorption after a 5 day flight, with no measurable effect on longitudinal bone growth. The increase in resorption might be explained by increased stress, as some effects were seen immediately preflight as well as early postflight.

Cosmos 1887

Radiographic and Bone Growth Studies

Cosmos 1887 radiographic studies showed a slowed longitudinal bone growth in the one monkey with nutritional restriction. There was little if any evidence for this in the other monkey. In addition, postflight x-rays revealed the presence of a hypermineralized growth arrest line at the growth plate, indicating that mineralization was impaired during the period of nutritional restriction. This will undoubtedly have an effect on global parameters of the long bones such as total mineral content or bending stiffness, but is not due to the effect of microgravity.

Cosmos 2229

Endocrine Studies

Cosmos 2229 endocrine studies suggest an increase in serum calcium immediately postflight, but it is not as convincing as the data from human studies obtained inflight. There is a clear decrease in 25 (OH) D during the postflight period, but beginning later, not immediately postflight. This may be a response to changes in dietary intake of vitamin D during the flight and postflight periods. There was no change in serum osteocalcin (an indicator of bone formation), but this parameter is not as sensitive as histomorphometry for quantification of changes in bone formation.

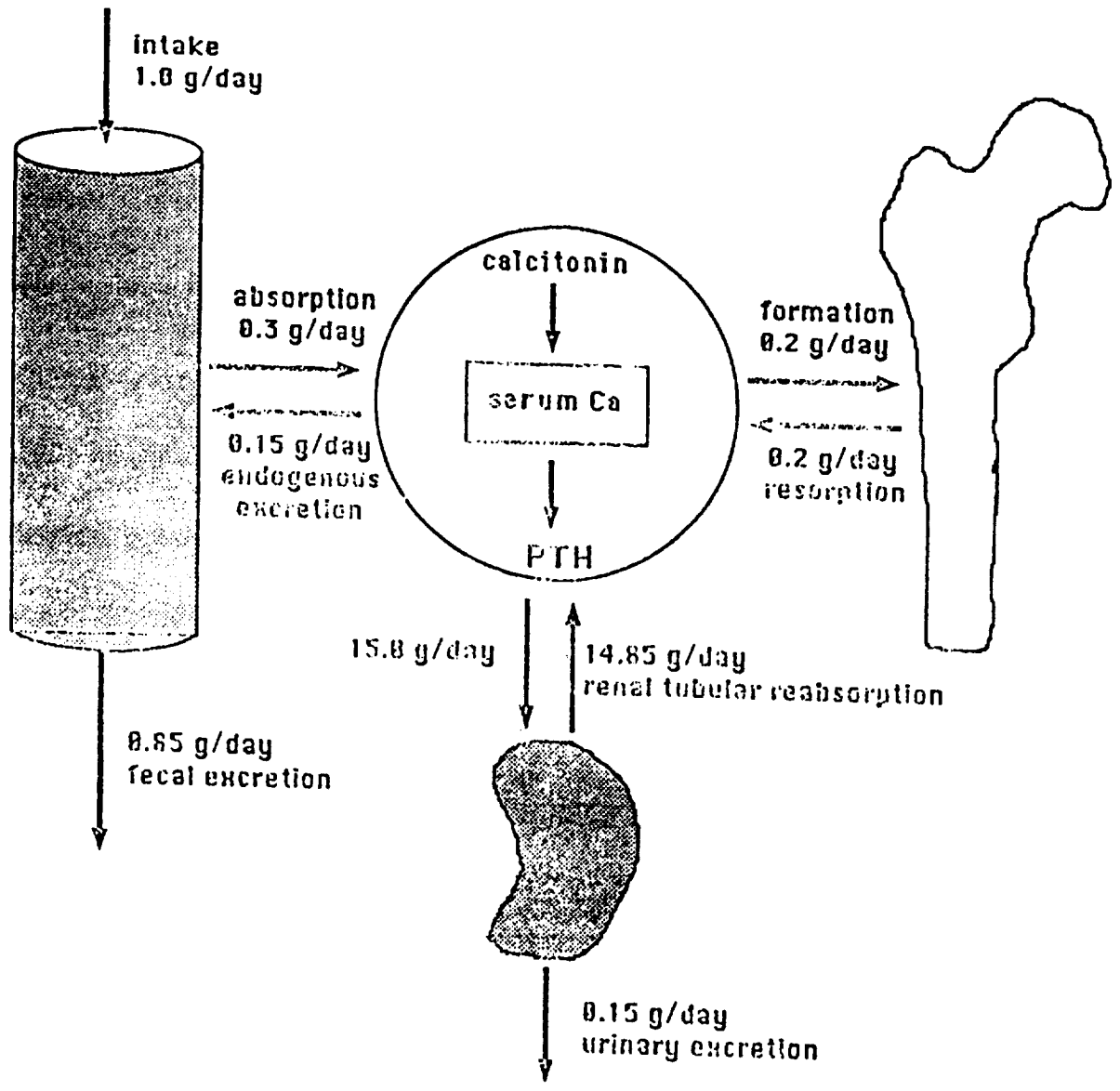


Figure 1.

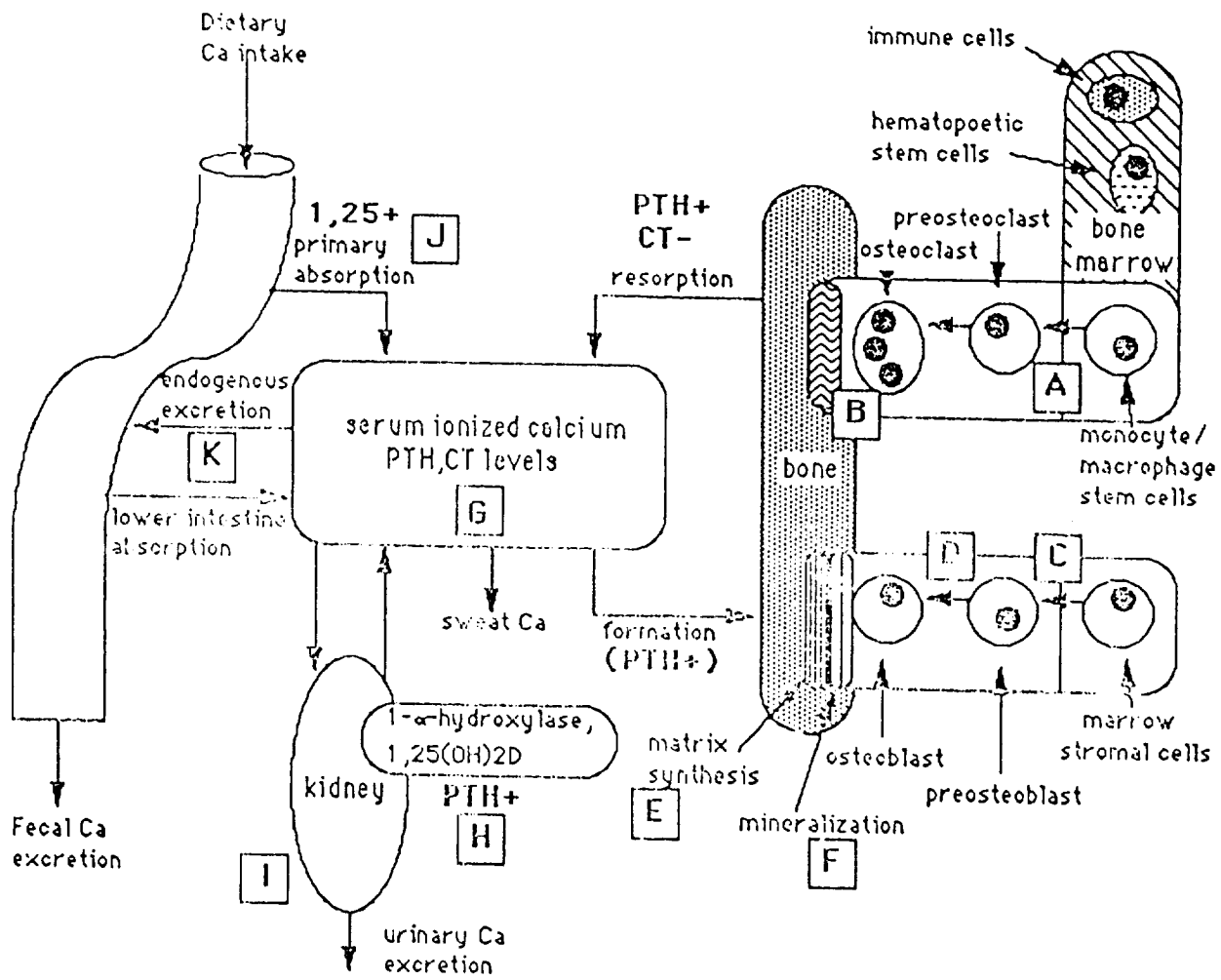


Figure 2.

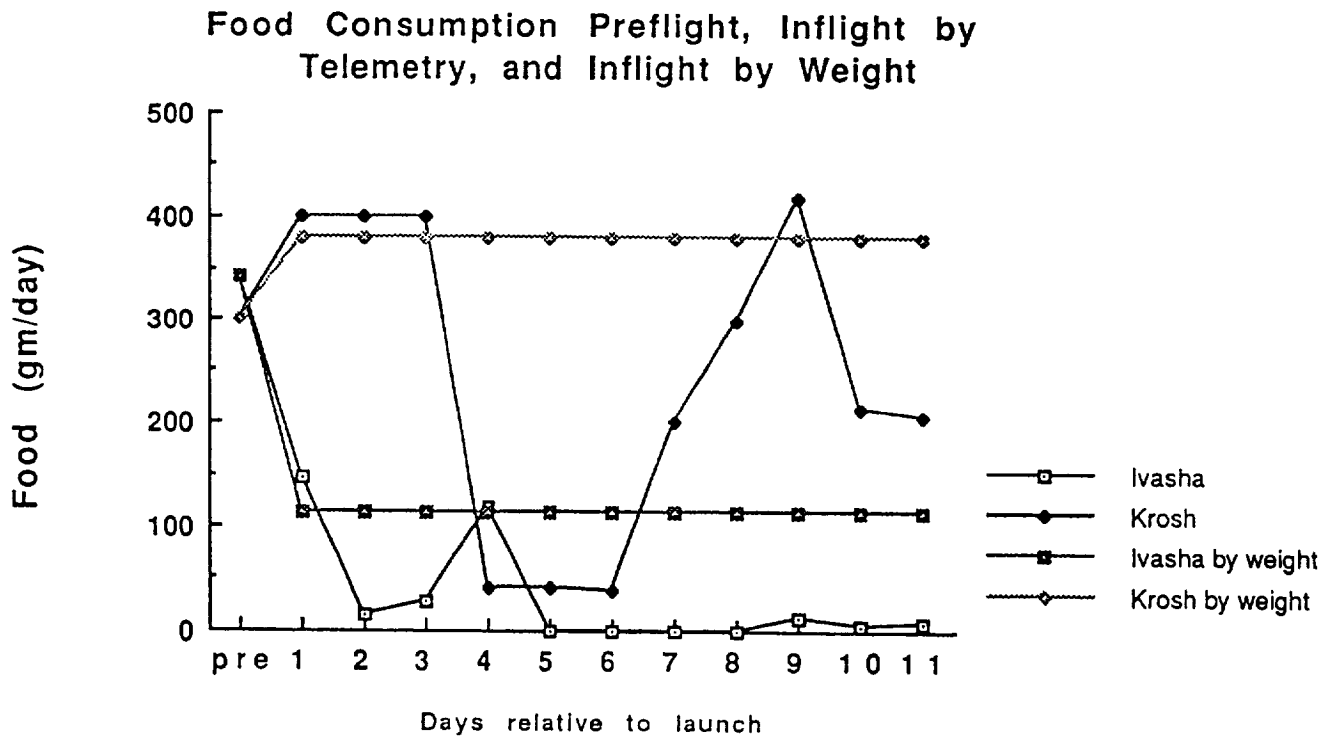


Figure 3.

CUMULATIVE CHANGE IN LENGTH

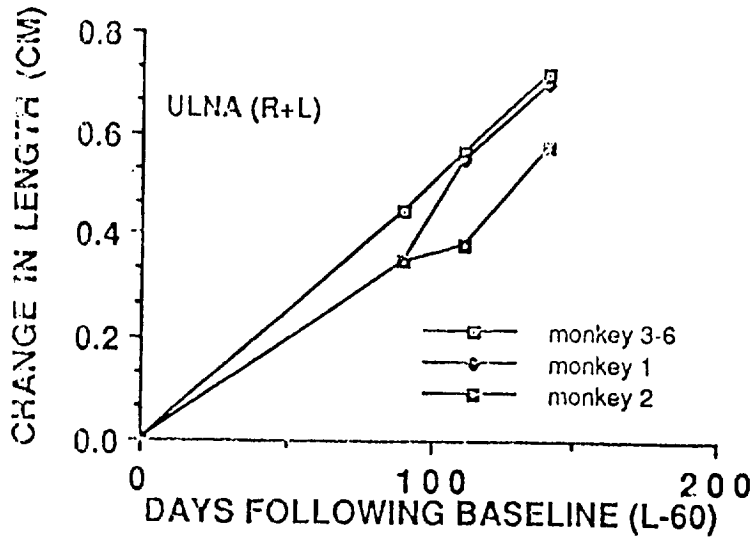
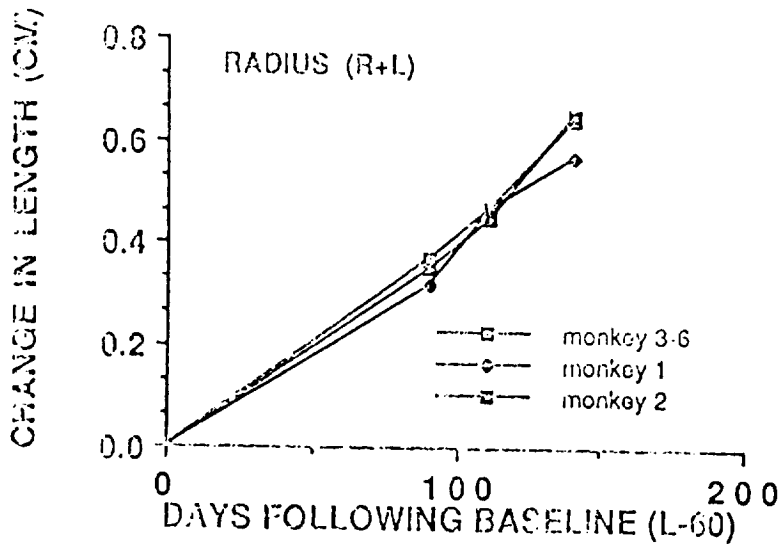
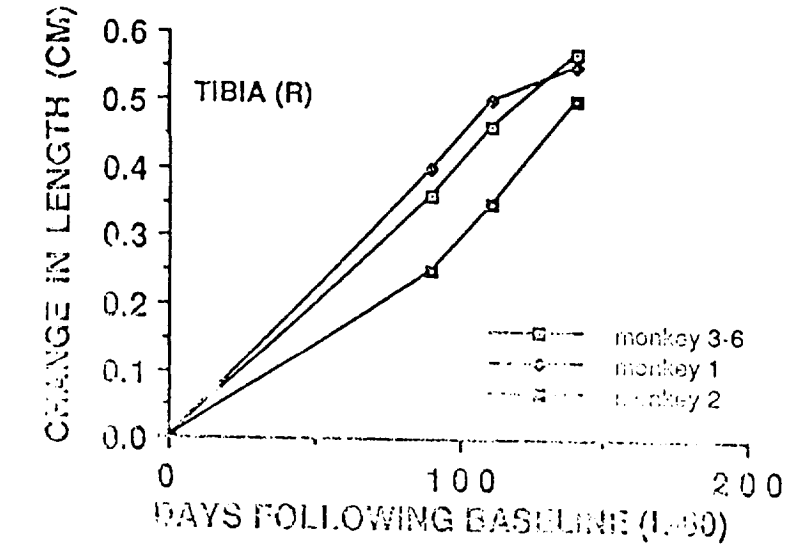


Figure 4.

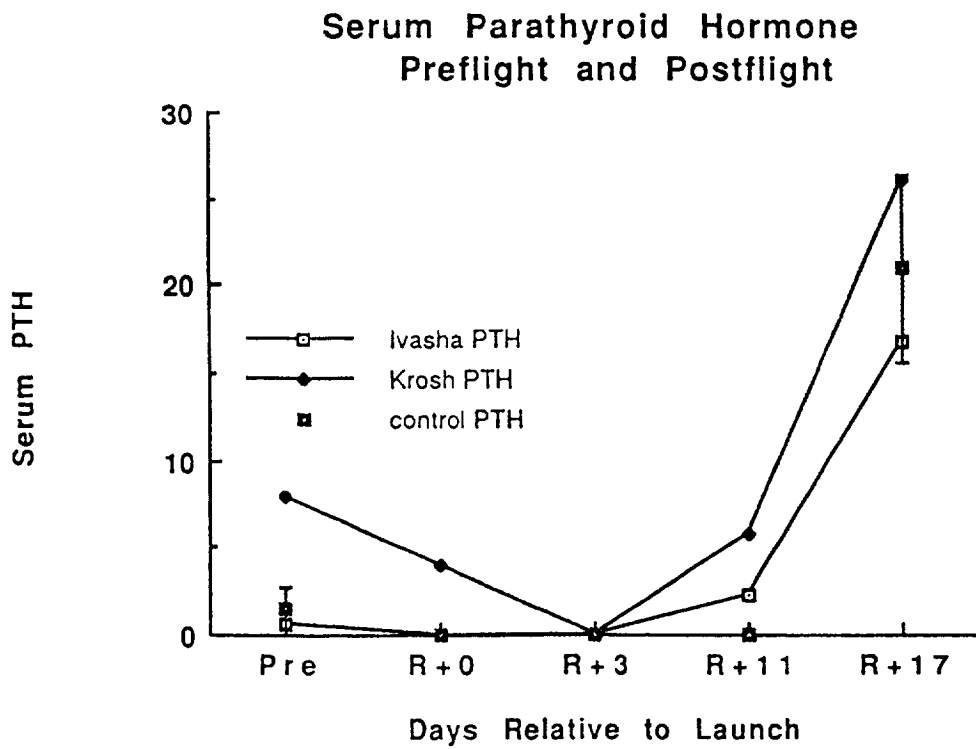
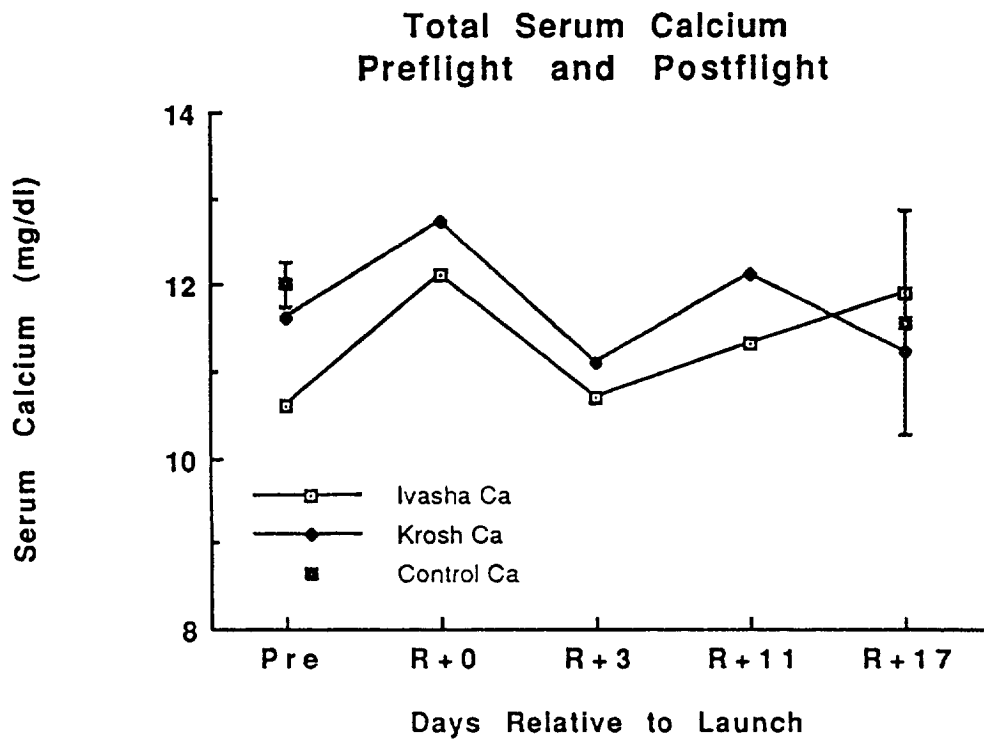
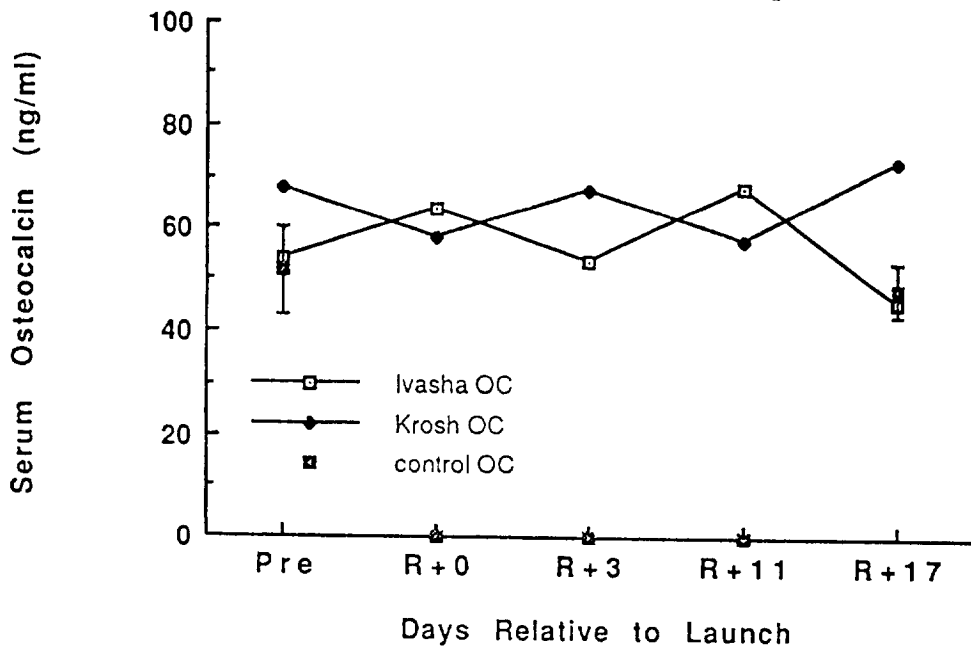


Figure 5.

Serum Osteocalcin Preflight and Postflight



Serum 25-hydroxy vitamin D Preflight and Postflight

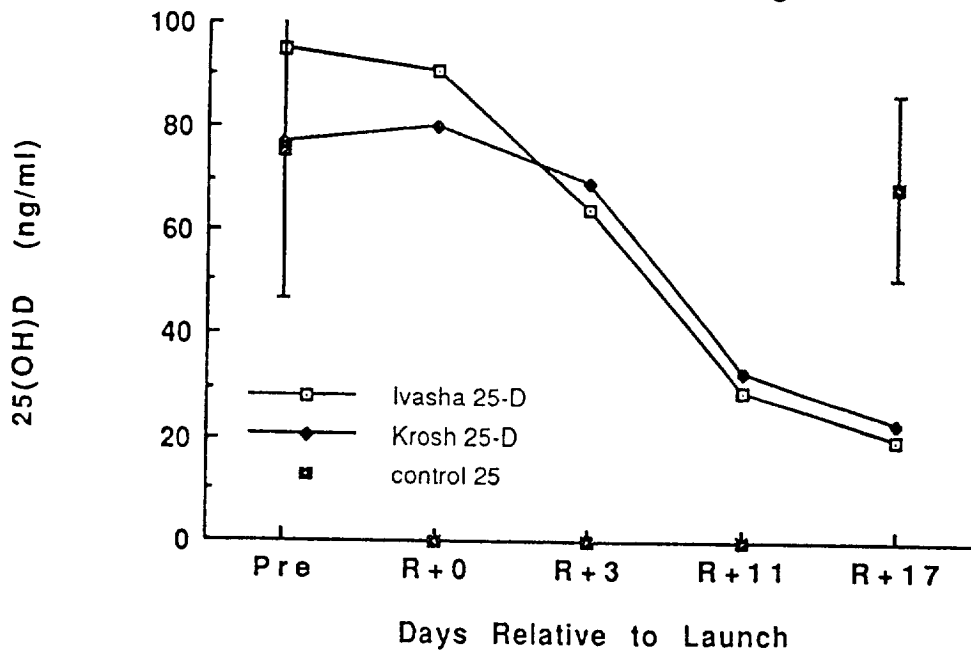


Figure 6.

EXPERIMENT K-8-01 (Part 3)

DEXA MEASUREMENTS: COSMOS 2229 RHESUS FLIGHT EXPERIMENT

Principal Investigator:

A. LeBlanc
Baylor College of Medicine
Waco, TX

Co-Investigators:

H. Evans
Krug Life Sciences
Houston, TX

L. Shackelford
Johnson Space Center
Houston, TX

S. West,
Baylor College of Medicine
Waco, TX

A. Rakhmanov
Institute of Biomedical Problems
Moscow, Russia

A. Bakulin
Institute of Biomedical Problems
Moscow, Russia

V. Oganov
Institute of Biomedical Problems
Moscow, Russia

DEXA MEASUREMENTS: COSMOS 2229 RHESUS FLIGHT EXPERIMENT

A. LeBlanc, H. Evans, L. Shackelford, S. West, A. Rakhmanov, A. Bakulin, V. Oganov

BACKGROUND

Previous flights involving animals and humans aboard Russian (MIR, Cosmos) and American spacecraft (Skylab, Spacelab) have documented that significant bone and muscle atrophy occurs during weightlessness requiring the development of effective and efficient countermeasures. In addition to the loss of bone and muscle, renal stones may also form during flight. During short duration flights, the loss of bone is of less concern. However, the potential for renal stone formation from hypercalcuria and the effects of significant muscle atrophy may still make some form of countermeasure desirable. This flight experiment resulted from the joint Russian and American collaboration to study the phenomenon of weightless induced bone and muscle atrophy. This collaboration has, over the last several years, focused on the rate of loss and recovery from long duration space flight in Cosmonauts. To supplement the human investigations, animal models have been deemed desirable to study mechanisms which require techniques which are either too invasive or complex for adequate study in crew members. The Rhesus monkey would appear to be an ideal candidate for this purpose.

Although the Cosmos 2229 flight was relatively short, 12 days; and therefore bone and muscle changes would be expected to be modest, significant muscle atrophy would be expected to occur based on muscle measurements performed on crew members of STS-35, 40 and 47. In addition, a number of disuse animal models have demonstrated rapid muscle atrophy during weightlessness and ground based simulation studies. Tail limb suspension of the rat demonstrated that maximal muscle atrophy of about 50% and 25% in the soleus and gastrocnemius respectively, occurs within 14-30 days (1-4). Rats flown in space aboard Russian spacecraft have shown similarly rapid loss in muscle mass and performance (5-6).

Young growing rats flown in space for 18-22 days have demonstrated less bone than ground controls (7-9). The observed bone changes returned to normal 27-29 days following flight. Previous reports have shown that bone turnover in the vertebrae of the rat decreases during flight, but was not apparent immediately post-flight becoming significant one week post flight (9). Similarly, losses observed in the distal epiphysis and head of the rat femur after 19 days in space, nearly doubled 6 days after flight (10). Thus, the rate of bone loss was actually greater early post flight than during the flight period itself, probably reflecting an alteration of bone turnover initiated during flight which continued during the post flight period. For this reason we measured the bone mineral density during the two time periods after flight in addition to the pre and immediately post-flight measurements. Although monkeys have been sent into space previously, these measurements are the first attempt to measure bone and muscle atrophy in a non-human primate after exposure to weightlessness.

HYPOTHESIS

It is hypothesized that short duration weightlessness will decrease bone remodeling and that this decrease will be apparent as a decrease in bone mineral immediately after flight or during the first few weeks following return to earth's gravity. Further, it is hypothesized that short duration weightlessness will result in significant muscle atrophy that will be rapidly recovered following return to one G gravity.

OBJECTIVE

The objective of this experiment was to determine, using regional and whole body dual energy x-ray absorptiometry (DEXA), if bone and lean body mass are reduced in the Rhesus monkey after exposure to short duration weightlessness.

METHODS

The DEXA scans were performed using a Hologic QDR-1000W instrument located at the Institute for Biomedical Problems in Moscow. The scans were performed by Drs. Bakulin and Rakhmanov from the above Institute. Three scanning protocols were employed: whole body, lumbar spine, left tibia. All scans were performed with the anesthetized animal in the supine position. The animals were immobilized with cloth arm and leg restraints. The total scanning time required was about 45 minutes. A copy of the raw scan data was returned to Houston on floppy discs for analysis. The data presented in this report were analyzed in the Nuclear Medicine Laboratory, Baylor College of Medicine, Houston Texas. The following acquisition and analysis protocols were employed: whole body infant acquisition and version 5.56 analysis software; adult spine acquisition and version 4.56, subregion analysis software; forearm acquisition and version 5.56, subregion forearm analysis software.

At the time of the DEXA scan, a consecutive number was assigned to each monkey in addition to the vivarium identification number. Both numbers are given in this report for convenience. The two flight monkeys were vivarium numbers 26151 (scan #5) and 27906 (scan #9). Three control animals that were housed in vivarium cages were 27803 (scan #1), 27907 (scan #2), and 25476 (scan #8). An additional control animal was housed in a chair restraint; this animal is identified as vivarium number 27892 (scan #12). Measurements were performed on two occasions pre-flight at about L-116/119 and L-53/57 days prior to launch; post-flight measurements were performed at about R+3/7, R+16/18, R+33/38, and R+53/57 days following recovery.

There were three groups of monkeys, chaired control, caged control and flight. For all analyses the data for the single chaired control was combined with the other controls resulting in two groups for analysis, flight and control. With a sufficient number of animals in each group and the same measurements performed at all time points, a repeated measures analysis of variance with group and time as factors would be the analytical model of choice. However, not all outcomes were measured at all time points and as few as three animals for both groups were measured at certain combinations of times and outcomes. Therefore a more simple model was chosen in order to maximize the use of the information available.

In order to determine changes during and after flight, four time points were used; the final pre-flight measurement (L-53/57) and the three post-flight times (R+3/7, R+16/18, R+33/38 days after recovery). From these, three pairs of time points were chosen for analysis, i.e., pre-flight to immediate post-flight (L-53/57 vs. R+3/7 days), post-flight to recovery #1 (R+3/7 vs. R+16/18 days), and post-flight to recover #2 (R+3/7 vs. R+33/38 days). Five body regions were statistically analyzed for changes in four types of measurements, i.e., bone mineral density in grams/cm²(BMD), bone mineral content in grams (BMC), lean body mass in grams, and body fat in grams. The difference between measurements for each animal and each time pair was calculated. The mean difference of the two groups was compared for each combination of region and measurement type for which data were available. These data were then tested using a standard analysis of variance. Since there were only two groups and mean differences were compared, the results are identical to a series of t-tests for each combination of factors.

RESULTS

Tables 1-3 give the bone mineral results for the spine, tibia, whole body, and whole body sub-regions for all monkeys and time points. Table 4 gives the fat and lean body mass results for all monkeys and time points. As discussed above in the methods, a subset of the data was chosen for statistical analysis. Tables 5-8 show the mean, standard error and number of animals of this subset for the control and flight groups. All p-values 0.1 or less are noted in the above tables. Because over 30 tests were performed, the probability of at least one comparison having a p-value less than one is approximately one. Therefore, the evaluation of the statistical significance of the results should be judged relative to consistency for a given outcome rather than considering the importance of a single p-value.

There was no evidence for bone loss, BMC or BMD, during the flight period, Tables 5 and 6. There was some evidence that BMC and BMD may have increased during the reambulation period relative to the control animals. There was evidence that lean tissue was lost in the arms and legs of the flight animals relative to controls during the flight period, Table 7. The total body change in lean tissue did not reach statistical significance, however, all four controls gained an average of 242 grams of lean tissue while flight monkey #26151 (scan #5) lost 192 grams and flight monkey #27906 (scan #9) gained 110 grams. During the reambulation post-flight period there was evidence of increased lean mass in the flight animals relative to controls. There were no significant changes in body fat in any of the groups tested.

SUMMARY AND CONCLUSIONS

Not unexpectedly, these results did not show significant bone loss during short duration flight in the Rhesus monkey. During the reambulation period, no bone loss was observed, instead there was some evidence for bone accretion above that observed in the control group, suggesting that if bone formation is decreased during weightlessness, it does not remain so following flight. These findings are similar to our results obtained in bed rested subjects which demonstrated evidence for increased bone formation following reambulation.

There was evidence of lean tissue loss in the arms and legs of the monkeys during flight. These losses are rapidly reversed following reambulation. These results are also similar to our findings in research subjects after short duration bed rest and in astronauts following short duration space flight (11-12).

We conclude that, given the constraints imposed by small sample size, our results suggest that the changes observed in the Rhesus monkey are compatible with those observed or expected from bed rest or weightless exposure of humans, suggesting that the Rhesus monkey may be a suitable model for bone and muscle investigations in weightlessness. However, additional flights of longer duration along with additional ground based studies are needed to adequately define this model.

REFERENCES

1. Booth, F.W. Time Course of Muscular Atrophy During Immobilization of Hindlimbs in Rats. *J. Appl. Physiol.: Respirat. Environ. Exercise Physiol.* 43(4):656-661, 1977.
2. Eurell, J.A., and L.E. Kazarian. Quantitative Histochemistry of Rat Lumbar Vertebrae Following Space Flight. *Am. J. Physiol.* 244:R315-R318, 1983.
3. Ilyina-Kakuyeva, E.I., Petrova N.V., and V.V. Portugalov. The Effects of Space Flight on the Skeletal Musculature and Nerve Apparatus of the Muscles (Morphologic and Cytochemical Study). Pages 100-106 in AM Genin, Ed., *The Effects of Dynamic Factors of Space Flight on Animal Organisms*. NASA Translation Document TM-75692.
4. Jee, W.S.S., Wronski T.J., Morey E.R., and D.B. Kimmel. Effects of Space Flight on Trabecular Bone in Rats. *Am. J. Physiol.* 24:R310-R314, 1983.
5. LeBlanc, A., March C., Evans H., Johnson P., Schneider V., and S. Jhingran. Bone and Muscle Atrophy with Suspension of the Rat. *J. Appl. Physiol.* 58(5): 1669-1975, 1985.
6. LeBlanc, A., Schneider V., Evans H., Wendt R., and T. Hedrick. Magnetic Resonance Imaging After Exposure to Microgravity. Results from Spacelab Mission, SL-J, Cocoa Beach, FLA, Nov. 8-10, 1993.
7. LeBlanc, A.D., Schneider V.S., Evans H.J., Pientok C., Rowe R., and E. Spector. Regional Changes in Muscle Mass Following 17 Weeks of Bed Rest. *J. Appl. Phys.* 73(5):2172-2178, 1992.
8. Morey-Holton, E., and T.J. Wronski. Animal Models for Simulating Weightlessness. *The Physiologist* 24(6):S45-S48, 1981.
9. Rogacheva, I.V., Stupakov G.P., Volozhim A.I., Ravlova M.N., and A.N. Polyakov. Rat Bone Tissue After Flight Aboard Cosmos-1129 Biosatellite. *Moscow Kosmicheskaya Biologiya I Aviakosmicheskaya Meditsina* (in Russian) 18:39-44, 1984.
10. Szilagyai, T., Szoor A., Takacs O., Rapcsak M., Oganov V.S., Skuratova S.A., Oganesyanyan S.S., Murashko L.M., and M.A. Eloyan. Study of Contractile Properties and Composition of Myofibrillar Proteins of Skeletal Muscles in the Cosmos-1129 experiment. *The Physiologist* 23:S67-S70, 1980.
11. Templeton, G.H., Padalino M., Manton J., Glasberg G., Silver J., Silver P., DeMartino G., Leconey T., Klug G., Hagler H., and J.L. Sutko. Influence of Suspension Hypokinesia on Rat Soleus Muscle. *J. Appl. Physiol.: Respirat. Environ. Exercise Physiol.* 56(2):278-286, 1984.
12. Yagodovsky, V.S., Triftanidid L.A., and G.P. Gorokhova. Space Flight Effects on Skeletal Bones of Rats (Light and Electron Microscopic Examination). *Aviat. Space Environ Med.* 47:734-738, 1976.

Table 1. Spine Scan Bone Mineral Results - Cosmos 2229

BMD ID #	Monkey ID #	Date	Days From Launch	Area cm ²	BMC gms	BMD gms/cm ²
1	27803	09/01/92	-119	17.621	7.942	0.451
1	27803	11/06/92	-53	18.445	8.429	0.457
1	27803	01/15/93	17	19.084	9.437	0.495
1	27803	01/26/93	28	20.632	9.648	0.468
1	27803	02/15/93	48	19.928	9.666	0.485
1	27803	03/07/93	68	20.713	9.751	0.471
2	27907	09/01/92	-119	14.550	6.380	0.438
2	27907	11/03/92	-56	15.020	7.300	0.486
2	27907	01/14/93	16	15.140	7.050	0.465
2	27907	01/26/93	28	16.040	7.320	0.456
2	27907	02/15/93	48	15.690	7.580	0.483
2	27907	03/07/93	68	15.660	7.290	0.466
3	1401	09/01/92	-11	18.761	8.413	0.449
3	1401	11/06/92	-53	19.414	9.501	0.489
3	1401	01/14/93	16	19.666	9.413	0.479
3	1401	01/28/93	30	19.366	9.207	0.475
3	1401	02/17/93	50	20.083	9.320	0.464
3	1401	03/08/93	69	21.120	10.029	0.475
5	26151	09/02/92	-118	19.139	9.100	0.476
5	26151	11/02/92	-57	19.569	10.065	0.514
5	26151	01/17/93	19	20.374	10.365	0.509
5	26151	01/27/93	29	19.930	10.580	0.531
5	26151	02/12/93	45	19.647	10.631	0.541
5	26151	03/04/93	65	20.034	10.491	0.524
6	25775	09/02/92	-118	19.013	9.680	0.509
6	25775	11/03/92	-56	19.734	10.426	0.528
6	25775	01/13/93	15	20.176	10.971	0.544
6	25775	01/28/93	30	20.335	11.018	0.542
6	25775	02/17/93	50	19.879	10.787	0.543
6	25775	03/08/93	69	20.335	10.446	0.514
8	25476	09/03/92	-117	20.942	10.894	0.520
8	25476	11/03/92	-56	21.624	11.696	0.541
8	25476	01/13/93	15	22.467	12.523	0.557
8	25476	01/28/93	30	21.517	11.658	0.542
8	25476	02/17/93	50	21.721	11.687	0.538
9	27906	09/03/92	-117	17.781	7.468	0.420
9	27906	11/02/92	-57	18.315	8.144	0.445
9	27906	01/17/93	19	18.086	8.223	0.455
9	27906	02/12/93	45	18.212	8.391	0.461
9	27906	03/04/93	65	18.881	8.789	0.466
12	27892	09/04/92	-116	18.101	8.179	0.452
12	27892	11/06/92	-53	18.900	9.318	0.493
12	27892	01/15/93	17	19.249	9.400	0.488

Table 2. Tibia Scan Bone Mineral Results - Cosmos 2229

BMD ID #	Monkey ID #	Date	Days From Launch	Area cm ²	BMC gms	BMD gms/cm ²
1	27803	09/01/92	-119	12.65	5.66	0.447
1	27803	11/06/92	-53	11.92	5.49	0.461
1	27803	01/15/93	17	12.02	5.53	0.460
1	27803	01/26/93	28	11.98	5.79	0.484
1	27803	02/15/93	48	12.06	5.24	0.435
1	27803	03/07/93	68	12.04	4.94	0.410
2	27907	09/01/92	-119	10.33	4.23	0.410
2	27907	11/03/92	-56	10.67	4.56	0.428
2	27907	01/14/93	16	10.68	4.50	0.422
2	27907	01/26/93	28	10.71	4.56	0.426
2	27907	02/15/93	48	10.83	4.50	0.416
2	27907	03/07/93	68	11.55	4.50	0.389
3	1401	09/01/92	-119	13.97	5.81	0.416
3	1401	11/03/92	-56	13.20	5.75	0.436
3	1401	01/14/93	16	13.53	6.12	0.452
3	1401	01/26/93	28	13.63	6.26	0.459
3	1401	02/15/93	48	13.68	6.32	0.462
3	1401	03/07/93	68	14.29	6.22	0.435
5	26151	09/02/92	-118	14.19	6.44	0.454
5	26151	11/02/92	-57	14.54	6.55	0.451
5	26151	01/17/93	19	14.80	6.82	0.461
5	26151	01/27/93	29	14.70	7.13	0.485
5	26151	02/12/93	45	14.62	6.82	0.467
5	26151	03/04/93	65	15.27	7.10	0.465
6	25775	09/02/92	-118	13.52	5.90	0.436
6	25775	11/03/92	-56	13.33	5.83	0.438
6	25775	01/13/93	15	13.29	5.79	0.436
6	25775	01/28/93	30	13.84	6.21	0.449
6	25775	02/17/93	50	13.93	6.33	0.454
6	25775	03/08/93	69	13.48	6.01	0.446
8	25476	09/03/92	-117	15.06	6.94	0.460
8	25476	11/03/92	-56	15.14	6.85	0.452
8	25476	01/13/93	15	14.67	6.50	0.443
8	25476	01/28/93	30	15.51	6.87	0.443
8	25476	02/17/93	50	15.55	6.95	0.447
9	27906	09/03/92	-117	13.91	5.01	0.361
9	27906	01/17/93	19	13.02	4.98	0.383
9	27906	01/27/93	29	12.29	4.78	0.389
9	27906	02/12/93	45	11.36	4.37	0.384
9	27906	03/04/93	65	12.39	4.98	0.402
12	27892	09/04/92	-116	12.51	5.27	0.421
12	27892	11/06/92	-53	12.87	5.78	0.449
12	27892	01/15/93	17	12.84	5.80	0.452

BMD ID #	Monkey ID #	Date	Days From Launch	Upper Body			Lower Body			Total Body		
				Area cm ²	BMC gms	BMD gms/cm ²	Area cm ²	BMC gms	BMD gms/cm ²	Area cm ²	BMC gms	BMD gms/cm ²
1	27803	09/01/92	-119	292.0	101.5	0.348	180.2	45.8	0.254	472.2	147.4	0.312
1	27803	11/06/92	-53	313.1	98.1	0.313	169.8	48.2	0.284	482.9	146.4	0.303
1	27803	01/15/93	17	312.0	95.5	0.306	197.3	55.2	0.280	509.3	150.7	0.296
1	27803	03/07/93	68	336.6	97.3	0.289	198.3	53.0	0.268	534.9	150.3	0.281
2	27907	09/01/92	-119	284.0	91.9	0.323	167.2	40.1	0.240	451.2	132.0	0.292
2	27907	11/03/92	-56	323.9	106.3	0.328	170.0	42.2	0.248	493.9	148.5	0.301
2	27907	01/15/93	17	308.0	84.1	0.273	181.9	45.0	0.247	489.9	129.1	0.263
2	27907	01/26/93	28	306.5	93.4	0.305	175.7	44.0	0.251	482.2	137.4	0.285
2	27907	02/15/93	48	307.9	76.5	0.249	169.5	43.3	0.255	477.4	119.8	0.251
2	27907	03/07/93	68	321.1	79.3	0.247	173.8	41.6	0.240	494.9	121.0	0.244
3	1401	09/01/92	-119	300.8	100.2	0.333	183.3	43.3	0.237	484.1	143.6	0.297
3	1401	11/06/92	-53	350.3	117.6	0.336	193.6	49.2	0.254	543.9	166.8	0.307
3	1401	01/14/93	16	346.7	115.8	0.334	192.4	52.1	0.271	539.1	167.9	0.311
3	1401	01/28/93	30	339.1	101.7	0.300	187.9	51.0	0.271	527.0	152.6	0.290
3	1401	02/17/93	50	348.2	94.9	0.273	187.0	49.3	0.264	535.1	144.2	0.269
3	1401	03/08/93	69	323.1	90.4	0.280	210.7	53.5	0.254	533.9	143.9	0.270
4	25588	09/02/92	-118	266.8	86.5	0.324	169.0	40.9	0.242	435.9	127.4	0.292
5	26151	09/02/92	-118	299.8	96.7	0.323	202.3	52.8	0.261	502.1	149.5	0.298
5	26151	11/02/92	-57	319.9	109.8	0.343	210.6	59.3	0.281	530.5	169.1	0.319
5	26151	01/17/93	19	305.0	85.9	0.282	200.5	59.4	0.297	505.5	145.3	0.287
5	26151	01/27/93	29	322.7	84.9	0.263	186.7	56.5	0.302	509.5	141.4	0.277
5	26151	02/12/93	45	358.2	107.3	0.300	193.4	54.4	0.281	551.6	161.7	0.293
5	26151	03/04/93	65	332.9	102.2	0.307	213.7	64.0	0.299	546.6	166.2	0.304
6	25755	09/02/92	-118	303.0	103.4	0.341	188.2	46.5	0.247	491.2	149.9	0.305
6	25755	11/03/92	-56	340.8	127.8	0.375	191.6	53.8	0.281	532.4	181.7	0.341
6	25755	01/13/93	15	348.0	117.2	0.337	189.9	50.1	0.264	537.9	167.3	0.311
6	25755	01/28/93	30	341.4	115.8	0.339	184.2	52.2	0.283	525.6	167.9	0.319
6	25755	02/17/93	50	317.6	117.9	0.371	202.4	57.7	0.285	520.0	175.6	0.338
6	25755	03/08/93	69	343.6	134.8	0.392	202.1	58.1	0.287	545.7	192.9	0.353
7	27856	09/03/92	-117	355.8	108.9	0.306	190.2	52.2	0.274	546.0	161.1	0.295
7	27856	11/02/92	-57	351.6	115.4	0.328	200.9	56.3	0.280	552.5	171.7	0.311
8	25476	09/03/92	-117	308.0	103.6	0.337	209.0	55.3	0.265	517.0	159.0	0.308
8	25476	11/03/92	-56	349.2	108.1	0.310	205.5	57.4	0.279	554.7	165.5	0.298
8	25476	01/13/93	15	357.3	109.1	0.305	216.7	62.2	0.287	574.0	171.3	0.298
8	25476	01/28/93	30	353.1	105.9	0.300	210.1	65.9	0.314	563.2	171.7	0.305
8	25476	02/17/93	50	360.3	102.7	0.285	218.6	61.9	0.283	578.9	164.6	0.284
9	27906	09/03/92	-117	259.8	75.0	0.289	155.5	35.5	0.229	415.2	110.6	0.266
9	27906	11/02/92	-57	307.7	102.6	0.334	159.5	40.0	0.251	467.1	142.6	0.305
9	27906	01/17/93	19	312.5	78.4	0.251	169.1	41.0	0.242	481.6	119.3	0.248
9	27906	02/12/93	45	327.7	93.5	0.285	157.6	39.9	0.253	485.3	133.4	0.275
9	27906	03/04/93	65	314.2	86.2	0.275	171.7	45.0	0.262	485.9	131.2	0.270
9*	27906	01/27/93	29	293.7	69.5	0.237	159.7	43.5	0.273	453.4	113.1	0.249
10	1417	09/04/92	-116	337.7	105.7	0.313	214.4	59.7	0.279	552.1	165.4	0.300
11	23838	09/04/92	-116	316.7	96.0	0.303	203.2	49.2	0.242	519.8	145.2	0.279
11	23838	11/06/92	-53	346.5	112.8	0.326	203.3	57.2	0.281	549.8	170.0	0.309
12	27892	09/04/92	-116	304.0	90.9	0.299	179.5	45.9	0.256	483.4	136.8	0.283
12	27892	11/06/92	-53	309.6	111.2	0.359	178.3	49.6	0.278	487.9	160.8	0.329
12	27892	01/15/93	17	295.7	92.3	0.312	188.0	54.9	0.292	483.6	147.2	0.304

* This data was not clear for the top half of the animal, sent to Hologic for evaluation.

+ Launch 12/29/92

Table 3B. Whole Body Scan Bone Mineral Results - Cosmos 2229

BMD ID #	Monkey ID #	Date	Days From Launch	Head			T-Spine			L-Spine			L-Ribs			R-Ribs		
				Area cm ²	BMC gms	BMD gms/cm ³	Area cm ²	BMC gms	BMD gms/cm ³	Area cm ²	BMC gms	BMD gms/cm ³	Area cm ²	BMC gms	BMD gms/cm ³	Area cm ²	BMC gms	BMD gms/cm ³
1	27803	09/01/92	-119	89.9	56.6	0.629	42.4	9.9	0.234	21.9	8.0	0.366	27.1	4.4	0.164	32.5	4.2	0.128
1	27803	11/06/92	-53	92.8	45.1	0.486	39.5	13.5	0.341	21.8	7.9	0.364	36.6	6.6	0.182	39.6	6.8	0.173
1	27803	01/15/93	17	91.1	41.1	0.452	37.8	11.8	0.312	18.3	7.3	0.398	27.9	5.7	0.206	39.2	6.4	0.162
1	27803	03/07/93	68	85.7	39.4	0.459	41.8	12.5	0.299	25.2	8.5	0.335	50.6	8.0	0.157	31.5	4.5	0.142
2	27907	09/01/92	-119	84.0	50.9	0.606	45.2	11.4	0.253	15.8	5.4	0.339	29.8	4.4	0.147	30.9	3.2	0.104
2	27907	11/03/92	-56	95.9	50.5	0.527	44.1	11.9	0.269	16.0	6.0	0.376	52.9	14.2	0.268	26.7	5.9	0.221
2	27907	01/15/93	17	92.9	32.6	0.351	46.0	14.5	0.316	16.5	6.6	0.399	26.6	5.0	0.190	38.3	7.8	0.205
2	27907	01/26/93	28	87.7	38.9	0.444	43.1	14.7	0.342	16.5	6.9	0.417	34.0	5.6	0.164	23.1	4.2	0.182
2	27907	02/15/93	48	88.1	25.2	0.286	45.0	11.6	0.258	15.8	6.0	0.379	36.2	7.4	0.205	20.2	4.0	0.200
2	27907	03/07/93	68	93.3	25.2	0.270	47.8	14.4	0.301	16.5	7.1	0.433	30.3	5.2	0.171	37.4	7.2	0.193
3	1401	09/01/92	-119	86.3	54.5	0.631	40.8	9.5	0.232	24.1	9.7	0.403	23.1	3.0	0.129	27.8	4.1	0.148
3	1401	11/06/92	-53	104.8	56.9	0.543	46.3	16.9	0.365	24.1	9.7	0.403	37.7	8.4	0.223	36.2	6.6	0.183
3	1401	01/14/93	16	96.0	56.2	0.585	42.7	12.9	0.302	25.2	9.1	0.362	44.3	9.4	0.223	33.6	5.9	0.177
3	1401	01/28/93	30	96.3	44.4	0.461	53.5	15.7	0.292	25.2	9.8	0.388	29.1	5.2	0.178	30.3	4.8	0.158
3	1401	02/17/93	50	95.4	32.8	0.344	49.8	13.3	0.267	27.0	9.8	0.365	40.2	7.8	0.194	21.1	3.1	0.147
3	1401	03/08/93	69	95.2	34.2	0.359	39.1	11.3	0.290	28.3	9.9	0.350	39.4	7.2	0.182	17.5	2.2	0.123
4	25588	09/02/92	-118	79.3	48.2	0.608	37.7	10.2	0.270	21.5	7.9	0.365	15.6	1.9	0.123	28.4	3.6	0.126
5	26151	09/02/92	-57	82.2	48.9	0.595	44.2	12.1	0.273	24.0	8.2	0.341	23.7	3.2	0.135	21.9	3.1	0.141
5	26151	11/02/92	-57	88.8	50.5	0.568	44.4	14.1	0.319	24.2	10.7	0.442	32.2	6.4	0.199	21.2	4.0	0.189
5	26151	01/17/93	19	96.0	31.2	0.325	50.0	17.8	0.355	22.8	9.0	0.396	24.6	4.4	0.178	21.0	3.2	0.151
5	26151	01/27/93	29	99.4	36.2	0.364	39.5	10.5	0.266	23.8	9.0	0.380	45.5	5.6	0.123	26.7	6.5	0.243
5	26151	02/12/93	45	96.6	37.1	0.385	41.1	18.2	0.443	21.4	11.8	0.552	48.5	8.7	0.180	62.6	12.2	0.195
5	26151	03/04/93	65	94.9	40.8	0.430	49.2	17.4	0.353	24.0	10.0	0.418	43.4	8.0	0.184	31.3	5.4	0.172
6	25775	09/02/92	-118	89.5	55.3	0.618	44.5	12.5	0.281	24.1	7.4	0.308	19.6	2.4	0.124	22.5	3.9	0.173
6	25775	11/03/92	-56	94.0	62.8	0.668	43.4	16.7	0.384	27.7	10.0	0.360	34.9	6.1	0.175	34.9	6.4	0.185
6	25775	01/13/93	15	98.9	50.1	0.507	41.5	14.6	0.351	27.3	11.0	0.404	30.7	5.5	0.179	37.3	7.9	0.211
6	25775	01/28/93	30	95.7	49.7	0.519	46.0	18.0	0.391	23.8	10.7	0.448	42.5	8.3	0.196	34.8	5.9	0.170
6	25775	02/17/93	50	84.2	57.9	0.688	38.3	12.6	0.331	23.6	10.1	0.428	38.5	10.3	0.268	15.9	2.1	0.133
6	25775	03/08/93	69	90.9	64.6	0.711	60.1	20.9	0.348	26.7	10.7	0.401	36.5	7.9	0.215	25.1	7.7	0.307
7	27856	09/03/92	-117	85.1	48.3	0.568	42.3	14.4	0.340	27.7	10.6	0.381	34.5	5.5	0.159	45.8	7.0	0.153
7	27856	11/02/92	-57	95.8	48.9	0.511	41.9	15.5	0.370	27.3	11.1	0.408	38.6	7.5	0.194	37.5	8.5	0.227
8	25476	09/03/92	-117	72.8	46.1	0.633	45.4	13.4	0.296	25.7	11.0	0.429	26.4	3.8	0.145	36.0	5.1	0.143
8	25476	11/03/92	-56	98.7	44.9	0.455	43.1	15.6	0.362	23.9	10.0	0.419	49.0	9.5	0.195	33.7	6.0	0.177
8	25476	01/13/93	15	105.9	42.3	0.399	46.8	15.8	0.339	18.3	7.6	0.416	38.0	7.8	0.204	29.9	7.9	0.263
8	25476	01/28/93	30	96.8	38.9	0.402	49.9	16.6	0.333	25.9	12.7	0.450	41.9	7.3	0.174	36.8	8.0	0.217
8	25476	02/17/93	50	100.5	36.8	0.367	52.5	17.8	0.339	25.3	10.6	0.419	40.2	8.4	0.210	29.4	7.6	0.257
9	27906	09/03/92	-117	79.7	41.3	0.519	39.7	9.5	0.240	17.3	5.3	0.305	24.9	3.3	0.134	28.1	4.1	0.145
9	27906	11/02/92	-57	89.8	50.3	0.560	47.8	14.2	0.298	18.9	6.7	0.354	38.6	8.1	0.210	27.6	5.1	0.184
9	27906	01/17/93	19	91.2	20.9	0.230	45.9	13.5	0.294	18.8	7.5	0.399	41.4	8.0	0.194	25.3	5.0	0.199
9	27906	02/12/93	45	90.9	32.4	0.357	39.1	15.0	0.383	27.7	12.0	0.434	65.0	14.9	0.229	33.0	8.2	0.247
9	27906	03/04/93	65	88.1	30.1	0.342	44.1	14.3	0.324	25.9	10.3	0.395	49.7	9.0	0.181	36.4	9.1	0.249
9*	27906	01/27/93	29	113.6	28.5	0.251	42.4	11.3	0.266	24.7	8.6	0.348	26.5	5.3	0.199	26.6	4.9	0.186
10	1417	09/04/92	-116	81.8	47.8	0.585	42.1	11.5	0.273	23.4	9.6	0.410	33.3	4.2	0.126	46.6	9.0	0.194
11	23838	09/04/92	-116	89.2	47.2	0.529	42.9	12.0	0.279	19.1	7.3	0.385	30.6	4.2	0.139	31.1	4.6	0.149
11	23838	11/06/92	-53	96.5	49.6	0.514	42.5	14.2	0.334	29.3	10.4	0.355	37.6	7.9	0.210	30.9	4.6	0.149
12	27892	09/04/92	-116	75.7	40.8	0.539	40.8	11.1	0.273	23.1	8.1	0.350	31.0	5.2	0.167	38.8	5.7	0.146
12	27892	11/06/92	-53	92.7	57.4	0.620	40.5	12.7	0.314	28.0	10.9	0.388	33.2	7.8	0.235	20.2	3.7	0.185
12	27892	01/15/93	17	84.7	36.2	0.428	43.6	15.0	0.345	23.1	8.7	0.376	24.3	4.4	0.181	22.3	4.0	0.179

Table 3. Whole Body Scan Bone Mineral Results - Cosmos 2229

BMD ID #	Monkey ID #	Date	Days From Launch	R-Arm			L-Arm			Pelvis		
				Area cm ²	BMC gms	BMD gms/cm ²	Area cm ²	BMC gms	BMD gms/cm ²	Area cm ²	BMC gms	BMD gms/cm ²
1	27803	09/01/92	-119	42.4	10.1	0.238	40.0	9.2	0.229	54.8	16.5	0.301
1	27803	11/06/92	-53	41.3	9.9	0.240	48.8	9.9	0.204	53.4	18.2	0.342
1	27803	01/15/93	17	44.5	10.8	0.243	54.7	12.8	0.235	67.3	21.9	0.326
1	27803	03/07/93	68	52.4	11.8	0.225	50.6	13.2	0.262	64.8	20.6	0.317
2	27907	09/01/92	-119	43.8	9.2	0.210	37.7	7.9	0.209	59.7	16.7	0.279
2	27907	11/03/92	-56	38.6	8.0	0.208	50.1	9.9	0.197	56.2	16.2	0.288
2	27907	01/15/93	17	45.8	9.7	0.212	42.9	7.9	0.185	58.2	18.1	0.311
2	27907	01/26/93	28	48.5	10.0	0.207	54.0	13.1	0.243	57.6	17.8	0.308
2	27907	02/15/93	48	48.0	10.4	0.216	55.8	12.2	0.219	54.1	17.1	0.316
2	27907	03/07/93	68	49.7	9.5	0.190	47.8	11.1	0.232	51.1	16.1	0.316
3	1401	09/01/92	-119	45.9	9.3	0.203	53.7	11.1	0.207	58.6	16.9	0.288
3	1401	11/06/92	-53	54.0	9.2	0.170	55.5	12.5	0.225	55.9	17.1	0.307
3	1401	01/14/93	16	51.4	11.1	0.216	56.6	12.0	0.212	62.9	19.7	0.313
3	1401	01/28/93	30	47.8	9.0	0.189	59.4	13.4	0.226	55.5	18.9	0.341
3	1401	02/17/93	50	49.0	10.6	0.217	75.4	19.6	0.260	61.6	19.1	0.309
3	1401	03/08/93	69	50.7	11.4	0.224	54.4	14.7	0.271	65.9	19.4	0.294
4	25588	09/02/92	-118	42.1	8.6	0.204	44.1	6.6	0.150	57.1	16.1	0.283
5	26151	09/02/92	-118	55.0	10.4	0.190	52.3	11.7	0.223	63.2	18.1	0.287
5	26151	11/02/92	-57	56.6	12.1	0.214	53.9	12.6	0.233	64.1	20.4	0.319
5	26151	01/17/93	19	43.5	9.3	0.215	49.1	11.7	0.238	62.5	22.0	0.353
5	26151	01/27/93	29	38.9	8.7	0.223	49.2	8.4	0.172	62.2	22.7	0.364
5	26151	02/12/93	45	46.9	10.4	0.222	42.4	9.3	0.220	50.5	17.0	0.338
5	26151	03/04/93	65	46.9	10.2	0.219	44.4	10.5	0.237	70.5	25.4	0.361
6	25775	09/02/92	-118	43.6	10.6	0.243	61.6	11.9	0.193	61.2	18.6	0.304
6	25775	11/03/92	-56	56.0	13.6	0.244	51.7	12.8	0.247	65.6	21.6	0.329
6	25775	01/13/93	15	61.4	15.0	0.244	54.1	13.7	0.253	61.9	19.5	0.315
6	25775	01/28/93	30	52.9	12.2	0.230	50.1	12.0	0.239	60.8	20.8	0.342
6	25775	02/17/93	50	50.1	12.0	0.238	67.1	12.8	0.191	67.6	24.9	0.368
6	25775	03/08/93	69	43.6	10.1	0.232	66.2	14.2	0.214	72.6	25.7	0.354
7	27856	09/03/92	-117	60.6	10.7	0.176	63.7	13.3	0.209	63.3	20.3	0.321
7	27856	11/02/92	-57	57.5	12.0	0.209	56.7	12.9	0.228	64.6	23.1	0.357
8	25476	09/03/92	-117	52.5	12.9	0.245	54.1	12.5	0.231	65.4	19.3	0.294
8	25476	11/03/92	-56	51.6	12.2	0.236	56.2	11.7	0.209	66.6	21.9	0.329
8	25476	01/13/93	15	53.1	13.8	0.259	72.7	15.9	0.218	64.8	23.3	0.359
8	25476	01/28/93	30	49.8	11.1	0.223	55.6	12.7	0.228	69.8	24.6	0.352
8	25476	02/17/93	50	51.4	11.2	0.218	64.2	11.1	0.172	69.9	24.0	0.343
9	27906	09/03/92	-117	33.7	6.4	0.191	38.1	5.4	0.143	53.6	14.3	0.267
9	27906	11/02/92	-57	43.1	8.4	0.196	44.8	10.4	0.231	54.3	16.2	0.299
9	27906	01/17/93	19	38.8	7.7	0.200	52.9	16.0	0.303	56.7	17.3	0.305
9	27906	02/12/93	45	34.3	5.9	0.172	44.2	6.6	0.149	51.5	15.5	0.301
9	27906	03/04/93	65	39.1	7.2	0.185	35.9	7.6	0.212	58.1	18.7	0.322
9*	27906	01/27/93	29	27.9	4.9	0.174	35.5	6.6	0.187	58.6	19.6	0.334
10	1417	09/04/92	-116	49.0	11.7	0.239	64.6	12.3	0.191	72.1	22.0	0.305
11	23838	09/04/92	-116	48.5	10.8	0.222	56.9	10.4	0.182	66.4	17.7	0.267
11	23838	11/06/92	-53	49.5	11.7	0.237	62.9	15.0	0.239	71.8	22.3	0.311
12	27892	09/04/92	-116	47.7	10.3	0.217	48.3	10.2	0.212	66.5	18.5	0.278
12	27892	11/06/92	-53	41.9	9.7	0.231	56.5	9.8	0.174	67.4	21.9	0.326
12	27892	01/15/93	17	48.8	11.3	0.231	50.4	13.1	0.259	67.7	21.6	0.320

+ Launch 12/29/92

* This data was not clear for the top half of the animal, sent to Hologic for evaluation

Table 3D. Whole Body Scan Bone Mineral Results - Cosmos 2229

BMD ID #	Monkey ID #	Date	Days from Launch	R-Leg			L-Leg		
				Area cm ²	BMC gms	BMD gms/cm ²	Area cm ²	BMC gms	BMD gms/cm ²
1	27803	09/01/92	-119	58.0	14.3	0.246	67.4	15.1	0.224
1	27803	11/06/92	-53	56.2	14.7	0.261	60.2	15.3	0.254
1	27803	01/15/93	17	62.9	15.9	0.254	67.2	17.4	0.258
1	27803	03/07/93	68	69.7	14.6	0.209	63.8	17.9	0.281
2	27907	09/01/92	-119	54.2	12.0	0.221	53.3	11.4	0.215
2	27907	11/03/92	-56	55.5	12.3	0.221	58.7	13.8	0.236
2	27907	01/15/93	17	57.5	12.5	0.217	67.1	14.6	0.218
2	27907	01/26/93	28	57.4	12.5	0.218	60.6	13.7	0.227
2	27907	02/15/93	48	55.6	13.1	0.236	59.8	13.1	0.218
2	27907	03/07/93	68	62.7	11.0	0.175	60.1	14.6	0.242
3	1401	09/01/92	-119	64.9	12.2	0.188	59.8	14.3	0.238
3	1401	11/06/92	-53	63.3	16.5	0.261	74.5	15.5	0.209
3	1401	01/14/93	16	63.9	16.1	0.252	65.6	16.4	0.249
3	1401	01/28/93	30	63.3	15.9	0.251	69.1	16.1	0.234
3	1401	02/17/93	50	60.5	13.3	0.221	64.8	16.9	0.261
3	1401	03/08/93	69	78.7	17.1	0.217	67.7	17.4	0.258
4	25588	09/02/92	-118	56.0	11.8	0.211	56.3	13.0	0.232
5	26151	09/02/92	-118	73.3	16.5	0.225	65.8	18.2	0.276
5	26151	11/02/92	-57	70.6	19.7	0.279	76.0	19.2	0.252
5	26151	01/17/93	19	65.9	20.5	0.311	72.1	16.9	0.235
5	26151	01/27/93	29	63.1	15.2	0.241	61.4	18.6	0.303
5	26151	02/12/93	45	72.7	19.5	0.268	70.2	17.9	0.254
5	26151	03/04/93	65	63.2	18.8	0.297	80.1	19.8	0.247
6	25775	09/02/92	-118	68.4	13.6	0.199	58.6	14.2	0.243
6	25775	11/03/92	-56	60.4	15.6	0.259	66.4	16.9	0.254
6	25775	01/13/93	15	62.1	15.3	0.246	65.8	15.4	0.233
6	25775	01/28/93	30	61.7	15.4	0.249	61.6	16.0	0.260
6	25775	02/17/93	50	67.9	15.3	0.225	67.3	17.8	0.264
6	25775	03/08/93	69	69.6	16.2	0.232	61.2	16.9	0.276
7	27856	09/03/92	-117	65.2	16.5	0.252	61.7	15.4	0.249
7	27856	11/02/92	-57	70.0	16.5	0.235	66.2	16.7	0.252
8	25476	09/03/92	-117	74.7	17.3	0.232	68.9	18.8	0.272
8	25476	11/03/92	-56	69.2	16.7	0.241	69.7	18.8	0.269
8	25476	01/13/93	15	82.9	18.5	0.224	69.0	20.4	0.296
8	25476	01/28/93	30	66.0	18.7	0.283	74.2	22.6	0.304
8	25476	02/17/93	50	75.1	16.9	0.226	73.6	20.9	0.284
9	27906	09/03/92	-117	53.0	10.4	0.197	48.8	10.8	0.220
9	27906	11/02/92	-57	53.5	11.5	0.216	51.7	12.3	0.237
9	27906	01/17/93	19	54.9	11.2	0.204	57.5	12.5	0.218
9	27906	02/12/93	45	51.7	12.0	0.232	54.5	12.4	0.229
9	27906	03/04/93	65	61.6	12.8	0.208	53.0	13.7	0.258
9*	27906	01/27/93	29	50.7	11.8	0.234	50.5	12.1	0.240
10	1417	09/04/92	-116	70.7	19.6	0.278	71.7	18.1	0.252
11	23838	09/04/92	-116	69.7	14.9	0.214	67.1	16.6	0.247
11	23838	11/06/92	-53	62.9	16.9	0.269	68.6	17.9	0.262
12	27892	09/04/92	-116	57.8	14.0	0.242	55.2	13.4	0.244
12	27892	11/06/92	-53	55.8	13.3	0.238	55.2	14.4	0.260
12	27892	01/15/93	17	61.2	16.4	0.268	59.1	16.8	0.285

+ Launch 12/29/92

* This data was not clear for the top half of the animal, sent to Hologic for evaluation.

Table 4. Whole Body Scan Soft Tissue Results - Cosmos 2229

BMD ID #	Monkey ID #	Date	Days from Launch	Whole Body		Arm		Leg	
				Lean gms	Fat gms	Lean gms	Fat gms	Lean gms	Fat gms
1	27803	09/01/92	-119	3470.8	309.7	245.3	17.5	405.2	48.1
1	27803	11/06/92	-53	3521.0	363.8	228.1	16.8	400.5	57.1
1	27803	01/15/93	17	3880.1	445.4	267.8	23.7	441.4	69.2
1	27803	03/07/93	68	4051.6	413.8	323.0	30.2	382.8	79.8
2	27907	09/01/92	-119	3331.4	337.3	249.1	21.7	337.2	56.8
2	27907	11/03/92	-56	3616.3	500.1	241.2	25.2	360.2	74.6
2	27907	01/15/93	17	3741.8	378.1	277.4	27.5	387.9	78.2
2	27907	01/26/93	28	3559.8	364.2	299.5	21.5	386.3	48.5
2	27907	02/15/93	48	3502.0	351.2	278.0	19.8	360.2	65.5
2	27907	03/07/93	68	3562.0	380.3	256.3	22.8	361.1	48.2
3	1401	09/01/92	-119	3315.1	528.9	252.2	29.9	352.7	57.1
3	1401	11/06/92	-53	3864.4	299.2	268.3	10.9	442.7	49.9
3	1401	01/14/93	16	3854.9	454.8	309.2	23.7	423.7	52.3
3	1401	01/28/93	30	4025.8	352.9	245.7	20.6	426.5	48.2
3	1401	02/17/93	50	4220.1	299.2	268.3	23.1	363.5	42.0
3	1401	03/08/93	69	3745.4	512.9	280.7	30.9	436.0	70.0
4	25588	09/02/92	-118	3137.1	236.5	223.8	16.9	339.1	38.6
5	26151	09/02/92	-118	3583.5	426.4	286.4	23.4	424.7	57.5
5	26151	11/02/92	-57	3721.5	448.2	329.0	35.8	439.9	84.0
5	26151	01/17/93	19	3529.6	317.2	228.0	25.4	433.7	38.4
5	26151	01/27/93	29	3749.0	288.5	227.6	25.3	392.6	67.4
5	26151	02/12/93	45	3860.9	362.2	270.0	24.4	467.0	62.4
5	26151	03/04/93	65	3928.1	466.6	268.4	20.3	483.3	54.0
6	25775	09/02/92	-118	3666.4	355.1	258.4	22.0	387.0	64.4
6	25775	11/03/92	-56	4026.6	487.3	329.1	34.9	466.4	63.4
6	25775	01/13/93	15	4331.6	311.4	338.2	27.4	468.9	58.4
6	25775	01/28/93	30	4150.9	378.7	303.8	26.3	421.0	63.2
6	25775	02/17/93	50	4095.5	339.1	324.4	21.6	383.5	84.3
6	25775	03/08/93	69	3975.7	244.0	269.4	23.7	406.1	52.8
7	27856	09/03/92	-117	3727.5	499.4	293.9	15.9	469.3	34.0
7	27856	11/02/92	-57	3897.0	419.7	299.1	33.7	476.6	38.2
8	25476	09/03/92	-117	3861.0	512.9	332.4	31.5	456.9	66.6
8	25476	11/03/92	-56	4433.0	394.9	310.7	28.1	434.5	61.6
8	25476	01/13/93	15	4534.8	392.1	319.3	18.4	458.5	93.6
8	25476	01/28/93	30	4386.8	542.1	289.1	23.8	497.0	71.9
8	25476	02/17/93	50	4620.9	288.6	299.9	25.1	453.8	79.9
9	27906	09/03/92	-117	2927.2	333.6	196.1	20.0	303.7	55.5
9	27906	11/02/92	-57	3101.8	367.0	245.8	24.2	324.2	56.6
9	27906	01/17/93	19	3211.0	459.4	222.6	25.3	318.7	67.3
9	27906	02/12/93	45	3557.2	245.5	215.2	15.8	376.4	54.7
9	27906	03/04/93	65	3444.7	317.8	220.9	18.8	399.8	52.7
9*	27906	01/27/93	29	3476.1	360.5	142.6	15.6	377.3	42.8
10	1417	09/04/92	-116	2746.1	200.6	262.3	29.2	483.3	76.6
11	23838	09/04/92	-116	4150.8	445.3	282.6	23.3	453.9	70.3
11	23838	11/06/92	-53	4246.2	397.9	286.1	27.1	472.1	61.8
12	27892	09/04/92	-116	3436.6	345.1	257.4	24.4	374.8	44.1
12	27892	11/06/92	-53	3280.5	304.4	244.9	17.1	369.1	25.5
12	27892	01/15/93	17	3665.0	321.7	271.5	21.9	425.7	30.2

Table 5. BMD (gms/cm²) at 4 times and 5 regions used for statistical testing. The differences between control and flight groups were tested for significance at 3 pairs of time points, Pre-Post, Post-Recovery #1, Post-Recovery #2.

Region	Control Monkeys				Flight Monkeys			
	Pre	Post	Rec1	Rec2	Pre	Post	Rec1	Rec2
Arm								
Mean	0.229	0.236	0.215	0.217	0.205	0.207	0.223	0.197
Standard Error	0.007	0.010	0.008	0.001	0.009	0.007	-	0.025
Number of Animals	4	4	2	2	2	2	1	2
Leg								
Mean	0.240	0.240	0.250	0.231	0.247	0.257	0.264	0.250
Standard Error	0.008	0.012	0.033	0.005	0.031	0.054	-	0.018
Number of Animals	4	4	2	2	2	2	1	2
Spine								
Mean	0.494	0.501	0.488	0.502	0.479	0.482	0.531*	0.501
Standard Error	0.017	0.020	0.027	0.018	0.035	0.027	-	0.040
Number of Animals	4	4	3	3	2	2	1	2
Tibia								
Mean	0.447	0.444	0.451	0.432	0.451	0.421	0.437	0.425
Standard Error	0.007	0.008	0.017	0.009	-	0.039	0.048	0.041
Number of Animals	4	4	3	3	1	2	2	2
Whole Body								
Mean	0.308	0.290	0.295	0.268	0.312	0.268	0.278	0.284†
Standard Error	0.007	0.009	0.010	0.017	0.007	0.020	-	0.009
Number of Animals	4	4	2	2	2	2	1	2

* - Spine, Post to Recovery #1, P = 0.064

† - Whole Body, Post to Recovery #2, P = 0.104

Table 6. BMC (gms) at 4 times and 3 regions used for statistical testing. The differences between control and flight groups were tested for significance at 3 pairs of time points, Pre-Post, Post-Recovery #1, Post-Recovery #2.

Region	Control Monkeys				Flight Monkeys			
	Pre	Post	Rec1	Rec2	Pre	Post	Rec1	Rec2
Spine								
Mean	9.18	9.60	9.54	9.64	9.10	9.29	10.58	9.51
Standard Error	0.93	1.12	1.25	1.18	0.96	1.07	-	1.12
Number of Animals	4	4	3	3	2	2	1	2
Tibia								
Mean	5.67	5.59	5.74	5.56	6.55	5.90	5.95	5.59
Standard Error	0.47	0.41	0.67	0.72	-	0.92	1.17	1.23
Number of Animals	4	4	3	3	1	2	2	2
Whole Body								
Mean	155.3	149.6	154.6	142.2	155.9	132.3	144.5	147.5*
Standard Error	4.6	8.6	17.2	22.4	13.2	13.0	-	14.1
Number of Animals	4	4	2	2	2	2	1	2

* - Whole Body, Post to Recovery #2, P = 0.006

Table 7. Lean Tissue mass (gms) for 4 times and 3 regions used for statistical testing. The differences between control and flight groups were tested for significance at 3 pairs of time points, Pre-Post, Post-Recovery #1, Post-Recovery #2.

Region	Control Monkeys				Flight Monkeys			
	Pre	Post	Rec1	Rec2	Pre	Post	Rec1	Rec2
Arm								
Mean	256	284	294	288	287	225*	227	242
Standard Error	18	12	5	11	42	3	-	27
Number of Animals	4	4	2	2	2	2	1	2
Leg								
Mean	391	428	442	407	382	376†	393	422‡
Standard Error	17	15	55	47	58	57	-	45
Number of Animals	4	4	2	2	2	2	1	2
Whole Body								
Mean	3712	3955	3973	4061	3411	3370	3749§	3709
Standard Error	250	198	413	559	310	159	-	152
Number of Animals	4	4	2	2	2	2	1	2

* - Arm, Pre to Post, P=0.026

† - Leg, Pre to Post, P=0.018

‡ - Leg, Post to Recovery #2, P=0.067

§ - Whole Body, Post to Recovery #1, P=0.049

Table 8. Fat Tissue mass (gms) for 2 times and 3 regions used for statistical testing. The differences between control and flight groups were tested for significance at Pre-Post.

	<u>Control Monkeys</u>		<u>Flight Monkeys</u>	
	Pre	Post	Pre	Post
Region				
Arm				
Mean	22	23	30	25
Standard Error	3	2	6	0
Number of Animals	4	4	2	2
Leg				
Mean	55	68	70	53
Standard Error	10	13	14	14
Number of Animals	4	4	2	2
Whole Body				
Mean	391	384	408	388
Standard Error	41	25	41	71
Number of Animals	4	4	2	2

EXPERIMENT K-08-2

REDUCTION OF OCULAR COUNTER-ROLLING BY ADAPTATION TO SPACE

Principal Investigator:

Bernard Cohen
Departments of Neurology and Physiology and Biophysics
Mount Sinai School of Medicine, New York

Co-Investigators:

Mingjia Dai
Departments of Neurology and Physiology and Biophysics
Mount Sinai School of Medicine, New York

Leigh McGarvie
Departments of Neurology and Physiology and Biophysics
Mount Sinai School of Medicine, New York

Inessa Kozlovskaya
Institute of Biomedical Problems
Moscow, Russia

Michoïl Sirota
Institute of Biomedical Problems
Moscow, Russia

Theodore Raphan
Department of Computer and Information Science
Brooklyn College, CUNY

with technical assistance from Victor Rodriguez,
Nicholas Pasquale and Philip Cook

REDUCTION OF OCULAR COUNTER-ROLLING BY ADAPTATION TO SPACE

Bernard Cohen, Mingjia Dai, Leigh McGarvie, Inessa Kozlovskaya, Michoïl Sirota, Theodore Raphan

SUMMARY

We studied the three-dimensional vestibulo-ocular reflex (VOR) of rhesus monkeys before and after the Cosmos Biosatellite 2229 Mission of 1992-1993. This included tests of ocular counter-rolling (OCR), the gain of the vestibulo-ocular reflex (VOR) and spatial orientation of velocity storage. A four-axis vestibular and oculomotor stimulator was transported to the Institute of Biomedical Problems in Moscow for the pre- and postflight ground-based testing. Twelve normal juvenile male rhesus monkeys were implanted surgically with eye coils and tested 60-90 days before space flight. Two monkeys (7906 and 6151), selected from the twelve as flight animals, flew from 12/29/92 to 1/10/93. Upon recovery, they were tested for 11 days along with three control animals.

Compensatory ocular torsion was produced in two ways: 1) Lateral head tilts evoked OCR through otolith-ocular reflexes. OCR was also measured dynamically during off-vertical axis rotation (OVAR). 2) Rotation about a naso-occipital axis that was either vertical or horizontal elicited torsional nystagmus through semicircular canal-ocular reflexes (Roll VOR). OCR from the otoliths was substantially reduced (70%) for 11 days after reentry on both modes of testing. The gain of the Roll VOR was also decreased, but less than OCR. These data demonstrate that there was a long-lasting depression of torsional or roll eye movements after adaptation to microgravity in these monkeys, especially those movements produced by the otolith organs.

The gain of the horizontal or yaw VOR was close to unity when the two animals were tested 1 and 2 days after landing, respectively. The VOR gain value was similar to those registered before flight. This result confirms previous findings from the 1989 COSMOS 2044 Mission (Cohen et al. 1992). It indicates that there are no long-term changes in the passive gain of the yaw VOR on return after adaptation to microgravity.

The gain of the vertical or pitch VOR were not changed if values from the up- and downward nystagmus were pooled. However, there was a slight, but statistically significant decrease in upward VOR gain ($p < 0.05$), and there was a slight but statistically significant increase in downward VOR gain ($p < 0.05$). This reduced the asymmetry of up-down nystagmus that had existed prior to flight in these monkeys. The downward gain returned to the preflight level for 6151, but not for 7906 7 days after reentry.

We also examined the spatial orientation of velocity storage, using optokinetic nystagmus (OKN) and after-nystagmus (OKAN), according to techniques developed previously (Raphan and Sturm, 1991; Dai et al. 1991). Before flight, the yaw axis eigenvector angle was 5° with regard to the spatial vertical for monkey 7906 when the animal was tilted 90° . That is, the yaw axis orientation vectors of velocity storage were closely aligned to the spatial vertical before flight. One day after landing the same test yielded an orientation vector angle of 28° re the spatial vertical, which was a significant shift of the yaw axis eigenvector toward the body axis. By 7 days after recovery, the orientation vector angle had returned to 7° re the spatial vertical, indicating that it was again closely aligned with gravity.

In summary, these experiments demonstrate that otolith-induced ocular torsion against gravity as well as canal-induced ocular torsion was reduced for sustained periods after reentry. There were no long-term changes in the horizontal VOR after reentry. Although the overall gain of vertical VOR was not changed, there was less up-down asymmetry after landing. Finally, the data support the

hypothesis that there is a shift in the yaw axis orientation vector of velocity storage from a gravitational to a body frame of reference as a result of adaptation to space.

INTRODUCTION

Adaptation to microgravity presents a unique set of challenges to the nervous system because the input from the canals and the otoliths are no longer in synergy. The demand for head angular movements in space flight is essentially unchanged, although stimulation of the semicircular canals with pitch and torsional head movements at high frequencies may be reduced because there is no locomotion (Grossman et al. 1988). Consistent with this, little change has been found in the angular horizontal VOR (see Cohen et al. 1992, for review). There is no information about the VOR in pitch and roll.

On the other hand, the otolith organs face a new set of circumstances. The continuous force of gravity is reduced to a negligible level, although linear accelerations associated with translation persist. (It should be noted, however, that the otoliths do not often encounter comparable force levels in microgravity to those on earth when the head moves in pitch and roll, where it frequently encounters changes in the order of 1g.) Therefore, a reinterpretation of otolith input has been proposed, in which linear force sensed by otolith organs is now interpreted primarily as translation (Young et al. 1986). The consequence is that when the head is tilted laterally (rolled) in microgravity, there should be 1) adaptive down regulation of OCR and 2) no internal representation of the vertical re a gravitational frame of reference.

OCR was measured by an after-image method (Fischer 1927) by Yakovleva et al (1982). The response of several subjects varied. The reduction in OCR lasted in two subjects, one for the right tilt and the other for the left tilt, for up to 14 days after landing. The recover took place only at the next test point of 36 days. In some subjects there was anti-compensatory torsion after landing, in the direction of the tilt ("paradoxical counter-rolling", Kornilova; personal communication). OCR was also measured from colored transparencies in the right eye of four subjects after Spacelab-1 Mission (Vogel and Kass 1986). The angles of OCR were expressed as a gain ratio which was reduced for all subjects for the left tilt 1 day after landing between 28% and 56%. Whereas, changes in gain on the right were inconclusive.

Rotation about axes tilted from the vertical (off-vertical axis rotation, OVAR) offers unique possibilities as a test for the integrity of canal-ocular and otolith-ocular reflexes. At the onset of rotation about a tilted axis, input to the central nervous system comes both from the semicircular canals and the otolith organs. The canals transduce angular acceleration at the onset and end of rotation, converting it into a signal related to head angular velocity (Goldberg and Fernandez 1971), and the otolith organs sense the linear acceleration (gravity) which continuously changes its direction re head position. From this the nervous system extracts an estimate of head velocity about the tilted axis (Benson and Bodin 1966, Cohen et al. 1983, Guedry 1965, Raphan et al. 1981, Raphan et al. 1979, Raphan and Schnabolk 1988, Young and Henn 1975). This estimate is utilized to activate the velocity storage integrator to generate continuous nystagmus and compensatory steady state eye velocities (Cohen et al. 1983, Raphan et al. 1981, Raphan and Schnabolk, 1988).

The signal arising in the otolith organs is also used to produce compensatory changes in eye position (Diamond et al. 1979) over otolith-ocular pathways (Baker and Berthoz 1974) as the head changes its position with regard to gravity. At a low angular speed, OVAR can be treated as semi-static stimulation (0.17 Hz at 60°/s, for example). Under this testing condition, as the otolith organs, particularly the utricles, are continuously reoriented with regard to gravity, the magnitude of OCR also changes continuously. The repetitive nature of the dynamic response allows averaging and robust estimation of changes in OCR as a function of gravity, i.e., as the axis of rotation is tilted at various angles from the upright. No other stimulus produces sinusoidal ocular torsion repetitively without involvement of the semicircular canals. Thus, it is possible to gain a dynamic measure of

OCR during OVAR as well as a measure of the steady state or bias level of yaw-axis OVAR nystagmus velocity generated through otolith activation.

In addition, there is a reason to believe that there could be alterations in spatial orientation after adaptation to microgravity. Dai et al. (1991) and Raphan and Cohen (1988) have demonstrated a mechanism in the vestibular system, "velocity storage", that is spatially oriented on earth. As a result, when yaw axis OKN is elicited with monkeys in tilted positions, the OKAN develops vertical and torsional components that tend to bring the axis of rotation of the eyes toward the spatial vertical. A similar mechanism has been found in humans during OKN (Gizzi et al. 1994). A hypothesis of the current experiments was that adaptation to microgravity would be associated with a shift in orientation of velocity storage from a gravitational axis to a body axis. In the COSMOS 2044 1989 mission, Cohen et al. (1992) found that one flight monkey lost its dumping mechanism after space flight. This supported the notion that the monkey had shifted its internal reference of vertical to its body axis and away from the spatial vertical in the period after reentry.

The current series of experiments was an extension of studies begun on the COSMOS 2044 flight (Cohen et al. 1992). Steps of velocity were used to test the gain of the horizontal and vertical VOR. OCR was elicited by static tilts and by OVAR. Finally, OKAN induced by yaw axis OKN delivered in tilted conditions, was used to test the orientation of the velocity storage system. Preliminary results on OCR have been reported elsewhere (Dai et al. 1993).

METHODS

General

Eye movements of two rhesus monkeys (6151 and 7906) that flew in space for 12 days on the COSMOS Biosatellite Flight 2229 were compared with their preflight eye movements, with the preflight data from 10 other monkeys that formed a control group, and with data obtained in the postflight period from three of the ten control monkeys. The flight animals were launched on 12/29/92 and recovered on 1/10/93. Testing extended for 11 days postflight.

Eye movements were measured in three dimensions with magnetic scleral search coils. Horizontal and vertical movements were sensed by a coil implanted in the frontal plane by the technique of Judge et al. (1980). Ocular torsion or roll about the optic axis was recorded with a magnetic scleral search coil implanted on the top of one eye using the technique described below. We studied OCR using static tilts of 90° and off-vertical axis rotation (OVAR). Advantages of OVAR are that it affords a measure of dynamic tilt without canal contamination, and that multiple cycles of recording of eye position change can be averaged to obtain a robust measure of alteration in eye position with regard to head position relative to gravity. We also measured the Roll VOR during steps of velocity about a naso-occipital axis with the animal prone and during sinusoidal oscillation with the animal upright.

Surgery

Fourteen male rhesus monkeys of approximately 4 kg were used in these experiments. The animals were also utilized in studies of activity in the vestibular nerve (Manning Correia and colleagues) and studies of linear acceleration on ocular movements (David Tomko and colleagues). Under anesthesia scleral search coils (16mm) were implanted under the conjunctiva in the frontal planes of both eyes to record horizontal and vertical eye position, and a roll coil was implanted on the top of the left eye of each animal to record torsional eye movements.

To implant the roll coil, the left eye was pulled down, and a lateral cut was made in Tenon's capsule about 2 mm below the tarsal plate. The dissection was carried down to the superior rectus muscle, which was identified and freed both medially and laterally. A three turn 12 mm coil was fashioned by passing the wire under the superior rectus muscle. The coil was pushed into place posteriorly, where it lay under the superior rectus muscle on the top of the eye. Anteriorly, it was sutured in place at about the level of the equator. A tension loop was pushed up into the pocket lateral to the superior rectus, and the coil wires were led through the lateral portion of Tenon's capsule.

The conjunctiva was then dissected free about 1 mm from the edge of the limbus, a deep pocket was opened with blunt and sharp dissection, and a 16 mm 3 turn coil was placed over the eye and sutured in place. A tension loop was placed into the pocket, lateral to the inferior rectus muscle, and the wires were led through the lateral portion of Tenon's capsule. The same frontal plane coil operation was carried out on the right eye without difficulty or special bleeding. The coil wires were led out of the orbit and sutured to the fascia overlying the temporal muscle, before being led to the top of the skull, where they were attached to a plug. Typical impedances of the coils were: Left eye roll coil 56 ohms; frontal eye coil 67 ohm.

Experimental Apparatus

A four axis vestibular and optokinetic stimulator (Neurokinetics of Pittsburgh) was transported from New York to the Institute of Biomedical Problems in Moscow for these experiments. The apparatus provided great flexibility to accomplish a variety of experimental paradigms. It had four axes driven by servo-motors that were independent and were under computer control. A picture of the apparatus is shown in Fig. 1. The animal rotator was enclosed in an optokinetic sphere, 122 cm in diameter, with 10° vertical black and white stripes. When rotated, the sphere produced full field motion that induced OKN. The rotator consisted of a "C" gimbal, through the center of which was a rotational axis to which the primate chair was attached. We shall designate the latter as the "chair axis". The chair axis was positionally controlled to provide $\pm 90^\circ$ of excursion. It produced pitch or roll of the animal, depending on whether the axis of rotation was coincident with the animal's interaural or naso-occipital axis, respectively. The gimbal axis produced rotation of the animal about an axis coincident with the axis of the surrounding optokinetic sphere. The gimbal axis could be controlled in either velocity or positional servo mode. The maximum acceleration and deceleration of the C gimbal and optokinetic sphere were $200^\circ/\text{s}^2$. The sphere and C gimbal were fixed to a spine that surrounded the sphere and was attached to two lateral posts. The spine was positionally controlled to pivot about a horizontal axis $\pm 180^\circ$.

The animal's chair could be positioned in four directions, 90° apart, with regard to the chair axis. For example, if it was facing out or in along the axis of rotation, the animal could be rotated around by $\pm 90^\circ$ about its naso-occipital axis. Likewise, if it were left or right ear in, it could be pitched by $\pm 90^\circ$ about its interaural axis. The monkey could also be continuously rotated with velocity steps around the primate axis. If it was upright, the rotation axis would be along the animal's head-feet (Z) axis. If the animal was tilted 90° on its side, rotation was around its interaural axis. If it was tilted 90° into a prone or supine position, the rotation would be along a naso-occipital axis. All these rotations were head-centered.

Although the C gimbal and optokinetic sphere axes were coaxial, they were independent of each other. This allowed us to rotate the visual surround and monkey at the same rate in some experiments to produce a relative stationary surround. In this paradigm, the vestibular system indicates that the head is moving, but the visual system indicates that it is stationary. We designate this as a "relative stationary surround". As a result, vestibular nystagmus is quickly suppressed, particularly that component attributable to velocity storage (Raphan et al. 1979; Waespe et al. 1983). The ability to rapidly suppress or "dump" nystagmus proved valuable in shortening the time of experiments during the postflight testing.

A final modification of the chair enabled us to position the animal about 38 cm from the axis of rotation. This provided the capability of centrifugation. Preliminary experiments were carried out using centrifugation at 200°/s in the head forward and backward conditions and with the animal facing outward. Under this velocity, a resultant force of about 18° re gravity was produced. Adequate ground-based data is not available for comparison with these results, and they will not be included in this report.

Thus, the entire apparatus could be tilted to any position while the animal pitched or rolled, or while the optokinetic sphere provided visual stimulation or the animal rotated about any axis through the center of the head.

Experimental Control And Data Acquisition

Eye position was recorded by a magnetic scleral search coil technique (Robinson 1963). During experiments animals sat in a primate chair. Their heads were fixed to a square plastic frame, 33 cm on a side, that held the field coils and was attached to the primate chair. The eyes were centered in the field coils. Voltages associated with eye position and with the position and velocity of the various axes were recorded through analog filters with a bandwidth of DC to 40 Hz. Eye positions, analog-differentiated velocities and stimulus data were displayed on a 8 channel chart recorder (Astromed) and an oscilloscope. A 486 PC computer was used to control the experiment and to take the data. Each stimulus paradigm was pre-designed and called in by a computer program specially designed for that experiment. The voltages associated with eye positions were sampled at 600 Hz and stimulus data were sampled at 150 Hz.

All settings of analog instruments remained the same throughout the Mission. The resistances of eye coils were measured in all experiments and there was no change before and after space flight. Therefore, we were able to compare eye movements of animals before and after flight.

Experimental Paradigm

Prior to all tests, yaw, pitch and roll velocity calibrations were done. The monkeys were placed upright, left ear 90° down and in prone positions, respectively, and rotated about a vertical axis at $\pm 30^\circ/\text{s}$ for 20 seconds while they viewed the stationary OKN stripes in light. Under this condition, the velocity gain (slow phase eye velocity/head velocity) of the combined visual-vestibulo-ocular reflex was assumed to be close to unity for the yaw and pitch eye velocities. The roll velocity gain was determined by comparing the output of the implanted roll coil from each monkey during torsional nystagmus to that of a similar "dummy" coil of the same size, mounted on a jig and moved in the same magnetic field. A positional calibration was first established for the "dummy" coil. This was then used to calibrate torsional eye position changes during the nystagmus, and to compare the velocity of the slow phases to the velocity of the stimulus. Using this technique the gain of the torsional VOR was about 0.6 for all monkeys. This agrees with data from other laboratories on the gain of the roll VOR in rhesus monkeys (Henn, personal communication). Regardless, it should be emphasized that the coil amplifier settings were the same before and after flight, and the coil resistances were unchanged. Therefore, the pre and postflight results could be compared to each other.

OCR was tested in two ways after a calibration in which the animal was rotated around a naso-occipital axis coincident with gravity while prone and in light. To test static OCR, the monkey was positioned upright in the darkness for 20 seconds and then tilted 90° to its left and right for another 20 seconds, respectively. Spontaneous torsional eye position were recorded for each of the three conditions. OCR was also studied during OVAR nystagmus induced by rotation at 60°/s. The experiment was done in the following way: First, the animal was upright and was rotated in light with a relative stationary surround, i.e., with the optokinetic sphere moving at 60°/s to dump the nystagmus induced by the semicircular canals at the onset of rotation. After the nystagmus had disappeared, the lights were turned off while the animal continued to rotate. The rotating axis was subsequently tilted with a speed of less than 5°/s to angles of 15°, 30°, 45°, 60°, 75° and 90° re gravity. Each tilt of the rotation axis was held for 36 seconds (6 cycles of rotation). During OVAR compensatory horizontal nystagmus developed and reached a steady state level. Since the animal's head was reoriented continuously with respect to gravity during OVAR, roll eye position was altered continuously in direction and magnitude (ocular counter rolling) at a frequency of 0.17 Hz. Two series of tests were done utilizing OVAR, one with animal rotating to its right and one to its left.

Animals were tested in two different experimental paradigms to evaluate the gain of the roll VOR. In the first paradigm, the animal was placed prone and rotated with a velocity step (200°/s²) about its naso-occipital axis in the darkness, at angular speeds of ±30°/s, ±45°/s, ±60°/s, ±75°/s and ±90°/s. In the second paradigm, the animal was upright and was oscillated sinusoidally over ±30° around its naso-occipital axis which was horizontal at frequencies of 0.025, 0.05, 0.077, 0.1 and 0.125 Hz. The cycles of sinusoidal oscillation varied, ranging from 5-10 cycles per frequency.

The horizontal and vertical VOR were tested in the conventional way. For the horizontal VOR, the monkey was in an upright position, and it was rotated at angular speeds of 30°/s, 60°/s, 90°/s and 120°/s about a spatial vertical axis which was coaxial with body axis. For the vertical VOR, the monkey was positioned left side 90° down and rotated with angular speeds of 30°/s, 45°/s, 60°/s, 75°/s and 90°/s around its interaural axis, which was spatially vertical. The VOR gain is flat at these velocities (Raphan et al. 1979; Matsuo and Cohen 1984).

DATA ANALYSIS

A velocity calibration was used to obtain a relative calibration for horizontal and vertical eye position. The individual slope of slow phases of eye position was calculated over the period of velocity calibration, and the slopes of eye position were averaged. The mean was then converted to a 15° eye position calibration. The baseline or zero eye position was determined by averaging eye position over a long period of spontaneous eye movements with the animal upright. For the calibration of horizontal and vertical eye movement, the gain, defined as eye velocity divided by stimulus velocity, was taken as unity (Cohen et al. 1992). As noted above, the gain for roll eye velocity was about 0.6. The preflight calibration was used throughout, since the gain of the postflight response might differ from the preflight response. Data analyses for both eye position and eye velocity were based on the converted eye position calibration.

When calculating static OCR, torsional eye positions were considered only if the eyes were not deviated more than ±10° horizontally or vertically from the midposition. The values of OCR for the monkey tilted ±90° laterally were referenced to the baseline torsional position in the upright position.

Dynamic OCR was also recorded in tilt positions from 15-90° during OVAR. 5 to 6 cycles of roll eye position data were averaged during OVAR nystagmus. The trigger signal came from the output of a potentiometer which registered the yaw axis rotation position. The mean roll eye position then was fitted with a sine function. The peak value of the fitted sine curve was taken as the amplitude of the OCR.

In the data analysis associated with slow phases of eye velocity, eye position data were digitally differentiated, and quick phases of nystagmus were removed by a histogram desaccading algorithm. The data was then smoothed by averaging each four points, which would reduce the sampling rate to 150 Hz. To calculate the gain of the horizontal, vertical or roll VOR from velocity steps about a vertical axis, the slow phases associated with first three nystagmus were marked and averaged, and then the gain was obtained by dividing mean eye velocity by the corresponding roll step stimulus velocity.

To calculate the gain of roll eye velocity from the naso-occipital oscillation about a horizontal axis, the eye velocities were first desaccaded. 5-10 cycles of slow phases of eye velocity were averaged, and the averaged data were fitted by a sinusoidal function. The peak value of the fitted curve was taken as the peak amplitude of the roll eye velocity. The gain then was obtained as the ratio of peak roll eye velocity versus peak oscillating velocity of the stimulus.

RESULTS

Static and Dynamic Ocular Counter-Rolling (OCR)

Static OCR in response to tilts of $\pm 90^\circ$ are shown in Table 1. Although there was no difference in the magnitude of OCR between left and right tilts across the five monkeys preflight and for the three controls postflight (right $6.4 \pm 0.9^\circ$, left $5.7 \pm 1.0^\circ$; $p=0.069$), we considered each side to be a separate trial in the statistical calculations. A striking finding was that OCR was dramatically reduced by about 70% after recovery from space flight in both flight monkeys, and there was no apparent recovery in the magnitude of torsion over 11 days of testing ($p < 0.001$, $n_1=10$, $n_2=10$). In contrast, there was no change in the ocular torsion of the three control monkeys when compared in the preflight and postflight period ($p=0.92$, $n_1=10$, $n_2=6$).

Dynamic OCR was assessed using OVAR. The roll component of eye movement showed a typical increase in the amplitude of sinusoidal modulation before flight as a function of tilt of the angle of rotation (see Fig 1A, ROLL POSI). In contrast, the magnitude of OCR was substantially reduced after flight (Fig. 2B, ROLL POSI). Changes shown in Fig. 2B for 6151 were similar to those found in 7906 and can be contrasted to the preflight OCR and the findings in the control monkeys. In each of the animals there was approximately $\pm 7^\circ$ of torsion when the axis of rotation was tilted 60° - 90° in the preflight or control postflight testing (Fig. 3A-E), whereas the maximum torsion induced by OVAR after flight was 2° - 3° (Fig. 3D, E).

The reduction of dynamic OCR in the entire group is summarized in Fig. 3F. The preflight OCR for the two flight monkeys fell more than two standard deviations below the preflight mean of 5 monkeys, a highly significant difference ($p < 0.001$, $n_1=5$, $n_2=7$). The reduction of dynamic OCR for 7906 was more than for 6151. Nevertheless, there was no recovery of OCR for both monkeys over the post-test period of 11 days. As with static OCR, the reduction in dynamic OCR after flight was 70%.

We considered various artifacts that might account for the reduction in OCR in the flight monkeys. Changes in the apparatus were ruled out by the same values for OCR pre and postflight for the control monkeys (Fig. 3A-C). It was postulated that there might be adhesions in the supraorbital area around the roll coil in the flight monkeys that was tethering the eye. One of the animals was anesthetized, and its eyes were tortured physically by grasping the conjunctiva at both sides of the limbus and moving the eye in roll. There was no difference in the physical force needed to move either eye. Moreover, adhesions that might have reduced the amount of eye movement before the mobility test and been broken by the physical movement were ruled out because there was no difference between the OCR before and after the mobility test. This demonstrated that the eye was not tethered in roll for these two monkeys after flight.

Roll VOR

The Roll VOR was measured in two experimental paradigms, with velocity steps with the monkeys prone while rotating about a vertical naso-occipital axis (Fig. 4A) and with sinusoidal oscillations with the monkeys upright rotating about a horizontal axis (Fig. 4B). The gain of the Roll VOR of 7906 was reduced about 50% and of 6151 about 15% in both modes of stimulation. Especially for 6151, this was less than the amount of reduction in OCR, which was about 60%. However, with the exception of 6151 at 30°/s step and 0.025 Hz oscillation, it was significantly different from the preflight means across all step velocities and frequencies, laying more than $\pm 2SD$ from the means of the five monkeys. In comparison, there was no reduction in the gain of the Roll VOR in the three control monkeys.

There were some differences between the two tests. In the velocity step test (Fig. 4A), only the vertical semicircular canals were stimulated, and there was no contribution from the otoliths, but activation was at a high frequency. In the oscillation experiments both the vertical canals and otoliths were activated to generate roll movements, but the mode was with low frequencies (0.025-0.125 Hz). This may account for the finding that the overall response to oscillation had a lower gain than that to the velocity step.

Vertical VOR

There was upward spontaneous nystagmus in both monkeys before flight. This is a common finding in normal rhesus monkeys. The spontaneous nystagmus in 6151 can be seen in the vertical velocity trace of Fig. 2, A. It was reduced when the animal was first tested, 2 days after reentry (Fig. 2, B). This was also true for 7906 when tested 1 day after landing.

The upward VOR gain of the monkeys before flight was 0.96 ± 0.03 . The downward gain was $0.75 \pm .04$. Thus both monkeys had an asymmetry of their VOR gains before flight, with the upward gain being greater than the downward gain. This was the same as other monkeys in the control pool. In the first postflight record, there was a decrease in the gain of the upward VOR to 0.90 ± 0.03 , and an increase in the downward VOR to 0.82 ± 0.03 for 1-2 days for both monkeys¹. These differences were small but statistically significant (decrease in upward gain: 7906, $p=0.04$, $n=5$ and 6151, $p=0.01$, $n=5$; increase in downward gain: 7906, $p=0.04$, $n=5$; 6151, $p=0.02$, $n=5$). If the gains for the up- and downward VOR were considered together, the differences in pre- and postflight gains equalized, and there was no difference in either 7906 ($p=0.78$, $n=10$, day 1) or 6151 ($p=0.74$, $n=10$, day 2) before and after flight.

¹Monkey 7906 was tested on Day 1 postflight, 22 hours after landing. Monkey 6151 was tested on Day 2 postflight, 55 hours after landing.

By 7 days of landing, there was no statistical difference in gain between pre- and postflight testing for the upward VOR in both monkeys (7906: $p=0.07$, $n=5$; 6151: $p=0.12$, $n=5$) or for the downward VOR in 6151 ($p=0.81$, $n=5$). Monkey 7906 still had an increased downward VOR gain ($p=0.03$, $n=5$).

In summary, there was a drop in the upward VOR gain 1-2 days after landing and an increase in the downward VOR gain. By 7 days the gain had returned to preflight level except for an increase in the downward VOR gain in one animal.

Horizontal VOR

The gain for the horizontal VOR was pooled for rotation to the right and left, since there was no gain difference between them. As shown in Table 3, there was no yaw gain difference between pre- and postflight testing, 1-2 days after landing for both 7906 ($p=0.65$) and 6151 ($p=0.22$). This confirms findings reported in the 1989 Mission (Cohen et al. 1992). There was also no change in the gain of the steady state horizontal velocities during OVAR, which were the same before flight and after landing (Fig. 2A, B, Horizontal Velocity).

Changes in Spatial Orientation

The yaw axis eigenvector of OKAN, derived from the feedback matrix of a velocity storage integrator, has been regarded as an internal representation of the vertical (Dai et al. 1991; Raphan and Sturm 1991). Before flight, the eigenvector angle re gravity for 7906, tested during yaw axis OKN at 90° of tilt, was 5° (Fig. 5A). This was close to the spatial vertical and was similar to other normal monkeys tested in a previous study (Dai et al 1991). Twenty-two hours after landing, the yaw axis eigenvector had moved significantly away from spatial vertical and was now 28° (Fig. 5B). This is consistent with the hypothesis that there is a tendency for the spatial orientation of OKAN to move toward a body axis as a result of adaptation to microgravity. By 7 days after landing, the eigenvector angle was 7° , having returned to its preflight level (Fig. 5C). Unfortunately, testing of the orientation of velocity storage was limited in 6151 after flight because it was sick after recovery and could not be tested until the second day, at which time there was no alteration in the spatial orientation.

DISCUSSION

The major finding of these experiments is that the torsional otolith-ocular reflex, induced by head tilt with regard to gravity, was substantially reduced in two flight monkeys after adaptation to space, and that the reduction in OCR persisted for a prolonged period after reentry. There was also a reduction in the gain of the Roll VOR, more in one monkey than in the other. The alteration in Roll VOR gain was to a lesser extent in both monkeys than the changes in OCR. The reduction in the gain of OCR measured dynamically during OVAR was the same as the reduction in gain of static OCR, measured in side down position. Thus, regardless of how the monkey was moved to a side down position, the counter-rolling in that position was reduced after space flight. In addition, the reduction in gain was not dependent on the yaw orientation vector of velocity storage but remained uniformly lower despite the fact that the orientation vector changed from 5° to 28° back to 7° . This supports the notion that the gain of the direct otolith ocular pathway is separate from the pathway responsible for velocity storage.

There are two types of afferents from the otoliths. One is phasic, carrying irregular activity from large fibers that innervate Type I hair cells that lie close to the striola. The firing rates of these cells typically adapt when the head is statically tilted, making them poor sensors of head position. However, their activity could be integrated to generate the position command for driving motoneurons (Cannon and Robinson 1987; Schnabolk and Raphan 1993). They also have a steep gain curve. As a result, their pulse-like activity could summate with the output of the integrator to be

useful during translation. The second type of afferent is generally of smaller diameter and carries regular fibers from Type II hair cells. These cells do not adapt, making them excellent sensors of head position. The gain adaptation in OCR that occurred in the two monkeys may have been the result of a reduction in the effect of the regular afferents, acting on direct otolith-ocular pathways. In addition, the roll gain control of the final position integrator (Cannon and Robinson 1987) as well as the cerebellum (Zee et al. 1980) may also have been responsible for producing the adaptation of OCR after space flight.

The phases of the OVAR-induced modulations in torsional eye position and in horizontal slow phase velocity were unaffected in the previous Cosmos space flight (Cohen, et al. 1992). The finding that the steady state levels of OVAR were also unaffected by space flight (Cosmos 2044 and 2229) implies that the otolith organs were sensing gravity correctly, and that the system that converts the patterns of position in the otolith afferents to drive velocity storage was intact. This suggests that the functional structure of the otolith afferents was not changed after flight. On the other hand, there were indications that canal-ocular as well as otolith-ocular torsional reflexes were adapted. This is surprising, since in these same animals, there was no change in the horizontal VOR gains, tested in a similar fashion. This implies that the factors that contribute to the adaptation of the Roll VOR are more dependent on gravity than are the horizontal or vertical VOR.

What is the reason for the striking changes in OCR as well as the significant, although less striking changes in the Roll VOR? Torsional head movements occur at low frequencies on earth, but probably the largest stimulus to torsional movement is lateral head tilt which activates OCR through gravity. In space, horizontal and vertical eye movements can be generated voluntarily or through canal reflexes. On the other hand, there are no voluntary torsional eye movements, and only negligible gravity is present. Therefore, maintenance of the roll reflex would depend only on roll-angular accelerations. One possibility is that there was relative inactivity of the torsional system in space, leading to a reduction in gain after reentry. Since the monkeys used in the Cosmos project were chaired and were not able to exercise freely, they may have made even fewer torsional head movements than astronauts or cosmonauts. If the changes in OCR were related to inactivity, there might be differences in the amount of OCR between monkeys and humans who were able to move more freely. Were this to be substantiated in future experiments, a program of head movements which produced compensatory torsional ocular movements might be a natural counter-measure.

An alternate possibility is that conflict is generated in space when the head is tilted either vertically or in roll because an otolith signal does not accompany the angular head movement. Therefore, the gain is adapted down. Although this would explain the reduction in the roll gain, it would not account for the relatively small changes observed in the vertical VOR gain. In this study, we have shown that the upward VOR gain was reduced and the downward VOR gain was enhanced while the upward spontaneous nystagmus was decreased after landing. The peak to peak vertical gain was essentially the same before and after flight, however.

The otolith organs may also play a role in spontaneous vertical eye movement. The present data show that the level of spontaneous vertical nystagmus varied after space flight, and level of vertical nystagmus contributed to the asymmetry of vertical VOR gain. Clement and Berthos (1990) demonstrated that there was a downward drift of the eyes after adaptation to space flight in humans. The two may be related. As yet, the effects of otolith on vertical eye movement have not been studied in humans or monkeys in space.

There are several steps that would aid in understanding these results: The reduction in OCR should be replicated in monkeys and studied in humans, and it should be correlated to behavior after landing. Motion analysis of head movements should be done to provide information about the content of natural head movements in space and after landing, particularly those around a naso-occipital axis. We would predict that there would be fewer torsional head movements in space than on earth. If a similar decrease occurs in OCR in humans as in monkeys, tasks should be designed so

that they do not involve the necessity for torsional eye velocities or changes in torsional eye position. Counter-measures, such as a program of torsional head movements in space, might be considered. Finally, the gain of the vertical and roll VOR should be studied systematically, as well as the equalization of the vertical asymmetry.

REFERENCES

1. Baker, R., and A. Berthoz. Organization of Vestibular Nystagmus in Oblique Oculomotor System. *J Neurophysiol.* 37: 195-217, 1974.
2. Benson, A.J., and M.A. Bodin. Interaction of Linear and Angular Accelerations on Vestibular Receptors in Man. *Aerosp Med.* 37: 144-154, 1966.
3. Cannon, S.C., and D.A. Robinson. Loss of the Neural Integrator of the Oculomotor System From Brain Stem Lesions in Monkey. *J Neurophysiol.* 5: 1383-1409, 1967.
4. Clement, G., and A. Berthoz. Cross-coupling Between Horizontal and Vertical Eye Movements During Optokinetic Nystagmus and Optokinetic Afternystagmus Elicited in Microgravity. *Acta Otolaryngol.* (Stockh) 109:179-187, 1990.
5. Cohen, B., J.I. Suzuki, and T. Raphan. Role of the Otolith Organs in Generation of Horizontal Nystagmus: Effects of Selective Labyrinthine Lesions. *Brain Res.* 276: 159-164, 1983.
6. Cohen, B., I. Kozlovskaya, Raphan T., Solomon D., Helwig D., Cohen N., Sirota M., and S. Yakushin. Vestibular Reflex of Rhesus Monkeys After Spaceflight. *J App Physiol.* (Supplement), 73: 121-131, 1992.
7. Dai, M., T. Raphan, and B. Cohen. Spatial Orientation of the Vestibular System: Dependence of Optokinetic After-nystagmus on Gravity (Abs). *J Neurophysiol.* 66: 1422-1439, 1991.
8. Dai, M.J., T. Raphan, and B. Cohen. Spatial Orientation of Velocity Storage During Post-rotatory Nystagmus (Abs). 21st Neuroscience Annual Meeting, Part 1, pp 314, 1991.
9. Dai, M.J., B. Cohen, Raphan T., McGarvie L., and I.B. Kozlovskaya. Reduction of Ocular Counter-rolling (OCR) After Spaceflight (Abs). 23rd Neuroscience Annual Meeting, Part 1, pp 343, 1993.
10. Diamond, S.G., Markham C.H., Simpson N.E., and I.S. Curthoys. Binocular Counterrolling in Humans During Dynamic Rotation. *Acta Otolaryngol.* 87:490-498, 1979.
11. Fischer, M.H. Messende Untersuchungen über die Gegenrollung der Augen und die Lokalisation der scheinbaren Vertikalen bei seitlicher Neigung des Gesamtkörpers bis zu 360°. I. Mitteilung. Neigung bis zu 40° (Untersuchungen an Normalen). *Albrecht von Graefes Arch Klin Ophthalmol.* 118, 633, 1927.
12. Gizzi, M., T. Raphan, and B. Cohen. Orientation of Human Optokinetic Nystagmus (OKN) to Gravity: A Model Based Approach (Abs). 23rd Neuroscience Annual Meeting, Part 1, pp 343, 1993.
13. Goldberg, J.M., and C. Fernandez. Physiology of the Peripheral Neurons Innervating Semicircular Canal of the Squirrel Monkey. I. Resting Discharge and Response to Constant Angular Accelerations. *J Neurophysiol.* 34: 635-660, 1971.

14. Grossman, G.E., Leigh R.J., Abel L.A., Lanska D.J., and S.E. Thurston. Frequency and Velocity of Rotational Head Perturbations During Locomotion. *Exp Brain Res.* 70: 470-476, 1988.
15. Guedry, F.E. Orientation of the Rotation Axis Relative to Gravity: Its Influence on Nystagmus and the Sense of Rotation. *Acta Otolaryngol. (Stockh)* 60: 30-48, 1965.
16. Judge, S.J., B.J. Richmond, and F.C. Chu. Implantation of Magnetic Search Coils for Measurement of Eye Position: An Improved Method. *Vision Res.* 20: 535-538, 1980.
17. Matsuo, V., B. Cohen, Raphan T., DeJong V., and V. Henn. Asymmetric Velocity Storage for Up and Down Nystagmus. *Brain Res.* 176: 159-164, 1979.
18. Matsuo, V. and B. Cohen. Vertical Optokinetic Nystagmus and Vestibular Nystagmus in the Monkeys: Up-down Asymmetry and Effects of Gravity. *Exp Brain Res.* 53: 197-216, 1984.
19. Raphan, T., V. Matsuo, and B. Cohen. Velocity Storage in the Vestibulo-ocular Reflex Arc (VOR). *Exp Brain Res.* 35: 229-248, 1979.
20. Raphan, T., Cohen B., and V. Henn. Effects of Gravity on Rotatory Nystagmus in Monkeys. *Annals of the New York Academy of Sciences* 374: 44-55, 1981.
21. Raphan, T., and B. Cohen. Organizational Principles of Velocity Storage in Three Dimensions: The Effect of Gravity on Cross-coupling of Optokinetic After-nystagmus. *Annals of the New York Academy of Sciences* 545: 74-92, 1988.
22. Raphan, T., and C. Schnabolk. Modeling Slow Phase Generation During Off-vertical Axis Rotation. *Annals of the New York Academy of Sciences* 545: 29-50, 1988.
23. Raphan, T. and D. Sturm. Modeling the Spatiotemporal Organization of Velocity Storage in the Vestibuloocular Reflex by Optokinetic Studies. *J Neurophysiol.* 66: 1410-1421, 1991.
24. Robinson, D.A. A Method of Measuring Eye Movement Using a Scleral Search Coil in a Magnetic Field. *IEEE Trans Biomed Eng.* 10: 137-145, 1963.
25. Schnabolk, C., and T. Raphan. Model of Three Dimensional Velocity-position Transformation in Oculomotor Control. 23rd Neuroscience Annual Meeting, Part 2, pp 1593, 1993.
26. Waespe, W., Cohen B., and T. Raphan. Role of the Flocculus and Paraflocculus in Optokinetic Nystagmus and Visual-vestibular Interactions: Effects of Lesions. *Exp Brain Res.* 50: 9-33, 1983.
27. Vogel, H. and J.R. Kass. European Vestibular Experiments on the Spacelab-1 Mission: 7. Ocular Counterrolling Measurements Pre-and Post-flight. *Exp Brain Res.* 64: 284-290, 1986.
28. Yakovleva, I.Ya., Kornilova L.N., Serix G.D., Tarasov I.K., and V.N. Alekseev. Results of Vestibular Function and Spatial Perception of the Cosmonauts for the 1st and 2nd Exploitation on Station of Salute 6. *Space Biology (CCCP)* 1:19-22, 1982.
29. Young, L.R., and V. Henn. Nystagmus Produced by Pitch and Yaw Rotation of Monkeys about Non-vertical Axes. *Fortschr Zool* 23: 235-246, 1975.

30. Young, L.R., Oman C.M., Watt D.G.D., Money K.E., Lichtenberg B.K., and R.V. Kenyon. M.I.T./Canadian Vestibular Experiments on the Spacelab-1 Mission: 1. Sensory Adaptation to Weightlessness and Readaptation to One-g: An Overview. *Exp Brain Res.* 64: 291-298, 1986.
31. Zee, D.S., Leigh R.J., and F. Mathieu-Millaire. Cerebellar Control of Ocular Gaze Stability. *Ann Neurol.* 7:37-40, 1980.

TABLE 1
 STATIC OCR

A. Flight Monkeys

	7906			6151			
Torsion	Pre	D1	D11	Pre	D2	D7	D11
to Right	7.0±1.7°	1.2±1.2°	2.1±0.5°	7.6±1.5°	1.6±1.6°	1.6±1.3°	1.7±1.3°
to Left	5.3±1.2°	2.2±1.1°	0.5±0.8°	5.3±1.3°	3.2±1.1°	1.4±1.0°	2.1±1.3°

B. Control Monkeys

	7803		7907		5775	
Torsion	Pre	Post	Pre	Post	Pre	Post
to Right	5.8±0.2°	5.8±0.9°	7.5±2.2°	6.9±1.9°	5.3±2.9°	5.7±2.4°
to Left	4.6±1.2°	6.9±2.7°	7.2±2.0°	6.5±2.3°	4.8±1.3°	4.8±2.0°

TABLE 1: Static OCR in two flight monkeys (**A**) and three control monkeys (**B**). Shown are the average deviation of the eyes before flight for 7906 and 6151 (Pre) and in the preflight period for the three control animals, 7803, 7907, and 5775 (Pre). The Post value for the control animals in B represents OCR taken in the postflight period. It was not different than that in the preflight period. In contrast, there was a substantial reduction in OCR (70%) postflight.

TABLE 2
Vertical VOR gain

Stimulus	30°/s		45°/s		60°/s		75°/s		90°/s	
	Up	Down								
7906 Pre	0.95	0.66	0.97	0.75	0.93	0.72	0.93	0.73	0.91	0.77
7906 Day1	0.90	0.83	0.88	0.82	0.85	0.78	0.93	0.79	0.88	0.78
7906 Day7	0.96	0.80	0.97	0.82	0.95	0.81	0.97	0.82	0.97	0.77
6151 Pre	0.97	0.77	0.97	0.78	0.97	0.72	1.00	0.81	1.00	0.74
6151 Day2	0.93	0.87	0.93	0.85	0.89	0.87	0.89	0.82	0.87	0.82
6151 Day7	0.96	0.78	0.97	0.75	0.97	0.73	0.96	0.80	0.97	0.75

TABLE 2: Gains of the vertical VOR in the pre- and postflight periods. The gains for the up-and downward VOR were listed separately due to the asymmetry of the vertical VOR gain before flight.

TABLE 3
Horizontal VOR gain

Stimulus	30°/s	60°/s	90°/s	120°/s
7906 Pre	0.98	0.94	1.00	1.00
7906 Day1	0.96	0.99	1.00	1.00
6151 Pre	0.98	1.00	1.00	1.00
6151 Day2	0.98	0.97	0.99	0.97

TABLE 3: Gains of the horizontal VOR in the pre- and postflight periods for monkeys. The gain for the horizontal VOR was averaged for the rotations to the right and to the left, since there was no gain difference between the two rotations.

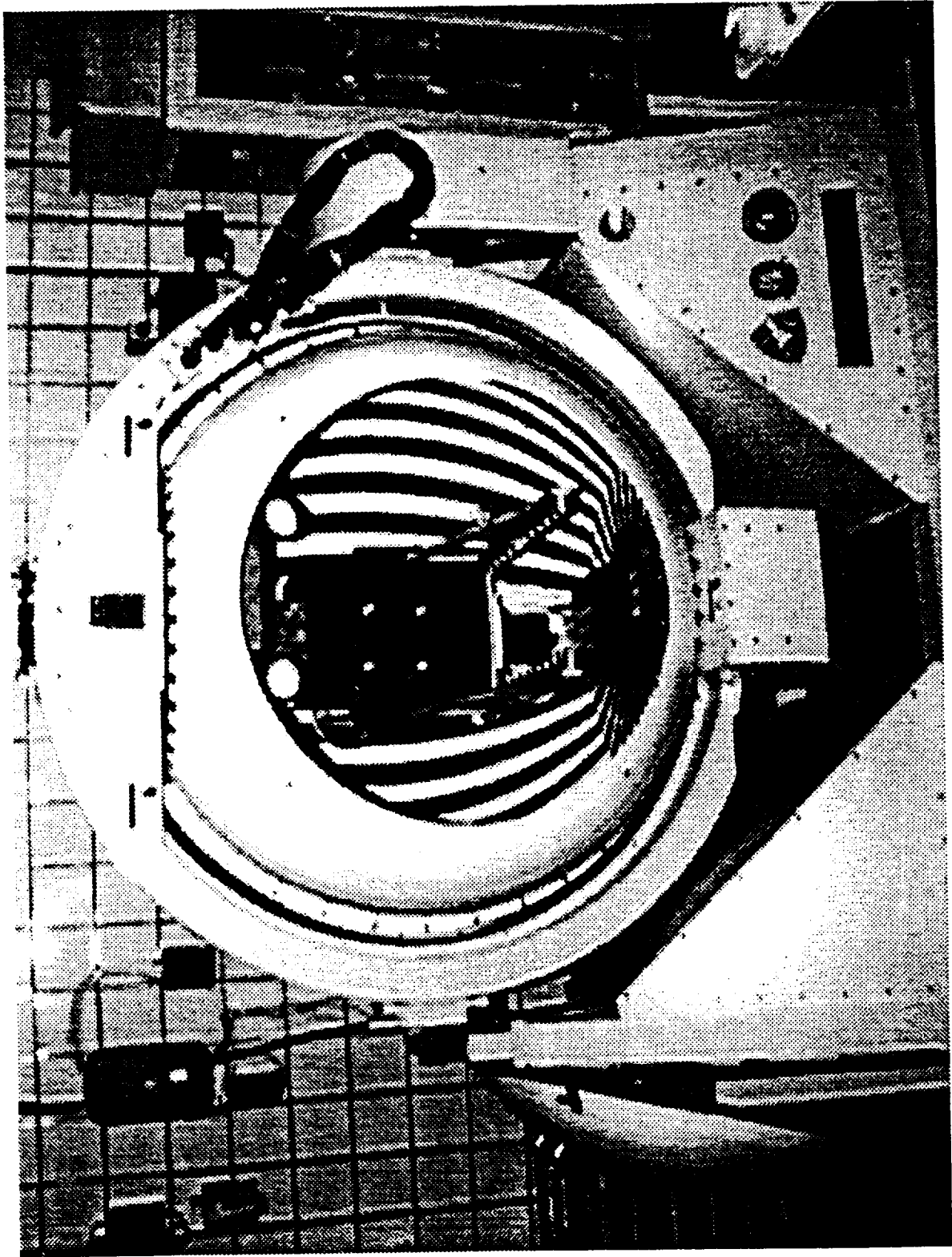


Figure 1: Four axis vestibular and optokinetic stimulator used in this series of experiments. See Methods for complete description of the apparatus.

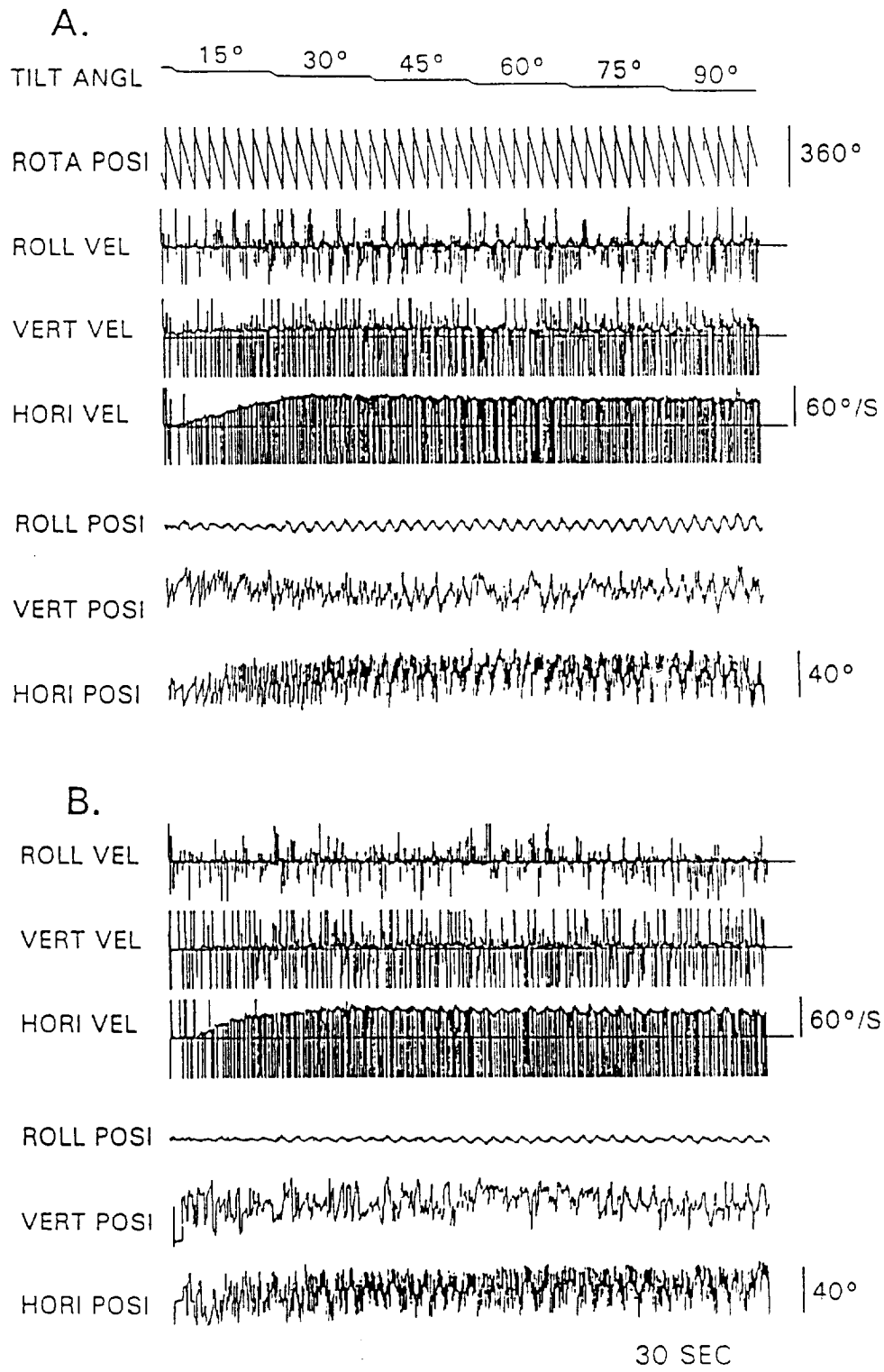


Figure 2: Nystagmus induced by rotation in darkness at $60^\circ/\text{s}$ about a tilted axis in darkness for 6151 before (**A**) and 7 days after (**B**) spaceflight. The animal was first rotated at $60^\circ/\text{s}$ about a vertical axis with the OKN drum in light inducing per-rotatory nystagmus whose slow phase velocity declined rapidly to zero (not shown). Then, the axis of rotation was tilted from 15° - 90° (Tilt Pos, first trace), while the yaw axis rotation continued (Yaw Pos, second trace), inducing nystagmus. Roll, vertical and horizontal eye velocity and position are shown, from top to bottom. Note the modulations in slow phase velocity (H Vel, fifth trace) and in roll eye position (Roll Posi, fifth trace) during the OVAR. Note the decrease in the modulation of roll position after flight (**B**). Note also that the steady state horizontal velocity was achieved both before and after flight, and that there was a reduction in vertical spontaneous nystagmus after flight.

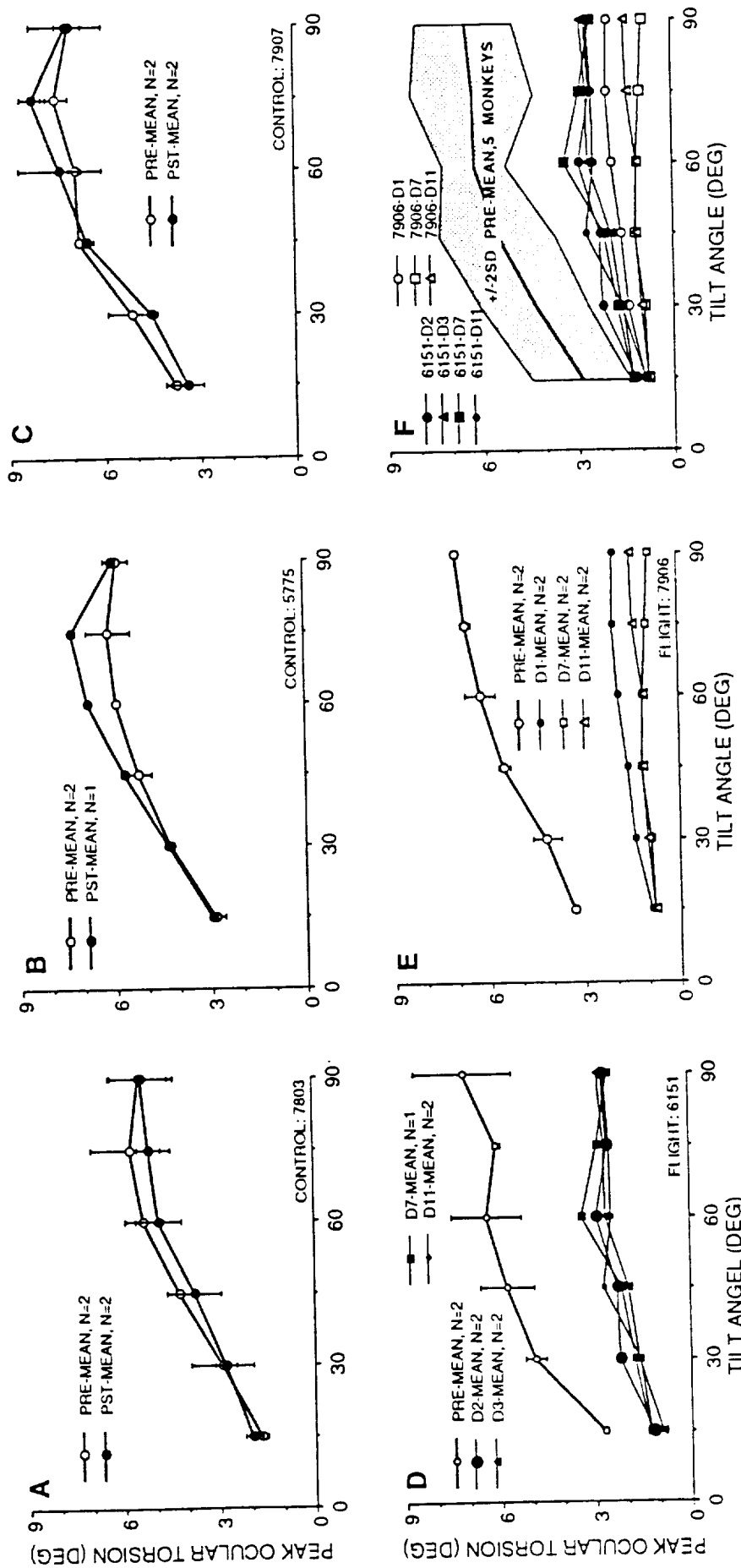


Figure 3: **A-E**, Graphs of preflight and postflight dynamic OCR induced by OVAR in three control monkeys (**A-C**) and the two flight monkeys (**D-E**). Five to six cycles were averaged for rotation to the right and to the left, and the means were combined into the value shown in the graph. The vertical error bar is $\pm 1SD$. Each control animal had a test 60-90 days before flight and after flight. The flight animals had a control test 60-90 days before flight and several tests after flight from the first (D1) to the eleventh day (D11). **F**, Mean and 2 standard deviation (shaded area) for control data from the 3 control animals and the preflight values for the flight animals. Note that the postflight data fell more than two SD from the mean at all tilt angles. This was a highly significant difference in unpaired t-tests.

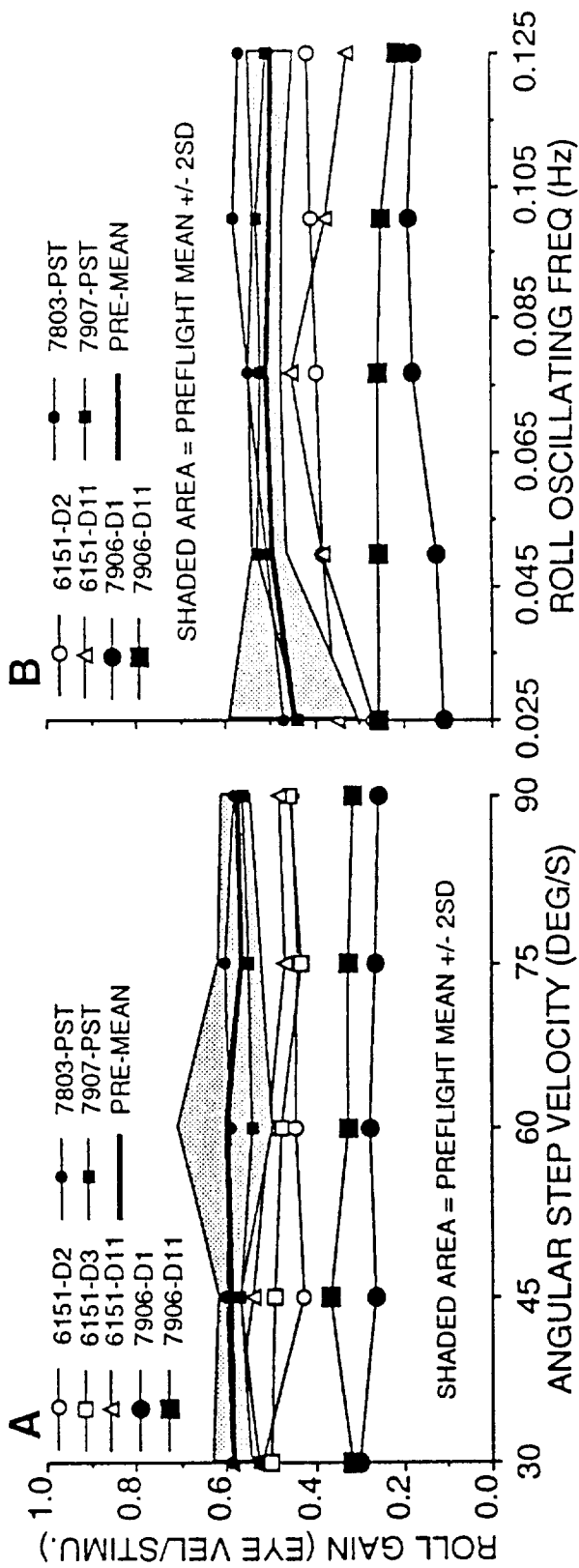


Figure 4: A, Graph of gain of Roll VOR induced by steps of velocity between 30 and 90°/sec. The mean for the preflight testing is shown by the heavy solid line (PRE-MEAN), which is surrounded by a shaded area representing \pm 2SD. There was a slight decrease in Roll VOR gain in 6151 after flight, and a larger decrease in the Roll VOR of 7906. B, Graph of gain of Roll VOR induced by sinusoids around a horizontal interaural axis. The shaded area shows the preflight mean \pm 2SD. After flight there was a decrease in the gain of the Roll VOR, more for 7906 than for 6151.

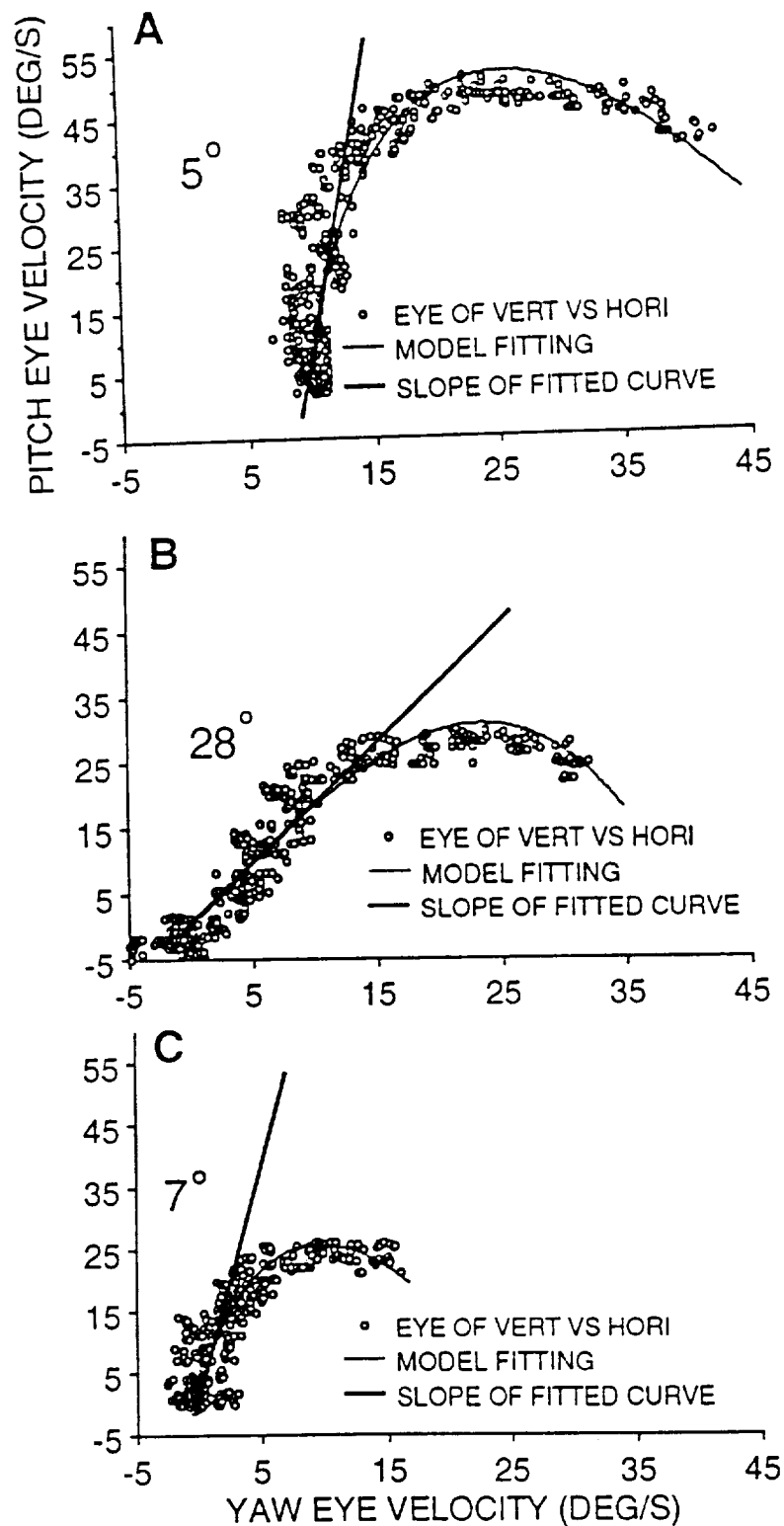


Figure 5: Phase plane graphs of vertical (ordinate) versus horizontal (abscissa) eye velocity for OKAN induced by yaw axis rotation with 7906 in a 90° tilted side down position. OKAN slow phase velocities began in each graph on the right and the velocities progressed toward zero in a curved fashion. The circles each represent the velocity of one slow phase. The solid curved line represents the fit of the data using a modified Levenberg-Marquardt algorithm. The straight line is the trajectory of the last part of the graph and shows the slope of the fitted curve as the data approached zero. **A**, Before flight, the yaw axis eigenvector had an angle of 5° from the vertical. **B**, Twenty-two hours after flight, the slope of the yaw axis eigenvector had shifted toward the body axis and was now 28° from the vertical. **C**, Several days later, the yaw axis eigenvector had returned to close to its original angle and now was deviated 7° from the vertical.

EXPERIMENT K-08-03

STUDIES OF VESTIBULAR NEURONS IN NORMAL, HYPER- AND HYPOGRAVITY

Principal Investigator:

Manning J. Correia
University of Texas Medical Branch
Galveston, Texas

STUDIES OF VESTIBULAR NEURONS IN NORMAL, HYPER- AND HYPOGRAVITY

Manning J. Correia

OVERVIEW

Ground Based Preflight Studies at UTMB Related to Cosmos Flight 2229 (BION 10)

11/1/92 - 8/22/92

- Established stereotaxic coordinates for medial vestibular nucleus, abducens nucleus and vestibular nerve then redesigned the head ring platform and microelectrodes to permit recordings from these deep neural structures.
- Completed development of surgical procedures to chronically implant orthodromic stimulation electrodes. Implanted two control rhesus monkeys at UTMB.
- Completed evaluation of eye movement measurement using ISCAN. Installed the ISCAN camera on the multi-axis rotator.
- Completed development of a system to permit active and passive head motion testing. Installed components on the multi-axis rotator.
- Participated in the development of the flight amplifier used to process neural signals during space flight.
- Evaluated several technologies used to produce a multiple microelectrode array. Developed and tested thin microelectrodes that were implanted as a bundle multiple microelectrode array in several flight candidates.
- Continued to develop computer programs in anticipation of recording from rectifying neurons (vestibular nuclei neurons).

Ground Based Preflight Studies at the Institute Biomedical Problems (IMBP) in Moscow Related to Cosmos Flight 2229 (BION 10)

8/22/92 - 9/6/92

- J. David Dickman (JDD), Ph.D. and Manning J. Correia (MJC), Ph.D. implanted microelectrode guide tube carrier platforms stereotaxically in 12 monkey flight candidates.

8/29/92 - 9/13/92

- Adrian A. Perachio (AAP), Ph.D., Denise Helwig and Samantha Edmonds implanted orthodromic stimulating electrodes in the bony labyrinths of 7 monkey flight candidates.

9/29/92 - 10/4/92

- AAP and JDD implanted 5 flight monkey candidates with orthodromic stimulating electrodes.

10/3/92 - 10/29/92

- MJC x-rayed all 12 flight candidates. MJC, AAP and JDD conducted electrophysiological studies to determine the stereotaxic coordinates of the vestibular nerve, the medial vestibular nucleus and the abducens nucleus.

11/11/92 - 11/21/92

- Studies were carried out to obtain preflight data from each of the flight monkey candidates. Recordings were obtained from monkeys 803, 775, 151, 907, 1401, and 856. From these monkeys, recordings were obtained from 35 horizontal canal afferents, 8 medial vestibular nucleus type II neurons, 8 medial vestibular nucleus type I neurons, 3 untyped medial vestibular nucleus neurons and one vertical medial vestibular nucleus neuron.

11/29/92 - 12/12/92

- Indwelling microelectrodes were implanted in several of the leading flight candidates.

Ground Based Preflight Studies at the Institute of Biomedical Problems (IMBP) Remote Facility in Plesetz Related to Flight 2229 (BION 10)

12/18/92 - 12/23/92

- Indwelling flight microelectrodes were implanted by JDD and AAP in other flight candidates. The location and number of Implants are summarized in the table below.

Flight Candidate Microelectrode Implants (Dec. 1992)			
Monkey	Location		
	Nerve	Nuclei	Cerebellum
803	multiple electrode (3)	multiple electrode (2)	single electrode (1)
907	single electrode (1)	single electrode (1)	single electrode (1)
151	single electrode (1)	single electrodes(4)	none
775	single electrode (1)	single electrode (1)	none
906	single electrode (1)	single electrodes(6)	single electrode (1)
892	multiple electrode (2)	multiple electrode (3) single electrodes(2)	single electrode (1)
476	none	single electrodes(3)	single electrode (1)

Inflight Studies Related to Cosmos Flight 2229 (BION 10)

12/26/92 - 12/23/92

- Studies were carried out in which recordings were made from the vestibular nerve and the vestibular nuclei in the two cosmonaut monkeys, 151 and 906.

Ground Based Postflight Studies at the Institute of Biomedical Problems (IMBP) in Moscow Related to Cosmos Flight 2229 (BION 10)

1/5/92 - 1/23/93

- Synchronous control studies were made on flight candidate monkeys 803 & 907. Recordings were obtained from 11 horizontal canal afferents from these monkeys.

- Postflight studies were carried out in which recordings were made from the vestibular nerve of the two cosmonaut monkeys, 151 and 906 as well as the vestibular nerve and vestibular nucleus of control monkeys 803, 907, 1401, 892. See Appendix 2. Recovery was on 1/10/93. First recordings were made on: 1/11/93-13 horizontal afferents recorded from monkey 906 and 5 afferents recorded from monkey 151; 1/12/93-5 afferents recorded from monkey 906 and 13 afferents recorded from monkey 151; 1/14/93-2 afferents recorded from monkey 906 and 10 afferents recorded from monkey 151; and on 1/21/93-10 afferents recorded from monkey 906 and 0 afferents recorded from monkey 151. During postflight tests on the control monkeys listed above, 12 horizontal canal afferents and 6 medial vestibular nucleus type I neurons were studied.

1/23/93 - 1/27/93

- Laboratory packed with the exception of the monkey multi-axis rotator.

5/3/93 - 5/7/93

- The monkey multi-axis rotator was disassembled, reassembled and packed for shipment to UTMB.

1/23/93 - 11/14/93

- Derived usable data from preflight, postflight and synchronous control tests. The results of those analyses are summarized in Tables 1-31 in Appendix 2. Graphical summary of these data are presented throughout the text that follows.

Presentations, Abstracts and Publications

1. Correia, M.J., A.A. Perachio, J.D. Dickman, and I.B. Kozlovskaya. Sensitivity Changes in Semicircular Canals Following Microgravity. World Space Congress, F1.2-M.1.02, p. 541, 1992.
2. Correia, M.J., A.A. Perachio, and J.D. Dickman. The Effects of Space Flight on the Inner Ear of Non Human Primates. Eleventh Annual Houston Conference on Biomedical Engineering Research, p. 131, 1993.
3. Correia, M.J., J.D. Dickman, A.A. Perachio, I.B. Kozlovskaya, and M.G. Sirota. Postflight Responses of Horizontal Semicircular Canal Afferents to Pulse Rotations, Cosmos 2229 symposium, Ames Research Center, 1993.

ABSTRACT

During the past year, pre-, in- and postflight studies were conducted in association with the Axon project for Bion 10 (Cosmos 2229). Recordings were made during pre- and postflight studies, from 118 horizontal semicircular canal afferents and 27 vestibular nucleus neurons in 7 rhesus monkeys; 137 pulse rotation protocols alone were executed (548 acceleration and deceleration responses were curve fit). Usable data was obtained from 127 horizontal afferents concerning their spontaneous discharge. Curve fits and analysis was made of sinusoidal and sum of sinusoidal responses from 42 and 35 horizontal afferents, respectively. Also recordings were made from neurons inflight from the two flight animals. The mean spontaneous rate varied from 128 spikes/sec. during preflight to 92 spikes/sec during postflight (day 5) - a change of 28%. In direct contrast to the results of Cosmos 2044, the best fitted neural adaptation operator (k) and the gain of the pulse response were decreased during post flight when compared to preflight. Surprisingly, the best fitted gain and k values for the sum of sines were slightly elevated during post flight tests. The gain and phase of single sine responses were compared for pre- and post flight tests and compared to a larger population of afferents (Miles and Braitman, 1980). In contrast to Cosmos 2044 results where on the first day of post flight testing the gains of the best fitted sine response were skewed toward the higher values of the Miles and Braitman distribution, the gain of the best fitted sine responses during the first day of

post flight testing (day 2) during Cosmos 2229 were exactly on the mode of the Miles and Braitman distribution. Thus, at least for the periodic stimuli, (pulses and sine waves) we found no change in gain and neural adaptation during post flight testing following Cosmos 2229. This conclusion is different from the one derived following the Cosmos 2044 flight (Correia et al., 1992). Cosmos flight 2229 differed from Cosmos flight 2044 in several significant ways: For example, during *preflight*, (1) The animals preflight training was different (less well trained on the gaze task) and (2) the animals were exposed to more experimental manipulations (surgical and rotational). *Inflight*, (1) the animals were required to make a pointing gesture (motor response) in association with eye movements to obtain reward, (2) the inflight diet was different (more balanced), (3) the feeder for one of the animals clogged following 9 days of flight resulting in evident dehydration and probably less head motion exposure in that monkey and (4) there was limited video taping of the monkeys in space. During *postflight*, (1) we were unable to test the flight animals until 26 hours postflight as compared to 14.5 hours during Cosmos 2044, (2) the animals received significantly more exposure to motion stimuli during postflight testing than during Cosmos 2044. These differences in the vestibular environment will require analysis of several parameters other than just neural and eye movement responses. For example, computer programs will have to be written and used to recover and quantitate the number of head movements made by each animal during flight. This activity is critical to the production of neural adaptation and increased gain.

METHODS AND RESULTS

Differences from Cosmos 2044 (Correia et al. 1992)

A summary of the neural recordings and stimulation protocols carried out on five control and two flight monkeys during preflight and postflight tests associated with Cosmos Flight 2229 are presented in Appendix 1. Because of time restrictions, two types of neurons were studied in association with this flight. These two types of neurons were horizontal (lateral) semicircular canal afferents and type I or type II vestibular nuclei neurons found in the medial vestibular nucleus. Rotation protocols used for study of the horizontal semicircular canal afferents were similar to those used during Cosmos Flight 2044 (Correia et al., 1992) except that the number of protocols were abbreviated to include: test of spontaneous discharge, pulse rotation test, sum of signs tests (bandwidth from 0.2 hertz to 1.0 hertz) and sinewave test (0.2 hertz). Rotation protocols for the vestibular nuclei neurons included: spontaneous sinusoidal discharge test, oscillations at 0.2 hertz, 0.5 hertz, 1.0 hertz; a pulse of constant velocity of 60 degrees per second and a sum of sines stimulus covering the band width from 0.02 hertz to 1.0 hertz.

Neurons in the vestibular nuclei and semicircular canal afferents were identified and functionally characterized by their responses to natural vestibular stimulation and to electrical stimulation of the vestibular nerve. The technique for the latter test required that a method be developed for chronic implantation of electrodes for stimulation across the bony labyrinth of awake rhesus monkeys. In a single monkey, the implantation technique used by Broussard et al (1992) was attempted. This technique requires dissection through the mastoid bone to locate the superior semicircular canal. An opening is made in the canal wall near the ampullae for the placement of one of a pair of stimulating electrodes. The reference electrode is placed near the posterior wall of the ear canal. The technique also involves exposure of the dura overlying the lateral tip of the dorsal paraflocculus. The technique was judged to be too difficult for our application and carried the added risk that vertical canal function might be compromised during the course of the entire project. Dr. Lisberger informed us that cathodal stimulation, such as would be used in our studies, might lead to bone growth and to the eventual occlusion of the implanted canal.

The approach we finally used was derived from a method reported by Minor and Goldberg (1991) for galvanic stimulation of the squirrel monkey labyrinth. This involves a placement of a single electrode into a hole drilled into the promontory near the round window. The tip of the electrode seals an opening made into the perilymphatic space. The electrode consists of a platinum plated,

teflon insulated silver wire (250 micron uncoated diameter) with a 1.0 mm exposed tip. The reference electrode is of similar material but with a longer tip exposure (3.0 mm). That electrode is placed into a hole drilled deep into the posterior attachment of the zygomatic arch.

Surgery was performed under general anesthesia and sterile conditions. In our facilities at UTMB, we successfully implanted three rhesus monkeys, two unilaterally and one bilaterally. The post auricular incision was made and the platyzma divided. The remaining underlying soft tissue of the ear canal was dissected to expose the external bony auditory meatus and the zygomatic arch. Two self-tapping, stainless steel screws were placed near the ear canal into the parietal bone, dorsal to the parietal-occipital ridge. The soft tissue was carefully dissected along the posterior wall of the meatus to level of the annulus. The tympanic membrane was incised inferiorly and posteriorly to gain entrance to the middle ear. In immature rhesus monkeys, the external meatus is so oriented as to allow direct visualization of the round window via this approach. In more mature animals, the canal is rotated forward relative to the basal skull, thus obscuring the promintory and the long process of the malleus, requiring further dissection.

Exposure of the round window in mature rhesus monkeys is achieved by drilling away the deepest most posterior wall of the external auditory meatus. This is best achieved with a diamond coated drill so as to minimize danger to the underlying facial nerve and middle ear ossicles. In a series of eleven unilaterally implanted rhesus monkeys, facial nerve damage occurred in only one animal. Following further exposure, the long process of the malleus and the facial nerve are visualized. The site of implantation of the stimulating electrode is posterior to the malleus. The facial nerve is displaced rostrally to protect it during implantation. The ossicles are not this disarticulated. The surface of the promontory is scraped to remove the periosteum and thinned with a diamond tipped round bur. A hole is then drilled in the center of the resulting concavity and the electrode tip is inserted, seated firmly at the shoulder formed by the teflon insulation. The wire is pushed against the posterior wall of the meatus and formed against the drilled surface. The external portion of the wire is wound around one of the skull screws and cemented to it with dental acrylic. The reference electrode is placed into the hole in the zygomatic arch, wound around the second screw and cemented in place. The two leads are then passed under the temporalis muscle and exteriorized at the head restraint implant with a curve needle. The wound is closed in layers with absorbable suture and the skin closed with silk suture material. Antibiotics are routinely administered perioperatively.

The animals implanted in Moscow generally recovered from surgery with no sequelae. One monkey, that was diagnosed as having meningitis at the time of surgery, was found to have a positional nystagmus postoperatively. Since this animal was tested only during the postoperative period, it was not possible to definitively assess the relationship of those symptoms to the implant. Another monkey was reported to have an ipsilateral head tilt and was acutely ataxic. Those symptoms resolved quickly. No vestibulo-ocular abnormalities were reported by other investigators in that animal. Afferent activity and vestibular nuclear responses were comparable to those of the remaining animals.

In Figure 1, an example of an entrained response of a horizontal semicircular canal afferent is illustrated. The latency of the action potential is less than 0.5 msec. This response was obtained during ground based testing and strongly argues that we recorded from primary afferents. No histological verification has been possible. Response thresholds ranged from the 30 to 100 microamps for single monophasic cathodal pulses. Diphasic responses were recorded in neurons located contralaterally at the stereotaxic location of the abducens nuclei. Cells in those areas discharge tonic/phasically with ipsilateral horizontal eye position/movement.

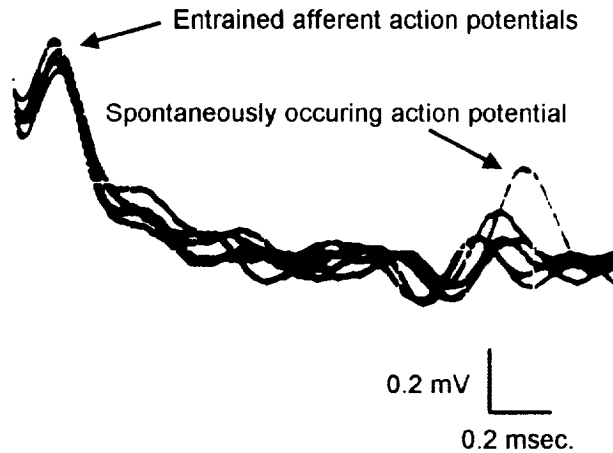


Figure 1. Entrained action potentials from a horizontal semicircular canal afferent. The orthodromic stimulation produced entrained action potentials with latencies less than 0.5 msec. Also observed at the right of the figure is a spontaneously occurring action potential.

Recordings were made from 86 neurons in control animals and 59 neurons in the flight animals. Thus 145 neurons were studied in total during pre- and postflight ground base tests. Neurons studied during flight have not yet been analyzed. The procedures for analysis of the data resulting from the rotation protocols that stimulated the horizontal semicircular canals have been published elsewhere (Correia et al., 1981, Correia et al., 1992). Briefly, this analysis can be stated as follows: pulse response analysis-using nonlinear curve fitting techniques, one model was (the adaptation model - Correia et al., 1992) was fit to each of the four pulse responses that occur during a given rotation pulse protocol. In some cases the responses were so noisy that the data was rejected. If the protocols were repeated, the protocol that yielded the histogram with the least noise was chosen. Data from repeated protocols was not included. That is, only one set of parameters from the four pulses is included for each neuron. For each sinusoidal rotation, curve fit techniques were used to estimate the gain and phase of each of the sinusoidal responses to head velocity. For the sum of sinusoidal stimuli, the total neural response was exposed to cross Fourier techniques to determine the gain and phase of the cycle histogram re head velocity. Mathematical functions based on the adaptation model (Thorson and Biederman-Thorson, 1974, Correia et al., 1981, Correia et al., 1992) was used to curve fit the pulse response and the frequency response data. The parameters derived from analysis of the time and frequency domain responses of the semicircular canal afferents was clustered into groups along the preflight and postflight time continuum and compared. As yet we have not been able to statistically compare the parameters. This will be the next step. However, descriptive first order statistics have been completed and they are presented in Appendix 2 and in the graphs that follow.

It should be noted that in *all* the figures that follow that during Cosmos 2229 during Postflight days 6 and 7 only control animals were tested.

Figure 2 presents mean gain values derived from best fitted responses to pulse stimulation. The numbers in the bars represent the number of afferents that comprise the mean. It can be seen that in contrast to Cosmos 2044 the postflight mean gains are depressed relative to preflight, synchronous and postflight controls (Postflight day 6).

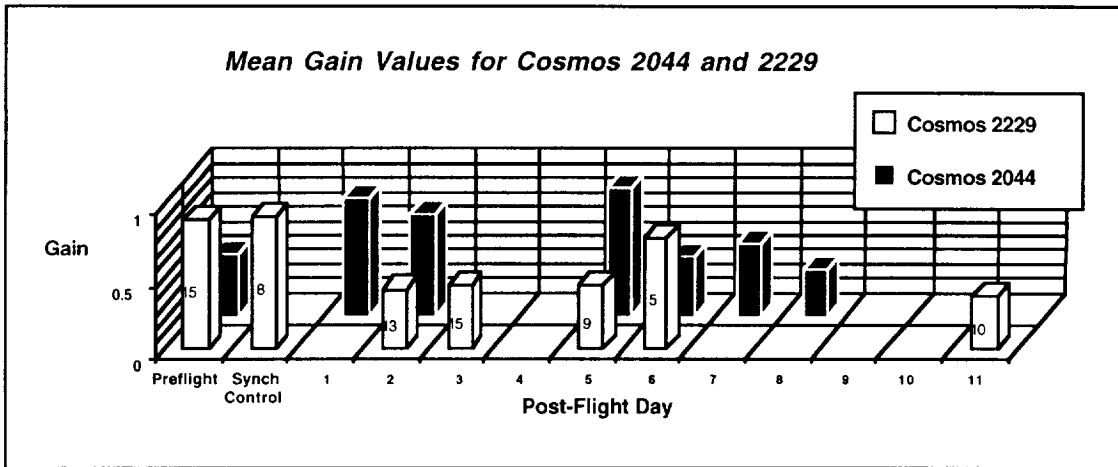


Figure 2. Mean Gain values for pulse responses of horizontal afferents during Cosmos 2044 and 2229.

As with the mean gain values, the parameter that represents the degree of neural adaptation (k), plotted in Figure 3 is depressed on postflight days 2, 3, and 5 when compared to preflight and postflight controls and when compared to comparable test days following Cosmos flight 2044.

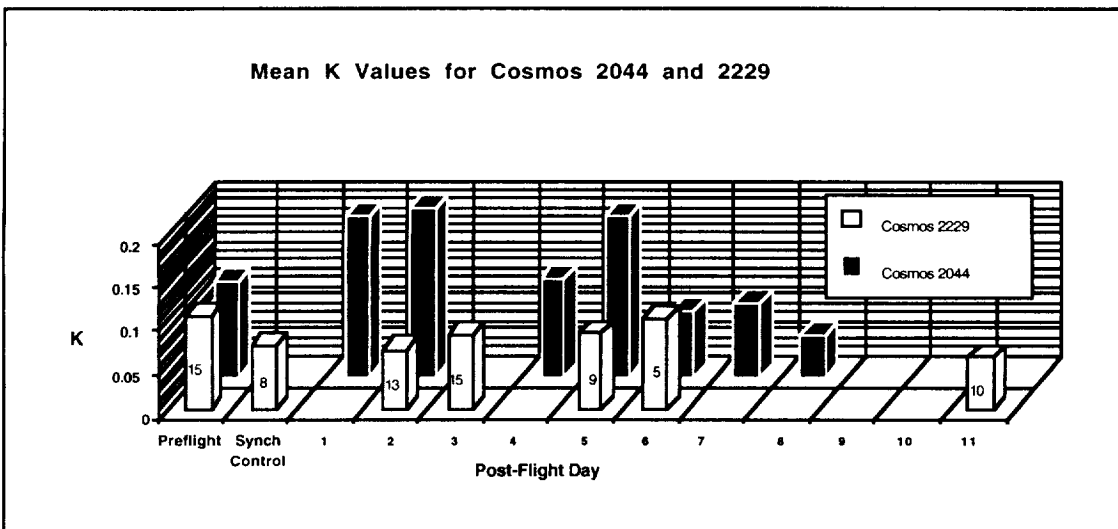


Figure 3. Mean neural adaptation (k) values for pulse responses of horizontal afferents during Cosmos 2044 and 2229.

Again, in contrast to the results derived from the postflight data following Cosmos 2044, the mean long time constant of the semicircular canal deduced from best fitted functions of the pulse histogram response and shown plotted in Figure 4, lengthened in the flight animals when compared to preflight, synchronous controls and postflight controls (postflight day 6).

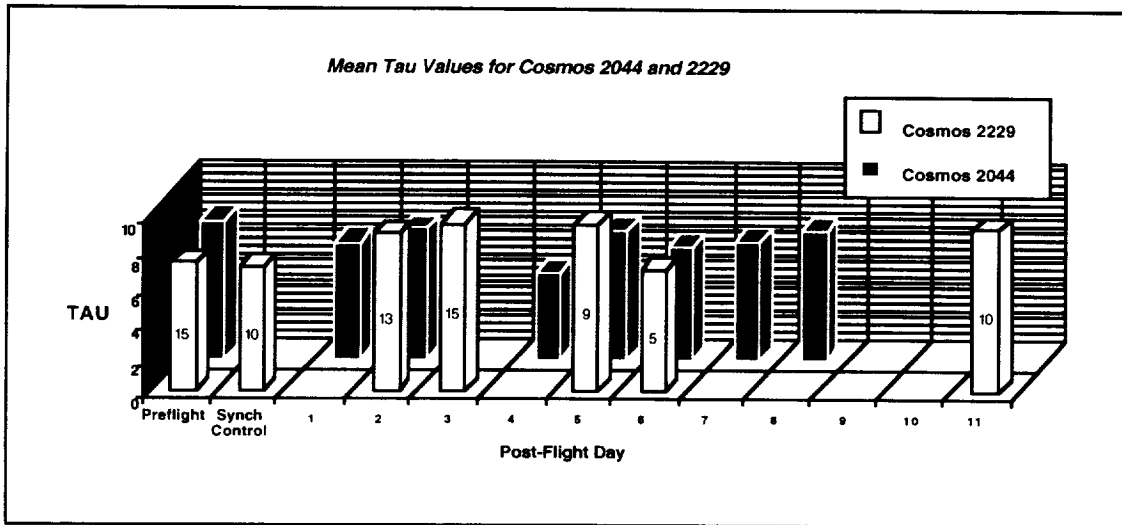


Figure 4. Mean Tau (deduced long time constant of the semicircular canal) values for pulse responses of horizontal afferents during Cosmos 2044 and 2229.

Like the data following Cosmos 2044, the mean baseline of the frequency of firing between pulses (DC level), plotted in Figure 5, was not much different during postflight testing when compared to control responses. The mean responses differed from 125 spikes/sec to 95 spikes/sec. These values fall around the mean firing rate determined by other investigators (e.g. ~100 spikes/sec. Miles and Braitman, 1981).

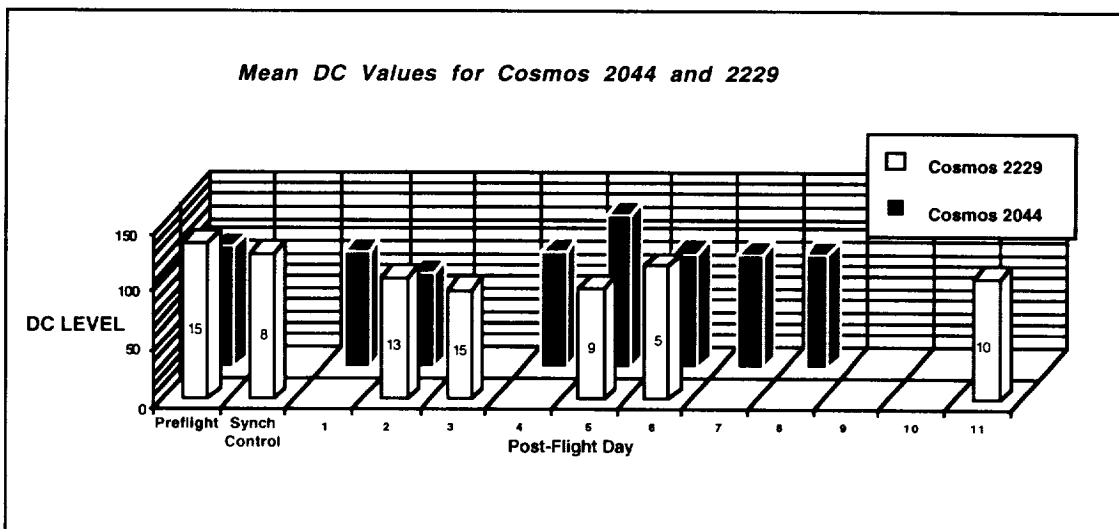


Figure 5. Mean spontaneous values (DC level) obtained as an asymptotic response following pulse rotations during Cosmos 2044 and 2229.

The mean spontaneous firing rate, plotted in Figure 6 was obtained from interspike interval histograms of spontaneous discharge prior to the first pulse rotation. The mean values showed depression during the postflight testing but like the mean DC level values, the firing rate was near 100 spikes/sec.

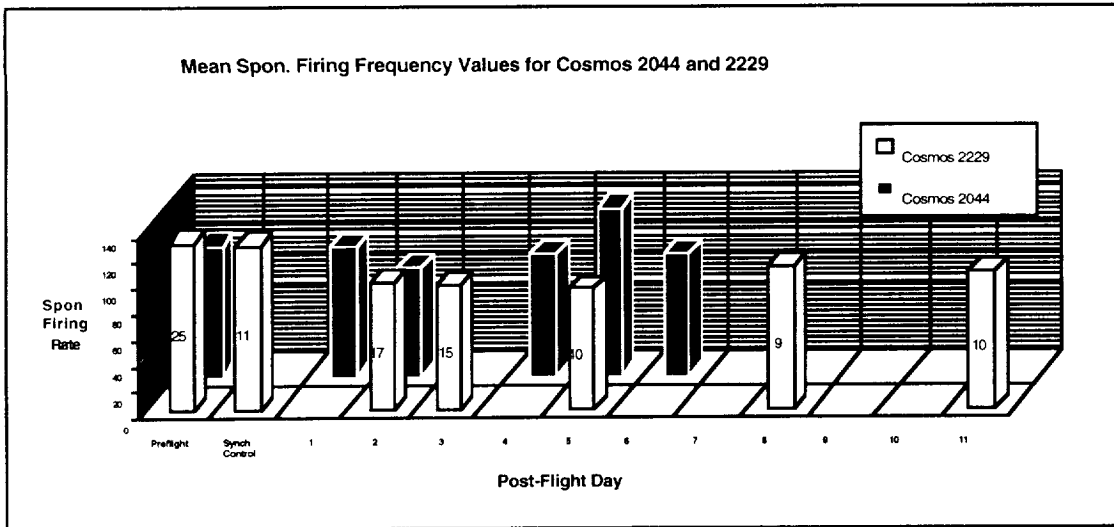


Figure 6. Mean frequency of firings values for spontaneously discharging horizontal afferents during Cosmos 2044 and 2229.

In the control animals the coefficient of variation (CV) for all afferents (see Table 8 in Appendix 2) ranged from 0.34 to 0.03. But the mean values for each day, (plotted in Figure 7) ranged from 0.09 to 0.15. That is, the mean CV of the afferents across days would be classified as regularly firing after the distribution of Louie and Kimm (1976). In this statistic our results during flight 2229 were almost identical to the results of flight 2044.

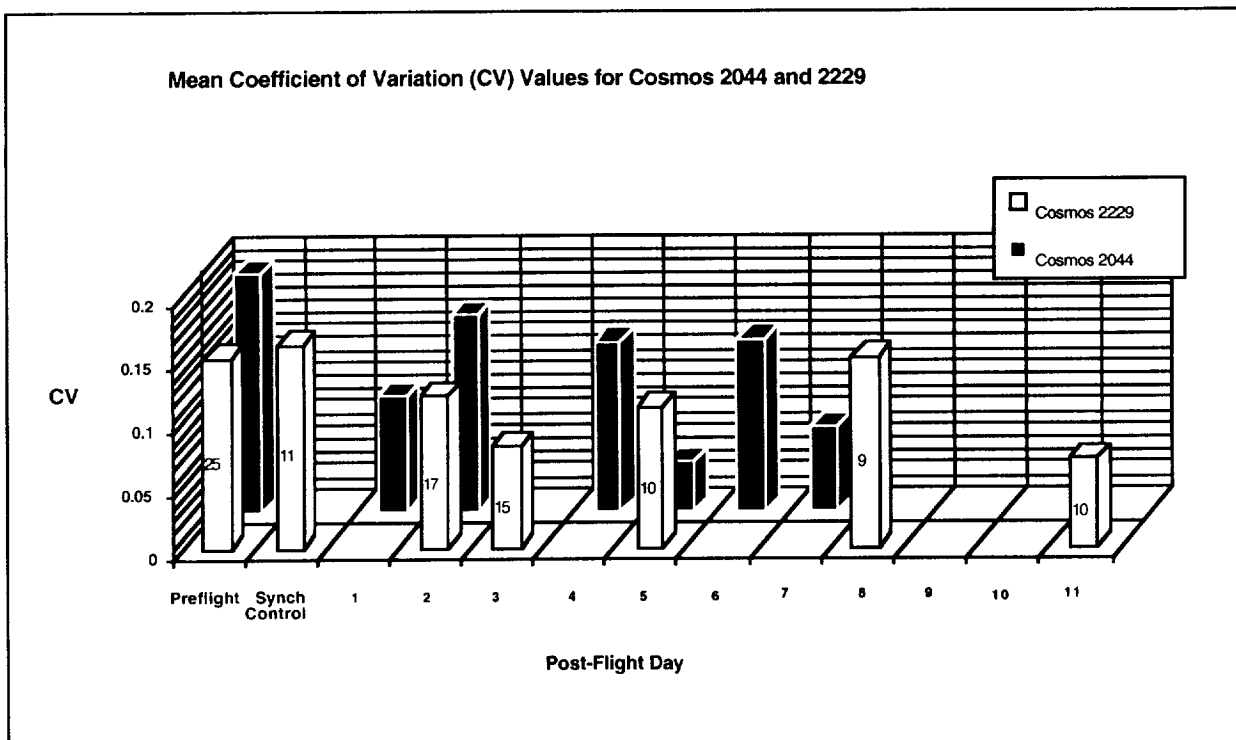


Figure 7. Mean coefficient of variation of spontaneously discharging horizontal afferents during Cosmos 2044 and 2229.

The best fitted parameters plotted in Figures 1-5 were derived from the equation:

$$r(t) = (G/t^k)[\gamma^*(-k, -t/\tau_L)e^{-t/\tau_L}] + DC; \text{ where } \gamma^*(a, t) = \int_0^t x^{a-1} e^{-x} dx \quad (1)$$

and $\gamma^*(a, t)$ is the incomplete gamma function (which is single-valued and finite in terms of a and t), G = gain, k = across frequency adaptation, τ_L (TAU) = cupula long time constant and DC = non stimulated (spontaneous) firing rate (Correia et al., 1981).

The Laplace transform of Eq. 1 with a term $(\tau_V s + 1)$, representing the response to cupula velocity at higher frequencies (Fernandez and Goldberg, 1971), is a transfer function of the form

$$H(s) = G s^{k+1} (\tau_V s + 1) (\tau_L s + 1)^{-1} \quad (2)$$

where G = the frequency independent gain ; k = the across frequency adaptation operator; $s = 1 + j\omega$; $\omega = 2\pi f$; τ_V = velocity time constant and τ_L = the long time constant of the semicircular canals. In the next 3 figures the parameters k , τ_V and τ_L are presented. These parameters represent best fitted values of Eq. 2 to a sum of sines frequency response.

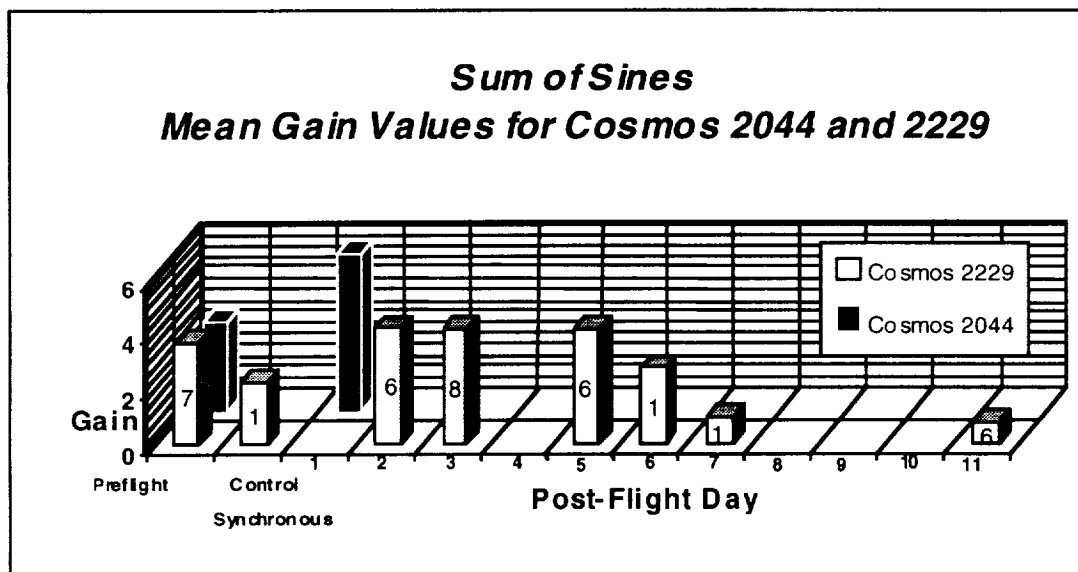


Figure 8. Mean best fitted values of G (frequency independent gain term) of cycle histogram response to sum of sines by horizontal afferents during Cosmos 2044 and 2229.

It is interesting that the frequency domain equivalent of the pulse response produces an increase in gain during post flight days 2, 3, and 5 relative to the pre- and post flight controls . The sum of sines differs from the pulse in that most of the frequency content is below 0.4 Hz and the sum of sines is an unpredictable stimulus.

In Figure 9 (below) it can be noted that while the mean value of k increases on the second post flight day, the increase is not nearly as dramatic as noted during Cosmos 2044 (black bars).

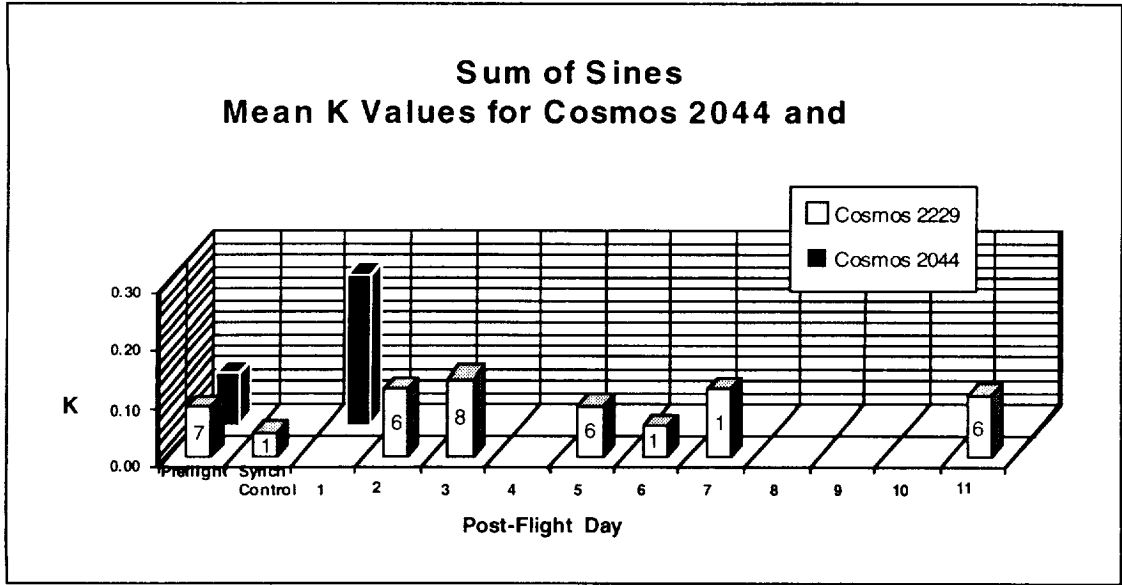


Figure 9. Mean best fitted values of K (across frequency neural adaptation operator) of cycle histogram response to sum of sines by horizontal afferents during Cosmos 2044 and 2229.

There does not appear to be a systematic change in the mean best fitted parameter τ_v shown plotted in Figure 10 below.

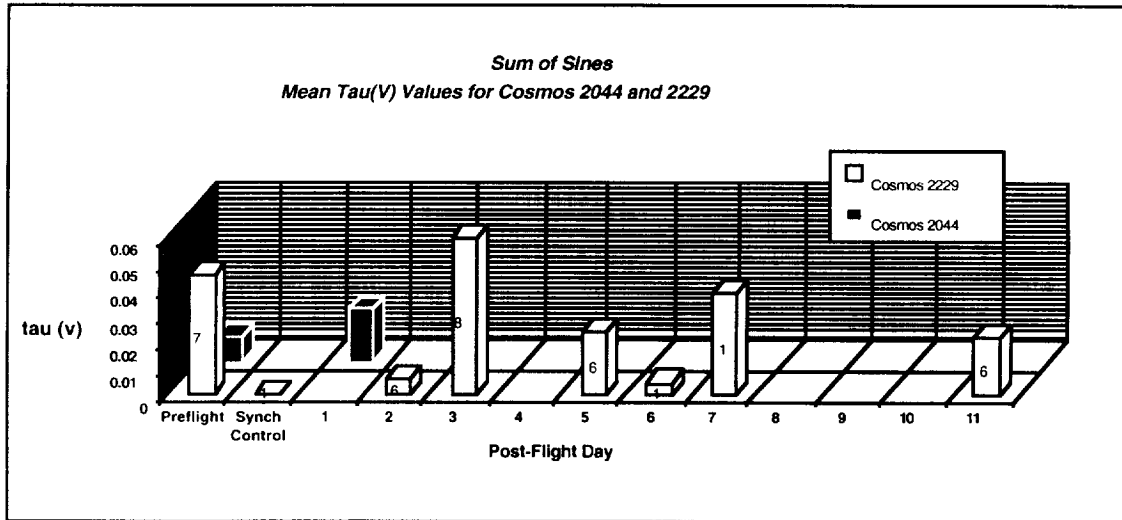


Figure 10. Mean best fitted values of τ_v (across frequency neural adaptation operator) of cycle histogram response to sum of sines by horizontal afferents during Cosmos 2044 and 2229.

During the first day of postflight testing during Cosmos 2044, the long time constant of the semicircular canal decreased as indicated by the black bars. During the first postflight day of Cosmos 2229, the parameter τ_L increased.

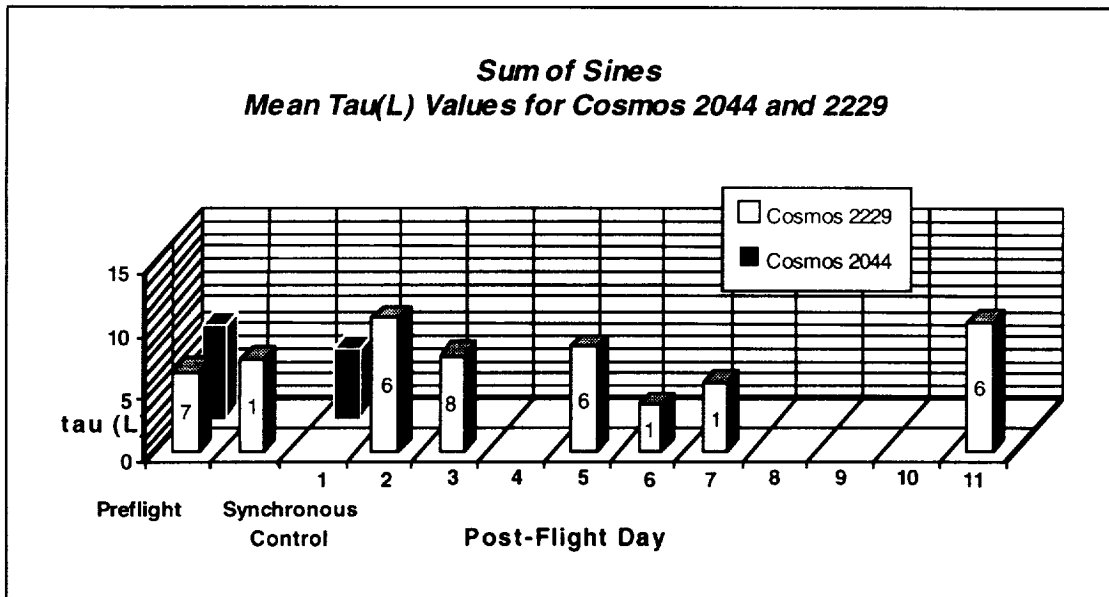


Figure 11. Mean best fitted values of τ_L (semicircular canal long time constant operator) of cycle histogram response to sum of sines by horizontal afferents during Cosmos 2044 and 2229.

The next 2 three dimensional bar histograms display gain values calculated from the best fitted sine function to the cycle histogram of the afferent response to a sinusoidal yaw rotation of 30°/sec. amplitude and 0.2 Hz frequency. As a reference, the histogram of gains from Miles and Braitman (1980) sinusoidal response to 0.2 Hz are presented. Presented in Figure 12 are the gains for the control monkeys during both Cosmos 2044 and 2229. It can be seen, for example that the distribution of gains from post -flight controls in Cosmos 2229 are similar to those published by Miles and Braitman (1980).

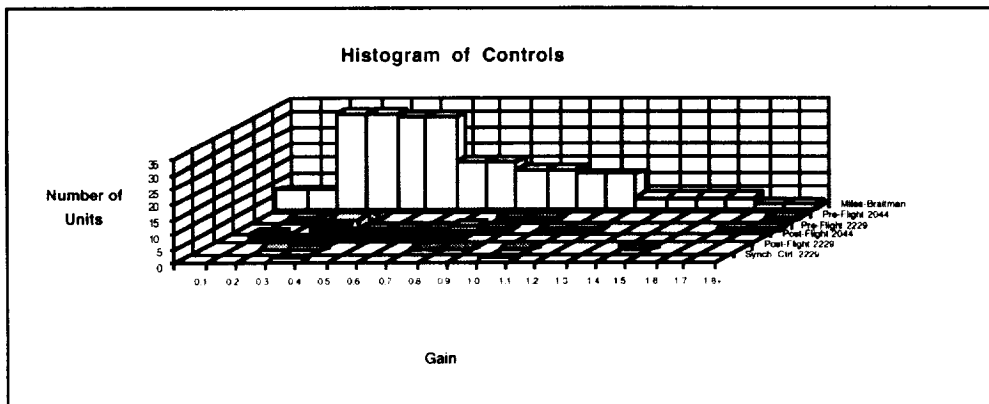


Figure 12. A three dimensional histogram of sinusoidal gains from control monkeys during testing associated with Cosmos 2044 and Cosmos 2229. The data of Miles and Braitman (1980) are presented for comparison.

Figure 13 presents the same type plot but postflight data from different days during Cosmos 2044 and 2229 are presented. The striking difference between the gains during Cosmos 2044 and 2229 can be observed by comparing postflight day 1 - Cosmos 2044 and postflight day 2 - Cosmos 2229. During Cosmos 2044, the gain values are skewed toward the higher end of the Miles and Braitman

distribution; during the first post flight test day (day 2) during Cosmos 2229, the values are directly in line with the central tendency values of Miles and Braitman (1980).

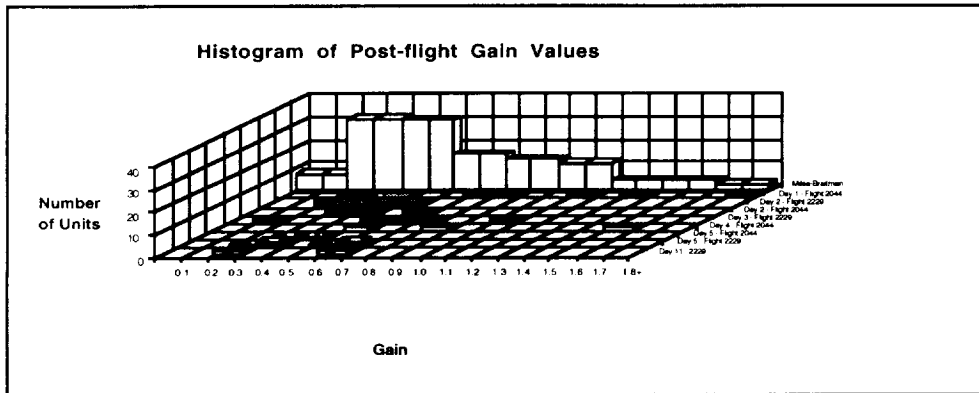


Figure 13. A three dimensional histogram of sinusoidal gains from flight monkeys during postflight testing associated with Cosmos 2044 and Cosmos 2229. The data of Miles and Braitman (1980) are presented for comparison.

DISCUSSION

In contrast to Cosmos 2044 results (Correia et al., 1992) where on the first day of post flight testing the gains of the best fitted pulse, sine and sum of sine response were skewed toward the higher values of the Miles and Braitman (1980) distribution, the gain of the best fitted sine and pulse responses during the first day of post flight testing (postflight day 2) during Cosmos 2229 were exactly on the mode of the Miles and Braitman (1980) distribution. Thus, at least for the periodic stimuli, (pulses and sine waves) we found no change in gain during post flight testing following Cosmos 2229. Moreover, during postflight day 1 during Cosmos 2044 we found an increased level of neural adaptation as reflected by an increased mean k value. After issuing the caveat that we only sampled a small number of afferents, we (Correia et al., 1992) suggested the increased gain could result from some non-vestibular factor secondary to space flight such as stress or changes in body calcium levels or some vestibular factor such as a strategy to obtain reward without having to make large head movements by increasing the semicircular canal gain. This latter speculation is predicated on the assumption that the monkeys during space flight make numerous head movements. Increase in neural adaptation would also logically follow from numerous head movements. Also, increased gain, increased k and irregular firing are correlated in semicircular canal afferents. Thus, we could have simply sampled a population of neurons with high G and k . But, most of the units we sampled were regularly firing. Analysis of the mean sinusoidal gain data from Cosmos 2229 (summarized in Figure 13), indicated that relative to postflight controls, the gain and k values were depressed, but relative to the data of Miles and Braitman (1980), the values were on the mean of their distribution. Future statistical comparisons will be necessary to determine if the mean gain and k values from flight 2229 and those of flight 2044 and those of Miles and Braitman (1980) are from the same population. The gain and particularly the neural adaptation observed during Cosmos 2044 was dramatic and showed a reversible trend with time following recovery. Why could these data be different from those of flight 2044? Cosmos flight 2229 differed from Cosmos flight 2044 in several significant ways: First, different monkeys were flight monkeys. Although during both flights the microgravity exposure was similar, several differences existed. For example, during *preflight*; (1) The animals' preflight training was different (the animals were less well trained on the gaze task) and (2) the animals were exposed to more experimental manipulations (surgical and rotational) and in flight 2229 the animals carried an indwelling electrode in one labyrinth. *Inflight*, (1) the animals were required to make a pointing gesture (motor response) in association with eye movements to obtain reward, (2) the inflight diet was different (more balanced), (3) the feeder for one of the animals clogged following 9 days of flight

resulting in evident dehydration and probably less head motion exposure in that monkey and (4) there was limited video taping of the monkeys in space. During *postflight*, (1) we were unable to test the flight animals until 26 hours postflight as compared to 14.5 hours during Cosmos 2044, (2) in the intervening interval between recovery and testing, and on subsequent postflight days, the animals received significantly more exposure to linear and angular motion stimuli than during Cosmos 2044.

Since gravity acts primarily on the otolith organs, it was a surprise that the gain and neural adaptation of the semicircular canals was increased following microgravity during Cosmos 2044. It may ultimately turn out that with a large sample of afferent data that gain and adaptation may not change. However, to fairly compare the results, we must prove that the angular head motion environment in flight was the same for Cosmos 2044 and 2229. To accurately compare the angular head motion environment will require analysis of several parameters other than just neural and eye movement responses. For example, it must be determined that during Cosmos flight 2229 that both monkeys made as many head movements during the gaze test as their counterparts during Cosmos flight 2044. The number of head movements made by each animal during both flight must be quantitated.

ACKNOWLEDGMENTS

The P.I. (M.J. Correia) and Co. Is (A.A. Perachio, J.D. Dickman, I.B. Kozlovskaya, and M.B. Sirota) of this work gratefully acknowledge the hard work and dedication of our colleagues at the Institute of Biomedical Problems in Moscow and particularly our American colleagues-James Connolly, Denise Helwig, Samantha Edmonds, Elizabeth Clark, Bill Little, Andy Couch, Carrie Sanchez and Stacie McMahan.

REFERENCES

1. Broussard, D.M., Bronte-Stewart H.M., and S.G. Lisberger. Expression of Motor Learning and the Response of the Primate Vestibulo-ocular Reflex Pathway to Electrical Stimulation. *J. Neurophysiol.*, 67:1493-1508, 1992.
2. Correia, M.J., Perachio A.A., Dickman J.D., Kozlovskaya I.B., Sirota M.G., Yakushin S.B., and I.N. Beloozerova. Changes in Monkey Horizontal Semicircular Canal Afferent Responses After Space Flight. *J. Appl. Physiol.*, 73(2):112S-120S.
3. Correia, M.J., Landolt, J.P., M.-D. Ni, Eden A.R., and J.L. Rae. A Species Comparison of the Linear and Nonlinear Transfer Characteristics of Primary Afferents Innervating the Semicircular Canals. In *The Vestibular System: Function and Morphology*. T. Gualtierotti, ed. (Springer-Verlag, New York, 1981), pp. 280-316.
4. Fernandez, C., and J.M. Goldberg. Physiology of Peripheral Neurons Innervating Semicircular Canals of the Squirrel Monkey. II. Response to Sinusoidal Stimulation and Dynamics of Peripheral Vestibular System. *J. Neurophysiol.* 34: 661-675, 1971.
5. Louie, A.W., and J. Kimm. The Response of 8th Nerve Fibers to Horizontal Sinusoidal Oscillation in the Alert Monkey. *Exp. Brain Res.* 24: 447-457, 1976.
6. Miles, F.A., and D.J. Braitman. Long-term Adaptive Changes in Primate Vestibuloocular Reflex. II. Electrophysiological Observations on Semicircular Canal Primary Afferents. *J. Neurophysiol.* 43:1426-1436, 1980.
7. Minor, L., and J.M. Goldberg. Vestibular Nerve Input to the Vestibulo-ocular Reflex: A Functional Ablation Study in the Squirrel Monkey. *J. Neurosci.*, 11:1636-1648, 1991.

8. Thorson, J., and M. Biederman-Thorson. Distributed Relaxation Processes in Sensory Adaptation. *Science*. 183: 161-172, 1974.

APPENDIX 1

A summary of the pre- and postflight testing. The Table on pages 149-155 chronicles the pre and postflight testing of all monkeys. The column type denotes whether the neuron was a lat. (horizontal) afferent, a type I or type II vestibularnuclear neuron and whether the neuron could be further classified as a pvp type neuron. The location column denotes the anterior-posterior and the lateral stereotaxic coordinates of the electrode tract. For example, ap0l10 means anterior-posterior 0 and lateral 10 mm from the midline of the skull. The protocol describes the test. The terms step and pulse are used interchangeably throughout this report.

Summary of individual neurons and experimental conditions observed during pre-and post flight testing

Time	cell	time	date	type	side	location	monkey	protocol	tape	footage
preflight	1	pre control	11/14/92	lat. aff.	left	ap0112	803	spon	1	2200
preflight	1	pre control	11/14/92	lat. aff.	left	ap0112	803	step	1	2250
preflight	1	pre control	11/14/92	lat. aff.	left	ap0112	803	ss	1	2300
preflight	1	pre control	11/14/92	lat. aff.	left	ap0112	803	sine0.2	1	2460
preflight	2	pre control	11/14/92	lat. aff.	left	ap0112	803	spon	1	2536
preflight	2	pre control	11/14/92	lat. aff.	left	ap0112	803	step	1	2600
preflight	2	pre control	11/14/92	lat. aff.	left	ap0112	803	step-rpt	1	2662
preflight	2	pre control	11/14/92	lat. aff.	left	ap0112	803	sine0.2	1	- 2727
preflight	2	pre control	11/14/92	lat. aff.	left	ap0112	803	ss	1	2770
preflight	2	pre control	11/14/92	lat. aff.	left	ap0112	803	sine1.0	1	2855
preflight	3	pre control	11/14/92	lat. aff.	left	ap0112	803	spon	1	2887
preflight	4	pre control	11/14/92	lat. aff.	left	ap0112	803	spon	1	2946
preflight	4	pre control	11/14/92	lat. aff.	left	ap0112	803	step	1	2946
preflight	5	pre control	11/14/92	lat. aff.	left	ap0112	803	spon	1	2982
preflight	5	pre control	11/14/92	lat. aff.	left	ap0112	803	step	1	3001
preflight	6	pre control	11/14/92	lat. aff.	left	ap0112	803	spon	1	3025
preflight	6	pre control	11/14/92	lat. aff.	left	ap0112	803	step	1	3040
preflight	6	pre control	11/14/92	lat. aff.	left	ap0112	803	sine0.2	1	3040
preflight	7	pre control	11/14/92	lat. aff.	left	ap0112	803	spon	1	-3170
preflight	7	pre control	11/14/92	lat. aff.	left	ap0112	803	step	1	- 3140
preflight	7	pre control	11/14/92	lat. aff.	left	ap0112	803	sine0.2	1	3190
preflight	7	pre control	11/14/92	lat. aff.	left	ap0112	803	ss	1	3230
preflight	7	pre control	11/14/92	lat. aff.	left	ap0112	803	ss-rpt	1	3305
preflight	7	pre control	11/14/92	lat. aff.	left	ap0112	803	sine1.0	1	3370
preflight	8	pre control	11/14/92	lat. aff.	left	ap0112	803	spon	1	3397
preflight	9	pre control	11/15/92	lat. aff.	left	ap0110	775	spon	1	3399
preflight	10	pre control	11/15/92	lat. aff.	left	ap0110	775	spon	1	3466
preflight	11	pre control	11/15/92	lat. aff.	left	ap0110	775	spon	1	3470
preflight	12	pre control	11/15/92	lat. aff.	left	ap0110	775	spon	1	3489
preflight	12	pre control	11/15/92	lat. aff.	left	ap0110	775	step	1	3566
preflight	12	pre control	11/15/92	lat. aff.	left	ap0110	775	step-rpt	1	3631
preflight	12	pre control	11/15/92	lat. aff.	left	ap0110	775	sine	1	3631
preflight	13	pre control	11/15/92	lat. aff.	left	ap0110	775	spon	1	3697
preflight	14	pre control	11/15/92	lat. aff.	left	ap0110	775	spon	1	3791
preflight	15	pre control	11/15/92	lat. aff.	right	ap0110	151	spon	1	3780
preflight	15	pre control	11/15/92	lat. aff.	right	ap0110	151	step	1	3810
preflight	16	pre control	11/16/92	lat. aff.	left	ap0110	907	spon	1	3880
preflight	16	pre control	11/16/92	lat. aff.	left	ap0110	907	step	1	-3900
preflight	16	pre control	11/16/92	lat. aff.	left	ap0110	907	sine0.2	1	- 3950
preflight	16	pre control	11/16/92	lat. aff.	left	ap0110	907	ss	1	3999
preflight	17	pre control	11/16/92	lat. aff.	left	ap0110	907	spon	1	4058
preflight	17	pre control	11/16/92	lat. aff.	left	ap0110	907	step	1	4089
preflight	17	pre control	11/16/92	lat. aff.	left	ap0110	907	stp-rpt	1	4173
preflight	17	pre control	11/16/92	lat. aff.	left	ap0110	907	sine0.2	1	4229
preflight	17	pre control	11/16/92	lat. aff.	left	ap0110	907	spon-rpt	1	4290
preflight	18	pre control	11/16/92	lat. aff.	left	ap0110	907	spon	1	4295
preflight	18	pre control	11/16/92	lat. aff.	left	ap0110	907	step	1	4313
preflight	18	pre control	11/16/92	lat. aff.	left	ap0110	907	step-rpt	1	4360
preflight	19	pre control	11/16/92	lat. aff.	left	ap0110	907	spon	1	4392
preflight	20	pre control	11/16/92	lat. aff.	left	ap0110	907	spon	1	4430
preflight	21	pre control	11/16/92	lat. aff.	left	ap0110	907	step	1	4486
preflight	22	pre control	11/16/92	lat. aff.	left	ap0110	907	step	1	4540
preflight	23	pre control	11/16/92	lat. aff.	left	ap0110	907	step	1	-4623
preflight	24	pre control	11/16/92	lat. aff.	left	ap0110	907	step	1	4643
preflight	25	pre control	11/16/92	lat. aff.	left	ap0110	907	step	1	4687

Summary of individual neurons and experimental conditions observed during pre-and post flight testing

preflight	25	pre control	11/16/92	lat. aff.	left	ap0110	907	step-rpt	1	4739
preflight	25	pre control	11/16/92	lat. aff.	left	ap0110	907	sine0.2	1	4780
preflight	25	pre control	11/16/92	lat. aff.	left	ap0110	907	ss	1	4816
preflight	26	pre control	11/16/92	lat. aff.	left	ap0110	907	step	1	4860
preflight	26	pre control	11/16/92	lat. aff.	left	ap0110	907	step-rpt	1	4908
preflight	26	pre control	11/16/92	lat. aff.	left	ap0110	907	sine0.2	1	4950
preflight	26	pre control	11/16/92	lat. aff.	left	ap0110	907	ss	1	4980
preflight	26	pre control	11/16/92	lat. aff.	left	ap0110	907	sine1.0	1	5046
preflight	27	pre control	11/16/92	lat. aff.	left	ap0110	907	step	1	5063
preflight	27	pre control	11/16/92	lat. aff.	left	ap0110	907	ss	1	5105
preflight	27	pre control	11/16/92	lat. aff.	left	ap0110	907	spon	1	5150
preflight	27	pre control	11/16/92	lat. aff.	left	ap0110	907	sine0.2	1	5170
preflight	27	pre control	11/16/92	lat. aff.	left	ap0110	907	sine1.0	1	5200
preflight	27	pre control	11/16/92	lat. aff.	left	ap0110	907	sine0.5	1	5248
preflight	28	pre control	11/16/92	lat. aff.	left	ap0110	907	step	1	5262
preflight	29	pre control	11/16/92	lat. aff.	left	p1110	1401	step	1	5290
preflight	29	pre control	11/16/92	lat. aff.	left	p1110	1401	sine0.2	1	5317
preflight	29	pre control	11/16/92	lat. aff.	left	p1110	1401	ss	1	5348
preflight	29	pre control	11/16/92	lat. aff.	left	p1110	1401	spon	1	6394
preflight	29	pre control	11/16/92	lat. aff.	left	p1110	1401	sine1.030	1	5410
preflight	29	pre control	11/16/92	lat. aff.	left	p1110	1401	sine0.5	1	5435
preflight	29	pre control	11/16/92	lat. aff.	left	p1110	1401	step-rpt	1	5457
preflight	29	pre control	11/16/92	lat. aff.	left	p1110	1401	step-rpt	1	5500
preflight	30	pre control	11/16/92	lat. aff.	left	p1110	1401	step	1	5553
preflight	30	pre control	11/16/92	lat. aff.	left	p1110	1401	step-rpt	1	5570
preflight	30	pre control	11/16/92	lat. aff.	left	p1110	1401	sine0.2	1	5620
preflight	30	pre control	11/16/92	lat. aff.	left	p1110	1401	step-rpt	1	5658
preflight	30	pre control	11/16/92	lat. aff.	left	p1110	1401	ss	1	5696
preflight	30	pre control	11/16/92	lat. aff.	left	p1110	1401	sine1.0	1	5743
preflight	30	pre control	11/16/92	lat. aff.	left	p1110	1401	sine0.5	1	5761
preflight	31	pre control	11/16/92	lat. aff.	left	p1110	1401	step	1	5775
preflight	31	pre control	11/16/92	lat. aff.	left	p1110	1401	ss	1	5823
preflight	31	pre control	11/16/92	lat. aff.	left	p1110	1401	sine0.2	1	5867
preflight	31	pre control	11/16/92	lat. aff.	left	p1110	1401	sine0.5	1	5898
preflight	32	pre control	11/17/92	mvnii	left	p412	151	sine0.2	1	5982
preflight	33	pre control	11/17/92	mvnii	left	p412	151	sine0.2	1	6000
preflight	34	pre control	11/18/92	mvni	left	p413	856	field pot.	1	6050
preflight	34	pre control	11/18/92	mvni	left	p413	856	sine0.2	1	6190
preflight	34	pre control	11/18/92	mvni	left	p413	856	sine0.5	1	6220
preflight	34	pre control	11/18/92	mvni	left	p413	856	sine1.0	1	6236
preflight	34	pre control	11/18/92	mvni	left	p413	856	elec. stim.	1	6249
preflight	35	pre control	11/18/92	mvnvert	left	p413	856	elec. stim.	1	6340
preflight	36	pre control	11/18/92	mvni	left	p413	856	elec. stim.	1	6360
preflight	36	pre control	11/18/92	mvni	left	p413	856	sine0.2	1	6370
preflight	37	pre control	11/18/92	mvni	left	p413	856	elec. stim.	1	6400
preflight	37	pre control	11/18/92	mvni	left	p413	856	sine0.2	1	6420
preflight	37	pre control	11/18/92	mvni	left	p413	856	sine0.2	1	6457
preflight	37	pre control	11/18/92	mvni	left	p413	856	sine0.5	1	6490
preflight	37	pre control	11/18/92	mvni	left	p413	856	sine1.0	1	6502
preflight	37	pre control	11/18/92	mvni	left	p413	856	sine1.0	1	6512
preflight	38	pre control	11/18/92	mvnii	left	p513	856	spon	1	6563
preflight	39	pre control	11/18/92	mvnii	left	p513	856	spon	1	6570
preflight	39	pre control	11/18/92	mvnii	left	p513	856	sine0.2	1	6592
preflight	39	pre control	11/18/92	mvnii	left	p513	856	sine0.2	1	6613
preflight	39	pre control	11/18/92	mvnii	left	p513	856	sine0.5	1	6633
preflight	39	pre control	11/18/92	mvnii	left	p513	856	sine1.0	1	6651

Summary of individual neurons and experimental conditions observed during pre-and post flight testing

preflight	39	pre control	11/18/92	mvnii	left	p5i3	856	sine 1.0	1	6661
preflight	39	pre control	11/18/92	mvnii	left	p5i3	856	sine0.5	1	6674
preflight	40	pre control	11/19/92	mvnii	left	p3i3	803	elec.stim	2	0
preflight	40	pre control	11/19/92	mvnii	left	p3i3	803	sine0.2	2	0
preflight	41	pre control	11/19/92	mvn	left	p3i3	803	elec.stim	2	148
preflight	42	pre control	11/19/92	mvn	left	p4i3	803	elec.stim	2	300
preflight	42	pre control	11/19/92	mvn	left	p4i3	803	sine0.2	2	300
preflight	43	pre control	11/19/92	mvni	left	p4i3	803	elec.stim	2	405
preflight	43	pre control	11/19/92	mvni	left	p4i3	803	sine0.2	2	474
preflight	44	pre control	11/19/92	mvni	left	p4i3	907	sine0.2	2	528
preflight	45	pre control	11/19/92	mvnii	left	p4i3	907	spon	2	643
preflight	46	pre control	11/19/92	mvni	left	p4i3	907	spon	2	654
preflight	47	pre control	11/19/92	mvni	left	p4i3	907	spon	2	711
preflight	48	pre control	11/19/92	mvni	left	p3i3	907	spon&elec	2	809
preflight	49	pre control	11/19/92	mnvipvp	left	p3i3	907	spon&elec	2	827
preflight	49	pre control	11/19/92	mnvipvp	left	p3i3	907	sine0.2	2	827
preflight	49	pre control	11/19/92	mnvipvp	left	p3i3	907	sine0.5	2	827
preflight	49	pre control	11/19/92	mnvipvp	left	p3i3	907	sine1.0	2	827
preflight	50	pre control	11/19/92	mvn	left	p3i3	907	spon	2	1140
preflight	50	pre control	11/19/92	mvn	left	p3i3	907	elec.stim	2	-1140
preflight	50	pre control	11/19/92	mvn	left	p3i3	907	sine0.2	2	-1140
preflight	51	pre control	11/19/92	mvnii	left	p3i3	907	sine0.2	2	1304
preflight	52	pre control	11/20/92	lat.aff.	left	ap0i10	1401	step	2	1537
preflight	52	pre control	11/20/92	lat.aff.	left	ap0i10	1401	step	2	1625
preflight	52	pre control	11/20/92	lat.aff.	left	ap0i10	1401	sine0.2	2	1707
preflight	52	pre control	11/20/92	lat.aff.	left	ap0i10	1401	ss	2	1749
preflight	52	pre control	11/20/92	lat.aff.	left	ap0i10	1401	sine1.0	2	1823
preflight	52	pre control	11/20/92	lat.aff.	left	ap0i10	1401	spon	2	1844
preflight	53	pre control	11/20/92	lat.aff.	left	ap0i10	1401	step	2	1866
preflight	53	pre control	11/20/92	lat.aff.	left	ap0i10	1401	sine0.2	2	1925
preflight	53	pre control	11/20/92	lat.aff.	left	ap0i10	1401	ss	2	1966
preflight	53	pre control	11/20/92	lat.aff.	left	ap0i10	1401	sine1.0	2	2034
preflight	53	pre control	11/20/92	lat.aff.	left	ap0i10	1401	spon	2	2054
preflight	53	pre control	11/20/92	lat.aff.	left	ap0i10	1401	sine0.5	2	2078
preflight	53	pre control	11/20/92	lat.aff.	left	ap0i10	1401	step rpt	2	2103
preflight	54	pre control	11/20/92	lat.aff.	left	ap0i10	1401	step rpt	2	2240
preflight	54	pre control	11/20/92	lat.aff.	left	ap0i10	1401	sine0.2	2	2298
preflight	54	pre control	11/20/92	lat.aff.	left	ap0i10	1401	ss	2	2336
preflight	54	pre control	11/20/92	lat.aff.	left	ap0i10	1401	sine1.0	2	-2401
preflight	54	pre control	11/20/92	lat.aff.	left	ap0i10	1401	sine0.5	2	-2418
preflight	54	pre control	11/20/92	lat.aff.	left	ap0i10	1401	spon	2	2442
preflight	55	pre control	11/20/92	lat.aff.	left	ap0i10	1401	step	2	2461
preflight	55	pre control	11/20/92	lat.aff.	left	ap0i10	1401	sine0.2	2	2518
preflight	55	pre control	11/20/92	lat.aff.	left	ap0i10	1401	ss	2	2558
preflight	55	pre control	11/20/92	lat.aff.	left	ap0i10	1401	sine1.0	2	2619
sync. cont.	56	sync control	1/9/93	lat.aff.	left	ap0i12	803	step	1	0
sync. cont.	56	sync control	1/9/93	lat.aff.	left	ap0i12	803	step rpt	1	136
sync. cont.	56	sync control	1/9/93	lat.aff.	left	ap0i12	803	step rpt	1	404
sync. cont.	57	sync control	1/9/93	lat.aff.	left	ap0i12	803	step	1	500
sync. cont.	58	sync control	1/9/93	lat.aff.	left	ap0i12	803	step	1	629
sync. cont.	59	sync control	1/9/93	lat.aff.	left	ap0i12	803	step	1	720
sync. cont.	59	sync control	1/9/93	lat.aff.	left	ap0i12	803	step rpt	1	797
sync. cont.	60	sync control	1/9/93	lat.aff.	left	ap0i12	803	step	1	876
sync. cont.	61	sync control	1/9/93	lat.aff.	left	ap0i12	803	step	1	-1209
sync. cont.	62	sync control	1/9/93	lat.aff.	left	ap0i12	803	step	1	1307
sync. cont.	63	sync control	1/9/93	lat.aff.	left	ap0i12	803	step	1	1440

Summary of individual neurons and experimental conditions observed during pre-and post flight testing

sync. cont.	64	sync control	1/10/93	lat.aff.	left	ap0110	907	step	1	1500
sync. cont.	64	sync control	1/10/93	lat.aff.	left	ap0110	907	step rpt	1	1600
sync. cont.	65	sync control	1/10/93	lat.aff.	left	ap019	907	step	1	1668
sync. cont.	65	sync control	1/10/93	lat.aff.	left	ap019	907	step rpt	1	1734
sync. cont.	65	sync control	1/10/93	lat.aff.	left	ap019	907	ss	1	1792
sync. cont.	65	sync control	1/10/93	lat.aff.	left	ap019	907	sine0.2	1	1871
sync. cont.	65	sync control	1/10/93	lat.aff.	left	ap019	907	spon	1	1840
sync. cont.	66	sync control	1/10/93	lat.aff.	left	ap019	907	ss	1	1960
sync. cont.	66	sync control	1/10/93	lat.aff.	left	ap019	907	step	1	- 2046
sync. cont.	66	sync control	1/10/93	lat.aff.	left	ap019	907	spon	1	2106
sync. cont.	66	sync control	1/10/93	lat.aff.	left	ap019	907	sine0.2	1	2137
postcont	67	post control	1/15/93	lat.aff.	left	ap0112	803	step	po1	5540
postcont	68	post control	1/15/93	lat.aff.	left	ap0112	803	step	po1	5578
postcont	68	post control	1/15/93	lat.aff.	left	ap0112	803	ss	po1	5620
postcont	68	post control	1/15/93	lat.aff.	left	ap0112	803	sine0.2	po1	5663
postcont	69	post control	1/15/93	lat.aff.	left	ap0112	803	step	po1	5689
postcont	70	post control	1/15/93	lat.aff.	left	ap0112	803	step	po1	5713
postcont	71	post control	1/15/93	lat.aff.	left	ap0112	803	step	po1	5756
postcont	71	post control	1/15/93	lat.aff.	left	ap0112	803	step rpt	po1	5781
postcont	72	post control	1/15/92	lat.aff.	left	ap0111	907	step	po1	- 5819
postcont	72	post control	1/15/92	lat.aff.	left	ap0111	907	ss	po1	- 5870
postcont	72	post control	1/15/92	lat.aff.	left	ap0111	907	sine0.2	po1	5913
postcont	72	post control	1/15/92	lat.aff.	left	ap0111	907	spon	po1	5937
postcont	72	post control	1/15/92	lat.aff.	left	ap0111	907	step	po1	5948
postcont	73	post control	1/15/92	lat.aff.	left	p1110	907	step	po1	6005
postcont	73	post control	1/15/92	lat.aff.	left	p1110	907	step	po1	6015
postcont	73	post control	1/15/92	lat.aff.	left	p1110	907	ss	po1	6046
postcont	73	post control	1/15/92	lat.aff.	left	p1110	907	sine0.2	po1	6058
postcont	74	post control	1/15/92	lat.aff.	left	p1110	907	step	po1	6113
postcont	75	post control	1/15/92	lat.aff.	left	p1110	907	step	po1	6144
postcont	76	post control	1/15/92	lat.aff.	left	p1110	907	step	po1	6153
postcont	76	post control	1/15/92	lat.aff.	left	p1110	907	ss	po1	6194
postcont	77	post control	1/15/92	lat.aff.	left	p1110	907	step	po1	6268
postcont	77	post control	1/15/92	lat.aff.	left	p1110	907	ss	po1	6304
postcont	78	post control	1/15/92	lat.aff.	left	p1110	907	ss	po1	6350
postcont	79	post control	1/16/93	mvni	left	p512	892	elec stim	po1	6500
postcont	79	post control	1/16/93	mvni	left	p512	892	sine0.2	po1	6549
postcont	79	post control	1/16/93	mvni	left	p512	892	sine0.5	po1	6578
postcont	79	post control	1/16/93	mvni	left	p512	892	sine1.0	po1	- 6591
postcont	79	post control	1/16/93	mvni	left	p512	892	step	po1	- 6609
postcont	79	post control	1/16/93	mvni	left	p512	892	ss	po1	6642
postcont	79	post control	1/16/93	mvni	left	p512	892	step rpt	po1	6681
postcont	79	post control	1/16/93	mvni	left	p512	892	step	po1	6710
postcont	80	post control	1/16/93	mvni	left	p313	1401	elec stim	po1	6730
postcont	80	post control	1/16/93	mvni	left	p313	1401	sine0.2	po1	6791
postcont	80	post control	1/16/93	mvni	left	p313	1401	sine0.5	po1	6817
postcont	80	post control	1/16/93	mvni	left	p313	1401	sine1.0	po1	6839
postcont	80	post control	1/16/93	mvni	left	p313	1401	step	po1	6859
postcont	80	post control	1/16/93	mvni	left	p313	1401	ss	po1	6892
postcont	80	post control	1/16/93	mvni	left	p313	1401	step	po1	6936
postcont	81	post control	1/16/93	mvni	left	p313	1401	elec stim	po1	6980
postcont	81	post control	1/16/93	mvni	left	p313	1401	step	po1	7010
postcont	81	post control	1/16/93	mvni	left	p313	1401	sine0.2	po1	7063
postcont	81	post control	1/16/93	mvni	left	p313	1401	sine0.5	po1	- 7088
postcont	81	post control	1/16/93	mvni	left	p313	1401	sine1.0	po1	7103
postcont	81	post control	1/16/93	mvni	left	p313	1401	ss	po1	7119

Summary of individual neurons and experimental conditions observed during pre-and post flight testing

postcont	81	post control	1/16/93	mvni	left	p3l3	1401	elec stim	po1	7160
postcont	82	post control	1/16/93	mvni	left	p3l3	1401	elec stim	po1	7185
postcont	82	post control	1/16/93	mvni	left	p3l3	1401	sine0.2	po1	7207
postcont	83	post control	1/16/93	mvni	left	p3l3	1401	elec stim	po1	7231
postcont	83	post control	1/16/93	mvni	left	p3l3	1401	sine0.2	po1	7246
postcont	83	post control	1/16/93	mvni	left	p3l3	1401	sine0.5	po1	7317
postcont	83	post control	1/16/93	mvni	left	p3l3	1401	sine1.0	po1	7330
postcont	83	post control	1/16/93	mvni	left	p3l3	1401	step	po1	-7348
postcont	83	post control	1/16/93	mvni	left	p3l3	1401	ss	po1	7380
postcont	84	post control	1/17/93	mvni	left	p3l3	907	elec stim	po2	0
postcont	84	post control	1/17/93	mvni	left	p3l3	907	sine0.2	po2	93
postcont	84	post control	1/17/93	mvni	left	p3l3	907	sine0.5	po2	185
postcont	84	post control	1/17/93	mvni	left	p3l3	907	sine1.0	po2	237
postcont	84	post control	1/17/93	mvni	left	p3l3	907	step	po2	294
postcont	84	post control	1/17/93	mvni	left	p3l3	907	step rpt	po2	360
postflight	1	flt. animals	1/11/93	lat.aff.	right	ap0l11	906		1	
postflight	2	flt. animals	1/11/93	lat.aff.	right	a1l11	906	step	1	0
postflight	2	flt. animals	1/11/93	lat.aff.	right	a1l11	906	step	1	100
postflight	2	flt. animals	1/11/93	lat.aff.	right	a1l11	906	ss	1	-220
postflight	2	flt. animals	1/11/93	lat.aff.	right	a1l11	906	step rpt	1	-322
postflight	2	flt. animals	1/11/93	lat.aff.	right	a1l11	906	sine0.2	1	413
postflight	3	flt. animals	1/11/93	lat.aff.	right	a1l11	906	spon	1	481
postflight	4	flt. animals	1/11/93	lat.aff.	right	a1l11	906	step	1	523
postflight	5	flt. animals	1/11/93	lat.aff.	right	a1l11	906	step	1	600
postflight	5	flt. animals	1/11/93	lat.aff.	right	a1l11	906	step	1	723
postflight	5	flt. animals	1/11/93	lat.aff.	right	a1l11	906	ss	1	796
postflight	5	flt. animals	1/11/93	lat.aff.	right	a1l11	906	sine0.2	1	890
postflight	5	flt. animals	1/11/93	lat.aff.	right	a1l11	906	spon	1	942
postflight	6	flt. animals	1/11/93	lat.aff.	right	a1l11	906	step rpt	1	983
postflight	6	flt. animals	1/11/93	lat.aff.	right	a1l11	906	step	1	1057
postflight	6	flt. animals	1/11/93	lat.aff.	right	a1l11	906	ss	1	1138
postflight	6	flt. animals	1/11/93	lat.aff.	right	a1l11	906	spon	1	1217
postflight	7	flt. animals	1/11/93	lat.aff.	right	a1l11	906	sine0.2	1	1250
postflight	8	flt. animals	1/11/93	lat.aff.	right	a1l11	906	step	1	1304
postflight	8	flt. animals	1/11/93	lat.aff.	right	a1l11	906	step	1	1376
postflight	8	flt. animals	1/11/93	lat.aff.	right	a1l11	906	ss	1	1447
postflight	8	flt. animals	1/11/93	lat.aff.	right	a1l11	906	spon	1	1517
postflight	9	flt. animals	1/11/93	lat.aff.	right	a1l11	906	sine0.2	1	1544
postflight	10	flt. animals	1/11/93	lat.aff.	right	a1l11	906	step	1	
postflight	11	flt. animals	1/11/93	lat.aff.	right	a1l11	906	step	1	1650
postflight	12	flt. animals	1/11/93	lat.aff.	right	a1l11	906	step	1	1709
postflight	12	flt. animals	1/11/93	lat.aff.	right	a1l11	906	step	1	1762
postflight	12	flt. animals	1/11/93	lat.aff.	right	a1l11	906	ss	1	1824
postflight	12	flt. animals	1/11/93	lat.aff.	right	a1l11	906	step rpt	1	1893
postflight	12	flt. animals	1/11/93	lat.aff.	right	a1l11	906	sine0.2	1	1956
postflight	13	flt. animals	1/11/93	lat.aff.	right	a1l11	906	spon	1	1995
postflight	14	flt. animals	1/11/93	lat.aff.	right	a2l9	151	step	1	2012
postflight	14	flt. animals	1/11/93	lat.aff.	right	a2l9	151	step	1	2070
postflight	14	flt. animals	1/11/93	lat.aff.	right	a2l9	151	ss	1	2127
postflight	14	flt. animals	1/11/93	lat.aff.	right	a2l9	151	sine0.2	1	2193
postflight	15	flt. animals	1/11/93	lat.aff.	right	a2l9	151	spon	1	2236
postflight	15	flt. animals	1/11/93	lat.aff.	right	a2l9	151	step	1	2248
postflight	16	flt. animals	1/11/93	lat.aff.	right	a2l9	151	ss	1	2315
postflight	16	flt. animals	1/11/93	lat.aff.	right	a2l9	151	sine0.2	1	2385
postflight	17	flt. animals	1/11/93	lat.aff.	right	a2l9	151	step	1	2386

Summary of individual neurons and experimental conditions observed during pre-and post flight testing

postflight	18	flt. animals	1/11/93	lat.aff.	right	a219	151	step	1	2440
postflight	19	flt. animals	1/12/93	lat.aff.	right	a1111	906	step	1	2475
postflight	19	flt. animals	1/12/93	lat.aff.	right	a1111	906	step	1	2500
postflight	19	flt. animals	1/12/93	lat.aff.	right	a1111	906	ss	1	2545
postflight	20	flt. animals	1/12/93	lat.aff.	right	a1111	906	step rpt	1	2606
postflight	20	flt. animals	1/12/93	lat.aff.	right	a1111	906	step	1	2640
postflight	21	flt. animals	1/12/93	lat.aff.	right	a1111	906	ss	1	2723
postflight	22	flt. animals	1/12/93	lat.aff.	right	a1111	906	step	1	2785
postflight	22	flt. animals	1/12/93	lat.aff.	right	a1111	906	step	1	2834
postflight	23	flt. animals	1/12/93	lat.aff.	right	a1111	906	step rpt	1	2889
postflight	24	flt. animals	1/12/93	lat.aff.	right	a219	151	step	1	2944
postflight	24	flt. animals	1/12/93	lat.aff.	right	a219	151	step	1	2950
postflight	24	flt. animals	1/12/93	lat.aff.	right	a219	151	ss	1	3007
postflight	24	flt. animals	1/12/93	lat.aff.	right	a219	151	step	1	3063
postflight	25	flt. animals	1/12/93	lat.aff.	right	a219	151	sine0.2	1	3101
postflight	25	flt. animals	1/12/93	lat.aff.	right	a219	151	step	1	3140
postflight	25	flt. animals	1/12/93	lat.aff.	right	a219	151	ss	1	3185
postflight	25	flt. animals	1/12/93	lat.aff.	right	a219	151	step rpt	1	3248
postflight	26	flt. animals	1/12/93	lat.aff.	right	a219	151	sine0.2	1	3301
postflight	27	flt. animals	1/12/93	lat.aff.	right	a219	151	step	1	3338
postflight	27	flt. animals	1/12/93	lat.aff.	right	a219	151	step	1	3385
postflight	27	flt. animals	1/12/93	lat.aff.	right	a219	151	ss	1	3430
postflight	28	flt. animals	1/12/93	lat.aff.	right	a219	151	sine0.2	1	3483
postflight	28	flt. animals	1/12/93	lat.aff.	right	a219	151	step	1	3518
postflight	28	flt. animals	1/12/93	lat.aff.	right	a219	151	step	1	3571
postflight	28	flt. animals	1/12/93	lat.aff.	right	a219	151	ss	1	3617
postflight	29	flt. animals	1/12/93	lat.aff.	right	a219	151	sine0.2	1	3669
postflight	30	flt. animals	1/12/93	lat.aff.	right	a219	151	step	1	3730
postflight	31	flt. animals	1/12/93	lat.aff.	right	a219	151	step	1	3823
postflight	31	flt. animals	1/12/93	lat.aff.	right	a219	151	step	1	3871
postflight	32	flt. animals	1/12/93	lat.aff.	right	a219	151	ss	1	3912
postflight	33	flt. animals	1/12/93	lat.aff.	right	a219	151	step	1	3962
postflight	33	flt. animals	1/12/93	lat.aff.	right	a219	151	step	1	3978
postflight	33	flt. animals	1/12/93	lat.aff.	right	a219	151	ss	1	4018
postflight	33	flt. animals	1/12/93	lat.aff.	right	a219	151	sine0.2	1	4069
postflight	34	flt. animals	1/12/93	lat.aff.	right	a219	151	spon	1	4103
postflight	35	flt. animals	1/12/93	lat.aff.	right	a219	151	step	1	4117
postflight	35	flt. animals	1/12/93	lat.aff.	right	a219	151	step	1	4157
postflight	36	flt. animals	1/12/93	lat.aff.	right	a219	151	ss	1	4200
postflight	36	flt. animals	1/12/93	lat.aff.	right	a219	151	step	1	4256
postflight	37	flt. animals	1/12/93	lat.aff.	right	a219	151	ss	1	
postflight	37	flt. animals	1/12/93	lat.aff.	right	a219	151	step	1	4331
postflight	38	flt. animals	1/14/93	lat.aff.	right	a118	151	ss	1	4374
postflight	38	flt. animals	1/14/93	lat.aff.	right	a118	151	step	1	4370
postflight	38	flt. animals	1/14/93	lat.aff.	right	a118	151	ss	1	4416
postflight	39	flt. animals	1/14/93	lat.aff.	right	a118	151	sine0.2	1	4463
postflight	39	flt. animals	1/14/93	lat.aff.	right	a118	151	step	1	4511
postflight	40	flt. animals	1/14/93	lat.aff.	right	a118	151	ss	1	4553
postflight	40	flt. animals	1/14/93	lat.aff.	right	a118	151	step	1	4590
postflight	40	flt. animals	1/14/93	lat.aff.	right	a118	151	ss	1	4640
postflight	40	flt. animals	1/14/93	lat.aff.	right	a118	151	sine0.2	1	4683
postflight	41	flt. animals	1/14/93	lat.aff.	right	a118	151	step	1	4716
postflight	41	flt. animals	1/14/93	lat.aff.	right	a118	151	step	1	4760
postflight	41	flt. animals	1/14/93	lat.aff.	right	a118	151	ss	1	4800
postflight	41	flt. animals	1/14/93	lat.aff.	right	a118	151	step rpy	1	4841
postflight	42	flt. animals	1/14/93	lat.aff.	right	a118	151	sine0.2	1	4878

Summary of individual neurons and experimental conditions observed during pre-and post flight testing

postflight	42	flt. animals	1/14/93	lat.aff.	right	a1l8	151	step	1	4930
postflight	43	flt. animals	1/14/93	lat.aff.	right	a1l8	151	step rpt	1	4947
postflight	44	flt. animals	1/14/93	lat.aff.	right	a1l8	151	step	1	4981
postflight	44	flt. animals	1/14/93	lat.aff.	right	a1l8	151	step	1	4989
postflight	44	flt. animals	1/14/93	lat.aff.	right	a1l8	151	ss	1	5026
postflight	44	flt. animals	1/14/93	lat.aff.	right	a1l8	151	step rpt	1	5060
postflight	45	flt. animals	1/14/93	lat.aff.	right	a1l8	151	sine0.2	1	5105
postflight	45	flt. animals	1/14/93	lat.aff.	right	a1l8	151	step	1	5132
postflight	45	flt. animals	1/14/93	lat.aff.	right	a1l8	151	ss	1	-5173
postflight	45	flt. animals	1/14/93	lat.aff.	right	a1l8	151	sine0.2	1	5216
postflight	46	flt. animals	1/14/93	lat.aff.	right	a1l8	151	spon	1	5240
postflight	47	flt. animals	1/14/93	lat.aff.	right	a1l8	151	step	1	5253
postflight	47	flt. animals	1/14/93	lat.aff.	right	a1l8	151	step	1	5295
postflight	48	flt. animals	1/14/93	lat.aff.	right	a1l11	906	ss	1	5330
postflight	48	flt. animals	1/14/93	lat.aff.	right	a1l11	906	step	1	5370
postflight	49	flt. animals	1/14/93	lat.aff.	right	a1l11	906	step rpt	1	5414
postflight	49	flt. animals	1/14/93	lat.aff.	right	a1l11	906	step	1	5434
postflight	49	flt. animals	1/14/93	lat.aff.	right	a1l11	906	ss	1	5470
postflight	50	flt. animals	1/21/93	lat.aff.	right	a2l11	906	sine0.2	2	5510
postflight	50	flt. animals	1/21/93	lat.aff.	right	a2l11	906	ss	2	
postflight	50	flt. animals	1/21/93	lat.aff.	right	a2l11	906	step	2	
postflight	51	flt. animals	1/21/93	lat.aff.	right	a2l11	906	sine0.2	2	
postflight	51	flt. animals	1/21/93	lat.aff.	right	a2l11	906	step	2	
postflight	51	flt. animals	1/21/93	lat.aff.	right	a2l11	906	ss	2	
postflight	52	flt. animals	1/21/93	lat.aff.	right	a2l11	906	sine0.2	2	
postflight	53	flt. animals	1/21/93	lat.aff.	right	a2l11	906	step	2	
postflight	53	flt. animals	1/21/93	lat.aff.	right	a2l11	906	step	2	
postflight	53	flt. animals	1/21/93	lat.aff.	right	a2l11	906	ss	2	
postflight	54	flt. animals	1/21/93	lat.aff.	right	a2l11	906	?	2	
postflight	54	flt. animals	1/21/93	lat.aff.	right	a2l11	906	step	2	
postflight	55	flt. animals	1/21/93	lat.aff.	right	a2l11	906	ss	2	
postflight	55	flt. animals	1/21/93	lat.aff.	right	a2l11	906	step	2	
postflight	56	flt. animals	1/21/93	lat.aff.	right	a2l11	906	ss	2	
postflight	57	flt. animals	1/21/93	lat.aff.	right	a2l11	906	step	2	
postflight	57	flt. animals	1/21/93	lat.aff.	right	a2l11	906	step	2	
postflight	58	flt. animals	1/21/93	lat.aff.	right	a2l11	906	ss	2	
postflight	58	flt. animals	1/21/93	lat.aff.	right	a2l11	906	step	2	
postflight	59	flt. animals	1/21/93	lat.aff.	right	a2l11	906	step	2	
postflight	59	flt. animals	1/21/93	lat.aff.	right	a2l11	906	ss	2	

APPENDIX 2

The 31 tables on pages 157-168 summarize data for each of the test procedures. The tables are further organized to summarize the responses to each of the test procedures (listed by afferent) on each test day such as during the preflight tests, during the synchronous control tests, and during each of the postflight test days when data were obtained. At the bottom of each table are presented first order summary statistics where appropriate.

Pulse Response

TABLE 1
Pulse Response - Pre-Flight (10-17-92 & 11-16-92 to 12-9-93)

Case	Curve 1				Curve 2				Curve 3				Curve 4				Average Inc. Gain				Average Dec. Gain								
	DC	K	K	DC	DC	K	K	DC	DC	K	K	DC	DC	K	K	DC	DC	K	K	DC	DC	K	K	DC	DC	K	K		
L 01o1701a		
L 01o1701b		
L 01o1701c		
L 01o1702a	-0.4155	7.1328	0.0882	101.5656	0.3820	6.5779	0.0163	102.9482	0.4507	8.4298	0.0000	101.2178	99.3106	-0.8899	6.2883	0.0789	100.4421	0.4214	7.5038	0.0682	102.0930	1.2406	3.2589	0.0242	156.3708	2.1748	10.006	0.2121	97.5811
L 03a1401a	-1.1234	7.8453	0.1986	183.5273	1.4988	5.5245	0.0157	156.3604	0.9933	0.9933	0.0328	156.3811		
L 03a1402a	2.2067	9.6983	0.2033	98.2926	2.1429	10.313	0.2208	98.8696		
L 03a1402b	
L 03a1404a	
L 03a1405a	
L 03a1406a	-1.3253	3.182	0.0000	151.5870		
L 03a1407a	-0.8237	3.8853	0.0000	143.0723	0.7533	6.4401	0.0374	141.8198	0.6130	4.7198	0.0000	145.3469	143.8768	-0.6327	4.8483	0.0289	143.4746	0.6632	5.5799	0.0187	143.5833	
R 51a1501a	
L 75a1504a	1.5134	9.2211	0.1598	80.9320	1.2947	6.1085	0.2845	68.8725		
L 75a1504b	
L 07a1801a	-1.7525	10.239	0.4874	124.8675	1.7469	9.0291	0.4024	122.2586	1.5845	6.8652	0.3921	131.2002	119.0914	-1.6806	10.477	0.4320	121.9795	1.6657	7.8572	0.3973	126.7284	
L 07a1802a	
L 07a1803a	-0.9705	6.1416	0.0981	164.1014	0.7761	5.9755	0.1561	165.1752	0.8387	6.6322	0.2478	161.4111	158.8814	-0.8619	4.9787	0.0637	161.8914	0.8064	7.8039	0.2020	163.2932	
L 07a1803b	-1.6439	4.0281	0.0000	120.5870	1.5306	9.0822	0.1698	117.4469	1.6624	5.7845	0.0919	123.7423	117.5148	-1.4558	4.9984	0.0000	119.0508	1.5995	7.4334	0.1369	120.5948	
L 07a1806a	
L 07a1807a	
L 07a1808a	
L 07a1809a	
L 07a1810a	
L 07a1810b	
L 07a1811a	
L 07a1811b	
L 07a1812a	-0.5397	6.3241	0.0562	140.9330	0.6254	12.757	0.0512	135.8798	0.6024	12.454	0.1319	139.0757	136.0342	-0.4861	7.2222	0.0549	136.4836	0.6198	12.806	0.0918	137.4778	
L 07a1813a	
L 01a1801a	
L 01a1801b	
L 01a1801c	
L 01a1802a	-0.5779	9.6917	0.1567	145.0000	0.5235	3.128	0.0000	147.0874	
L 01a1802b	-0.5947	3.4463	0.0000	142.8078	
L 01a1802c	
L 01a1803a	-0.3152	5.7	0.0000	111.4161	0.3230	9.3387	0.0000	110.1897	0.3343	8.8109	0.0000	112.9107	111.1201	-0.2903	11.502	0.0639	111.2681	0.3287	8.0748	0.0000	111.5537	
L 01a2004a	
L 01a2004b	-0.8232	3.5003	0.0740	155.0890	1.1588	5.959	0.0917	154.1314	1.1484	7.4675	0.1529	151.5107	151.1228	-0.8428	4.3845	0.1109	153.1094	1.1531	6.7123	0.1223	152.8211	
L 01a2005a	
L 01a2005b	-0.3193	8.2552	0.0931	130.3882	0.7314	17.875	0.0250	111.3644	0.3935	8.1509	0.0000	127.9710	127.0024	-0.3412	7.8978	0.0870	128.8933	0.5825	13.063	0.0125	119.6877	
L 01a2006a	
L 01a2006b	-0.4892	11.666	0.4433	153.0725	0.9133	3.746	0.0458	155.7657	0.8828	12.248	0.1630	145.1741	160.3664	-0.6831	11.814	0.3217	158.7195	0.8981	7.997	0.1044	150.4689	
L 01a2007a	-1.0981	2.3914	0.2029	164.0958	0.9417	6.4114	0.0750	161.3007	0.9790	4.8058	0.0403	157.1922	155.1292	-0.8887	4.0984	0.0579	159.8125	0.9604	5.0086	0.0577	159.2465	
MEAN	0.8232	6.2285	0.1143	142.1417	1.0425	8.0576	0.0966	129.3905	0.8665	7.3728	0.1172	130.8088	134.9078	-0.8065	6.8701	0.1103	141.0378	0.9782	7.4483	0.1002	131.0418	
ST. DEV.	0.4631	2.8662	0.1551	21.6397	0.5475	3.7184	0.1080	29.3851	0.5221	3.147	0.1246	26.1836	20.1932	0.4220	2.8925	0.1233	21.8008	0.5226	2.8873	0.1120	26.8652	
N	15	15	15	15	15	15	15	15	15	15	15	15	15	15	15	15	15	15	15	15	15	15	15	15	15	15	15	15	15
SEM	0.0454	0.1129	0.0263	0.3101	0.0493	0.1286	0.0219	0.3614	0.0482	0.1183	0.0235	0.3411	0.0528	0.1647	0.0289	0.3745	0.0433	0.1134	0.0234	0.3113	0.0452	0.1062	0.0209	0.3246	0.0452	0.1062	0.0209	0.3246	

Pulse Response

TABLE 2
Pulse Response - Synchronous Control (1-9-83 to 1-10-83)

UNIT	Curve 1				Curve 2				Curve 3				Curve 4				Average Inc.				Average Dec.								
	GAIN	Δ	Δ	DC	GAIN	Δ	Δ	DC	GAIN	Δ	Δ	DC	GAIN	Δ	Δ	DC	GAIN	Δ	Δ	DC	GAIN	Δ	Δ	DC	GAIN	Δ	Δ	DC	
L 03c0901a	-1.0421	4.2521	0.1051	138.0470	0.9455	26.163	0.1406	127.4103	1.0468	5.8041	0.0208	134.8712
L 03c0901b	0.0446	8.6511	0.0000	130.0422
L 03c0901c
L 03c0902a	-1.1119	5.3636	0.1526	140.1345	0.1818	6.6552	0.0000	140.0000
L 03c0902b	-0.9136	2.0836	0.0000	164.5718
L 03c0903a	-1.8117	4.546	0.0497	153.3475	1.4938	3.4043	0.0123	147.8993	1.2172	7.4226	0.1230	142.0520
L 03c0904a	-1.1487	1.8713	0.0580	130.8689	1.0548	8.9874	0.2445	121.3475	1.1319	4.9241	0.1383	116.9827
L 03c0904b	-0.9843	4.17	0.1170	120.2544
L 03c0905a	-0.8752	4.7275	0.2984	136.1300
L 03c0906a	-0.4553	1.7019	0.0868	53.1023
L 03c0907a
L 03c0908a	-0.3323	3.1711	0.0000	104.0870	0.3063	2.9193	0.0000	105.2517	1.3871	16.869	0.2556	114.4782
L 07c1001a	-1.0179	4.8937	0.0517	146.0618	1.2252	7.3702	0.1070	134.3165	0.9840	6.8274	0.1005	137.0171
L 07c1001b	0.8284	40.352	0.0000	102.3157
L 07c1002a	-0.2682	6.5101	0.0000	100.2647	0.3284	6.4404	0.0000	100.4426
L 07c1002b	-0.8410	4.0218	0.0341	128.5819	1.0594	8.6418	0.0659	125.2216	0.9892	5.5356	0.0693	127.6030
L 07c1003a
L 07c1003b
L 07c1003c
MEAN	0.8903	3.9427	0.0803	128.7801	0.8953	8.3316	0.0815	128.7781	0.8289	10.778	0.0709	120.9167
ST. DEV.	0.3781	1.4775	0.0842	28.5490	0.4792	7.8571	0.0804	13.8170	0.4389	10.964	0.0850	15.4889
N	12	12	12	12	7	7	7	7	10	10	10	10	5	5	5	5	5	5	5	5	13	13	13	13	9	9	9	9	9
SEM	0.0512	0.1013	0.0242	0.4530	0.0989	0.4004	0.0430	0.5310	0.0662	0.3311	0.0292	0.3936	
													0.6341	0.0999	0.207	0.0535	0.8341	0.0471	0.0693	0.0225	0.4046	0.0669	0.378	0.0331	0.4422	0.9222	7.1218	0.0722	125.9306

Pulse Response

TABLE 3
Pulse Response - Pulse-Fight Day 2 (1-11-83)

Pulse	Curve 1				Curve 2				Curve 3				Curve 4				Average Inc.				Average Dev.			
	GAIN	I	K	DC	GAIN	I	K	DC	GAIN	I	K	DC												
R 06c1101a	0.3971	9.3428	0.0000	129.6178	-0.1181	6.2437	0.0592	124.1026	-0.2563	9.8951	0.0052	127.0000	0.3503	13.537	0.0208	127.0000	0.3587	11.44	0.0104	128.3088	-0.1872	8.0694	0.0317	125.5513
R 06c1102a
R 06c1102e	0.5008	9.2185	0.0287	112.0816	-0.3728	4.9926	0.0386	108.5857	-0.3708	7.7444	0.0989	110.1776	0.4796	11.939	0.0433	110.0000	0.4902	10.578	0.0380	111.0408	-0.3718	6.3585	0.0493	109.3817
R 06c1103a
R 06c1103e	-1.0035	1.8266	0.2287	68.4754
R 06c1105a
R 06c1105e	0.3634	7.8656	0.0248	124.1607	-0.4082	10.427	0.0000	120.0000	-0.4056	9.6673	0.0369	116.4590	0.5898	10.619	0.0000	120.0000	0.4866	9.2424	0.0124	122.0804	-0.4058	10.047	0.0185	118.2285
R 06c1106a	0.3649	11.811	0.0526	120.7111	-0.2287	7.6198	0.1131	119.7221	-0.2921	17.477	0.0795	122.2796	0.3690	6.6155	0.0124	120.9043	0.3870	9.2131	0.0325	120.8077	-0.2604	12.548	0.0983	121.0009
R 06c1107a
R 06c1108a	0.3397	12.938	0.0585	125.4427	-0.1717	4.2239	0.0727	120.5247	-0.3763	17.013	0.1570	124.1263	0.3885	8.595	0.0755	120.0000	0.3631	10.616	0.0670	122.7214	-0.2740	10.619	0.1149	122.3255
R 06c1108e
R 06c1110a	0.9315	6.4472	0.1086	91.9747	-1.0891	8.5007	0.0094	90.0000	-0.7067	7.1062	0.0000	85.4837	0.8908	4.0849	0.4065	112.7193	0.9112	5.2681	0.2566	102.3470	-0.8978	7.8035	0.0047	87.7419
R 06c1111a	0.4959	7.0482	0.0838	140.7837	0.4959	7.0482	0.0838	140.7837
R 06c1112a	0.2893	8.515	0.0000	110.6316	-0.1896	8.4459	0.0682	107.0000	-0.2905	8.0316	0.0536	107.0000	0.3149	3.4212	0.0000	114.3209	0.3021	5.9681	0.0000	112.4763	-0.2736	8.2388	0.0614	107.0000
R 06c1113a
R 51c1101a	0.2491	21.15	0.1320	63.6601	-0.1897	4.4541	0.0154	61.3223	-0.2527	6.9523	0.0553	63.7192	0.3069	7.512	0.0000	62.0000	0.2780	14.331	0.0660	62.9401	-0.2292	5.7032	0.0354	62.5208
R 51c1102a	0.5496	5.8583	0.1593	114.9683	-0.5905	5.2922	0.1847	110.2709	0.5496	5.8583	0.1593	114.9683	-0.5905	5.2922	0.1847	110.2709
R 51c1103a	0.2310	13.477	0.0718	61.0000	-0.2088	14.578	0.1104	59.0000	-0.2594	7.5999	0.0000	58.6991	0.2310	13.477	0.0718	61.0000	-0.2541	11.089	0.0552	58.3486
R 51c1104a	0.4849	11.074	0.0824	106.8724	0.4849	11.074	0.0824	106.8724
R 51c1105a
MEAN	0.4323	10.37	0.0667	108.4936	-0.3965	7.1313	0.0716	97.8733	-0.3771	9.6759	0.0672	102.8215	0.4610	8.2905	0.0698	110.8681	0.4432	9.5094	0.0732	108.8537	-0.4250	7.8632	0.0819	98.2586
ST. DEV.	0.1880	4.1827	0.0499	24.8077	0.3532	3.6406	0.0678	26.1181	0.1563	4.2006	0.0643	24.5377	0.1975	3.8088	0.1388	20.4858	0.1785	2.9781	0.0722	24.1528	0.2848	3.0788	0.0703	25.2337
N	12	12	12	12	10	10	10	10	10	10	10	10	8	8	8	8	8	12	12	12	12	11	11	11
SEM	0.0361	0.1704	0.0186	0.4151	0.0594	0.1908	0.0280	0.5111	0.0395	0.205	0.0254	0.4954	0.0556	0.2375	0.0465	0.5855	0.0352	0.1438	0.0224	0.4095	0.0489	0.1595	0.0241	0.4586
																					0.4158	8.971	0.0687	104.8454

Pulse Response

TABLE 4
Pulse Response - Post-Flight Day 3 (11-12-83)

Pulse Response	Curve 1				Curve 2				Curve 3				Curve 4				Average Inc.				Average Dec.													
	GAIN	T	K	DC	GAIN	T	K	DC	GAIN	T	K	DC	GAIN	T	K	DC																		
R 06c1214e	0.3772	11.878	0.0000	111.5303	-0.2537	14.756	0.0954	112.0000	-0.3395	10.424	0.0639	112.9932	0.3858	8.1561	0.0000	111.8267	0.3815	10.017	0.0000	111.7295	-0.2868	12.358	0.0787	112.4506										
R 06c1214e																																		
R 06c1215a	0.4804	11.088	0.1302	137.1729	-0.3238	3.2983	0.0761	126.5631	-0.5181	8.9505	0.1073	133.2148	0.5420	14.763	0.2024	133.0000	0.5112	12.926	0.1863	135.0685	-0.4210	8.1244	0.1117	130.8680										
R 06c1215a																																		
R 06c1216a	0.4379	14.923	0.0083	109.8733	-0.2617	11.498	0.2273	106.7153	-0.3744	15.805	0.1182	109.2550	0.3630	13.691	0.0481	113.5597	0.4105	14.307	0.0262	111.7185	-0.3181	13.668	0.1728	107.9852										
R 06c1217a	0.3872	14.396	0.0000	105.0654	-0.2172	8.2276	0.0000	105.7105	-0.2558	5.534	0.0000	103.6375	0.2067	6.8703	0.0000	108.0000	0.3970	10.815	0.0000	106.5427	-0.2395	8.8808	0.2000	104.6740										
R 06c1217a																																		
R 06c1218a																																		
R 51c1206a	0.5049	11.1	0.1230	86.8458	-0.5222	12.77	0.0631	90.5675	-0.4705	7.5629	0.1026	85.4418	0.5217	6.8672	0.0805	86.0000	0.5133	8.9635	0.1018	85.4226	-0.4894	10.186	0.0629	86.0047										
R 51c1207a	0.1282	11.19	0.1912	60.0000	-0.1300	5.3517	0.0000	56.8753	-0.1529	3.8888	0.0336	58.4394	0.1550	7.7039	0.0371	59.0000	0.1416	9.4166	0.1142	58.5000	-0.1415	4.3703	0.2166	56.6574										
R 51c1207a																																		
R 51c1208a	0.7131	14.097	0.1515	77.0818	-0.4418	3.4934	0.0269	75.8387										0.7131	14.097	0.1515	77.0818	-0.4418	3.4934	0.0269	75.8387									
R 51c1209a	0.7861	22.256	0.2722	68.9035	-0.7998	3.9073	0.2893	63.7725	-0.9351	24.656	0.3451	77.8924	1.1446	14.394	0.3768	67.9524	0.8654	18.325	0.3245	68.4280	-0.9675	14.282	0.3172	70.6325										
R 51c1210a	0.5503	7.8306	0.0000	98.0551	-0.5401	1.7222	0.0559	112.7361	-0.8743	5.1445	0.0338	114.9877	0.7696	4.0534	0.0000	114.0000	0.6600	5.842	0.0000	106.0276	-0.7072	3.4334	0.0448	113.8618										
R 51c1210a																																		
R 51c1212a																																		
R 51c1213a	0.1994	15.582	0.0652	51.3553	-0.1469	11.021	0.1230	52.1476	-0.1655	6.7444	0.0000	52.1086	0.2166	10.65	0.0714	51.9621	0.2080	12.116	0.0683	51.8697	-0.1562	8.8827	0.0615	52.1781										
R 51c1214a																																		
R 51c1215a																																		
R 51c1216a	0.5615	7.2442	0.0322	99.3973	-0.5027	5.5549	0.0130	96.0157	-0.5147	6.9398	0.0467	94.1453	0.5351	4.9926	0.0000	97.9282	0.5483	6.1184	0.0161	98.6633	-0.5087	6.0974	0.0299	95.0809										
R 51c1217a																																		
R 51c1218a	0.8513	16.845	0.0988	144.2215	-0.5950	3.3352	0.0944	145.7813	-0.7524	5.9673	0.0620	155.4045	0.7058	6.8713	0.1106	148.7001	0.7786	11.858	0.1047	145.4608	-0.6737	4.6513	0.0782	150.5829										
R 51c1219a	0.3509	5.8637	0.0178	70.8881	-0.2548	5.4715	0.0354	67.2858	-0.3183	6.4282	0.0184	67.8813	0.3195	8.3391	0.1035	70.3391	0.3352	7.1014	0.0009	70.6141	-0.2666	5.9504	0.0274	67.5836										
R 51c1220a	0.4447	19.85	0.1915	101.0000	-0.3095	9.4473	0.0915	102.1764	-0.3629	8.262	0.0677	102.5974	0.4265	10.674	0.0361	101.0000	0.4358	15.262	0.1136	101.0000	-0.3362	8.8547	0.0786	102.3869										
R 51c1220a																																		
MEAN	0.4838	13.193	0.0916	94.3665	-0.3771	7.1323	0.0651	94.1561	-0.4642	8.8875	0.0816	97.5384	0.4855	9.0635	0.0820	97.1823	0.4928	11.308	0.0883	95.0605	-0.4186	7.8173	0.0814	95.0723										
ST. DEV.	0.2037	4.9609	0.0879	27.2265	0.1941	4.1238	0.0635	27.9607	0.2522	5.0357	0.0924	29.4118	0.2710	3.5077	0.1061	28.9257	0.2278	3.6377	0.0681	27.6694	0.2140	3.6647	0.0616	28.1039										
N	14	14	14	14	14	14	14	14	14	14	14	14	14	14	14	14	14	14	14	14	14	14	14	14	14									
SEM	0.0322	0.1545	0.0212	0.3727	0.0315	0.1451	0.0206	0.3750	0.0386	0.1828	0.0234	0.4172	0.0400	0.1441	0.0251	0.4137	0.0341	0.1362	0.0212	0.3757	0.0330	0.1371	0.0204	0.3767										

Pulse Response

TABLE 5

Pulse Response - Post-Flight Day 5 (11-14-53)

REFLECTION	Curve 1			Curve 2			Curve 3			Curve 4			Average Inc.			Average Dec.								
	GAIN	K	DC	GAIN	K	DC	GAIN	K	DC	GAIN	K	DC	GAIN	K	DC	GAIN	K	DC						
R 06c1418a	0.5520	7.3488	0.0539	143.5039	-0.4481	9.0711	0.0809	139.0000	-0.4554	5.3215	0.0181	135.7669	0.5801	8.335	0.0487	139.0780	0.5661	7.8419	0.0513	141.2898	-0.4523	7.1983	0.0485	137.3835
R 06c1420a	0.3441	13.532	0.1154	98.3431	-0.2580	5.1782	0.0067	98.6656	-0.3281	8.5215	0.0581	98.9763	0.3747	14.525	0.1970	100.0000	0.3594	14.028	0.1582	98.1716	-0.2931	8.8489	0.0314	97.8210
R 51c1421a	0.7600	13.188	0.0464	79.5173	-0.5324	4.4052	0.0947	79.5173	-0.5179	15.985	0.2841	80.0000	0.9589	3.9641	0.0325	78.9179	0.8959	8.588	0.0395	78.9174	-0.5252	10.195	0.1194	79.7587
R 51c1423a
R 51c1424a
R 51c1425a	0.4194	10.587	0.0000	77.9694	-0.3748	2.3328	0.0000	78.7878	0.4194	10.587	0.0000	77.9694	-0.3748	2.3328	0.0000	78.7878
R 51c1425a
R 51c1426a	0.3542	12.293	0.1326	111.2541	-0.3824	5.6478	0.0813	108.3304	-0.4328	5.8282	0.0270	112.5027	0.3578	4.5768	0.0645	119.0206	0.3580	8.4349	0.0986	115.1374	-0.4078	5.637	0.0442	110.4198
R 51c1427a	0.1815	6.734	0.0000	58.4764	-0.1248	5.6828	0.0989	55.0579	-0.2252	22.801	0.1551	57.7468	0.1987	7.9448	0.0107	58.1225	0.1901	7.3394	0.0054	57.2895	-0.1750	14.232	0.1270	58.4023
R 51c1428a
R 51c1429a	0.6539	10.935	0.0773	77.8983	-0.6548	12.504	0.2434	78.0000	-0.6808	13.635	0.1980	80.0000	0.7784	17.611	0.2127	80.0000	0.7182	14.273	0.1450	78.9492	-0.6678	13.069	0.2212	79.5000
R 51c1430a	0.5950	11.108	0.0804	92.8470	-0.2527	2.7071	0.1289	86.0800	0.5950	11.108	0.0804	92.8470
R 51c1431a	0.3832	20.879	0.1554	119.3101	-0.3385	6.4954	0.0418	121.0689	-0.3505	7.1334	0.0000	122.7848	0.3944	10.139	0.0573	119.1683	0.3888	15.408	0.1084	119.2392	-0.3435	6.8144	0.0208	122.2158
MEAN	0.4893	11.821	0.0735	95.4517	-0.3891	6.4118	0.0784	94.7532	-0.4054	10.218	0.1084	98.7298	0.5204	9.5849	0.0891	98.8150	0.4934	10.843	0.0758	95.8467	-0.3880	7.8702	0.0903	84.2028
ST. DEV.	0.1853	4.0841	0.0547	25.9275	0.1625	3.1058	0.0764	27.2056	0.1485	6.7307	0.1010	25.7694	0.2675	5.0009	0.0812	28.9879	0.2084	3.0852	0.0563	25.8068	0.1485	4.1452	0.0782	26.2055
N	9	9	9	9	9	9	9	9	9	9	9	9	9	9	9	9	9	9	9	9	9	9	9	9
SEM	0.0478	0.224	0.0280	0.9658	0.0504	0.2203	0.0345	0.9520	0.0483	0.3243	0.0397	0.6345	0.0739	0.3185	0.0407	0.7691	0.0508	0.1945	0.0284	0.5659	0.0428	0.2262	0.0313	0.5578

TABLE 6

Pulse Response - Post-Flight Day 6 (11-15-53)

REFLECTION	Curve 1			Curve 2			Curve 3			Curve 4			Average Inc.			Average Dec.								
	GAIN	K	DC	GAIN	K	DC	GAIN	K	DC	GAIN	K	DC	GAIN	K	DC	GAIN	K	DC						
L 03c1515a
L 03c1516a
L 03c1517a
L 03c1519a
L 03c1520a
L 07c1501a	-0.9186	4.4045	0.0942	131.2077	1.2352	8.4238	0.0832	120.0000	1.2100	3.884	0.0412	128.4114	-1.2070	7.2593	0.2180	122.6370	-1.0628	5.8319	0.1551	126.9224	1.2256	6.6588	0.0672	124.2057
L 07c1501a
L 07c1502a	-1.1701	8.832	0.2957	117.5980	1.0648	3.8647	0.1473	113.3886	1.7923	12.536	0.5338	114.9521	-1.1701	8.832	0.2957	117.5980	1.3986	8.2008	0.3408	114.1704
L 07c1503a	-0.7480	3.2568	0.0235	102.8084	0.8578	5.7204	0.0000	97.7881	0.8968	15.877	0.1254	103.1659	-0.7480	3.2568	0.0235	102.8084	0.7772	10.789	0.0427	100.4820
L 07c1505a	-0.3808	4.4436	0.0087	108.0948	0.3872	5.4608	0.0000	106.1003	0.3888	8.7877	0.0787	107.4101	-0.3808	4.4436	0.0087	108.0948	0.3885	8.1243	0.0394	108.7552
L 07c1507a	-0.2921	4.7628	0.0000	128.0421	0.2750	6.4958	0.0000	128.1780	0.2882	8.9419	0.0317	128.7815	-0.2872	6.9048	0.0715	128.0000	-0.2797	5.8538	0.0358	128.0211	0.2816	6.7189	0.0159	128.4903
MEAN	-0.7019	5.1399	0.0844	118.7504	0.7680	6.1931	0.0481	112.8932	0.8668	9.2073	0.1822	118.1442	0.7371	7.0821	0.1438	124.3185	-0.7283	5.8396	0.1038	118.8881	0.8163	7.7002	0.1051	114.4187
ST. DEV.	0.3872	2.1418	0.1238	12.2882	0.4188	2.0438	0.0688	11.1923	0.6027	4.8878	0.2110	11.2891	0.6645	0.2507	0.1022	2.3780	0.3997	2.0841	0.1220	11.1170	0.4821	1.8981	0.1332	11.1163
N	5	5	5	5	5	5	5	5	5	5	5	5	5	5	5	5	5	5	5	5	5	5	5	5
SEM	0.1212	0.2827	0.0704	0.7011	0.1281	0.2859	0.0524	0.6691	0.1553	0.4413	0.0819	0.6720	0.4078	0.2503	0.1598	0.7710	0.1280	0.2887	0.0688	0.6688	0.1403	0.2754	0.0730	0.6688

Pulse Response

TABLE 7
Pulse Response - Post-Flight Day 11 (11-21-83)

Run	Curve 1				Curve 2				Curve 3				Curve 4				Average Inc.				Average Dec.			
	GAIN	1	2	DC	GAIN	1	2	DC	GAIN	1	2	DC	GAIN	1	2	DC	GAIN	1	2	DC	GAIN	1	2	DC
R 06c2101a	0.5560	11.929	0.1317	144.9898	-0.4646	6.5806	0.1015	145.0000	-0.4817	8.0088	0.0837	147.6385	0.8207	7.0568	0.1186	147.5811	0.5884	8.483	0.1252	144.2854	-0.4732	7.5887	0.0976	146.3183
R 06c2102a	0.1637	4.889	0.0000	123.2332	-0.1324	1.7803	0.0000	112.9868	100.1172	0.1637	4.888	0.0000	123.2332	-0.1324	1.7803	0.0000	112.9866
R 06c2103a	0.2816	10.539	-0.0000	99.8148	-0.2208	8.81	0.0595	88.8913	100.1172	0.2816	10.539	0.0000	99.8148	-0.2208	8.81	0.0595	87.8957
R 06c2104a	0.6483	16.644	0.1278	135.0000	-0.5083	16.548	0.1602	136.3037	-0.1728	15.991	0.1173	97.0000	0.3055	7.0596	0.0305	137.9872	0.8278	11.644	0.0638	135.4988	-0.5407	12.568	0.0801	137.4789
R 06c2105a	0.3410	8.1832	0.0000	128.0232	-0.1631	8.2358	0.1877	128.0000	-0.2209	8.9885	0.0785	128.7718	0.2763	8.4484	0.0245	131.6427	0.3102	8.9208	0.0123	130.3330	-0.1920	8.1022	0.1331	128.8659
R 06c2106a	0.1475	10.089	0.0000	67.0000	-0.1687	8.2602	0.0598	66.0000	-0.2211	15.526	0.0857	68.1612	0.1603	3.1156	0.0000	88.0000	0.1839	8.6024	0.0000	86.0000	-0.1928	11.863	0.0728	67.0806
R 06c2107a	0.3819	8.0583	0.0000	131.9548	-0.2538	6.1776	0.0351	128.7954	-0.3783	14.177	0.0585	136.5542	0.3657	6.7153	0.0158	133.7008	0.3788	7.8698	0.0080	132.8278	-0.3161	10.177	0.0473	133.1748
R 06c2108a	0.1133	7.1088	0.0000	63.4880	-0.1469	19.106	0.1249	63.8057	-0.1588	15.725	0.0825	63.0000	0.1664	10.828	0.0980	83.0000	0.1408	8.888	0.0485	83.4445	-0.1528	17.415	0.1037	63.4528
R 06c2110a	0.7218	10.31	0.1416	56.0890	-0.7815	3.9513	0.0000	45.8638	-0.8348	3.8461	0.0000	47.4898	0.8808	4.5655	0.1835	55.5557	0.7013	7.4375	0.1826	55.8224	-0.7882	3.5887	0.2080	46.5687
R 06c2111a	0.4256	11.233	0.0211	115.0000	-0.2508	5.1801	0.0189	111.8070	-0.2812	11.053	0.0638	112.0170	0.3728	11.175	0.0089	112.0000	0.3883	11.304	0.0155	113.5000	-0.2711	8.4217	0.0514	111.8120
MEAN	0.3801	10.11	0.0422	108.5573	-0.3067	8.5048	0.0748	103.8253	-0.3705	11.231	0.0688	104.4734	0.3957	7.2878	0.0535	105.6184	0.3763	8.5756	0.0452	108.8681	-0.3267	9.3554	0.0674	104.5750
ST. DEV.	0.2117	3.0651	0.0636	32.9912	0.2058	5.4731	0.0683	34.2929	0.2248	4.4285	0.0408	37.2510	0.1859	2.5807	0.0648	35.3884	0.2041	1.985	0.0568	33.3888	-0.2143	4.5667	0.0434	34.7407
N	10	10	10	10	10	10	10	10	9	9	9	8	9	9	9	9	10	10	10	10	10	10	10	10
SEM	0.0460	0.1751	0.0252	0.5744	0.0454	0.2339	0.0258	0.5856	0.0527	0.2338	0.0224	0.8782	0.0482	0.1785	0.0283	0.6808	0.0452	0.1412	0.0238	0.5778	-0.0483	0.2137	0.0208	0.5884
																					0.3822	9.28	0.0583	105.1227

Spontaneous Rate

TABLE 8

Spontaneous Rate - Pre-Flight

Filename	Mean ISI (ms)	SP Rate (S/s)	CV
01o1701a	---	---	---
01o1701e	---	---	---
01o1701i	6.93	144.30	0.23
01o1702a	9.99	100.10	0.04
03a1401a	5.85	170.94	0.17
03a1402a	10.52	95.06	0.16
03a1402e	9.85	101.52	0.14
03a1404a	---	---	---
03a1405a	---	---	---
03a1406a	7.86	127.23	0.20
03a1407a	6.97	143.47	0.05
51a1501a	9.13	109.53	0.07
75a1504a	10.05	99.50	0.17
75a1504e	12.33	81.10	0.30
07a1601a	8.68	115.21	0.25
07a1602a	6.12	163.40	0.06
07a1602e	6.10	163.93	0.06
07a1603a	7.99	125.16	0.18
07a1603e	9.34	107.07	0.17
07a1606a	39.25	25.48	0.09
07a1607a	9.59	104.28	0.20
07a1608a	5.85	170.94	0.24
07a1609a	9.24	108.23	0.03
07a1610a	6.46	154.80	0.25
07a1610e	6.98	143.27	0.25
07a1611a	7.08	141.24	0.26
07a1611e	8.05	124.22	0.22
07a1612a	7.17	139.47	0.03
07a1613a	---	---	---
01a1601a	6.81	146.84	0.27
01a1601e	6.59	116.41	0.34
01a1601i	7.28	137.36	0.28
01a1602a	7.05	141.84	0.10
01a1602e	6.83	146.41	0.10
01a1602i	7.72	129.53	0.10
01a1603a	6.99	111.23	0.03
01a2004a	5.95	166.07	0.06
01a2004e	6.30	158.73	0.10
01a2005a	7.83	127.71	0.05
01a2005e	7.90	126.58	0.05
01a2006a	6.35	119.76	0.25
01a2006e	6.6	151.52	0.14
01a2007a	6.45	155.04	0.15
mean	6.69	128.85	0.15
st dev	5.31	29.07	0.09
n	38.00	38.00	38.00
sem	0.66	0.14	0.01

TABLE 9

Spontaneous Rate - Post Flight Day 1

Filename	Mean ISI (ms)	SP Rate (S/s)	CV
03c0901a	7.03	142.25	0.06
03c0901e	7.00	142.86	0.06
03c0901m	7.05	141.84	0.06
03c0901i	6.88	145.35	0.06
03c0902a	7.06	141.84	0.30
03c0903a	6.79	147.28	0.17
03c0904a	7.68	130.21	0.25
03c0904e	8.83	113.25	0.30
03c0905a	7.29	137.17	0.19
03c0906a	7.69	130.04	0.28
03c0906e	11.72	85.32	0.55
03c0907a	8.44	118.48	0.17
03c0908a	9.47	105.60	0.04
07c1001a	7.38	135.50	0.12
07c1001e	7.35	136.05	0.12
07c1002a	9.94	100.60	0.02
07c1002e	9.88	101.21	0.02
07c1003a	7.85	127.39	0.07
mean	8.07	126.75	0.16
st dev	1.37	16.41	0.14
n	18.00	18.00	18.00
sem	0.07	0.24	0.02

TABLE 10

Spontaneous Rate - Post Flight DAY 2

Filename	Mean ISI (ms)	SP Rate (S/s)	CV
06c1101a	7.91	126.42	0.03
06c1102a	8.63	115.87	0.04
06c1102e	9.00	111.11	0.03
06c1103a	12.23	81.77	0.18
06c1104a	10.91	91.66	0.14
06c1105a	10.30	97.09	0.15
06c1105e	9.77	102.35	0.15
06c1106a	8.16	122.55	0.03
06c1107a	16.20	61.73	0.34
06c1108a	7.96	125.31	0.03
06c1109a	16.62	53.71	0.51
06c1110a	11.56	86.36	0.17
06c1111a	7.32	136.61	0.04
06c1112a	9.49	105.37	0.03
06c1112e	9.60	104.17	0.03
06c1113a	11.16	89.61	0.37
51c1101a	15.84	63.13	0.03
51c1102a	9.25	108.11	0.06
51c1103a	16.45	60.79	0.03
51c1104a	9.27	107.87	0.04
mean	10.66	97.58	0.12
st dev	3.26	23.88	0.14
n	20.00	20.00	20.00
sem	0.08	0.24	0.02

Spontaneous Rate

TABLE 11

Spontaneous Rate - Post Flight DAY 3			
Flarename	Mean ISI (ms)	SP Rate (SP/s)	CV
06c1214a	8.84	113.12	0.03
06c1214e	9.09	110.01	0.03
06c1215a	7.38	135.50	0.06
06c1216a	8.87	112.74	0.04
06c1217a	9.21	108.58	0.04
06c1217e	9.05	110.50	0.04
51c1206a	12.03	83.13	0.04
51c1206e	11.96	83.61	0.03
51c1207a	18.96	58.96	0.04
51c1207e	17.66	58.56	0.04
51c1208a	13.22	75.64	0.31
51c1208e	14.98	66.78	0.20
51c1210a	10.12	96.81	0.22
51c1213a	19.02	52.58	0.03
51c1215a	7.96	125.63	0.12
51c1216a	10.24	97.66	0.03
51c1218a	6.60	151.52	0.06
51c1219a	14.13	70.77	0.03
51c1220a	10.06	99.21	0.05
mean	11.44	95.93	0.06
st dev	3.63	27.60	0.06
n	19.00	19.00	19.00
sem	0.10	0.28	0.01

TABLE 12

Spontaneous Rate - Post Flight DAY 6			
Flarename	Mean ISI (ms)	SP Rate (SP/s)	CV
06c1419a	7.11	140.65	0.03
06c1420a	10.14	98.62	0.04
51c1421a	13.16	75.99	0.33
51c1425a	12.63	79.18	0.26
51c1426a	8.72	114.68	0.05
51c1426e	8.94	111.88	0.05
51c1427a	13.37	74.79	0.04
51c1428a	17.54	57.01	0.04
51c1428e	17.87	55.96	0.07
51c1429a	12.40	80.65	0.06
51c1430a	10.42	95.97	0.27
51c1431a	8.29	120.63	0.04
mean	11.72	92.18	0.11
st dev	3.46	26.15	0.11
n	12.00	12.00	12.00
sem	0.16	0.43	0.03

TABLE 13

Spontaneous Rate - Post Flight DAY 9			
Flarename	Mean ISI (ms)	SP Rate (SP/s)	CV
03c1515a	14.05	71.17	0.03
03c1516a	17.42	57.41	0.73
03c1517a	7.36	135.87	0.10
03c1520e	9.57	104.49	0.16
07c1501a	7.79	128.37	0.10
07c1501e	7.34	136.24	0.09
06c1502e	8.68	115.21	0.16
07c1503a	9.77	102.35	0.06
07c1505a	9.25	106.11	0.03
07c1507a	7.85	127.39	0.03
mean	9.91	106.66	0.15
st dev	3.29	26.61	0.21
n	10.00	10.00	10.00
sem	0.16	0.52	0.05

TABLE 14

Spontaneous Rate - Post Flight DAY 11			
Flarename	Mean ISI (ms)	SP Rate (SP/s)	CV
06c2102a	7.06	141.64	0.06
06c2103a	8.67	115.34	0.03
06c2104a	10.21	97.94	0.03
06c2105a	7.31	136.60	0.07
06c2106a	7.66	130.55	0.04
06c2107a	15.25	65.57	0.03
06c2108a	7.45	134.23	0.03
06c2109a	16.80	59.52	0.04
06c2110a	20.39	49.04	0.32
06c2111a	8.80	113.64	0.04
mean	10.96	104.43	0.07
st dev	4.76	34.71	0.09
n	10.00	10.00	10.00
sem	0.22	0.58	0.03

Sum of Sines

TABLE 15

Sum of Sines Protocols - Pre-Flight (11-14-82 to 12-9-82)

total neurons = 7

Frequency		0.0293		0.0879		0.2051		0.3809							
ear	FILENAME	gain	phase	gain	phase	gain	phase	gain	phase	G	k	tau.V	tau.L	MSE	
L	03a1401b	0.2800	80.3990	0.7200	23.3340	0.7600	23.3640	0.8300	36.2630	2.0650	0.0721	0.2491	2.7290	1.33E-02	
L	03a1402b	***	***	***	***	***	***	***	***	***	***	***	***	***	
L	03a1407b	***	***	***	***	***	***	***	***	***	***	***	***	***	
L	03a1407f	0.4400	48.7050	0.6100	24.6950	0.7000	12.9190	0.6800	7.1110	3.3030	0.0320	0.0000	4.8730	3.70E-04	
L	07a1601b	***	***	***	***	***	***	***	***	***	***	***	***	***	
L	07a1610b	***	***	***	***	***	***	***	***	***	***	***	***	***	
L	07a1611b	***	***	***	***	***	***	***	***	***	***	***	***	***	
L	07a1612b	0.3700	38.0860	0.5000	19.9640	0.5500	13.4000	0.5800	12.1250	4.9170	0.1030	0.0000	9.2460	1.13E-04	
L	01a1601b	***	***	***	***	***	***	***	***	***	***	***	***	***	
L	01a1602b	0.3700	48.2020	0.5100	22.5190	0.5700	18.4460	0.6300	18.9400	3.9880	0.1070	0.0403	7.0890	1.94E-04	
L	01a1603b	0.2500	32.9740	0.3100	14.2050	0.3100	5.5030	0.3100	4.3610	2.4410	0.0020	0.0047	7.8470	5.55E-05	
L	01a2004b	***	***	***	***	***	***	***	***	***	***	***	***	***	
L	01a2005b	***	***	***	***	***	***	***	***	***	***	***	***	***	
L	01a2006b	0.4400	57.5410	0.5800	34.0490	0.7800	25.8270	0.8300	24.1720	4.8460	0.1920	0.0229	6.8270	8.59E-04	
L	01a2007b	0.3600	44.4870	0.5100	9.0640	0.6600	#####	0.7900	#####	***	***	***	***	***	
STATISTICS		gain	phase	gain	phase	gain	phase	gain	phase	G	k	tau.V	tau.L	MSE	
MEAN		0.3586	50.0563	0.5343	21.1186	0.6157	11.9160	0.6643	5.2526	3.5917	0.0847	0.0528	6.4352	2.48E-03	
ST. DEV.		0.0724	15.5353	0.1258	7.9718	0.1584	14.1037	0.1847	33.3278	1.2048	0.0665	0.0074	2.3087	5.30E-03	
N		7	7	7	7	7	7	7	7	6	6	6	6	6	6
SEM		0.0384	0.5631	0.0507	0.4033	0.0569	0.5365	0.0614	0.8247	0.1829	0.0430	0.0520	0.2532	1.21E-02	

TABLE 16

Sum of Sines Protocols - Synchronous Controls (1-8-83 to 1-10-83)

total neurons = 1

Frequency		0.0293		0.0879		0.2051		0.3809							
ear	FILENAME	gain	phase	gain	phase	gain	phase	gain	phase	G	k	tau.V	tau.L	MSE	
L	07c1002b	0.2200	37.6450	0.2800	18.9080	0.0300	9.7090	0.3100	5.7590	2.2000	0.0430	0.0000	7.4190	4.01E-05	
L	07c1003b	***	***	***	***	***	***	***	***	***	***	***	***	***	
STATISTICS		gain	phase	gain	phase	gain	phase	gain	phase	G	k	tau.V	tau.L	MSE	
MEAN		0.2200	37.6450	0.2800	18.9080	0.0300	9.7090	0.3100	5.7590	2.2000	0.0430	0.0000	7.4190	4.01E-05	
ST. DEV.		0.0000	0.0000	0.0000	0.0000	0.0000	0.0000	0.0000	0.0000	0.0000	0.0000	0.0000	0.0000	0.0000	0
N		1	1	1	1	1	1	1	1	1	1	1	1	1	1
SEM		0.0000	0.0000	0.0000	0.0000	0.0000	0.0000	0.0000	0.0000	0.0000	0.0000	0.0000	0.0000	0.0000	0

TABLE 17

Sum of Sines Protocols - Post Flight Day 2 (1-11-83)

total neurons = 6

Frequency		0.0293		0.0879		0.2051		0.3809							
ear	FILENAME	gain	phase	gain	phase	gain	phase	gain	phase	G	k	tau.V	tau.L	MSE	
R	06c1102b	0.3900	33.4080	0.4400	21.2040	0.4800	14.8150	0.5200	14.4350	5.5570	0.0970	0.0297	11.5620	2.35E-04	
R	06c1106b	***	***	***	***	***	***	***	***	***	***	***	***	***	
R	06c1106b	0.2500	31.7430	0.3200	20.7750	0.3400	12.9110	0.3800	9.7150	3.8010	0.0990	0.0000	11.4105	1.12E-04	
R	06c1108b	0.2500	32.7230	0.3100	20.8840	0.3500	13.4920	0.3800	10.9630	3.8890	0.1090	0.0000	11.6672	7.70E-05	
R	06c1112b	0.2800	35.2010	0.3200	16.0630	0.3500	11.3730	0.3700	11.1070	3.5970	0.0880	0.0000	10.5208	2.97E-05	
R	51c1101b	0.2100	34.8150	0.2500	14.9520	0.2900	6.8780	0.2700	5.0350	2.1755	0.0255	0.0000	8.0624	1.21E-04	
R	51c1102b	0.2900	47.0570	0.4600	38.2450	0.6400	29.7180	0.7300	25.4460	5.9963	0.2820	0.0000	10.4932	9.06E-04	
STATISTICS		gain	phase	gain	phase	gain	phase	gain	phase	G	k	tau.V	tau.L	MSE	
MEAN		0.2750	35.7912	0.3500	22.0205	0.4100	14.8645	0.4350	12.7835	4.1693	0.1168	0.0050	10.6193	2.47E-04	
ST. DEV.		0.0619	5.8592	0.0820	8.3928	0.1310	7.7756	0.1655	6.9086	1.3966	0.0863	0.0121	1.3547	3.30E-04	
N		6	6	6	6	6	6	6	6	6	6	6	6	6	6
SEM		0.0415	0.3965	0.0477	0.4828	0.0603	0.4647	0.0678	0.4381	0.1971	0.0490	0.0184	0.1940	3.03E-03	

Sum of Sines

TABLE 18

Sum of Sines Protocols - Post Flight Day 3 (1-12-83)

total neurons = 8

ID	FILENAME	0.0293		0.0879		0.2051		0.3809		G	k	tau V	tau L	MSD
		gain	phase	gain	phase	gain	phase	gain	phase					
R	51c1206b	0.3600	39.5360	0.4800	23.5260	0.5600	14.2580	0.5900	10.0700	4.3218	0.1014	0.0000	8.0026	3.70E-04
R	51c1207b	0.1100	32.7550	0.1400	19.9343	0.1600	12.5860	0.1600	7.5270	1.7962	0.1205	0.0350	12.0030	2.99E-05
R	51c1209b	0.3100	61.6880	0.5300	45.7570	0.8000	38.4280	0.9600	32.9780	5.6336	0.3539	0.0000	7.8378	9.90E-04
R	51c1210b	0.4500	52.7780	0.6000	32.5680	0.7000	22.2800	0.7300	22.0900	3.8624	0.1050	0.0663	5.7020	8.33E-04
R	51c1214b	***	***	***	***	***	***	***	***	***	***	***	***	***
R	51c1216b	0.4300	35.1300	0.5300	18.0820	0.5600	12.0630	0.8000	8.1310	5.3480	0.0746	0.0000	9.4252	1.15E-04
R	51c1218b	0.5200	60.9930	0.6300	34.3380	0.8100	23.3630	0.8500	16.8570	4.2850	0.1510	0.0011	5.6630	3.38E-03
R	06c1214b	0.2800	27.2340	0.2400	8.7000	0.3300	6.5380	0.2100	27.0350	1.7020	0.1695	0.2514	6.7120	2.81E-03
R	06c1215b	0.7500	38.6490	0.8700	25.6400	0.8200	20.7320	0.8600	17.8130	6.0480	0.0130	0.1191	7.0320	6.89E-03
STATISTICS		gain	phase	gain	phase	gain	phase	gain	phase	G	k	tau V	tau L	MSD
MEAN		0.4013	43.5954	0.5025	26.0682	0.5963	18.7848	0.6225	17.7876	4.1245	0.1361	0.0580	7.7960	1.93E-03
ST. DEV.		0.1884	13.1992	0.2278	11.3892	0.2422	9.8357	0.3044	9.2099	1.8428	0.1001	0.0687	2.1238	2.36E-03
N		8	8	8	8	8	8	8	8	8	8	8	8	8
SEM		0.0543	0.4534	0.0597	0.4218	0.0815	0.3920	0.0690	0.3793	0.1602	0.0395	0.0372	0.1822	6.07E-03

TABLE 19

Sum of Sines Protocols - Post Flight Day 5 (1-14-83)

total neurons = 8

ID	FILENAME	0.0293		0.0879		0.2051		0.3809		G	k	tau V	tau L	MSD
		gain	phase	gain	phase	gain	phase	gain	phase					
R	51c1421b	0.4500	47.6670	#####	23.8790	0.6400	18.0500	0.7200	18.8500	5.0150	0.1240	0.0312	7.9290	5.00E-04
R	51c1423b	***	***	***	***	***	***	***	***	***	***	***	***	***
R	51c1424b	***	***	***	***	***	***	***	***	***	***	***	***	***
R	51c1425b	0.1700	58.6760	0.3000	14.4220	0.3400	13.7400	0.3900	5.4700	1.3860	0.0150	0.0000	3.9900	1.34E-03
R	51c1426b	0.2300	35.6620	0.2700	18.3830	0.3000	9.2420	0.3100	8.3640	2.5240	0.0530	0.0000	8.8030	5.37E-05
R	51c1429b	0.6200	39.2860	0.7800	23.5840	0.9000	16.5800	0.9600	14.8180	9.2420	0.1430	0.0000	10.6700	3.14E-04
R	51c1431b	0.2900	51.8320	0.3800	24.1930	0.4100	17.8730	0.4500	19.9790	2.2297	0.0474	0.0829	5.5048	1.44E-04
R	06c1420b	0.2400	34.4860	0.3000	22.8490	0.3400	17.6960	0.3700	18.4740	4.3530	0.1440	0.0263	13.2760	2.07E-05
STATISTICS		gain	phase	gain	phase	gain	phase	gain	phase	G	k	tau V	tau L	MSD
MEAN		0.3333	44.6018	59.5017	21.2183	0.4883	15.5307	0.5383	13.9925	4.1250	0.0877	0.0234	8.3288	3.96E-04
ST. DEV.		0.1895	9.6978	#####	3.9601	0.2358	3.4753	0.2635	6.4965	2.8526	0.0580	0.0324	3.3781	4.96E-04
N		6	6	6	6	6	6	6	6	6	6	6	6	6
SEM		0.0686	0.5190	2.0053	0.3317	0.0808	0.3107	0.0856	0.4248	0.2815	0.0394	0.0300	0.3062	3.71E-03

TABLE 20

Sum of Sines Protocols - Post Flight Day 6 (1-15-83)

total neurons = 1

ID	FILENAME	0.0293		0.0879		0.2051		0.3809		G	k	tau V	tau L	MSD
		gain	phase	gain	phase	gain	phase	gain	phase					
L	07c1501b	***	***	***	***	***	***	***	***	***	***	***	***	***
L	07c1502b	***	***	***	***	***	***	***	***	***	***	***	***	***
L	07c1505b	***	***	***	***	***	***	***	***	***	***	***	***	***
L	07c1507b	***	***	***	***	***	***	***	***	***	***	***	***	***
L	07c1508b	0.3900	61.2390	0.6400	31.1720	0.7400	14.1180	0.7900	13.1660	2.7421	0.0523	0.0040	3.6669	6.06E-04
L	03c1516b	***	***	***	***	***	***	***	***	***	***	***	***	***
L	03c1518b	***	***	***	***	***	***	***	***	***	***	***	***	***
STATISTICS		gain	phase	gain	phase	gain	phase	gain	phase	G	k	tau V	tau L	MSD
MEAN		0.3900	61.2390	0.6400	31.1720	0.7400	14.1180	0.7900	13.1660	2.7421	0.0523	0.0040	3.6669	6.06E-04
ST. DEV.		0.0000	0.0000	0.0000	0.0000	0.0000	0.0000	0.0000	0.0000	0.0000	0.0000	0.0000	0.0000	0
N		1	1	1	1	1	1	1	1	1	1	1	1	1
SEM		0.0000	0.0000	0.0000	0.0000	0.0000	0.0000	0.0000	0.0000	0.0000	0.0000	0.0000	0.0000	0

Sum of Sines

TABLE 21

Sum of Sines Protocols - Post Flight Day 7 (1-18-93)

total neurons = 1

Frequency		0.0293		0.0879		0.2051		0.3809						
ear	FILENAME	gain	phase	gain	phase	gain	phase	gain	phase	G	k	tau V	tau L	MSE
L	92c1601b	***	***	***	***	***	***	***	***	***	***	***	***	***
L	01c1601b	***	***	***	***	***	***	***	***	***	***	***	***	***
L	01c1602b	***	***	***	***	***	***	***	***	***	***	***	***	***
L	01c1604b	3.0700	54.0910	5.1600	30.1210	5.5100	19.4080	6.4200	20.8810	0.9620	0.1173	0.0385	5.4995	4.59E-05
STATISTICS		gain	phase	gain	phase	gain	phase	gain	phase	G	k	tau V	tau L	MSE
MEAN		3.0700	54.0910	5.1600	30.1210	5.5100	19.4080	6.4200	20.8810	0.9620	0.1173	0.0385	5.4995	4.59E-05
ST. DEV.		0.0000	0.0000	0.0000	0.0000	0.0000	0.0000	0.0000	0.0000	0.0000	0.0000	0.0000	0.0000	0
N		1	1	1	1	1	1	1	1	1	1	1	1	1
SEM		0.0000	0.0000	0.0000	0.0000	0.0000	0.0000	0.0000	0.0000	0.0000	0.0000	0.0000	0.0000	0

TABLE 22

Sum of Sines Protocols - Post Flight Day 11 (1-21-93)

total neurons = 6

Frequency		0.0293		0.0879		0.2051		0.3809						
ear	FILENAME	gain	phase	gain	phase	gain	phase	gain	phase	G	k	tau V	tau L	MSE
R	06c2101b	0.1400	73.8120	0.1700	19.1320	0.2400	21.5990	0.2200	21.6820	0.0000	0.0590	0.0718	4.2580	1.04E-13
R	06c2102b	0.4000	37.2170	0.5100	28.5430	0.6200	23.5580	0.7000	23.6410	0.0001	0.2140	0.0224	15.8620	1.63E-14
R	06c2104b	0.2300	30.9860	0.2700	14.3720	0.2900	8.7490	0.2900	7.1110	2.9420	0.0480	0.0031	10.4350	1.40E-05
R	06c2105b	0.4100	33.0500	0.5300	21.0970	0.5800	17.1940	0.6200	15.2290	0.0001	0.1340	0.0134	13.1940	1.47E-14
R	06c2106b	0.1600	48.9780	0.2600	13.9430	0.2900	13.2710	0.3100	14.2840	1.7730	0.0770	0.0108	6.3430	7.15E-04
R	06c2108b	***	***	***	***	***	***	***	***	***	***	***	***	***
R	06c2109b	***	***	***	***	***	***	***	***	***	***	***	***	***
R	06c2111b	0.2500	32.4000	0.3200	19.9780	0.3500	14.5400	0.3600	12.5940	0.0000	0.1100	0.0076	12.0430	6.37E-15
STATISTICS		gain	phase	gain	phase	gain	phase	gain	phase	G	k	tau V	tau L	MSE
MEAN		0.2650	42.7405	0.3433	19.5108	0.3950	16.5018	0.4167	15.7568	0.7858	0.1070	0.0215	10.3558	1.22E-04
ST. DEV.		0.1161	16.5762	0.1453	5.3267	0.1631	5.5077	0.1954	6.0740	1.2723	0.0614	0.0255	4.3477	2.91E-04
N		6	6	6	6	6	6	6	6	6	6	6	6	6
SEM		0.0566	0.6786	0.0635	0.3647	0.0673	0.3911	0.0737	0.4108	0.1880	0.0413	0.0266	0.3475	2.84E-03

Sine Protocol
0.2051 Hz

TABLE 23
Pre-Flight (11-14-93 to 12-9-93)

Site	FEQUANCY	gain	phase
L	01c1702d	0.43	9.8810
L	03a1401d	1.02	19.2150
L	03a1402d	2.26	25.6480
L	03a1407d	0.70	12.1920
L	75a1504d	***	***
L	01a1801d	***	***
L	01a1802d	0.60	21.0840
L	01a1803d	0.31	16.7600
L	01a1803h	***	***
L	07a1801d	1.64	36.8490
L	07a1802d	0.77	22.3990
L	07a1810d	0.36	10.6120
L	07a1811d	0.38	9.1950
L	07a1812d	0.57	12.1480
L	01a2004d	1.12	25.9100
L	01a2005d	0.39	13.1760
L	01a2006d	0.81	24.8050
L	01a2007d	***	***
STATISTICS			
MEAN		0.81	18.1667
ST. DEV.		0.56	12.4152
N		14	14
SEM		0.05	0.2517

TABLE 26
Post-Flight Day 3 (1-12-93)

Site	FEQUANCY	gain	phase
R	51c1206d	0.56	14.5580
R	51c1207d	0.18	11.7780
R	51c1208d	1.02	11.1400
R	51c1210d	0.71	21.0360
R	51c1211d	***	***
R	51c1216d	0.81	10.6730
STATISTICS			
MEAN		0.61	13.8370
ST. DEV.		0.31	4.2974
N		5	5
SEM		0.11	0.4146

TABLE 29
Post-Flight Day 7 (1-16-93)

Site	FEQUANCY	gain	phase
L	01c1801d	***	***
L	01c1802d	0.74	14.7970
L	01c1803d	***	***
L	01c1804d	***	***
L	01c1804h	0.29	18.1610
L	82c1801d	***	***
STATISTICS			
MEAN		0.52	16.4790
ST. DEV.		0.32	2.3787
N		2	2
SEM		0.28	0.7712

TABLE 27
Post-Flight Day 5 (1-16-93)

Site	FEQUANCY	gain	phase
R	51c1421d	0.60	20.7930
R	51c1424d	0.52	26.9100
R	51c1425d	0.35	21.7340
R	51c1428d	0.20	11.0700
R	51c1429d	0.66	16.4580
R	06c1420d	0.34	18.7500
STATISTICS			
MEAN		0.45	19.2656
ST. DEV.		0.18	5.3325
N		6	6
SEM		0.07	0.3849

TABLE 30
Post-Flight Day 6 (1-17-93)

Site	FEQUANCY	gain	phase
L	07c1701d	0.81	3.8540
STATISTICS			
MEAN		0.81	3.8540
ST. DEV.		0.00	0.0000
N		1	1
SEM		0.00	0.0000

TABLE 24
Synchronous Control (1-9-93 to 1-10-93)

Site	FEQUANCY	gain	phase
L	07a1002d	0.31	10.1680
L	07a1003d	1.09	18.7090
STATISTICS			
MEAN		0.70	14.4385
ST. DEV.		0.55	6.0394
N		2	2
SEM		0.37	1.2288

TABLE 28
Post-Flight Day 6 (1-15-93)

Site	FEQUANCY	gain	phase
L	03c1516d	0.37	25.2260
L	07c1501d	1.42	23.2340
L	07c1502d	1.44	42.1080
STATISTICS			
MEAN		1.08	30.1887
ST. DEV.		0.61	10.3704
N		3	3
SEM		0.26	1.0734

TABLE 31
Post-Flight Day 11 (1-21-93)

Site	FEQUANCY	gain	phase
R	06c2101d	***	***
R	06c2102d	0.61	24.4030
R	06c2102h	***	***
R	06c2104d	0.28	9.2520
STATISTICS			
MEAN		0.45	18.8275
ST. DEV.		0.23	10.7134
N		2	2
SEM		0.24	1.8366

TABLE 25
Post-Flight Day 2 (1-13-93)

Site	FEQUANCY	gain	phase
R	06c1102d	0.49	14.9520
R	06c1105d	0.58	16.4380
R	06c1106d	0.34	11.6900
R	06c1108d	0.34	10.5890
R	06c1112d	0.37	10.7400
R	51c1101d	0.26	8.8000
R	51c1103d	0.27	9.1140
STATISTICS			
MEAN		0.38	11.7461
ST. DEV.		0.11	2.8756
N		7	7
SEM		0.05	0.2423

EXPERIMENT K-08-04 (Part 1)

FUNCTIONAL NEUROMUSCULAR ADAPTATION TO SPACE FLIGHT

Principal Investigator:

V. Reggie Edgerton
University of California at Los Angeles
Los Angeles, CA

Co-Investigators:

Roland R. Roy
University of California at Los Angeles
Los Angeles, CA

John A. Hodgson
University of California at Los Angeles
Los Angeles, CA

FUNCTIONAL NEUROMUSCULAR ADAPTATION TO SPACE FLIGHT

V. Reggie Edgerton, Roland R. Roy, John A. Hodgson

INTRODUCTION

The following tasks were proposed for the Cosmos project during 1993:

- 1) Complete recordings of all preflight candidates during performance of a foot pedal motor control task while in the space capsule mock-up.
- 2) Complete recordings of all preflight candidates during locomotion and postural tasks.
- 3) Complete recordings of 24-hour spontaneous cage activity in the two flight monkeys before and after flight and of at least three control (non-flight) monkeys after the flight has been completed.
- 4) Complete recordings of the foot pedal and motor control tasks during flight and postflight as scheduled.
- 5) Complete recordings of the vertical drop test pre, during and postflight for the two flight and three control monkeys.
- 6) Complete recordings of locomotion and posture tests of the two flight monkeys postflight.
- 7) Complete recordings of locomotion and postural tests of at least three control (non-flight) monkeys during the postflight period.
- 8) Recalibrate buckles of the two flight and of at least three control monkeys postflight.
- 9) Complete analysis of the 24 hour EMG recordings of all monkeys.
- 10) Complete analysis of the foot pedal, locomotor and postural motor control tasks for the two flight and three control monkeys.

It was proposed that efforts in the first postflight year be concentrated on the two flight animals and three postflight animals.

RESULTS

Table 1 summarizes the results of preflight recording from the flight pool and indicates ranking determined for this experiment.

Animals 906 and 151 were flown. No preflight 24 hr cage activity or chair trial data was available from 151 following reimplantation of the defective soleus electrode. The first postflight data available for monkey 906 was 25 days after recovery.

24 Hour Cage Activity

Figure 1 shows 24 successive histograms for (a) soleus and (b) medial gastrocnemius throughout a 24 hour period beginning at 12 noon. The first (leftmost) bin, containing the counts of baseline activity has been removed from each histogram. Circadian changes in activity are very clear, with some hours, particularly during the night showing no EMG activity. Activities in other animals showed similar changes throughout the day but with very different absolute values and different relationships between soleus and medial gastrocnemius amplitudes.

Table 2 illustrates this for three juvenile animals from the Cosmos flight pool and compares them with three adult animals recorded at the NASA Ames research facility.

Figure 2 summarizes these findings. Though no significant differences were observed due to the large differences in EMG amplitudes recorded from individuals, the juvenile animals appeared to show lower levels of overall EMG activity than adults.

Force Recordings

Preflight chair trials demonstrated that all but two of the implanted force transducers were functional. The two defective transducers had a circuit to ground, indicating a breakdown of electrical insulation. One problem which became apparent during the tests on the remaining transducers was drift to such a degree that compensation modules had to be switched in order to bring the transducer output into a measurable range.

Table 3 summarizes the drift of transducers during our recordings and indicates the compensation modules found to bring the traducers within a usable range.

Figure 3 shows data from one preflight chair trial. The four implanted muscles show normal patterns of EMG activity with force in the medial gastrocnemius muscle following a similar pattern to the EMG activity. Forces during this trial were in the range of 0-1kg, significantly lower than the estimated force output of a monkey medial gastrocnemius muscle (>15kg). At these force levels, the lever excursion was maximal, indicating that the monkey was exerting force against the lever stop. The first second of the trace indicates a sequence where the lever was moved through most of its range then allowed to return to its original position. There was very little force developed in the medial gastrocnemius muscle during this period and this corresponds to a period of barely detectable EMG in the muscle. There are, however corresponding bursts of activity in the soleus and vastus lateralis muscles. It is highly probable that the soleus muscle developed sufficient force alone to overcome the forces in the lever with vastus lateralis providing extensor torques at the knee. The inset on the right hand side of figure 3 shows the first second of activity displayed at a higher gain. The higher peak in the middle of the force record corresponds to the lever press and indicated that medial gastrocnemius developed less than 50gm of force.

Animal 151 had a defective force transducer which was not connected during flight. At the time of launch the transducer on animal 906 had drifted to such a degree that it was outside of the measurable range for the duration of the flight. Postflight chair trials and calibrations indicated that all the transducers tested were still functional.

The trial on 906 indicated that the transducer was in good condition following the flight. The low levels of force recorded by the transducer during these trials may, as in the preflight trials, indicate that the soleus muscle was generating most of the torque around the ankle.

These findings demonstrate that transducer life is sufficient to provide data for preflight, flight and postflight recordings.

Chair Trial EMG Activity

Successful chair trial recordings were made on animal 906 preflight, on both animals during flight and postflight. Flight data presented two significant problems. The monkeys performed the motor tasks very poorly during flight, providing very little data to analyze and the EMG amplifiers were set at high gains resulting in clipped signals (Figure 4). Analysis of the EMG data was conducted despite the clipped signals and this should be borne in mind when interpreting the data.

Figure 5 tracks amplitudes of soleus and medial gastrocnemius EMG activity in the two flight animals. Animal 906 shows a significant drop in EMG activity in both muscles on the second day in space relative to preflight conditions. Soleus activity appeared to recover only slightly on days 4 and 6 whereas medial gastrocnemius appeared to return to preflight levels. Postflight activity more than 3 weeks after recovery indicates an incomplete recovery of soleus activity and a postflight depression of medial gastrocnemius activity. Preflight activity levels for animal 151 were not available but show a reverse of the trends seen in animal 906. Soleus activity remained at high levels during the flight, even increasing on days 4 and 6 and fell on return to earth. In contrast, medial gastrocnemius activity was low during the flight and immediately postflight and recovered slightly after 3 weeks.

The previous Bion flight (Cosmos 2044) had indicated a significant change in the relationship between soleus and gastrocnemius activity following space flight. We compared this relationship in the current flight by calculating a ratio of mean medial gastrocnemius amplitude to mean soleus amplitude. The findings are illustrated in figure 6. In monkey 151 the ratio of medial gastrocnemius to soleus was low during flight and immediately postflight. This indicated low levels of medial gastrocnemius activity relative to soleus. Three weeks after recovery the ratio has increased substantially, indicating that medial gastrocnemius activity rose relative to soleus. In animal 151 preflight levels and those 3 weeks after recovery had similar, relatively low values. During flight the ratio increased substantially, suggesting that soleus activity decreased relative to medial gastrocnemius activity.

DISCUSSION

The following list summarizes the tasks completed during 6 week preflight recording visit to IMBP in Moscow.

- Modification of EMG connector to improve the reliability of EMG recording.
- 24 hour cage activity recording from all flight candidate animals with the exception of 151 and 1417. Recordings from 151 indicated that the soleus EMG implant had shifted and was no longer recording activity from the soleus muscle. The electrode was reimplanted but no further 24 hour recordings were made.
- Attempts were made to record from flight candidates during the foot lever task. There were intermittent problems with the space capsule mock-up which prevented recordings from some monkeys. Other animals did not perform the foot lever task during recording.
- Force transducer calibrations on all flight candidate animals.
- Time constraints during this visit did not permit the posture, locomotion and drop tests to be conducted during this visit.

The animals chosen for flight were #151 and #906. Neither animal was high on our priority list (see Table 1). Nevertheless, both animals provided valuable information.

The following list summarizes the tasks completed during 4 week postflight recording visit to IMBP in Moscow

- Postflight recordings from flight animals.
- Postflight recordings on 3 control (non-flight) animals.
- Recalibration of force transducers on 1 flight and 4 control (non-flight) animals.
- Attempts were made to record EMG and video data from the flight animals during postflight locomotion and postural activity. EMG data were unusable due to poor reception of the telemetered EMG signal.
- Time constraints during this visit did not permit the 24 hour cage activity and drop tests to be conducted during this visit.

Normal Cage EMG Activity

Normal cage activity recorded in the juvenile monkeys at IMBP in Moscow show large differences in the levels of EMG activity recorded from different individuals and different relationships between soleus and medial gastrocnemius muscles in those individuals. These findings parallel those made at NASA Ames on adult animals indicating that, for EMG studies, each animal must be used as its own control.

Force Transducer Performance

Eight of 10 force transducers were operational before flight and of the 5 transducer tested postflight, all were operational, indicating a potential high probability of success with these transducers in the future.

The low levels of force recorded from the medial gastrocnemius muscle during chair trial activities suggests that a majority of the torque around the ankle may have been generated by the soleus muscle during these trials. The drop in soleus EMG activity in animal 906 flight suggests that this situation may change during flight so that more of the torque may be generated by medial gastrocnemius.

Flight EMG Recordings

The flight EMG recordings suggest that significant changes in muscle control may occur in space flight. The very different observations made in the two animals is somewhat puzzling. The lack of preflight data for animal 151 and of postflight data close to recovery for animal 906 makes comparison with our previous flight (Cosmos 2044) difficult. Animal 151 shows a drop in soleus amplitude from the post recovery recording to the 25 day post recovery recording, in contrast to our observations on flight 2044 where soleus amplitude increased for several days after recovery. A tempting suggestion would be that the soleus and gastrocnemius channels on animal 151 were reversed at some stage of the experimental procedure. This would bring observations on animal 151 more into line with the observations made on animal 906 and with the animal recorded in our previous flight. At the present time we have no verification of such a switch.

It is also clear from our recordings that levels of EMG recorded during space flight can attain values similar to those measured on earth. Amplifier gain settings should therefore probably not be changed for space flight.

TABLE 1

EDGERTON - MONKEY RANKINGS AS OF 11/1/92

Rank	Animal Number	Comments
1-5	1401, 27892, 25775, 27856, 27803	At this time, these animals are of equal ranking. All flight recorded leg EMGs and the TFT appear to be intact. Performance on the motor task and implant viability should be considered at the time of the final selection.
6	25476 "Houdini"	Currently all leg EMG electrodes and the TFT are working in this animal. However the TFT has been repaired and the durability of the repair is questionable. Also, it is likely that he will get to and damage his implants again.
7	27906	Soleus EMG exhibits an intermittent dropout.
8	26151	Force buckle has leakage to ground. Do not ground animal if connected to force transducer amplifier, unless you receive prior approval from John Hines.
9	27907	Force buckle has high noise level. Recordings are useless.
10	27838	Animal does not perform foot lever task

TABLE 2

Total Daily Muscle Activity

Monkey Number	Medial Gastrocnemius (mVs)	Soleus (mVs)
I738 (adult)	914	1166
M009 (adult)	935	1970
411 (adult)	1355	1462
M27803 (juv.)	1671	1671
M27892 (juv.)	358	262
M27906 (juv.)	54	499

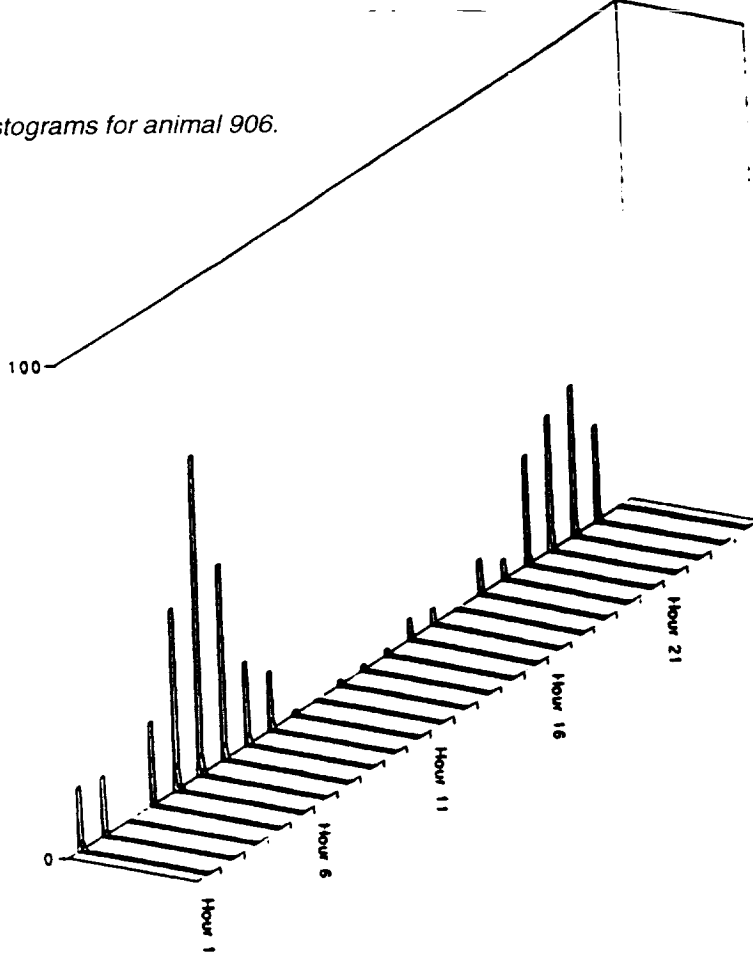
TABLE 3

ANIMAL #	FORCE TRANSDUCER OFFSET		
	DATE	OFFSET(V)	COMP.MOD
27803	10/8/92	0	17
	10/15/92	-.7	
	10/21/92	-.55	
	10/26/92	-1.2	
27907	10/7/92	10	19
	10/21/92	10	19
	10/30/92	10	19
		3.5	11
1401	10/7/92	0	24
	10/20/92	-2.5	
	10/26/92	-2.8	
	10/30/92	-1.9	
25588	10/21/92	.8	23
26151	10/21/92	1.8	16
	10/27/92	1.2	
	10/29/92	3.6	
27856	10/6/92	Dropout	22
	10/22/92	10	22
	10/26/92	-0.5	19

ANIMAL #	FORCE TRANSDUCER OFFSET		
	DATE	OFFSET(V)	COMP.MOD
27906	10/9/92	0	11
	10/20/92	1.3	
	10/27/92	0.2	
27838	10/12/92	0.5	15
	10/20/92	-0.5	
	10/30/92	1	
25476	10/14/92	1	25
	10/21/92	-1.4	
	10/27/92	-1.4	
	10/28/92	-1.7	
25775	10/8/92	-5	20
	10/20/92	-5	
	10/27/92	-5	
	10/30/92	-5	
1417			Not tested.
27892	10/13/92	-2	18
		0	19
	10/20/92	-3.7	18
		-1.5	19
	10/29/92	-2.8	19

24-hour cage activity amplitude histograms for animal 906.

Soleus



Medial
Gastrocnemius

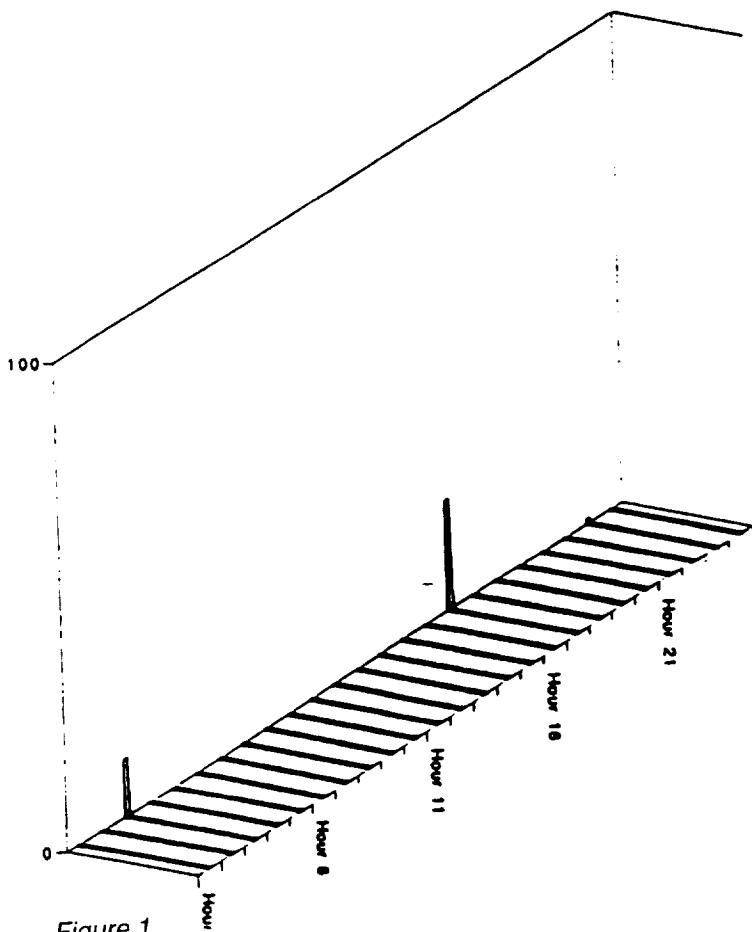


Figure 1.

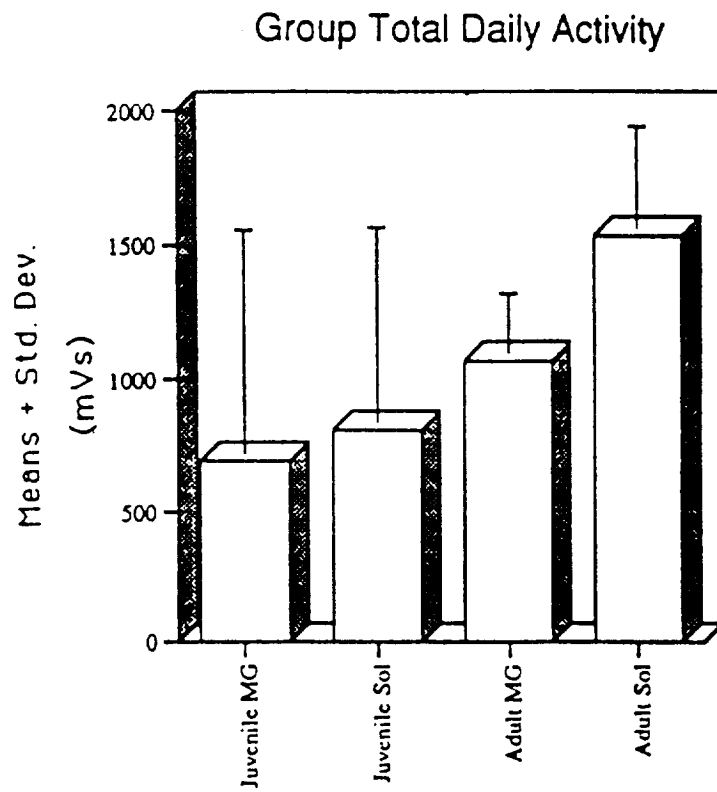


Figure 2. Group total daily activity.

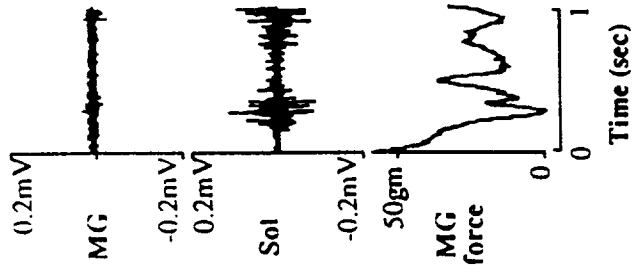
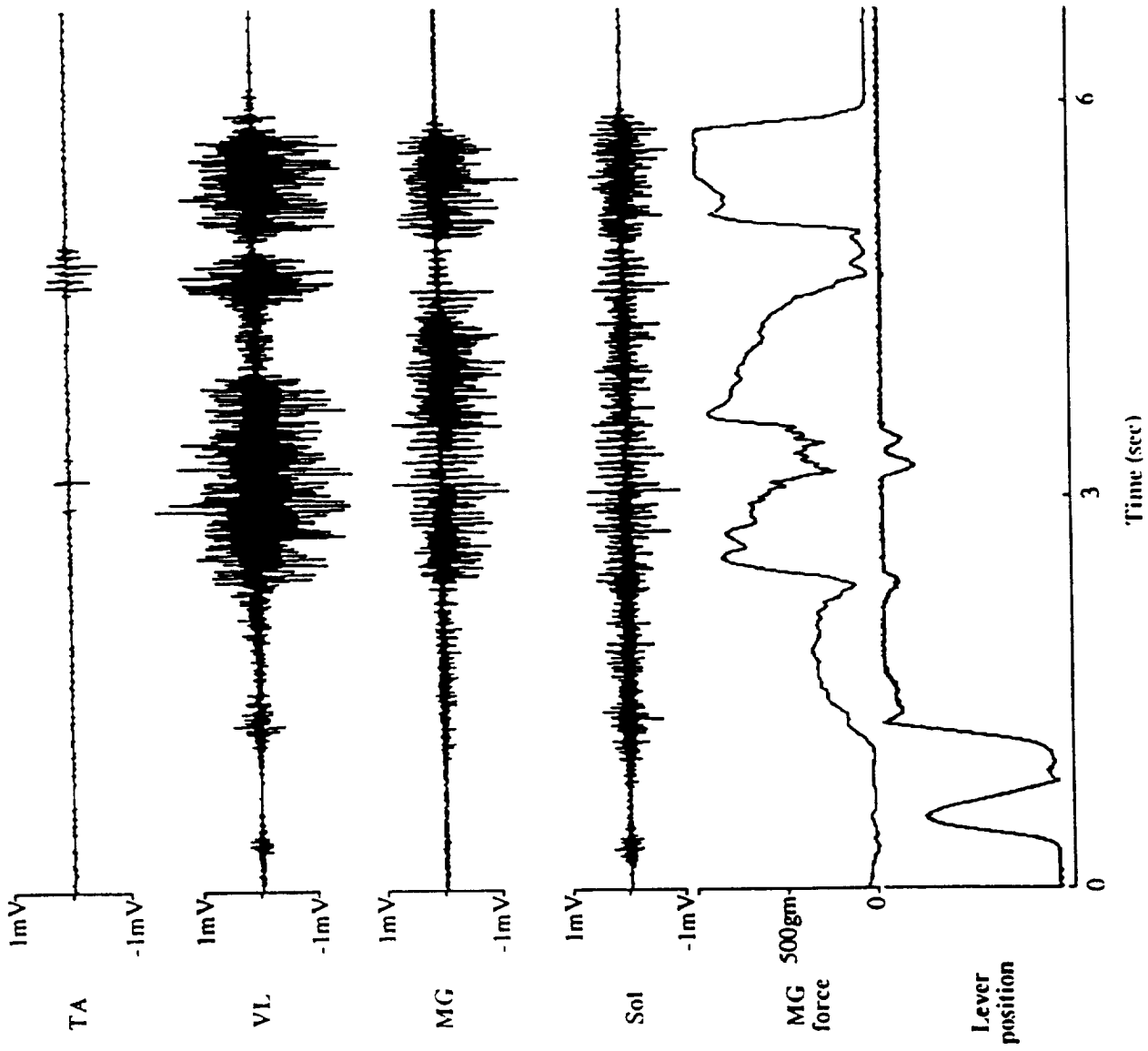


Figure 3. Preflight chair trail animal 892.

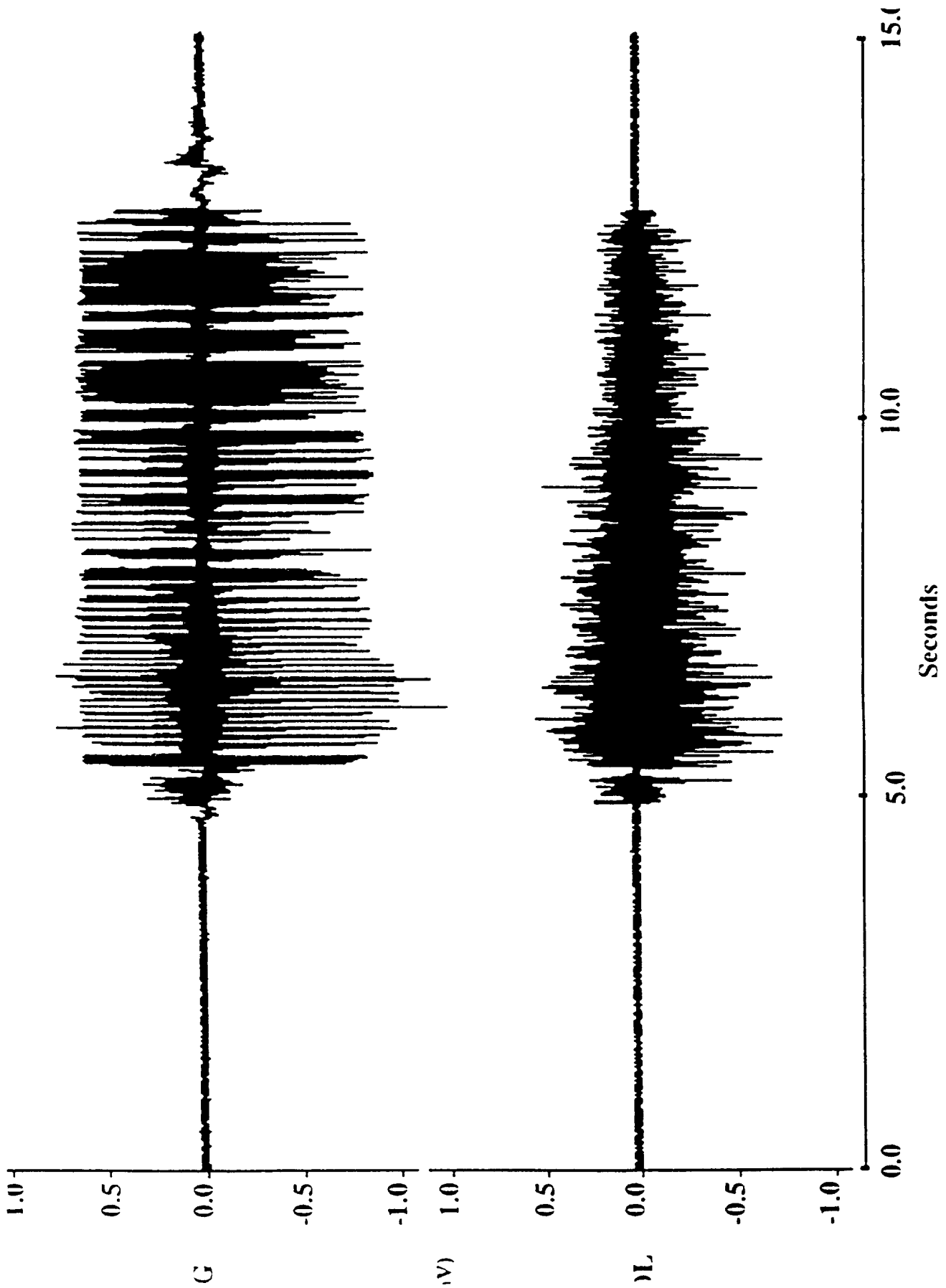


Figure 4. Flight data at 4000 gain.

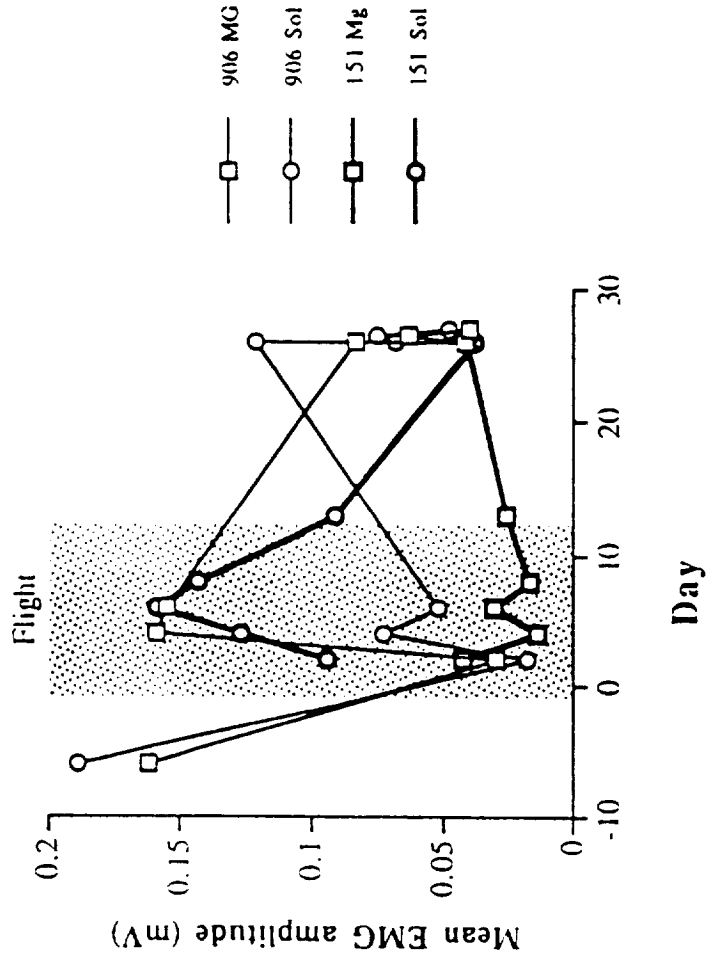


Figure 5. EMG amplitude changes inflight monkeys.

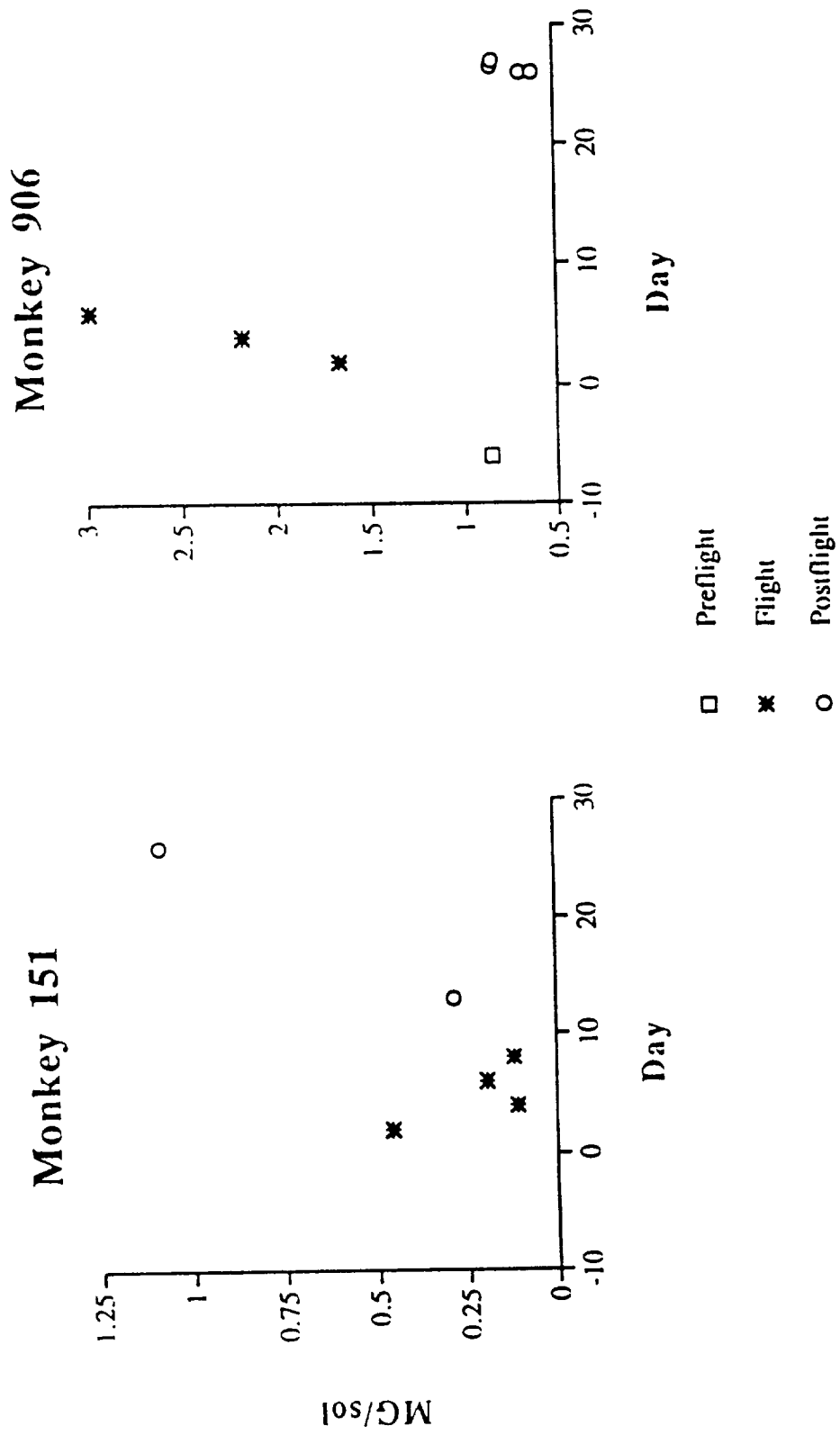


Figure 6. Ratio of soleus and MG mean amplitudes.

EXPERIMENT K-8-04 (Part 2)

MORPHOLOGIC AND METABOLIC PROPERTIES OF SINGLE MUSCLE FIBERS
IN HINDLIMB MUSCLES OF THE RHESUS

Principal Investigator:

Sue C. Bodine-Fowler
UCSD School of Medicine and VA Medical Center
San Diego, CA

Co-Investigators:

David J. Pierotti
UCSD School of Medicine and VA Medical Center
San Diego, CA

V. Reggie Edgerton
University of California at Los Angeles
Los Angeles, CA

MORPHOLOGIC AND METABOLIC PROPERTIES OF SINGLE MUSCLE FIBERS IN HINDLIMB MUSCLES OF THE RHESUS

Sue C. Bodine-Fowler, David J. Pierotti, V. Reggie Edgerton

INTRODUCTION

The maintenance of skeletal muscle properties appears to be related, in part, to the amount of external loading imposed on the muscular system. A reasonably clear picture of how hindlimb muscles of rats respond to unloading has unfolded over the last several years. However, relatively little is known about other mammals. In the rat, within 7 days after the onset of zero gravity, i.e., space flight, or the elimination of weight support by the hindlimbs, i.e., hindlimb suspension, there is considerable muscle atrophy and a small increase in the percent of fibers that express fast myosin isoforms principally within slow muscles. The response of individual muscle fibers to decreased loading conditions seems to be dependent on the function of the muscle and on the original myosin type of the fiber. For example, extensor muscles such as the soleus (Sol) and medial gastrocnemius (MG) atrophy to a greater extent than flexor muscles such as the tibialis anterior (TA) and extensor digitorum longus. A differential response also can be seen in fibers that express slow myosin versus those that express fast myosin.

Two issues that have arisen from the results of the studies on rats are: 1) what are the physiological signals which trigger these adaptations, and 2) how do these responses in the rat compare to those in other mammals both qualitatively and quantitatively? The monkey may be an excellent model for identifying the physiological factors that initiate the atrophic and related changes that occur in muscles, as well as increasing our understanding of how the nervous system adjusts to microgravity and the associated changes such as muscle atrophy. For example, previous studies suggest that the maintenance of muscle mass is related to: 1) the proportion of the muscle, i.e., the motor pool, recruited and 2) the muscle loading conditions at any given recruitment level. In the monkey, electromyographic (EMG) activity and force can be measured from individual muscles during specific motor tasks that the monkey has been trained to perform. Moreover, EMG and tendon force data can be correlated with biochemical and morphological measurements acquired from the same muscles using biopsy techniques.

In a previous Cosmos mission (2044) we found that a 14-day space flight had little effect on fiber size in the Sol and MG muscles, whereas, there appeared to be a slight decrease in size in the TA. In each of the flight animals the mean fiber size in the postflight biopsies increased relative to preflight values. An increase in fiber size over the same period of time was also observed in four control monkeys that were the same age and approximately the same weight as the flight monkeys. The relative increase in size was related to the body weight of the monkey at the time of the pre and postflight biopsies. The mean fiber succinate dehydrogenase activity appeared to decrease in the MG, whereas, there was no apparent effect of space flight on the Sol and TA muscles.

The purpose of the present study was to further define the effects of space flight on selected morphologic and metabolic properties of single muscle fibers from selected extensor (soleus, medial gastrocnemius and vastus lateralis) and flexor (tibialis anterior) muscles of the Rhesus monkey in order to extend the findings of Cosmos 2044.

METHODS

Biopsy Procedures

Muscle biopsies were taken from two independent sites in the Sol, MG, TA, and VL muscles using an open biopsy technique. The biopsy sites were selected to ensure that the same muscle fibers were not sampled during the pre and postflight biopsies and that regions with similar fiber type distributions were sampled. The first (preflight) biopsies were taken 90-98 days prior to launch, and the second (postflight) biopsies were taken 3-5 days after the recovery of the capsule. All biopsies were taken from the right leg since the left leg was implanted with EMG electrodes. A list of the monkeys and the dates of the biopsies are given in Table 1.

The biopsies were taken while the animal was under a general anesthesia. Under sterile conditions, one incision was made to the lateral aspect of the thigh to give access to the VL, one incision was made on the medial side of the lower leg to give access to the Sol and MG muscles, and one incision was made on the anterior side of the leg to give access to the TA muscle. Using blunt dissection, the belly of each muscle was exposed and a small cut was made in the overlying fascia. A #15 blade was used to remove a piece of muscle tissue which was approximately 10 mm long and 5 mm wide. The sample weighed between 100 to 2000 mg. The muscle sample was pinned to a piece of cork at approximately its *in situ* length and frozen in isopentane cooled with liquid nitrogen. The fascia and skin were closed with absorbable sutures (Vicryl™).

Tissue Analysis

Fiber cross-sectional area and succinate dehydrogenase (SDH) activity were determined for individual fibers (50-80 fibers) in 10 μ m cross sections taken from each of the biopsy samples. Tissue sections were analyzed on a computer-assisted image analysis system (Universal Imaging, Image I). To measure SDH activity, repeated digitized images were taken of a single tissue section every 2 min over a period of 14 min while the tissue was incubated in a medium without the substrate, succinate. A medium with succinate then was added and repeated scans were taken every 2 min over the next 14 min. Reaction rates for each fiber were based on a linear regression line determined from the 8 points acquired with the medium containing substrate (Figure 1). Although the absolute optical density readings may vary slightly from day to day, the slope or reaction rate is not affected.

The medium for determining SDH activity contained: 100 mM phosphate buffer (pH=7.6), 1.5 mM sodium azide, 3 mM 1-methoxyphenazine methylsulfate, 1.5 mM nitro blue tetrazolium, 5.5 mM EDTA-disodium salt, and 58 mM succinate disodium salt. This incubation medium is a modification of the one used for the rat muscle and has been optimized for the monkey muscle. The reaction rates for fibers in the monkey were approximately 5 times slower than those in the rat.

Fibers were classified as type I (slow), type IIa (fast) or type IIb (fast) based on monoclonal antibodies specific for myosin heavy chains. Type I fibers were positive for antibodies #8 and 35; type IIa fibers were positive for antibodies #13, 35 and 71; and type IIb fibers were positive for antibodies #13 and 71 (Figure 2) . The type I fibers were darkly stained in the myosin ATPase reaction at an acidic pH (pH=4.35) and lightly stained at a basic pH (pH=10.0). The type IIa and IIb fibers were lightly stained in the myosin ATPase reaction at an acidic pH and darkly stained at a basic pH. In the Sol and MG muscles, a subset of fibers coexpress both slow and fast myosins (Figures 2 and 3). These hybrid fibers (i.e., slow and fast) are darkly stained after preincubation at both an acidic (pH=4.35) and basic (pH=10.0) pH in the myosin ATPase reaction.

To access for differences in fiber cross-sectional area after space flight, a sample of 200 to 500 fibers were measured from tissue cross-sections stained with an antibody specific for laminin, a protein in the basal lamina surrounding the muscle fiber. Significant differences between the means of the pre and postflight biopsies for each animal were tested using paired t-tests ($p < 0.05$).

Ground Based Experiments

To determine the effects of restraint at 1G, five male monkeys weighing between 3.5 to 4.1 Kg (mean 3.7 ± 0.23 Kg) were placed in a replication of the flight chair and restrained for 14-days to simulate the flight duration. All ground based experiments were performed at the NASA/Ames Research Center. Muscle biopsies were taken from the SOL, MG, TA, and VL approximately 2-weeks prior to the restraint and 3 days after the 14-day restraint period (Table 2).

RESULTS AND DISCUSSION

Fiber Cross-Sectional Area

Table 3 gives the mean fiber cross-sectional areas for fibers sampled from the SOL, MG and TA of the two flight monkeys (151 and 906). In both monkeys the TA muscle showed significant muscle atrophy. In contrast, the SOL and MG in monkey 906 significantly increased in size over the period between the two biopsies, whereas these same muscles showed significant atrophy in monkey 151. In control monkeys that were sampled at the same time as the flight monkeys and were part of the flight pool, the SOL, MG and TA showed significant growth or maintained their size over the period between the first and second biopsies (Table 4).

Preliminary results from the ground restraint experiments suggest that the SOL, and possibly the MG, exhibit significant atrophy after restraint at 1G for 14-days in a chair similar to the one flown on the Cosmos missions (Table 5).

The results from monkey 906 are similar to those found for the two monkeys flown in Cosmos 2044. Monkey 151 had significant atrophy in all muscles sampled and this may be related to the low activity level of this animal while in space. The response of monkey 151 appears to be more similar to that seen in monkeys that are restrained at 1G. The response observed in monkey 906 and the two monkeys flown in Cosmos 2044 may be related to their activity level or to some movement they performed while in space. The position of the foot may be such that the tibialis anterior is placed in a shortened position while in space or the animals may be pressing on the rigid lever and performing some type of isometric exercise which is preventing the atrophy. These results emphasize the need to have a measure of the activity level of the animals while in space. In addition, a record of the foot position and a force sensor on the stationary foot lever would be useful in trying to interpret the results.

SDH Activity

Succinate dehydrogenase activity and fiber cross-sectional area were determined in a sample of 50 to 80 fibers from each muscle. Each fiber was classified as type I, IIa, IIb or hybrid based on its staining to a panel of myosin monoclonal antibodies. The mean SDH activities for the flight and control monkeys are shown in Figures 4-6.

In control monkeys (907,803,775 and 1401), SDH activity decreased in the SOL over the ~90-day period between the pre and post biopsies. In the flight monkeys, mean SDH activity decreased in monkey 151 and increased in monkey 906. The MG and TA muscles showed significant decreases in SDH activity in both flight monkeys. In controls, the mean SDH activity was generally higher in the post biopsies than the pre biopsies.

The relationship between SDH, fiber size and fiber type is illustrated for each of the muscles in flight monkey 151 (Figures 7-9), flight monkey 906 (Figures 10-12) and control monkey 803 (Figures 13-15). In the SOL of 151 one can see that there was a decrease in SDH in all fiber types, however, the decrease in size was restricted to the type IIa and hybrid fibers. In contrast, in the SOL of 906 all fiber types exhibited an increase in SDH activity and the fast and hybrid fibers increased in size. In the MG of 151 there was a decrease in size and SDH activity in all fiber types. In the MG of 906 there was an increase size and a decrease in SDH activity in all fiber types. In the TA of 151 the decrease in SDH activity was restricted to the type I and IIa fibers and the decrease in size was restricted to the type IIb fibers. In the TA of 906, all fiber types showed a decrease in SDH activity and size. In muscles such as the MG and TA which contain type I, IIa, and IIb fibers; the type IIb fibers were generally the largest in size and had the lowest SDH activity.

CONCLUSIONS

The use of the open biopsy procedure allowed us to obtain better samples which were larger and contained a greater number of fibers that could be analyzed. The results from monkey 906 are similar to those obtained from the two flight animals flown in Cosmos 2044. Although monkey 151 lost considerably more body weight than 906, the increased amount of atrophy, especially in the SOL and MG, may be a result of the inactivity and not the loss of body weight. In future flights, it would be helpful if the position of the animals foot was recorded and if a strain gauge was mounted on the right foot lever to monitor the activity and force produced by the right limb.

Additional data is being collected on the fiber type percentages in each of the biopsies to determine if there has been a shift in the percentage of fibers expressing fast myosin. This is being done using the myosin antibodies and 2-D gel electrophoresis. In addition, we are completing the analysis on the monkeys that were restrained at 1G for 14-days and on one more control monkey. Also, we have started the analyses of the biopsies taken from the VL. These data will be available in January, 1994.

TABLE 1
PRE- AND POSTFLIGHT BIOPSY SCHEDULE

MONKEY	GROUP	DATE PRE	BW (Kg)	DATE POST	BW (Kg)
803	CONTROL	9/22/92	3.90	1/15/93	4.29
907	CONTROL	9/22/92	3.30	1/14/93	3.90
1401	CONTROL	9/23/92	4.10	1/14/93	4.14
588	RESERVE	9/23/92	3.60	3/7/93	
775	CONTROL	9/24/92	4.55	1/13/93	4.57
151	FLIGHT	9/24/92	4.10	1/15/93	4.00
476	RESERVE	9/25/92	4.60	1/15/93	4.83
856	DIED	9/25/92	4.60	NONE	
1417	RESERVE	9/28/92	4.60	3/7/93	
906	FLIGHT	9/28/92	3.30	1/13/93	3.65
838	RESERVE	9/29/92	5.10	NONE	
892	CONTROL	9/29/92	3.40	1/15/93	4.06

BODY WEIGHTS (Kg) OF FLIGHT MONKEYS

MONKEY	30-SEPT-92	24-DEC-92	10-JAN-93
151	4.10	4.70	4.00
901	3.30	3.85	3.65

Launch: December 29, 1992; Recovery: January 10, 1993

TABLE 2
SCHEDULE OF GROUND BASE EXPERIMENTS

MONKEY	RESTRAINT	DATE PRE	BW (Kg)	DATE POST	BW (Kg)
150	14-DAY	4/20/92	3.7	5/21/92	3.5
148	14-DAY	5/5/92	3.5	6/5/92	3.4
149	14-DAY	5/5/92	4.10	6/5/92	3.9
90-009	9-DAY	5/26/92	3.80	7/13/92	3.65
90-008	14-DAY	5/26/92	3.6	7/13/92	

TABLE 3
MEAN FIBER CROSS-SECTIONAL AREA (μm^2)
FLIGHT MONKEYS

Monkey 151

		SOLEUS		MG		TA	
		PRE	POST	PRE	POST	PRE	POST
MEAN		868	1652	1539	1361	2487	1952
SD		394	442	609	455	927	646
n		195	167	436	387	286	310

Monkey 906

		SOLEUS		MG		TA	
		PRE	POST	PRE	POST	PRE	POST
MEAN		2018	2271	1175	1976	2128	1507
SD		407	565	298	690	830	566
n		215	234	294	453	322	331

Means are expressed in square microns; SD, standard deviation; n, number of fibers sampled per biopsy. Preflight biopsies were taken September 24 (151) and 28 (906) 1992, approx. 98 days prior to the launch which occurred on December 29, 1992. Postflight biopsies were taken January 13 (906) and (151) 1993, approx. 3 days (906) and 5 days (151) after the recovery of the biosatellite.

TABLE 4

MEAN FIBER CROSS-SECTIONAL AREA (μm^2) CONTROL MONKEYS

		Monkey 907					
		SOLEUS		MG		TA	
		PRE	POST	PRE	POST	PRE	POST
MEAN		2268	2374	1975	2647	2916	2941
SD		397	448	626	832	1220	1120
n		65	55	77	63	62	70

		Monkey 803					
		SOLEUS		MG		TA	
		PRE	POST	PRE	POST	PRE	POST
MEAN		2613	3252	2140	2988	2338	3206
SD		609	642	450	727	768	637
n		64	58	68	68	88	64

		Monkey 775					
		SOLEUS		MG		TA	
		PRE	POST	PRE	POST	PRE	POST
MEAN		3028	3689	2301	2611	3165	2660
SD		613	910	439	871	1353	1294
n		46	910	439	871	1353	1294

Means are expressed in square microns; SD, standard deviation; n, number of fibers sampled per biopsy.

A larger number of fibers is being measured for each of these muscles. Additional data is being collected on 2 more control (1401 and 892) animals.

TABLE 5

MEAN FIBER CROSS-SECTIONAL AREA (μm^2)
GROUND RESTRAINT EXPERIMENT

Monkey 150

	SOLEUS		MG		TA	
	PRE	POST	PRE	POST	PRE	POST
MEAN	1599	1447	1304	1105	1567	1551
SD	349	342	442	491	575	453
n	217	247	277	294	206	214

Monkey 148

	SOLEUS		MG		TA	
	PRE	POST	PRE	POST	PRE	POST
MEAN	1167	1332	NA	NA	NA	NA
SD	325	246				
n	395	461				

Monkey 149

	SOLEUS		MG		TA	
	PRE	POST	PRE	POST	PRE	POST
MEAN	1581	1414	NA	NA	NA	NA
SD	318	397				
n	413	495				

Means are expressed in square microns; SD, standard deviation; n, number of fibers sampled per biopsy.

NA, not available at this date. Data is being collected for the MG and TA.

SDH RATE REACTION

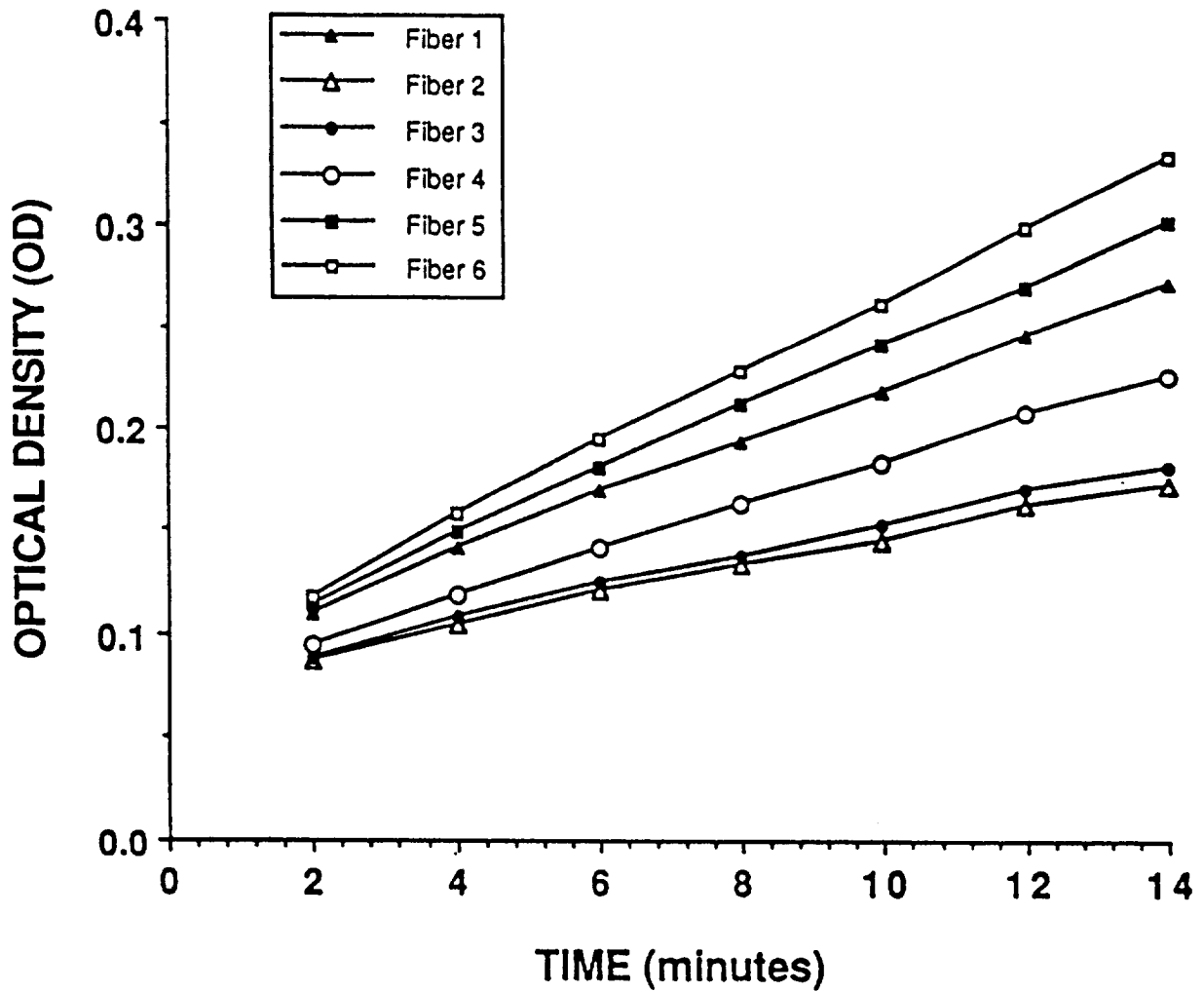


Figure 1: Calculation of SDH activities for fibers in the medial gastrocnemius of the monkey. Muscle cross-sections were incubated in a medium that has been modified to give optimal staining of monkey tissue (see Methods). The SDH activities (OD/min) were calculated as the slope of the line (OD/min). The regression lines had a correlation coefficient equal to 0.98 or better.

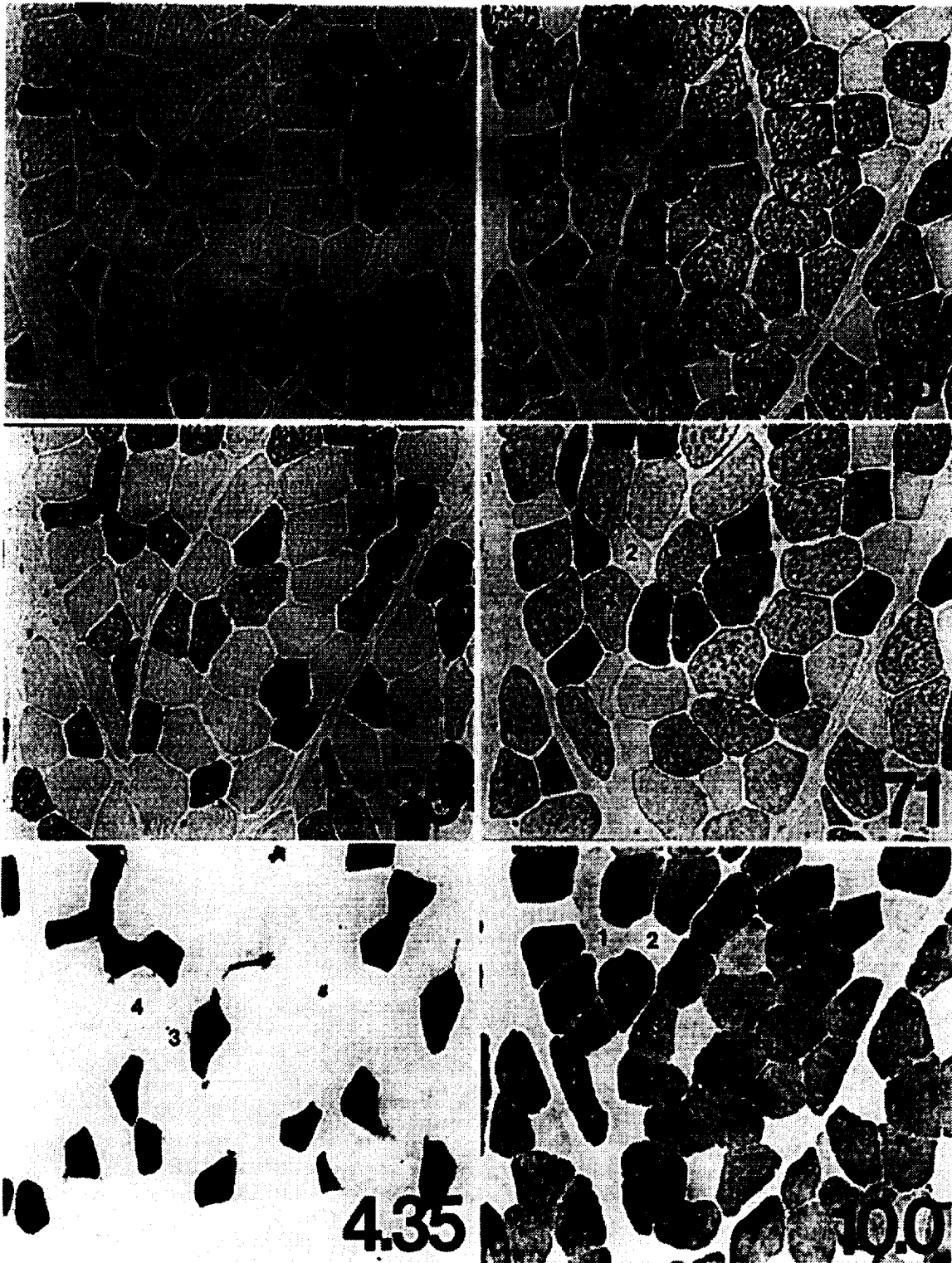


Figure 2 : Serial cross-sections taken from the medial gastrocnemius muscle. Sections were reacted with monoclonal antibodies specific for myosin heavy chains. Antibody 8 labels type I myosin; 13 labels all type II; 35 labels type I and IIa; and 71 labels type IIa and IIb. Sections were also tested for myosin ATPase activity. Sections were pre incubated at an acidic (pH=4.35) and a basic (pH=10.0) pH. The numbered fibers correspond to the various fiber types found in the MG: (1) hybrid, expressed both slow and fast myosins; (2) type I; (3) type IIa; (4) type IIb.

Figures 3(a) and 3(b): Serial cross-sections taken from the soleus muscle. Sections were reacted with monoclonal antibodies specific for myosin heavy chains. Antibody 8 labels type I myosin; 13 labels all type II; 35 labels type I and IIa; and 71 labels type IIa and IIb. Sections were also tested for myosin ATPase activity. Sections were pre incubated at an acidic (pH=4.35) and a basic (pH=10.0) pH. Serial section were also stained with hemotoxylin and eosin for general cellular morphology and labeled with a monoclonal antibody specific to laminen. Laminen labeled sections were used to measure fiber cross-sectional area in a sample of fibers. The numbered fibers correspond to the various fiber types found in the SOL: (1) type I; (2) hybrid, expressed both slow and fast myosins; (3) type IIa; and 4) hybrid. Occasionally type IIb fibers were found in the SOL.

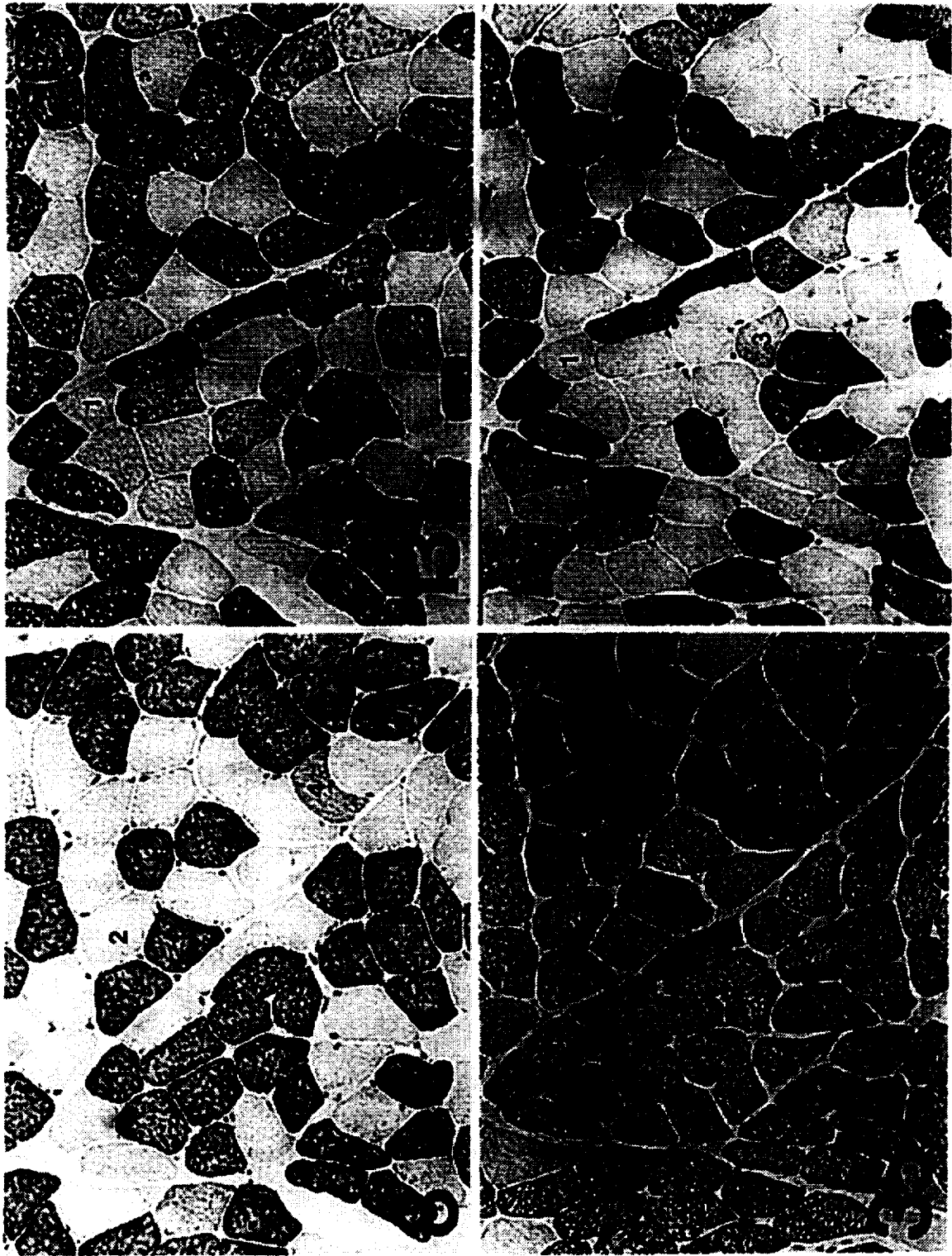


Figure 3(a).

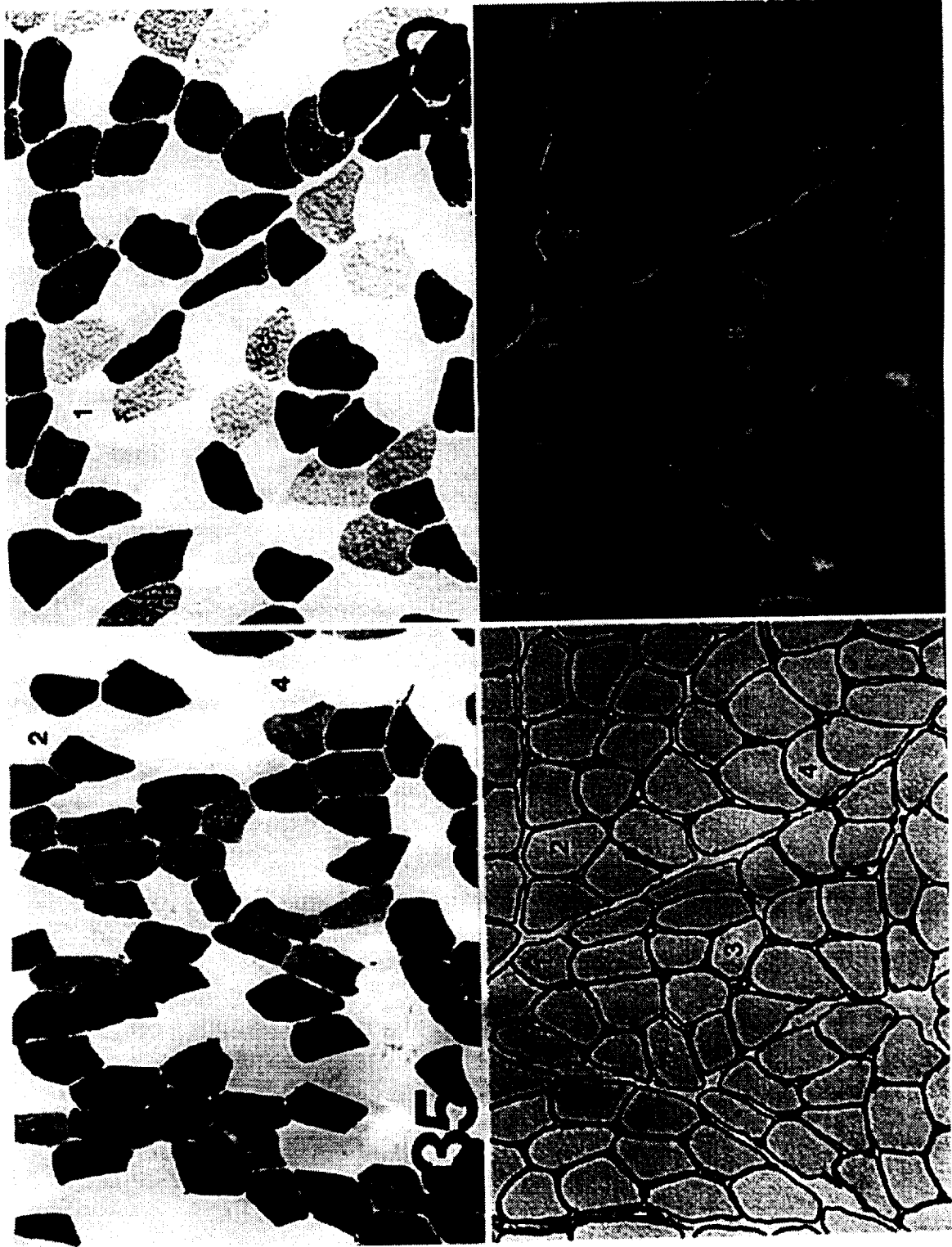


Figure 3(b).

Figures 4–6: Bar graphs showing the mean succinate dehydrogenase (SDH) activity (OD/min) and standard deviation for a sample of fibers in the pre (hatched) and postflight (empty) biopsies. The number of fibers sampled is indicated in each bar. The flight monkeys were 151 and 906. Monkeys 907, 803, 775 and 1401 served as controls and were members of the flight candidate pool. The body weights of the control monkeys were similar to the flight monkeys (see Table 1).

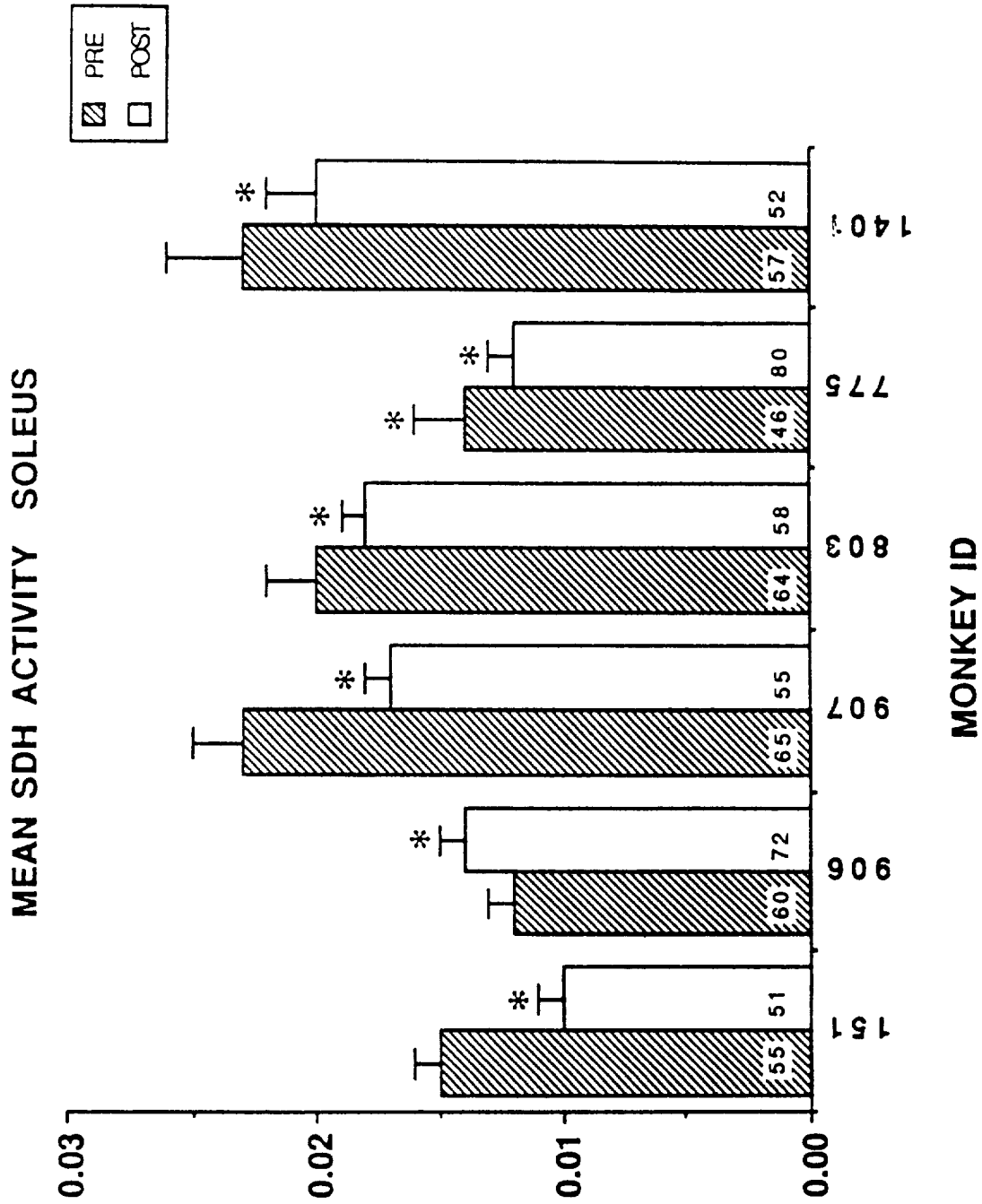


Figure 4.

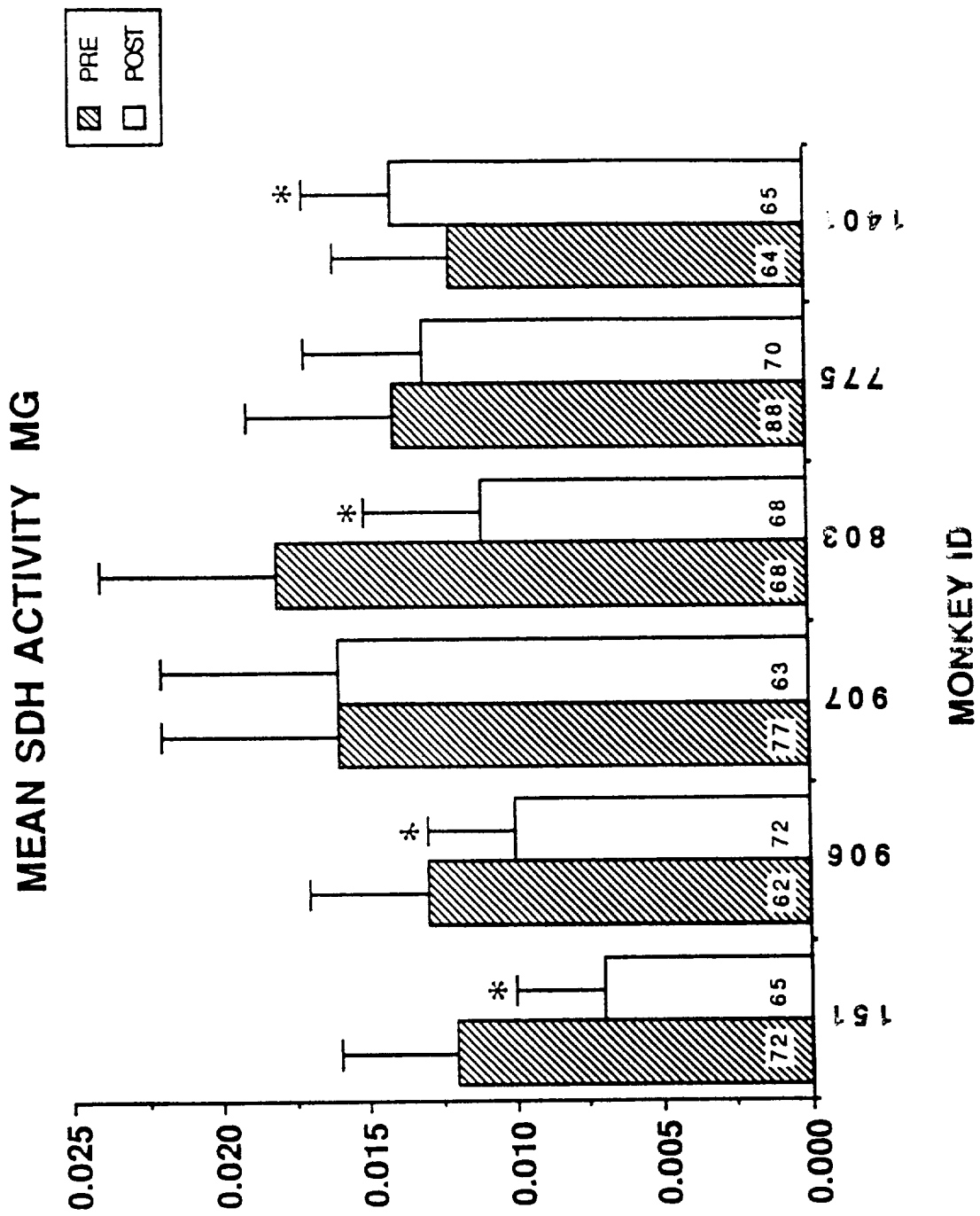


Figure 5.

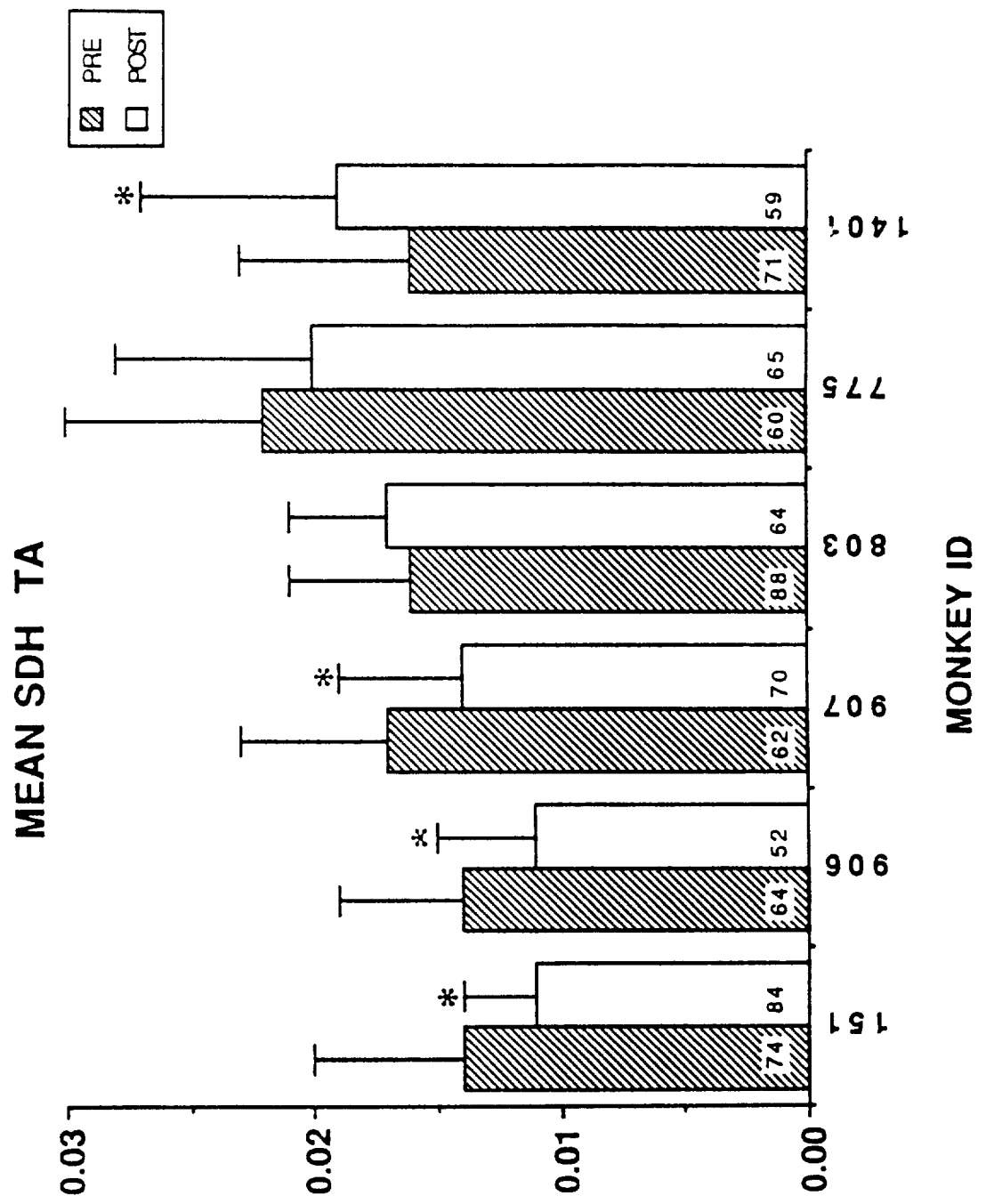


Figure 6.

Figures 7–15: Plot of the relationship between SDH activity (OD/min) and fiber cross-sectional area (μm^2) in the SOL, MG and TA of each of the flight monkeys (151 and 906) and one control (803). Each fiber was classified according to its labeling profile for the myosin monoclonal antibodies. The type of fiber is denoted by the symbols shown in the legends.

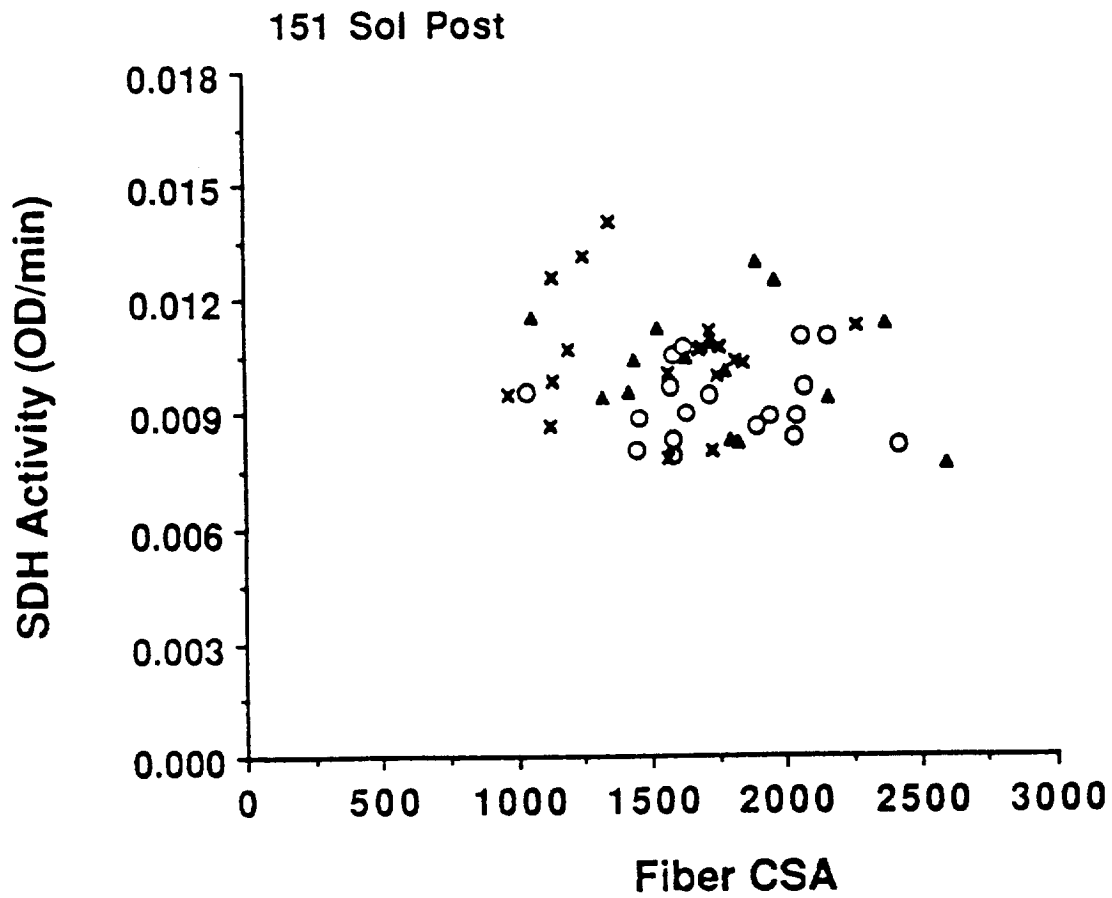
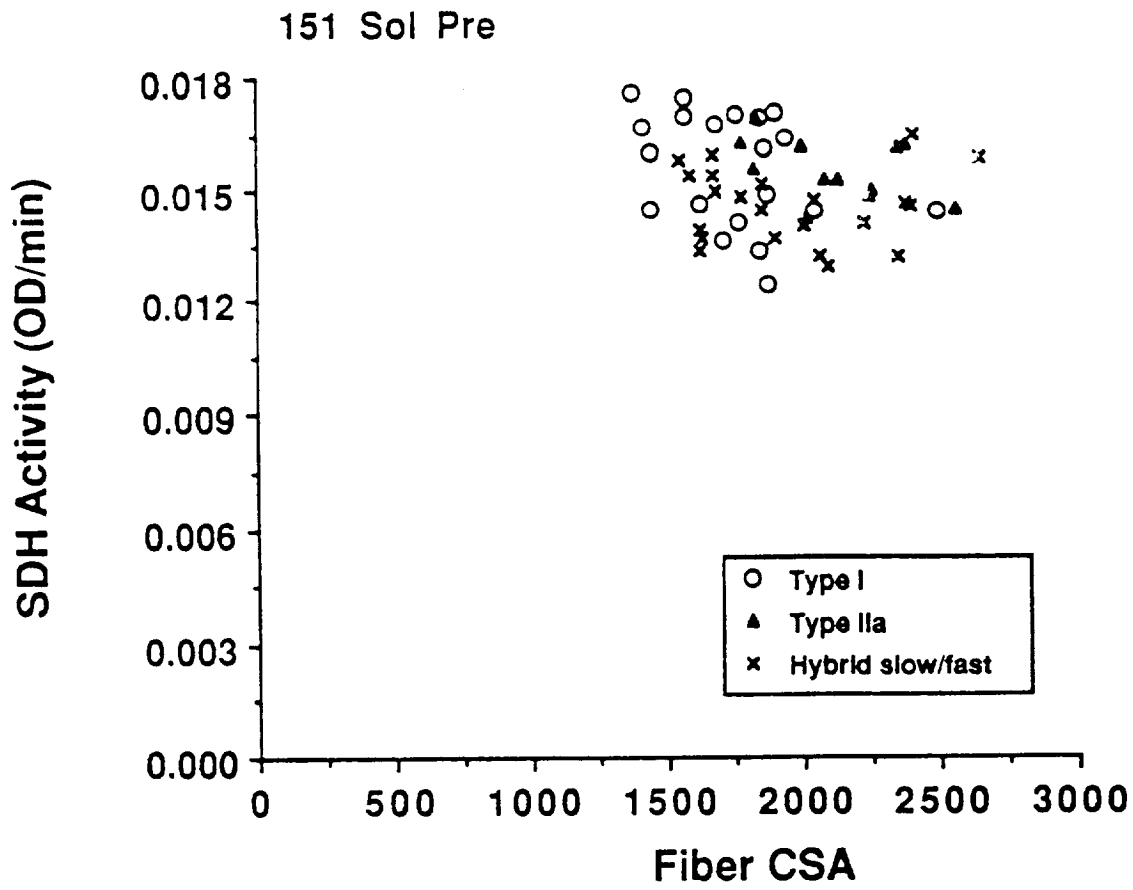


Figure 7.

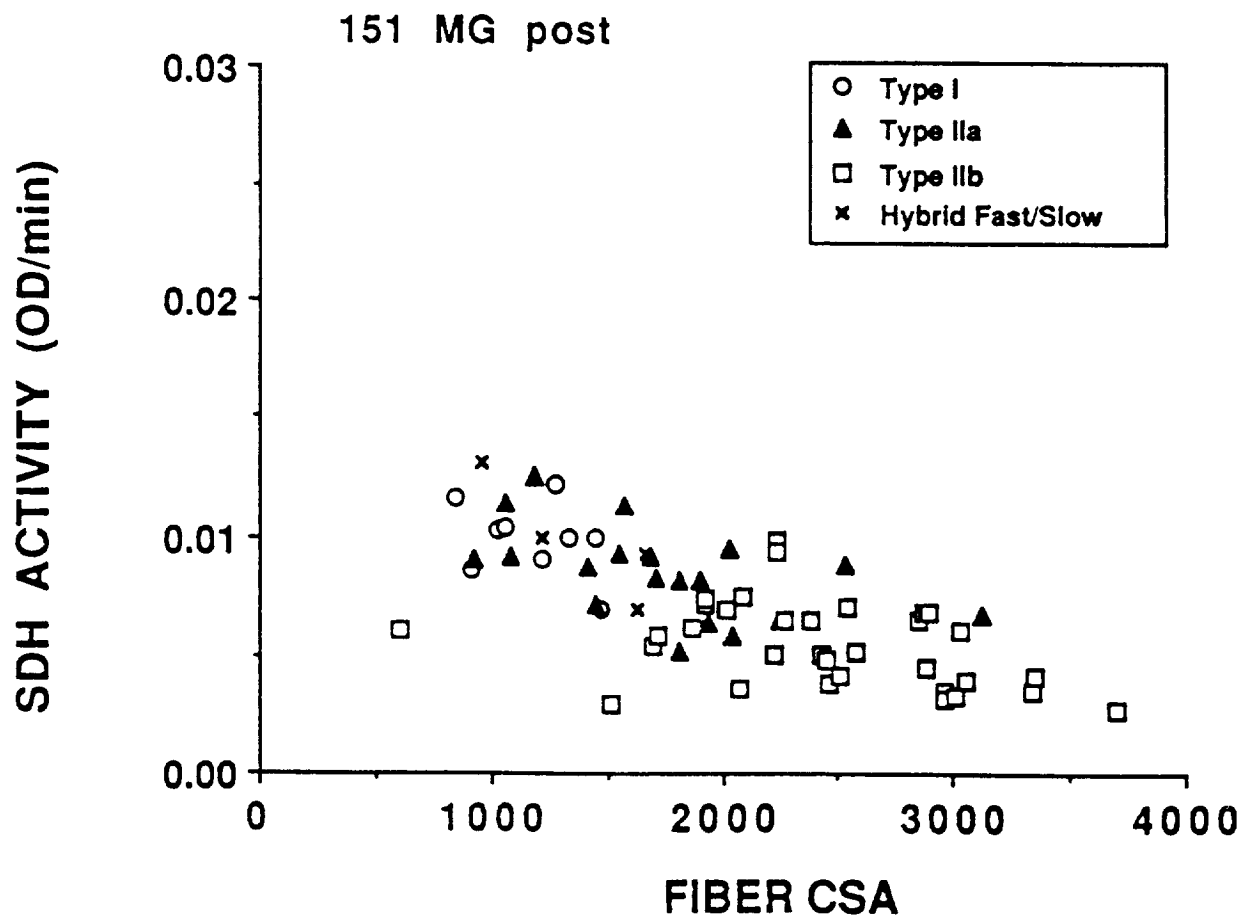
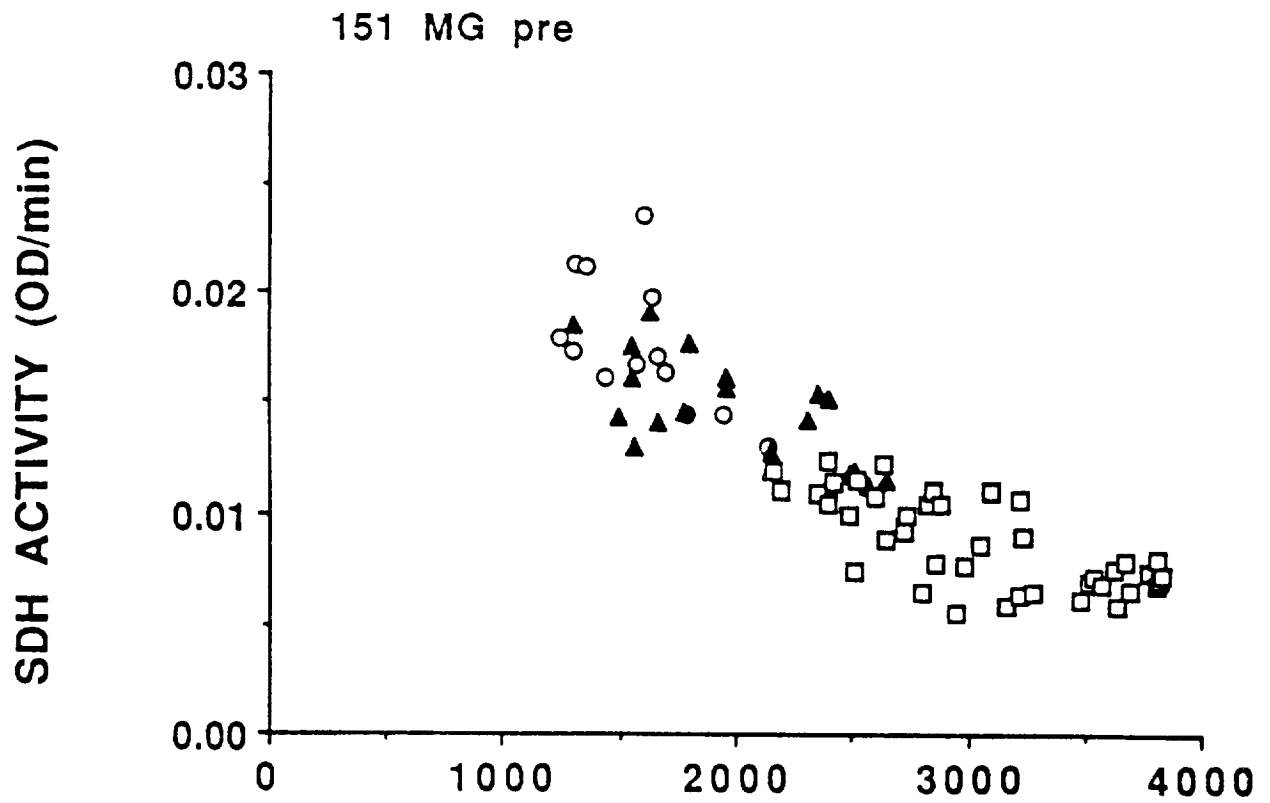


Figure 8.

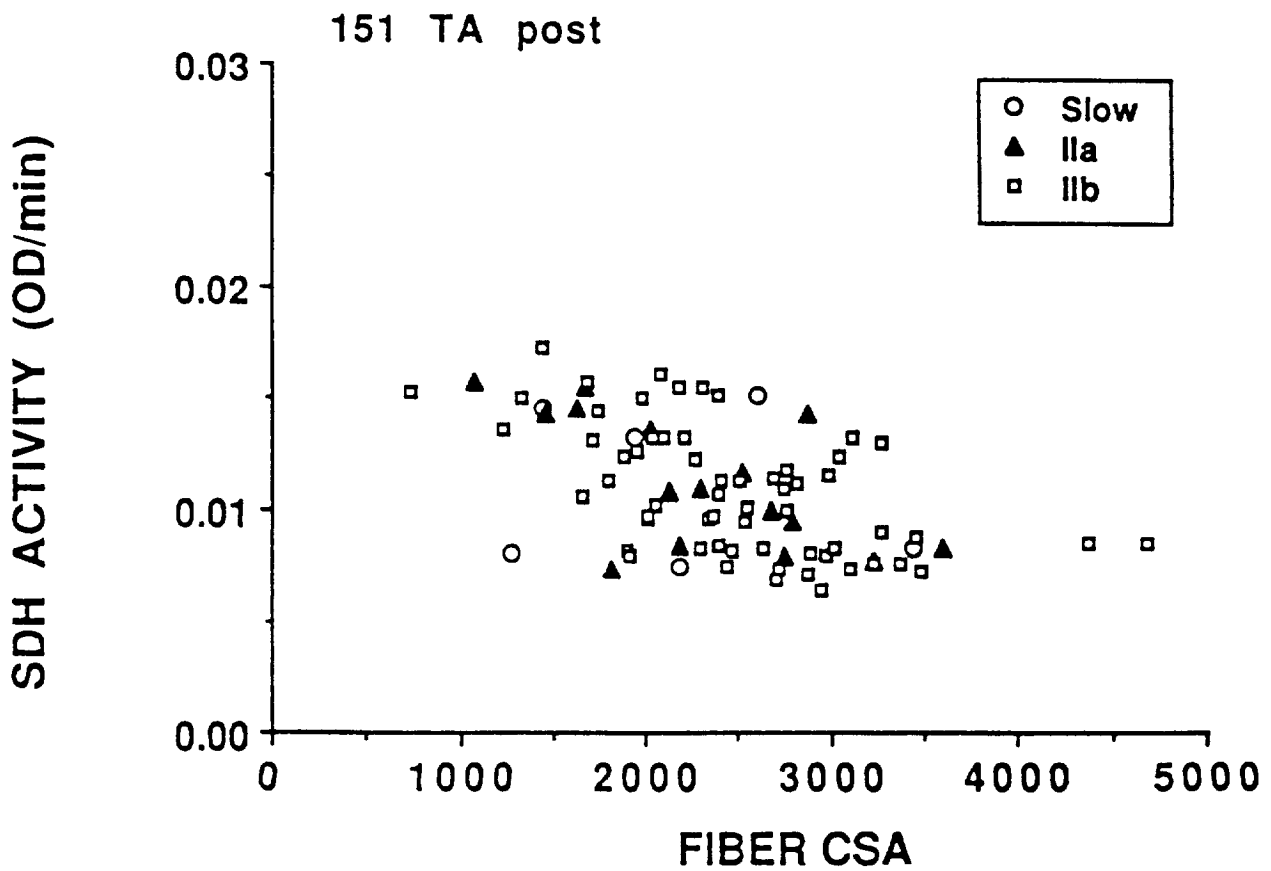
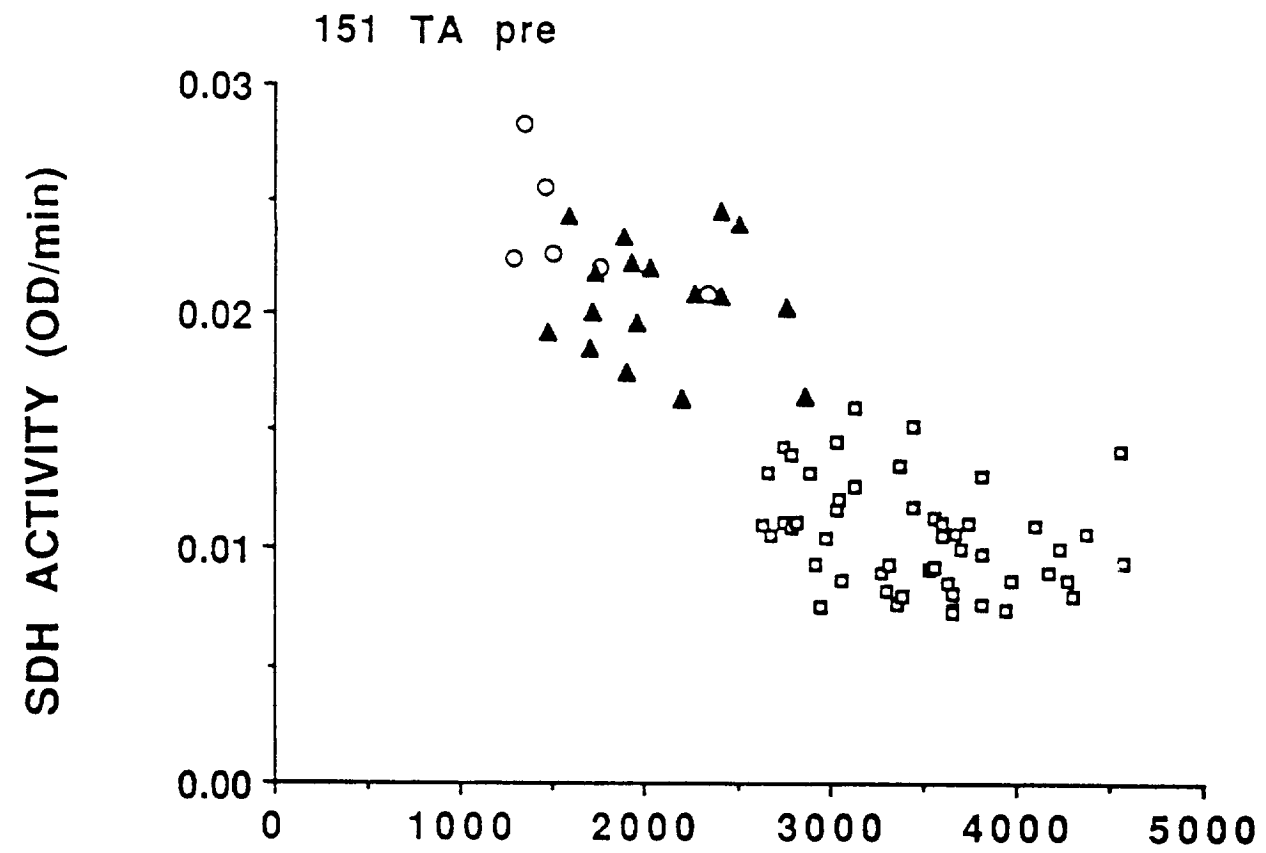


Figure 9.

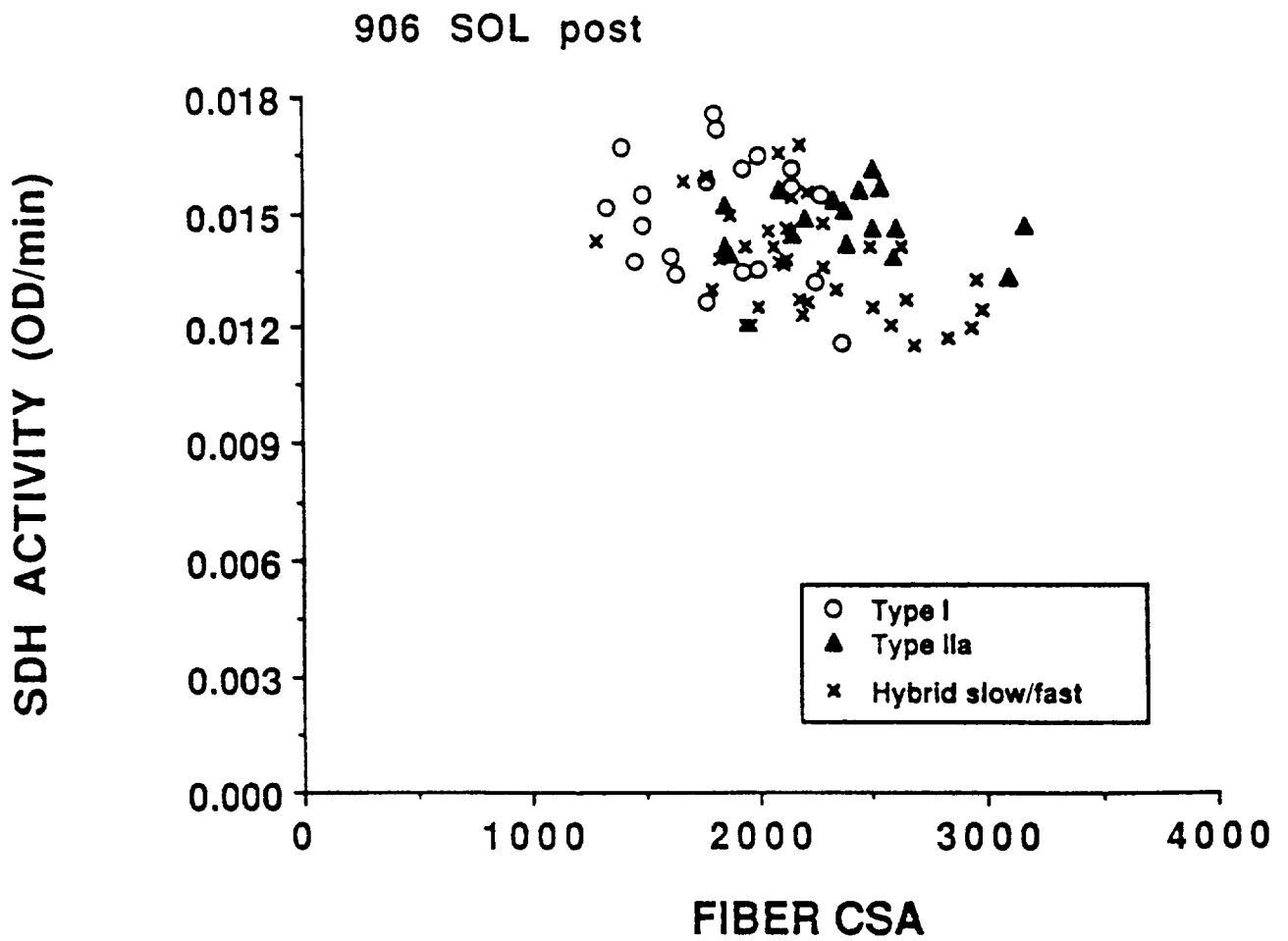
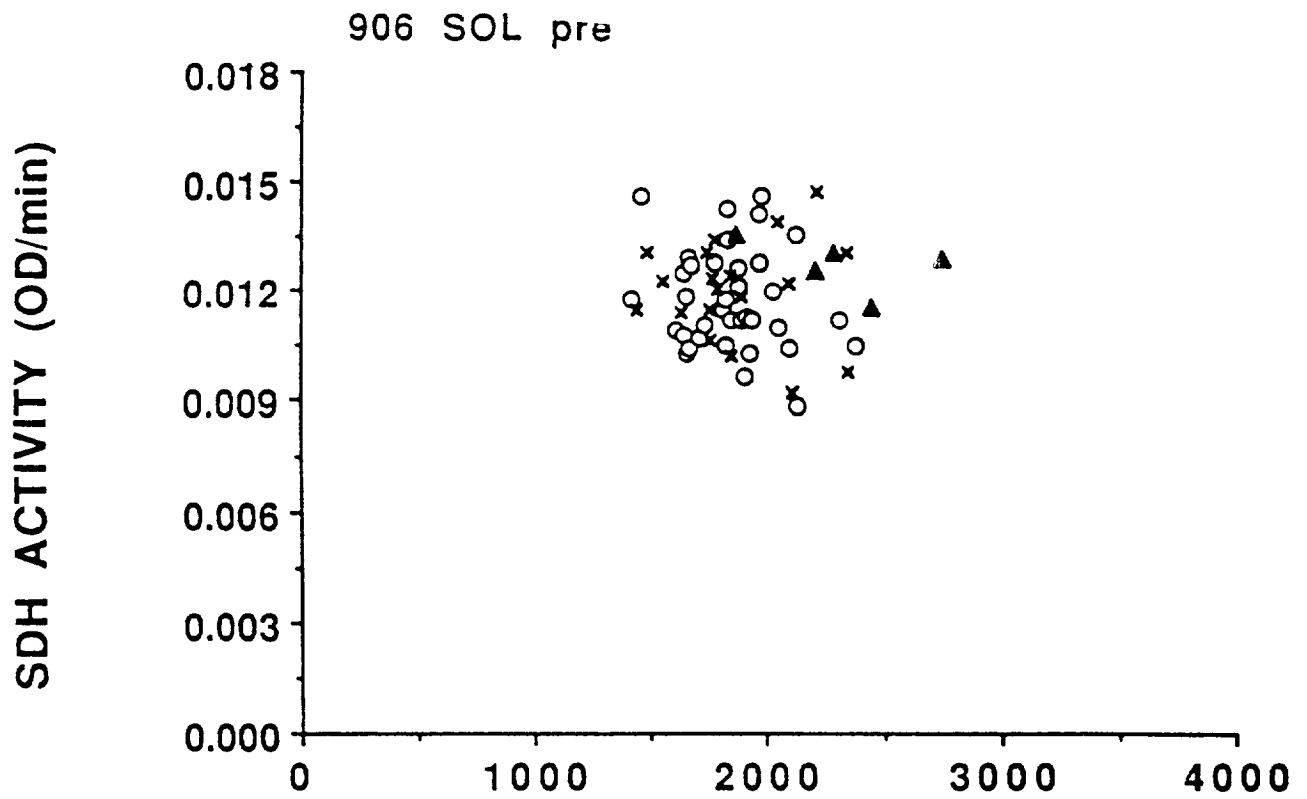


Figure 10.

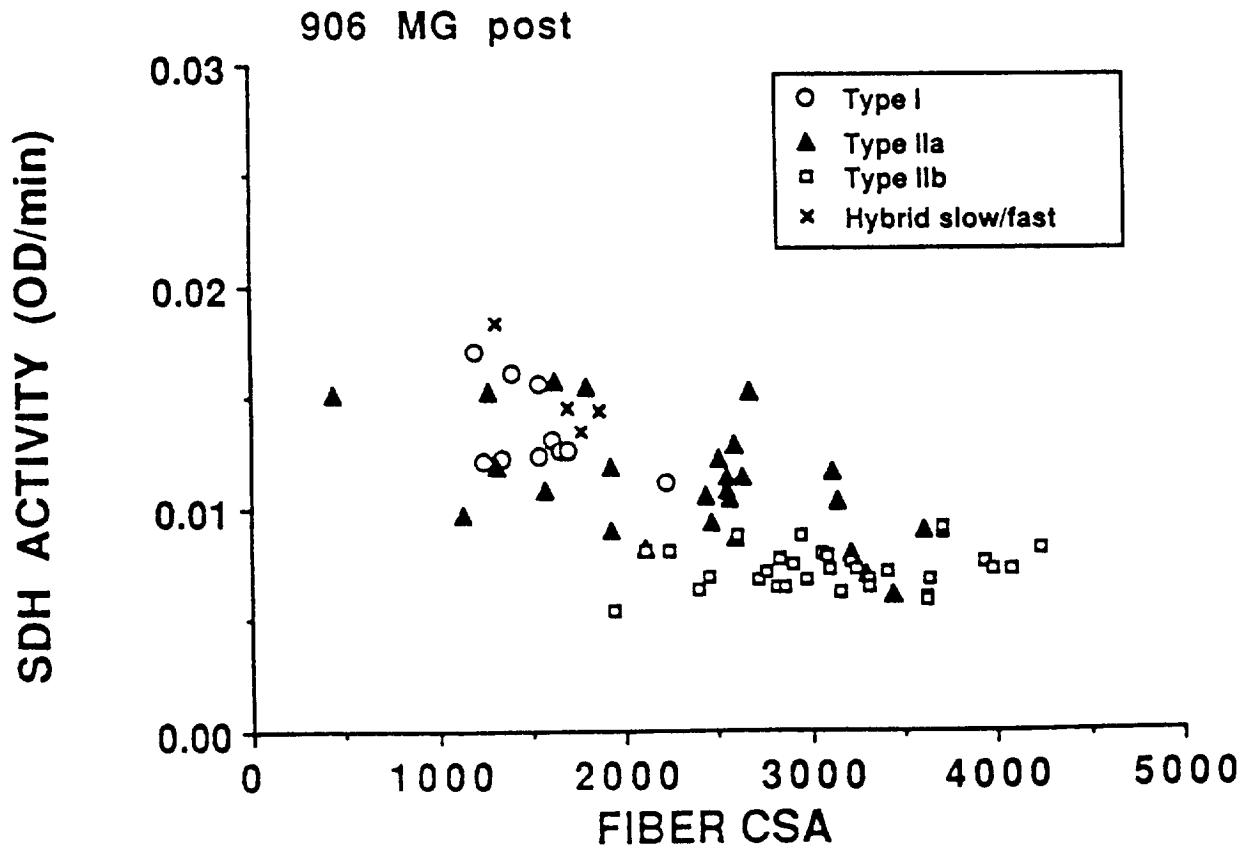
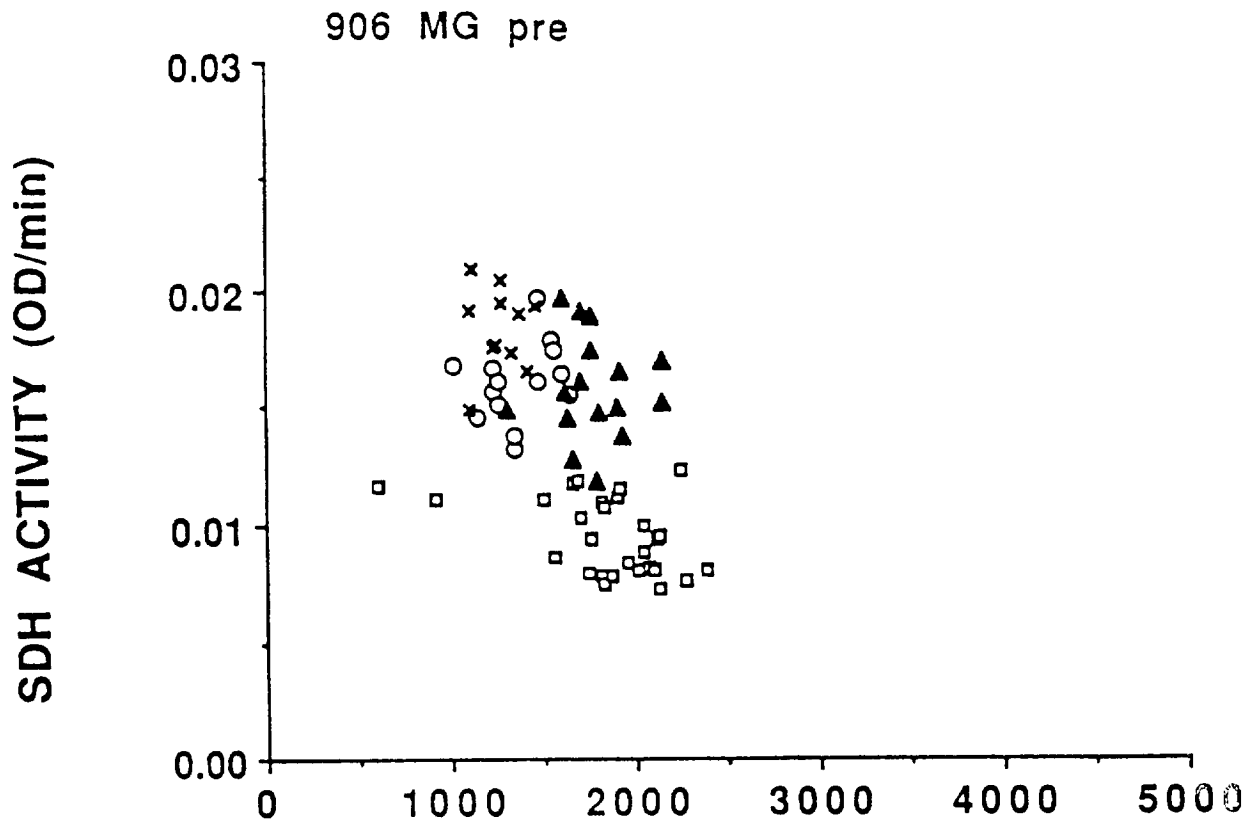


Figure 11.

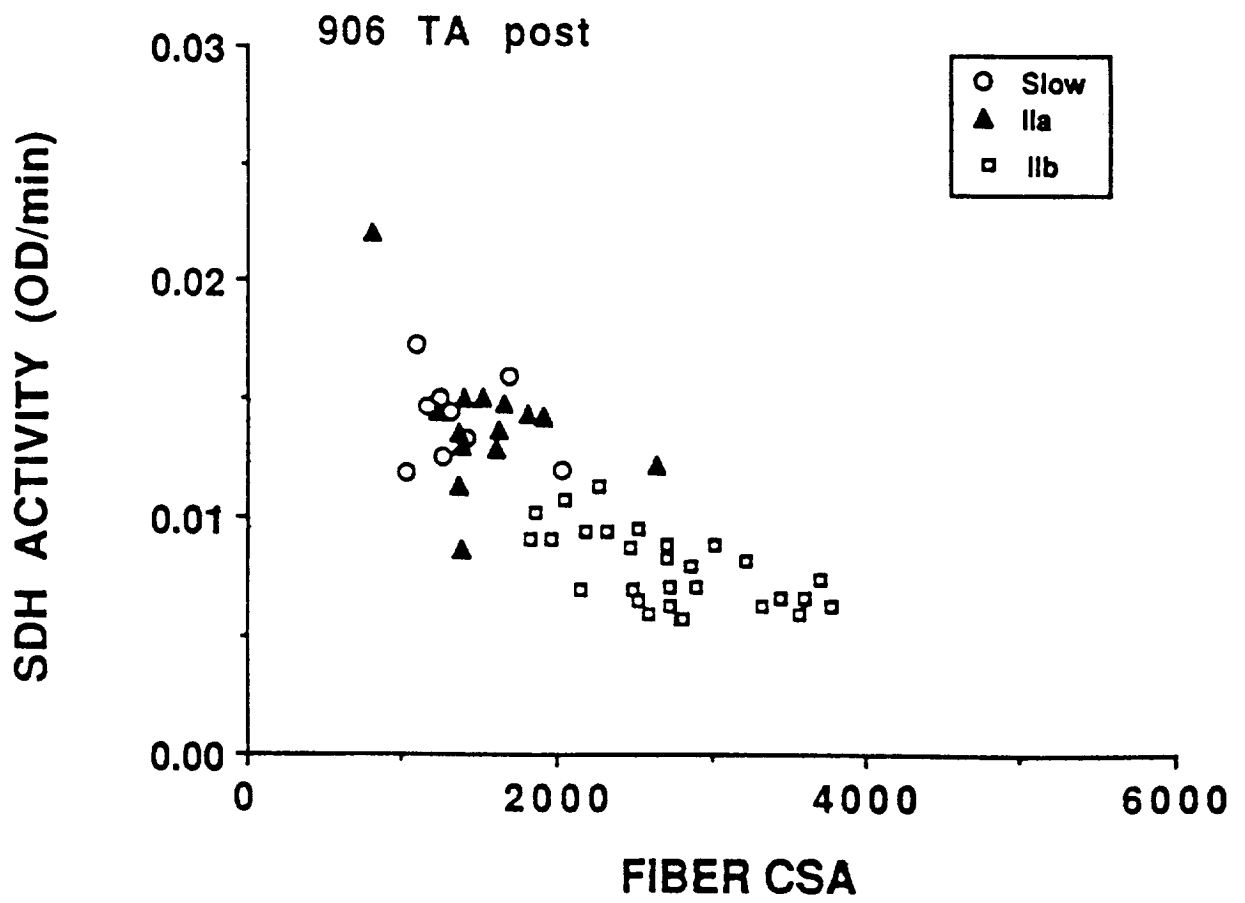
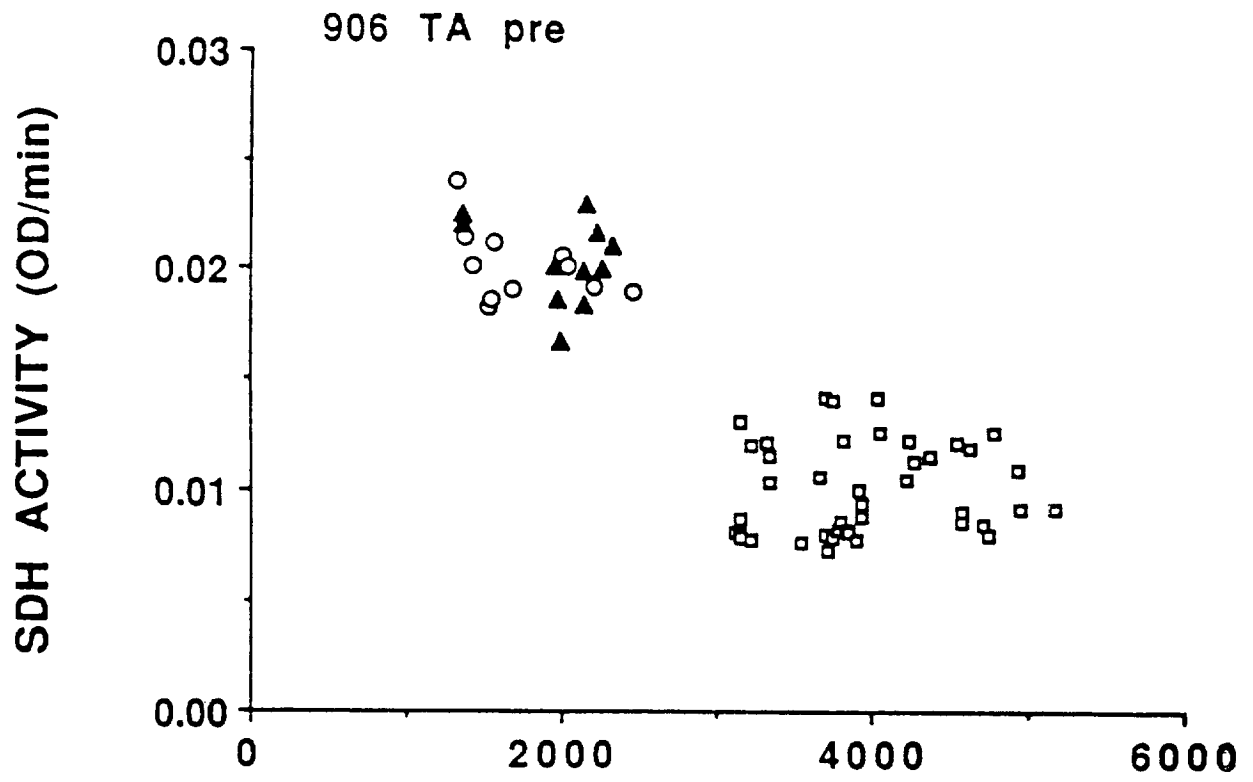


Figure 12.

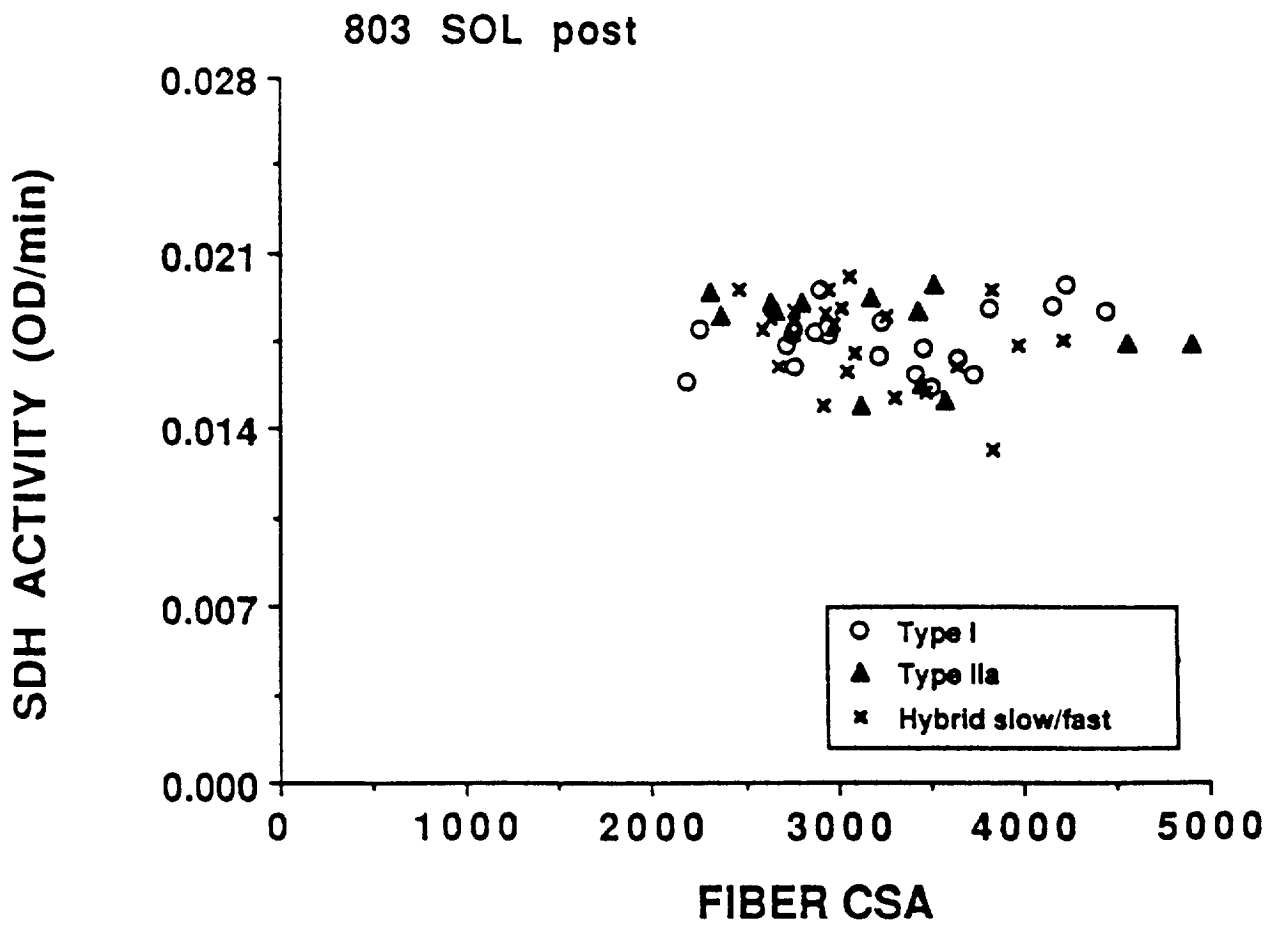
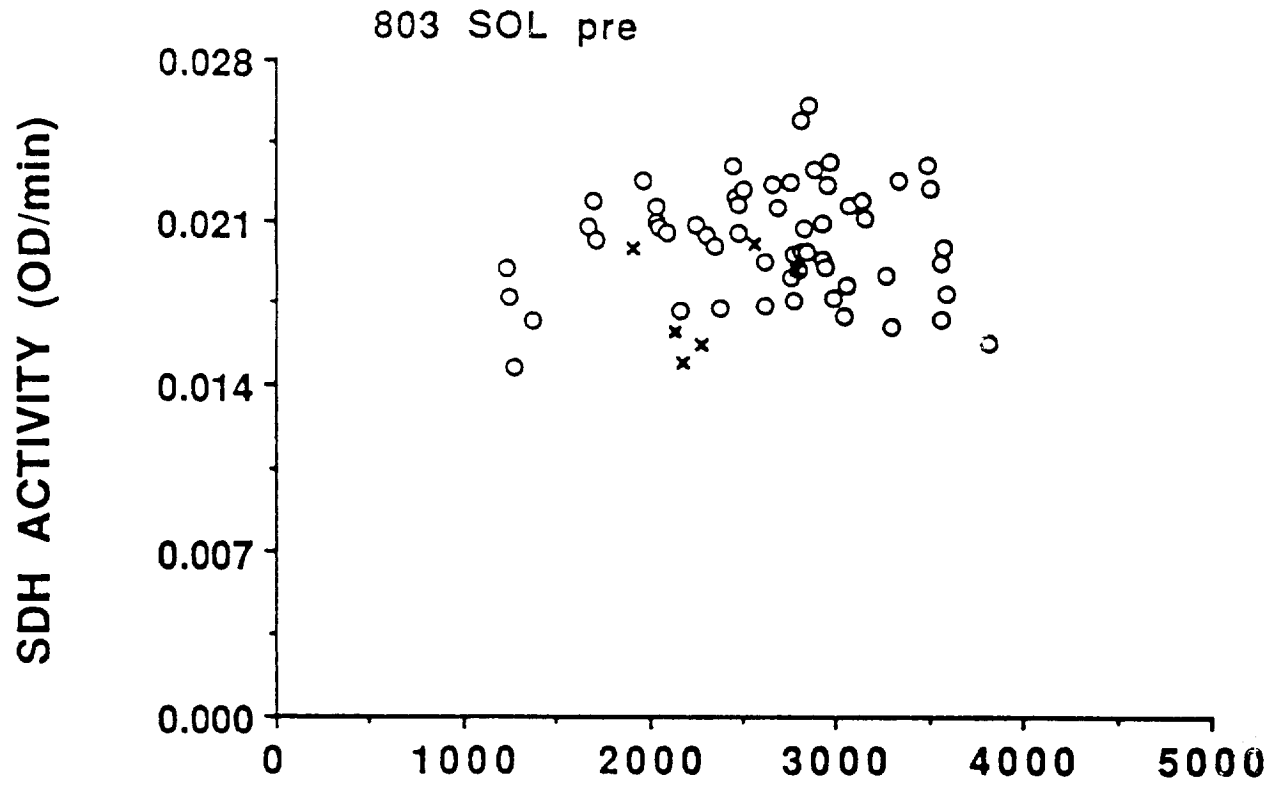


Figure 13.

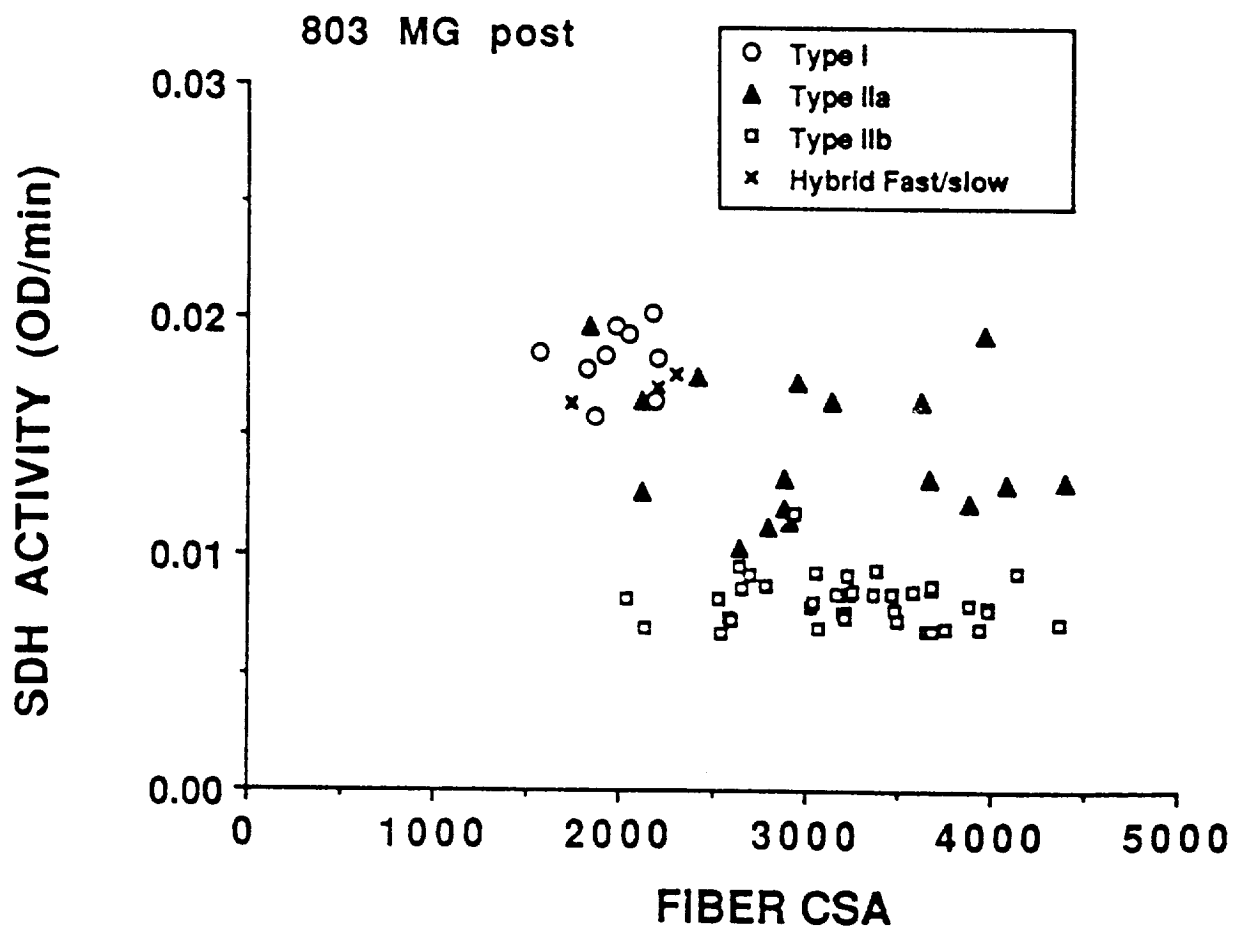
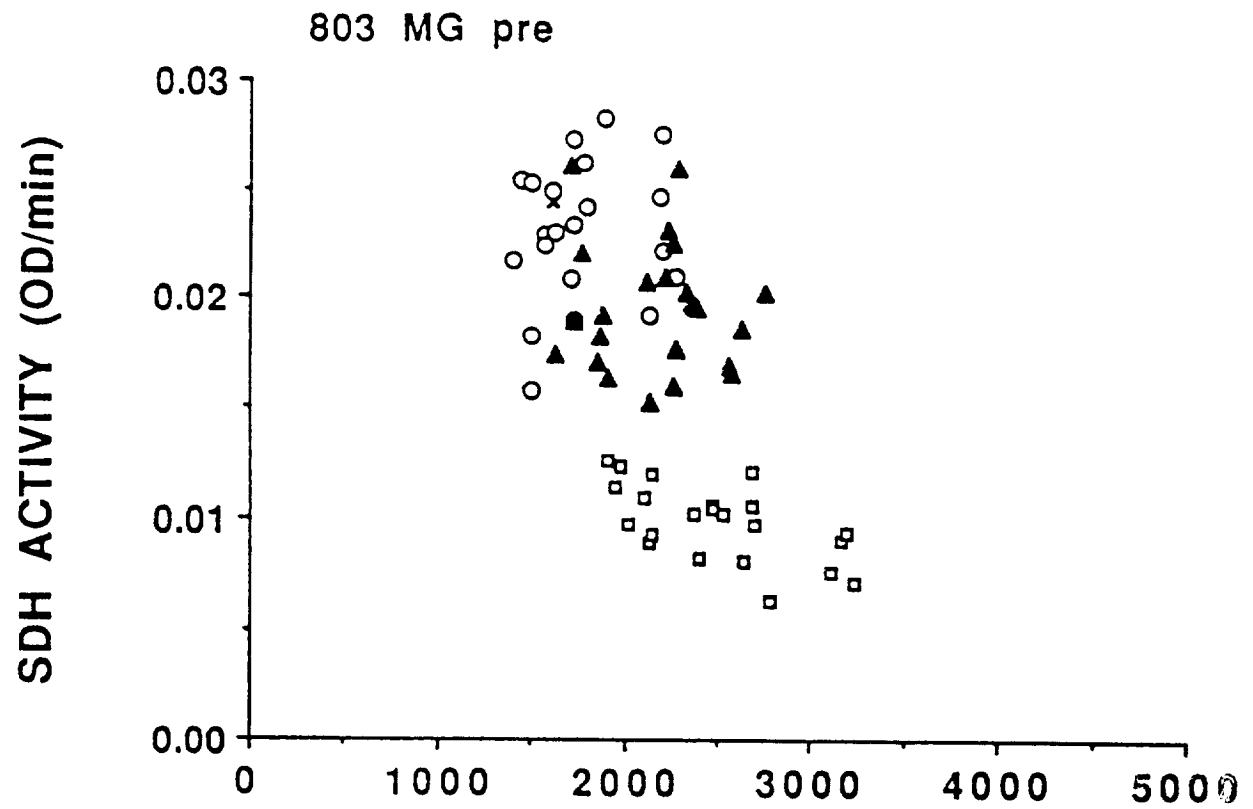


Figure 14.

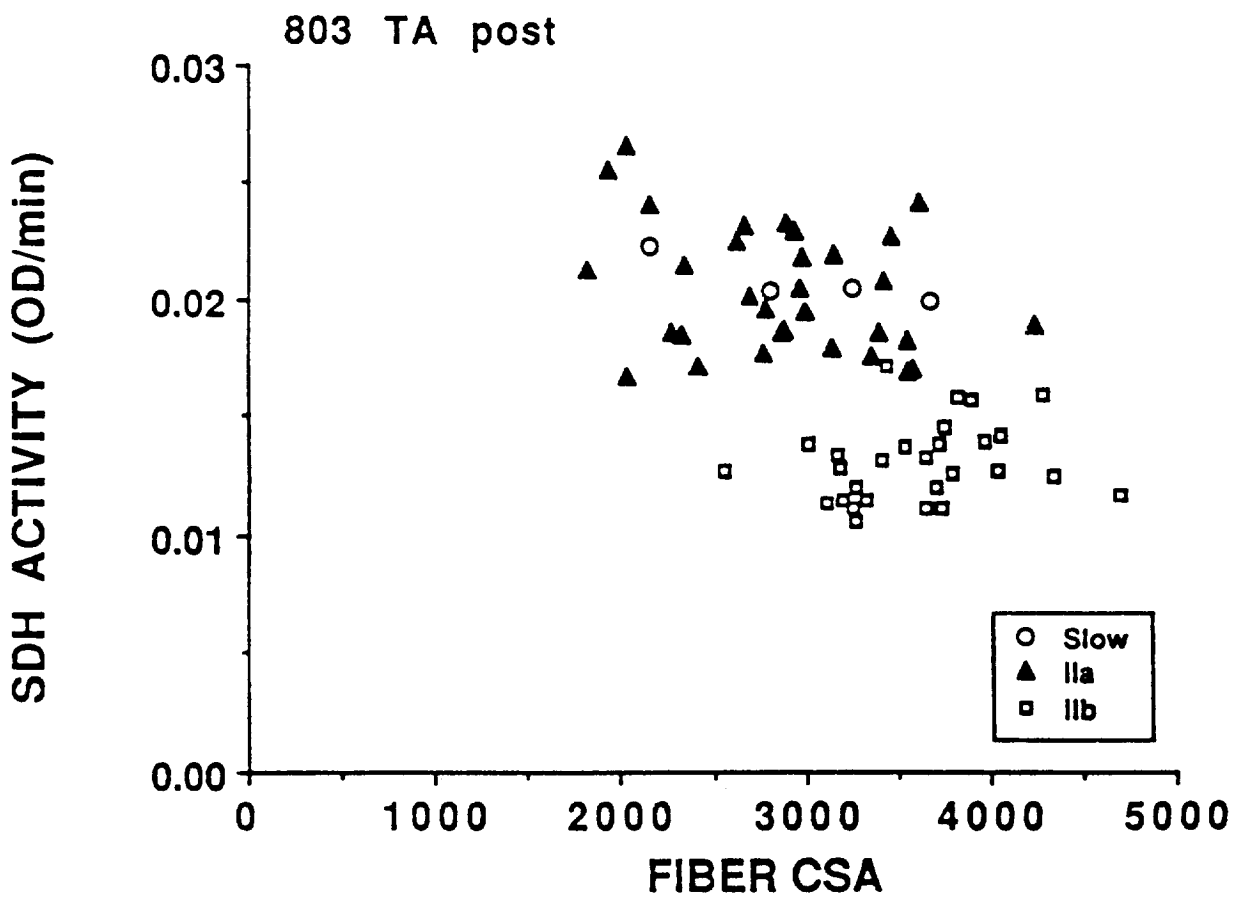
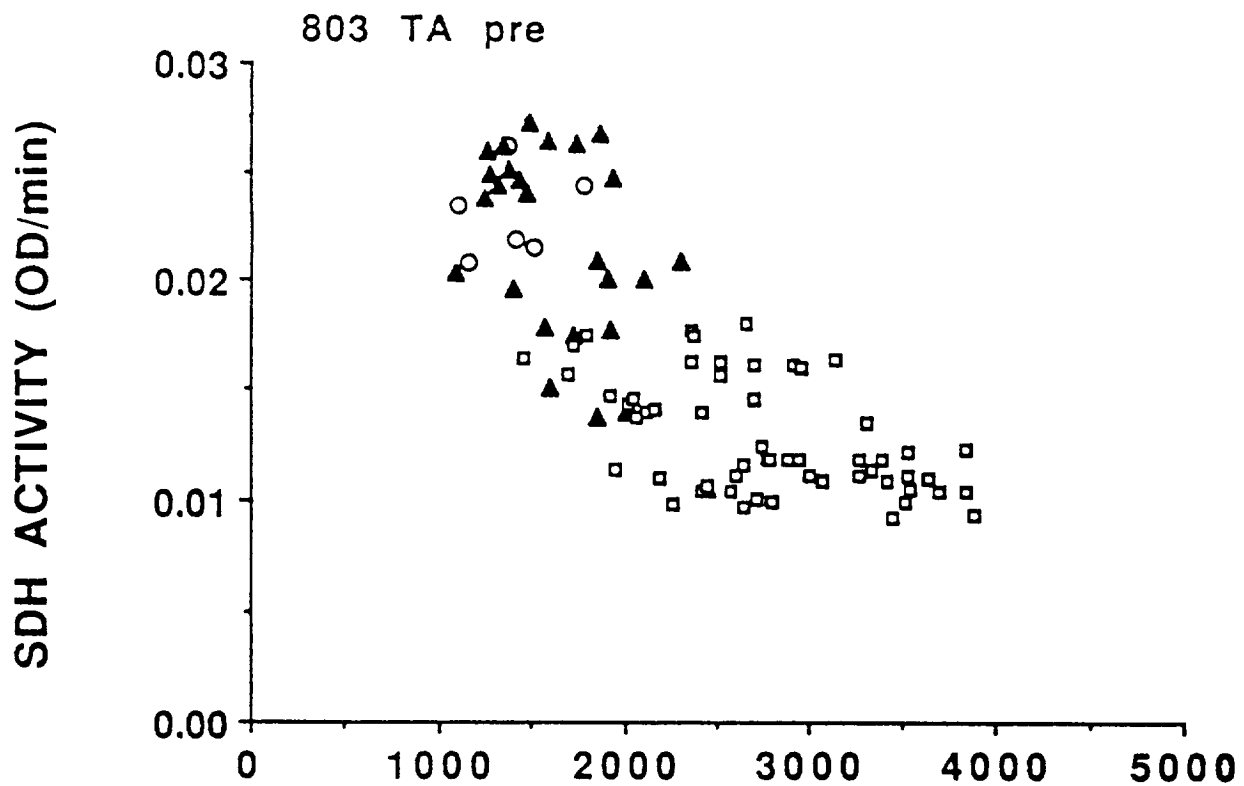


Figure 15.

EXPERIMENT K-8-05

CIRCADIAN RHYTHMS AND TEMPERATURE REGULATION
IN RHESUS MONKEYS DURING SPACE FLIGHT

Principal Investigator:

C.A. Fuller
University of California
Davis, California

Co-Investigators:

T. M. Higgins
University of California
Davis, California

D.W. Griffin
University of California
Davis, California

V. Klimovitsky
Institute of Biomedical Problems
Moscow, Russia

A. Alpatov
Institute of Biomedical Problems
Moscow, Russia

V. Magedov
Institute of Biomedical Problems
Moscow, Russia

CIRCADIAN RHYTHMS AND TEMPERATURE REGULATION IN RHESUS MONKEYS DURING SPACE FLIGHT

C.A. Fuller, T.M. Higgins, D.W. Griffin, V. Klimovitsky, A. Alpatov, V. Magedov

INTRODUCTION

Mammals have developed the ability to maintain homeostasis, i.e., a relatively constant internal environment, despite most variations encountered in their everyday environment. For example, as homeotherms mammals maintain a relatively constant body temperature. The most prominent variation encountered in the terrestrial environment is the daily alternation of light and dark. The evolution of the circadian timing system (CTS) has allowed animals to coordinate their internal time with the external environment. This physiological system enables an organism to anticipate and prepare for daily (and yearly) alterations in the environment.

Living organisms have evolved under the unvarying level of earth's gravity. Physiological and behavioral responses to changes in gravity are not completely understood. Exposure to altered gravitational environments (i.e., via hyperdynamic fields or space flight) has pronounced effects on physiological and behavioral systems, including body temperature regulation and circadian rhythms.

The Bioflights in the late 1950's provided the first temperature data from a primate in microgravity (Graybiel et al., 1959). Although many problems existed in interpretation of data (i.e., axillary instead of core temperature, short flight duration, highly stressed animals, etc.), there was a suggestion of a general decline in body temperature during the flights.

The earliest record of primate temperature data during space flight is that of Biosatellite III (Hahn et al., 1971). Although this animal was compromised, three applicable observations are apparent from the data: 1) there was a depression in body temperature during the flight, 2) the circadian rhythm of body temperature persisted but was "free-running" and not entrained to the ambient light-dark cycle and, 3) there were substantial changes in the sleep-wake behavior, including shifts in the phase-angle relationship to the LD cycle (with synchrony to 24-hour maintained) and fragmentation of the sleep-wake cycle (Hanley and Adey, 1971; Hoshizaki, et al., 1971). The loss of synchronization of the temperature rhythm while the sleep rhythm remained synchronized suggests that the altered gravitational field had a selective effect on the circadian timekeeping system. These data are consistent with our current understanding of the mammalian circadian timekeeping system. The circadian clock regulating the temperature rhythm is different from the clock regulating behaviors such as drinking and rest-activity (Fuller, et al., 1981). Some of the recent Soviet Cosmos monkeys also showed a decrease in body temperature of 0.50-0.75 °C, with a suggestion of altered phase-control of the temperature rhythms.

This program examined the influence of microgravity on temperature regulation and circadian timekeeping systems in Rhesus monkeys. Animals flown on the Soviet Biosatellite Cosmos 2229 were exposed to 11 2/3 days of microgravity. The circadian patterns temperature regulation, heart rate and activity were monitored constantly. This experiment has extended previous observation from Cosmos 1514 (Sulzman et al., 1986) and 2044 (Fuller, et al., 1993a), as well as provided insights in the physiological mechanisms that produce these changes.

METHODS

Two male Rhesus monkeys (151 and 906), weighing 3.5 and 4.0 kg, were used in three experimental paradigms to study the effects of microgravity on circadian rhythms and temperature regulation. The animals were studied in a 3-5 day baseline control experiment verifying all procedures and collecting baseline data prior to the flight of the Biosatellite. The animals were flown for 11 2/3 days on the Biosatellite and subsequently studied in a 3 day postflight experiment which began 13 days after the flight. Six weeks after recovery, a second, longer control study was performed, but the data are not yet available for analysis. In all conditions, the animals were housed in a 24 hour light-dark cycle (LD 16:8; lights on 08:00-24:00). The primates were fed 250 gram meals twice each day (08:00-10:00 and 18:00-20:00) and performed behavioral tests four times per day (08:00, 13:00, 16:00 and 21:00). The atmosphere in flight was maintained at sea level partial pressures and barometric pressure. The animals were extensively trained to sit in a chair-like restraint device for the duration of the experiments.

Measured parameters for each animal included: brain temperature, axillary temperature, head skin temperature, thigh skin temperature, axillary temperature, heart rate, motor activity, and ambient temperature at the upper portion of the chair. Except for brain temperature (which was collected at one minute intervals), data were collected at 10 minute intervals. All data were stored on a battery operated data logger (Vitalog, modified by L&M Electronics).

The heart rate was derived from the Soviet EKG signal by a U.S.-supplied R-wave detector (L&M Electronics). The axillary temperature measurements were taken from the output signals of a German biotelemetry transmitter (BTS BT) implanted in the axilla of each animal. The activity measurements were derived from a piezoelectric transducer (L&M Electronics) attached to a harness over the animals chest. Brain temperature was recorded by means of an electrode implanted superior to the caudate nucleus (A15; L10, V-25mm; Snider & Ledd, 1961) using a microbead thermistor encased in 25 gauge stainless steel tubing. The rest of the temperatures were measured via thermistors (YSI series 400 probes). The head skin temperature sensor was attached to the temple of the animals. The thigh and ankle skin temperature sensors were super-glued to the animals skin in those locations. To provide strain relief, the leg sensors were then taped in place. The ambient temperatures were measured at the top of the restraint system.

After each experiment the data were transferred to a microcomputer for analysis and storage. The analysis of the data included: examination and plotting of the raw data files, phase, waveform, period and statistical analysis. The statistical analyses yielded daily 24 hour means, light means, dark means and standard errors. Phase analysis was performed by fitting a sine wave to 24 hours of data using the least squares technique to compute circadian phase and amplitude. Waveform analysis was performed by repetitive waveform reduction. Period analysis was performed by the periodogram technique. Data were subjected to analysis of variance for repeated measures and the individual values compared using the Tukey test.

RESULTS

Circadian rhythms persisted in both subjects in all three conditions (preflight, flight, postflight). There was an increase in ambient temperature during the last three days of the flight. This increase was such that several of the temperature sensors (skin and ambient) reached the upper maximum of their range. This fact will bias the data from these sensors at this time such that maxima and means will be higher than actually reported. In addition, some alteration of the waveform of the data also occurred, which may slightly bias the circadian analysis of the data. To avoid any confounding influence this increase may have had, to examine variables across comparable lengths of time of collection, and to examine the response of the thermoregulatory system to the increased ambient temperature, the following data were examined: preflight days 2-3; flight days 2-3 (early), 7-8 (mid), 11-12 (late); and postflight day 2-3. Analysis of the data at intervals over the course of flight also

allowed a preliminary examination of the acute vs. chronic effects of the space flight environment. Average data for each measured variable are given in Table 1. The summary of the responses of each animal is described individually by variable below. All values given are 2-day means with standard errors.

Brain Temperature

This is the first of the Cosmos bioflights to measure brain temperature in a non-human primate. As mentioned previously, this variable was recorded at one minute intervals, allowing a very precise delineation of the daily rhythm in brain temperature. Averaged data from each animal is presented as a histogram in Figure 2. The average phase of the brain temperature was 15.1 ± 0.12 hours preflight. The phase is advanced from the position of 16.6 ± 0.23 hours which was seen on days 2-3 of flight. There was a slight delay to 17.0 ± 0.38 hours by days 7-8 of flight and a return back to an earlier time during days 11-12 (16.6 ± 0.85 hours). Postflight the average phase of the brain temperature rhythm was 14.4 ± 0.39 hours. The phase of brain temperature was significantly earlier postflight than during any other interval ($p < 0.05$).

The amplitude of the brain temperature rhythm was 0.85 ± 0.01 °C preflight. This was slightly larger than the 0.76 ± 0.03 °C exhibited early in the flight. There was a slight decrease to 0.70 ± 0.05 °C by midflight with an increase to 0.86 ± 0.11 °C by the end of the flight. The postflight brain temperature amplitude was 0.74 ± 0.08 °C.

Mean brain temperature was 38.73 ± 0.20 °C preflight, comparable to the 38.80 ± 0.15 °C seen at the start of flight. Average brain temperature decreased slightly (to 38.56 ± 0.3 °C) by midflight and returned back to preflight levels (38.82 ± 0.11 °C) by the end of flight. The pattern was generated by the response of animal M151. While the average brain temperature of M906 remained between 38.95 and 39.01, M151's average brain temperature fell from 38.63 °C at the start of flight to 38.1 °C midflight. It returned back to 38.3 °C during the last two days of flight. Postflight mean brain temperature averaged 39.02 ± 0.06 °C.

Axillary Temperature

Axillary temperature data is reported as a frequency output of the sensor, and not as absolute body temperature. The frequency output of the sensor decreased as body temperature increased. The raw plots of axillary temperature thus show high body temperatures as occurring during the dark (the reverse of the actual body temperature rhythm for this diurnal species). This is also the reason that the phases (which are the time of the acrophase of a sine wave fitted to 24 h of data) of axillary temperature occur during the dark period. Further, axillary temperature was not recorded in animal M151 during the preflight experiment, nor was it recorded from either subject postflight. The following data are shown graphically in Figure 3.

Animal M906 had an average phase of the axillary temperature rhythm of 3.45 ± 0.03 hours preflight. The average axillary temperature phase inflight for M906 and M151 began at 4.62 ± 0.18 hours. This delayed slightly by midflight to 5.07 ± 0.39 hours. A further delay to 6.10 hours was seen on day 11 of flight. The data from day 12 of flight was not complete enough to perform a curve fitting.

The amplitude of the axillary temperature rhythm for M906 preflight was 16.41 ± 0.14 . For both animals, the average axillary amplitude was 14.0 ± 1.54 on days 2-3 of flight, 14.7 ± 0.87 on days 7-8 and 15.0 ± 3.11 on days 11-12.

Mean axillary temperature showed a slight decrease at midflight, compared to early and late flight. This is shown by the slightly higher average frequency recorded at this time.

Head Skin Temperature

This variable also showed a later phase inflight than preflight. Preflight phase was $14.9 \text{ h} \pm 0.74$ hours; inflight than preflight. Preflight phase was $14.9 \text{ h} \pm 0.74$ hours; inflight phase began at 16.4 ± 0.79 hours, delayed to 18.0 ± 0.16 hours by midflight and slightly advanced to 17.8 ± 1.65 hours by late flight. Postflight the average phase of the head temperature rhythm was 14.63 ± 1.27 hours. This response was seen in both animals. The phase of this variable became very unstable during the high ambient temperatures seen during the last three days of flight. Results of data analysis are plotted in Figure 4.

The amplitude of the head skin temperature rhythm decreased from preflight to early flight (0.59 ± 0.13 °C to 0.35 ± 0.09 °C). As flight advanced the amplitude increased to 0.56 ± 0.06 °C. During the late flight, there was a further increase in this amplitude (1.01 ± 0.18 °C) as the animals were increasing blood flow to the skin in order to thermoregulate in the face of the thermal load of the increased ambient temperature. The postflight amplitude was 0.82 ± 0.17 °C.

The use of vasomotion was also seen in the average head skin temperature, which rose from a relatively constant level (33.53 ± 1.69 °C pre; 33.86 ± 0.85 °C d2-3; 33.59 ± 0.78 °C d7-8) to 36.59 ± 0.4 °C on d11-12. Postflight the mean head skin temperature was 34.17 ± 1.29 °C.

Thigh Skin Temperature

This variable was not measured during the preflight or postflight conditions. The following data are presented as a histogram in Figure 5. During flight the average phase of the upper leg skin temperature was fairly stable (18.5 ± 1.63 hours d2-3; 18.1 ± 1.22 hours d7-8; 18.2 ± 1.71 hours d11-12).

This pattern was also seen in the mean thigh skin temperatures; averages were 32.64 ± 0.63 °C for d2+3; 33.69 ± 0.36 °C for d7-8; and 36.59 ± 0.40 °C for d11-12.

Ankle Skin Temperature

These data are presented graphically in Figure 6. The phase of the ankle skin temperature rhythm was very different during space flight. Preflight the average phase was 15.0 ± 2.55 hours; while postflight it was 21.41 ± 2.95 hours. However, during space flight, the average ankle skin temperature phase was 6.9 ± 3.53 hours on d2-3; 6.1 ± 3.73 hours on d7-8; and 18.7 ± 1.84 hours during the high ambient temperature of d11-12.

The amplitude of the rhythm was also initially increased in space flight (1.0 ± 0.63 °C preflight; 3.16 ± 1.17 °C d2-3). The amplitude decreased to 1.04 ± 0.45 °C on d7-8. There was a slight increase to 1.34 ± 0.46 °C on days 11-12. Postflight ankle skin temperature amplitude averaged 1.64 ± 0.79 °C.

Mean ankle skin temperature again reflected the vasomotor response to the ambient temperature. Mean skin temperature at this site was 26.8 ± 1.88 °C preflight, 27.35 ± 0.84 °C d2-3 of flight, 26.83 ± 0.4 °C d7-8 of flight. It rose to 35.5 ± 0.55 °C during d11-12 of flight. Postflight mean ankle skin temperature averaged 32.06 ± 1.21 °C. Mean ankle skin temperature was significantly high during late flight than during either preflight or midflight ($p < 0.05$).

Heart Rate

Figure 7 is a plot of the average heart rate circadian phase, amplitude and 24 hour mean for each animal in five experimental data sets. Preflight, the animals had an average phase of approximately 14.9 ± 0.94 hours. At the start of flight, the average phase was 12.7 ± 0.28 hours. This delayed to

17.9±2.43 hours at midflight and advanced back to 15.1±1.35 hours at the end of flight (during the high ambient temperature). Postflight, the average phase of the heart rate rhythm was 13.0±0.52 hours.

The average amplitude of the heart rate rhythm was larger preflight (30.1±4.29 bpm) than at the start of flight (10.6±2.51 bpm). This increased slightly midflight (12.1±3.44 bpm) and late in the flight (12.5±2.22 bpm). The postflight amplitude average 11.2±1.10 bpm. A statistical difference was revealed by ANOVA ($p<0.025$). A Tukey test revealed that the preflight amplitude differed from all flight amplitudes as well as from the postflight amplitude.

Mean heart rate during the preflight experiment was 144.8±17.41 bpm. This was higher than the average heart rate during days 2-3 of flight (128.7±3.46 bpm), days 7-8 (117.2±20.1 bpm) and days 11-12 (108.0±17.0 bpm). Postflight, the daily mean heart rate was 144.1±7.5 bpm. It should be noted that while the average heart rate for both animals was smaller inflight than preflight, the drop was noticeably larger in M151. This animal also exhibited a decrease in food consumption and activity level over the flight.

Activity

The activity measurement is a relative one, depending on the placement and sensitivity of the sensor used. As such, activity levels and amplitudes can only directly be compared within the course of a single experiment. The average phase of activity rhythm of the two animals was 15.6±0.23 hours preflight, as shown in Figure 7. This is close to the value of 16.1±.35 hours seen during days 2-3 of flight. However, by days 7-8 of flight the average phase of the activity rhythm had delayed to 19.6±.51 hours. As was the case with the phase of the heart rate rhythm, this advanced (to 17.2±.42 hours) during the last 2 days of flight. Postflight the average activity phase was 14.7±0.37 hours. Activity phase showed a statistically significant difference ($p<0.005$). The phase at midflight was significantly later than preflight, early in the flight, during late flight, and during the postflight experiment.

During flight the amplitude of the activity rhythm rose from 120.4±27.43 counts/10 minutes during days 2-3 to 173.9±27.41 counts/10 minutes on days 7-8. The mean activity amplitude remained high at the end of the flight (172.1±30.62 counts/10 minutes).

Mean activity levels rose slightly from 662.5±26.7 counts/10 minutes on days 2-3 to 687.0±131.2 counts/10 minutes on days 7-8. Mean activity levels then decreased to 582.1±160.5 counts/10 minutes during the last two days of flight. This pattern of average activity was driven by animal M906 who exhibited an increase followed by a slight decrease in activity. M151 exhibited a continued steady decline in activity level over the course of the flight.

Ambient Temperature

Mean ambient temperature was 25.2±0.24 °C preflight. From early to midflight it remained relatively stable (24.9±0.31 °C; 25.6±0.78 °C), but rose significantly during the late flight (31.5±0.24 °C; $p<0.005$). Postflight the mean ambient temperature was 27.24±1.19 °C. These data are presented in Figure 8.

DISCUSSION

Temperature Regulation

Previous experiments have shown that skin temperatures are reduced in space flight. This, in concert with a reduced heart rate and activity level, combined with reduced food intake of the animals during the flight suggest a decrease in metabolism; analysis of metabolic rate using the double-labeled water

method revealed a decrease of up to 40% in these two subjects during space flight (Fuller et al., 1993b). In this experiment, both head and ankle skin temperatures were lower inflight (early and mid) than during the postflight experiment, despite the fact that ambient temperature was higher in the postflight experiment. However, during the preflight experiment, head skin temperature was lower than during flight. Ankle skin temperature was higher preflight than at the start of flight, but decreased at midflight to the preflight level. These data continue to suggest that the thermoregulatory system is operating at a lowered level while the organism is in a microgravity environment. However, there were variations between the animals and analysis of the second postflight data will be required to more completely understand these responses.

Circadian Timing System

Several previous observations of different organisms suggest that the circadian timing system is composed of two or more central pacemakers. The limited data sets that are available from space flight experiments suggest that these pacemakers show differential responses to the microgravity environment.

The pacemaker involved in regulating the timing of variables such as heart rate and motor activity consistently evidence appropriate 24 hour rhythms in the presence of a 24 hour light-dark cycle. Various reports have suggested the possibility of a phase angle shift but not a change in period. In contrast, the pacemaker that is involved with the circadian regulation of parameters such as body temperature does not show such stability. Frequent reports have indicated that temperature rhythms in the microgravity environment, even in the presence of a light-dark cycle have non-24 hour or significantly altered 24 hour rhythms. While such robust changes were not observed in this flight, there were deviations from the 24 hours patterns in some of the temperature variables, most notably in ankle skin temperature.

CONCLUSION

The data that were collected during this experiment further confirm that temperature regulation, metabolism and circadian timing are altered in the microgravity environment of space flight. Increased knowledge of these alterations will assume increasing importance as our forays into this environment increase in frequency and duration.

ACKNOWLEDGMENTS

We would like to thank our Soviet colleagues for their involvement and support of this project, especially Drs. V. Ya. Klimovitsky, A.M. Alpatov, E.A. Ilyin, A. Truzennikov, Y. Evstartov, M. Kaplansky, V. Magedov, and B. Perepech, at the Institute of Biomedical Problems. In the U.S., the role that Jim Connolly played as Project Manager was key to the successful U.S. participation in the flight. We also wish to acknowledge the participation of other individuals at Ames Research Center, especially: Mike Skidmore, Rod Ballard, Mike Souza, Denise Helwig, Samantha Edmonds and Dick Grindeland, support personnel Richard Mains and Edward Luzzi. This work was supported by NASA Grant NAG2-587.

REFERENCES

1. Fuller, C.A., 1984a, *Aviat. Space Environ. Med.* 55:226-330.
2. Fuller, C.A., Horowitz, J.M., Horwitz, B.A., 1977a. *J. Appl. Physiol.* 42:154-158.
3. Fuller, C.A., Horwitz, B.A., and Horowitz J.M., 1977b. *J. Appl. Physiol.* 42:74-79.
4. Fuller, C.A., Horwitz, B.A., and Horowitz J.M., 1975. *Am. J. Physiol.* 228: 1519-1524.

5. Fuller, C.A., Tremor, J., Connolly, J.P. and Williams, B.A., 1981. *Physiologist* 24:S111-112.
6. Fuller, C.A., Hoban-Higgins T.M., Griffin, D.W. and Murakami, D.M. 1992. COSPAR, in press.
7. Fuller, C.A., Hoban-Higgins, T.M., Alpatov A. and Klimovitsky, V. 1993a. In: COSMOS 2044 Biosatellite Mission Description and U.S. Final Reports of Monkey, Rat and Radiation Experiments. NASA, 1994.
8. Fuller, C.A., Stein, T.P., Griffin, D.W., Dotsenko, M., Truzennikov, A. and Korolkov, V. 1993b. In: COSMOS 2229 Final Results Symposium, Moscow, 1993.
9. Giacchino, J., Horowitz, J.M., and Horwitz, B.A., 1979. *J. Appl. Physiol.* 46:1049-1053.
10. Graybiel, A., Homes, R.H., Beischer, D.E., Champlin, G.E., Pedigo, G.P., Hixson, C., Davis, T.R.A., Barr, N.L., Kistler, W.G., Niven J.E., Wilbrager, E., Stullken, D.E., Augerson, W.D., Clarke, R., Berrian, J.H., 1959. *Aerospace Med.* 30:871-931.
11. Hahn, P.M., Hoshizaki, T., and Adey, W.R., 1971. *Aerospace Med.* 42: 295-304.
12. Hanley, J., and Adey, W.R., 1971. *Aerospace, Med.* 42:204-313.
13. Horowitz, J.M., Schertel, E.R., and Horwitz, B.A., 1979. *The Physiologist* 22:S57-S58.
14. Hoshizaki, T., Durham. R., and Adey, W.R., 1971. *Aerospace Med.* 42:288-295.
15. Oyama, J., 1971. In: *Regulatory Biology: Depressed Metabolic States*. NASA TM-X-69354, pp. 27-51.
16. Oyama, J., 1975. *COSPAR Life Scis. Space Res. XIII*. P.H.A. Sneath, eds., Akademik-Verlag (Berlin) p. 2-17.
17. Oyama, J. and Chan, L., 1973. *Fed. Proc.* 32:392.
18. Schertel, E.R., Horowitz, J.M., and Horwitz, B.A., 1980. *J. Appl. Physiol.* 49:663-668.
19. Smith, A.H., 1975. In: *Foundations of Space Biology and Medicine*. M. Calvin and O. Gazonko, eds. NASA (Washington, D.C.), p. 125-172.
20. Sulzman, F.M., Fuller, C.A., Moore-Ede, M.C., Klimovitsky, V., Magedov, V., and Alpatov, A.M., 1986. In: *Final Reports of U.S. Monkeys and Rat Experiments Flown on the Soviet Satellite COSMOS 1514*, eds. R.C. Mains and W.W. Gomersall, NASA (Moffett Field), p. 71.
21. Weir, J. B., deB., 1949. *J. Physiol. (London)*, 109:1-9.

TABLE 1

ACTIVITY				HEART RATE			AXILLARY TMP			BRAIN TMP		
PREFLIGHT	PHASE	AMP	MEAN	PHASE	AMP	MEAN	PHASE	AMP	MEAN	PHASE	AMP	MEAN
AVERAGE	15.59	179.78	435.37	14.87	30.11	144.80	3.45	16.41	532.13	15.05	0.85	38.73
SEM	0.23	110.74	281.09	0.94	4.29	17.41	0.03	0.14	3.05	0.12	0.01	0.20
FLIGHT-EARLY												
AVERAGE	16.06	120.43	662.53	12.69	10.59	128.73	4.61	13.97	533.08	16.58	0.76	38.80
SEM	0.35	27.42	26.66	0.28	2.51	3.46	0.18	1.54	2.45	0.23	0.03	0.15
FLIGHT-MID												
AVERAGE	19.62	173.93	686.98	17.89	12.14	117.22	5.07	14.67	543.13	16.95	0.70	38.56
SEM	0.51	27.41	131.17	2.43	3.44	20.12	0.39	0.87	3.11	0.38	0.05	0.30
FLIGHT-LATE												
AVERAGE	17.23	172.06	582.13	15.07	12.45	107.96	6.10	14.98	535.50	16.64	0.86	38.82
SEM	0.42	30.62	160.48	1.35	2.22	16.99	0.39	3.11	3.11	0.85	0.11	0.11
POSTFLIGHT												
AVERAGE	14.70	201.20	419.19	12.99	11.21	141.37				14.39	0.74	39.02
SEM	0.37	29.27	93.94	0.52	1.10	7.46				0.59	0.08	0.06
SKIN AND AMBIENT TEMPERATURES												
HEAD SKIN TMP				THIGH SKIN TMP			ANKLE SKIN TMP			AMBIENT TMP		
PREFLIGHT	PHASE	AMP	MEAN	PHASE	AMP	MEAN	PHASE	AMP	MEAN	PHASE	AMP	MEAN
AVERAGE	14.88	0.59	33.53				14.98	0.99	26.80	11.99	0.56	25.18
SEM	0.74	0.13	1.69				2.55	0.63	1.88	3.74	0.10	0.24
FLIGHT-EARLY												
AVERAGE	16.35	0.35	33.86	18.48	1.09	32.64	6.88	3.16	27.35	14.12	0.32	24.86
SEM	0.79	0.09	0.85	1.63	0.15	0.63	3.53	1.17	0.84	5.43	0.09	0.31
FLIGHT-MID												
AVERAGE	17.97	0.56	33.59	18.12	0.73	32.31	6.12	1.04	26.83	20.03	0.28	25.57
SEM	0.16	0.06	0.78	1.22	0.07	0.36	3.73	0.45	0.40	1.84	0.09	0.78
FLIGHT-LATE												
AVERAGE	17.80	1.01	36.59	18.15	1.20	36.11	18.69	1.34	35.53	18.07	0.87	31.51
SEM	1.65	0.18	0.40	1.71	0.23	0.36	1.84	0.46	0.55	1.57	0.49	0.24
POSTFLIGHT												
AVERAGE	14.63	0.82	34.17				21.41	1.64	32.06	18.03	0.52	27.24
SEM	1.27	0.17	1.29				2.95	0.79	1.21	2.34	0.21	1.19

Circadian phase and amplitude and 24 hours means for each variable. Values are given for days 2 and 3 of the preflight experiment, days 2, 3, 7, 8, 11, and 23 of the flight, and days 2 and 2 of the postflight experiment. The data are averaged and given with standard errors for: preflight, early flight (d2-3), midflight (d7-8), late flight (d11-12) and postflight. All phases are in hours. Activity amplitude and mean are in counts per 10 minute interval. Heart rate amplitude and mean are in beats per minute (bpm). Amplitude and mean values for all temperatures other than axillary are in °C axillary temperature is reported as the frequency output of the sensor. A higher frequency is indicative of a lower temperature.

Figure 1(a), (b), (c), and (d): The complete data set for one animal (M906) for recorded during the flight of COSMOS 2229. All variables are plotted vs. time of day. The light-dark cycle is indicated by the light and dark bars at the top of the graph. Data shown include: brain temperature (in °C), axillary temperature (in frequency of the sensor), head skin, thigh skin, and ankle skin temperatures (in °C), heart rate (in beats per minute), activity (in counts per 10 minute interval) and ambient temperatures (in °C). Brain temperature was recorded at 1 minute intervals. All other data were recorded at 10 minute intervals. The frequency of the axillary temperature sensor increases as temperature decreases, thus higher values, indicating a decreased temperature, are seen at night. Data records begin when the animals were placed in the BIOS chamber, Launch which occurred on 12/29/92 at 1630 hours. Landing and recovery occurred on 1/10/93 at 0716.

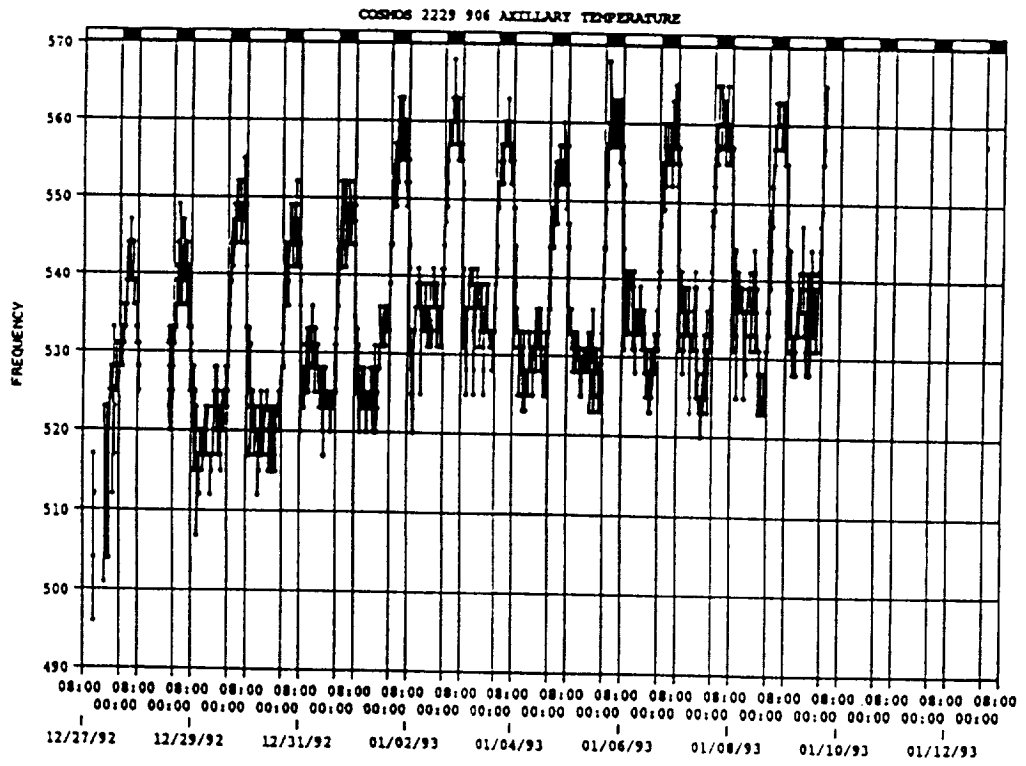
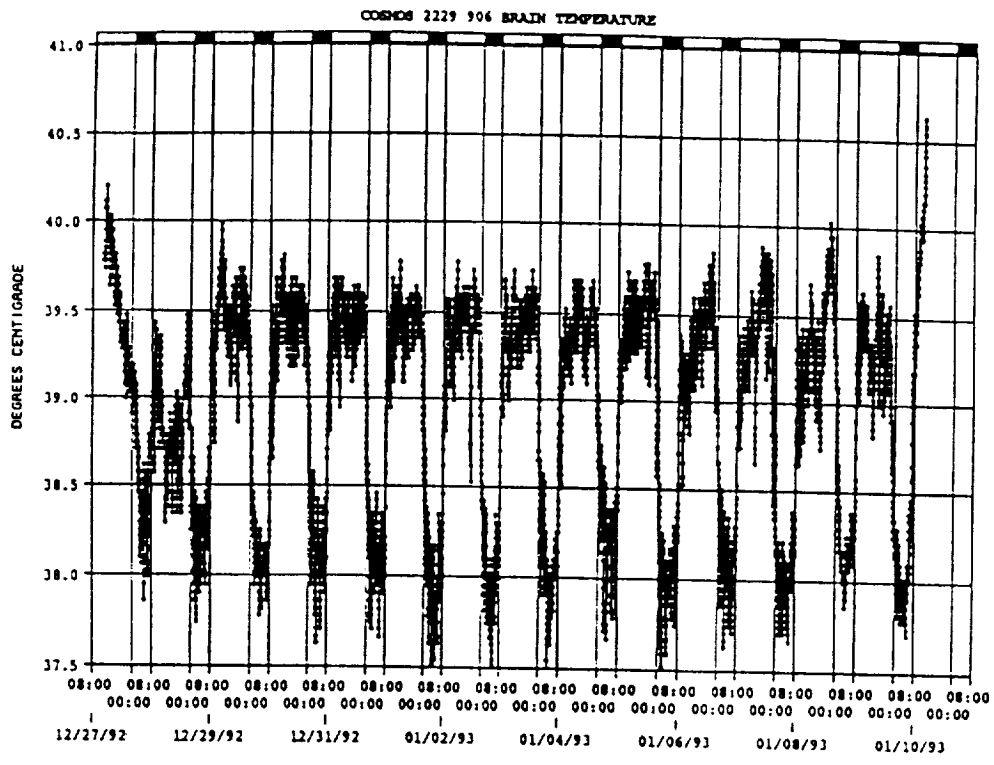


Figure 1(a).

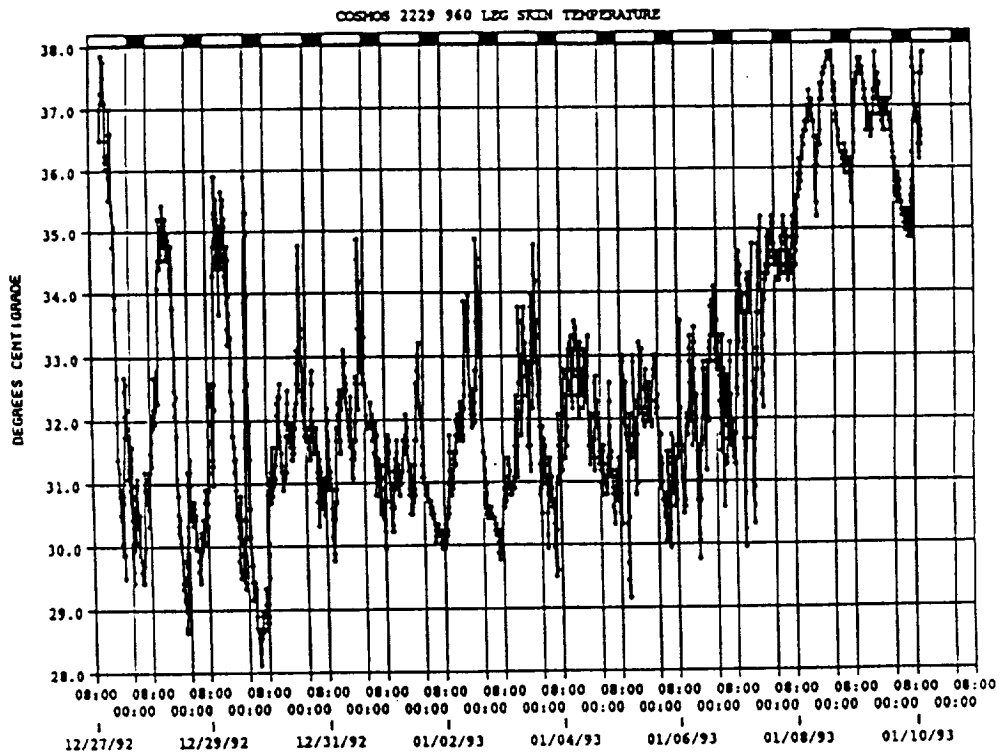
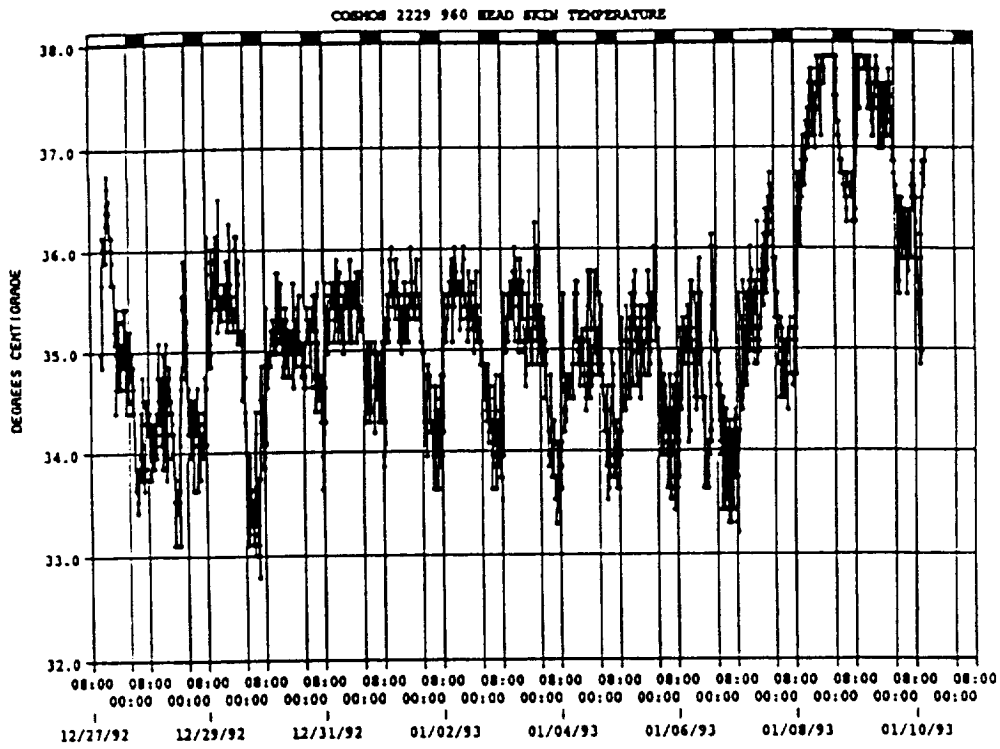


Figure 1(b).

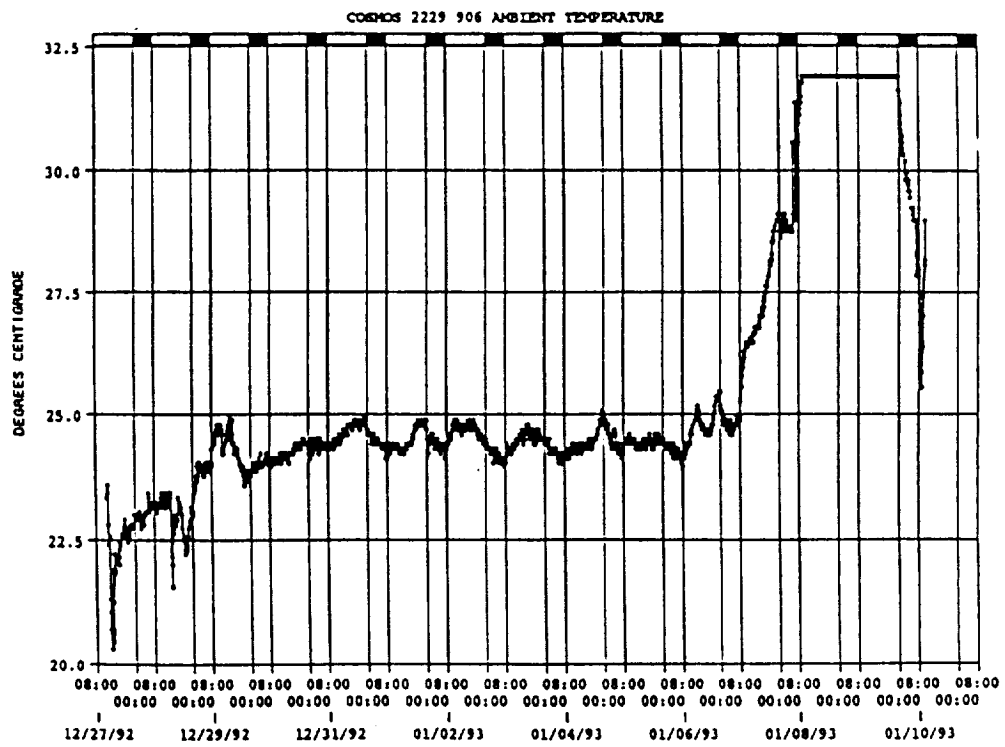
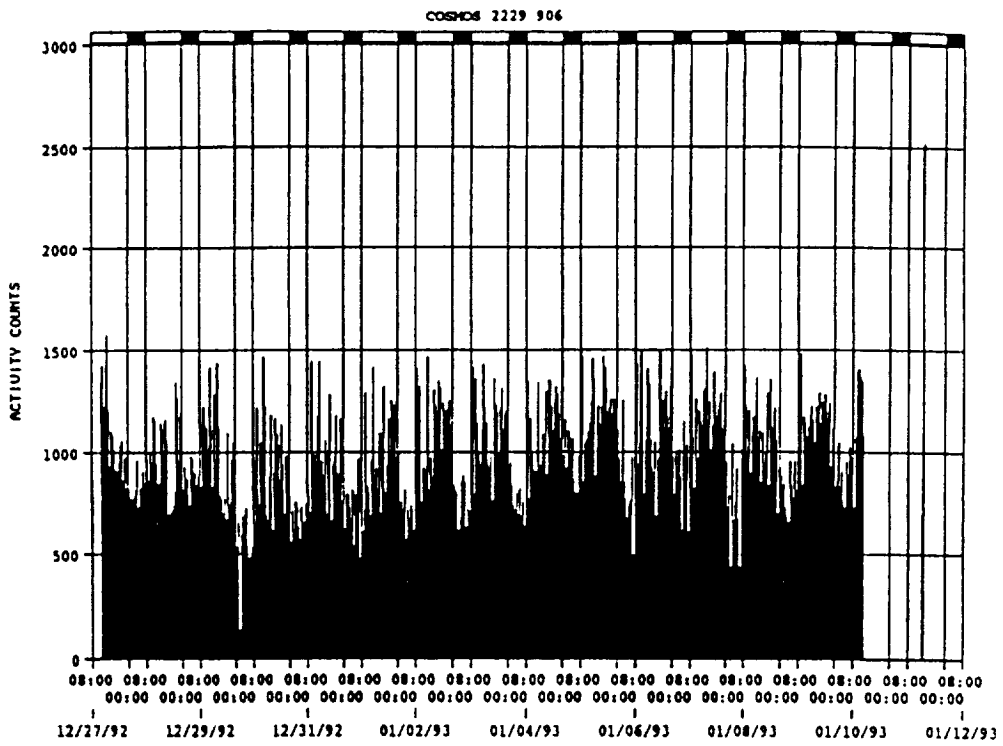


Figure 1(d).

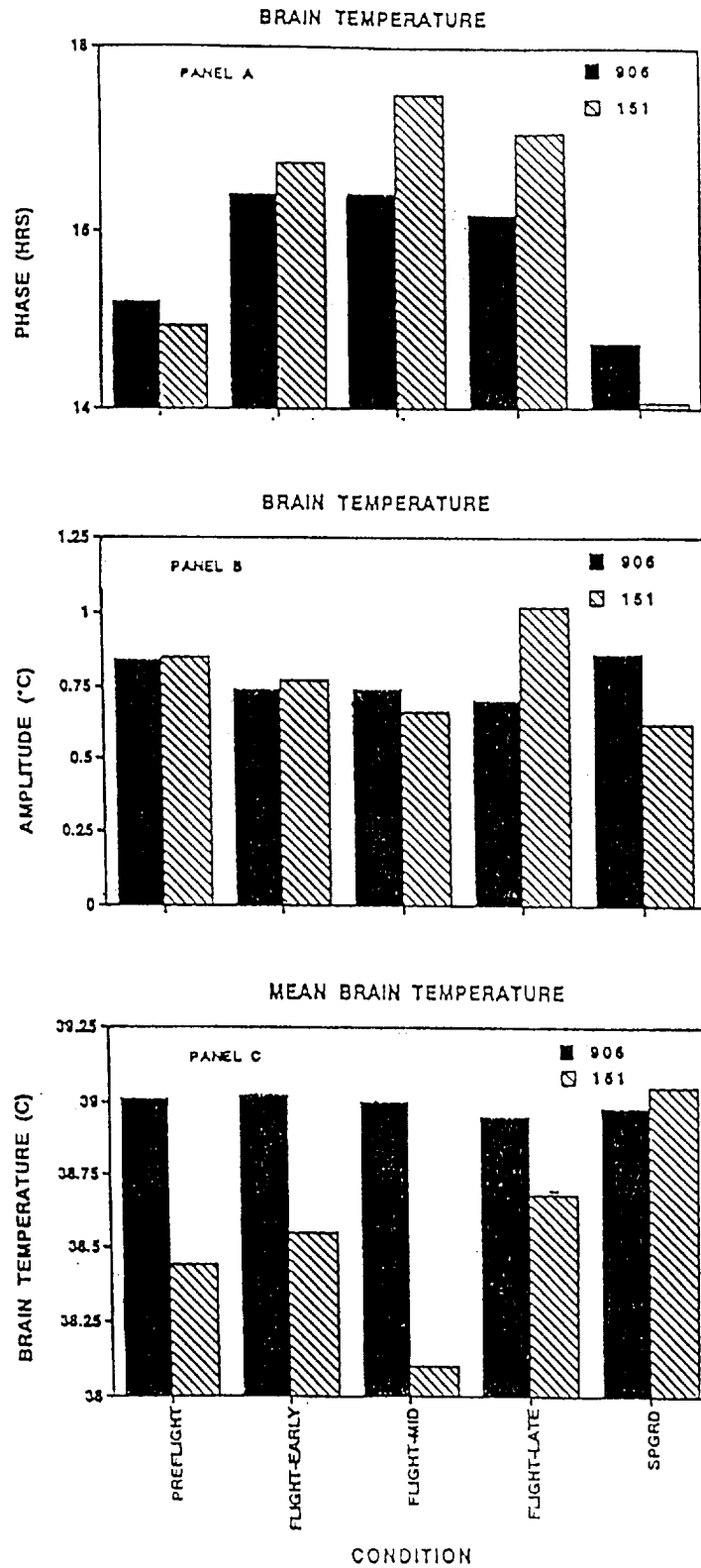


Figure 2: Brain temperature data. These data are two day means from: days 2 and 3 of preflight, days 2 and 3 of flight (early), days 7 and 8 of flight (mid), days 11 and 12 of flight (late) and days 2 and 3 of the short postflight experiment that was conducted 10 days after flight (spgrd). Panel A: Average circadian phase (in hours). Panel B: Average amplitude of the circadian rhythm of heart rate (in °C). Panel C: Average mean heart rate (in °C)

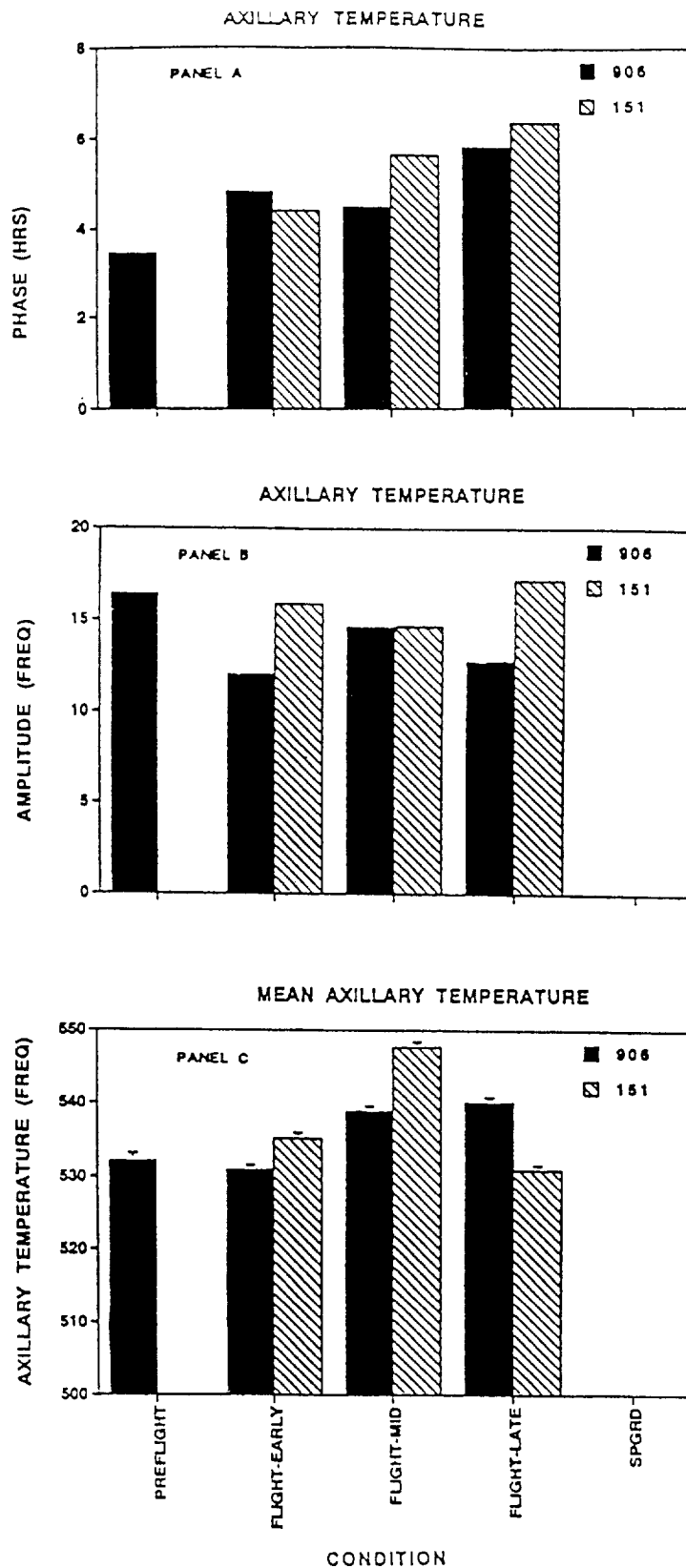


Figure 3: Axillary temperature data is present as described in Figure 2. The axillary temperature is reported as the frequency of the output of the sensor, and which has an inverse relationship to actual temperature. Therefore, the highest values of frequency occur during the night, the time of the minimum body temperature.

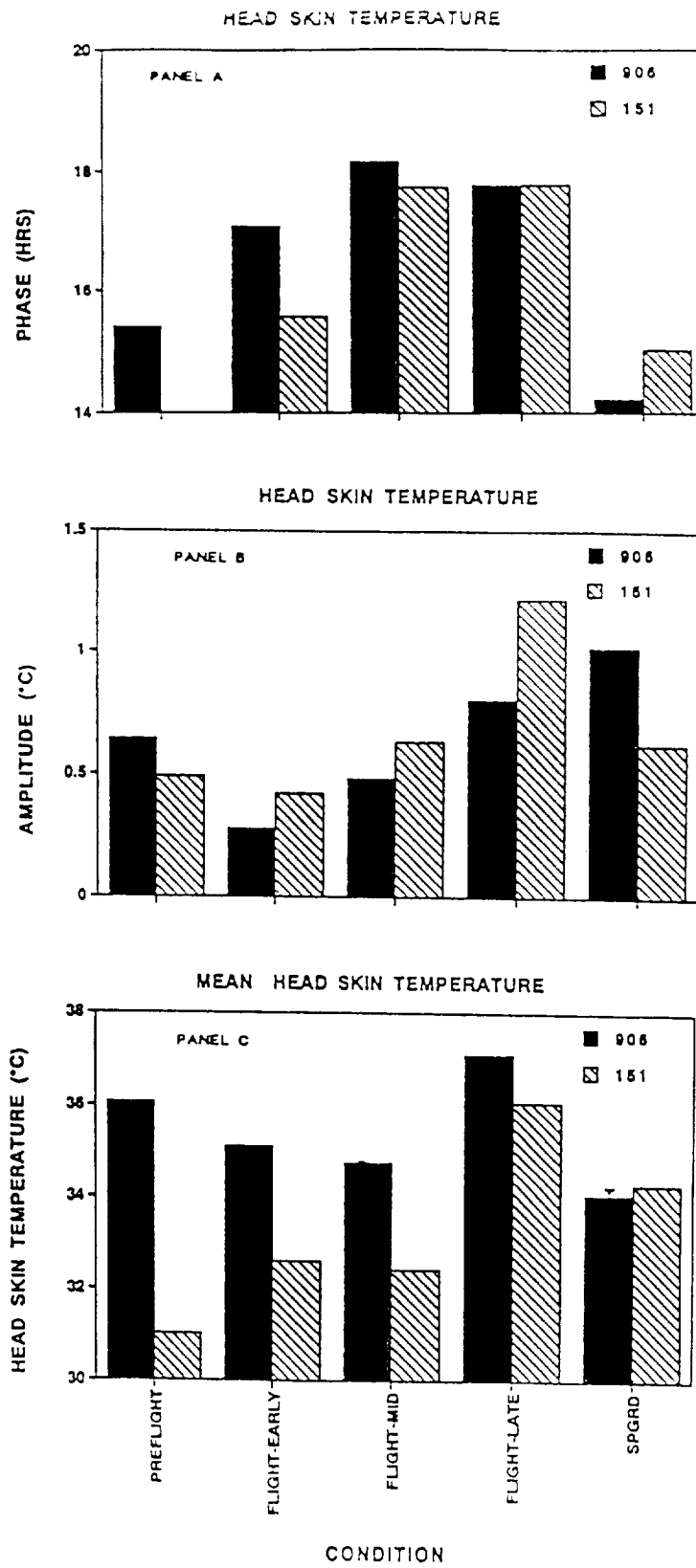


Figure 4: Head skin temperature data is presented as described in Figure 2.

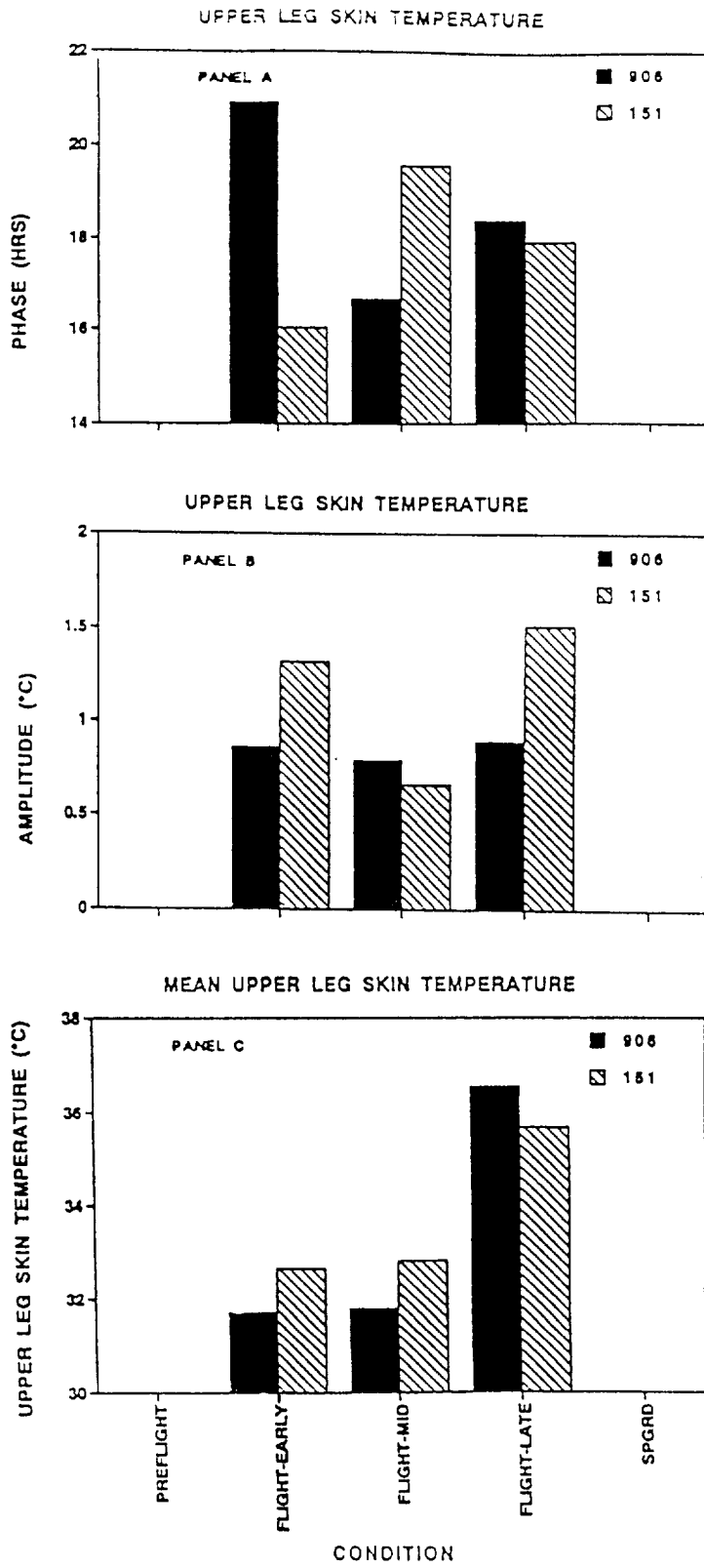


Figure 5: Thigh skin temperature data is presented as described in Figure 2.

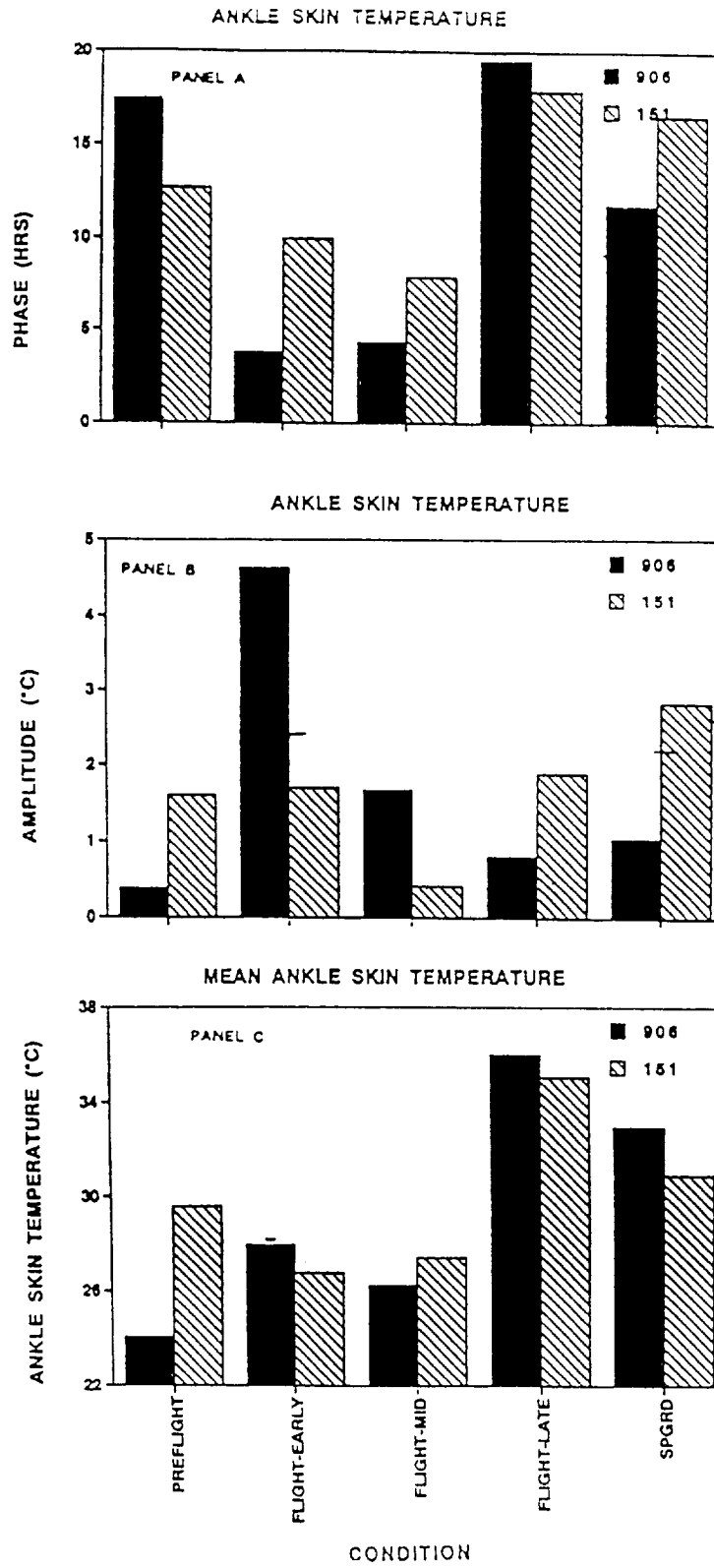


Figure 6: Ankle skin temperature data is presented as described in Figure 2.

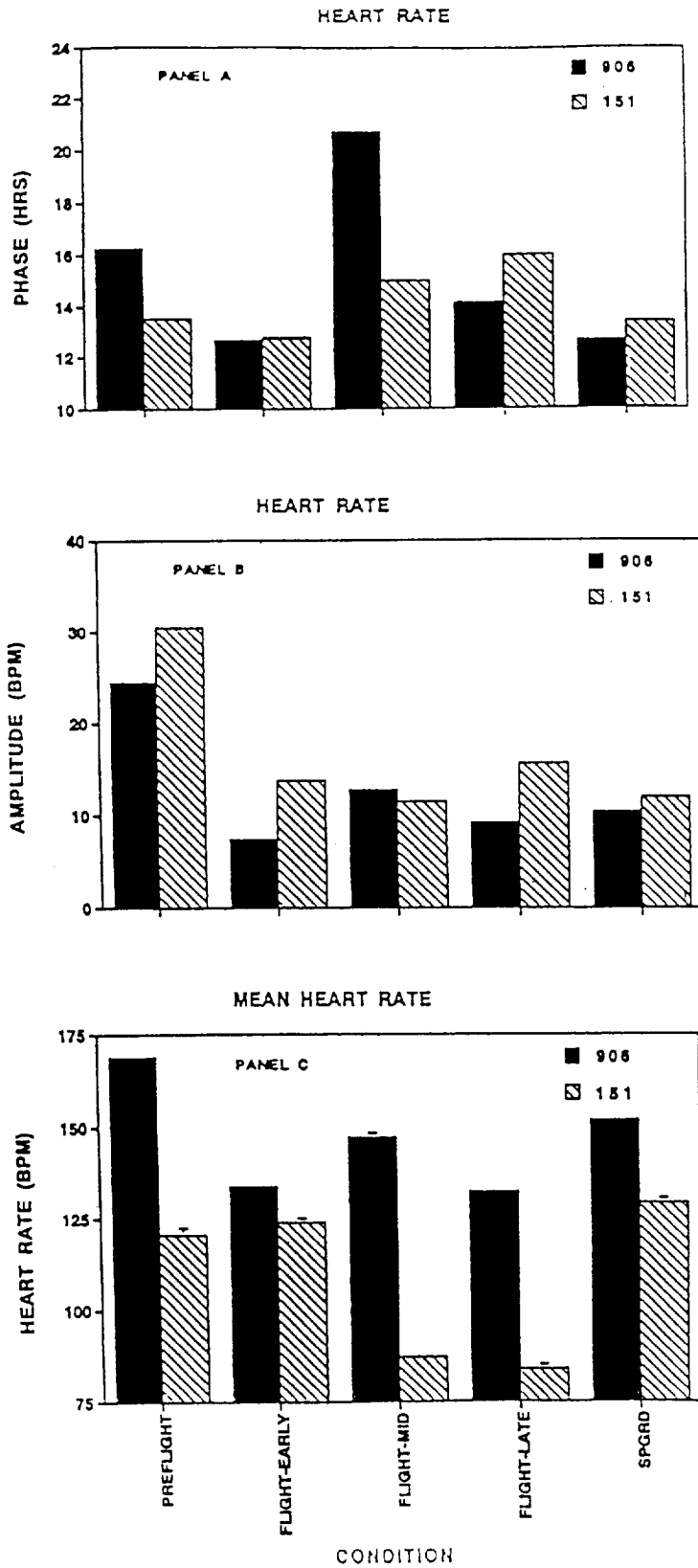


Figure 7: Heart rate data are shown as described in Figure 2. Heart rates are in beats per minute.

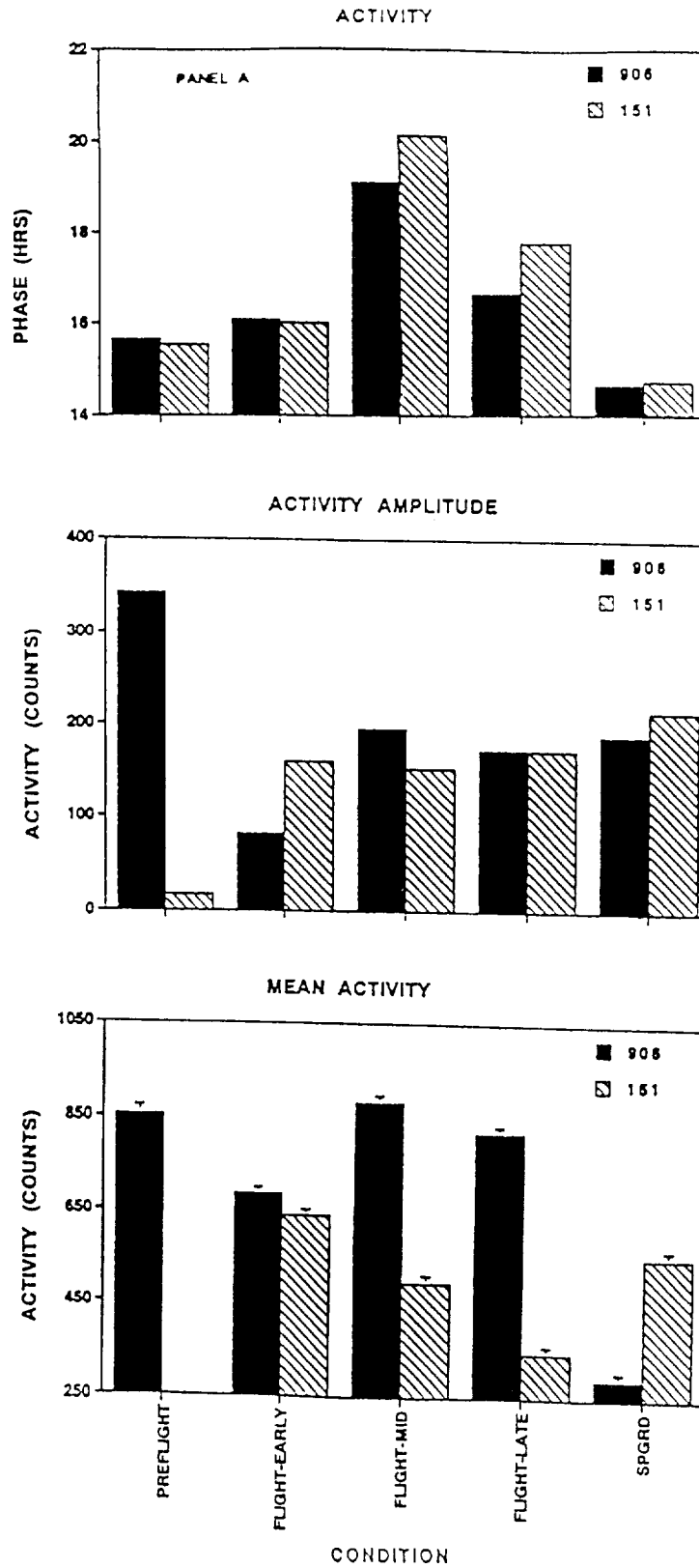


Figure 8: Activity data is presented as described in Figure 2. Activity levels are in counts per 10 minute interval.

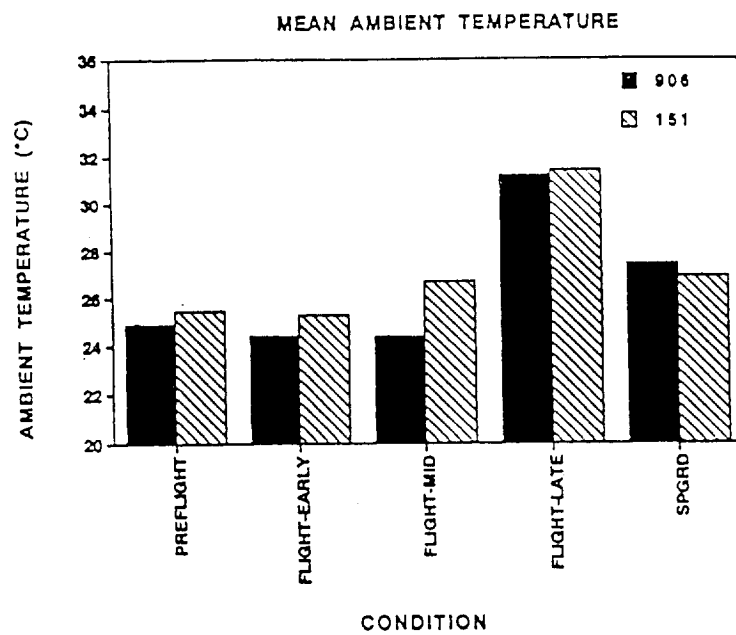


Figure 9: Mean ambient temperature data for each condition (°C).

EXPERIMENT K-8-06

RHESUS MONKEY METABOLISM DURING SPACE FLIGHT:
MEASUREMENT OF ENERGY EXPENDITURE USING THE DOUBLY
LABELED WATER ($^2\text{H}_2^{18}\text{O}$, DLW) METHOD

Principal Investigator:

C.A. Fuller
University of California
Davis, CA

Co-Investigators:

T.P. Stein
University of Medicine and Dentistry of
New Jersey-School of Osteopathic Medicine
Stratford, NJ

D.W. Griffin
University of California
Davis, CA

V.I. Korolkov
Institute of Biomedical Problems
Moscow, Russia

M.A. Dotsenko
Institute of Biomedical Problems
Moscow, Russia

RHESUS MONKEY METABOLISM DURING SPACE FLIGHT: MEASUREMENT OF ENERGY EXPENDITURE USING THE DOUBLY LABELED WATER ($^2\text{H}_2^{18}\text{O}$, DLW) METHOD

C.A. Fuller, T.P. Stein, D.W. Griffin, V.I. Korolkov, M.A. Dotsenko

SUMMARY

Energy expenditure was determined by the doubly labeled water (DLW: $^2\text{H}_2^{18}\text{O}$) method in two Rhesus during space flight (151, 906) and 4 ground control monkeys (75, 803, 892 and 907). Urine was used to sample body water. Energy expenditure was measured for the two flight monkeys over a four day period preflight. Three days preflight the monkeys were redosed with $^2\text{H}_2^{18}\text{O}$. The urine was sampled again preflight and immediately postflight. For the four ground controls monkeys, energy expenditure was measured over a four day period, and for one monkey again after a 13 day period to simulate the flight period. In addition, flight data was available from one monkey flown previously on Cosmos 2044 (2483). The mean energy expenditure for the ground control determinations was 88.8 ± 5.9 kcal/kg/day ($n=6$). The energy expenditure values for the monkey 892, with both 4 day and thirteen day determinations were the same (83.6 vs. 77.6 kcal/kg/day). The mean inflight energy expenditure values (59.9 ± 4.6 kcal/kg/day ($n=3$)) were significantly less than the preflight values. The approximate 30% decrease is significant ($p < 0.05$). This limited data base is consistent with a decrease in energy expenditure in chair adapted Rhesus monkeys during space flight.

INTRODUCTION

Although more than 30 years have elapsed since the first manned space flight, the effect of space flight on energy metabolism is still not known (Lane, 92). The question is of interest for both practical and theoretical reasons. Practically it is important to know energy expenditure as part of the overall health maintenance program for the crew, especially during long term missions are provided with enough energy. Yet, Gazonko has argued on theoretical grounds that gravity should have no direct effect at the cellular level because processes at that level are diffusion controlled (Gazonko et al., 80). The effect of microgravity on the whole organism's energy expenditure is not known.

Secondly, the energy costs of living in an environment lacking the force of earth's gravity are unknown. *A priori*, one would expect the energy requirements at 0 g to be less because of the absence of work related to opposition of gravity (Grigoriev and Egorov, 92; Rambaut et al., 77). However, the available evidence based on data collected during the Skylab missions suggest that human energy expenditure may be increased during space flight (Rambaut et al., 77). By analyzing food and water intake, urine and fecal output, and changes in body weight, the Skylab investigators reached the unexpected conclusion that energy expenditure during space flight was about 5% greater than at 1 g (Rambaut et al., 77; Leonard, 83).

Possible explanations are an increased workload during space flight, or as Rambaut et al. suggested, a progressive decrease in metabolic efficiency (Rambaut et al., 77). It is likely to be very difficult to distinguish between these two possibilities in human crew members since the activity component may be different during space flight than it is on the ground. Energy expenditure can be regarded as the sum of two components, the basal metabolic rate and the energy costs of activity. The problem is how to measure energy expenditure with sufficient precision during space flight in a non-invasive manner which will not interfere with any other investigations or take any time. The combination of the chair adapted monkey and the doubly labeled water method meet these criteria.

The use of the chair adapted monkey model should ensure that the activity levels should be similar on the ground and during space flight. The doubly labeled water expenditure ($^2\text{H}_2^{18}\text{O}$) method for measuring energy expenditure is simple, non-invasive and highly accurate. The method was originally described by Lifson in 1955 and applied to man by Schoeller in 1982 (Lifson and McClintock, 66; Schoeller and van Santen, 82). If $^2\text{H}_2^{18}\text{O}$ is given orally, it mixes with the body water in about 3 hours (8). The two isotopes then leave the body at different rates. (^2H leaves as water, mainly in the urine, whereas ^{18}O leaves both as water and exhaled C^{18}O_2).

Thus the turnover rate of isotopic hydrogen and oxygen labeled water differ, and that difference is proportional to the rate of CO_2 production. The method has been validated in man, in normal animals, in animals in metabolically perturbed states, and in animals in the grossly non-steady state such as a complete fast. It has been used to measure the energy cost of the flight of birds as well as of free ranging wild animals. Thus, the method has been shown to be widely applicable. The principal sources of error with the method are the pre-dose enrichment expressed in delta units and the fractionation effect = 1.047 for CO_2 . For this study we assumed that the isotope distribution space is equal to the TBW. In man, the total body water (TBW) is assumed to be equal to the ^{18}O isotope distribution space divided by 1.01 (Schoeller et al., 82).

ENERGY EXPENDITURE

The rate of isotope loss from the body was calculated from equation 2.

$$k_{\text{O}} \text{ or } k_{\text{H}} = (\ln \delta_{\text{pre}} - \ln \delta_{\text{post}})/t \quad (2)$$

where δ_{pre} and δ_{post} are the differences in isotopic enrichment of the sample and the pre-dosing background for ^{18}O or ^2H on pre- and postflight respectively and k_{O} and k_{H} are the fractional H_2^{18}O and $^2\text{H}_2\text{O}$ turnover rates.

The rate of carbon dioxide production was calculated from equation 3 (Schoeller et al., 86).

$$r\text{CO}_2 = 0.481N(1.01k_{\text{O}} - 1.04k_{\text{H}}) - 0.0258N(k_{\text{O}} - k_{\text{H}}) \quad (3)$$

where $r\text{CO}_2$ is the rate of CO_2 production in mol/day and N is the total body water in moles.

The Weir equation (4) was used to convert the rate of CO_2 production into energy expenditure values.

$$\text{EE} = 3.941\text{VO}_2 + 1.106\text{VCO}_2 - 2.17\text{U} \quad (4)$$

$$r\text{CO}_2 = \text{VCO}_2 / 22.4 \quad (5)$$

$$\text{RQ} = \text{VCO}_2 / \text{VO}_2 \quad (6)$$

RESULTS

Two pair calculations were used for calculating out the data. The values from individual animals are given in Table 3. Table 4 shows summary results by group.

The mean energy expenditure of 59.9 ± 4.6 found during flight for the three flight monkeys represents about a 30% decrease from the 88.8 ± 5.9 ($n=7$, includes both values for #892) level of the ground controls ($p < 0.05$).

DISCUSSION

Although the data base is small, the values are reasonable and the reproducibility of the energy expenditure values where duplicate determinations were done is good. This is particularly true of the flight monkeys on this mission. It is reassuring that the flight values from this flight (Cosmos 2229) match the flight value from the previous Cosmos 2044 mission which was primarily an experimental mission designed to see if the doubly labeled water method could be gotten to work under the limitations of space flight. Even though only one suitable postflight urine was collected on Cosmos 2044 for monkey 2483, the inflight energy expenditure value is similar to that of 906 and 151.

The 4 day ground control energy expenditures show about the range of variation expected. Although data are only available for one 15+ day ground control monkey (892), the value agrees well with the 4 day value on the same animal and with the mean value for the other 4 day determinations. Thus one can have reasonable confidence in the data base and in drawing conclusions from it even though the actual number of animals is small.

The difference in energy expenditure between the 3 flight animals and the ground controls is statistically significant ($p < 0.05$, t-test). Energy expenditure was reduced by 33% inflight. It follows therefore that space flight does not result in an increase in energy expenditure. Where differences are suspected as from the Skylab missions, the previously postulated increase most likely reflects a higher degree of activity and work load. However, the decrease in energy expenditure is surprisingly large.

These conclusions are necessarily tentative because of the small number of subjects. To validate the results and the conclusions drawn therefrom, it would be necessary to increase the number of ~17 day ground controls by 4 to 5 and the number of flight animals by 2 to 3.

ACKNOWLEDGMENTS

We would like to thank our Soviet colleagues for their involvement and support of this project, especially Drs. M. Dotsenko, A. Korolkov, A. Truzennikov, I. Kozlovskaya, E.A. Ilyin, V. Magedov, and B. Perepech, at the Institute of Biomedical Problems. In the U.S., the role that Jim Connolly played as Project Manager was key to the successful U.S. participation in the flight. We also wish to acknowledge the participation of the many other individuals at Ames Research Center, especially: Mike Skidmore, Rod Ballard, Denise Helwig, Samantha Edmonds and Dick Grindeland, support personnel Richard Mains and Edward Luzzi. We also wish to thank the support staff at the California Primate Research Center at UC Davis and at University of Medicine and Dentistry of New Jersey, particularly Maria Leskiw, who were essential for the development of procedures and supporting analysis for this experiment. This work was supported by NASA Grant NAG2-587.

REFERENCES

1. Gazenko, O.G., A.M. Genin, E.A. Ilyina-Kakueva, A.S. Ushakov, and A.D. Egorov. Physiological Mechanisms of Adaptation to Weightlessness. *Biol. Bull. Acad. Sci., USSR*, 7: 1-12, 1980.
2. Grigoriev, A.I., and A.D. Egorov. General Mechanisms of the Effect of Weightlessness on the Human Body. *Advances in Space Biology and Medicine*. Ed. S.J. Bonting. 2:1-43, 1992.
3. Huss-Ashmore, R., J.L. Goodman, T.E. Sibiya, and T.P. Stein. Energy Expenditure of Young Swazi Women as Measured by the Doubly Labeled Water Method. *Europ. J. Clin. Nutr.* 43:737-748, 1989.
4. Jones, P.J., A.L. Winthrop, D.A. Schoeller et al. Evaluation of the Doubly Labeled Water Method for Measuring Energy Expenditure During Changing Nutrition. *Am. J. Clin. Nutr.* 47: 799-804, 1988.
5. Lane, H.W. Energy Requirements for Spaceflight. *J. Nutr.* 122:13-18, 1992.
6. Leonard, J.I. Quantitation of Tissue Loss During Prolonged Spaceflight. *Am. J. Clin. Nutr.* 38: 667-679, 1983.
7. Lifson, N., and R. McClintock. Theory of Use of Turnover Rates of Body Water for Measuring Energy and Material Balance. *J. Theor. Biol.* 12:46-74, 1966.
8. Rambaut, P.C., C.S. Leach, and J.I. Leonard. Observations in Energy Balance in Man During Spaceflight. *Am. J. Physiol.* 233:R208-R212, 1977.
9. Schoeller, D.A., W. Dietz, E. van Santen, and P.D. Klein. Validation of Saliva Sampling for Total Body Water Determination by H₂¹⁸O dilution. *Am. J. of Clin. Nutr.* 35:591-594, 1982.
10. Schoeller, D.A. and E. van Santen. Measurement of Energy Expenditure in Humans by Doubly Labeled Water Method. *J. Appl. Physiol.* 63:955-959, 1982.
11. Schoeller, D.A., E. Ravussin, Y. Schutz, K.J. Acheson, P. Baertschi, and E. Jequier. Energy Expenditure by Doubly Labeled Water: Validation in Humans and Proposed Calculation. *Am. J. Physiol.* 250:R823-R830, 1986.
12. Stein, T.P., R.W. Hoyt, M. O'Toole, R.G. Settle, and W.D.B. Hiller. *Am. J. Clin. Nutr.* 45: 534-539, 1987.

TABLE 1
 Protocol and Sample Collection Schedule
 (Monkeys 151, 916 and 892)

Sample	Purpose	Time (hr)
1	preflight baseline	<0
2	3 hrs post DLW for TBW	3
3	6 hrs post DLW for TBW	6
4	9 hrs post DLW for TBW	9
5	12 hrs post DLW for TBW	12
6	pretest for DLW calculation	15
7	pretest for DLW calculation	15
8	posttest for DLW calculation	3 days
9	posttest for DLW calculation (dup.)	3 days
10	preflight for DLW calculation	4 days
11	preflight for DLW calculation (dup.)	4 days
12	postflight for DLW calculation	~17 days
13	postflight for DLW calculation (dup.)	~17 days

TABLE 2
 Protocol and Sample Collection Schedule
 (Monkeys 75 and 907)

<u>Sample</u>	<u>Purpose</u>	<u>Time (hr)</u>
1	pretest baseline	<0
2	3 hrs post DLW for TBW	3
3	6 hrs post DLW for TBW	6
4	9 hrs post DLW for TBW	9
5	12 hrs post DLW for TBW	12
6	pretest for DLW calculation	15
7	pretest for DLW calculation	15
8	posttest for DLW calculation	~3 days
9	posttest for DLW calculation	~3 days

TABLE 3

Calculated Energy Expenditure Values by the 'Two Pair' Method:
Individual Animal Data

Monkey #	Group	Urines	EE	Mean EE
803	Control 4 days	4 - 11 6 - 12	75.4 106.3	90.9
75	Control 4 days	6 - 11 6 - 12	88.3 62.3	75.3
907	Control 4 days	1 - 11 5 - 12	96.5 57.8	77.2
892	Control 4 days	3 - 10	83.6	83.6
892	Flight Control (~15d)	12 - 23 13 - 24	61.3 93.8	77.6
151	Preflight 4 days	6 - 10 7 - 11	97.3 100.1	98.7
151	Flight ~17 days	12 - 14 13 - 15	56.0 55.0	55.5
906	Preflight 4 days	6 - 10 7 - 11	126.0 111.1	118.6
906	Flight ~17 days	12 - 14 13 - 15	69.4 41.2	55.3
2483 (2044)	Flight	B'5 - B'7	69.3	69.3

The numbers in the Urines column are the sample numbers of the urine specimens used for calculating the Energy Expenditures and Mean Energy Expenditures (EE) expressed as kcal/kg/day.

TABLE 4

Summary of Energy Expenditure Values: Group Data

	<u>Control (4 day)</u>	<u>Control (~17 day)</u>	<u>Flight (~17 day)</u>
	98.7 (#151)	77.6 (#892)	55.3 (#151)
	118.6 (#906)		55.3 (#906)
	77.2 (#907)		69.1 (B')
	83.6 (#892)		
	90.9 (#803)		
	75.3 (#75)		
Mean	90.7	77.6	59.9
SEM	6.6		4.6

Values are Mean Energy Expenditure expressed as kcal/kg/day.
Corresponding monkey identification numbers are in parentheses.

EXPERIMENT K-8-07

COSMOS 2229 RHESUS MONKEY IMMUNOLOGY STUDY

Principal Investigator:

Gerald Sonnenfeld
University of Louisville Schools of Medicine and Dentistry
Louisville, KY

Co-Investigators:

Stephanie Davis
University of Louisville Schools of Medicine and Dentistry
Louisville, KY

Gerald R. Taylor
NASA Johnson Space Center
Houston, TX

Adrian D. Mandel
NASA Ames Research Center
Moffett Field, CA

Andrei Lesnyak
Institute of Biomedical Problems
Moscow, Russia

Boris B. Fuchs
Institute of Human Morphology
Moscow, Russia

COSMOS 2229 RHESUS MONKEY IMMUNOLOGY STUDY

Gerald Sonnenfeld, Stephanie Davis, Gerald R. Taylor, Adrian D. Mandel, Andrei Lesnyak,
Boris B. Fuchs

SUMMARY

The purpose of the Cosmos 2229 11 and 1/2 day mission was to begin experiments to determine the suitability of the rhesus monkey as a surrogate for humans in space research. In this study, experiments examining the effects of space flight on immunological responses of rhesus monkeys were performed to gain insight into the effect of space flight on resistance to infection. Experiments were performed on tissue samples taken from the monkeys before and immediately after flight. Additional samples were obtained approximately one month after flight for a postflight restraint study. Two types of experiments were carried out throughout this study. The first experiment examined the responsiveness of rhesus bone marrow cells to recombinant human granulocyte/macrophage colony stimulating factor (GM-CSF). In the second experiment, monkey peripheral blood and bone marrow cells were stained using a variety of antibodies directed against cell surface antigenic markers. Human reagents that cross-reacted with monkey tissue were utilized for the bulk of the studies. Results from both studies indicated that there were changes in immunological function attributable to space flight. Bone marrow cells from flight monkeys showed a significant decrease in their response to CSF-GM when compared to the response of bone marrow cells from non-flight control monkeys. Antibody staining of both blood and bone marrow cells from flight monkeys showed alterations in leukocyte subset distributions when compared to antibody staining patterns of non-flight controls. These results suggest that the rhesus monkey will be a useful surrogate for humans in future studies which examine the effect of space flight on immune response, particularly when conditions do not readily permit human study.

INTRODUCTION

Data from studies reported over the past several years have indicated that various alterations in immunological parameters occur after space flight (Barone and Caren, 1984; Cogoli, 1981 and 1984; Durnova et al., 1978; Gould et al., 1987a; Konstantinova et al., 1985; Lesnyak and Tashputalov, 1981; Mandel and Balish, 1977; Sonnenfeld et al., 1990; Talas et al., 1983 and 1984; Taylor et al., 1983 and 1984). Immunological changes similar to those observed after space flight have been reported in various ground base studies, including antiorthostatic suspension of rats (Caren et al., 1980; Gould and Sonnenfeld, 1987b; Rose et al., 1984; Sonnenfeld, et al., 1982). These changes involve alterations in lymphoid organ size (Durnova et al., 1976), alterations in the production of interferons (Talas et al., 1983 and 1984; Gould et al., 1987a), and alterations in lymphocyte activation (Cogoli et al., 1981 and 1984).

The 11.5 day Cosmos 2229 space flight attempted to further explore space flight effects on immune response. Immunological parameters similar to those parameters affected in rats after similar flights, including Cosmos 2044, were chosen for study in Cosmos 2229. Results from the Cosmos 2044 study had shown that space flight inhibited the ability of GM-CSF to stimulate colony formation in rat bone marrow cells, and altered various leukocyte subset population distributions, such as the CD4+ and CD8+ cell subsets (Sonnenfeld et al., 1992). These studies and recent ground-based studies establishing immunological techniques for handling rhesus monkey cells (Sonnenfeld et al., 1993) made possible testing of the hypothesis that the rhesus monkey could be used as a surrogate for humans in future studies. This could be of great advantage, since rhesus monkey and human immune systems have been shown to be closely related. The purpose of the current study was to further validate use of the rhesus monkey as a model for humans in future space flight testing.

The areas of immunological importance examined in the Cosmos 2229 flight were represented by two sets of studies. The first set of studies determined the effect of space flight on the ability of bone marrow cells to respond to granulocyte/monocyte colony stimulating factor (GM-CSF). GM-CSF is an important regulator in the differentiation of bone marrow cells of both monocyte/macrophage and granulocyte lineages and any change in the ability of these cells to respond to GM-CSF can result in altered immune function (Waheed and Shadduck, 1979).

A second set of studies determined space flight effects on the expression of cell surface markers on both spleen and bone marrow cells. Immune cell markers included in this study were those for T-cell, B-cell, natural killer cell, and interleukin-2 populations. Variations from a normal cell population percentage, as represented by these markers, can be correlated with alterations in immunological function (Jackson and Warner, 1986). Cells were stained with fluorescein-labelled antibodies directed against the appropriate antigens, and then analyzed using a flow cytometer.

MATERIALS AND METHODS

Two juvenile male rhesus monkeys (*Macacca mulatta*) were born at the Soviet Primate Center in Sukhumi, Georgia and sustained throughout the duration of studies reported in this paper at the Institute of Biomedical Problems in Moscow, Russia. The monkeys were flown under chair restraint for 11.5 days during the Cosmos 2229 (Bion 10) flight from December 19, 1992 to January 10, 1993. Details concerning flight conditions, condition of monkeys pre- and postflight, as well as maintenance procedures for all animals used in this study, are described in the Mission Description section of this technical memorandum.

Tissue sampling from the monkeys for preflight studies occurred approximately 1.5 months prior to flight. Tissue sampling was also done at various time periods after flight, from 1 to 12 days postflight recovery. Two types of tissue samples were obtained: peripheral blood and bone marrow. Additional samples were obtained from monkeys for a postflight study examining the possible role of restraint in those effects observed after space flight. The restraint study was carried out 40 days post-recovery for the same duration of time as the flight. Other controls involved the testing of bone marrow and blood obtained from flight-pool monkeys as well as the testing of bone marrow and blood samples from two standard vivarium control monkeys (#s 85 and 3224) at regular intervals throughout each experimental period. Results from the testing of standard vivarium control monkeys indicated when changes in test values were due to a failure of experimental procedure. The sampling schedule is given in the results section of this report.

Bone marrow samples were obtained through needle biopsy of the posterior of the head of the humerus (left or right) of monkeys under Ketamine/Xylazine anesthesia. Each bone marrow sample was transferred to a 15 ml polypropylene centrifuge tube containing McCoy's medium (Gibco BRL, Grand Island, NY) supplemented with antibiotics, sodium bicarbonate, hepes buffer, L-glutamine, and fungizone. Bone marrow cells were centrifuged and resuspended in supplemented McCoy's medium with 10% FBS (as a washing step). Cell counts were obtained on a hemocytometer, using trypan blue dye exclusion for determination of viability. One $\times 10^5$ bone marrow cells/mL were resuspended in a 2% methylcellulose solution prepared in supplemented McCoy's media containing 30% FBS (Shadduck and Nagabhushnam, 1971). Medium for experimental group cultures contained a concentration of 40 ng/ml recombinant human GM-CSF (a gift of Dr. Steven Gillis, Immunex Research and Development Corp, Seattle, WA). The GM-CSF was from lot 620-028-5, and had a specific activity of at least 5×10^7 units/mg protein. For each animal tested, five 35 mm tissue culture dishes, each containing 1 ml of the bone marrow cell suspension, were set up for control (- CSF) and for experimental (+ CSF) groups. Dishes containing suspended cells were incubated in a 37 °C incubator with 5% CO₂ (Shadduck and Nagabhushnam, 1971). After 7 days of incubation, 10 microscope fields from each petri dish were evaluated for the number of colonies formed, a colony represented by aggregates of 50 or more cells (Sonnenfeld, et al., 1990). The GM-CSF data was analyzed using a pooled estimate of variance and linear contrast analysis.

The following procedure was implemented to evaluate cell surface antigenic markers on bone marrow cells (Jackson and Warner, 1986). One x 10⁶ bone marrow cells, suspended in supplemented McCoy's media with 10% FBS, was allocated to each microcentrifuge tube. Cell suspensions were centrifuged for 1.5 min at 1,000 x g, supernatant removed, and 5 µl of the appropriate antibody added to each microcentrifuge tube. Background values were taken into account by including a microcentrifuge tube containing cells, but no antibody, for each animal tested. Cells and antibody (or no antibody) were allowed to incubate at 4 °C for 25 min. Antibodies used in this study were obtained from Becton-Dickinson Immunocytometry Systems, San Jose, CA, except as noted below:

1. Leu 2a (CD-8, cytotoxic T lymphocyte)
2. Leu 3a (CD-4, helper T lymphocyte)
3. Leu 4 (CD-3 signal transducer for T lymphocyte)
4. Leu 11 a (CD-16, Natural killer cell/monocyte)
5. Anti-human IgM (B cell - purchased from Sigma Chemical Co., St. Louis, MO)
6. Anti-monkey IgG (B cell - purchased from Organon-Teknika Corp. W. Chester, PA)
7. Anti-monkey IgG F(ab)' (B cell - purchased from Organon-Teknika Corp.)
8. Goat anti-rabbit IgG (Purchased from Accurate Chemical Co., Westbury, NY)
9. No antibody added.

After the 25 minute incubation, red blood cells were lysed for 6 minutes at room temperature with one ml of lysing solution/microcentrifuge tube (8.26 g ammonium chloride, 1.00 g potassium bicarbonate, 37 mg of tetrasodium EDTA brought to 1 L with distilled water, pH 7.4). Cell suspensions were then centrifuged for 1.5 min at 1,000 x g, and resuspended in FTA buffer (BBL Microbiology Systems, Cockeysville, MD), pH 7.4, containing 0.1% sodium azide. Cell suspensions were again centrifuged for 1.5 min at 1,000 x g, supernatant removed, and cells fixed by resuspension in 0.5 ml of 1% paraformaldehyde prepared in FTA buffer. The staining procedure for peripheral blood was exactly the same as for bone marrow except that 20 µl of heparin-treated blood was placed into each microcentrifuge tube and then stained.

Fixed cells from blood and bone marrow staining were maintained at 4 °C, flown to the United States at this temperature, and later analyzed at the University of Louisville to determine the presence of antigenic markers using a Profile II flow cytometer (Coulter Electronics, Hialeah, FL). Lymphocytic and myelogenous regions were gated on three-part differentials using forward vs. side scatter plots.

Statistical analysis of bone marrow cell response to GM-CSF was accomplished by using a pooled estimate of variance in the hypothesis testing of differences between two group means. Flow cytometry results from antibody stained peripheral blood and bone marrow cells were analyzed using linear contrast and factorial anova. Alpha was set *a priori* at $p \leq 0.05$

RESULTS

Effect of Space Flight on the Response of Bone Marrow Cells to GM-CSF

Bone marrow cells from some monkeys within the pool of flight animals showed a lower than normal response to human GM-CSF prior to flight (Table 1). Bone marrow from monkeys exposed to space flight showed decreases in the ability to form colonies in response to GM-CSF when compared bone marrow cells from standard vivarium control monkeys (Table 2). As time progressed, recovery towards the normal GM-CSF developed, but suppression of colony formation occurred again at 12 days post landing (Table 2). There was also significant variability in the response of bone marrow from standard vivarium control monkeys to GM-CSF across the pre- and postflight testing periods (figures 1, 2, and 3). Except in the postflight restraint study (Tables 1, 2,

and 3), there was always an increase in colony formation if GM-CSF was present in the cultures when compared to control cultures (- CSF) from the same animal.

Effect of Space Flight on the Percentage of Cells Expressing Cell Surface Antigenic Markers

Results from antibody staining of peripheral blood and bone marrow were very similar in the pattern of response. Data from anti-monkey IgG only rather than data from both this antibody and the other positive control antibody used in the staining study, anti-monkey IgG F(ab')₂, is included since the data were very similar. All given cell population percentages have had background values subtracted through gating against unstained cell populations. Prior to flight, several of the flight pool animals showed significant differences in stained cell population percentages for the different surface antigens (Tables 4-10). For all leukocyte surface markers tested, a decreased expression of the surface antigens occurred immediately after flight (recovery + 1 day, and recovery + 2 days), followed by a shift toward more normal values at recovery + 3 days. A return to suppression occurred at recovery + 12 days (Tables 11-17). There was also variability in the flow cytometry data from standard vivarium control monkeys within and across pre- and postflight testing periods (Tables 11-17).

Effect of Postflight Restraint on the Percentage of Cells Expressing Cell Surface Antigenic Markers:

Flow cytometry data from the antibody staining of both peripheral blood leukocyte and bone marrow have been included in the tables section because of differences in the response of these two cell types. Restraint of the flight animals resulted in decreases in the percentage of peripheral blood leukocytes carrying the CD-8 marker and in the percentage of bone marrow cells carrying the HLA-DR marker (Tables 18-31). These were the only changes observed in the response of flight animals to restraint, but restrained controls showed other alterations (Tables 18-31).

DISCUSSION

Results of the current study suggest that space flight affects immunological parameters of the rhesus monkey. This study suggests that the bone marrow cell response to colony stimulating factor, as well as leukocyte subset cell population distributions of both peripheral blood and bone marrow leukocytes, were altered after space flight. It is worth noting that most immunological parameters examined in Cosmos 2229 were suppressed for some period of time after flight. Immunological results from Cosmos 2229 differed from previous Cosmos flights involving rats in that the number of bone marrow colonies formed in response to colony stimulating factor was depressed, but leukocyte population percentages found from antibody staining showed both increases and decreases after flight (Sonnenfeld et al., 1992). A number of possible explanations can be given to account for comparative discrepancies between the results of Cosmos 2229 and previous flights. Among these explanations are species difference and differences in flight conditions which, regardless of species difference, may have had some immunological impact. Further experimentation is required to answer these questions.

All immune parameters tested in the study of flight monkeys appeared to return towards a more normal level by 3 days post-landing; however, by 12 days post-landing, these responses were again suppressed. This second drop occurring after recovery could have been due to stress on the monkeys due to increases in scientific testing and handling of the animals. There were differences in the level, but not the pattern, of immune response observed in each of the two flight monkeys. These differences may be explained by the dehydration and reduced food intake experienced by one of the flight monkeys both during and immediately after flight.

There were experimental difficulties observed in both pre- and post-flight experiments. First, there were unusual responses of bone marrow to GM-CSF and unusual leukocyte phenotyping in some flight pool animals monkeys prior to flight support preflight levels of immunosuppression

(Sonnenfeld et al., 1993). Explanations for the unusual preflight immunological responses of the flight pool animals could include the nutritional status of these monkeys, or immunosuppression caused by stresses from increased handling. Additionally, prenatal conditions and nurturing of the monkeys could have had important influences on pre- and postflight results. Second, there were differences across testing periods in the response of standard vivarium control monkey bone marrow cells to GM-CSF as well as differences in the results of cell population staining percentage. This variation from testing time to testing time has not been observed in previous studies (Sonnenfeld et al., 1993). Results from standard vivarium control monkey samples were included as baseline values to insure that those changes observed after flight were directly due to space flight and not to possible problems with experimental procedure. Despite the changes observed in these vivarium control values across testing times, when differences between results from standard vivarium control and flight animals occurred, they were of similar proportions. This allowed for interpretation of the flight data, and reinforced the need for this type of standard vivarium control in future flight experiments.

After the flight, both flight animals were placed in flight chairs in an attempt to determine the effect of restraint on immunological parameters measured in this study. Data from the study of the response of bone marrow from restrained flight animals to GM-CSF were uninterpretable because bone marrow taken from standard vivarium control monkeys at corresponding time periods in the restraint study showed no response to GM-CSF. However, it appeared that restraint of the flight animals resulted in only some of the immunological changes in leukocyte phenotypes that were altered by space flight. Some of the restrained animals had changes in immune parameters that were different from those observed after space flight. Therefore, restraint probably played some small role in those immunological changes observed after space flight, but, certainly, was not responsible for the majority of the changes which occurred after flight.

SUMMARY AND CONCLUSIONS

The current study indicates that exposure of rhesus monkeys to space flight resulted in inhibition of the response of bone marrow cells to GM-CSF and depression of the percentage of peripheral blood and bone marrow leukocyte antibody markers. B cells, bearing surface immunoglobulin, appeared to be less affected than were T cells. As time progressed following landing, the flight monkeys appeared to recover their immune responses; however, postflight testing possibly contributed to a second drop in immunological response. Restraint appeared to play some role in the effect of space flight on immune response, but restraint alone was not responsible for all of the immunological changes observed after flight.

Despite experimental difficulties, immunological results from the Cosmos 2229 space flight provide interesting new data suggesting that space flight indeed affects some immune responses of rhesus monkeys. These results indicate there may be an effect of species difference when comparing the immunological impact of space flight on monkeys and rats, as well as possible effects of stress and microgravity. The importance of these and other factors having possible immunological implications should be determined and taken into consideration for the design of future studies involving space flight. Further experimentation is required to establish the degree to which these and other factors are involved in changes resulting from space flight, mechanisms for these changes, and possible measures which can be used to abrogate or mediate such influences.

ACKNOWLEDGMENTS

The authors wish to thank Drs. I. Kozlovskaya and V. Korolkov as well as the entire Russian Cosmos team for their excellent support throughout these studies. Without their efforts, this paper would not be possible. We would also like to thank Mr. James Connolly, Ms. Denise Helwig, Ms. Samantha Edmonds, the late Dr. Rodney W. Ballard, and the NASA Ames Research Center Cosmos Support Staff for their constant support and invaluable assistance. This work was supported in part by NASA grant number NAG2-707.

REFERENCES

1. Barone, R.B., and L.D. Caren. The Immune System: Effects of Hypergravity and Hypogravity. *Aviat. Space Environ. Med.*, vol. 55, 1984, pp. 1063-1068.
2. Berry, W.D., J.D. Murphy, G.R. Taylor, and G. Sonnenfeld. The Relationship of Dihydroxyvitamin D to Cellular Immunity in Simulated Weightlessness. In Preparation, 1990.
3. Caren, L.B., A.D. Mandel, and J.A. Nunes. Effect of Simulated Weightlessness on the Immune System in Rats. *Aviat. Space Environ. Med.*, vol. 51, 1980, pp. 251-256.
4. Cogoli, A. Hematological and Immunological Changes During Space Flight. *Acta Astronautica*, vol. 8, 1981, pp. 995-1002.
5. Cogoli, A., P. Tschopp, P. and Fuchs-Bislin. Cell Sensitivity to Gravity. *Science*, vol. 225, 1984, pp. 228-230.
6. Durnova, G.N., A.S. Kaplansky, and V.V. Portugalov. Effect of a 22-day Space Flight on Lymphoid Organs of Rats. *Aviat. Space Environ. Med.*, vol. 47, 1976, pp. 588-591.
7. Gould, C.L., M. Lyte, J.A. Williams, A.D. Mandel, and G. Sonnenfeld. Inhibited Interferon-gamma but Normal Interleukin-3 Production from Rats Flown on the Space Shuttle. *Aviat. Space Environ. Med.*, vol. 58, 1987a, pp. 983-986.
8. Gould, C.L., and G. Sonnenfeld. Enhancement of Viral Pathogenesis in Mice Maintained in an Antiorthostatic Suspension Model - Coordination with Effects on Interferon Production. *J. Biol. Regulators Homeostatic Agents*, vol. 1, 1987b, pp. 33-36.
9. Jackson, A.L., and N.L. Warner. Preparation, Staining and Analysis by Flow Cytometry of Peripheral Blood Leukocytes. In: *Manual of Clinical Laboratory Immunology*, 3rd ed., N.K. Rose, H. Friedman, and J.L. Fahey, eds., American Society for Microbiology, Washington, D.C., 1986, pp. 226-235.
10. Konstantinova, I.V., E.N. Antropova, M.P. Rykova, O.A. Guseva, A.T. Lesnyak, I.E. Vorotnikova, and E.F. Vasilyeva. Cell-mediated and Humoral Immunity in Cosmonauts Exposed to Space Flight Factors. *Vestnik, Akad. Med. Nauk CCCP*, No. 8, 1985, pp. 51-58.
11. Konstantinova, I.V., and B.B. Fuchs. The Immune System Under Extreme Condition: Space Immunology. Nauka, Moscow, 1988.
12. Lesnyak, A.T., and R.Y.U. Tashputalov. Effects of Space Flight on Leukocyte Transformation in Cosmonauts' Peripheral Blood. *Komich. Biol.*, vol. 1, 1981, pp. 32-34.
13. Mandel, A.D., E. and Balish. Effect of Space Flight on Cell-mediated Immunity. *Aviat. Space Environ. Med.*, vol. 48, 1977, 1051-1057.
14. Rose, A., J.M. Steffen, X. J. Musacchia, A.D. Mandel, and G. Sonnenfeld, G. Effect of Antiortho-static Suspension on Interferon-alpha/beta Production by the Mouse. *Proc. Soc. Exp. Biol. Med.*, vol. 177, 1984, pp. 253-256.
15. Shadduck, R.K., and N.G. Nagabhushanam. Granulocyte Colony Stimulating Factor I. Response to Acute Granulocytopenia. *Blood*, vol. 38, 1971, pp. 14-22.

16. Sonnenfeld, G., E.R. Morey, J.A. Williams, and A.D. Mandel. Effect of a Simulated Weightlessness Model on the Production of Rat Interferon. *J. Interferon Res.*, vol. 2., 1982, pp. 467-470.
17. Sonnenfeld, G., A.D. Mandel, I.V. Konstantinova, G.R. Taylor, W.D. Berry, S.R. Wellhausen, A.T. Lesnyak, and B.B. Fuchs. Effects of Space Flight on Levels and Activity of Immune Cells. *Aviat. Space Environ. Med.*, vol. 61, 1990, 648-653.
18. Sonnenfeld, G., L. Schaffar, D.A. Schmitt, D.A. Koebel, and B.A. Smith. Interferon Production by and Leukocyte Phenotyping of Rhesus Monkey Lymph Node and Peripheral Blood Cells. *J. Interferon Res.*, vol. 13, 1993, 259-265.
19. Sonnenfeld, G., A.D. Mandel, I.V. Konstantinova, W.D. Berry, G.R. Taylor, A.T. Lesnyak, B.B. Fuchs, and A.L. Rakhmievich. Spaceflight Alters Immune Cell Function and Distribution. *J. Appl. Physiol.*, vol. 73, 1992, 191S-195S.
20. Talas, M., L. Baktai, I. Stoger, K. Nagy, L. Hiros, I. Konstantinova, M. Rykova, I. Mozgovaya, O. Guseva, and V. Kozharinov. Results of Space Experiment Program "Interferon" I. Production of Interferon In-vitro by Human Leukocytes Aboard Space Laboratory Soyuz-6 ("Interferon-I") and Influence of Space Flight on Lymphocyte Function of Cosmonauts ("Interferon-III"). *Acta Microbiol. Hungarica*, vol. 30, 1983, pp. 53-61.
21. Talas, M., L. Baktai, I. Stoger, K. Nagy, L. Hiros, I. Konstantinova, M. Rykova, L. Mozgovaya, O. Guseva, and V. Kozharinov. Results of the Space Experiment Program "Interferon". *Acta Astronautica*, vol. 11, 1984, pp. 379-386.
22. Taylor, G.R., and J.R. Dardano. Human Cellular Immune Responsiveness Following Space Flight. *Aviat. Space Environ. Med.*, vol. 54 suppl. 1, 1983, pp. 555-559.
23. Taylor, G.R., L.S. Neal, and J.R. Dardano. Immunological Analysis of U.S. Space Shuttle Crewmembers. *Aviat. Space Environ. Med.*, vol. 57, 1986, pp. 213-217.
24. Waheed, A., and R.K. Shadduck. Purification and Properties of L Cell Derived Colony stimulating factor. *J. Lab. Clin. Med.*, vol. 94, 1979, pp. 180-194.

TABLE 1

Preflight Response of Bone Marrow Cells to GM-CSF

Animal #	Condition During Flight	# Colonies - CSF	# Colonies + CSF
85	Standard Vivarium Control	0	8
3224		0	6
151	Flight	5	25
906		3	2
476	Flight Pool Control	0	0
775		0	2
856		2	14
907		0	43

Statistical considerations:

Significance, $p < 0.05$, determined using a pooled estimate of variance for a two-tailed t-test.

Standard vivarium control monkeys (#s 85 and 3224)* vs standard vivarium control monkeys (#s 85 and 3224)**: $9.902 \times 10^{-3} < 0.05$.

Flight monkey (#151)* vs flight monkey (#151)**: $14.142 < 4.303$

Flight pool control monkey (# 856)* vs flight pool control monkey (# 856)**: $8.49 > 4.303$

Flight pool control monkey (#907)* vs flight pool control monkey (#907)**: $330.41 > 4.303$

*: - GM-CSF

** : + GM-CSF

TABLE 2

Postflight Response of Bone Marrow Cells to GM-CSF

Animal #	Condition During Flight	# Colonies - CSF	# Colonies + CSF
85	Standard Vivarium Control at R + 3	15	37
3224		19	41
151	Flight at R + 3	22	16
906		17	17
775	Flight Pool Control at R + 3	11	19
476	Flight Pool Control at R + 5	7	31
775		19	25
838	Flight Pool Control at R +10	11	14
1324		10	11
85	Standard Vivarium Control at R + 12	11	16
3224		5	13
151	Flight at R + 12	8	22
906		6	10

Statistical considerations:

Significance, $p < 0.05$, determined using a pooled estimate of variance for a two-tailed t-test.

TABLE 2 - Continued

Standard vivarium control monkeys at R + 3 (#s 85 and 3224)* vs standard vivarium control monkeys at R + 3 (#s 85 and 3224)**: $8.07 \times 10^{-3} < 0.05$.

Standard vivarium control monkeys at R + 3 (#s 85 and 3224)* vs standard vivarium control monkeys at R + 12 (#s 85 and 3224)**: $5.13 \times 10^{-3} < 0.05$.

Standard vivarium control monkeys at R + 3 (#s 85 and 3224)** vs flight pool control monkeys at R + 10 (#s 85 and 1324)**: $4.39 \times 10^{-3} < 0.05$.

Standard vivarium control monkeys at R + 3 (#s 85 and 3224)** vs flight pool control monkeys at R + 5 (#s 775 and 476)**: $0.0464 < 0.05$.

Standard vivarium control monkeys at R + 12 (#s 85 and 3224)** vs flight pool control monkeys at R + 5 (#s 775 and 476)**: $0.0283 < 0.05$.

Standard vivarium control monkeys at R + 3 (#s 85 and 3224)* vs flight pool control monkeys at R + 10 (#s 85 and 1324)*: $0.0438 < 0.05$.

Standard vivarium control monkeys at R + 3 (#s 85 and 3224)* vs flight monkeys at R + 12 (#s 151 and 906)*: $0.0233 < 0.05$.

Standard vivarium control monkeys at R + 3 (#s 85 and 3224)** vs flight monkeys at R + 12 (#s 151 and 906)**: $0.034 < 0.05$.

Standard vivarium control monkeys at R + 12 (#s 85 and 3224)* vs flight monkeys at R + 3 (#s 151 and 906)*: $0.0493 < 0.05$.

Standard vivarium control monkeys at R + 3 (#s 85 and 3224)** vs flight monkeys at R + 3 (#s 151 and 906)**: $4.15 \times 10^{-3} < 0.05$.

Flight monkeys at R + 12 (#s 151 and 906)* vs flight monkeys at R + 3 (#s 151 and 906)*: $0.0217 < 0.05$.

Flight pool control monkeys at R + 5 (#s 476 and 775)** vs flight pool control monkeys at R + 10 (#s 476 and 775)**: $0.0219 < 0.05$.

Flight pool control monkeys at R + 10 (#s 838 and 1324)* vs flight monkeys at R + 12 (#s 151 and 906)*: $0.0443 < 0.05$.

TABLE 2 - Continued

Flight pool control monkeys at R + 10 (#s 838 and 1324)* vs flight monkeys at R + 3 (#s 151 and 906)*: $0.0359 < 0.05$.

Flight pool control monkeys at R + 5 (#s 476 and 775)** vs flight monkeys at R + 3 (#s 151 and 906)**: $0.0317 < 0.05$.

*: - GM-CSF

** : + GM-CSF

TABLE 3

Effect of Postflight Restraint on the Response of Bone Marrow Cells to GM-CSF

Animal #	Condition	# Colonies - CSF	# Colonies + CSF
85	Standard Vivarium Control	5	7
3224		4	5
151	Flight + Restraint	2	2
906		4	8
803	Flight Pool Control + Restraint	8	5
907		8	10
588	Vivarium Control	12	24
1417		6	7

*Significance, $p < 0.05$, compared to standard vivarium control group (- GM-CSF)

**Significance, $p < 0.05$, compared to standard vivarium control group (+ GM-CSF)

There was no significance, $p < 0.05$, within groups comparing - GM-CSF to + GM-CSF.

TABLE 4

Preflight Staining of Peripheral Blood with Anti-HLA-DR

Animal #	Condition During Flight	% Lymphoid Cells Stained
85	Standard Vivarium Control	28.1
3224		14.3
151	Flight	9.6
906		0
476	Flight Control Pool	7.2
775		4.7
803		0
856		0
858		0.1
892		0
907		2.5
1404		0.2

*Significance, $p < 0.05$, between standard vivarium control monkeys (#s 85 and 3224) and individual flight monkeys

TABLE 5

Preflight Staining of Peripheral Blood with Leu-2a (CD 8)

Animal #	Condition During Flight	% Lymphoid Cells Stained
85	Standard Vivarium Control	3.2
3224		8.8
151	Flight	14.3
906		0
476	Flight Control Pool	2.3
775		1.0
803		0
856		0.6
858		0
892		0
907		0.1
1404		0.3

*Significance, $p < 0.05$, between standard vivarium control monkeys (#s 85 and 3224) and individual flight monkeys

TABLE 6

Preflight Staining of Peripheral Blood with Leu-3a (CD 4)

Animal #	Condition During Flight	% Lymphoid Cells Stained
85	Standard Vivarium Control	1.4
3224		0.8
151	Flight	5.8
906		0
476	Flight Control Pool	0.6
775		0.8
803		0
856		1.0
858		1.8
892		0
907		0.2
1404		0

*Significance, $p < 0.05$, between standard vivarium control monkeys (#s 85 and 3224) and individual flight monkeys

TABLE 7

Preflight Staining of Peripheral Blood with Leu-4 (CD 3)

Animal #	Condition During Flight	% Lymphoid Cells Stained
85	Standard Vivarium Control	0.6
3224		5.9
151	Flight	3.6
906		0
476	Flight Control Pool	1.2
775		0
803		0
856		3.1
858		1.6
892		0
907		0
1404		0.5

*Significance, $p < 0.05$, between standard vivarium control monkeys (#s 85 and 3224) and individual flight monkeys

TABLE 8

Preflight Staining of Peripheral Blood with Leu-11a (CD 16)

Animal #	Condition During Flight	% Lymphoid Cells Stained
85	Standard Vivarium Control	1.5
3224		3.6
151	Flight	9.2
906		0
476	Flight Control Pool	1.8
775		1.4
803		0
856		0.4
858		0.4
892		1.1
907		0.4
1404		2.0

*Significance, $p < 0.05$, between standard vivarium control monkeys (#s 85 and 3224) and individual flight monkeys

TABLE 9

Preflight Staining of Peripheral Blood with Anti-Human IgM

Animal #	Condition During Flight	% Lymphoid Cells Stained
85	Standard Vivarium Control	50.1
3224		40.2
151	Flight	32.1
906		39.9
476	Flight Control Pool	56.6
775		64.3
803		56.6
856		38.7
858		81.4
892		51.9
907		63.3
1404		77.2

*Significance, $p < 0.05$, between standard vivarium control monkeys (#s 85 and 3224) and individual flight monkeys

TABLE 10

Preflight Staining of Peripheral Blood with Anti-Monkey IgG

Animal #	Condition During Flight	% Lymphoid Cells Stained
85	Standard Vivarium Control	48.4
3224		69.8
151	Flight	63.5
906		32.4
476	Flight Control Pool	49.4
775		32.0
803		84.4
856		69.1
858		89.9
892		87.9
907		19.3
1404		71.8

*Significance, $p < 0.05$, between standard vivarium control monkeys (#s 85 and 3224) and individual flight monkeys

TABLE 11

Postflight Staining of Peripheral Blood with Anti-HLA-DR

Animal #	Condition During Flight		% Lymphoid Cells Stained
85	Standard Vivarium Control	R + 3	0
85		R + 12	3.1
3224		R + 3	2.0
3224		R + 12	0.2
151	Flight	R + 2*	0
151		R + 3**	20.0
151		R + 12	0.2
906		R + 1	0
906		R + 2*	3.0
906		R + 3**	5.0
906		R + 12	0.2
476		Flight Control Pool	R + 5***
775	R + 5***		11.0
838	R + 10		40.0
1324	R + 10		8.0

*Significance, $p < 0.05$, between standard vivarium control monkeys at R + 3 (#s 85 and 3224) and R + 2 flight monkeys (#s 906 and 151)

**Significance, $p < 0.05$, between standard vivarium control monkeys at R + 3 (#s 85 and 3224) and R + 3 flight monkeys (#s 906 and 151)

***Significance, $p < 0.05$, between standard vivarium control monkeys at R + 3 (#s 85 and 3224) and R + 3 flight monkeys (#s 476 and 775)

TABLE 12

Postflight Staining of Peripheral Blood with Leu-2a (CD 8)

Animal #	Condition During Flight		% Lymphoid Cells Stained
85	Standard Vivarium Control	R + 3	13.7
85		R + 12	4.1
3224		R + 3	0
3224		R + 12	0
151	Flight	R + 2	0
151		R + 3	19.6
151		R + 12	0
906		R + 1	0.3
906		R + 2	1.2
906		R + 3	1.1
906		R + 12	0
476		Flight Control Pool	R + 5
775	R + 5		5.6
838	R + 10		1.1
1324	R + 10		22.3

*Significance, $p < 0.05$, between standard vivarium control monkeys at R + 3 (#s 85 and 3224) and flight monkey groups

**Significance, $p < 0.05$, between standard vivarium control monkeys at R + 12 (#s 85 and 3224) and flight monkey groups

TABLE 13

Postflight Staining of Peripheral Blood with Leu -3a (CD 4)

Animal #	Condition During Flight		% Lymphoid Cells Stained
85	Standard Vivarium Control	R + 3	9.5
85		R + 12	1.3
3224		R + 3	4.1
3224		R + 12	0.2
151	Flight	R + 2	5.2
151		R + 3	15.6
151		R + 12	0
906		R + 1	0.3
906		R + 2	0.8
906		R + 3	4.1
906		R + 12	0
476		Flight Control Pool	R + 5
775	R + 5		2.8
838	R + 10		2.4
1324	R + 10		8.3

*Significance, $p < 0.05$, between standard vivarium control monkeys at R + 3 (#s 85 and 3224) and flight monkey groups

**Significance, $p < 0.05$, between standard vivarium control monkeys at R + 12 (#s 85 and 3224) and flight monkey groups

TABLE 14

Postflight Staining of Peripheral Blood with Leu-4 (CD 3)

Animal #	Condition During Flight		% Lymphoid Cells Stained
85	Standard Vivarium Control	R + 3	11.3
85		R + 12*	1.3
3224		R + 3	0
3224		R + 12*	0.2
151	Flight	R + 2**	0
151		R + 3*	22.7
151		R + 12*	0
906		R + 1*	0
906		R + 2**	2.3
906		R + 3*	10.1
906		R + 12*	0
476		Flight Control Pool	R + 5**
775	R + 5**		0
838	R + 10		5
1324	R + 10		14.6

*Significance, $p < 0.05$, between standard vivarium control monkeys at R + 3 (#s 85 and 3224) and flight monkey groups

**Significance, $p < 0.05$, between standard vivarium control monkeys at R + 12 (#s 85 and 3224) and flight monkey groups

TABLE 15

Postflight Staining of Peripheral Blood with Leu-11a (CD 16)

Animal #	Condition During Flight		% Lymphoid Cells Stained
85	Standard Vivarium Control	R + 3	10.1
85		R + 12	2.3
3224		R + 3	0
3224		R + 12	0.2
151	Flight	R + 2	0
151		R + 3	7.2
151		R + 12	0
906		R + 1	0.8
906		R + 2	4.0
906		R + 3	3.5
906		R + 12	0.8
476		Flight Control Pool	R + 5
775	R + 5		7.0
838	R + 10		0.8
1324	R + 10		12.7

*Significance, $p < 0.05$, between standard vivarium control monkeys at R + 3 (#s 85 and 3224) and flight monkey groups

**Significance, $p < 0.05$, between standard vivarium control monkeys at R + 12 (#s 85 and 3224) and flight monkey groups

TABLE 16

Postflight Staining of Peripheral Blood with Anti-Human IgM

Animal #	Condition During Flight		% Lymphoid Cells Stained
85	Standard Vivarium Control	R + 3	54.4
85		R + 12	33.3
3224		R + 3	47.3
3224		R + 12	14.7
151	Flight	R + 2	26.6
151		R + 3	72.3
151		R + 12	16.5
906		R + 1	4.0
906		R + 2	25.7
906		R + 3	30.0
906		R + 12	13.3
476		Flight Control Pool	R + 5
775	R + 5		49.6
838	R + 10		45.2
1324	R + 10		24.4

*Significance, $p < 0.05$, between standard vivarium control monkeys at R + 3 (#s 85 and 3224) and flight monkey groups

**Significance, $p < 0.05$, between standard vivarium control monkeys at R + 12 (#s 85 and 3224) and flight monkey groups

TABLE 17

Postflight Staining of Peripheral Blood with Anti-Monkey IgG

Animal #	Condition During Flight		% Lymphoid Cells Stained
85	Standard Vivarium Control	R + 3	78.5
85		R + 12	49.3
3224		R + 3	71.2
3224		R + 12	56.8
151	Flight	R + 2*	56.3
151		R + 3	83.0
151		R + 12	58.0
906		R + 1	47.8
906		R + 2*	60.3
906		R + 3	65.8
906		R + 12	60.5
476		Flight Control Pool	R + 5
775	R + 5		45.5
838	R + 10		37.3
1324	R + 10		46

*Significance, $p < 0.05$, between standard vivarium control monkeys at R + 3 (#s 85 and 3224) and flight monkey groups

**Significance, $p < 0.05$, between standard vivarium control monkeys at R + 12 (#s 85 and 3224) and flight monkey groups

TABLE 18

Effect of Restraint on Staining of Peripheral Blood with Anti-HLA-DR

Animal #	Condition During Flight	% Lymphoid Cells Stained
85	Standard Vivarium Control	27.5
3224		0.8
151	Flight + Restraint	8.6
906		25.2
803	Flight Pool + Restraint	13.4
907		2.9
588	Vivarium Control	16.7
1417		4.6

*Significance, $p < 0.05$, between standard vivarium control monkeys (#s 85 and 3224) and restraint monkey groups or vivarium control group monkeys

TABLE 19

Effect of Restraint on Staining of Bone Marrow with Anti-HLA-DR

Animal #	Condition During Flight	% Lymphoid Cells Stained
85	Standard Vivarium Control*	15.4
3224		16.6
151	Flight + Restraint*	3.8
906		4.0
803	Flight Pool + Restraint*	12.6
907		9.0
588	Vivarium Control	40.6
1417		39.3

*Significance, $p < 0.05$, between standard vivarium control monkeys (#s 85 and 3224) and restraint monkey groups or vivarium control group monkeys

TABLE 20

Effect of Restraint on Staining of Peripheral Blood with Leu-2a (CD -8)

Animal #	Condition During Flight	% Lymphoid Cells Stained
85	Standard Vivarium Control	11.7
3224		0.9
151	Flight + Restraint	4.8
906		11.1
803	Flight Pool + Restraint	21.8
907		0.8
588	Vivarium Control	1.6
1417		2.2

*Significance, $p < 0.05$, between standard vivarium control monkeys (#s 85 and 3224) and restraint monkey groups or vivarium control group monkeys

TABLE 21

Effect of Restraint on Staining of Bone Marrow with Leu-2a (CD -8)

Animal #	Condition During Flight	% Lymphoid Cells Stained
85	Standard Vivarium Control	3.8
3224		10.1
151	Flight + Restraint	0
906		0.8
803	Flight Pool + Restraint	0
907		2.8
588	Vivarium Control	4.4
1417		0

*Significance, $p < 0.05$, between standard vivarium control monkeys (#s 85 and 3224) and restraint monkey groups or vivarium control group monkeys

TABLE 22

Effect of Restraint on Staining of Peripheral Blood with Leu-3a (CD -4)

Animal #	Condition During Flight	% Lymphoid Cells Stained
85	Standard Vivarium Control	6.2
3224		0
151	Flight + Restraint	0
906		7.6
803	Flight Pool + Restraint	0
907		0
588	Vivarium Control	0
1417		1.3

*Significance, $p < 0.05$, between standard vivarium control monkeys (#s 85 and 3224) and restraint monkey groups or vivarium control group monkeys

TABLE 23

Effect of Restraint on Staining of Bone Marrow with Leu-3a (CD -4)

Animal #	Condition During Flight	% Lymphoid Cells Stained
85	Standard Vivarium Control	1.5
3224		0
151	Flight + Restraint	4.4
906		0.6
803	Flight Pool + Restraint	0
907		5.7
588	Vivarium Control	0
1417		0

*Significance, $p < 0.05$, between standard vivarium control monkeys (#s 85 and 3224) and restraint monkey groups or vivarium control group monkeys

TABLE 24

Effect of Restraint on Staining of Peripheral Blood with Leu-4 (CD -3)

Animal #	Condition During Flight	% Lymphoid Cells Stained
85	Standard Vivarium Control	14.6
3224		0
151	Flight + Restraint	11.4
906		23.4
803	Flight Pool + Restraint	3.0
907		0
588	Vivarium Control	10.6
1417		26.8

*Significance, $p < 0.05$, between standard vivarium control monkeys (#s 85 and 3224) and restraint monkey groups or vivarium control group monkeys

TABLE 25

Effect of Restraint on Staining of Bone Marrow with Leu-4 (CD -3)

Animal #	Condition During Flight	% Lymphoid Cells Stained
85	Standard Vivarium Control	21.4
3224		10.3
151	Flight + Restraint	39.9
906		13.7
803	Flight Pool + Restraint	17.6
907		18.5
588	Vivarium Control	13.5
1417		45.4

*Significance, $p < 0.05$, between standard vivarium control monkeys (#s 85 and 3224) and restraint monkey groups or vivarium control group monkeys

TABLE 26

Effect of Restraint on Staining of Peripheral Blood with Leu-11a (CD -16)

Animal #	Condition During Flight	% Lymphoid Cells Stained
85	Standard Vivarium Control	15.8
3224		0
151	Flight + Restraint	10.2
906		14.2
803	Flight Pool + Restraint	1.6
907		0
588	Vivarium Control	1.6
1417		2.6

*Significance, $p < 0.05$, between standard vivarium control monkeys (#s 85 and 3224) and restraint monkey groups or vivarium control group monkeys

TABLE 27

Effect of Restraint on Staining of Bone Marrow with Leu-11a (CD -16)

Animal #	Condition During Flight	% Lymphoid Cells Stained
85	Standard Vivarium Control	6.6
3224		25.9
151	Flight + Restraint	8.9
906		30.9
803	Flight Pool + Restraint	10.0
907		16.3
588	Vivarium Control	13.0
1417		26.6

*Significance, $p < 0.05$, between standard vivarium control monkeys (#s 85 and 3224) and restraint monkey groups or vivarium control group monkeys

TABLE 28

Effect of Restraint on Staining of Peripheral Blood with Anti-Human IgM

Animal #	Condition During Flight	% Lymphoid Cells Stained
85	Standard Vivarium Control	63.6
3224		74.6
151	Flight + Restraint	40.5
906		82.6
803	Flight Pool + Restraint	51.5
907		72.8
588	Vivarium Control	54.8
1417		62.7

*Significance, $p < 0.05$, between standard vivarium control monkeys (#s 85 and 3224) and restraint monkey groups or vivarium control group monkeys

TABLE 29

Effect of Restraint on Staining of Bone Marrow with Anti-Human IgM

Animal #	Condition During Flight	% Lymphoid Cells Stained
85	Standard Vivarium Control	53.3
3224		71.7
151	Flight + Restraint	84.5
906		86.0
803	Flight Pool + Restraint	58.9
907		84.8
588	Vivarium Control	46.9
1417		83.9

*Significance, $p < 0.05$, between standard vivarium control monkeys (#s 85 and 3224) and restraint monkey groups or vivarium control group monkeys

TABLE 30

Effect of Restraint on Staining of Peripheral Blood with Anti-Monkey IgG

Animal #	Condition During Flight	% Lymphoid Cells Stained
85	Standard Vivarium Control	85.7
3224		79.2
151	Flight + Restraint	81.8
906		87.1
803	Flight Pool + Restraint*	68.5
907		72.9
588	Vivarium Control	58.5
1417		74.0

*Significance, $p < 0.05$, between standard vivarium control monkeys (#s 85 and 3224) and restraint monkey groups or vivarium control group monkeys

TABLE 31

Effect of Restraint on Staining of Bone Marrow with Anti-Human IgM

Animal #	Condition During Flight	% Lymphoid Cells Stained
85	Standard Vivarium Control	70.7
3224		70.6
151	Flight + Restraint	76.1
906		51.2
803	Flight Pool + Restraint	36.8
907		74.4
588	Vivarium Control	78.5
1417		42.3

*Significance, $p < 0.05$, between standard vivarium control monkeys (#s 85 and 3224) and restraint monkey groups or vivarium control group monkeys

EXPERIMENT K-8-08

ADAPTATION TO MICROGRAVITY OF OCULOMOTOR REFLEXES (AMOR):
OTOLITH-OCULAR REFLEXES

Principal Investigator:

D.L. Tomko
NASA Ames Research Center
Moffett Field, CA

Co-Investigators:

I.B. Kozlovskaya
Institute of Biomedical Problems
Moscow, Russia

G.D. Paige
University of Rochester Medical School
Rochester, NY

A.M. Badakva
Institute of Biomedical Problems
Moscow, Russia

“What might have been is an abstraction
Remaining a perpetual possibility
Only in a world of speculation.
What might have been and what has been
Point to one end, which is always present.
Footfalls echo in the memory
Down the passage which we did not take
Towards the door we never opened.”
(Eliot, 1943)

Rod Ballard’s help was critical in opening the door that transformed this project from possibility to reality. We are grateful to him. We wish he were here with us to accept our thanks, and to share with us the fruits of our labor. We miss him, and will always remember him fondly.

We thank all the named and unnamed contributors, in the United States and Russia, without whose support this study would have been impossible. Principal members of the engineering team who designed, built, tested and operated the Portable Linear Sled at Ames Research Center (ARC) and at the Institute of Biomedical Problems (IMBP) included Jim Alwyn, Leonid Dunavetsky, Dennis Matsuhira, Alex Medvinsky, Tom Skundberg, Dave Squires, John Temple, Will Vallotton, and Tom Wynn. Vladimir Magedov of the IMBP assisted materially in laboratory set-up there. We are grateful to Shawn Bengston, Jim Clifford, and Cuong Ha for tireless and critical support in data collection and analysis. Russian scientists Natalia Miller, Michael Sirotta, and Dmitri Zalkind assisted in experiment conduct. Animal Health Technician support was crucial, and of high quality, both at ARC and IMBP. We are grateful to Ginny Reyna and Denice Helwig for excellent organizational support. We are especially grateful to Jim Connolly and Frank Sulzman without whose enthusiastic support and encouragement these studies would not have been done. Most importantly, every person involved in this project was congenial and good-natured, frequently under stressful circumstances. All deserve much credit for their enthusiasm, skills, and contributions to the accomplishment of a complex task in a limited time.

ADAPTATION TO MICROGRAVITY OF OCULOMOTOR REFLEXES (AMOR): OTOLITH-OCULAR REFLEXES

D.L. Tomko, I.B. Kozlovskaya, G.D. Paige, A.M. Badakva,

ABSTRACT

Vestibular otoliths sense linear head motion and head tilt relative to Earth gravity, while canal receptors provide a signal of angular head motion. An important use of these signals is to produce linear and angular vestibulo-ocular reflexes (LVORs and AVORs) that stabilize eye position in space, providing inertial stability for vision during head motion. LVORs occur during linear head motion that on Earth vectorially sums with gravity. AVORs are produced during angular head motion; on Earth, head pitch or roll stimulates vertical canals and modulates otolith outputs. In contrast, head yaw usually stimulates only canals.

Rationale and Objectives

It was hypothesized that after microgravity exposure would elicit adaptive changes in otolith-related functions and that there would be alterations in: 1) LVORs during translational head motion, and 2) AVORs produced on Earth by canal and otolith stimulation together (during pitch or roll). The experimental objectives were to characterize before and after space flight: 1) LVOR responses to linear acceleration along various axes and 2) AVOR responses during head yaw, pitch, or roll.

Method

Scleral search coils and head-holders were surgically implanted in 12 rhesus monkeys (9/92) to enable characterization of LVORs and AVORs preflight (10/92) and postflight (1/93) in the 2 flight animals (M151 and M906) and 3 controls (M775, M883 and M907). Using a specially constructed Portable Linear Sled, LVORs were studied during 1.0 and 5.0 Hz (+0.35 and +0.50 g pk, Noise <0.001 g) Earth-horizontal head motion in darkness (LVOR), and during viewing of a head fixed (VSLVOR) or an Earthfixed (VLVOR) visual scene. Motion was delivered along the inter-aural (IA), naso-occipital (NO), and dorso-ventral (DV) head axes, as well as along intermediate, oblique ones. Angular VORs were recorded during sinusoidal yaw, pitch, or roll motion (0.50-5.0 Hz, 50o/sec) delivered manually with Earth-fixed visual targets (VVOR) during yaw and pitch, and with animal-fixed visual targets during roll. PC-based programs were used for data acquisition and analysis; Response gain and phase were calculated, along with gaze position and vergence state. The gain and phase of differentiated, de-saccaded eye position recordings were calculated using Fourier analysis.

Results

Preflight LVORs and AVORs were similar to previous results in squirrel monkeys. LVORs compensatory for head displacement were recorded during IA, DV, NO, and intermediate axis motion. All responses were affected by vergence state (visual target distance). NO responses were affected also by gaze direction. During motion along axes oblique to the IA, DV, and NO axes, responses were organized with respect to the axes of motion. AVORs during yaw and pitch had roughly compensatory gains, while torsional gains of between 0.4 and 0.7 were recorded. AVOR and LVOR response characteristics of the two flight monkeys before and after the 11 day Cosmos 2229 flight were compared.

Postflight linear VORs

Postflight, during IA motion (5 Hz, 0.5g), M906 showed a roughly 2/3 reduction in the slope of the function relating horizontal LVOR sensitivity to vergence that had not recovered by R+391 hours. Under the same conditions, M151 showed almost identical responses pre- and postflight.

During DV motion (5 Hz, 0.5g) M906 showed from 35-60% reduction in the slope of the function relating vertical LVOR sensitivity to vergence that had not recovered by R+391 hours. Under the same conditions, M151 showed responses immediately postflight that were almost identical to preflight values, and subsequently had reductions of 30-50%.

Pre- and postflight responses during NO motion for M151 were similar to one another, while responses of M906 were smaller and more variable postflight. This was the case as well for motion along oblique axes between NO and DV.

During motion along axes between IA and DV, eye movements of flight monkey M151 were clearly misaligned with the motion axis immediately postflight, and had probably recovered by R+388 hours. In M906, pre- and postflight eye movements showed similar changes, but not so dramatically.

Postflight angular VORs

Immediately postflight, M151 and M906 had about a 20% drop in AVOR gain in response to head pitch, and a slight drop in AVOR gain in response to head yaw postflight. Both recovered within 3 days postflight. M906 had a roughly 50% drop in AVOR gain in response to head roll that had not recovered at R+390 hours, the last day of postflight testing. M151, and the control animals had similar AVOR roll gains pre- and postflight.

Conclusions

1. Both flight monkeys had lower AVOR gain in response to pitch and yaw head movements immediately postflight. M906 had a 50% reduction in AVOR gain in response to roll, while M151 had similar AVOR roll gains pre- and postflight.
2. During IA and DV head motion at 5 Hz (0.5 g), M906 had large reductions in the slope of the function relating LVOR sensitivity to vergence that did not recover by R+391 hours. Under the same conditions, M151 showed almost similar responses pre- and postflight.
3. During NO head motion, pre- and postflight responses for M151 were similar to one another, while responses of M906 were smaller and more variable postflight.

INTRODUCTION

Vestibular Physiology and Space Flight: Rationale

Vestibular reflexes resulting from stimulation of the gravity sensing otoliths are those most likely to be changed by space flight. The vestibular otoliths are arrays of linear accelerometers whose output signals allow the brain to determine the head's orientation relative to Earth's gravity. In addition, linear head motion (for example, during postural sway or locomotion) generates a linear acceleration that vectorially sums with gravity to produce an otolith signal. Linear head motion (along the inter-aural, dorso-ventral or naso-occipital axes) on Earth or in space produces LVORs that compensate for head motion, providing a stable inertial frame of reference for vision.

BACKGROUND

Present State of Knowledge

The Angular Vestibulo-ocular reflex (AVOR)

The function of the AVOR is to stabilize the eye in space during angular head motion. The reflex performs this function by producing eye movements that are compensatory for head movements (i.e., 180° out of phase with head movements). For frequencies in the physiological range of motion, yaw, pitch or roll of the head in the dark results respectively in horizontal (HVOR), vertical (VVOR) or torsional (TVOR) eye movements with gains of roughly 0.9, 0.9, and 0.6 (respectively) (c.f., Carpenter, 1977; Collewijn, 1985; Paige & Tomko, 1987). Further, the VOR is under adaptive control and its gain may be modified by visual experience (cf., Gonshor & Jones, 1976; Lisberger & Miles, 1980; Miles et al, 1980; Paige, 1983a; Paige et al, 1987). Even a monkey's experience in the test apparatus has a major influence on VOR gain (Buttner et al 1981). These VOR modifications are presumed to be driven by mismatched visual and vestibular cues during head movement, resulting in visual image motion and subsequent adaptive changes to reduce that image slip. Visual-vestibular mismatch might arise as a result of disease, or artificially, as in space flight.

Effect of Linear Acceleration on AVOR

Reflex eye movement control during pitch or roll head motion differs from that during yaw (discussed in Staab et al 1988). First, during most head yaw, position does not change relative to gravity, activating only semicircular canals, so long as motion is about an axis near the head's center (Viirre et al, 1986). But in most natural pitch and roll motion, head position relative to gravity does change, activating both otoliths and canals. Second, head yaw is mechanically symmetric; leftward and rightward motion requires the same amount of energy, and the same motor control strategy. In pitch or roll, however, upward head motion requires pulling the head's mass against gravity, while downward motion requires that the head's mass be braked against gravity. This asymmetry necessitates differing motor strategy and different energy expenditure during upward and downward motion.

Vertical VORs have been studied less than horizontal ones, though there has recently been increased interest in them (e.g., Anderson & Liston, 1983; Matsuo et al, 1984; Tomko et al, 1984, 1988). In most experiments, pitch around the inter-aural axis is delivered to the subject in the Earth-horizontal plane, while the subject lies on his side stimulating only the vertical semicircular canals (e.g., Benson et al, 1971; Darlot et al, 1981; Matsuo & Cohen, 1984). Under such conditions, vertical VOR gain is less than that of the horizontal VOR and there are asymmetries in upward and downward eye movements.

A recent study (Tomko et al, 1984; 1988) compared vertical VORs during on-side pitch with those during upright pitch (i.e., subject sitting upright). Vertical VOR gain was about 15% less (0.05 to 4.0 Hz) when the subject was pitched on his side than when upright. Vertical VOR gain during upright pitch was near that of the horizontal VOR of the same subjects. As well, vertical VOR asymmetries seen in the on-side condition were significantly reduced when the subject was upright. These findings have been replicated in squirrel monkeys, and were extended to roll and the torsional VOR during roll (Paige & Tomko, 1987). They suggest that vertical VORs are driven synergistically by otoliths and canals.

Evidence indicates that interactions between otolith responses to linear motion or gravity and semicircular canal responses to angular motion are important to eye movement control (e.g., Benson, 1974). More recently, it has been shown in a variety of species that the dynamic response characteristics of the VOR produced by angular accelerations are affected by head position with respect to gravity (e.g., Anderson & Liston, 1983; Arrott & Young, 1987; Collewijn, 1985; Fuller,

1985; Sirota et al, 1987a; 1987b). It has been shown that eye movements can be evoked by off-vertical axis rotation (OVAR) consisting of a sustained, or bias and a sinusoidal component. In man (Benson & Bodin, 1966) the sinusoidal component dominates, but in the monkey (Raphan et al, 1979) and cat (Harris, 1987) a large bias component is present. Post-rotational responses are also modified by gravity. The time constant of post rotational nystagmus is drastically reduced after OVAR (b) with the fastest response declines observed when the axis of apparent motion is perpendicular to gravity. It is thought that otolith stimulation underlies the sustained nystagmus during OVAR and the modification of post-rotational after OVAR. Correia & Money (1970) showed that nystagmus similar to that of intact animals could be induced in canal plugged cats during OVAR. It has also been shown that after macular ablation post rotational time constants were independent of tilt angle (Igarashi et al, 1980).

In addition, otolith inputs are important to the vertical opto-kinetic reflex (VOKR). Igarashi and colleagues (1978) showed that selective macular lesions increased VOKR slow phase velocity in squirrel monkeys. Matsuo and Cohen (1984) have demonstrated that velocity storage (Cohen et al, 1977) for VOKR is different when an animal is on-side than it is when it is upright, implying an otolith input to velocity storage as well. More recent work (Raphan & Cohen, 1988) has amplified that finding, and describes gravity effects on OKR in terms of a 3-D spatial model.

In addition, flight experiments have indicated that exposure to microgravity affects both the vertical vestibulo-ocular and opto-kinetic reflexes (Clement et al, 1986; Vieville et al, 1986). In one subject during space flight, the gain of the VVOR was reduced for the first four days before recovering its preflight value, and VOKR underwent both a gain change and a reversal of its normal up-down asymmetry. In another (postflight) study (Parker et al, 1985; Reschke & Parker, 1987), horizontal eye movements were elicited by head roll, indicating that there existed a kind of cross-coupling between otoliths and canals which had been induced by adaptation to microgravity. Neither exact mechanisms nor the long term consequences of any of the above findings are understood. It is likely, however, that eye movement control and visual mechanisms are influenced by somatic and vestibular stimuli, including those from otoliths.

Linear VOR (LVOR)

Previous studies in humans (Benson & Bodin, 1966a; 1966b; Niven et al, 1965; Young, 1967) and animals (e.g., Barmack, 1981) have described eye movements elicited by linear accelerations. None have looked in a systematic way at the variety of orientations and axes for delivery of linear stimuli. Furthermore, none have described an LVOR which might sum with the angular one during vertical head rotations, and which might account for the above described on-side versus upright pitch phenomenon (Tomko et al, 1988). This latter possibility was the motivation for a series of experiments investigating eye movement responses to linear accelerations (Paige & Tomko, 1987; 1988a; 1988b; Tomko & Paige, 1988). In those studies, horizontal, vertical, and torsional eye positions were recorded using the scleral search coil technique (Robinson, 1963) in adult squirrel monkeys. Linear sinusoidal stimuli (0.5-5.0 Hz, 0.36g peak) were delivered along the animals' naso-occipital (NO), dorso-ventral (DV) and inter-aural (IA) axes. For each stimulus axis, 4 of the following six animal positions were tested: upright, inverted, nose up or down, and left or right ear down. Gains (o/sec/g) and phases (eye velocity re head velocity) were calculated.

Two LVORs, horizontal LVORs during IA and vertical LVORs during DV motion were "compensatory" (tending to keep the eye fixed on a visual target), with eye velocity opposing head velocity (phase near 180o), presumably aiding maintenance of gaze fixation under normal conditions. Gains for both reflexes rose from 15 to 30o/sec/g as frequency increased from 0.5 to 5.0 Hz. A non-compensatory torsional LVOR during IA and vertical LVOR during NO motion were recorded with smaller gains (8-15o/sec/g) than the compensatory reflexes. However, vertical eye movements are clearly produced by NO accelerations, and may be related to the gain difference between upright and on-side pitch described in the preceding section. It seems probable that vertical

eye movements produced by NO linear acceleration result from otolith stimulation, and we surmise that these dynamic otolith-ocular reflexes interact with vertical-canal mediated ones, perhaps in the same way that linear VORs affect the gain of horizontal angular VORs (Viirre et al, 1986). An important finding from the above experiments is that for all axes of motion, no systematic modification of gain or phase was observed as a function of head orientation. Thus, in the squirrel monkey, the LVORs from 0.5 to 5.0 Hz behave as a set of specific vectorially-defined reflexes analogous to the angular VORs. This is counter to previous assumptions that the otoliths behave as gravity sensors and simply register the angle of tilt, or the simulated angle of tilt induced by linear acceleration. While this is certainly true for low frequencies of linear motion, results at 0.5 Hz and above illustrate that in this important and physiologic range of linear head motion, otoliths provide true linear motion cues which drive eye movements in a compensatory manner, analogous to the angular VOR.

In the same set of experiments, eye movements were recorded during linear oscillations in the light, while monkeys looked at the container wall (visual suppression, or VSLVOR). Compared to LVOR gains in darkness, the VSLVOR gain of horizontal eye movements during IA and of vertical eye movements during DV oscillations dropped to near 0 at 0.5 Hz. However, gain rose as frequency increased, to nearly double that of darkness at 5 Hz. Geometric considerations likely explain these seemingly peculiar results. As target distance approaches infinity, no eye movements are required to maintain stable visual images during linear head movement. As target distance moves near, however, the eyes must increasingly compensate for linear head motion to maintain a stable image. Since visual influences on eye movements are nearly gone at 5 Hz (Paige, 1983a), we surmised that a measure of target distance (TD), likely vergence dependent, biased the VSLVOR for fixation on the container wall (TD=20 cm.), thereby requiring greater gain. Darkness presumably allowed distant 'fixation' and smaller gains. When vergence was measured during oscillations (binocular coils), vergence angle and gain were closely linked. In a related phenomenon, during NO oscillations above 0.5 Hz, responses depended on gaze angle with respect to the axis of motion (e.g., responses were rightward during right gaze, upward during up gaze, etc.). This unique switching in the LVOR is consistent with a compensatory, TD- and gaze-dependent model.

Effects of μ -gravity or μ -gravity simulation on eye-head movement coordination and the AVOR

Existing ground-based data (Tomko et al, 1988; Paige & Tomko, 1987; 1988a; 1988b) clearly show that important components of VORs are controlled by otolith organs; Flight experiments in animals and humans (Clement et al, 1986; Grigoryan et al, 1986; Kozlovskaya et al, 1985; Kozlovskaya et al, 1984; Shipov et al, 1986; Sirota et al, 1987a; Vieville et al, 1986) also indicate potentially important changes in vestibular eye control mechanisms during adaptation to microgravity.

Soviet investigators (e.g., Shipov et al, 1986) have done studies on effects of space flight on an eye-head coordination paradigm (Bizzi et al, 1971; 1972) 'gaze fixation reaction', or GFR). In GFR, subjects visually acquire targets which appear in the visual field, usually on a horizontal meridian. Execution of this task includes a stereotypical sequence of events beginning with a saccade toward the target, a head movement in the same direction beginning after the saccade starts, and a compensatory (VOR) during the head movement, which brings head and eyes in a coordinated fashion to the target. This task therefore tests saccades, head movements and their coordination by the VOR. Similar experiments have been performed on humans and rhesus both in flight (e.g., Kozlovskaya et al, 1985) and in microgravity simulations (e.g., Grigoryan et al, 1986). Thus, eye-head coordination is a rich source of information about how vestibular and motor controls adapt to microgravity (Shipov et al, 1986).

Soviet experiments have shown dramatic, though not always consistent changes in the components of the GFR during adaptation to microgravity, following return to Earth gravity, and in microgravity simulations. There are changes in the amplitude and performance of saccades and of head

movements, changes in VOR gain and impairment of task accuracy. After long duration space flight, "the postflight saccadic amplitude in all (N=14) cosmonauts was elevated and overshoot the target by 10-20 degrees. In contrast, the amplitudes and velocities of head movements were sharply decreased. The VOR velocity was still further decreased, approaching 0 on the 3rd day postflight" (Grigoryan et al, 1986). Task latencies were almost doubled, and the subjects used many corrective eye and head saccades. Time to full recovery is not given. Findings in one group of bed rest subjects (duration=120 days) showed similar underactive saccades and reduced VOR gain (0.5-0.8) which recovered to normal after 14 days (Grigoryan et al, 1986). A second group showed the opposite, overactive saccades and increased VOR gains (1.3-1.9). Another report on results from cosmonauts (Kozlovskaya et al, 1985) indicates that they divide into two groups as well, one including cosmonaut investigators in which the GFR contained significantly smaller amplitude head movements, and a second in which head movement amplitudes increased. In both groups, there were postflight increases in VOR gain, 30-40% increases in positional errors during task execution, & acquisition latencies increased by 70-80 msec.

Experiments on rhesus (Shipov et al, 1986) showed that "on the first flight day (22 hours after launch) the saccadic amplitudes were noticeably increased. The increase persisted postflight. Simultaneously, the velocities of compensatory eye movements increased considerably." That is to say, horizontal VOR gains of 1.3 to 1.5 were measured.

Two conclusions can be drawn from Soviet experiments. 1) There are dramatic changes in coordination of eye and head movements during and following adaptation to microgravity, first in head movement and saccade amplitudes, and second in VOR gain. The results are somewhat inconsistent and contradictory. Some of this may be due to small sample sizes and some may be due to problems with EOG calibration or drift. 2) These studies have been restricted to horizontal head and eye movements. Vertical head and eye movements, which have not been studied are of great interest because normal vertical head movements stimulate the otoliths on Earth, but not in space. In addition, vertical eye and head movements have been shown to be asymmetric (Staab et al, 1988; Tomko et al, 1988), possibly due to gravity, and might be expected to be as dramatically effected as horizontal movements.

Neurophysiological correlates of adaptation to μ -gravity

Limited and poorly controlled experiments in frog otolith units hint at a possible sensitivity shift of vestibular neurons (Gualtierotti et al, 1972). Soviet experiments have recorded from vestibular nuclei neurons, and more recently from vestibular nerve, along with the VOR during adaptation to weightlessness. Increased sensitivity to head movements was reported to occur early in flight (Sirota et al, 1987a; 1987b).

OBJECTIVES AND HYPOTHESES

The VOR has two components. Eye movements are induced by angular accelerations that stimulate semicircular canal receptors, and by linear accelerations that stimulate otolith receptors. In altered gravity, normal head movements result in an altered stimulus pattern to the otolith organs; if compensatory VORs are to be maintained (i.e., eye movements equal and opposite to head movements) then a specific adaptation of VOR responses to linear accelerations must occur. The objective of the experiments was to characterize VOR adaptation to microgravity and recovery post-flight in rhesus monkey. This objective was achieved by recording and analyzing eye movements during passively applied linear and angular motion in the light and dark pre- and postflight.

Hypothesis 1) If otoliths and semicircular canals synergistically control eye position during angular head rotations, the dynamic response characteristics of the angular VOR will change in microgravity, and this change will re-adapt postflight.

Hypothesis 2) If otolith reflexes (LVORs) during translational accelerations require a background acceleration equivalent to Earth gravity for normal operation, then LVOR dynamic response characteristics should be altered in microgravity, and this change will re-adapt postflight.

Hypothesis 3) If inertial forces, as transduced by the otoliths, can signal gravity or linear acceleration, then adaptation to weightlessness will favor an interpretation of inertial forces as linear acceleration over gravity (tilt/translation reinterpretation hypothesis).

Experiments addressed the following questions. First, what are the dynamic response characteristics of angular VORs pre- and postflight? What is the effect of static head position on angular VOR? Do otolith organs bias the angular VOR, and how does space flight change this? Second, what are the dynamic response characteristics of LVORs during translational motion delivered passively before and after space flight? How are they influenced by visual stimuli? What are the effects of: static head position re motion, vergence and target distance, stimulus frequency, and how are they changed by flight?

METHODS

Animals and Surgical Procedures

Experimental subjects were 12 juvenile (4-5 kg) Rhesus (*Macacca mulatta*) monkeys. Preflight vestibulo-ocular reflexes were studied in each between October 8 and 19, 1992. Eleven of the 12 animals were each available for a total of two 2-3 hour periods preflight. The 12th was available for a single session. Animals M151 and M906 were exposed to 278.5 hours of "weightlessness" during Cosmos Biosatellite flight 2229, launched at 4:30PM Moscow time on December 29, 1992 and recovered at 7:00AM Moscow time on January 10, 1993. Following the flight, M151 and M906 were tested in 5 and 6, respectively, 2-3 hour periods. Three animals (M775, M803 & M907) were available as ground-based controls.

In an initial aseptic surgical procedure using inhalational anesthetic, silver-silver chloride electro-oculogram (EOG) electrodes (e.g., Bond & Ho, 1970) were implanted bi-temporally for other studies. A 10 cm. diameter plastic ring was secured to the skull with a perimeter circle of surgical stainless steel screws. An attempt was made to orient the head-holder's top surface near parallel to the stereotaxic horizontal plane. Three screws attached to the ring were used as a painless point of attachment to immobilize the head, and to insure that head position placement could be repeated from one day to another. Printed circuit (PC) boards attached to the head ring contained EOG and neural amplifiers, and provided access to 20 chronically implanted metal guide tubes for insertion of microelectrodes into either vestibular nuclei or nerve. All EOG-, EMG- and micro-electrodes used by other investigators were terminated within the head-holder.

To enable 3-d eye movement recording, scleral search coils were implanted in each animal (Robinson, 1963) in a second aseptic surgical procedure using inhalational anesthetic. Prefabricated coils (16 mm diameter) were sutured to the frontal plane of the sclera concentric to the limbus bilaterally to record horizontal and vertical eye position. A coil to measure ocular torsion was fabricated in situ, sutured to the sclera orthogonal to the first on top of the globe. Estimated torsion coil diameters at implant ranged from 10 to 12.5 mm. Twisted pair coil leads exited the orbit laterally and subcutaneously, leaving a loop of wire over the eye to allow unrestricted ocular motility. Coil leads were tunneled subcutaneously over the skull and terminated on a PC-board connector attached to the head-holder.

In experiments at Ames Research Center, animals were maintained in an AAALAC accredited Animal Care Facility staffed by a full time veterinarian and licensed animal health technicians. All

experiment protocols were reviewed and approved by an Institutional Animal Care and Use Committee prior to the studies.

Eye Movement Recording and Calibration

Horizontal and vertical eye position were obtained by demodulating the AM signal (in quadrature) from the eye coils mounted in the eye's frontal plane, while torsional position was obtained by demodulating the signal induced in the horizontally mounted coils. Eye position was recorded (resolution $<0.1^\circ$, DC-150 Hz) using a Robinson (1963) type system (CNC Model R2PWDR driver operating at 98 KHz (vertical) and 147KHz (horizontal), with R2PHDT and R2PHDT-M2 demodulators). Vergence was calculated by adding the right and left eye horizontal positions in a hardware summing amplifier prior to recording, or in software during data analysis.

Prior to the conduct of each experiment, prefabricated test coils of the same diameter as those implanted in the monkeys were mounted in a plastic test jig mounted in the magnetic field coils. To insure that the calibrations were as close to the actual experimental set-up with the monkey present, the test jig was attached to a plastic head ring identical to ones implanted on the monkey, including PC boards, plugs and connectors. With test coils located at roughly the same position in the field as on the monkeys' eyes, test coil orientation was systematically varied using a calibrated protractor. The system was calibrated so that horizontal and vertical positions of $+50^\circ$ were equal to $+10V$, while torsional positions of $+10^\circ$ were set to equal $+10V$. The CNC system provided linear measures of coil position over this range, as shown in Figure 1.

Vestibular Stimulation

Apparatus and stimuli

A specially designed and constructed Portable Linear Sled (PLS) was the stimulating device. It consists of three sub-systems: 1) inside a gimbaled, light-tight Specimen Test Container (STC, Figure 3), the subject was seated (Figure 2) in a plexiglas chair, 2) a carriage supported by air bearings and 'floating' on ceramic rails (Figure 4), and 3) a gantry that enables repositioning the translational axis from Earth-horizontal to Earth-vertical (Figure 5). A photograph of the device in use at the IMBP is shown in Figure 6. The PLS was designed to deliver low noise ($<10^{-3}$ g) linear motion (1.0-5.0 Hz, 1.0 g peak) to 4-5 Kg Rhesus monkeys. The gimbaled STC described below permitted the manual delivery of roughly sinusoidal yaw, pitch or roll at frequencies from about 0.5 to 2.0 Hz with modest peak amplitudes ($50^\circ/\text{sec}$). In addition, the gimbaled mount was used to reorient the animal in the STC with respect to the linear motion.

Linear motion was delivered to the seated monkey through its inter-aural (IA), dorso-ventral (DV), and naso-occipital (NO) axes (re the head). All stimuli were 1.0 and 5.0 Hz sinusoids. The data reported in the present report were collected at 5.0 Hz at 0.5g peak acceleration. A small amount of additional data were collected at 1.0 and 5.0 Hz, 0.35g peak. Eye movements were measured during NO, DV, and IA linear motion in as many of the cardinal positions as time allowed to test the effects of static head position on the LVOR.

All translational stimuli were delivered parallel to the Earth's surface using the PLS described below. Stimuli were delivered to the animal in darkness (LVOR), with an interior light switched on to permit the animal to view the STC's inside walls providing a head-fixed visual surround (VSLVOR) or with the animal viewing the laboratory through the STC's porthole during stimulation to provide visual-vestibular interaction using an Earth-fixed visual surround (VLVOR).

Specimen Test Container (STC)

The STC, its axes of motion, and attachment to the carriage are shown diagrammatically in Figure 2. After the subject was comfortably seated in a primate chair, the head was fixed in a standard position using the surgically implanted head-holder ring shown in Figure 3. The body was cushioned by foam padding to eliminate hard pressure points and to reduce body motion during stimulation. Orthogonal (horizontal and vertical) pairs of Helmholtz coils in which the animal's eyes were centered were firmly attached to the chair. A dovetail assembly was then attached to the back of the chair (not shown in figure) to enable mounting the chair in the STC.

The chair and subject are shown positioned in the STC (in Figure 2A from the top, in 2B from the side, and in 2C from the front). The subject's head was at the center of two manually operated STC rotational axes (labeled pitch/roll in 2C, and yaw in 2D). The STC consists of concentric cylinders; the monkey chair was attached to the inner sleeve, and the outer sleeve mounted to the pitch/roll rotational axis shown in Figure 2C. Rotation of the inner sleeve was used to reposition the subject re the Earth-horizontal axis, making it either pitch or roll. The gimbal-mounted STC was mounted on a round plate which could be firmly attached to the sled carriage by a bolt circle. When loosened, this plate could be relatively smoothly moved by hand to provide subject yaw.

Air-bearing carriage and sled mechanism

The basic mechanical components of the PLS are shown diagrammatically in Figure 4 (in A, from the side and in B, from the end). The STC described in Figure 2 is shown attached to the carriage. Mounted on the inner surface of each end of the carriage are five air bearings that 'float' on the two stationary ceramic rails as shown. Mounted on the center of the bottom inner surface of the carriage are the magnets of the linear motor used to drive the sled. The motor secondary also is mounted to the stationary base. The translational motion axis is indicated in 4A. It was possible to re-position the subject in any orientation re translation using the STC rotational axes described above.

Earth-horizontal and Earth-vertical operation

Figure 5 shows how the completed PLS was designed to provide either Earth-horizontal or Earth-vertical translational motion. Figure 5A shows Earth-horizontal position, while 5B shows the hand-operated gantry rolling along a track in the floor to reposition the sled into the Earth-vertical position (Figure 5C). However, due to scheduling constraints associated with the testing of the flight animals, data were only collected with the sled operating in the Earth-horizontal position.

DATA RECORDING AND ANALYSIS

Data recording

All data recording was performed by a portable personal computer together with laboratory I/O enhancements (analog-to-digital and digital-to-analog converters, clock, and digital I/O capabilities). Eye position, sled acceleration, and gimbal angular velocity were recorded digitally (sampled at 200 Hz). Analog events were recorded as time of event and interleaved within the digital record, such that all signals and events taking place during experiments were recorded for analysis.

Data analysis

Eye position signals were digitally differentiated and smoothed to yield velocities. A sample of angular VOR recorded during 10 seconds of yaw is illustrated in Figure 7. In all traces, rightward and upward movement are positive. The stimulus trace (labeled HWT) and the horizontal position of the right eye are shown in the top panel. In the center panel, the right eye horizontal velocity (HE1 VSM) is displayed, and in the bottom panel, the vertical position (VE1) and velocity (VSM) of the

right eye are shown. Eye position signals were specifically filtered semiautomatically to remove fast phases, as shown in Figure 8A for the same data as shown in Figure 8A. The analysis software enabled selection of desired cycles of data for further analysis as illustrated. All stimulus and response signals were subjected to Fourier analysis (Figure 8B and Table 2). The fundamentals from harmonic analyses were used to calculate gains (response/stimulus amplitudes) and phases (response-stimulus phase angle) for each cycle.

A similar sample of data in Figure 9 illustrates a 5 second sample of 5 Hz, 0.5g pk inter-aural oscillation. Labels are as in Figure 7; In the top trace, ACC is sled acceleration; HE1&HE2 are right and left horizontal eye position; In the center trace, HE1&VE1 VSM are right eye horizontal and vertical eye velocity; in the bottom trace, TE1&TE1 VSM indicate torsional position and velocity, and VER is the vergence. Figure 10 illustrates the criteria for choice of stimulus cycles used for further analysis at the higher stimulus frequencies. Responses were not de-saccaded, but any response within half a cycle of a saccade was rejected.

PRE- AND POSTFLIGHT TEST SCHEDULE, COMPONENTS AND CONSTRAINTS

The complete pre- and postflight test schedule is shown in Table 1. A word is in order regarding the components and constraints on data collection, since they had an important impact on the ability to complete the entire experimental protocol. Each experimental session was limited to from 1 to 3 hours, including the time required to chair the animal and return it to the animal room. The longest sessions were the two preflight experiments on each subject, and the very last postflight session (R+388 and R+391 hours) on the flight monkeys. Other sessions varied from 1 to 2 hours.

Following set-up and calibration, each session began with angular VOR measurements with Earth fixed targets for yaw and pitch using manually-produced sinusoids of between 0.5 and 1.0 Hz (50o/sec Pk). This was done to check the calibration of the coils, since the gain of both these reflexes should be close to 1.0 under these conditions. Roll AVOR was measured during viewing of animal fixed visual targets due to mechanical limitations of the gimbal positioning mechanism.

Data collection generally began with IA stimulation at 1.5 Hz (0.35g) and 5 Hz (0.35&0.50g). Similar measures were then performed during NO stimulation. For the most part, all remaining data in each session were collected using 5 Hz, 0.5g stimuli. In some sessions, to deliver motion along oblique axes between NO and DV, stimulation proceeded after static reorientation of the subject around the pitch axis (steps of +10,20,30,45,70 & 90o). In other sessions, to deliver motion along oblique axes between IA and DV, stimulation proceeded after static reorientations around the subject's roll axis (steps of +10,20,30, 45,70 & 90o). The shortest sessions were the ones immediately postflight, and generally no more than 1/3 of the protocol could be completed.

RESULTS

Vestibulo-Ocular Reflexes During Angular Motion (AVORS)

In Figure 11, horizontal, vertical and torsional (during yaw, pitch and roll) gains (left column) and phases (right column) are plotted for pre- and postflight observations for both flight monkeys M151 and M906. Each point represents the average response to 10-20 cycles of stimulation (+1 SD). Angular stimuli varied from 0.5 to 1.0 Hz due to the fact that the sinusoids were manually-delivered. Results were similar regardless of the exact frequency; harmonic distortion was typically less than 5%. Examples typical of the quality of the stimulus delivered are shown in the pitch data of Figures 12 and 13 (top traces). All gains were normalized to 1.0 relative to the averaged preflight sessions.

Horizontal AVOR in response to head yaw with Earth-fixed targets

Both animals showed a slight drop in postflight AVOR responses to head yaw postflight, but responses pre- and postflight were similar for all tests conducted. Again, phases were flat over time, and compensatory for both subjects.

Vertical AVOR in response to head pitch with Earth-fixed targets

M906 showed an almost 20% drop in AVOR gain in response to head pitch immediately postflight, which recovered by postflight day 4, falling again by postflight day 4. M151 had a 30% reduction in VVOR gain during pitch that recovered and then later dropped again as did that of M906. Phases were flat over time, and compensatory for both animals.

Typical 10 second samples of preflight and immediately postflight data collected during pitch with an Earth-fixed visual scene are shown in Figures 12 and 13 respectively. In both figures, the top panel shows right eye horizontal and vertical position (HE1&VE1, respectively), along with the pitch velocity (VWT VSM). The center trace of each figure illustrates the right eye horizontal and vertical velocity (HE1&VE1 VEL), while the bottom trace shows the desaccaded velocity record. There is an obvious qualitative difference between the pre- and postflight vertical position traces.

Torsional AVOR in response to head roll with head-fixed targets

M906 had a roughly 50% drop in AVOR gain in response to head roll that had not recovered by R+390 hours. The absolute value of torsional gain in M906 was 0.4, so the gain drop postflight is on the order of 50%, rather large. M151 showed no change in the torsional gain during head roll between pre- and postflight.

Vestibulo-Ocular Reflexes During Linear Motion (LVORS)

Typical ground-based results were similar to previous results in squirrel monkeys (Paige & Tomko, 1991a; 1991b; Tomko & Paige, 1992). There were eye movements during IA, DV and NO motion that were compensatory for head displacement. As reported previously, these responses were affected by vergence state (visual target distance), with increased LVOR sensitivity for closer fixation. NO responses were affected also by gaze direction.

Inter-aural (IA) axis motion

Figures 14 and 15 plot the right eye's horizontal and torsional sensitivity as a function of calculated vergence angle for monkeys M151 and M906 during inter-aural (IA) stimulation. Each point represents the sensitivity measured from a single 5 Hz, 0.5g stimulus cycle. In both figures, LVOR and VSLVOR data (solid and open points, respectively) are presented together, since they are part of a continuum. For simplicity in comparing pre- and postflight data, a best fitting lines was calculated for each data set. That best-fitting line is indicated, along with the fit parameters (A is the Y intercept, M the slope, and R the product-moment correlation coefficient). The upper left panel in each figure represents combined data from the two days of preflight testing for each animal. Each additional panel of Figures 14 and 15 represents the results from a single day of postflight testing, and the exact time of the start of the recording session is listed in each panel. For example, R+50 hours means that the session began at 9:00AM, January 13, 1993, 50 hours after recovery.

Inspection of Figures 14 and 15 shows that at 5 Hz, 0.5 g, M906 had a roughly 2/3 reduction in the slope of the function relating horizontal sensitivity to vergence that had not recovered by R+391 hours. Under the same conditions, M151 showed almost identical responses pre- and postflight.

Small non-compensatory torsional responses were present in response to IA stimulation, and were affected only slightly by vergence state, as has been reported for squirrel monkeys (Paige & Tomko, 1991a). It is interesting that these responses were increased slightly immediately postflight, and were gradually reduced over the roughly 16 days after recovery. This is especially striking for the data of M906, whose postflight Avers in response to head angular roll were reduced dramatically postflight, suggesting different adaptation mechanisms for the two conditions (AVER and LVOR). The difference may have to do with the frequency of stimulation, since the angular stimuli were delivered at significantly lower frequencies than the linear stimuli. This might be consistent with a suggestion, based on work in the squirrel monkey, that there may be two populations of otolith afferents, one high-pass and one low-pass filtered, the first associated with translational otolith responses and the second related suggesting different adaptation mechanisms for the two conditions (AVOR and LVOR). The difference may have to do with the frequency of stimulation, since the angular stimuli were delivered at significantly lower frequencies than the linear stimuli. This might be consistent with a suggestion, based on work in the squirrel monkey, that there may be two populations of otolith afferents, one high-pass and one low-pass filtered, the first associated with translational otolith responses and the second related to tilt responses.

Pre- and postflight time framework data for a single control animal (M907) in response to IA stimulation at 5 Hz (0.5g) are shown in Figure 15A. A best-fitting regression line relating horizontal sensitivity to vergence angle is plotted and the fit statistics are listed in each panel using the same labeling conventions as above.

Dorso-ventral (DV) axis motion

A second pair of figures, 16 and 17 plot the sensitivity of vertical eye movements to DV motion in a similar way to those for IA stimulation in Figures 14 and 15. Data were collected during the same sessions as those in Figures 14 and 15. All notations are the same as in the preceding two figures. Horizontal sensitivity for each stimulus cycle is also plotted; Results show that as ideally should be the case, there is little or no horizontal response to vertical motion, as was the case in previously published work on the squirrel monkey (Paige & Tomko, 1991a; 1991b).

Changes in vertical responses to DV stimulation are similar to the pattern of changes in horizontal sensitivity to IA motion postflight, shown in Figure 14 and 15. Inspection of Figures 16 and 17 shows that with DV stimuli at 5 Hz, 0.5 g, M906 showed from 35-60% reduction in the slope of the function relating vertical LVOR sensitivity to vergence that had not recovered by R+391 hours. Under the same conditions, M151 showed responses immediately postflight that were almost identical to preflight values, and subsequently had reductions of 30-50%.

Pre- and postflight time framework data for a single control animal (M907) in response to DV stimulation at 5 Hz (0.5g) are shown in Figure 17A. A best-fitting regression line relating vertical sensitivity to vergence angle is plotted and the fit statistics are listed in each panel using the same labeling conventions as above.

Motion along axes between IA and DV

In past work in squirrel monkey (Clifford et al, 1990), we have reported that when linear motion is delivered along axes intermediate between IA and DV, there is an appropriate addition of horizontal and vertical responses to produce a resultant eye motion that is parallel to the plane of the head motion, a behaviorally useful response that maintains ocular stability referenced to the head motion.

To illustrate this effect visually, vertical eye velocity is plotted in Figure 18 as a function of horizontal eye velocity for a sample of responses to IA (18A) and DV (18B) motion from preflight data of M906. Each of the two panels in Figure 18 consists of two components. In the upper trace of each, horizontal and vertical eye velocities are plotted as a function of time; in the X-Y plot beneath,

the vertical velocity for each cycle indicated (see methods) is plotted as a function of the horizontal velocity for the same cycle. Visual inspection allows the conclusion that during IA motion (18A), eye velocity is purely horizontal, while during DV motion (18B), velocity is purely vertical.

In Figure 19, a similar display is shown for responses during motion along an axis exactly intermediate between IA and DV, that is, with the head statically tilted around the roll axis by $\pm 45^\circ$ prior to delivery of the linear motion. The parameters of a least squares fit to these data are shown in the lower left corner of the top and bottom panels, and indicate statistically resultant eye motion within 2° to 3° of the applied linear motion.

Representative samples of pre- and postflight results for the two flight animals are shown in Figures 20 (M151) and 21 (M906). Plotting conventions are as in Figures 18 and 19. In each figure, examples of preflight (A&B), immediately postflight (C&D), and about 2 weeks postflight (E&F) data are shown for motion along axes between IA and DV. For M151 (Figure 20), the static head roll tilt was $\pm 25^\circ$ preflight (A&B) and $\pm 30^\circ$ for both postflight measures (C, D, E, F). For M906 (Figure 21), the static head roll was $\pm 45^\circ$ for all six examples shown. In Figure 20 (M151), the superimposed lines in the X-Y plots indicate the expected motion axes for the two conditions. In Figure 21 (M906), the superimposed lines result from least squares regressions to the plotted data, with the fit parameters in the lower left corner of each panel.

Comparison of pre- and postflight responses in Figures 20 and 21 shows that immediately postflight, M151's total eye velocity deviated substantially from the axis of linear motion, overshooting by 15 to 20° with either positive or negative static roll tilt. This finding indicates might be due either to an inappropriate signal of head tilt, or to an increased sensitivity of the vertical LVOR under these conditions. Data for this same animal at two weeks postflight appear similar to his preflight data. A similar comparison of pre- and postflight responses of M906 shows generally appropriate total eye velocity axis orientation using the same paradigm.

Motion along axes between IA and DV was delivered to the flight subjects prior to the flight along many axes (see methods). The experiment was repeated postflight, but unfortunately along a substantially reduced number of axes due to data collection time constraints discussed in the methods section. It was not possible to perform an experiment comparable in scope to the preflight measurements until over 2 weeks postflight (see schedule and methods), so only example data such as shown in Figures 20 and 21 C&D are available for characterization of immediate postflight responses.

Figures 22 and 23 show the data for this experiment performed preflight, at R+50 or R+53 hours, and at R+388 or R+391 hours (for M151 and M906 respectively). Data for each day are represented in three plots vertically, A, B, and C. All data points represent the mean ± 1 SD for data gathered at a single condition. Averages of cycles with vergences $< 4^\circ$ are circles, and those with vergences $> 4^\circ$ are triangles). In plot A, horizontal sensitivity is plotted as a function of the angle of the axis between IA and DV along which motion was delivered. With a static roll tilt of 0° (IA axis stimulation) horizontal response is maximal, and falls off roughly as a function of the cosine of angular roll tilt, until at $\pm 90^\circ$ (DV axis stimulation) the horizontal response is reduced to near zero. In plot B for each day, vertical sensitivity is plotted in a similar fashion. Now, at a static roll tilt of 0° (IA axis stimulation), the vertical response is minimal, and grows as a function of the sine of angular roll tilt until at $\pm 90^\circ$ (DV axis stimulation) the vertical response is maximal. To construct plot C, for each cycle of data included in A&B, the arctangent of the ratio of vertical sensitivity to horizontal sensitivity was calculated, and cycles for each axis of motion between IA and DV were averaged (± 1 SD). The arctangent values are plotted as a function of the angle of the motion axis between IA and DV in C. Ideally, these data should fall on a 45° line, indicating resultant eye motion exactly parallel to the axis of motion.

Figure 22 shows a summary of data for M151. Note that at R+50 hours, plot C shows the marked overshoot in vertical sensitivity for $\pm 30^\circ$ of static roll tilt that was illustrated in Figure 20. Note that by R+388 hours, the function is similar to the preflight data. The paucity of data at the immediate postflight session is evident.

The data summary for M906 shown in Figure 23 illustrate the finding already presented that both horizontal and vertical sensitivity for this animal were decreased postflight for equivalent vergence states (Plots A and B). They also show a marked overshoot (same direction as M151) from the expected with a 45° reorientation of the axis of motion during the R+53 hour session. Again, there are few data points for that day. These data are in contrast to the data shown in Figure 21C&D showing reasonable agreement at R+22 hours. Furthermore, the orientation of the eye velocity axis at R+391 hours, as shown in Figure 23C is clearly different from the preflight plot. Further analysis will be required to sort out these differences.

Pre- and postflight time framework data for one of the control animals (M907) in response to motion along axes between IA and DV at 5 Hz (0.5g) are shown in Figure 24 for comparison with the data from the flight animals. Data are plotted in a fashion similar to the data of Figures 22&23 for the flight animals. Labeling conventions are as in the above figures.

Motion along the naso-occipital (NO) axis and along axes between NO and DV

Linear vestibulo-ocular reflexes generated during high frequency (>1 Hz) linear motion along a naso-occipital axis have been shown to be interesting and complex in squirrel monkeys, especially in their interaction with visual mechanisms (for discussion, see Paige & Tomko, 1991b). In brief, the sensitivity of the VORs required during such motion increases not just as intended target distance from the subject decreases, but also as gaze position in space becomes more eccentric. With gaze directed straight ahead (along the visual axis), there is no requirement for compensatory eye movements other than a vergence VOR in which the eyes converge and diverge (i.e., move 180° out of phase with one another) at the fundamental stimulus frequency to enable steady fixation on the visual target, as the head moves toward and away from the target. During target fixation to the right or left during forward motion along the NO axis, eye motion must be to the right or left respectively, that is to say 180° out of phase. The basic finding is similar in rhesus monkeys, and is illustrated by preflight recordings from animals M151 and M906 in Figures 25 and 26 parts A through D. Horizontal sensitivity and phase are plotted in parts A&B as a function of horizontal eye position in the orbit. Vertical sensitivity and phase are plotted in a parallel fashion in parts C&D. Each point represents the sensitivity or phase in response to a single cycle of NO stimulation; open points are from VSLVOR trials (head fixed visual targets), and closed points are from LVOR (dark) trials. The slight deviations from zero in their inflection points are due to slight deviations in the placement of the head-holders; if placed so that the head were oriented straight ahead (with no static yaw) and roughly in the place of the horizontal semicircular canals, both the horizontal and vertical functions would be organized around orbital zero.

In additional studies in the squirrel monkey, we found that when motion occurred along axes between NO and IA or between NO and DV, the functions described above we organized parallel to the axis of motion, that is to say, relative to gaze in space, rather than to eye position in the head (for further discussion see Tomko & Paige, 1992). For the COSMOS 2229 experiments, we used motion along axes between NO and DV, since those axes change the orientation of the head with respect to gravity, as was the case for axes between IA and DV. The head was therefore statically re-oriented using varying amounts of head pitch (see methods for details). Preflight results are shown in Figures 25 and 26 (parts E through H) for the two flight monkeys for linear motion after the head was pitched -10° (nose down). Note that the horizontal sensitivity and phase plots are similar to the "unpitched" shifted about 10° toward the nose up direction.

Postflight data for these same conditions are plotted in Figures 27 and 28 for the two flight monkeys. It can be seen by comparing Figures 27 and 25 that pre- and postflight responses for M151 were similar to one another in this experiment, while comparing Figures 28 and 26 shows that responses of M906 were smaller and more variable postflight. Whether this difference for M906 is real requires further analysis. Since M906 had reduced sensitivities to linear motion postflight, the increased variability might be related to the increased uncertainty in calculating sensitivity and phase due to the fact that the responses were small.

CONCLUSIONS

There were interesting changes in vestibulo-ocular control in both flight monkeys following the Cosmos 2229 flight. No clear pattern has emerged, as is apparent from the table on the following page where a synopsis of the findings is presented. Each animal exhibited changes in oculomotor function; some changes were common to both monkeys, while others occurred in a single subject.

Both flight monkeys had lower AVOR gain in response to pitch and yaw head movements immediately postflight. M906 had a 50% reduction in AVOR gain in response to roll, while M151 had similar AVOR roll gains pre- and postflight. Since pitch and roll angular motion involve otolith activation, changes in these functions postflight probably indicate changes in otolith function or in interpretation of otolith output by central mechanisms associated with adaptation to microgravity.

During IA and DV head motion at 5 Hz (0.5g), M906 had large reductions in the slope of the function relating LVOR sensitivity to vergence that did not recover by R+391 hours. Under the same conditions, M151 showed similar responses pre- and postflight, but may have had similar reductions in sensitivity during recovery. A reduction in sensitivity to linear motion such as shown by M906 might be the result of an adaptive strategy to reduce dissonance between oculomotor and visual mechanism due to adaptation processes in microgravity. It is interesting to note in this regard that M151 exhibited signs of space motion sickness (anorexia and lethargy during flight), while M906 did not. Perhaps the adaptive strategies of M151 were less robust or effective than those of M906, leaving M151's postflight responses less changed than those of M906.

During Earth-horizontal linear motion along axes between IA and DV (with the head statically tilted in roll), both monkeys showed a tendency for the overall orientation of eye velocity to be not parallel to the axis of motion. This very interesting result would appear to indicate some change in otolith response associated with adaptation to microgravity. One possible explanation might be that the otoliths are providing an inappropriate signal of head tilt; a second might be that otoliths are providing increased sensitivity of the vertical LVOR under these conditions. This would be interesting if this were the case, since both monkeys showed a reduction in sensitivities to pure IA and DV motion.

During NO head motion, pre- and postflight responses for M151 were similar to one another, while responses of M906 were smaller and more variable postflight.

Correct analysis and interpretation of data from visual receptors during normal behavior depends on precise oculomotor control. Our results are consistent with previous reports that there are important changes in oculomotor control during adaptation to microgravity.

SYNOPSIS OF FINDINGS

	ANGULAR RESPONSES			LINEAR RESPONSES			AXES BETWEEN IA&DV	AXES BETWEEN NO&DV
	YAW	PITCH	ROLL	IA	DV	NO		
M151	SAME	REDUCED	SAME	SAME	VERGENCE FUNCTION REDUCED AFTER DELAY	SAME	CHANGED	SAME
M906	SAME	REDUCED	REDUCED	VERGENCE FUNCTION REDUCED TO R+388	VERGENCE FUNCTION REDUCED TO R+388	SMALLER AND MORE VARIABLE	CHANGED?	CHANGED?

REFERENCES

1. Anderson, J.H., and S.L. Liston. Asymmetry in the Human Vertical Vestibuloocular Reflex. *Abst. Assn. Res. Otolaryngol.* 6:82, 1983.
2. Arrott, A.P., and L.R. Young. Perception of Linear Acceleration in Weightlessness. In *Scientific Results of the D-1 Mission, DFVLR*, 1987.
3. Barmack, N.H. A Comparison of the Horizontal and Vertical Vestibulo-ocular Reflexes of the Rabbit. *J. Physiol. (Lond.)* 314:547-564, 1981.
4. Barmin, V.A., Kreidich Yu. V., and I.B. Kozlovskaya. Influence of Optokinetic Stimulation and Immersion on the Eye-head Coordination in Man. *The Physiologist*, 26:Suppl:S83-S85, 1983.
5. Benson, A.J. Modification of Response to Angular Accelerations. *Hndbk Sensory Physiology*, ed. Kornhuber, V6(2):281-320, 1974.
6. Benson, A.J., and M. Bodin. Interactions of Linear and Angular Accelerations on Vestibular Receptors in Man, *Aerospace Med.* 37:144-158, 1966a.
7. Benson, A.J., and M.A. Bodin. Effect of Orientation to the Gravitational Vertical on Nystagmus Following Rotation about a Horizontal Axis. *Acta Oto-Laryngol.* 61:517-526, 1966b.
8. Benson, A.J., and F.E. Guedry. Comparison of Tracking-task Performance and Nystagmus During Sinusoidal Oscillation in Yaw and Pitch. *Aerosp. Med.* 42:593-601, 1971.
9. Bizzi, E., Kalil R.E., and V. Tagliasco. Eye-head Coordination in Monkeys: Evidence for Centrally Patterned Organization. *Science* 173:452-454, 1971.
10. Bizzi, E., Kalil R.E., and P. Morasso. Two Modes of Active EyeHead Coordination in Monkeys. *Brain res.* 40:45-48, 1972.
11. Bond, H.W., and P. Ho. Solid Miniature Silver-Silver Chloride Electrodes for Chronic Implantation. *EEG Clin. Neurophysiol.* 28:206-208, 1970.
12. Buttner, U.W., Henn V., and L.R. Young. Frequency Response of Vestibulo-ocular Reflex (VOR) in the Monkey. *Aviat. Space Environ. Med.* 52:73-77, 1981.
13. Carpenter, R.H.S. (1977) *Movements of the Eyes.* Pion, London.
14. Clément, G., Viéville T., Lestienne, F. and A. Berthoz. Modifications of Gain Asymmetry and Beating Field of Vertical Optokinetic Nystagmus in Microgravity. *Neuroscience Letters* 63:271-274, 1986.
15. Clifford, J.O, Paige G.D., and D.L. Tomko. Effect of Roll Tilt on Eye Movements During 5 Hz Interaural Linear Acceleration. *Neurosci. Abstr.*, 16, 736, 1990.
16. Cohen, B, Matsuo V., and T. Raphan. Quantitative Analysis of the Velocity Characteristics of Optokinetic Nystagmus and Optokinetic After-nystagmus. *J. Physiol. (Lond.)* 270:321-344, 1977.

17. Collewijn, H. Integration of Adaptive Changes of the Optokinetic Reflex, Pursuit and the Vestibulo-ocular Reflex. in *Adaptive Mechanisms in Gaze Control: Facts & Theories*, Berthoz, A., Melvill Jones, G. (eds.) Elsevier Science Publishers: Amsterdam, 51-69. 59:185-196, 1985.
18. Correia M.J. and K.E. Money. The Effect of Blockage of all Six Semicircular Canal Ducts on Nystagmus Produced by Dynamic Linear Acceleration in the Cat. *Acta Oto-Laryngol* 69:7-16, 1970.
19. Darlot, C., Lopez-Barneo J., and D. Tracey. Asymmetries of Vertical Vestibular Nystagmus in the Cat. *Exp. Brain Res.* 41:420-426, 1981.
20. Eliot, T.S., Burnt Norton, Harcourt, Brace & World, Inc., New York, 1943 Fuller, C. Early Adaptation to Altered Gravitational Environments in the Squirrel Monkey. *The Physiologist* 28: S201 - S202, 1985.
21. Gonshor, A., and G. Melvill Jones. Short-term Adaptive Changes in the Human Vestibulo-ocular Reflex arc. *J. Physiol.*, 376: 361-379, 1976.
22. Grigoryan, R., O. Gazenko, Kozlovskaya I., Barmin V., and Yu. Kreidich. The Vestibulo-cerebellar Regulation of Oculomotor Reactions in Micro-gravitational Conditions. in Keller, E., Zee, D. (eds.) *Adaptive Mechanisms in Visual & Oculomotor Systems*, Pergamon Press, New York, 121-127, 1986.
23. Gualtierotti, T., Bracchi F., and E. Rocca. Orbiting Frog Otolith Experiment (OFO-A) Final Report of the Data Reduction & Control Experimentation. Piccin Medical Books, Milan. 1972.
24. Haddad, F.B., Paige G.D., Doslak M.J., and D.L. Tomko. Practical Method, and Errors, in 3-D Coil Eye Movement Measurements. *Invest. Ophthalmol. & Vis. Sci. (ARVO Suppl.)*, 1988.
25. Harris, L.R. (1987) Vestibular and Optokinetic Eye Movements Evoked in the Cat by Rotation about a Tilted Axis. *Exp. Brain Res.* 66:522-532, 1987.
26. Igarashi, M., Takahashi T., Kubo T., Alford B.R., and W.K. Wright. Effect of Off-vertical Tilt and Macular Ablation on Postrotatory Nystagmus in the Squirrel Monkey. *Acta Oto-Laryngol* 90:93-99, 1980.
27. Igarashi, M., Takahashi M., Kubo T., Levy J.K., and J.L. Homick. Effect of Macular Ablation on Vertical Optokinetic Nystagmus in the Squirrel Monkey. *ORL* 40:312-318, 1978.
28. Kozlovskaya, I.B., Barmin V.A., Kreidich Yu.V., and A.A. Repin. The Effects of Real and Simulated Microgravity on Vestibulo-oculomotor Interaction. *The Physiologist* 28(6 Suppl.) S51-S56, 1985.
29. Kozlovskaya, I.B., Babaev B.M., Barmin V.A., Beloozerova I.N., Kreidich Yu.V., and M.G. Sirota. The Effect of Weightlessness on Motor and Vestibulo-motor Reactions. *The Physiologist*, 6:111-114, 1984.
30. Lisberger, S.G., and F.A. Miles. Role of Primate Medial Vestibular Nucleus in Long-term Adaptive Plasticity of Vestibuloocular Reflex. *J. Neurophysiol.* 43:1725-1745, 1980.
31. Matsuo, V., and B. Cohen. Vertical Optokinetic Nystagmus and Vestibular Nystagmus in the Monkey: Up-Down Asymmetry and Effects of Gravity. *Exp. Brain Res.* 53:197-216, 1984.

32. Niven, S.I., Hixson C.W. and M.J. Correia. Elicitation of Horizontal Nystagmus by Periodical Linear Acceleration. Nav. Aerospace Med. Inst. Rpt. NAMI-953, 1965.
33. Oman, C.M., Lichtenberg B.K., Money K.E., and R.K. McCoy. MIT/Canadian Vestibular Experiments on Spacelab-1. IV. Space Motion Sickness: Symptoms, Stimuli, and Predictability. Exp. Brain Res. 64:347-357, 1986.
34. Paige, G.D. Vestibuloocular Reflex and its Interactions with Visual Following Mechanisms in the Squirrel Monkey. I. Response characteristics in Normal Animals. J. Neurophysiol. 49:134-151, 1983a.
35. Paige, G.D., and D.L. Tomko. Canal-otolith Interactions in the Vestibulo-ocular Reflex (VOR). Invest. Ophthalmol. & Vis. Sci. (ARVO Suppl.), 28:332, 1987.
36. Paige, G.D., and D.L. Tomko. Visual-vestibular Interactions in the Linear Vestibulo-ocular Reflex. Invest. Ophthalmol. & Vis Sci. (ARVO Suppl.), 1988a.
37. Paige, G.D., and D.L. Tomko. Linear Vestibulo-ocular Reflex (LVOR) of Squirrel monkey. II. Visual-vestibular Interactions. Neurosci. Abstr., 1988b.
38. Paige, G.D., and D.L. Tomko. The Linear Vestibulo-ocular Reflex in Squirrel Monkey. I. Basic Characteristics. J. Neurophysiol., 65(5), 1170-1182, 1991a.
39. Paige, G.D., and D.L. Tomko. The Linear Vestibulo-ocular Reflex in Squirrel Monkey. II. Visual-vestibular Interactions and Kinematic Considerations. J. Neurophysiol., 65(5), 1183-1196, 1991b.
40. Parker, D.E., Reschke M.F., Arrott A.P., Homick J.L., and B.K. Lichtenberg. Otolith Tilt-Translation Reinterpretation Following Prolonged Weightlessness: Implications for Preflight Training. Aviat. Space Environm. Med. 56:601-606, 1985.
41. Raphan, T., and B. Cohen. Organizational Principles of Velocity Storage in Three Dimensions: The Effect of Gravity on Cross-coupling of Optokinetic After-nystagmus (OKAN). Ann. New York Acad. Sci., in press. 1988.
42. Raphan, T, Matsuo V., and B. Cohen. Velocity Storage in the Vestibulo-ocular Reflex Arc (VOR). Exp. Brain Res. 35:229-248, 1979.
43. Reschke, M.F., and D.E. Parker. Effects of Prolonged Weightlessness on Self-Motion Perception and Eye Movements Evoked by Pitch and Roll. Aviat. Space Environm. Med. 58(9,Suppl.):A153-158, 1987.
44. Robinson, D.A. A Method of Measuring Eye Movements Using Ascleral Search Coil in a Magnetic Field. IEEE Trans. Biomed. Electron. 10:137-145, 1963.
45. Shipov, A.A., Sirota M.G., Beloozerova I.N., Babaev B.M., and I.B. Kozlovskaya. Results of the Tests on the Primate VestibuloVisualmotor Reactions in Biocosmos Experiments. in Keller, E.L., & Zee, D.S. (eds.) Adaptive Mechanisms in Visual & Oculomotor Systems, Pergamon Press, New York, 129-132, 1986.
46. Sirota, M.G., Babaev B.M., Beloozerova I.B., Nyrova A.N., and S.B. Jakushin. Characteristics of Vestibular Reactions to Canal and Otolith Stimulation at an Early Stage of Microgravity. Physiologist, Suppl. 30:S82-S84, 1987a.

47. Sirota, M., Babaev B., Beloozerova I., Nirova A., Jakushin S., and I. Kozlovskaja. Neuron Activity of Nucleus Vestibularis during Coordinated Movement of Eyes and Head in Microgravitation. Abstr. & pres., Symp. on Gravitational Physiol., Intl. Union of Physiol. Sci., Nitra, Czechoslovakia. 1987b.
48. Staab, J.P., Wall C., Robinson F.R., and D.L. Tomko, An Analysis fo Asymmetries in Cat Vertical Eye Movements Generated by Sinusoidal Pitch. *Aviat. Space Environm. Med* 58(9, Suppl.): A189-191, 1988.
49. Tomko, D.L., G.D. Paige. Linear Vestibulo-ocular Reflex (LVOR) during Motion Along Axes from Naso-occipital (NO) to Interaural (IA). in: *Annals of the New York Academy of Sciences*, Vol. 656, 233-241, 1992.
50. Tomko, D.L., Wall III C. , and F.R. Robinson. Vertical Eye Movements and Vertical Semicircular Canal Responses in Cat during Normal Pitch and during Pitch with the Animal Positioned on its Side. *Neurosci. Abstr.* 10(2):539, 1984.
51. Tomko, D.L., Wall III C., Robinson F.R., and J.P. Staab. Influence of Gravity on Cat Vertical Vestibulo-ocular Reflex. *Exp. Brain Res.* 69:307-314, 1988.
52. Vallotton, W., Matsuhira D., Wynn T., and J. Temple. Portable Linear Sled (PLS) for Biomedical Research. in *NASA Conference Publication 3205, 27th Aerospace Mechanisms Symposium*. 1993.
53. Viéville, T., Clément, G., Viéville T., Lestienne F., and A. Berthoz. Adaptive Modifications of the Optokinetic and Vestibulo-ocular Reflexes in Micro-gravity. in E. Keller & D. Zee (eds.) *Adaptive Mechanisms in Visual and Oculomotor Systems*. Pergamon Press, pp. 97-106, 1986.
54. Viirre, E., Tweed D., Milner L., and T. Vilis. A Reexamination of the Gain of the Vestibuloocular Reflex. *J. Neurophysiol.* 56:439-450, 1986.
55. Young, L.R. Effects of Linear Acceleration on Vestibular Nystagmus. 3rd Symp. Role of Vestib. Organs in Space Exploration NASA SP-152:383-391, 1967.

TABLES AND FIGURES

TABLE 1 - ANALYSIS OF FIGURE 7 DATA

VOR/ANALYSIS V1.01 M906R.000 11-29-1993
 NAME: M906
 TEST: , CAL. FACTOR: 5.0, A/D: 200 Hz, TOTAL TIME: 8.73
 DESACCADED AT 0.635 SEC IN EPOCH # 1
 DATA FILE: 10-10-92 10:38:17 280 BLOCKS (SECTORS)
 HEADER MESSAGE:
 NA 10-OCT-92 10:38:17 M906

===== CYCLE RESULTS (HANDFIT) =====											
CYC	STIMULUS (HWT)				RESPONSE (HE1)				(HE2)		
	DC	AMP	PHI	RMS	DC	AMP	PHI	RMS	GAIN	PHA	EXTRA
1	-0.43	50.94	-95.7	3.1	0.00	50.94	-275.7	4.6	1.00	0.0	-4.2
2	-0.16	47.85	-88.3	2.2	0.00	50.94	-275.7	4.5	1.06	-7.3	-18.1
3	0.91	46.69	-99.0	2.9	0.00	50.94	-275.7	2.9	1.09	3.4	-5.5
4	-0.02	46.16	-103.2	4.7	0.00	50.94	-275.7	5.6	1.10	7.5	-12.9
5	0.82	48.12	-102.2	4.5	0.00	50.94	-275.7	5.3	1.06	6.6	0.6
AVERAGE											
	0.22	47.95	-97.7	3.5	0.00	50.94	-275.7	4.6	1.06	2.0	-8.0
SD											
	0.61	1.85	6.0	1.1	0.00	0.01	0.0	1.0	0.04	6.0	7.4
===== CYCLE RESULTS (FOURIER) =====											
CYC	DC	AMP	PHI	RMS	DC	AMP	PHI	RMS	GAIN	PHA	FREQ
1	-0.43	50.94	-95.7	3.1	-0.01	58.48	85.9	3.2	1.15	1.5	0.746
2	-0.16	47.85	-88.3	2.2	0.94	54.10	92.4	3.2	1.13	0.8	0.769
3	0.91	46.69	-99.0	2.9	-2.14	52.26	79.2	1.8	1.12	-1.7	0.746
4	-0.02	46.16	-103.2	4.7	-0.35	54.44	80.7	4.8	1.18	3.9	0.714
5	0.82	48.12	-102.2	4.5	-2.90	55.96	79.0	4.3	1.16	1.3	0.746
AVERAGE											
	0.22	47.95	-97.7	3.5	-0.89	55.05	83.4	3.5	1.15	1.1	0.744
SD											
	0.61	1.85	6.0	1.1	1.58	2.33	5.7	1.2	0.02	2.0	0.020
===== GRAND AVERAGE =====											
	0.54	48.01	-103.4	2.6	-1.34	55.23	77.9	2.2	1.15	1.3	
HARM	AMP	PHI	AMP	PHI							
0	0.54	0.00	-1.34	0.00							
1	48.01	-103.40	55.23	77.91							
2	1.00	-134.38	0.70	22.45							
3	2.11	-51.16	2.15	118.50							
4	0.80	-147.41	0.72	63.93							
5	1.84	-32.72	0.62	171.57							
6	0.55	-90.55	0.36	94.19							
7	1.18	-30.48	0.84	117.45							
8	0.44	-79.83	0.37	143.07							
9	0.69	-37.28	0.82	167.15							
10	0.32	-78.87	0.33	120.24							
HARMONIC DISTORTION											
7.29%				5.06%							

TABLE 2 - PRE-AND POST-FLIGHT TEST SCHEDULE

PRE-FLIGHT TEST DATES		POST-FLIGHT TEST DATES							POST-FLIGHT CONTROLS	
MONK#	1st	2nd	1/11	1/12	1/13	1/14	1/17	1/21	1/26	
*M151	10/13/92	10/14/92		R+50	R+74		R+171	R+254	R+388	
M401	10/15/92	10/16/92								
M417	10/19/92	NONE								
M476	10/10/92	10/11/92								
M588	10/15/92	10/16/92								
M775	10/17/92	10/18/92								1/18 1/22
M803	10/12/92	10/14/92								1/16 1/21
M838	10/08/92	10/09/92								
XM856	10/12/92	10/13/92								
M892	10/08/92	10/09/92								
*M906	10/10/92	10/11/92	R+22	R+53		R+101	R+173	R+248	R+391	
M907	10/17/92	10/18/92								1/25

*FLIGHT MONKEY
XDeceased

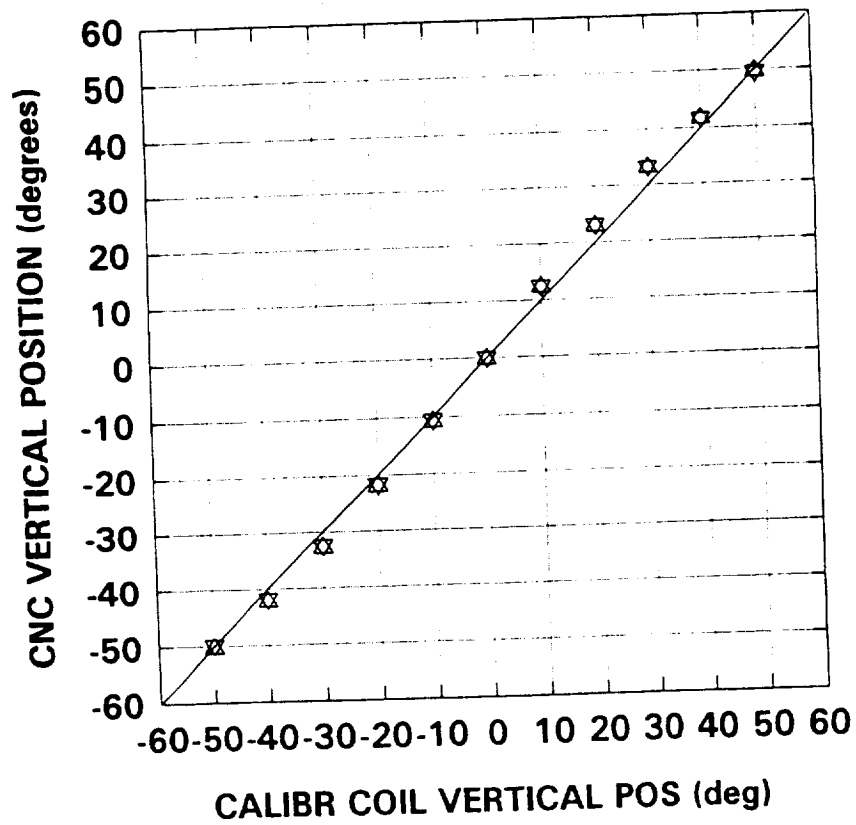
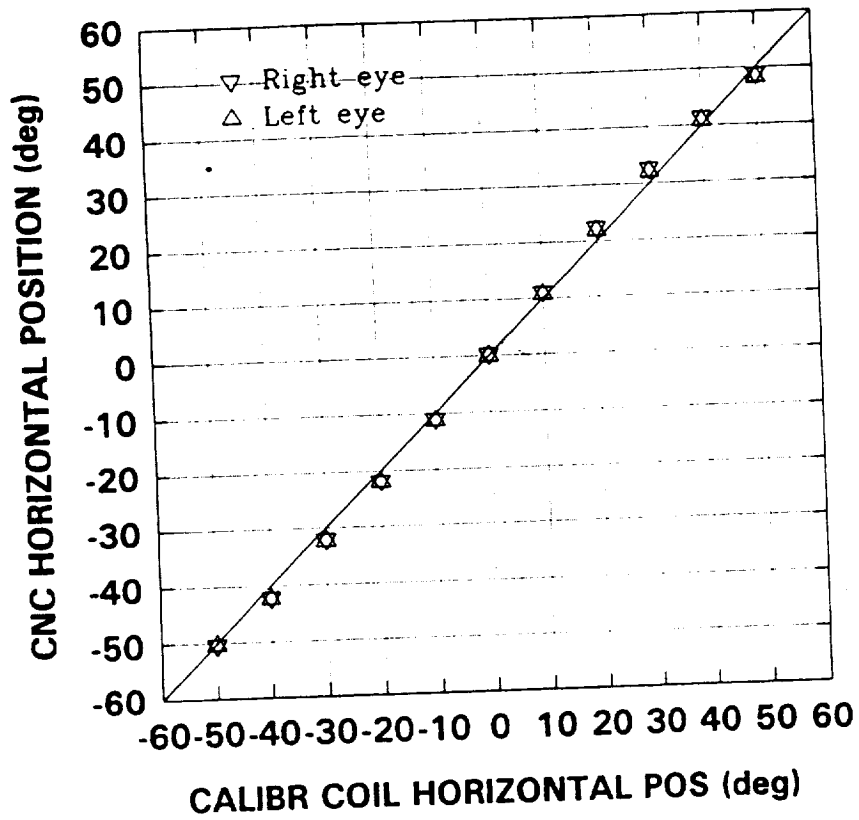


Figure 1. Eye coil calibration data.

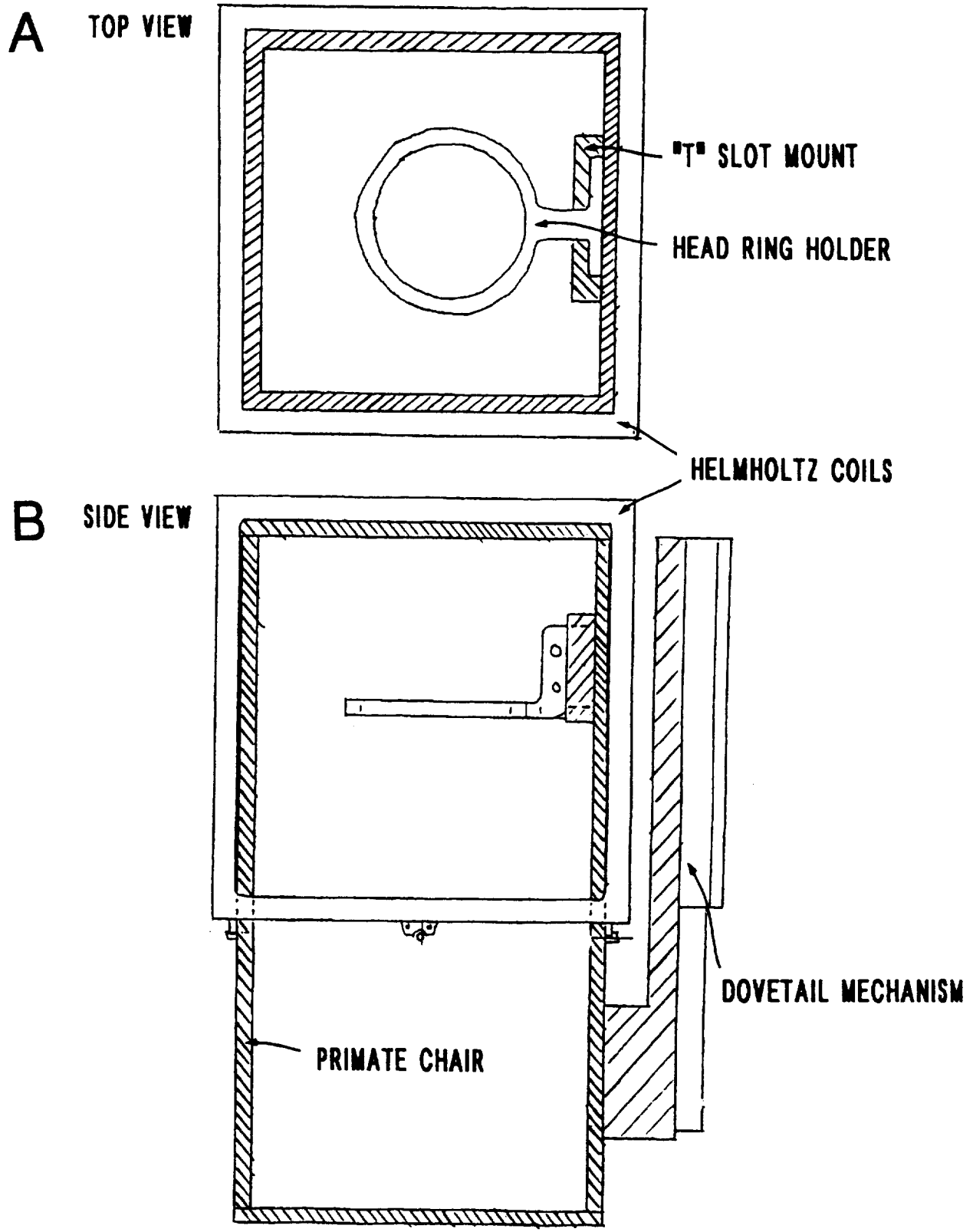


Figure 2. Primate chair and Helmholtz coils.

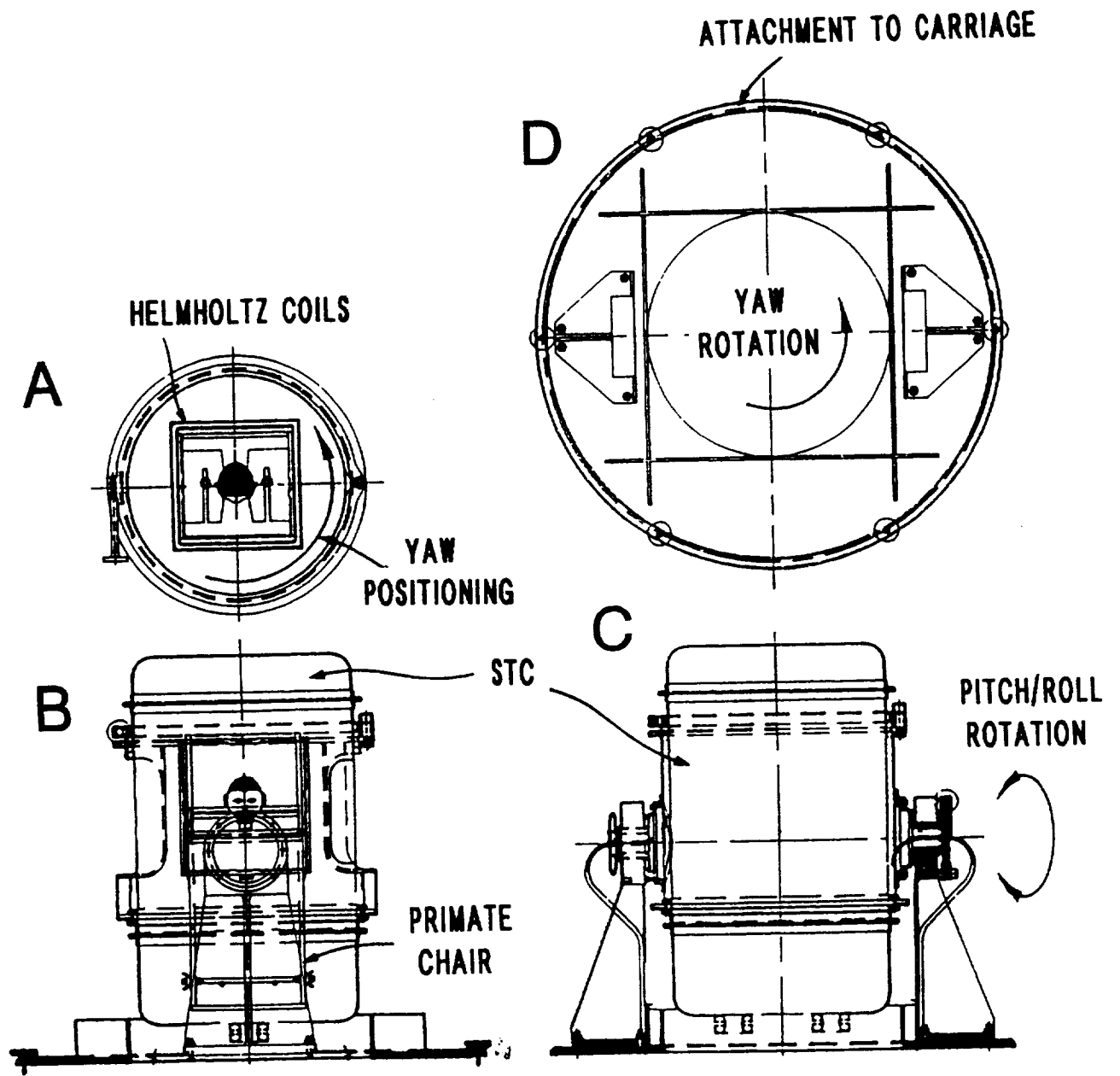


Figure 3. Specimen test container and Gimbal mount.

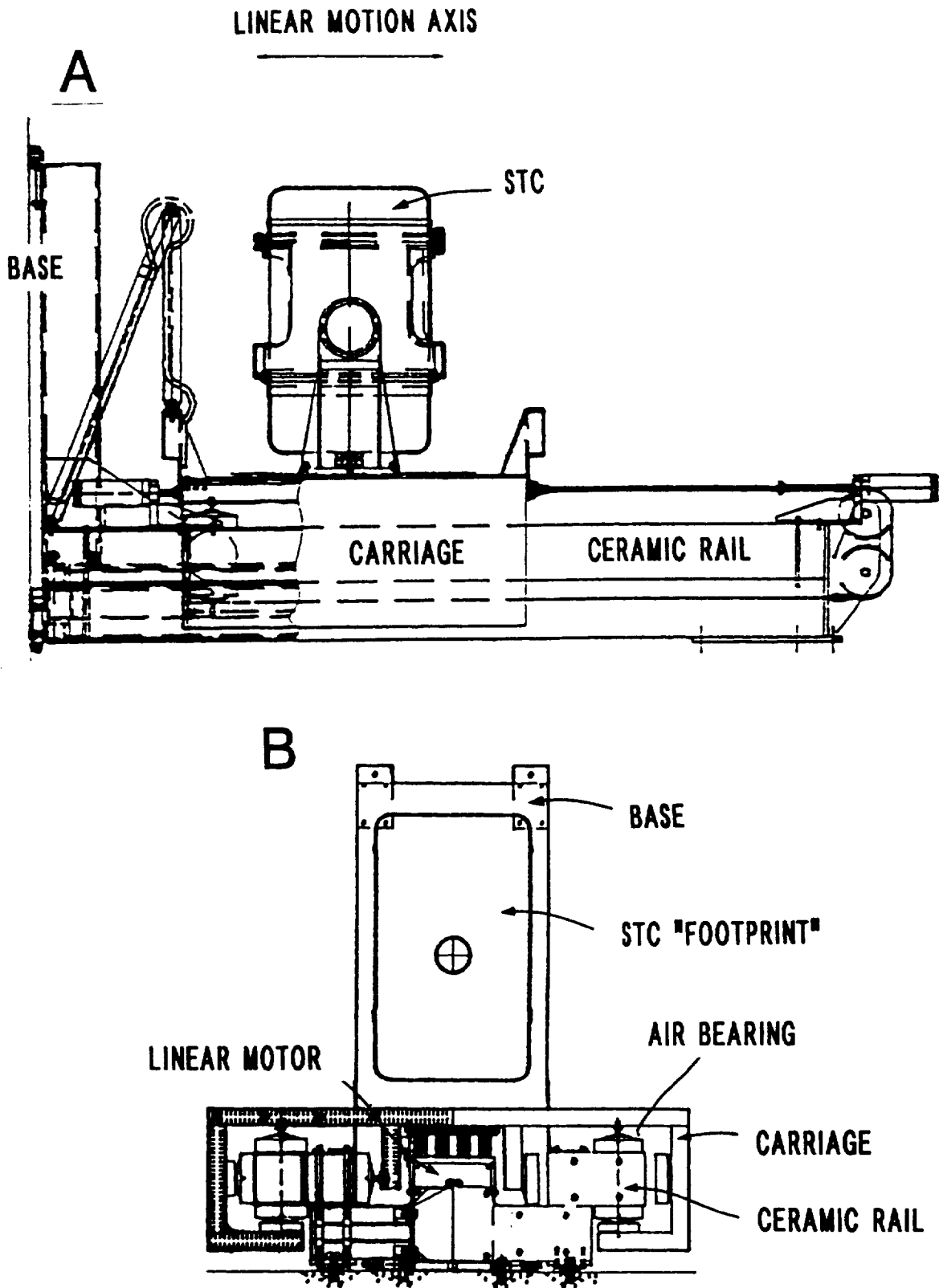


Figure 4. Portable linear sled (PLS).

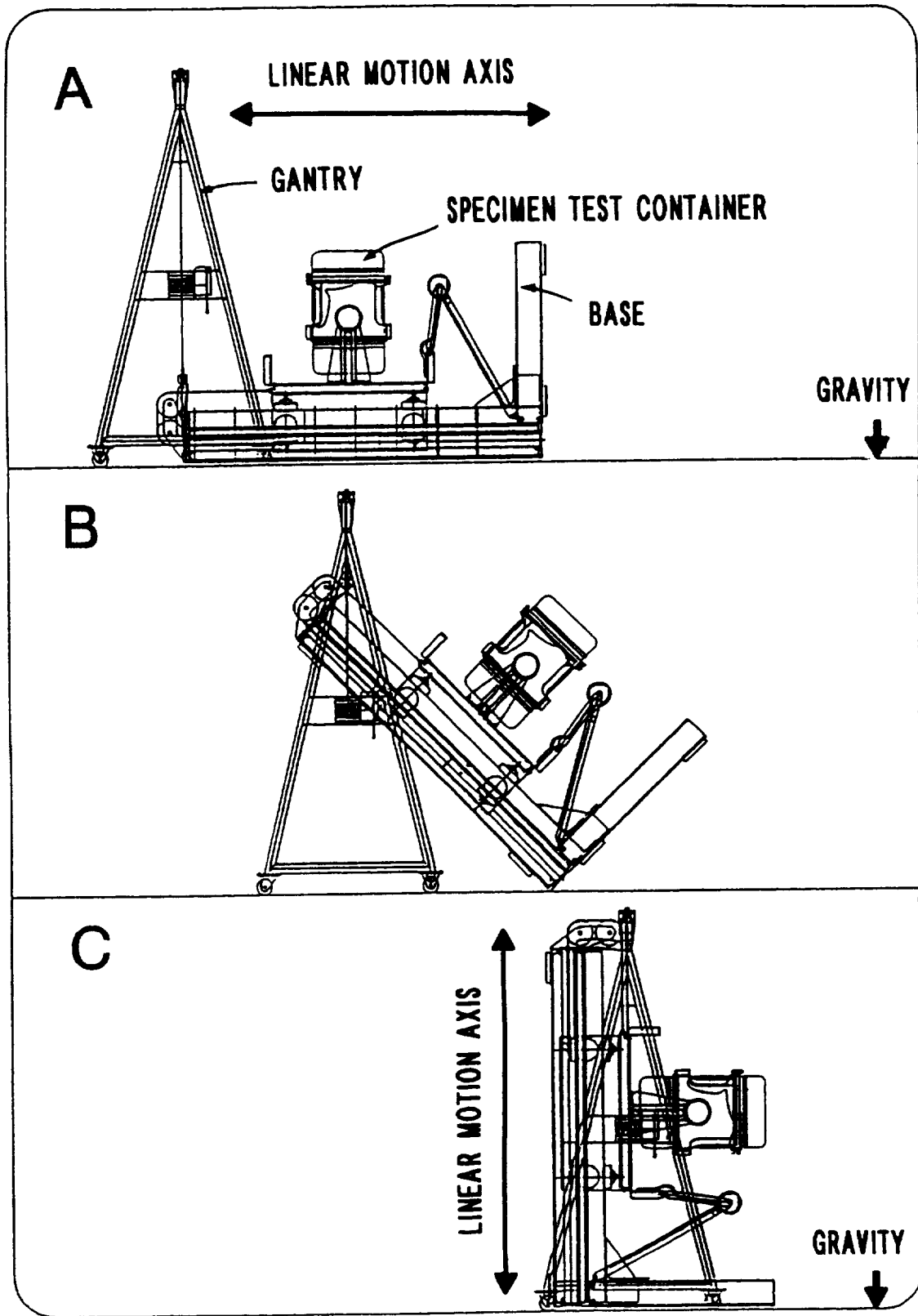


Figure 5. PLS operating modes.

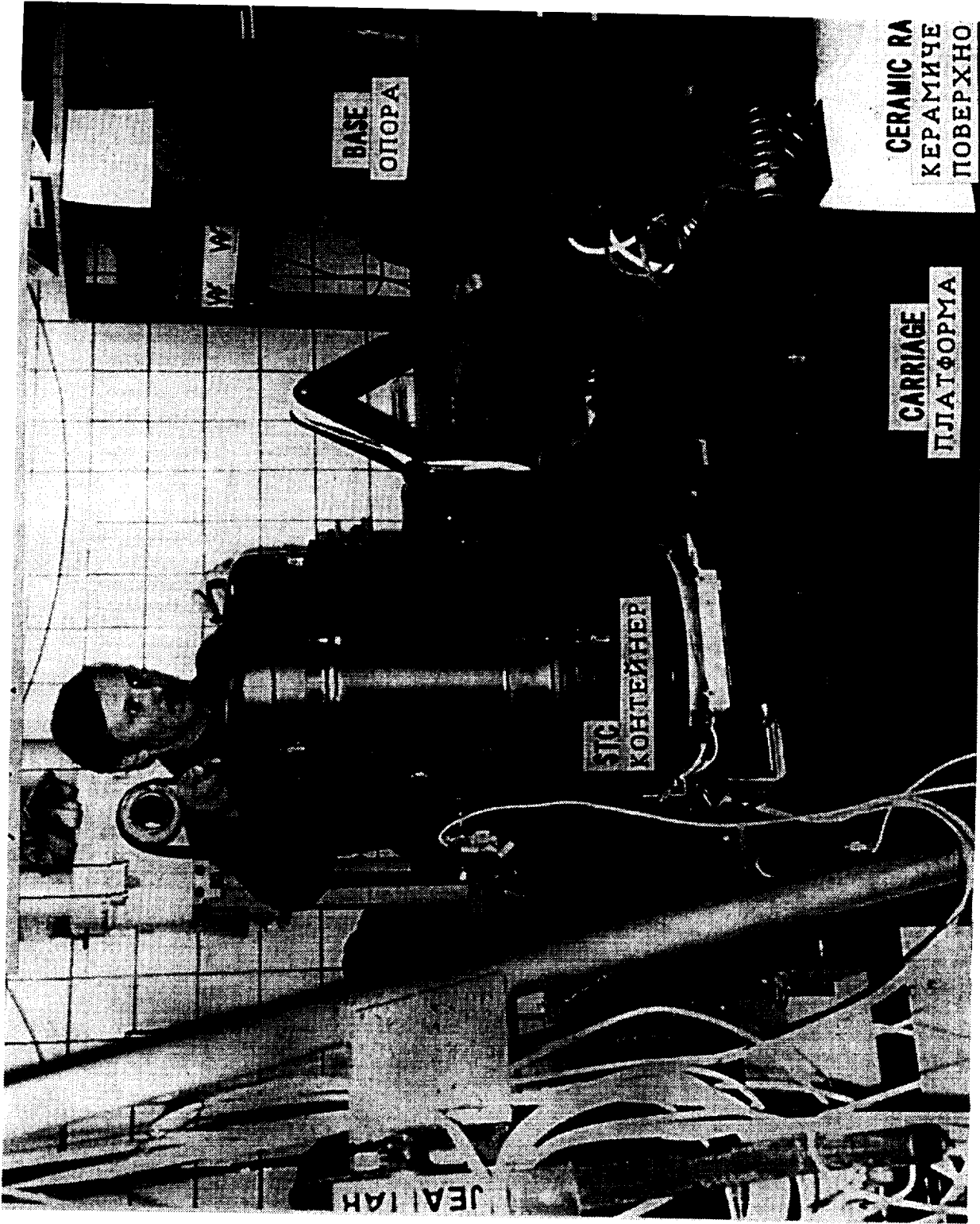


Figure 6. PLS operation at Institute for Biomedical Problems.

11-29-1993

M906R.000

DATA ANALYSIS (VOR VER: 1.01)

EXP DATE: 10-10-92 TIME: 10:38:17 A/D: 200Hz
HWT 11.30.0 HE1 5.0 VE1 6.5.0
PLOT RESOLUTION: 2000.0 PW: 0.1 0.3 0.2 0.1 0.4 0.3
COMMENT #1: NA 10-OCT-92 10:38:17 M906
COMMENT #2:
COMMENT #3:

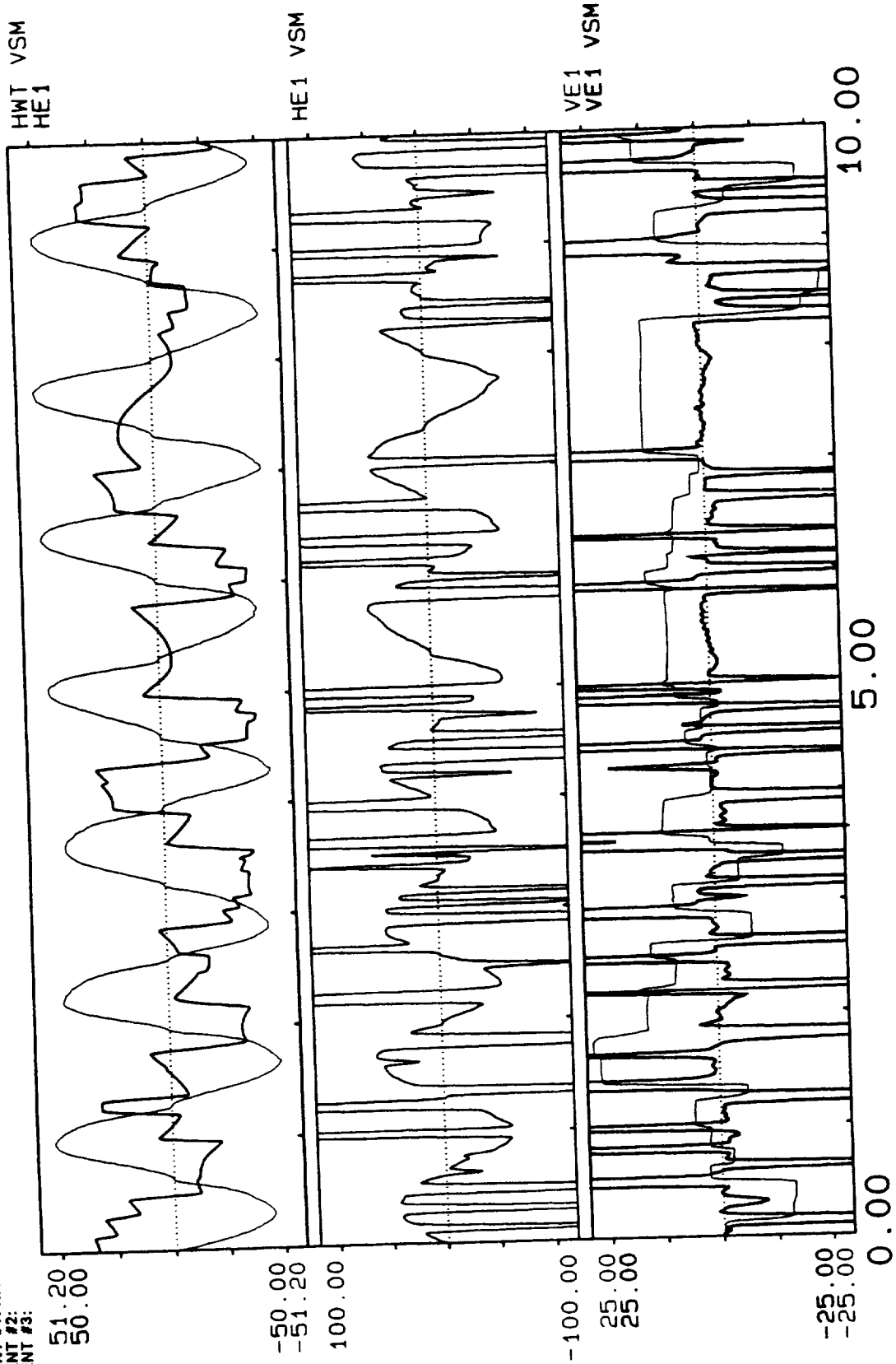
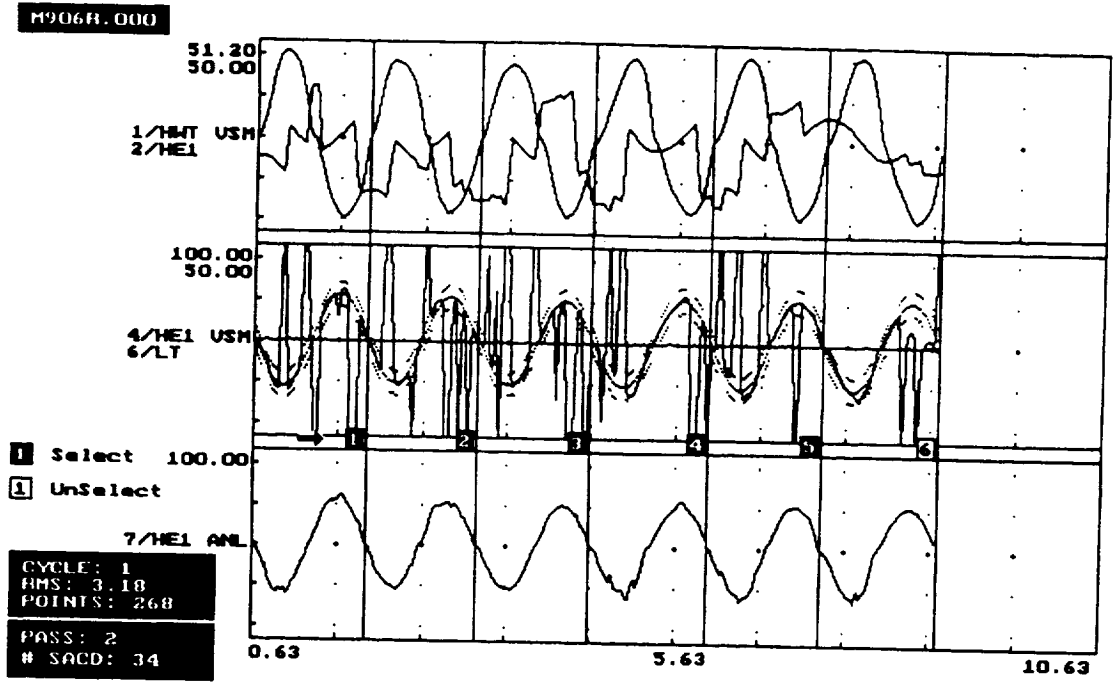


Figure 7. Pre-flight yaw responses for M906.

A



B

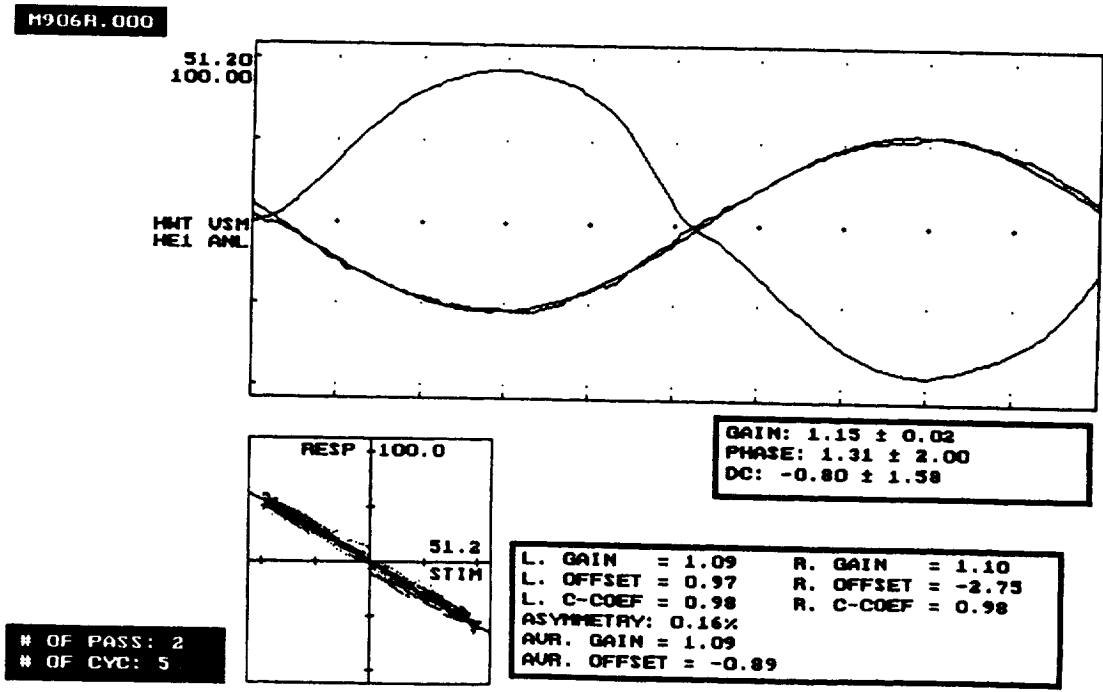


Figure 8. Analysis of figure 7 data.

11-28-1993

M151R.006

DATA ANALYSIS (VOR VER: 1.01)
EXP DATE: 10-13-92 TIME: 14:32:24 A/D: 200HZ
ACC 14.0.1 HE1 5.0 HE2 8.5.0 VE1 6.5.0 TE1 7.1.0 VER 15.5.0
PLOT RESOLUTION: 2000.0 PW: 0.1 0.3 0.5 0.2 0.4 0.1 0.4 0.6 0.3
COMMENT #1: NA 13-OCT-92 14:32:24 M151
COMMENT #2:
COMMENT #3:

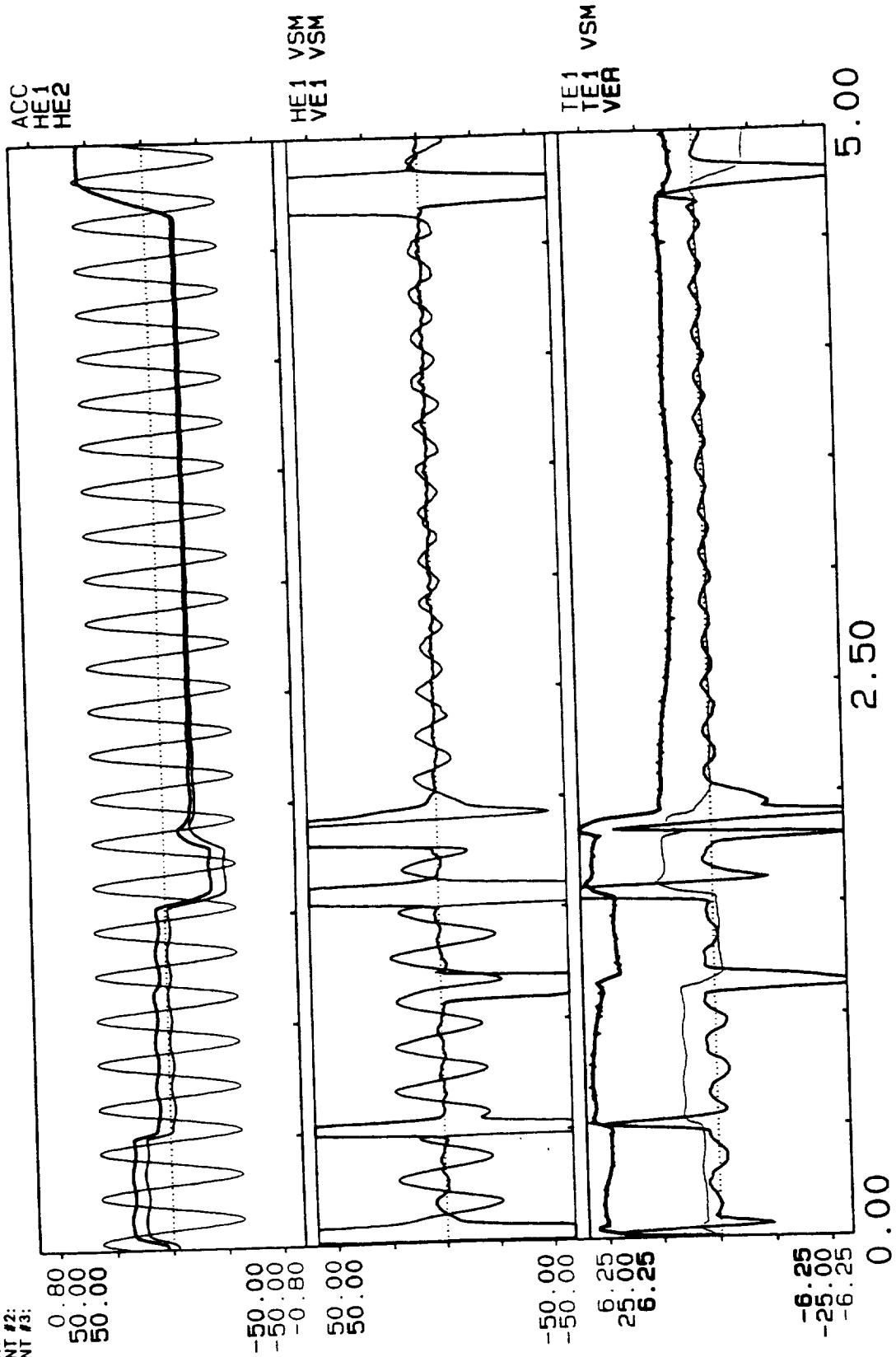


Figure 9. Pre-flight IA response for M151.

ML51R.006

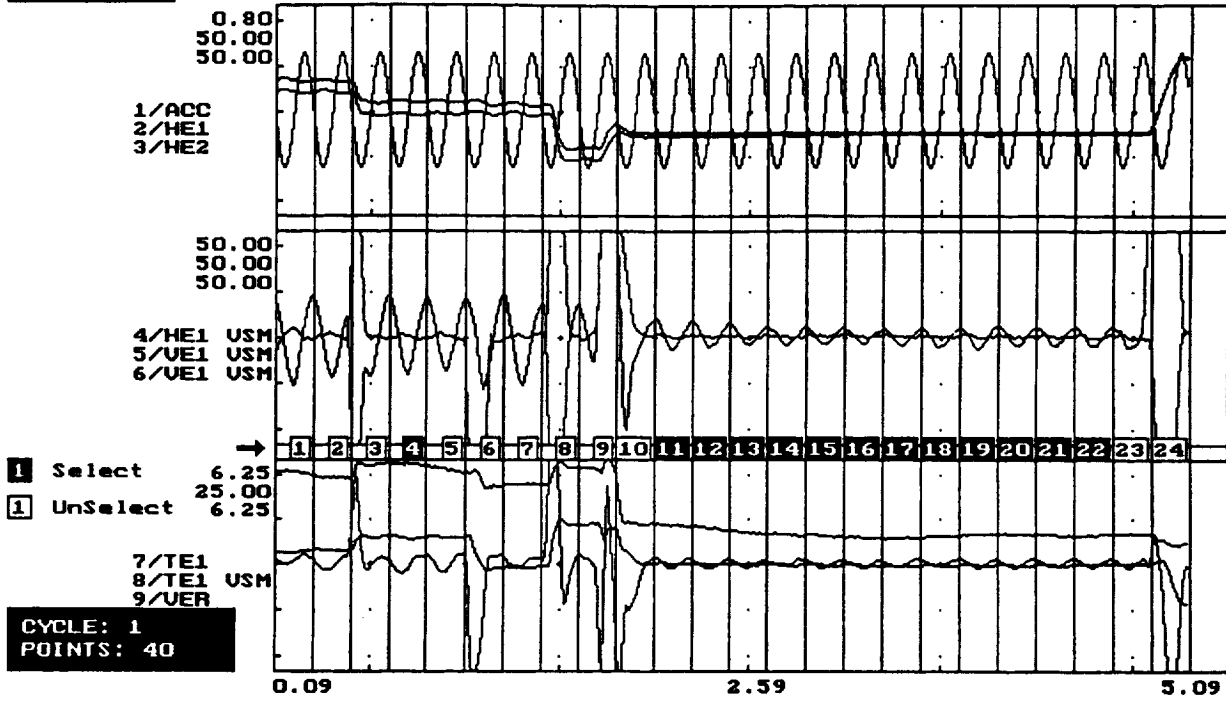


Figure 10. Analysis of figure 9 data.

COSMOS 2229 ANGULAR VESTIBULO-OCULAR REFLEX RESPONSES TO MID-FREQUENCY STIMULI (0.5-1.0 Hz)

• M151 ◇ M906

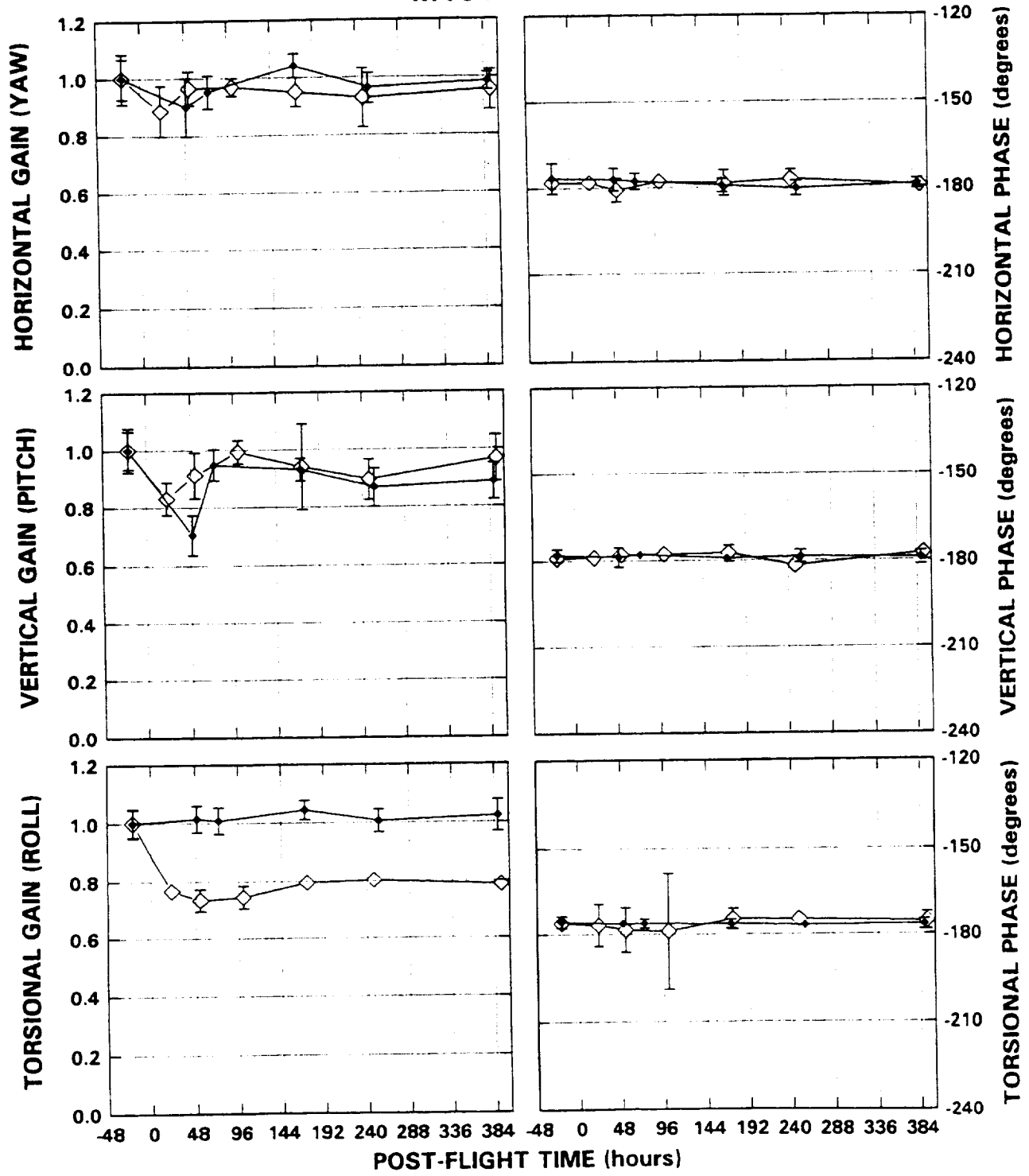


Figure 11. Pre- and post-flight AVORS for M151 and M906.

09-15-1993

M906R.001

DATA ANALYSIS (VOR VER: 1.01)
EXP DATE: 10-10-92 TIME: 10:39:03 A/D: 200Hz
VWT 1230.0 HEI 5.0 VE1 6.0
PLOT RESOLUTION: 2000.0 PW: 0.1 0.3 0.5 0.2 0.4 0.1 0.3
COMMENT #1: NA 10-OCT-92 10:39:03 M906
COMMENT #2:
COMMENT #3:

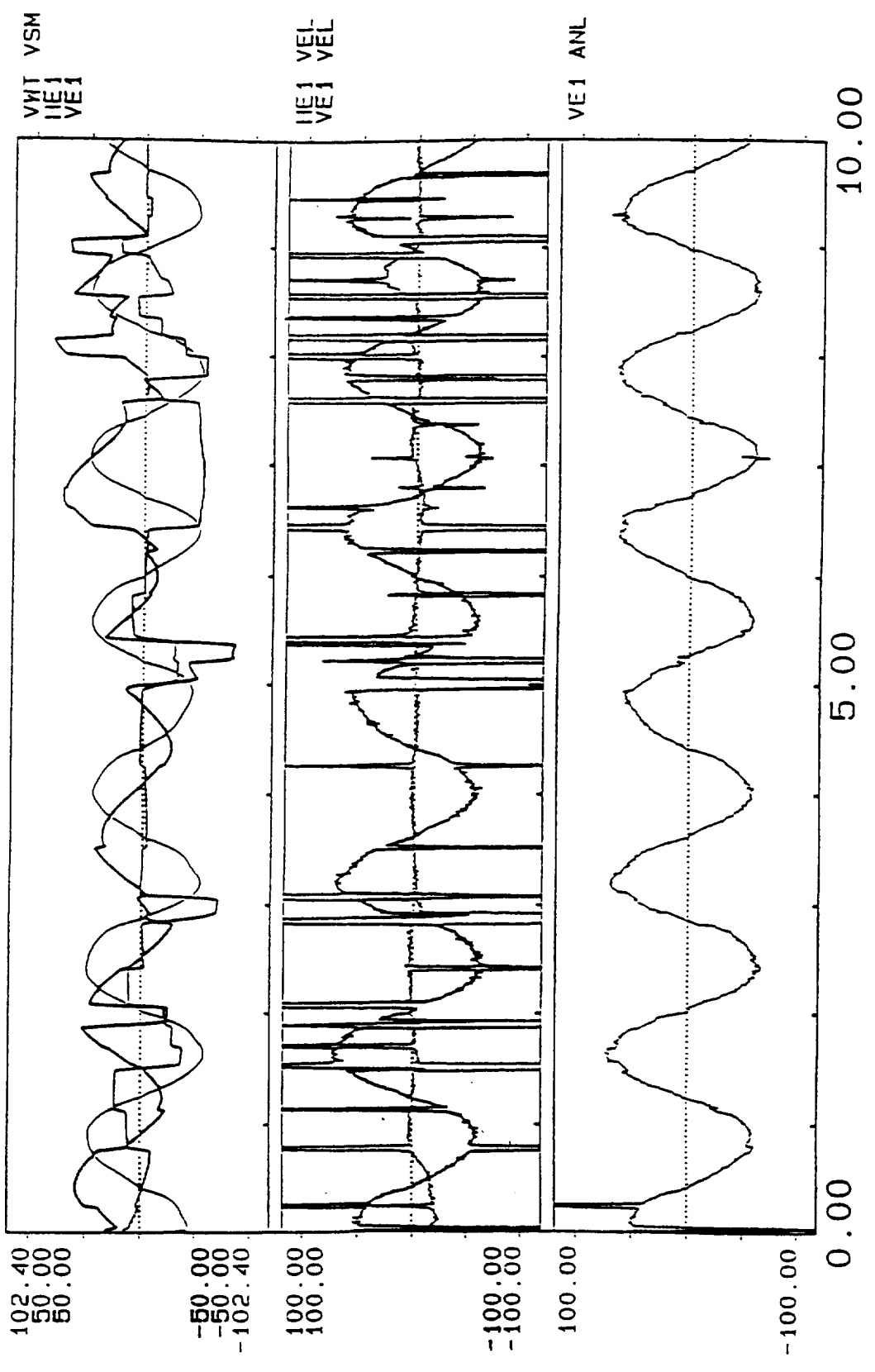


Figure 12. Sample of pre-flight AVOR responses to pitch for M906.

09-15-1993

M906R.062

DATA ANALYSIS (VOR VER: 1.01)

EXP DATE: 01-11-93 TIME: 06:30:14 A/D: 200Hz
VWT 1230.0 HEI 6.0 VE1 6.0
PLOT RESOLUTION: 2000.0 PW: 0.1 0.3 0.5 0.2 0.4 0.1 0.3
COMMENT #1: NA 11-JAN-93 06:30:14 M906
COMMENT #2:
COMMENT #3:

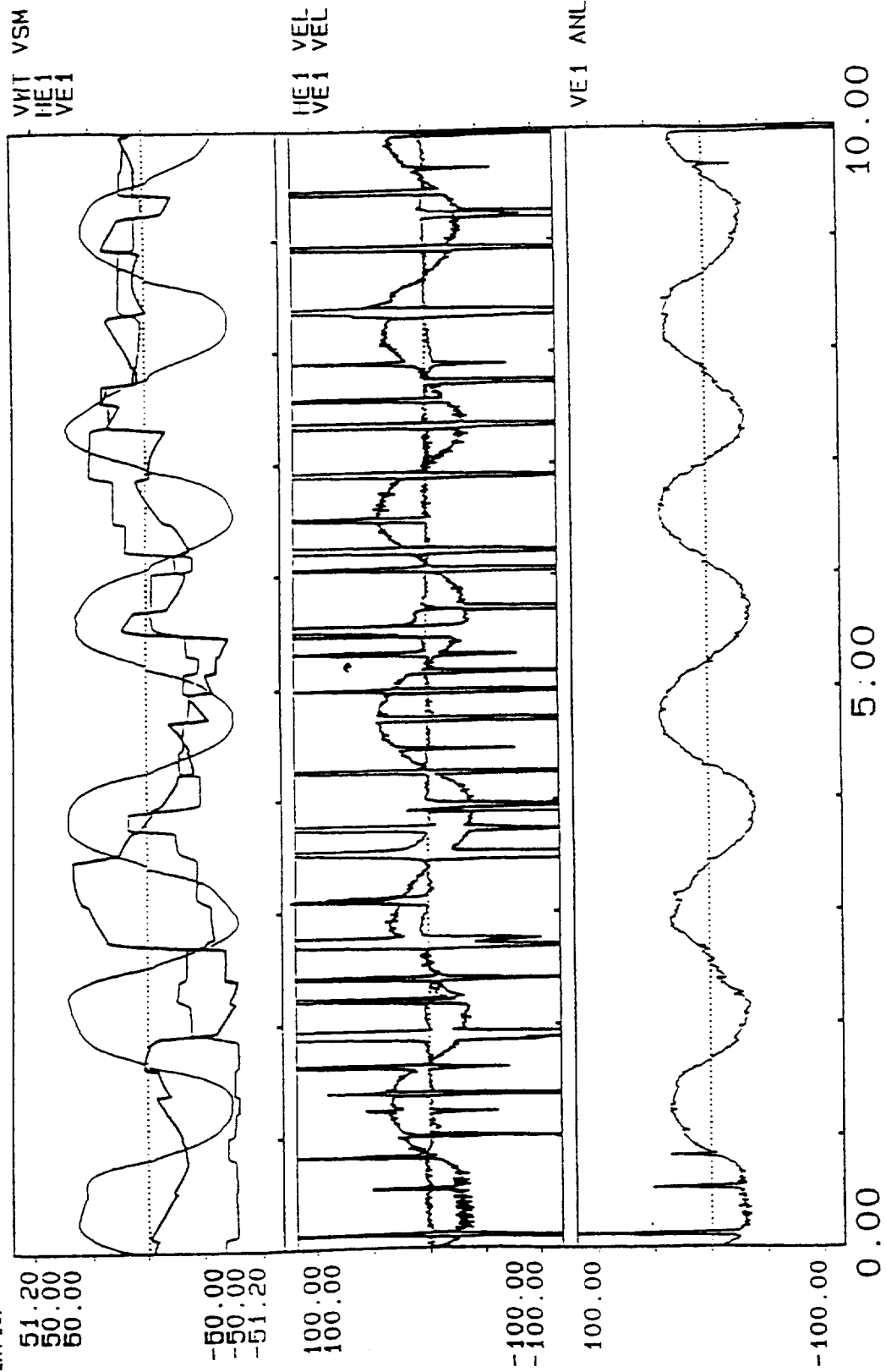


Figure 13. Sample of post-flight AVOR response to pitch for M906.

COSMOS 2229
M151, INTERAURAL 5 Hz, 0.5g STIMULUS

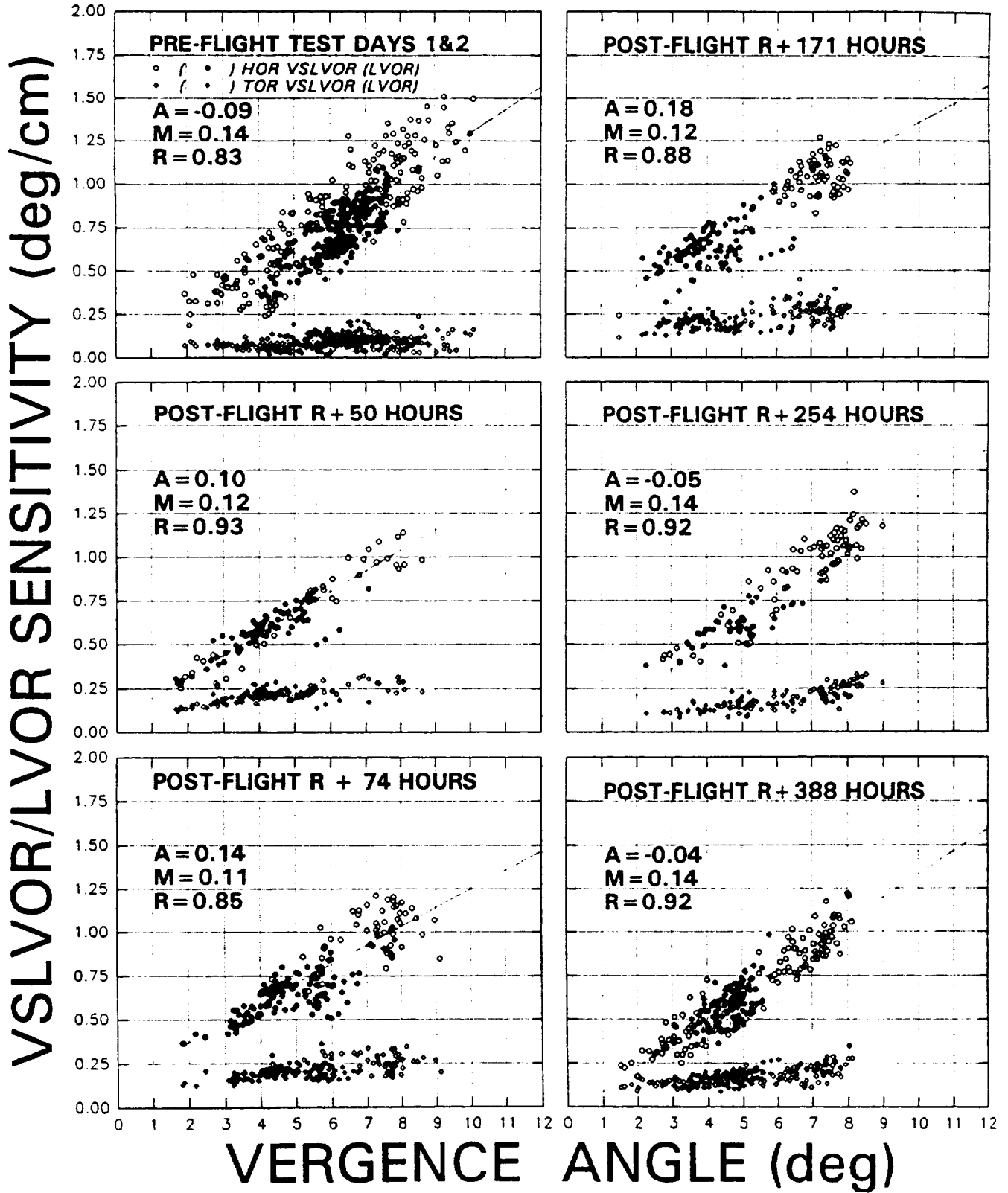


Figure 14. Pre- and post-flight horizontal and torsional sensitivity re vergence for M151 during IA stimulation.

M906, INTERAURAL 5 Hz, 0.5g STIMULUS

VSLVOR & LVOR SENSITIVITY (deg/cm)

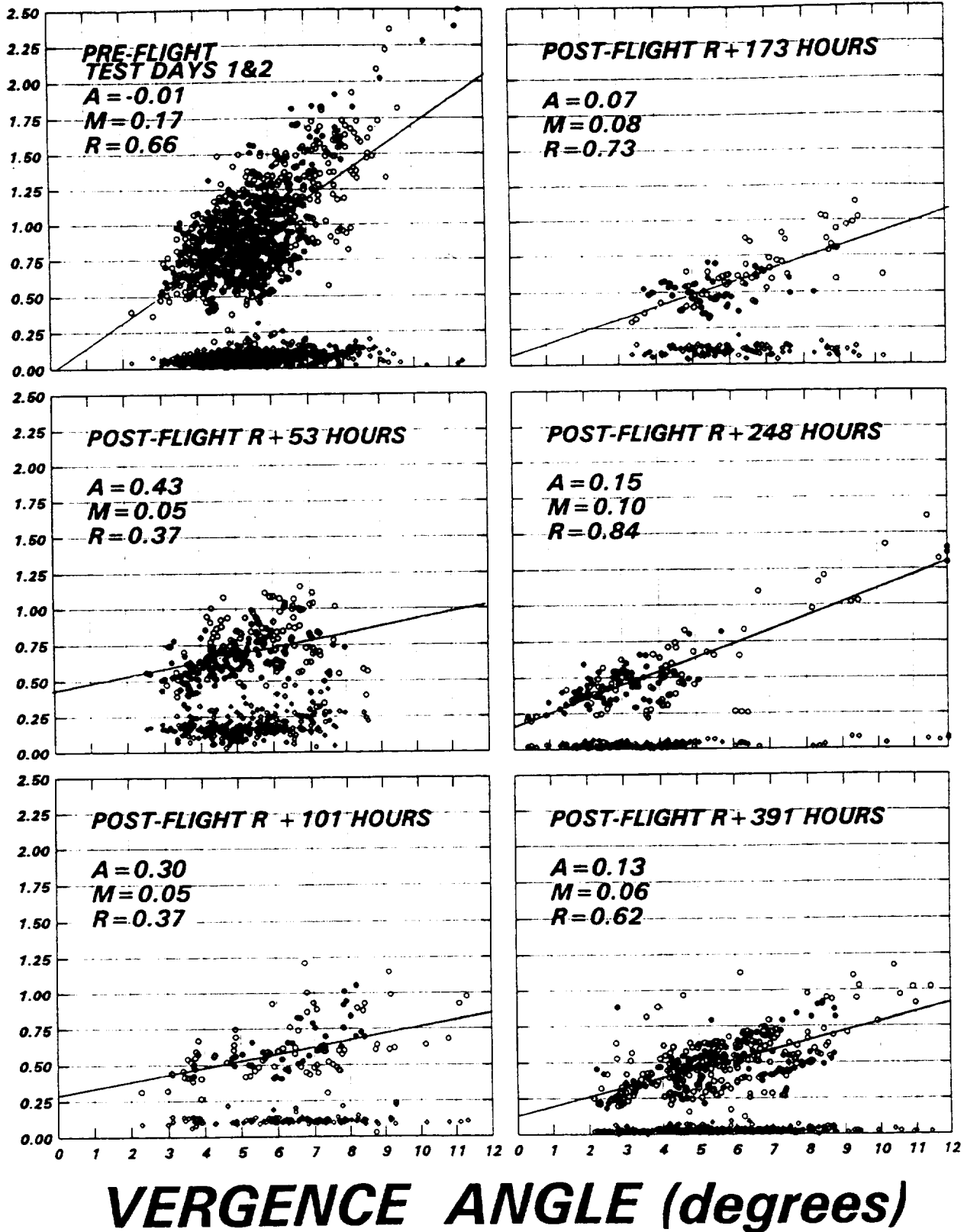
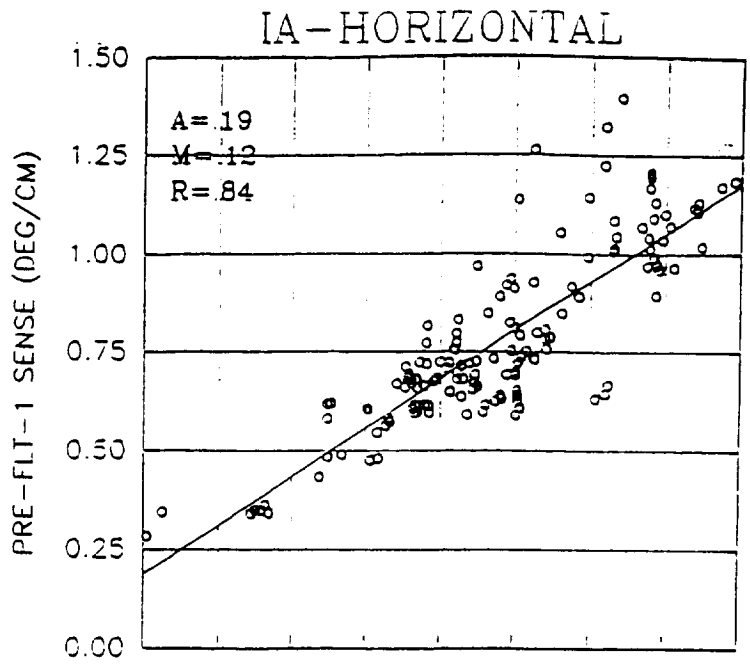


Figure 15. Pre- and post-flight horizontal and torsional sensitivity re vergence for M906 during IA stimulation.

A



B

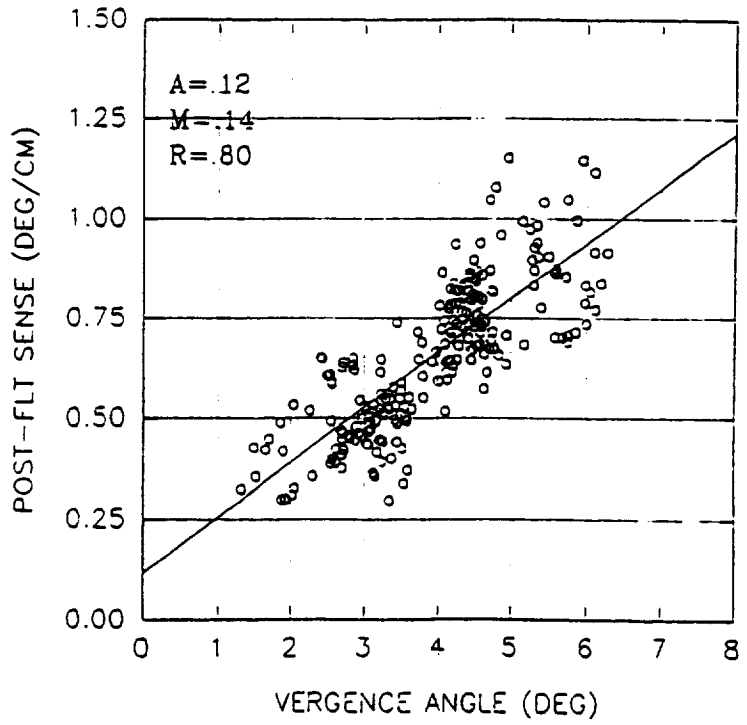


Figure 15(a). M907 pre- and post-flight control data.

COSMOS 2229
M151, DORSOVENTRAL-PRONE 5 Hz, 0.5g STIMULUS

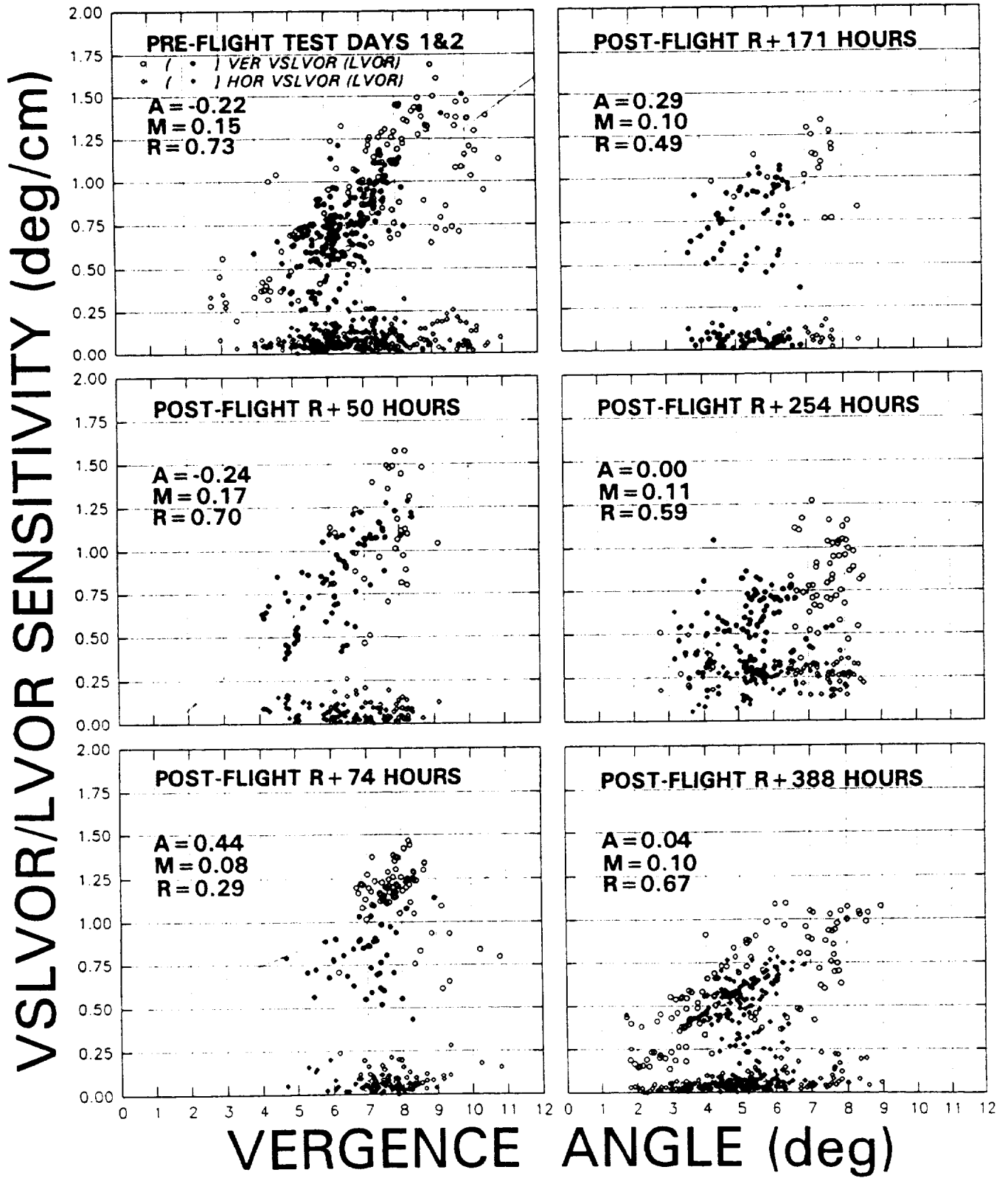


Figure 16. Pre- and post-flight vertical and horizontal sensitivity re vergence for M151 during DV stimulation.

COSMOS 2229
M906, DORSOVENTRAL-PRONE & SUPINE 5 Hz, 0.5g STIMULUS

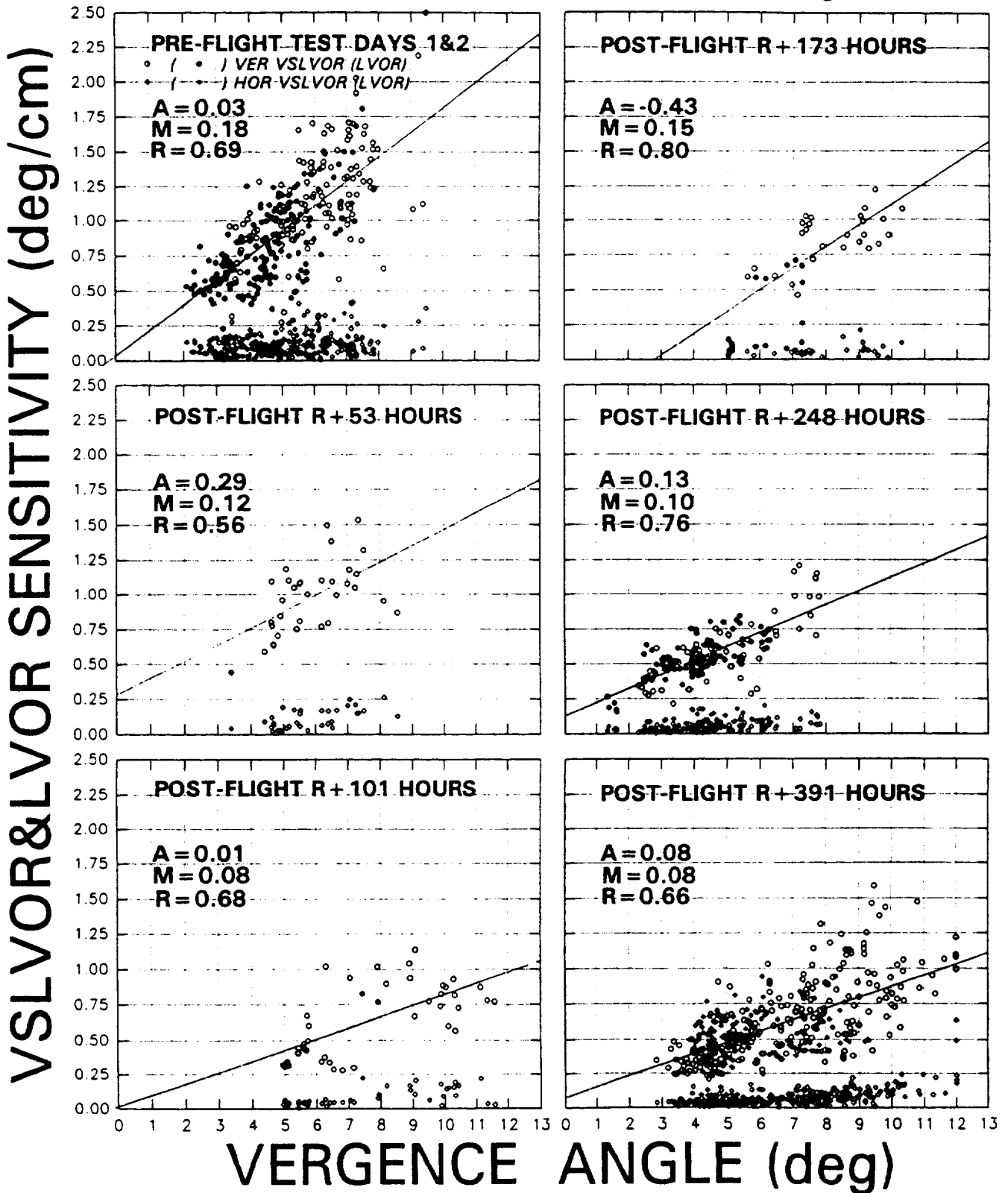
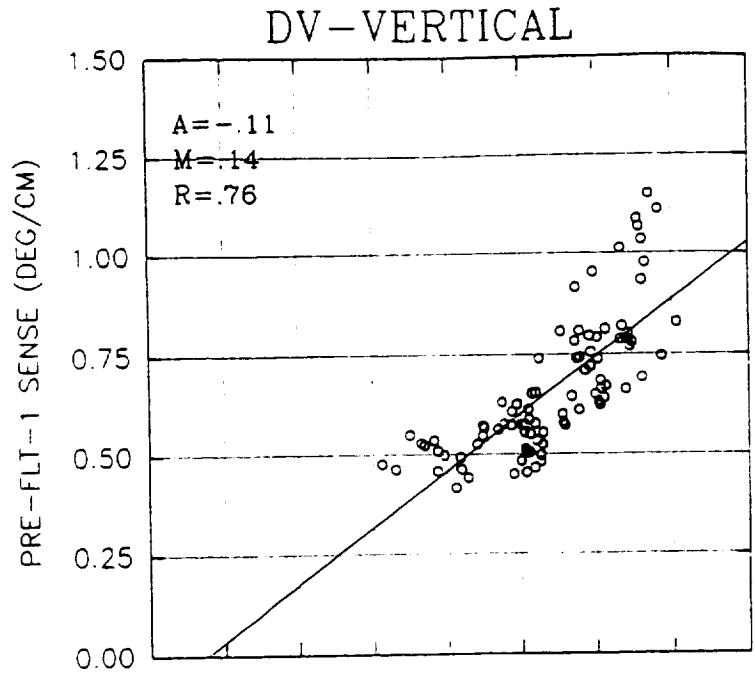


Figure 17. Pre- and post-flight vertical and horizontal sensitivity re vergence for M906 during DV stimulation.

A



B

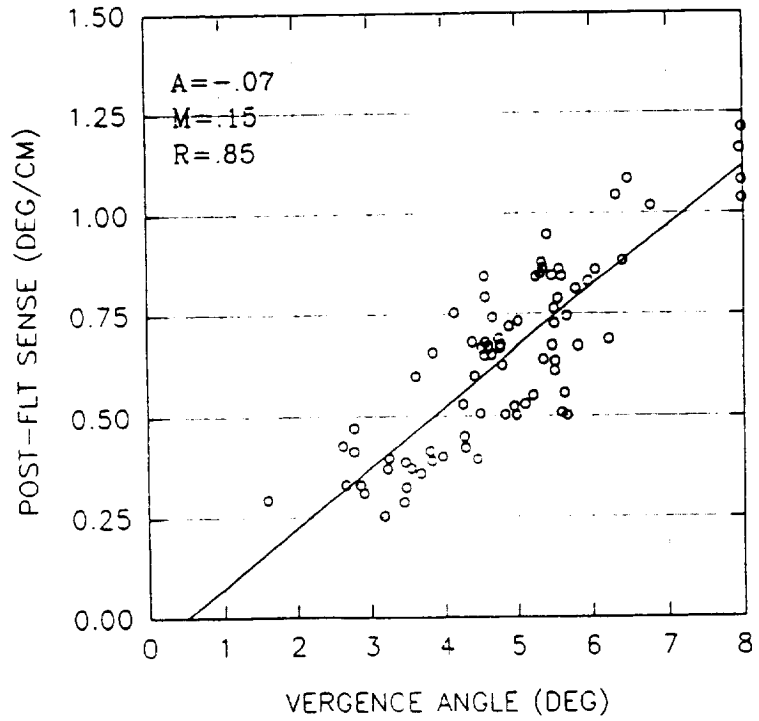


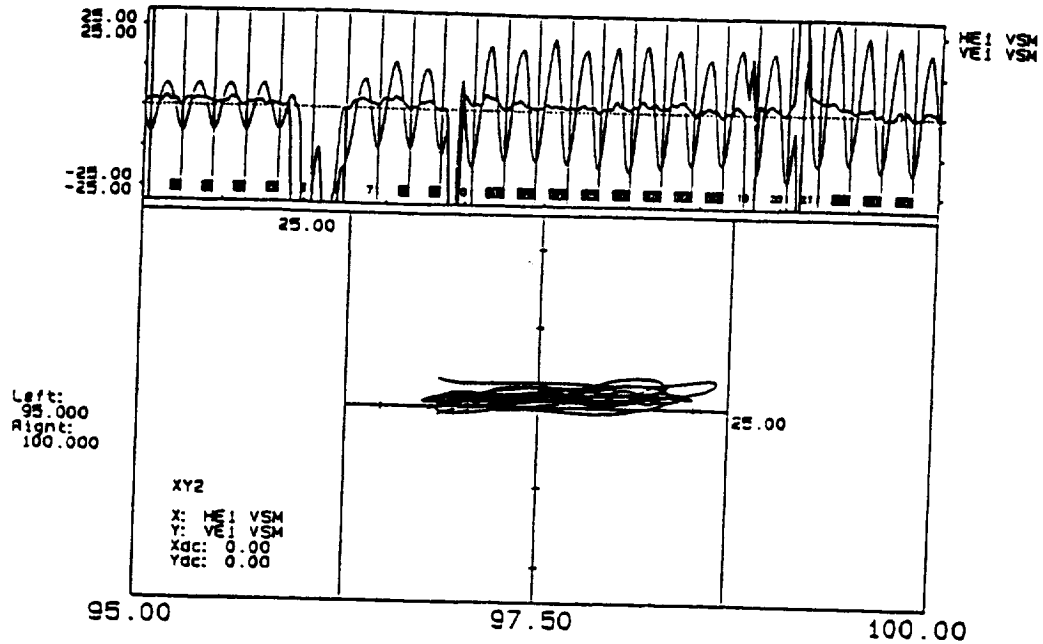
Figure 17(a). M907 pre- and post-flight control data.

DATA ANALYSIS (VOR VER: 1.01)
 EXP DATE: 10-1-92 TIME: 18:23:48 ADR: 2004
 MEI: 0.5 VEI: 0.5
 PLOT RESOLUTION: 2000.0 PPR: 0.5 0.4 0.3
 COMMENT #1: NA 11-OCT-92 18:23:48 1800
 COMMENT #2:
 COMMENT #3:

M906R.053

11-30-1993

A



DATA ANALYSIS (VOR VER: 1.01)
 EXP DATE: 10-1-92 TIME: 18:14:08 ADR: 2004
 MEI: 0.5 VEI: 0.5
 PLOT RESOLUTION: 2000.0 PPR: 0.5 0.4 0.3
 COMMENT #1: NA 11-OCT-92 18:14:08 1800
 COMMENT #2:
 COMMENT #3:

M906R.051

11-30-1993

B

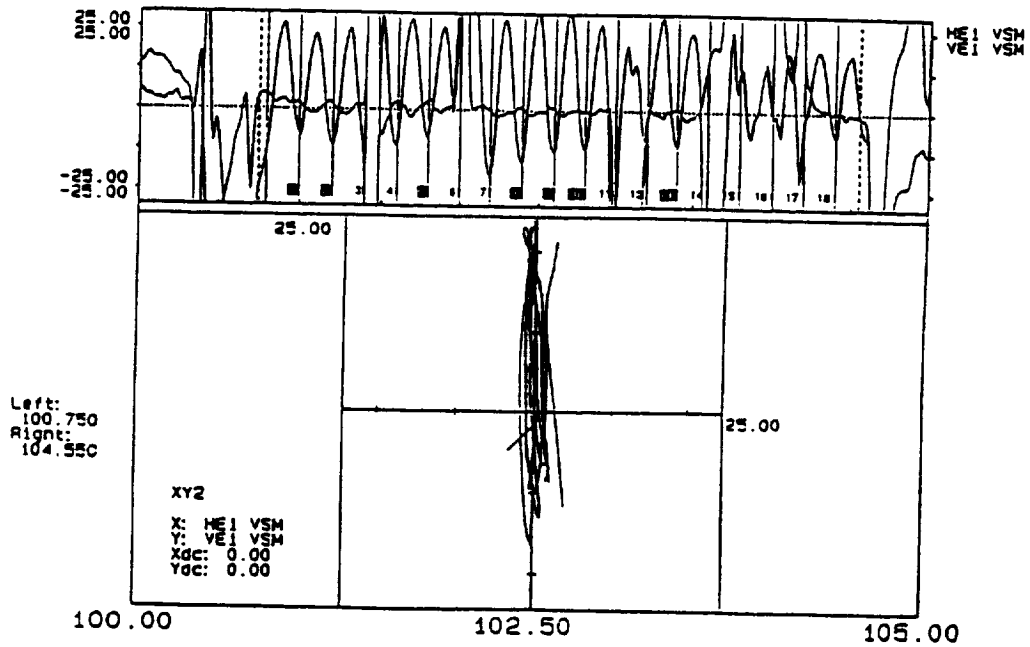
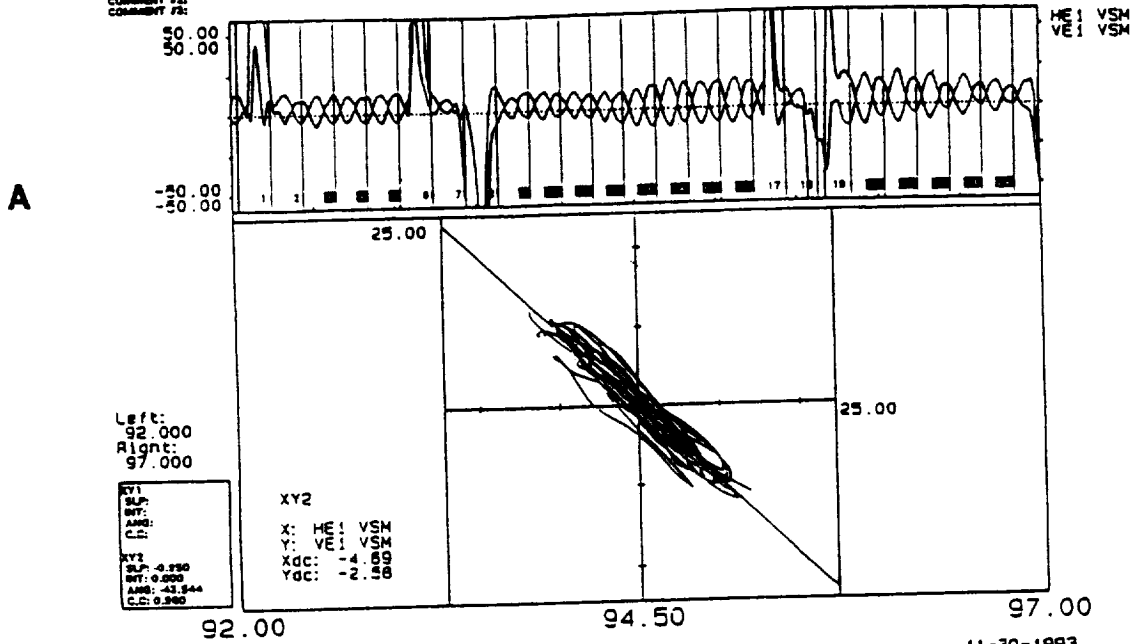


Figure 18. Right eye vertical sensitivity plotted as a function of horizontal sensitivity for IA(A) and DV(B) stimulation.

DATA ANALYSIS (VOR VER: 1.01)
 EXP DATE: 10-11-92 TIME: 15:42:28 ADR: 2500Hz
 HE1 S.S.D VE1 S.S.D
 PLOT RESOLUTION: 2000.0 PPH: 0.3 0.4 0.3
 COMMENT #1: NA 11-OCT-92 15:42:28 M906
 COMMENT #2:
 COMMENT #3:

M906R.059

11-30-1993



DATA ANALYSIS (VOR VER: 1.01)
 EXP DATE: 10-11-92 TIME: 15:44:44 ADR: 2500Hz
 HE1 S.S.D VE1 S.S.D
 PLOT RESOLUTION: 2000.0 PPH: 0.3 0.4 0.3
 COMMENT #1: NA 11-OCT-92 15:44:44 M906
 COMMENT #2:
 COMMENT #3:

M906R.060

11-30-1993

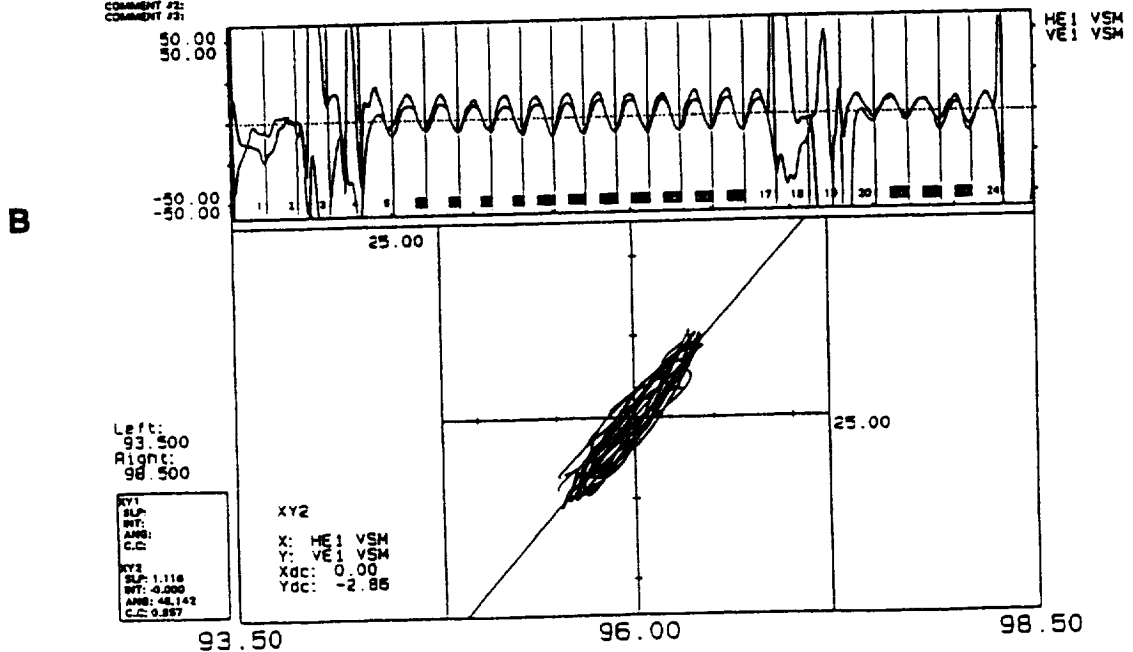


Figure 19. Right eye vertical sensitivity plotted as a function of horizontal sensitivity for motion along axes 45° between IA and DV.

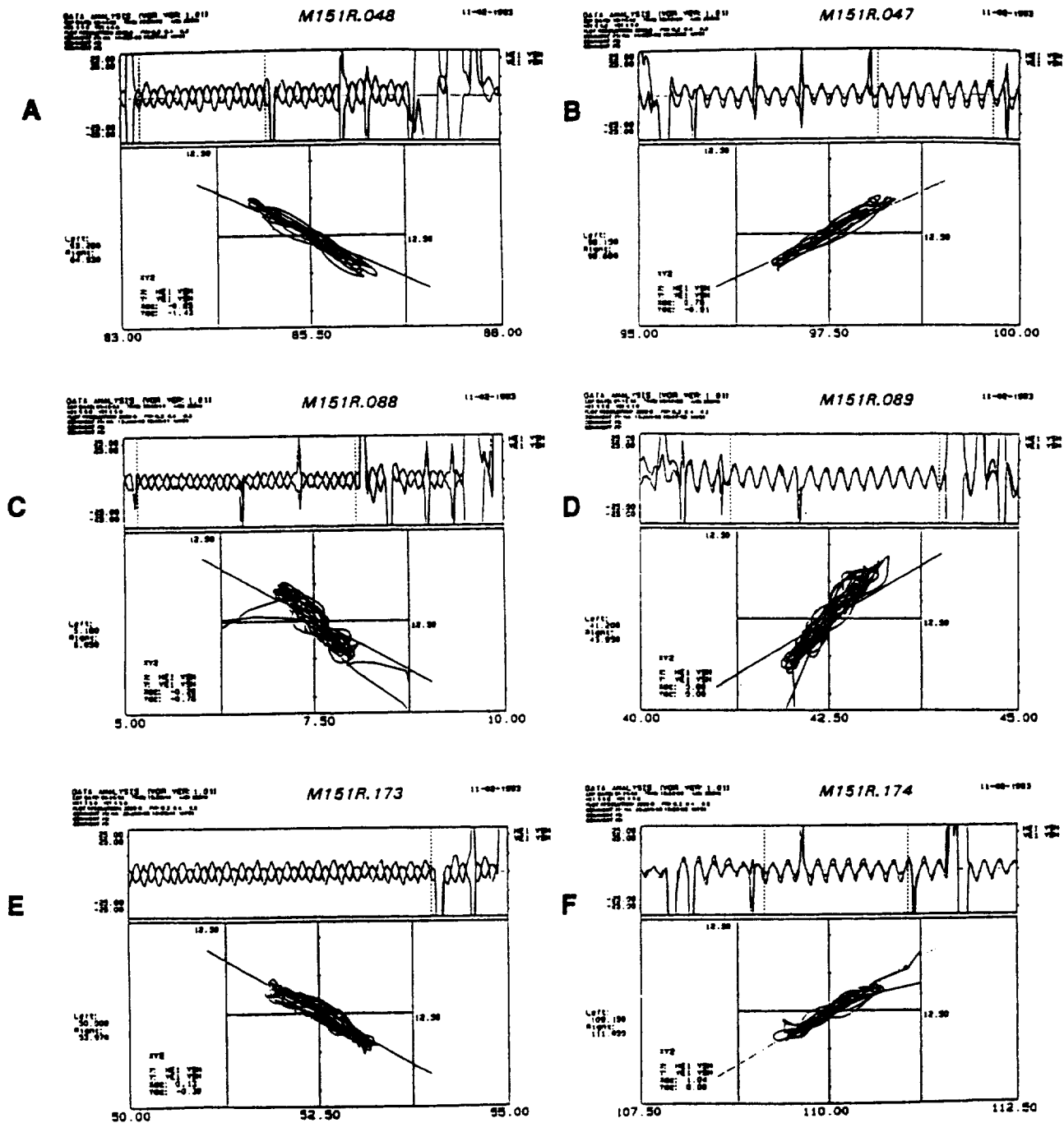


Figure 20. Right eye vertical sensitivity plotted as a function of horizontal sensitivity for motion along axes between IA and DV for M151 pre-flight (A&B) immediately post-flight (C&D) and at about 2 weeks post-flight (E&F).

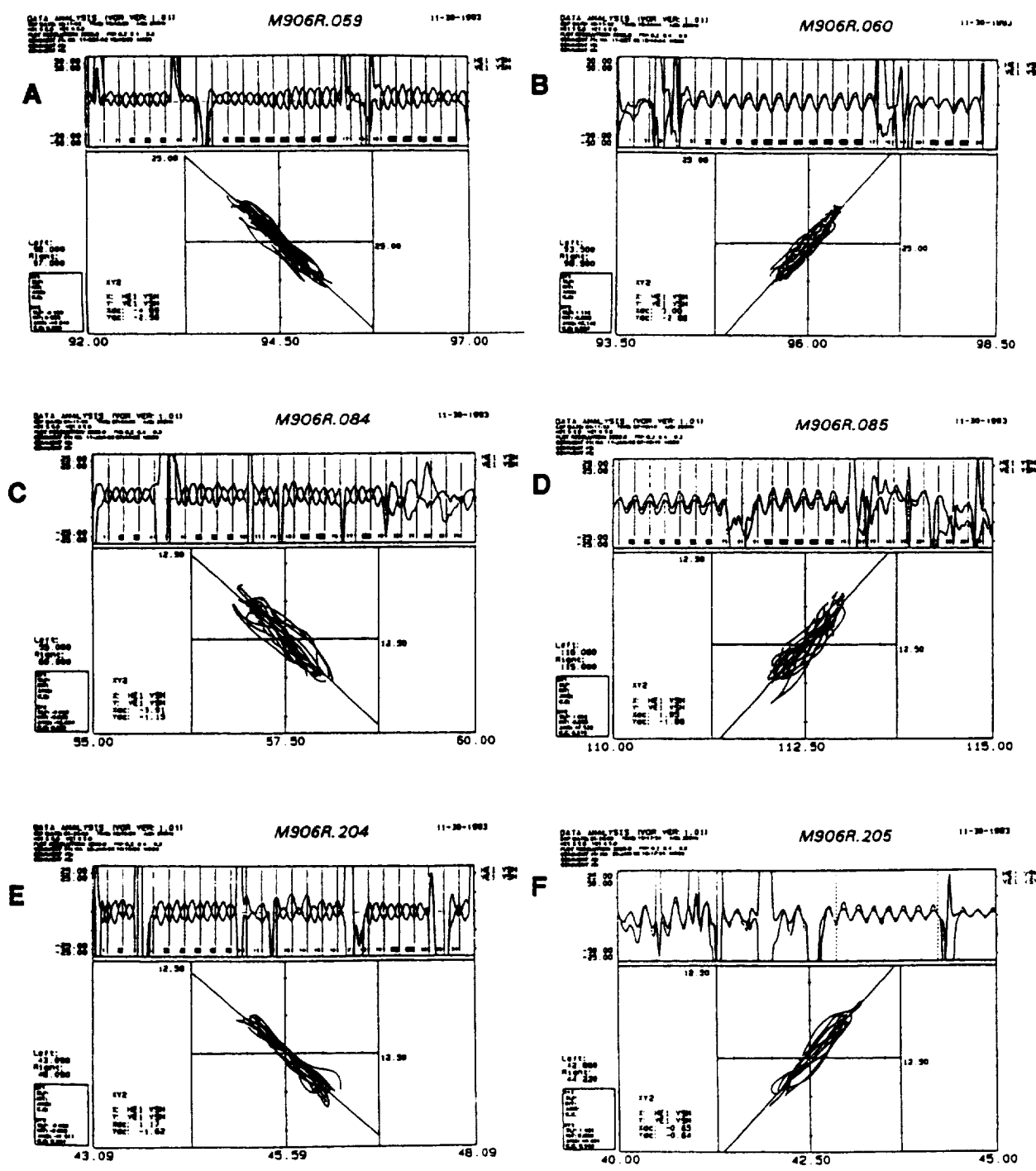


Figure 21. Right eye vertical sensitivity plotted as a function of horizontal sensitivity for motion along axes between IA and DV for M906 pre-flight (A&B) immediately post-flight (C&D) and at about 2 weeks post-flight (E&F).

R + 388

R + 50

PRE-FLIGHT

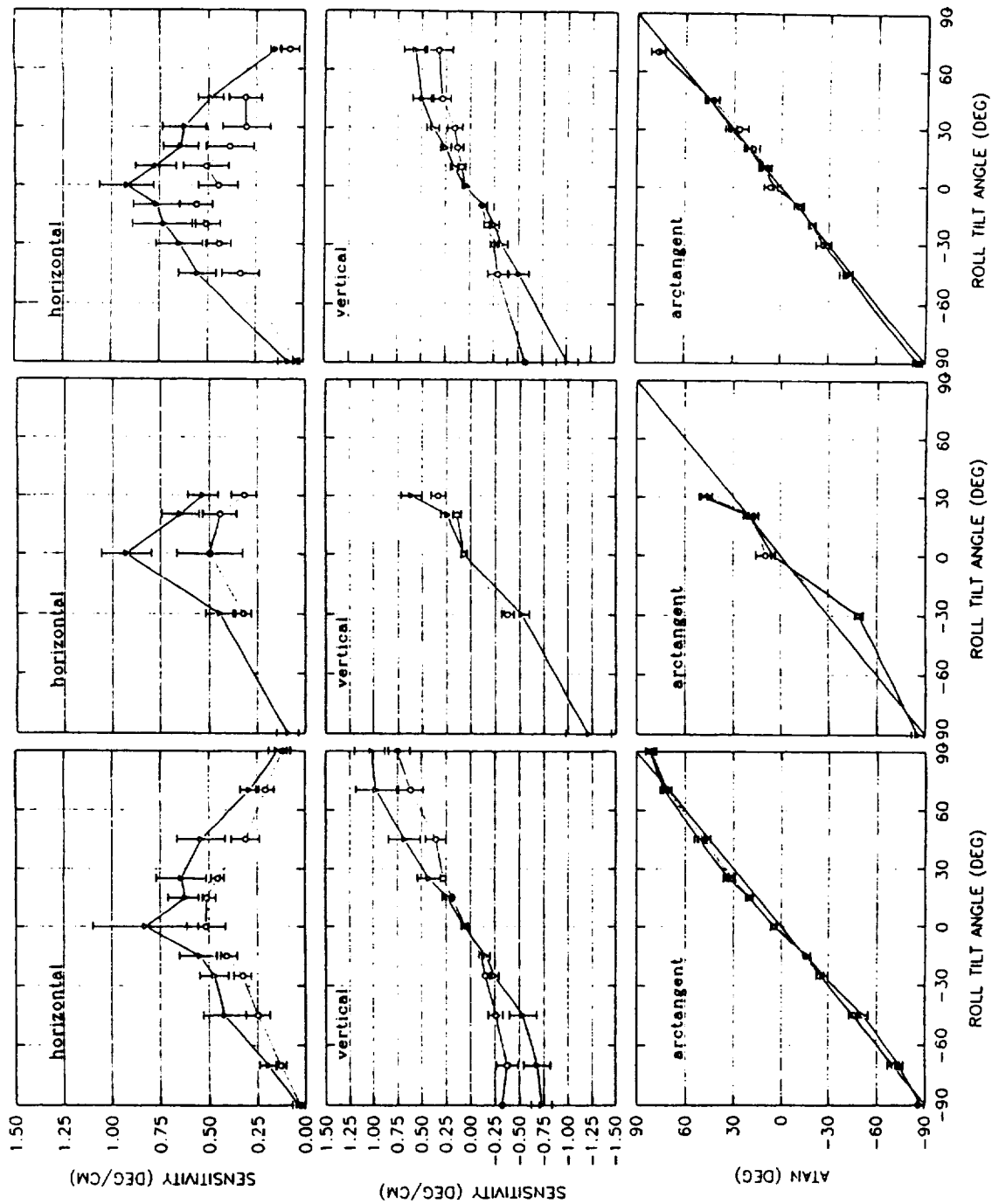


Figure 22. Motion along axes between IA and DV (M151).

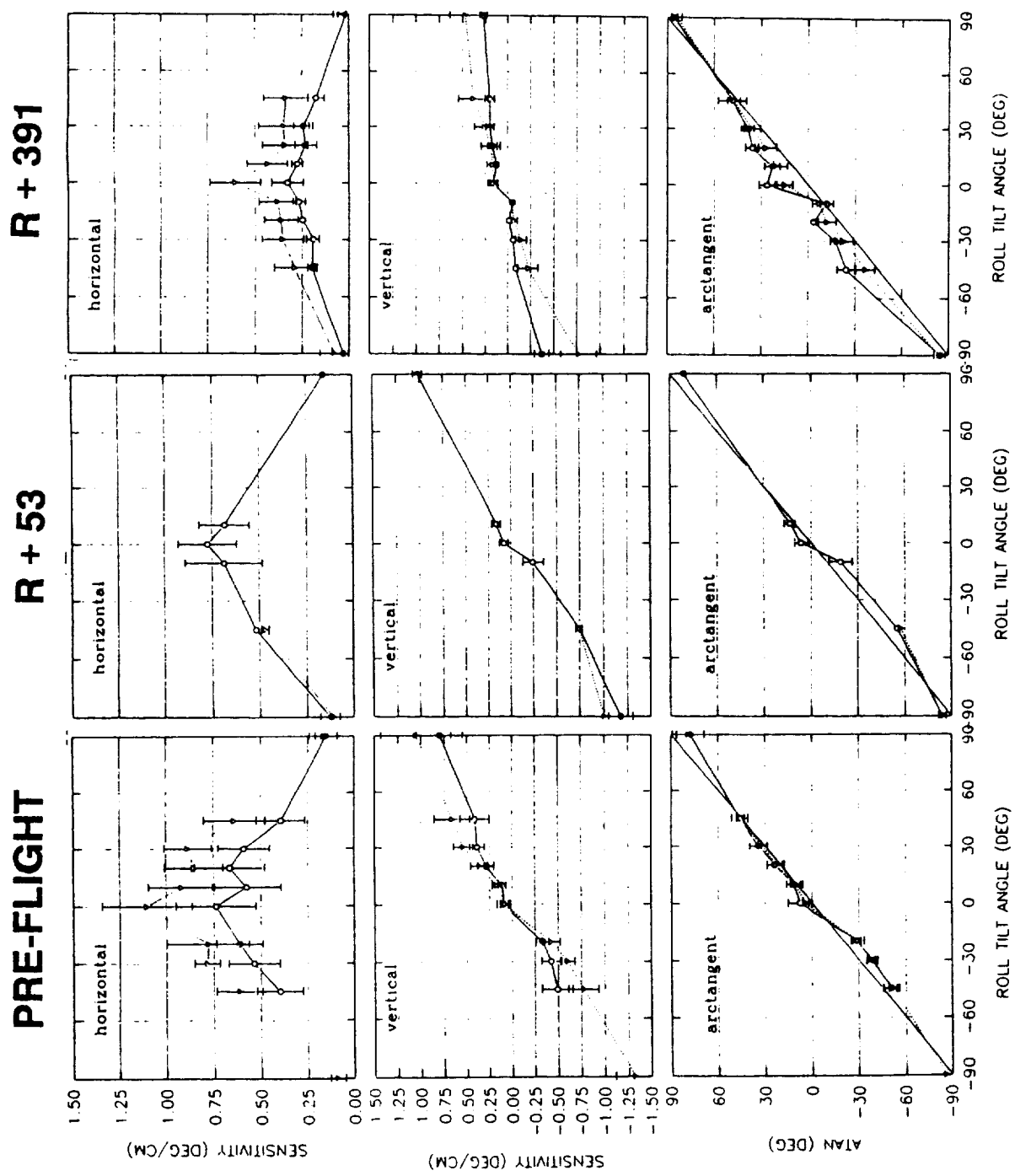


Figure 23. Motion along axes between IA and DV (M906).

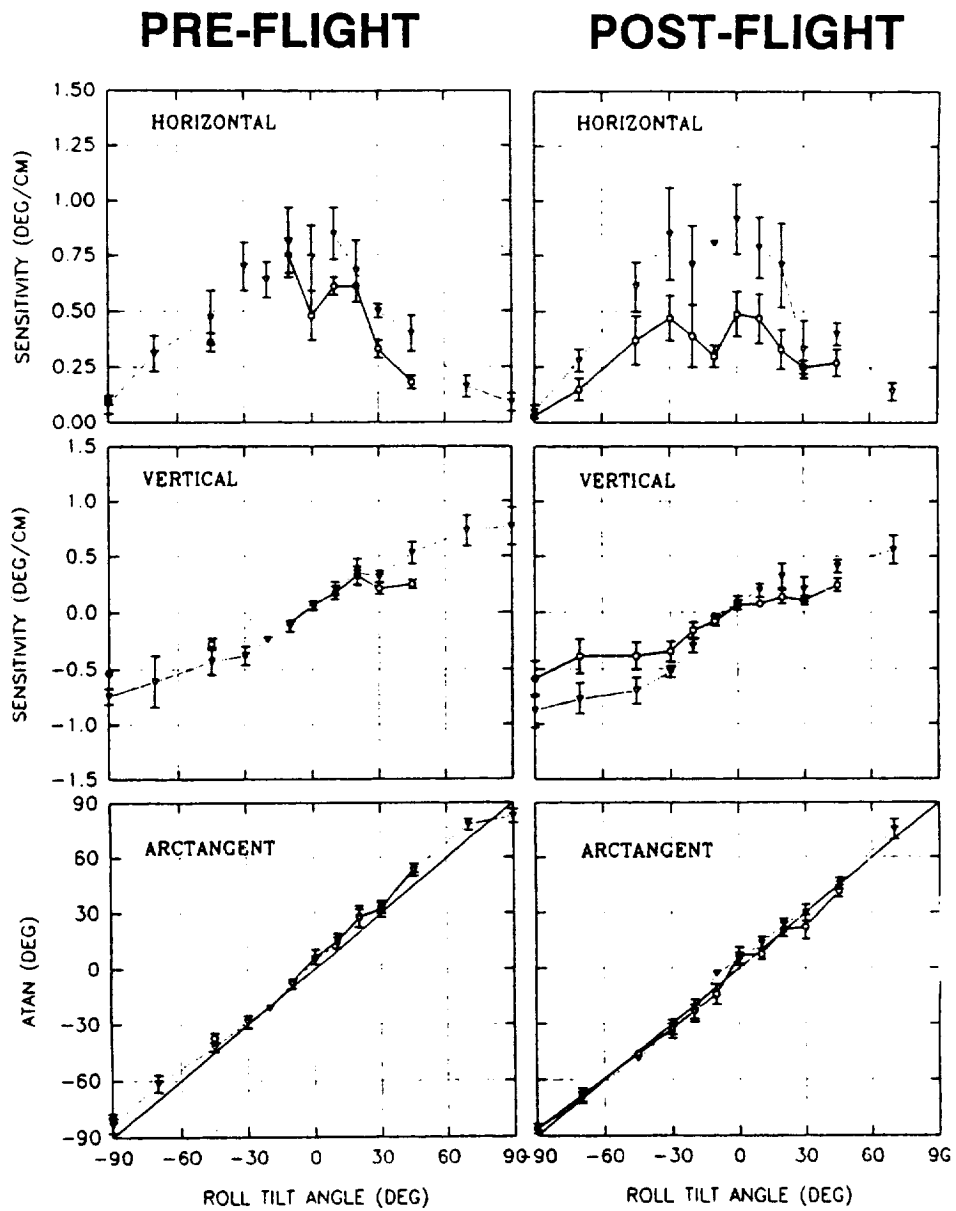


Figure 24. Motion along axes between IA and DV (M907).

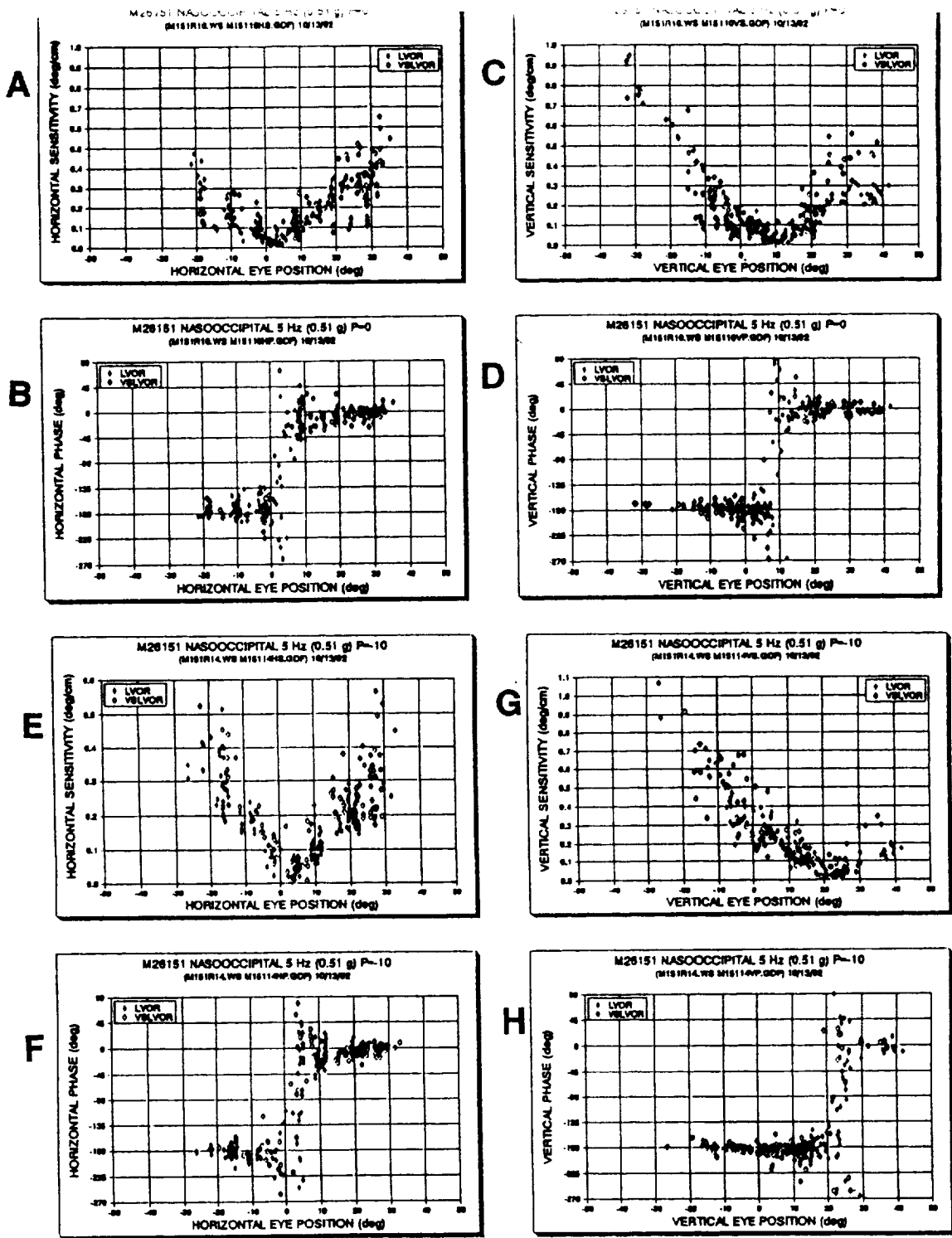


Figure 25. Motion along the NO axis and along one axis between NO and DV. Pre-flight measures for M151.

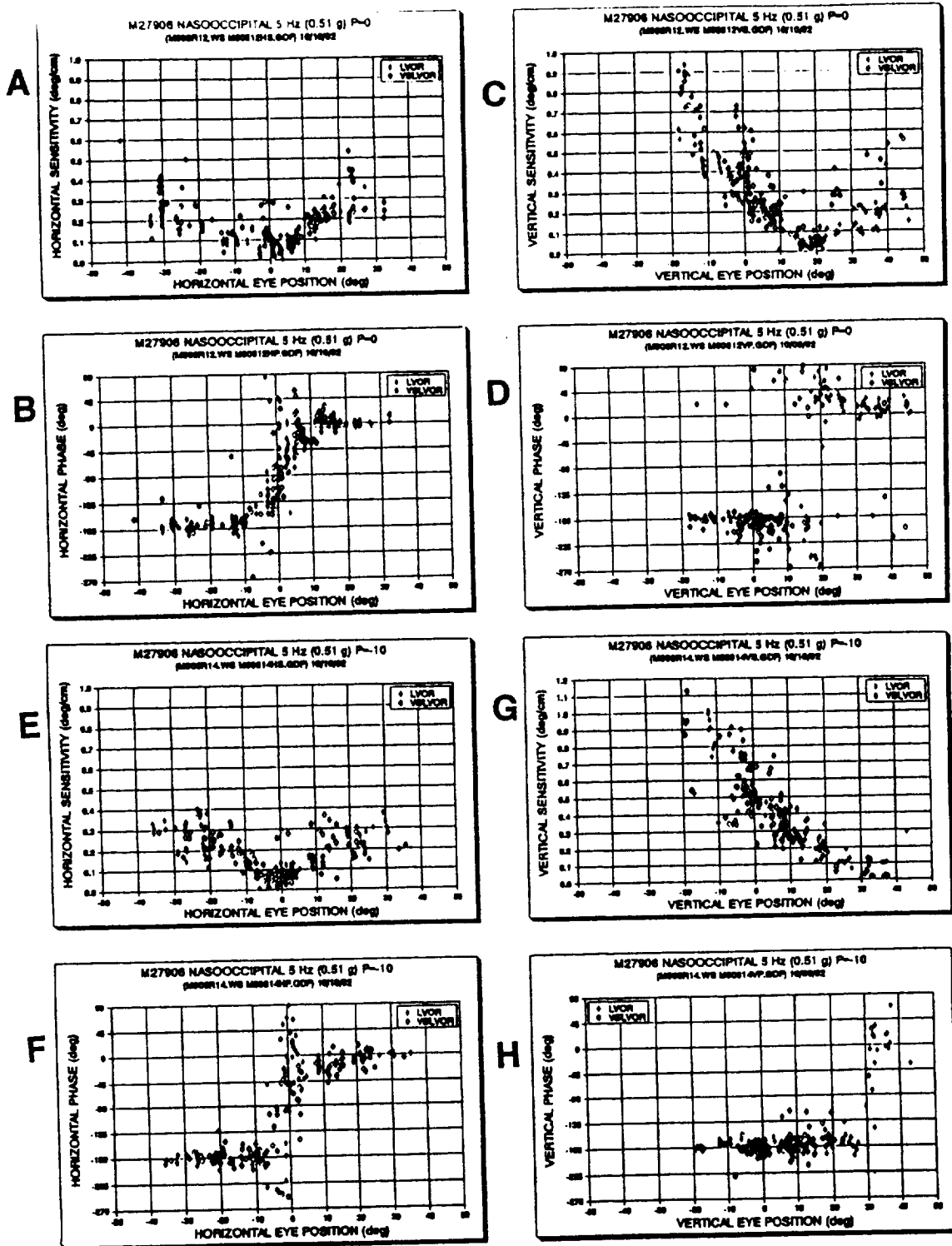


Figure 26. Motion along the NO axis and along one axis between NO and DV. Pre-flight measures for M906.

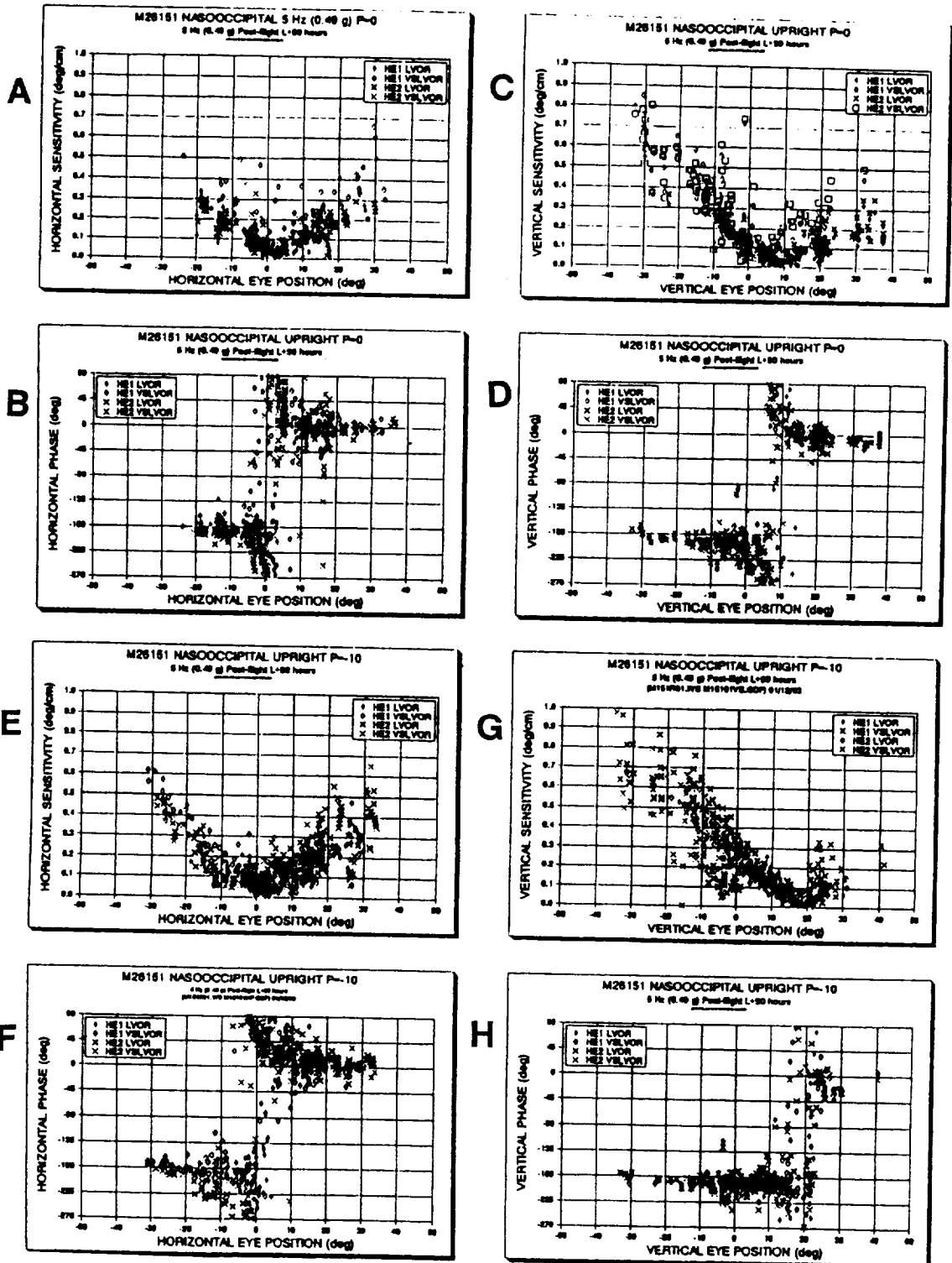


Figure 27. Motion along the NO axis and along one axis between NO and DV. Post-flight measures for M151.

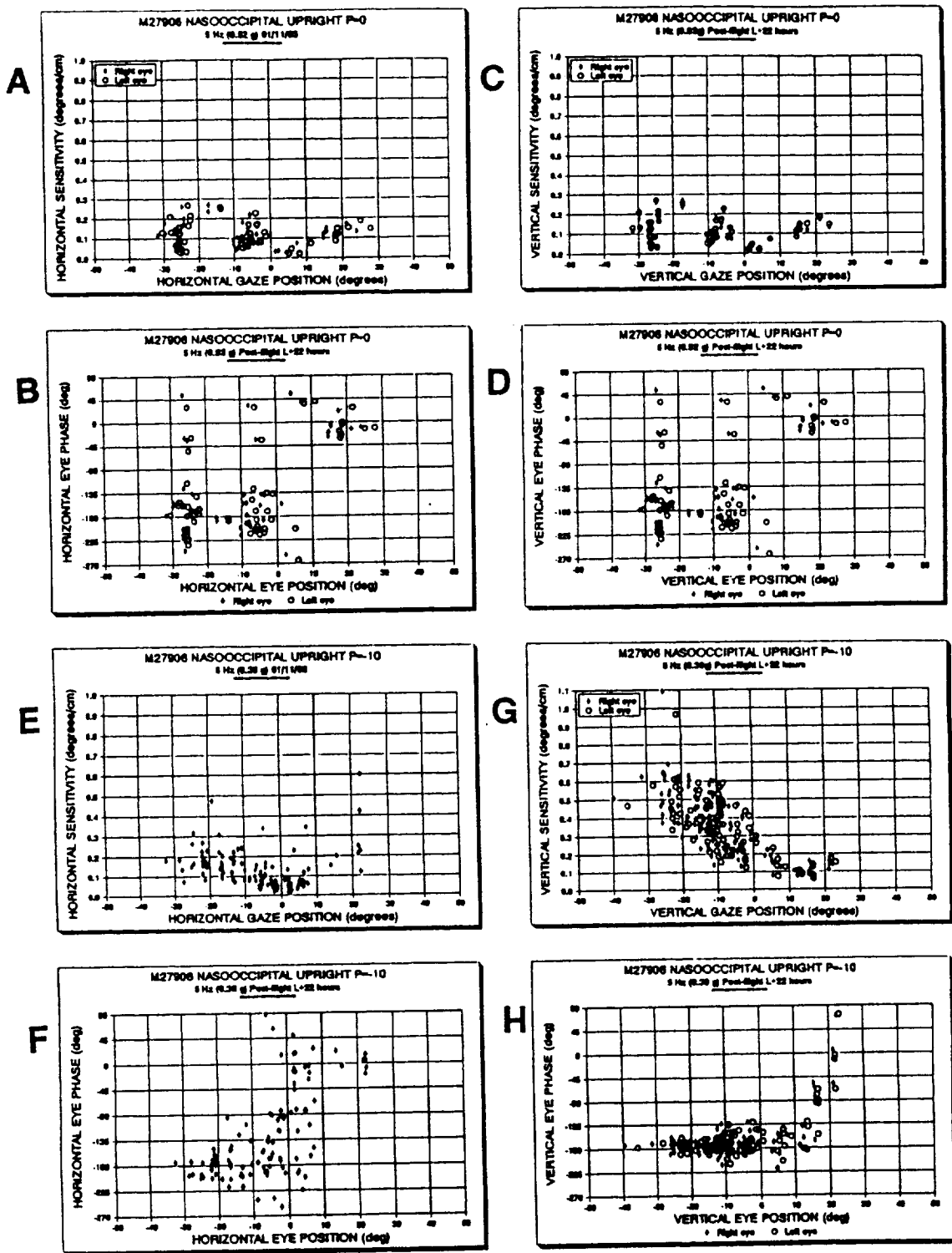


Figure 28. Motion along the NO axis and along one axis between NO and DV. Post-flight measures for M906.

GROUND SUPPORT REQUIREMENTS FOR
PORTABLE LINEAR SLED FOR COSMOS 92
EXPERIMENT K-0-08 "ADAPTATION TO
MICROGRAVITY OF OCULOMOTOR
REFLEXES (AMOR): OTOLITH-OCULAR
REFLEXES"

1. DESCRIPTION OF DEVICE

1.1. The purpose of the Portable Linear Sled (PLS) is to provide to vestibular researchers horizontal and vertical linear oscillations from 1.0 to 5.0Hz frequency and sinusoidal acceleration from 0 to +/-1g.

1.2. The PLS consists of an electro-mechanical sled, 94.4" long x 54.32" wide x 53.56" high (2398.78x1379.73x1360.42mm), an "A" shaped hoist for changing its orientation, and five racks, 19" wide x 30" deep x 60" high (482.6x762x1524mm) in which control, safety, science data acquisition systems, power supply, and an air compressor are installed.

1.3. The sled itself is shown in Figure 1 from the end (A) and from the side (B and C). It's purpose is to provide vibration free linear oscillations for animals up to the size of an 8-10kg Rhesus monkey. It is designed to operate in either a horizontal position (shown in B), so that Specimen Test Container (STC) oscillations are parallel to the ground, or vertically (shown in C), so that STC oscillations are perpendicular to the ground.

1.4. The sled must be firmly attached to a surface with low levels of ambient vibration ($\leq 0.001g$) during operation. The attachment must enable the sled to be quickly changed from the horizontal to vertical position and vice versa.

1.5. The two additional components are not shown in Figure 1. First, as shown in Figure 2, there is a manually operated, "A" shaped hoist designed to be used during experiments to quickly change the position of the sled from horizontal (A) to vertical (C) with the motion axis locked, but with the animal subject inside the STC.

1.6. The second additional component is the above-mentioned five rack set. Three racks hold the control system, safety system, amplifiers, power supply, and air compressor for the operation of the PLC. Two additional racks hold equipment for science data collection and analysis.

1.7. The following are physical dimensions and characteristics of the room in which the PLS must operate, and its electrical power requirements, based on the design described above.

2. ROOM REQUIREMENTS

2.1. The room has to be large enough for placement of, access to and maintenance of the PLS. An area of at least 10'x16.5' (3.04m x 5.02m) is required for the sleds placement and maintenance. An area of at least 14.5'x7.01' (4.40m x 2.13m) is required for racks placement and maintenance. The height of the room must be at least 9.87' (3m).

2.2. The floor on which the sled is mounted must have ambient vibrations $\leq 0.001g$. Therefore, it is desirable to place the air compressor rack in a room separate from the room where the PLS is placed or at a distance of at least $\geq 30.4'$ (10m) from the sled.

2.3. Racks holding control system, safety system, and science data acquisition system must be placed so that the operator can visually monitor the PLS during operation. It is desirable that distance between the racks and sled be no more than 20' (6.1m).

2.4. The room has to be large enough to accommodate additional equipment for PLS adjustment and maintenance, and accommodations for technicians' work benches (2-4 employees).

2.5. The room for the PLS placement must not be near any heavy equipment which will cause mechanical or electrical noise (e.g., an elevator, a welder, etc.). There should be no directional acoustic noise sources in the room (so that there are no directional cues to the animal subject).

2.6. The PLS room has to have shutters or blinds that will allow control of ambient natural lighting at any time that the experimenters wish.

2.7. An ambient temperature in the PLS room must be range from 64°F (18°C) to 72°F (22°C). Relative humidity has to be 30-70%.

3. POWER SUPPLY REQUIREMENTS

3.1. A 380V AC, 50Hz separate feeder has to be provided for the PLS power supply. Transformation of this power supply to the voltage required for the PLS operation will be provided by the PLS equipment.

3.2. The PLS operation with power rating of 20kW (90A current) must be provided: 55A-for linear motor, 20A-for control system, safety system, and air compressor, 15A-for science data acquisition system.

3.3. Normal PLS operation requires separate physical grounding with single-point grounding of linear motor, control and safety systems, and science data acquisition system.

3.4. A feeder switchboard for 380V, 50Hz power supply and at least four convenience-outlets for 220V, 50Hz must be provided in the PLS room.

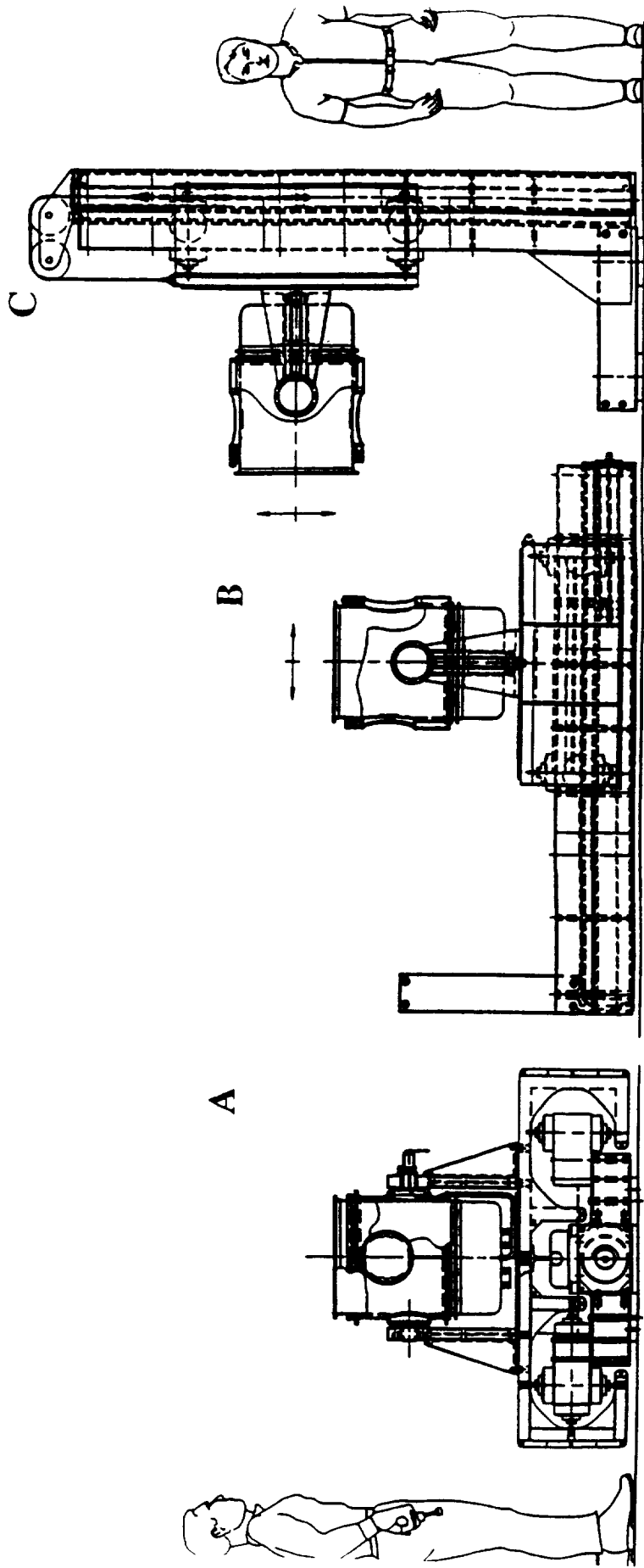


Figure 1.

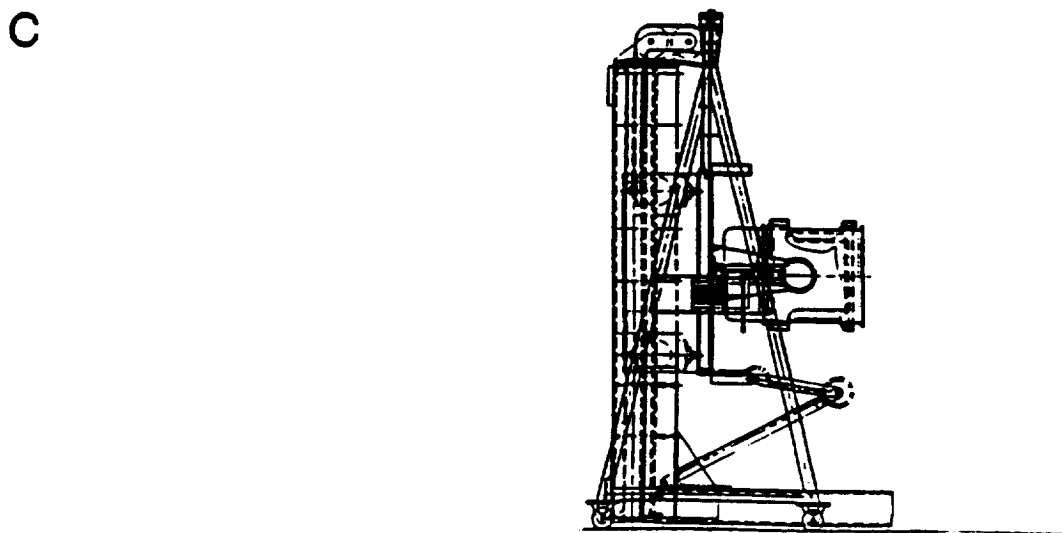
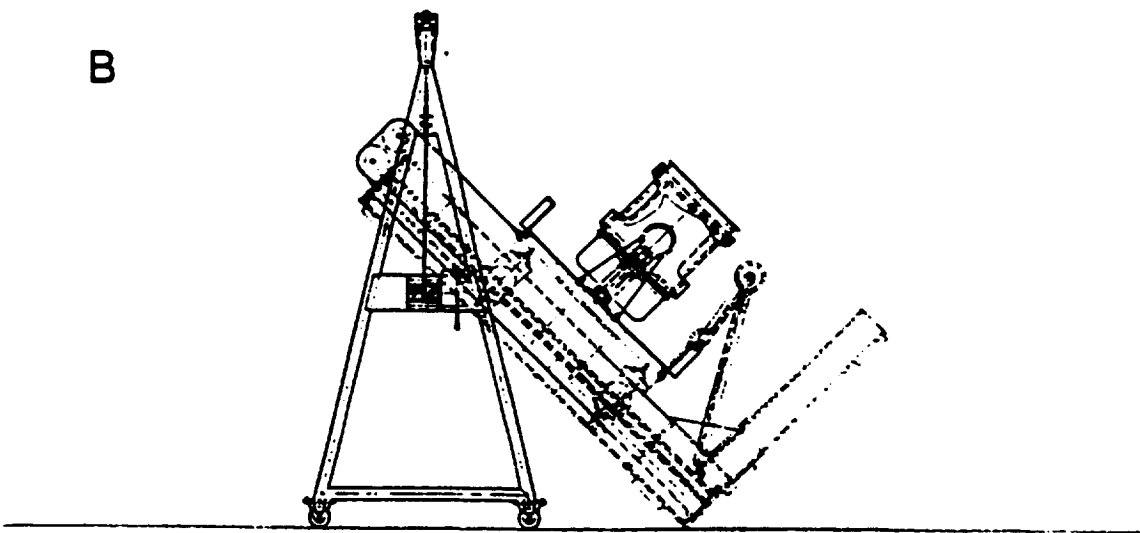
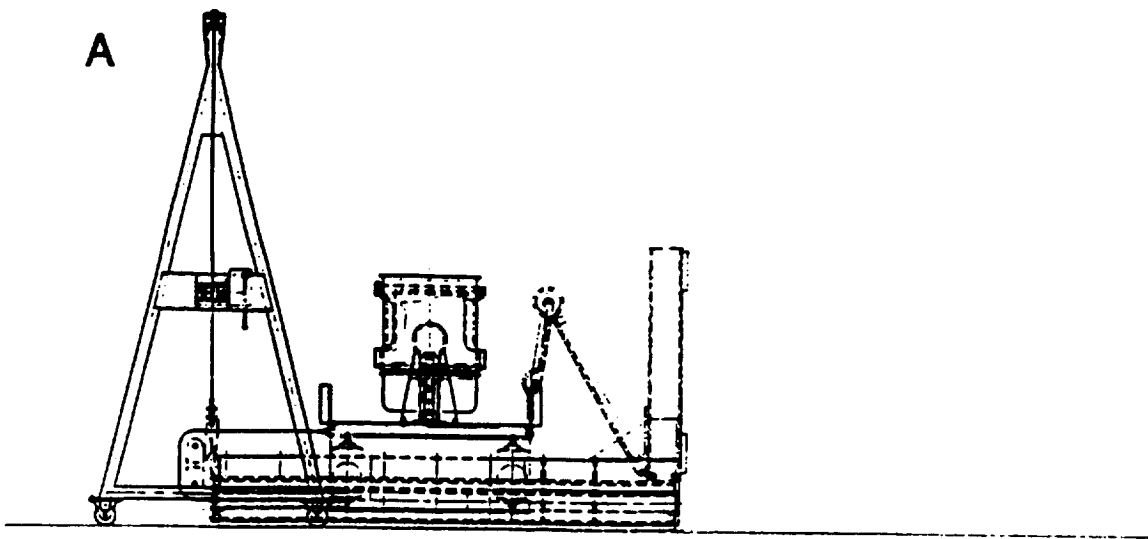


Figure 2.

SUPPLEMENTAL DATA ANALYSIS

PLASMA HORMONE CONCENTRATIONS IN RHESUS
MONKEYS AFTER SPACE FLIGHT

Principal Investigator:

R.E. Grindeland
NASA Ames Research Center
Moffett Field, CA

Co-Investigators:

V.R. Mukku
Genentech, Inc.
South San Francisco, CA

K.L. Gosselink
NASA Ames Research Center
Moffett Field, CA

R. Dotsenko
Institute of Biomedical Problems
Moscow, Russia

PLASMA HORMONE CONCENTRATIONS IN RHESUS MONKEYS AFTER SPACE FLIGHT

R.E. Grindeland, V.R. Mukku, K.L. Gosselink, and R. Dotsenko

SUMMARY

Human beings and rats reveal changes in plasma concentrations of several hormones after space flight. Growth hormone⁸ and testosterone^{2,4} are decreased whereas thyroid hormones have been reported to be increased,³ decreased,^{2,4} or unchanged in⁸ various flights¹. Calcitonin was reduced and parathyroid hormone increased in plasma of Cosmos 2044 rats¹. Rat adrenal steroid levels have typically been markedly elevated in both control and space flight rats after flight, with no significant differences between groups.^{2,7} In order to further our understanding of the effects of microgravity on endocrine function, we have now investigated the circulating levels of growth hormone, insulin-like growth factor I (IGF-I), thyroid hormones, cortisol, and testosterone in young male rhesus monkeys (4 g) following 12.5 days in space. Results of those studies are reported here.

METHODS

Blood was collected and the heparinized plasma or serum was separated and frozen for immunoassays and growth hormone bioassay. Cortisol, testosterone and thyroid hormones were measured by radioimmunoassay (RIA) using kits from Diagnostic Products Corp., Los Angeles, CA. Serum IGF-I was measured by RIA using antiserum and recombinant human IGF-I produced in-house (Genentech, Inc.) and growth hormone was measured by an in vitro bioassay (Genentech, Inc.). Blood samples were obtained about 7 weeks preflight and at 0, 3, 11, and 17 days after flight and at similar times following a space flight simulation 45 days after recovery from space. Samples were obtained at comparable times from control animals (n=4) and flight animals (n=2).

RESULTS

Cortisol concentrations showed a suggestive decrease on days 3 and 11 after flight, but at all other sampling times did not differ from preflight values or from those of control animals (Fig. 1). During the ground based simulation at 45 days after Recovery neither control nor flight monkeys showed significant changes in cortisol levels. (Fig. 2)

As expected with sexually immature monkeys, testosterone levels were low, ranging from 0.1 to 0.38 ng/ml for all animals. On the day of Recovery (R+0), flight monkeys sustained a 50% decrease in plasma testosterone, but were at all other times similar to preflight and control monkey values (Fig. 3). The simulation study yielded inconsistent effects on circulating levels of testosterone in all monkeys (Fig. 4).

Thyroxine (T₄) concentrations fell in the two flight monkeys 11 days after flight, but were otherwise unaffected by space flight (Fig. 5). Following R+45 day simulation both control and flight monkeys showed a transitory decrease of about 25% in plasma thyroxine which remained low in flight monkeys for 20 days but returned to preexperimental levels in control animals (Fig. 6).

Triiodothyronine (T₃), concentrations were reduced 80% at R+0 days and 30% at R+3 days with a subsequent resumption of control levels (Fig. 7). The simulation had no effect on T₃ concentrations in plasma (Fig. 8).

During the simulation at R+45 days half of the control and flight monkeys showed reduced levels of growth hormone (GH) whereas the other half did not (Fig. 9). However, following flight both monkeys (151, 906) showed marked and protracted reductions in GH levels; the decreases ranged from 50 to 92% and remained at these levels at 0, 3, 11 and 17 days after flight (Fig. 10, 11). The two flight animals yielded virtually identical responses post flight.

Insulin-like growth factor I (IGF-I) levels were reduced in flight monkey 151 at 0 and 3 days after flight but approached control concentrations on days 11 and 17 (Fig. 12). In contrast, IGF-I concentrations in monkey 906 were reduced at all sampling times after flight-days 0, 3, 11, and 17 (Fig. 13). Control and flight monkeys showed inconsistent responses to the R+45 day simulation (Fig. 14).

DISCUSSION

In all monkeys cortisol concentrations varied from 500 to nearly 1000 nm/l, values comparable to those of chaired or tethered animals (5, 8), with only suggestive decreases on days 3 and 11 post flight. More importantly, there were no increases immediately following flight or simulated flight, suggesting that corticotrophin and cortisol secretion were minimally affected by these treatments compared to the usual sampling conditions for preflight and control monkeys. Testosterone levels fell 50% on the day of recovery from flight, which is consistent with testosterone levels of post flight (2,4,8), or hindlimb suspended (7) rats. However, this finding in flight monkeys must necessarily be tempered by the low levels of hormone in these sexually immature animals and by the large standard error for testosterone concentrations of control monkeys. Thyroid hormones revealed a dichotomy in their responses to space flight. Thyroxine (T₄) titers were marginally decreased only on day 11 following flight, suggesting at most, a transitory decrease in thyroxine. In contrast, both flight monkeys showed an 80% reduction in triiodothyronine (T₃) on day 0, a 30% decrease on day 3, and returned to control concentrations on days 11 and 17. A further disparity between T₄ and T₃ was seen in the R+45 day simulation in which both flight and control monkeys showed a 25% decrease in T₄ without parallel change in T₃ concentrations.

Plasma growth hormone levels in the monkey tend to be very labile. In a study by Meyer and Knobil (5) exposure of monkeys to a new environment raised plasma concentrations from about 1 ng/ml to greater than 50 ng/ml. It has also been shown that tethered, cannulated monkeys have higher basal levels of plasma GH and respond more to growth hormone releasing factor than do chaired monkeys (4). In the present study control and flight monkeys after the R+45 day simulation showed highly variable concentrations of GH, which may reflect subtle differences in handling or environmental conditions. However, both flight monkeys showed suppression of GH at Recovery day 0 (50-60%), about an 80-90% suppression on days 3 and 11 after flight, and 75-80% decrease 17 days after flight. The consistent responses of the flight animals, which was not shown in the simulation study, and the variable levels shown by control animals, argue rather cogently that space flight does suppress GH secretion in these animals. Further support for a microgravity effect on GH can be adduced from the circulating levels of insulin-like growth factor I (IGF-I), which were reduced in one flight monkey at 0 and 3 days after flight and in the other monkey at 0, 3, 11 and 17 days after flight. The low levels of IGF-I found at day 0 further suggest that the concentrations of IGF-I were also reduced significantly in flight because of the rather slow rate at which changes occur in circulating IGF-I levels.

With only two space flight subjects to test it is impossible to draw statistically rigorous conclusions, but the data certainly suggest that space flight inhibits secretion of T₃, GH and IGF-I and may have lesser, transitory effects on T₄ and testosterone. The persistence of GH and IGF-I effects for up to 17 days following flight clearly indicate a significant, lasting effect of microgravity on hypothalamic regulation of GH secretion and/or the somatotrophic cells of the anterior pituitary gland.

REFERENCES

1. Arnaud, S.B., P. Fung, I.A. Popova, E.R. Morey-Holton, and R.E. Grindeland. Circulating Parathyroid Hormone and Calcitonin in Rats after Spaceflight. *J. Appl. Physiol. Suppl.* 73:169S-173S, 1992.
2. Grindeland, R.E., I.A. Popova, M. Vasques, and S.B. Arnaud. Cosmos 1887 Mission Overview: Effects of Microgravity on Rat Body and Adrenal Weights and Plasma Constituents. *FASEB J.* 4:105-109, 1990.
3. Leach, C.S., and P.C. Ranbaut. Biochemical Responses of the Skylab Crew: An Overview. In: *Biomedical Results from Skylab*, R.S. Johnson and L.F. Dietlein (eds.) Library of Congress Cataloging in Publications Data, Washington, D.C., pp 204-216, 1977.
4. Merrill, A.H., Jr., E. Wang, R.E. Mullens, R.E. Grindeland, and I.A. Popova. Analyses of Plasma for Metabolic and Hormonal Changes in Rats flown on board Cosmos 2044. *J. Appl. Physiol. Suppl.* 73:1325-1355, 1992.
5. Meyer, V. and E. Knobil. Growth Hormone Secretion in the Unanesthetized Rhesus Monkey in Response to Noxious Stimuli *Endocrinol.* 80:163-71, 1967.
6. Quabbe, H.J., S. Bunge, T. Walz, M and B. Bratzke. Plasma Glucose and Free Fatty Acids Modulate the Secretion of Growth Hormone, but not Prolactin, in the Rhesus and Java Monkey. *J. Clin. Endocrinol Metab.* 70:908-15, 1990.
7. Tipton, C.M., R.E. Grindeland, C.R. Woodman, K. Gasselink, J.K. Linderman, and V.R. Mukku. Hormonal and Metabolic Responses of Hypophysectomized Rats with Head-down Suspension In. *Union. Physiol. Sciences Symposium (Barcelona)*, 1993.
8. Vasques, M., R.E. Grindeland, M. Martinelli, and R. Furlanetto. Effects of 7 days of Microgravity on Plasma Hormone Levels. *Physiologist* 31:A104, 1988.
9. Wheeler, M.D., R.E. Schutzengel, S. Barry, and D.M. Styne. Changes in Basal and Stimulated Growth Hormone Secretion in the Aging Rhesus Monkey: A Comparison of Chair Restraint and Tether and Vest Sampling. *J. Clin. Endocrinol Metab.* 71:1501-7, 1990.

Cosmos 2229 Flight Samples

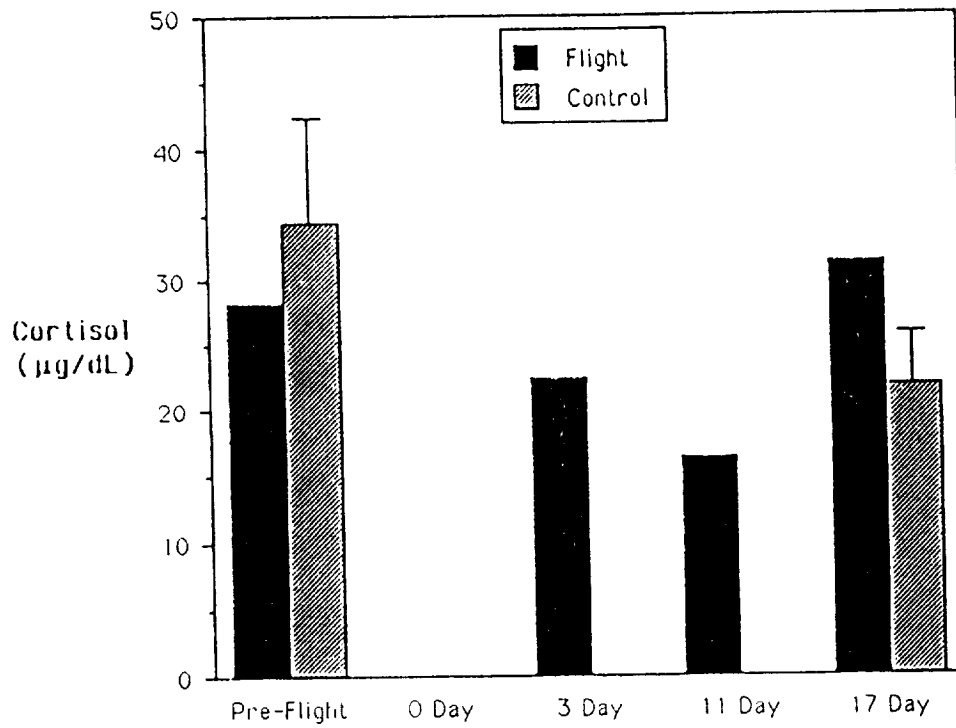


Figure 1: Mean Plasma cortisol concentration (ng/dl) of space flight (n=2) monkeys before and after space flight.

Cosmos 2229 R+45 Simulation

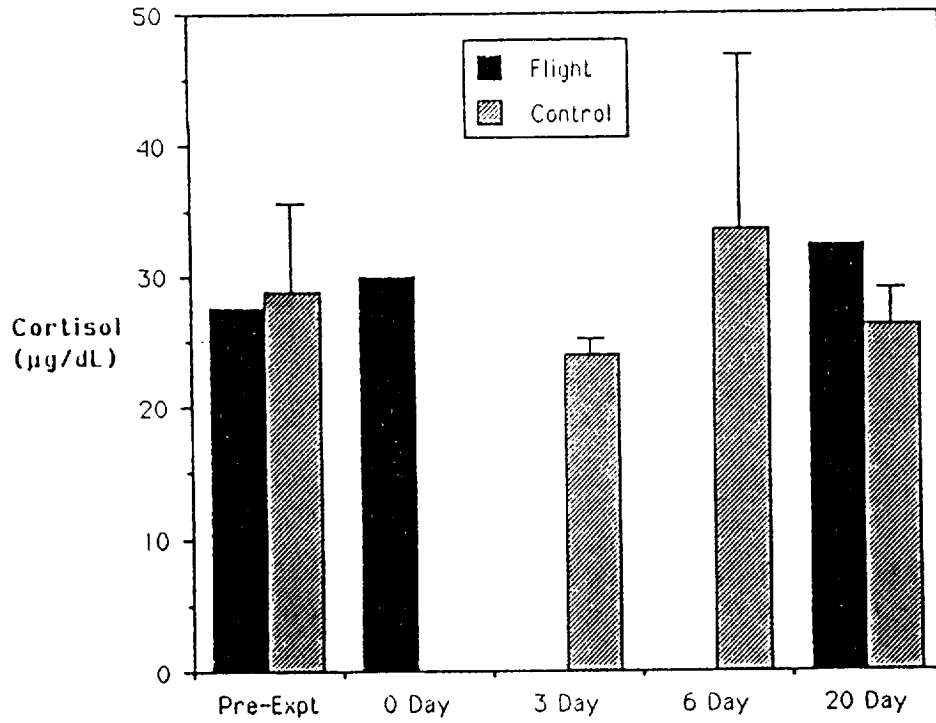


Figure 2: Plasma corticosterone concentrations (ng/dl) of space flight (n=2) and cortisol (n=4) monkeys before and after simulated space flight.

Cosmos 2229 Flight Samples

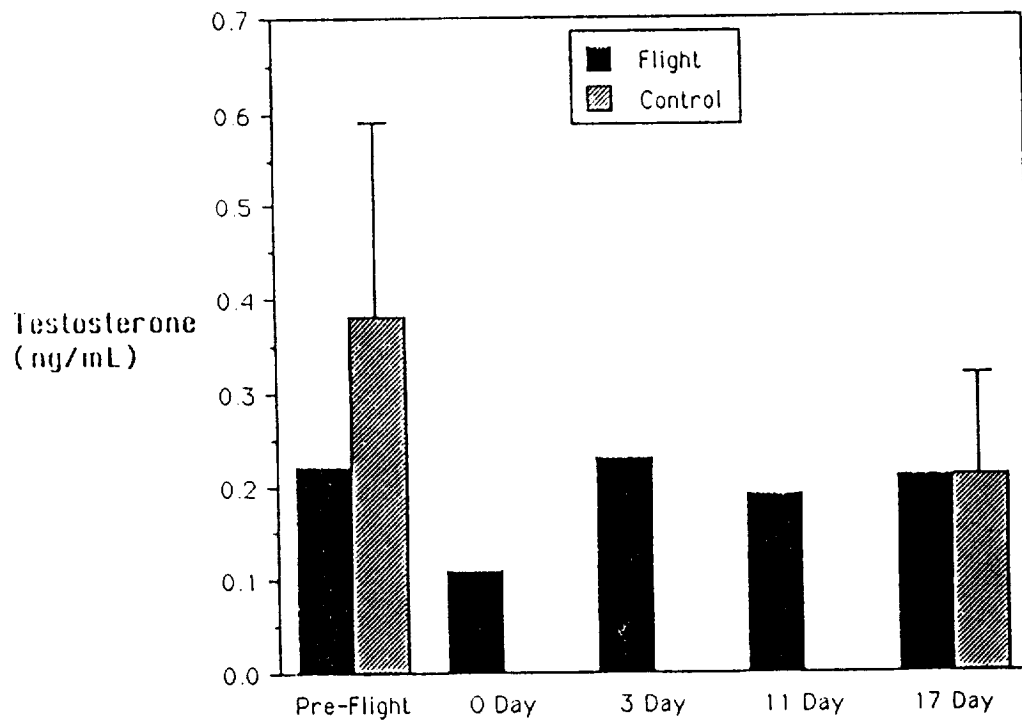


Figure 3: Mean Plasma testosterone concentration (ng/ml) of space flight (n=2) and control (n=4) monkeys before and after space flight.

Cosmos 2229 R+45 Simulation

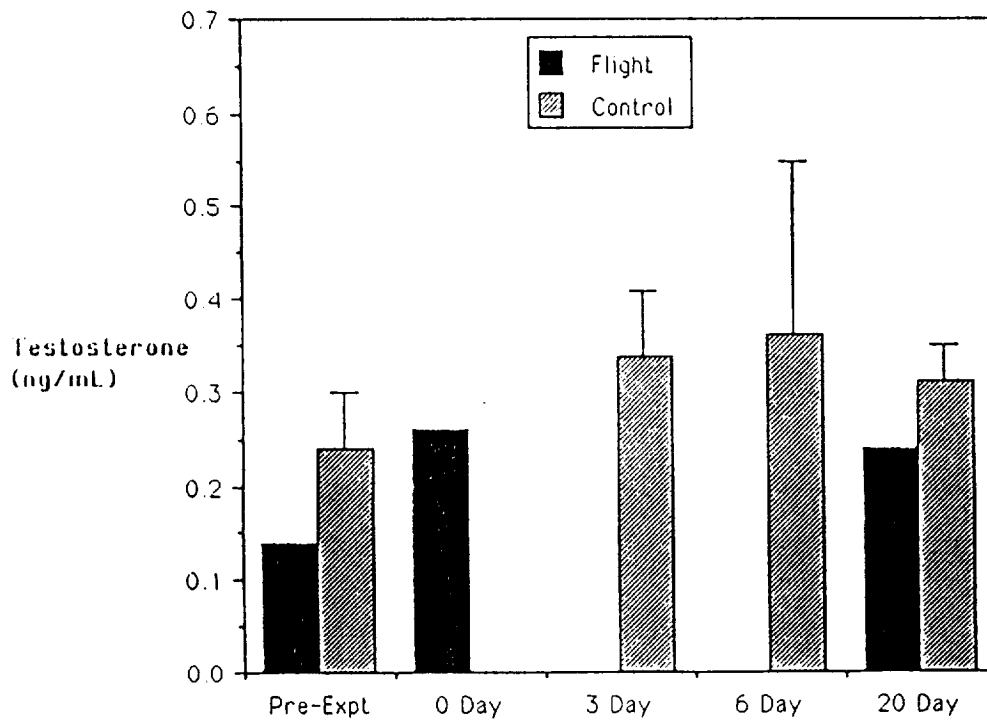


Figure 4: Plasma testosterone concentration (mg/ml) of space flight (n=2) and control (n=4) monkeys before and after simulated space flight.

Cosmos 2229 Flight Samples

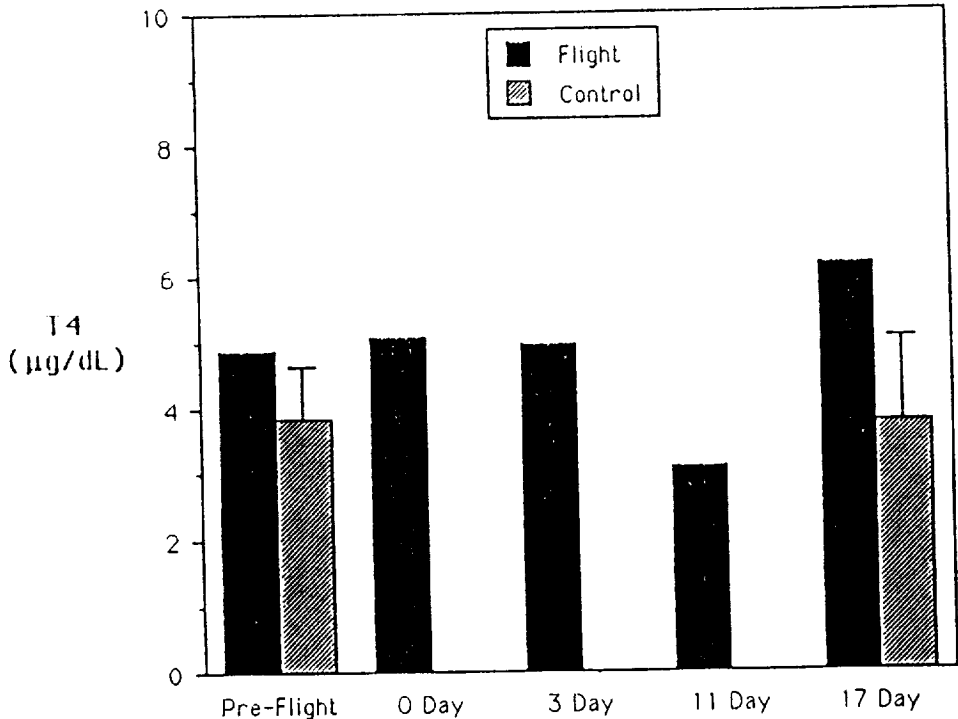


Figure 5: Mean thyroxine concentration (ug/dl) of space flight (n=2) and control (n=4) monkeys before and after space flight.

Cosmos 2229 R+45 Simulation

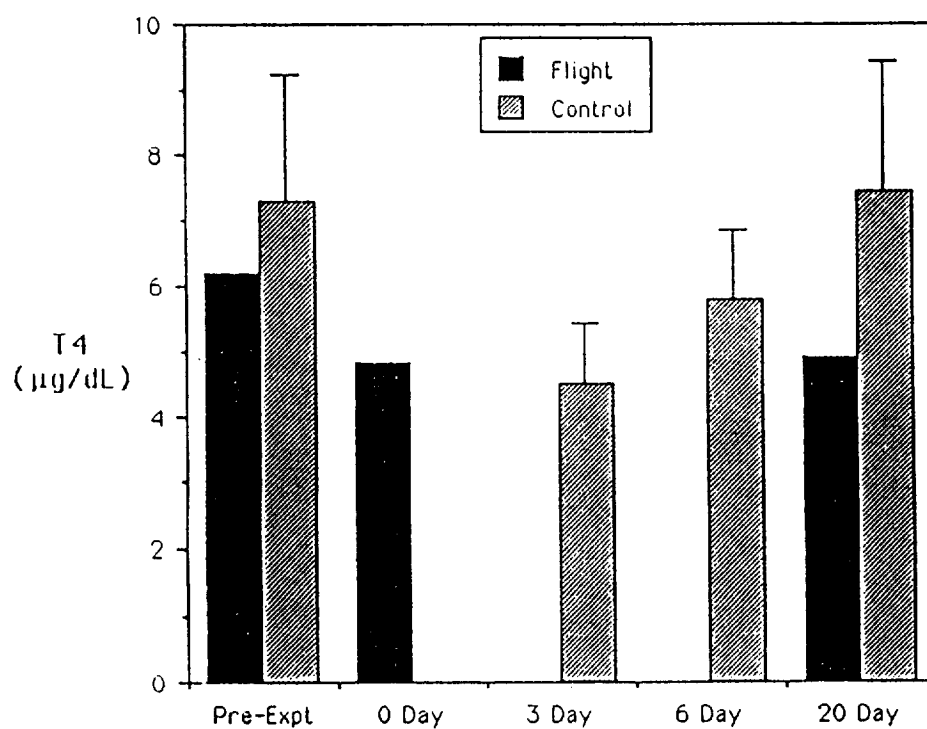


Figure 6: Plasma thyroxine levels of (ug/dl) monkeys before and after simulated space flight.

Cosmos 2229 Flight Samples

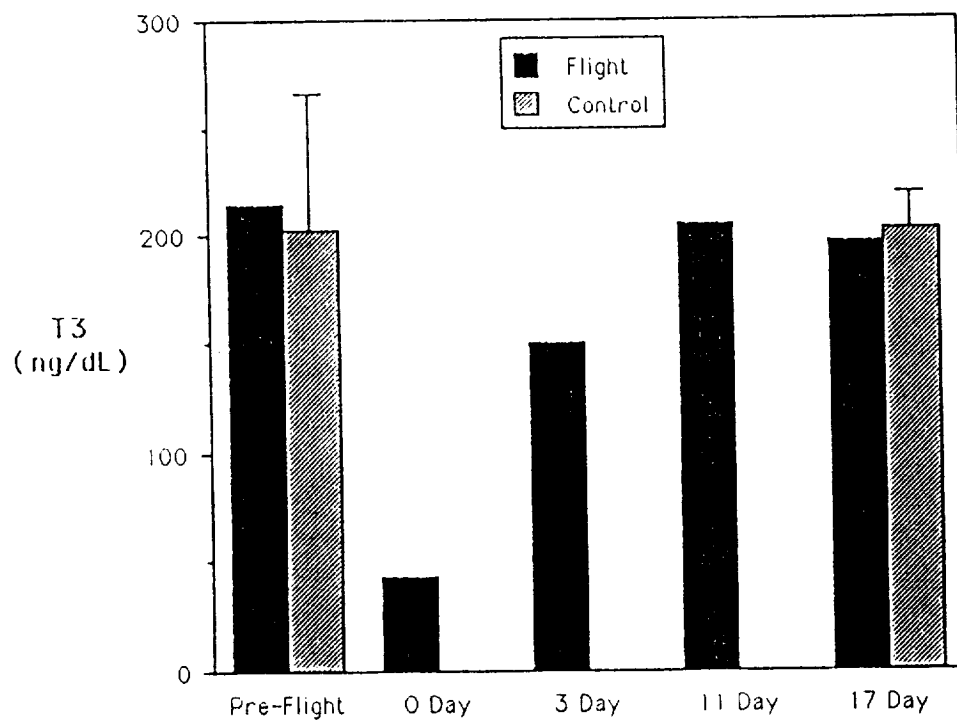


Figure 7: Triiodothyronine concentrations (ng/dl) of space flight (n=2) and control (n=4) monkeys before and after space flight.

Cosmos 2229 R+45 Simulation

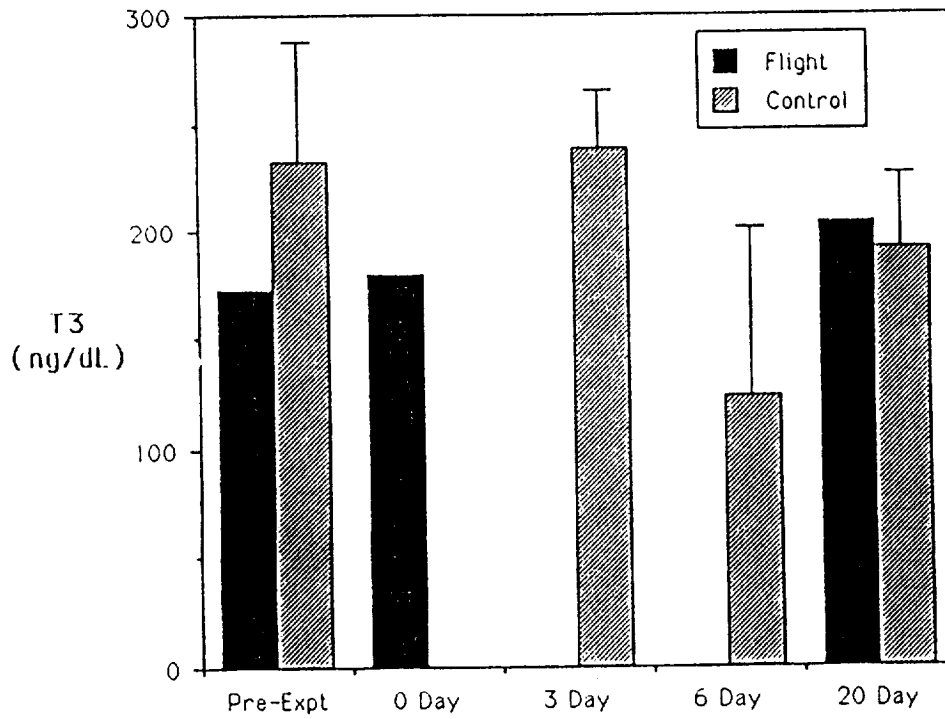


Figure 8: Plasma triiodothyronine concentrations (ng/dl) of flight (n=2) and control (n=4) of monkeys before and after simulated space flight.

Serum GH Levels after RL45 Simulation

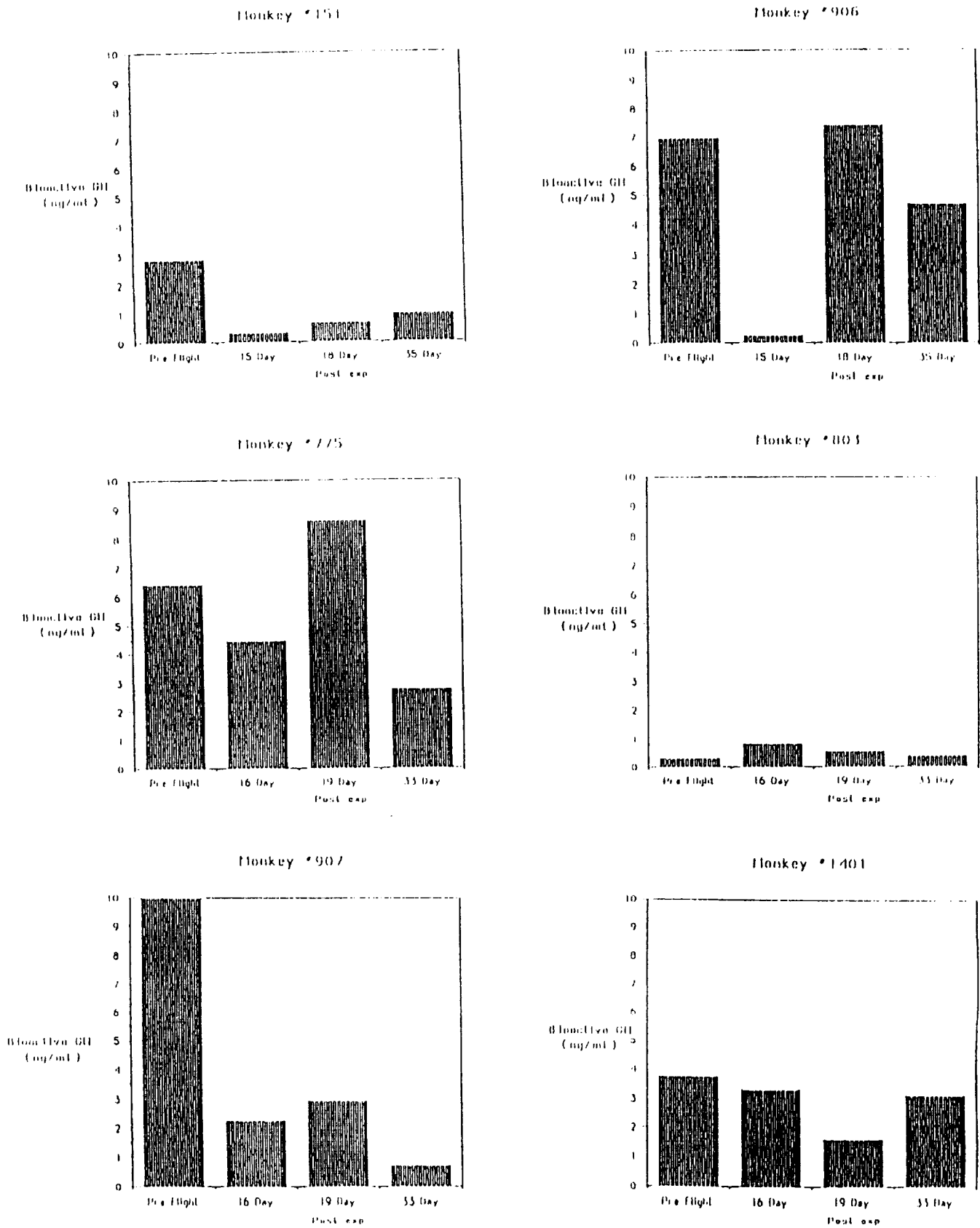


Figure 9: Serum GH concentrations of space flight monkeys (151, 906; top panels) and control monkeys before and after simulated space flight.

Serum GH in Monkey #151
pre- and post-flight

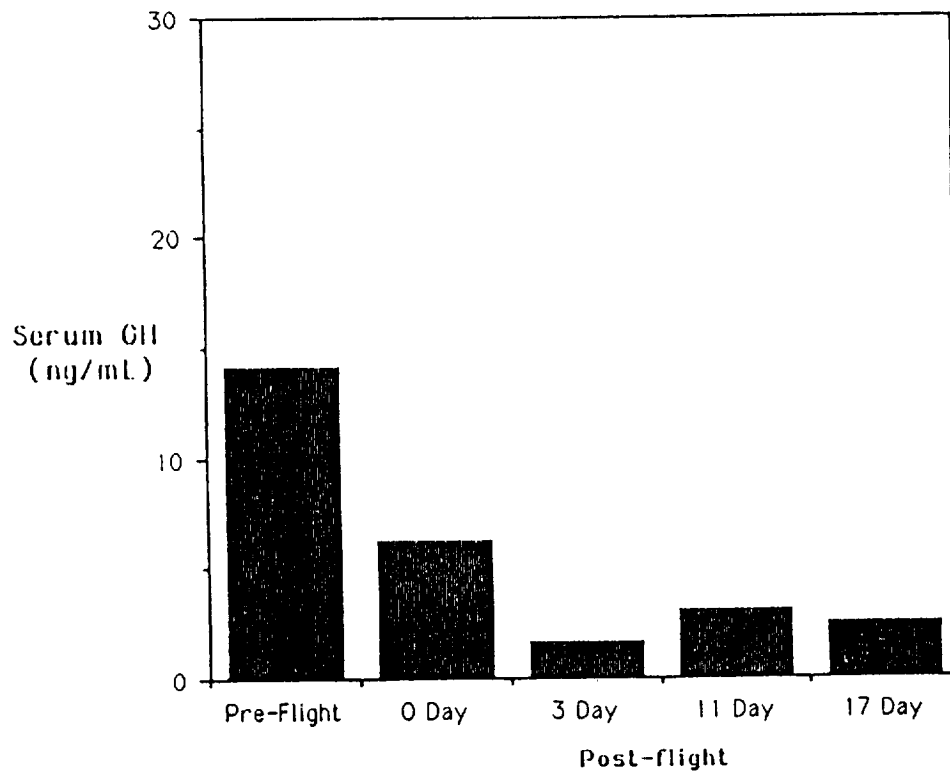


Figure 10: Serum GH concentrations (ng/ml) of space flight monkey 151 before and after space flight.

Serum GH in Monkey #906
pre- and post-flight

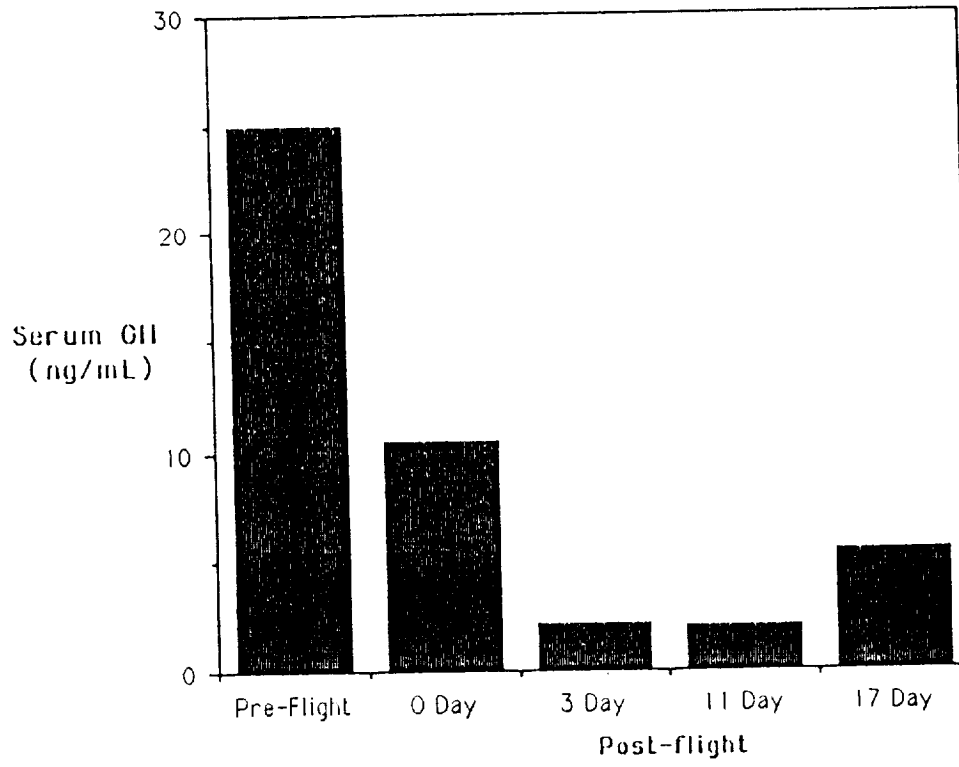


Figure 11: Serum GH concentrations (ng/ml) of space flight monkey 906 before and after space flight.

Serum IGF-1 in Monkey #151
pre- and post-flight

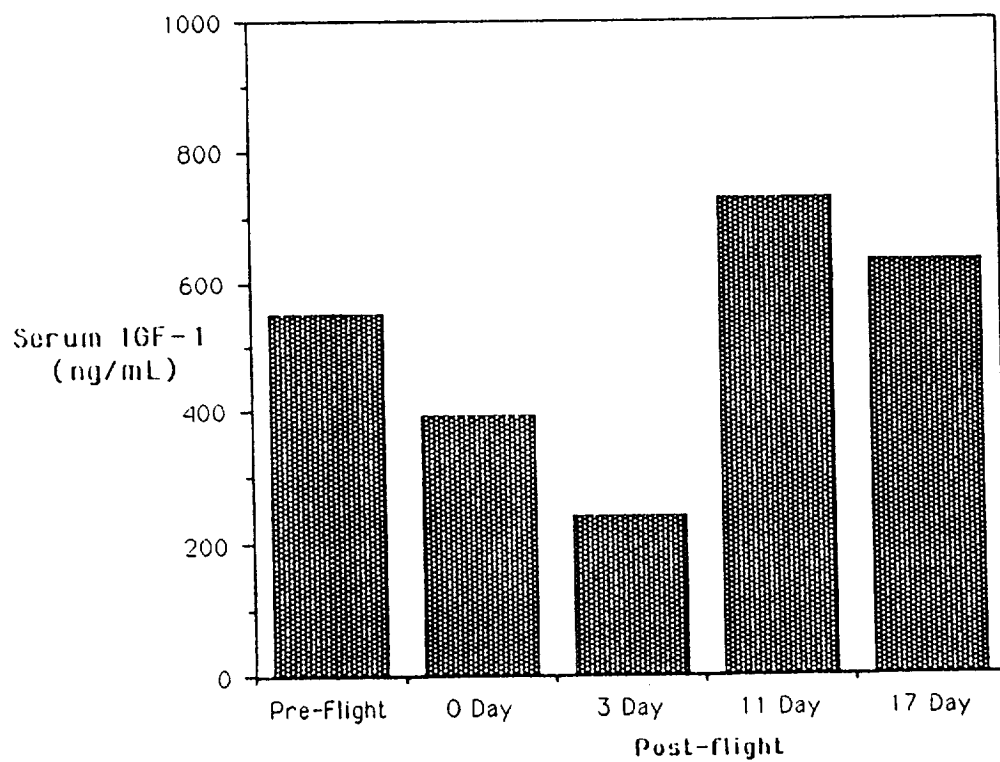


Figure 12: Serum IGF-1 concentrations (ng/ml) of space flight monkey 151 and control monkeys (n=4) before and after space flight.

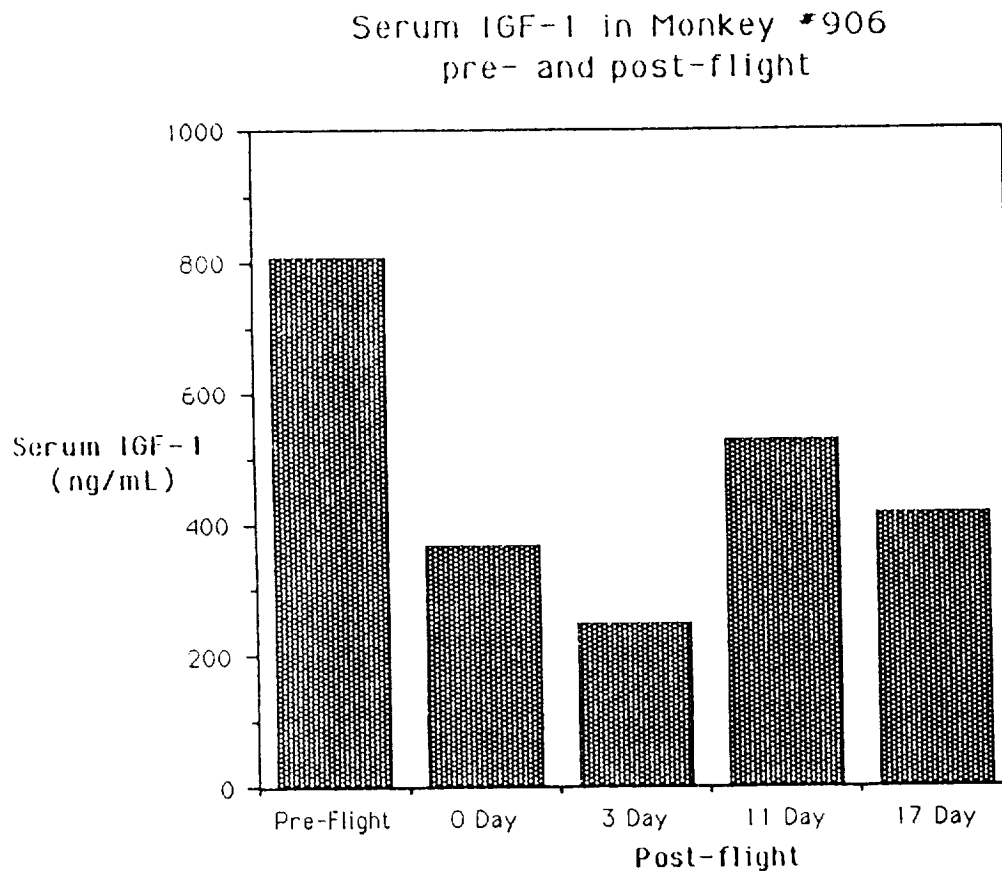


Figure 13: Serum IGF-1 levels (ng/ml) of space flight monkey 906 and control (n=4) monkeys before and after space flight.

Serum IGF-I Levels after R45 Simulation

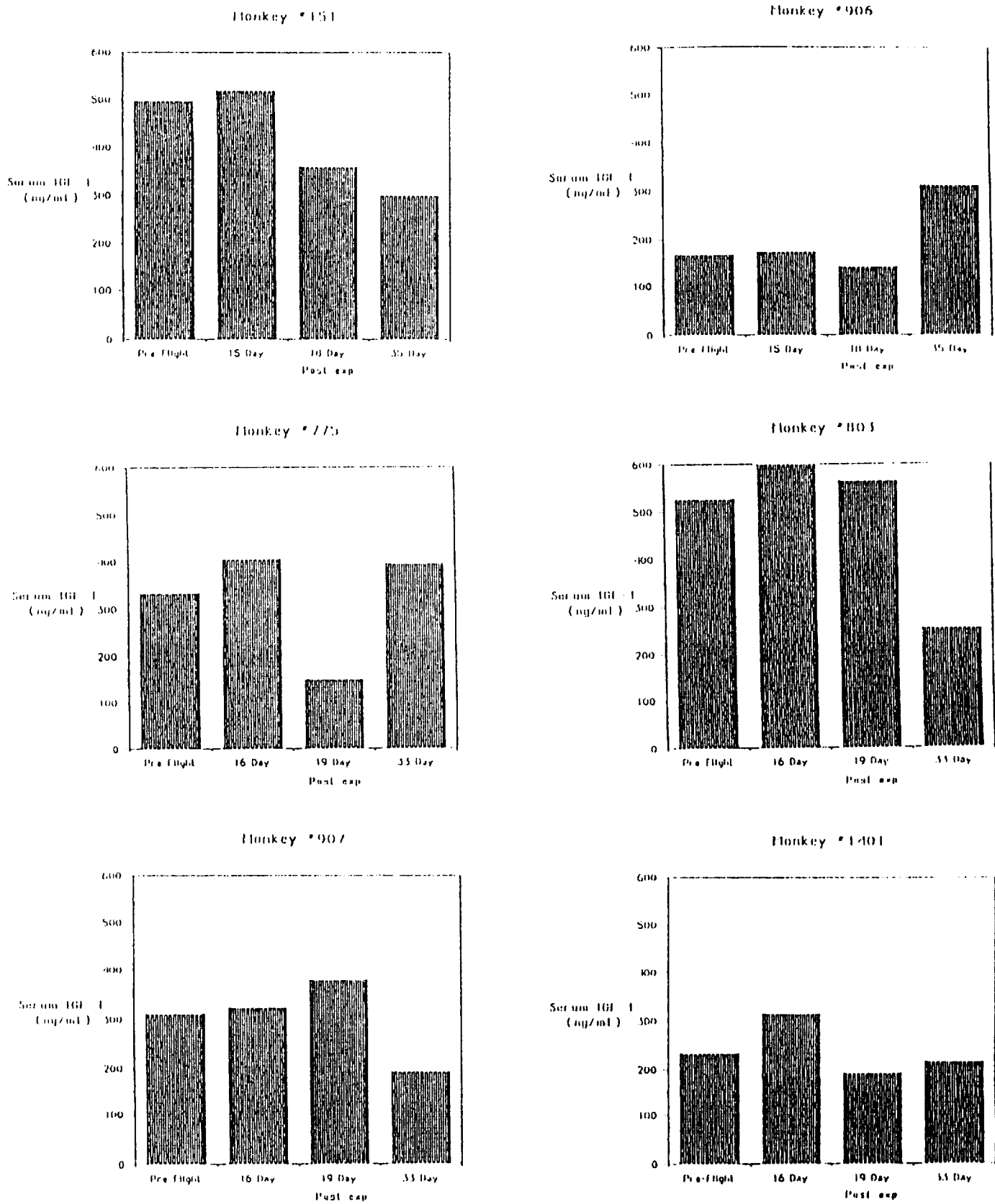


Figure 14: Serum IGF-I levels (ng/ml) of space flight monkeys (#151, 906; top panels) and control monkeys before and after simulated space flight.

REPORT DOCUMENTATION PAGE

Form Approved
OMB No. 0704-0188

Public reporting burden for this collection of information is estimated to average 1 hour per response, including the time for reviewing instructions, searching existing data sources, gathering and maintaining the data needed, and completing and reviewing the collection of information. Send comments regarding this burden estimate or any other aspect of this collection of information, including suggestions for reducing this burden, to Washington Headquarters Services, Directorate for Information Operations and Reports, 1215 Jefferson Davis Highway, Suite 1204, Arlington, VA 22202-4302, and to the Office of Management and Budget, Paperwork Reduction Project (0704-0188), Washington, DC 20503.

1. AGENCY USE ONLY (Leave blank)	2. REPORT DATE April 1997	3. REPORT TYPE AND DATES COVERED Technical Memorandum	
4. TITLE AND SUBTITLE Final Science Reports of the U.S. Experiments Flown on the Russian Biosatellite Cosmos 2229		5. FUNDING NUMBERS 106-30-43	
6. AUTHOR(S) James P. Connolly, Michael G. Skidmore, and Denice A. Helwig, Editors			
7. PERFORMING ORGANIZATION NAME(S) AND ADDRESS(ES) Ames Research Center Moffett Field, CA 94035-1000		8. PERFORMING ORGANIZATION REPORT NUMBER A-976106	
9. SPONSORING/MONITORING AGENCY NAME(S) AND ADDRESS(ES) National Aeronautics and Space Administration Washington, DC 20546-0001		10. SPONSORING/MONITORING AGENCY REPORT NUMBER NASA TM-110439	
11. SUPPLEMENTARY NOTES Point of Contact: James P. Connolly, Ames Research Center, MS 240A-3, Moffett Field, CA 94035-1000 (415) 604-6483			
12a. DISTRIBUTION/AVAILABILITY STATEMENT Unclassified-Unlimited Subject Category 55		12b. DISTRIBUTION CODE	
13. ABSTRACT (Maximum 200 words) Cosmos 2229 was launched on December 29, 1992, containing a biological payload including two young male rhesus monkeys, insects, amphibians, and cell cultures. The biosatellite was launched from the Plesetsk Cosmodrome in Russia for a mission duration of 11.5 days. The major research objectives were: •Study adaptive response mechanisms of mammals during flight •Study physiological mechanisms underlying vestibular, motor system and brain function in primates during early and later adaptation phases. American scientists and their Russian collaborators conducted 11 experiments on this mission which included extensive preflight and postflight studies with rhesus monkeys. Biosamples and data were subsequently transferred to the United States. The U.S. responsibilities for this flight included the development of experiment protocols, the fabrication of some flight instrumentation and experiment-specific ground-based hardware, the conducting of preflight and postflight testing and the analysis of biospecimens and data for the U.S. experiments. A description of the cosmos 2229 mission is presented in this report including preflight, on-orbit and postflight activities. The flight and ground-based bioinstrumentation which was developed by the U.S. and Russia is also described, along with the associated preflight testing of the U.S. hardware. Final Science Reports for the experiments are also included.			
14. SUBJECT TERMS Cosmos, Biosatellite		15. NUMBER OF PAGES 384	
		16. PRICE CODE A16	
17. SECURITY CLASSIFICATION OF REPORT Unclassified	18. SECURITY CLASSIFICATION OF THIS PAGE Unclassified	19. SECURITY CLASSIFICATION OF ABSTRACT	20. LIMITATION OF ABSTRACT